Organoaluminum Mediated Interrupted Nazarov Reaction

by

Yonghoon Kwon

A thesis submitted in partial fulfillment of the requirements for the degree of

Doctor of Philosophy

Department of Chemistry

University of Alberta

© Yonghoon Kwon, 2015

Abstract

Five-membered carbocycles are highly prevalent motifs in natural products and pharmaceutical drugs. Finding routes towards these moieties has been an attractive area of pursuit in synthetic organic chemistry. The Nazarov reaction is one that has been widely used to access cyclopentenone compounds. Interrupting the Nazarov reaction intermediate from its typical pathway has also emerged as a valuable tool to synthesize highly functionalized cyclopentanones. This dissertation contributes to expand the scope of the interrupted Nazarov reaction and hopefully opens door for the synthesis of 6-membered carbocycles and 1,4-diketones beyond functionalizing 5-membered carbocycles.

Recent developments in the interrupted Nazarov reaction are summarized in Chapter 1. The strategy of trapping Nazarov intermediates using heteroatom and π-nucleophiles in both an inter- and intramolecular fashion provides increased molecular complexity with enhanced step economy.

Chapter 2 describes the first example of a Nazarov reaction mediated by triorganoaluminum reagents. Use of these organoaluminum compounds allowed incorporation of simple alkyl and phenyl groups, as well as cyano and azido moieties. Details of using diethyl zinc as a trapping reagent in the Nazarov reaction are also discussed as a comparison to the organoaluminum reactions.

Efforts to find alternative Nazarov substrates involving the use of organoaluminum reagents were also carried out. A divinyl carbinol was found to undergo a domino Oppenauer oxidation/Nazarov cyclization.

During the study of the organoaluminum mediated interrupted Nazarov reaction, unexpected α-hydroxy cyclopentanones were formed upon unintentional exposure to atmospheric oxygen. Chapter 3 provides details of the aluminum enolate oxidation and its tactical use in the Nazarov cyclization.

The oxygen-trapping event in the Nazarov reaction was a realization of double interrupted Nazarov reaction: a nucleophilic addition followed by the resulting enolate addition to an electrophile. Inspired by the double functionalization, we hunted for other interesting electrophiles. Chapter 4 tells the story of these multi-component organoaluminum interrupted Nazarov reactions using masked aldehydes and carbenoids.

Chapter 5 describes the oxidative interruption of the Nazarov reaction. The use of potassium permanganate enabled the synthesis of *syn* 1,4-diketones via a decarbonylative decomposition of the Nazarov oxyallyl intermediate. Preliminary results of diatomic chlorination and bromination of the oxyallyl cation intermediate are also included in this chapter.

Preface

Part of Chapter 2 of this thesis has been published as Y. Kwon, R. McDonald, and F. G. West, "Organoaluminum-Mediated Interrupted Nazarov Reaction," *Angewandte Chemie International Edition*, **2013**, *52*, 8616–8619. I was responsible for the experimental work, the data collection, and characterization of compounds as well as the manuscript composition. R. MacDonald provided X-ray data for compounds **3a**, **3h**, **7a**, **8a'** and **11a** (numbering from Chapter 2). F. G. West was the supervisory author and was involved with concept formation and manuscript composition.

Chapter 3 of this thesis has been published as Y. Kwon, O. Scadeng, R. McDonald, and F. G. West, "α-Hydroxycyclopentanones via One-Pot Oxidation of the Trimethylaluminum-Mediated Nazarov Reaction with Triplet Oxygen," *Chemical Communications*, **2014**, *50*, 5558–5560. I was responsible for the experimental work, the data collection, and characterization of compounds as well as the manuscript composition. O. Scadeng assisted with preparation of compound **1h** and contributed to manuscript edits. R. MacDonald provided X-ray data for compounds **4a**, **4e**, and **5g** (numbering from Chapter 3). F. G. West was the supervisory author and was involved with concept formation and manuscript composition.

Part of Chapter 5 of this thesis will be published as Y. Kwon, D. J. Schatz, and F. G. West, "1,4-Diketones from Cross-conjugated Dienones: Potassium Permangate Interrupted Nazarov Reaction," *Manuscript in preparation*. I was responsible for the experimental work, the data collection, and characterization of compounds as well as the manuscript composition. D. J. Schatz contributed to the synthesis of **1e**, **1g**, and **1i** as well as repeating some of the reactions (numbering from Chapter 5). F. G. West was the supervisory author and was involved with concept formation and manuscript composition.

Dedication

For my wife, mother, and father

Acknowledgements

First and foremost, I sincerely thank my supervisor, F. G. West, for everything he has done for me. I truly enjoyed the freedom he provided to me in my research endeavours. His “massage” made my random and speculative ideas become real. For the past five years coming to our lab has been pleasant and exciting. I wish I could continue having this fun (research) experience with him. I almost cried when I acknowledged him at CSC conferences. I will miss his soft charisma.

I would like to thank past and present West group members, especially the hard working crews. You are very pleasant to be around! I would like to thank Hayley Wan for encouraging my teaching. Your genial tone with gentle smile made me less nervous when I started teaching. You are the most approachable person in this department!

I would like to express my gratitude to all of the NMR, IR, mass spec, and X-ray service labs. We graduate students are blessed because we have the best support staff.

I would like to thank my undergraduate supervisor, Jean Burnell. I was very lucky to be one of your students. Your inspiring lectures led me to change my major from physical education to chemistry without hesitation. My undergraduate research experience under your supervision was enough to survive in graduate school.

To my wife: Many good things have happened since 2003. For the past 12 years, I have been able to be mentally strong and healthy because I have been loved. Can you make better breakfast from now on, please? To my mom, dad, and brother: Can I acknowledge you at home? I am running out of space on this page. In retrospect, our domestic education could not be any better. Thank you for all of your support and love.

Table of Contents

Chapter 1. The Interrupted Nazarov Reaction 1
  1.1 The Nazarov Cyclization 1
  1.2 The Interrupted Nazarov Reaction 3
    1.2.1 Interruption with Carbon Nucleophiles 4
      1.2.1.1 Intramolecular Olefin Trapping 4
      1.2.1.2 Intramolecular Arene Trapping 7
      1.2.1.3 Intermolecular Arene Trapping 11
      1.2.1.4 Intermolecular Olefin Trapping 14
      1.2.1.5 [4+3] Cycloadditions 18
    1.2.2 Reductive Nazarov Reaction 19
    1.2.3 Heteroatoms 20
    1.2.4 Skeletal Rearrangement 25
    1.2.5 Electrophilic Trapping 26
  1.3 Conclusion 28

Chapter 2. Organoaluminum Mediated Nazarov Reactions: Interrupted to Oxidative Processes 29
  2.1 Introduction 29
    2.1.1 Organoaluminum Reagents as Nucleophiles 29
    2.1.2 Organoaluminum as a Medium for Redox Process 32
  2.2 Results and Discussion 36
    2.2.1 Organoaluminum Mediated Interrupted Nazarov Reaction 36
    2.2.2 Meerwein-Ponndorf-Verley Like Interrupted Nazarov Reaction 51
    2.2.3 Organozinc Interrupted Nazarov Reaction 52
    2.2.4 Domino Oppenauer Oxidation/Electrocyclization 57
  2.3 Conclusion 60
  2.4 Future Directions 61
  2.5 Experimental 62
    2.5.1 General Information 62

2.5.2 Experimental Procedures and Characterization for the Organoaluminum Mediated Interrupted Nazarov Reaction 63
2.5.3 Experimental Procedures and Characterization for the Diethylzinc Interrupted Nazarov Reaction 79
2.5.4 Experimental Procedures and Characterization for the Domino Oppenauer Oxidation/Electrocyclization 83
Chapter 3. Synthesis of α-Hydroxycyclopentanones *via* One-Pot Oxidation of the Trimethylaluminum-Mediated Nazarov Reaction with Triplet Oxygen 86
3.1 Introduction 86
3.2 Results and Discussion 87
3.3 Mechanistic Proposal 94
3.4 Conclusion 97
3.5 Future Directions 97
3.6 Experimental 100
3.6.1 General Information 100
3.6.2 Experimental Procedures and Characterization for the Synthesis of α-Hydroxycyclopentanones 100
Chapter 4. Multi-Component Organoaluminum Interrupted Nazarov Cyclization 108
4.1 Introduction 108
4.2 Results and Discussion 109
4.2.1 Organoaluminum-Mediated Interrupted Nazarov Reaction and Electrophilic Trapping with Aldehydes 109
4.2.2 Ring Expansion Strategy: Interrupted Nazarov Reaction and Simmons-Smith Type Cyclopropanation 119
4.3 Conclusion 128
4.4 Future Plans 129
4.5 Experimental 131
4.5.1 General Information 131
4.5.2 Experimental Procedures and Characterization for One-Pot Organoaluminum Mediated Interrupted Nazarov Reaction and Electrophilic Quenching with Aldehydes. 131

4.5.3 Experimental Procedures and Characterization for the Domino Interrupted Nazarov Reaction/Cyclopropanation 139

Chapter 5. Synthesis of 1,4-diketones: Potassium Permanganate Interrupted Nazarov Reactions 143

5.1 Introduction 143

5.1.1 Oxidative Cleavage of Olefins 143

5.2 Results and Discussion 147

5.2.1 Potassium Permanganate Interrupted Nazarov Reaction 147

5.2.2 Halogen Interrupted Nazarov Reactions 155

5.2.3 Alternative Routes to Nazarov Intermediates and Oxidative Cleavage 161

5.3 Conclusion 165

5.4 Future Directions 166

5.5 Experimental 168

5.5.1 General Information 168

5.5.2 Experimental Procedures and Characterization for Potassium Permanganate Interrupted Nazarov Reaction 168

5.5.3 Experimental Procedures and Characterization for Halogen Interrupted Nazarov Reaction 177

References 179

Appendix I: Selected NMR Spectra (Chapter 2) 186

Appendix II: Selected NMR Spectra (Chapter 3) 216

Appendix III: Selected NMR Spectra (Chapter 4) 237

Appendix IV: Selected NMR Spectra (Chapter 5) 258

Appendix V: X-ray Crystallographic Data for Compound **3a** (Chapter 2) 271

Appendix VI: X-ray Crystallographic Data for Compound **3h** (Chapter 2) 276

Appendix VII: X-ray Crystallographic Data for Compound **7a** (Chapter 2) 281

Appendix VIII: X-ray Crystallographic Data for Compound **8a’** (Chapter 2) 286

Appendix IX: X-ray Crystallographic Data for Compound **11a** (Chapter 2) 291

Appendix X: X-ray Crystallographic Data for Compound **7a’** (Chapter 2) 296

Appendix XI: X-ray Crystallographic Data for Compound **4a** (Chapter 3) 301

Appendix XII: X-ray Crystallographic Data for Compound **4e** (Chapter 3) 306

Appendix XIII: X-ray Crystallographic Data for Compound **5e** (Chapter 3)..................311

Appendix XIV: X-ray Crystallographic Data for Compound **5g** (Chapter 3) 316

Appendix XV: X-ray Crystallographic Data for Compound **4a** (Chapter 4)...................321

Appendix XVI: X-ray Crystallographic Data for Compound **3f** (Chapter 4) 326

Appendix XVII: X-ray Crystallographic Data for Compound **8a** (Chapter 4) 330

Appendix XVIII: X-ray Crystallographic Data for Compound **9a** (Chapter 4)...............334

Appendix XIX: X-ray Crystallographic Data for Compound **14a** (Chapter 4) 339

Appendix XX: X-ray Crystallographic Data for Compound **3a** (Chapter 5)...................344

Appendix XXI: X-ray Crystallographic Data for Compound **5a** (Chapter 5) 348

List of Tables

Table 2-1 Catalytic MPV Reduction by Alkylaluminum Reagents.................................. 33
Table 2-2 Optimization of $AlMe_3$-Mediated Interrupted Nazarov Reaction 38
Table 2-3 $AlMe_3$-Mediated Nazarov Cyclization 39
Table 2-4 Optimization of $ZnEt_2$ Interrupted Nazarov Reaction. 54
Table 2-5 $ZnEt_2$ Interrupted Nazarov Reaction 56
Table 2-6 Screening Condition for the Oxidative Nazarov Reaction 59
Table 3-1 Trimethylaluminum Mediated Nazarov Cyclization and Oxidation of Resulting Aluminum Enolate 90
Table 4-1 $AlMe_3$ Mediated Interrupted Nazarov Reaction and Electrophilic Addition of Formaldehyde 112
Table 4-2 $AlMe_3$ /CH_2I_2 Mediated Interrupted Nazarov Reaction and Cyclopropanation. 122
Table 5-1 Screening Conditions for the $KMnO_4$ Interrupted Nazarov Reaction............ 150
Table 5-2 Synthesis of 1,4-Diketones via $KMnO_4$ Interruptions of the Nazarov Intermediates 152

List of Figures

Figure 2.1 ORTEP Drawing of **3h** 41

Figure 2.2 Assignment of **3k** and **3k'**. 43

Figure 2.3 rOe Experiment for **3l** and Chemical Shift Comparison to 1-Methylnaphthalene. 44

Figure 2.4 ORTEP Drawing of **7a** 46

Figure 2.5 ORTEP Drawing of **8a'** 47

Figure 2.6 ORTEP Drawing of **11a'** 49

Figure 2.7 ORTEP Drawing of **7a'** 55

Figure 3.1 Natural Products Flammulinolide B and C 88

Figure 3.2 ORTEP Drawing of **4a** 92

Figure 3.3 ORTEP Drawing of **4e** and **5e** 93

Figure 4.1 Projection of the Prins Reaction to the Interrupted Nazarov Reaction 110

Figure 4.2 ORTEP Drawing of **4a** 114

Figure 4.3 ORTEP Drawing of **3f** 114

Figure 4.4 ^{1}H NMR Chemical Shift Correlations of **6a**, **6a'**, and **7a** 115

Figure 4.5 ^{1}H NMR Chemical Shift Correlations for **8a** and **9a** 116

Figure 4.6 ORTEP Drawing of **8a** and **9a** 117

Figure 4.7 ^{1}H NMR Chemical Shift Correlations for **10a** and **11a** and 6-Membered Transition State 119

Figure 4.8 Structural Similarity of TMS Enol Ether and Aluminum Enolate 121

Figure 4.9 Diagnostic 2D NMR Correlations of **13a** 124

Figure 4.10 ORTEP Drawing of **14a** 125

Figure 5.1 ORTEP Drawing of **3a** 151

Figure 5.2 ORTEP Drawing of **5a** 158

Figure 5.3 ^{1}H NMR study of **5a** and **6a** 159

List of Schemes

Scheme 1.1 Vorländer's Ketol 1

Scheme 1.2 Transformation of Divinylacetylene **3** to Cyclopentenone **4** 2

Scheme 1.3 Nazarov's Initial Proposed Route to Cyclopentenone **4** 2

Scheme 1.4 Mechanism of the Nazarov Reaction 3

Scheme 1.5 The Interrupted Nazarov Reaction 4

Scheme 1.6 Homologous Prins Type Interrupted Nazarov Reaction 5

Scheme 1.7 Distal Olefin Participation in the Interrupted Nazarov Reaction. 6

Scheme 1.8 Attempted Synthesis of Angular Triquinane via the Interrupted Nazarov Reaction 6

Scheme 1.9 Cascade Polycyclization. 7

Scheme 1.10 Scope of Arene Traps in the Intramolecular Interrupted Nazarov Reaction. 8

Scheme 1.11 Dichlorocyclopropane Substrates and Intramolecular Arene Trapping. 9

Scheme 1.12 Enantioselective Intramolecular Arene Trapping... 9

Scheme 1.13 Interrupted Imino-Nazarov Cyclization of 1-Aminopentadienyl Cation and Intramolecular Arene trapping. 10

Scheme 1.14 Tetrahydroquinoline-Fused Cyclopentenone 11

Scheme 1.15 Intermolecular Arene Trapping 12

Scheme 1.16 Tius's Indole Interrupted Nazarov Reaction 12

Scheme 1.17 Nazarov Cyclization of Allenyl Vinyl Ketones with Nitrogen Heterocyles. 13

Scheme 1.18 Heteroarylation Pathway of Acyclic Dienone **61** 13

Scheme 1.19 Allyltrimethylsilane Trapping 14

Scheme 1.20 Allyltriisopropylsilane Trapping 15

Scheme 1.21 Efficient Lewis Acid $TiCl_4$ in the Allylation 15

Scheme 1.22 Vinyl Sulfide Trapping in the Interrupted Nazarov Reaction 16

Scheme 1.23 Nazarov Reactions of Allenyl Vinyl Ketone with Electron-Rich Alkenes. 16

Scheme 1.24 Homologous Mukaiyama Reaction 17

Scheme 1.25 Formal Homologous Aldol Reactions: Electron Rich Arene Trapping 17

Scheme 1.26 Intramolecular [4+3] Cycloaddition. 18

Scheme 1.27 Domino Nazarov/Intermolecular [4+3] Cycloaddition Reactions. 18
Scheme 1.28 The Reductive Nazarov Cyclization. 19
Scheme 1.29 Reductive Cyclization of **87** in the Presence of Et_3SiD. 20
Scheme 1.30 *trans* Relative Stereochemistry in the Silyl Enol Ether Product. 20
Scheme 1.31 Intramolecular Oxygen Trapping in the Interrupted Nazarov Reaction...... 21
Scheme 1.32 Intermolecular Alcohol Trapping. 21
Scheme 1.33 Intermolecular Trapping with Trifluoroacetate. 22
Scheme 1.34 Interrupted Vinylogous Iso-Nazarov Reaction. 22
Scheme 1.35 Amine Interrupted Nazarov Reaction. 23
Scheme 1.36 Intramolecular Azide Trapping. 24
Scheme 1.37 Intermolecular Azide Trapping. 24
Scheme 1.38 Intermolecular Azide Capture via [3+3] Cycloaddition to Triazine **113** 24
Scheme 1.39 Nazarov Cyclization/Wagner-Meerwein Sequence. 25
Scheme 1.40 Spirocycle Formation from Nazarov Substrate **118**. 26
Scheme 1.41 Nazarov Cyclization/Electrophilic Fluorination. 27
Scheme 1.42 Asymmetric Nazarov Cyclization/Bromination Sequence. 27
Scheme 1.43 Tandem Nazarov Cyclization/Michael Addition. 28
Scheme 2.1 Organoaluminum-Mediated C-Glycoside Synthesis. 30
Scheme 2.2 Organoaluminum Mediated Regioselective/Stereoselective Substitution Reaction of Epoxy Alcohol. 30
Scheme 2.3 Alkylative Displacement and Cyclization of Allyl Phosphate Esters. 31
Scheme 2.4 Organoaluminum Induced Umpolung Reactions of N-Alkoxyenamines. 32
Scheme 2.5 Oppenauer Oxidation and MPV Reduction. 32
Scheme 2.6 Catalytic Oppenauer Oxidation with $AlMe_3$ 34
Scheme 2.7 Catalytic MPV Reduction with Aluminum Alkoxide. 34
Scheme 2.8 Catalytic Oppenauer Oxidation by Aluminum Alkoxide. 35
Scheme 2.9 Catalytic Asymmetric MPV Reduction. 36
Scheme 2.10 Proposed Organoaluminum Based Nazarov Reaction. 37
Scheme 2.11 Electronic Effect of Aromatic Substituents on the Regioselectivity. 42
Scheme 2.12 Possible Formation of Phenonium Ion 42
Scheme 2.13 Steric Effect of β-Substituents on the Regioselectivity 43

Scheme 2.14 Al(i-Bu)$_3$ Mediated Reductive Nazarov Reaction. 45
Scheme 2.15 AlEt$_3$ Mediated Interrupted Nazarov Reaction. 45
Scheme 2.16 Et$_2$AlCN Mediated Interrupted Nazarov Reaction. 47
Scheme 2.17 AlPh$_3$ Mediated Interrupted Nazarov Reaction. 48
Scheme 2.18 Intramolecular Azide Trapping. 48
Scheme 2.19 Base-Induced Epimerization of **11a'** 49
Scheme 2.20 Unsuccessful Vinylaluminum Reaction. 50
Scheme 2.21 Use of Ethylenediamine in Generation of Diethylalkynyl Aluminum. 51
Scheme 2.22 The MPV Alkynylation of Aldehydes. 51
Scheme 2.23 Proposed MPV-Type Interrupted Nazarov Reaction. 52
Scheme 2.24 Unsuccessful Delivery of Alkynyl Functionality. 52
Scheme 2.25 Organozinc Interrupted Nazarov Reaction. 53
Scheme 2.26 Reactivity of ZnEt$_2$ on a Nazarov Substrate. 53
Scheme 2.27 AlMe$_3$-Catalyzed Alcohol Oxidation. 57
Scheme 2.28 Domino Oppenauer Oxidation/Nazarov Cyclization. 58
Scheme 2.29 Oxidation of 6m with AlMe$_3$ and Nitrobenzaldehyde. 60
Scheme 2.30 Additive Effect on the Suppression of 1,2-addition. 61
Scheme 2.31 Study of Ethyl Migration on Unsymmetrical Dienone **1j** 62
Scheme 3.1 Organoaluminum Mediated Interrupted Nazarov Reaction. 87
Scheme 3.2 Unexpected Finding: α-Hydroxycyclopentanones. 87
Scheme 3.3 Aluminum Enolate Reaction under Photochemical Condition and Autoxidation. 88
Scheme 3.4 One-Pot Interrupted Nazarov Reaction/Oxidation of the Aluminum Enolate. 89
Scheme 3.5 Use of Davis Oxaziridine. 94
Scheme 3.6 The Formation of Aluminum Enolate. 95
Scheme 3.7 Autoxidation of Trimethylaluminum. 95
Scheme 3.8 Alcohol Oxidation by *tert*-Butyl Hydroperoxide and AlMe$_3$. 96
Scheme 3.9 Proposed Mechanism for the Aluminum Enolate Oxidation. 97
Scheme 3.10 Future Plan: One-Pot 1,4-Addition and Aluminum Enolate Oxidation. 98

Scheme 3.11 Diethylaluminum 2,2,6,6-Tetramethylpiperidine Mediated Crossed Aldol Reaction. 98

Scheme 3.12 Future Plan: Aluminum Amide and Triplet Oxygen. 99

Scheme 3.13 Control Experiment: Rubottom Oxidation. 99

Scheme 4.1 Modes of Bond Formation in the Nazarov Reaction. 108

Scheme 4.2 One-Pot Oxidation of the Trimethylaluminum-Mediated Nazarov Reaction with Triplet Oxygen. 109

Scheme 4.3 Domino Prins Reaction/Organoaluminum Carbocation Capture. 110

Scheme 4.4 Double Interrupted Nazarov Reaction. 111

Scheme 4.5 $AlMe_3$-Mediated Interrupted Nazarov Reaction of **1e** 113

Scheme 4.6 $AlEt_3$ Mediated Interrupted Nazarov Reaction in Paraformaldehyde. 115

Scheme 4.7 Reductive Nazarov Reaction in Paraformaldehyde 116

Scheme 4.8 Double Interrupted Nazarov Reaction with $AlMe_3$ and Paraldehyde. 118

Scheme 4.9 First Organoaluminum-Mediated Cyclopropanation. 120

Scheme 4.10 Organoaluminum Mediated Cyclopropanation. 120

Scheme 4.11 Domino Interrupted Nazarov Reaction/Cyclopropanation 121

Scheme 4.12 Test Substrate **1b** and **1d** 123

Scheme 4.13 Autoxidation Product **14a** and **15a** and Rationale for Formation of a Peroxyacetal in the Case of **14a**. 124

Scheme 4.14 Potential Equilibrium of Peroxides. 125

Scheme 4.15 Derivatization of Peroxides to β-Hydroxy-Cyclohexanones. 126

Scheme 4.16 Oxidative Rearrangement of Bicyclo[3.1.0]alkan-1-ols. 126

Scheme 4.17 Blanco's Control Experiment. 127

Scheme 4.18 Proposed Mechanism for the Autoxidation of **13a** 127

Scheme 4.19 Free Radical Reactions of Cyclopropanol. 128

Scheme 4.20 Interrupted Nazarov Reaction/Cyclopropanation with Et_2AlCl and CH_2I_2. 129

Scheme 4.21 Intermolecular Interrupted Nazarov Reaction and Carbenoid Quenching. 130

Scheme 5.1 Ozonolysis. 143

Scheme 5.2 Lemieux-Johnson Oxidation of *trans*-Stilbene to Benzaldehyde. 144

Scheme 5.3 OsO_4/$NaIO_4$ Promoted Oxidative Cleavage of Allylic Alcohol. 144

Scheme 5.4 Effects of 2,6-lutidine on the Lemieux-Johnson Oxidation. 145
Scheme 5.5 Oxidative Cleavage of Olefins Using OsO_4 and Oxone. 145
Scheme 5.6 Oxidative Cleavage of Allylic Alcohols Using $RuCl_3$ and $NaIO_4$. 146
Scheme 5.7 Homogeneous Permanganate Oxidation of *trans*-Stilbene to Benzaldehyde. 146
Scheme 5.8 Proposed Permanganate Interrupted Nazarov Reaction. 148
Scheme 5.9 Proposed **Mechanism A** for the $KMnO_4$ Interrupted Nazarov Reaction.... 154
Scheme 5.10 Proposed **Mechanism B** for the $KMnO_4$ Interrupted Nazarov Reaction.. 155
Scheme 5.11 Examples of Halide Interrupted Nazarov Cyclizations from West and Burnell.. 156
Scheme 5.12 A Fortuitous Finding: Chlorine Interrupted Nazarov Reaction. 156
Scheme 5.13 Chlorine Interrupted Nazarov Reaction. 157
Scheme 5.14 Bromine Interrupted Nazarov Reaction. 159
Scheme 5.15 Proposed Mechanism of Formation of the Bromonium Ion. 160
Scheme 5.16 Use of Hydrogen Fluoride with $KMnO_4$ in the Nazarov Reaction. 160
Scheme 5.17 Alternative Routes to the Oxyallyl Cation. 161
Scheme 5.18 [4+3] Cycloaddition using Föhlisch Conditions. 162
Scheme 5.19 Competing Favorskii Rearrangement.. 162
Scheme 5.20 Oxidative Cleavage of the Base-Induced Oxyallyl Cation. 163
Scheme 5.21 Control of Enolization Using a α,α'-Substituted Ketone........................ 163
Scheme 5.22 Noyori Reaction Conditions.. 164
Scheme 5.23 Oxidative Cleavage of the Iron-Carbonyl-Induced Oxyallyl Cation. 165
Scheme 5.24 Future Work on Screening Oxidants.. 166
Scheme 5.25 Bromination of Enones.. 167

List of Symbols and Abbreviations

^1H	proton
^{13}C	carbon-13
Å	Angstrom
ABq	AB quartet
Ac	acetyl
Ac_2O	acetic anhydride
acac	acetylacetonate
APCI	Atmospheric Pressure Chemical Ionization (mass spectrometry)
app.	apparent (spectral)
APPI	Atmospheric Pressure Photoionization (mass spectrometry)
aq	aqueous solution
Ar	aryl
Bn	benzyl
Boc	*tert*-butyloxycarbonyl
br	broad (spectral)
Bu	butyl
ºC	degrees Celsius
Calcd	calculated
cat.	indicates that the reagent was used in a catalytic amount
cm^{-1}	wave numbers
COSY	H-H correlation spectroscopy
conc.	concentrated
d	day(s); doublet (spectral)
DBU	1,8-diazabicyclo[5.4.0]undec-7-ene
DCE	1,2-dichloroethane
DCM	dichloromethane
dd	doublet of doublets (spectral)
ddd	doublet of doublets of doublets (spectral)
ddddd	doublet of doublets of doublets of doublets of doublets (spectral)

DIBAL-H	diisobutylaluminum hydride
DMS	dimethyl sulfide
dq	doublet of quartets (spectral)
dqdd	doublet of quartets of doublets of doublets (spectral)
dr	diastereomeric ratio
dt	doublet of triplets (spectral)
E^+	an unspecified electrophile
EDG	electron-donating group
ee	enantiomeric excess
EI	electron impact (mass spectrometry)
ESI	electrospray inonization (mass spectrometry)
Et	ethyl
EtOAc	ethyl acetate
equiv	equivalent(s)
EWG	electron-withdrawing group
g	gram(s)
h	hour(s)
Hex	hexyl
HMBC	heteronuclear multiple bond coherence (spectral)
HOMO	highest occupied molecular orbital
HSQC	heteronuclear single quantum coherence (spectral)
HPLC	high performance liquid chromatography
HRMS	high resolution mass spectrometry
hν	light
Hz	hertz
i-Bu	isobutyl
i-Pr	isopropyl
IR	infrared
J	coupling constant
J_{AB}	coupling constant between protons A and B
L	liter(s); unspecified ligand

LA	Lewis acid
LAH	lithium aluminum hydride
LDA	lithium diisopropylamide
M	molar
m	multiplet (spectral)
M^+	generalized Lewis acid or protic acid; molecular ion
Me	methyl
mg	milligram(s)
MHz	megahertz
min	minute(s)
mL	milliliter(s)
mmol	millimole(s)
Moc	methoxycarbonyl
mol	mole(s)
mp	melting point
MPV	Meerwein–Ponndorf–Verley
MS	molecular sieves
Ms	methanesulfonyl
m/z	mass to charge ratio
NFSI	*N*-fluoro-*o*-benzenedisulfonimide
NMR	nuclear magnetic resonance
n-Pr	normal propyl
Nu	an unspecified nucleophile
ORTEP	Oak Ridge thermal-ellipsoid plot
PCC	pyridinium chlorochromate
Ph	phenyl
PMB	4-methoxybenzyl
PMP	4-methoxyphenyl
ppm	parts per million
Pr	propyl
PTC	phase-transfer catalysis

q	quartet (spectral)
R	generalized alkyl group of substituent
R_f	retention factor (in chromatography)
rOe	rotating-frame Overhauser enhancement
rt	room temperature
rxn	reaction
s	singlet (spectral)
sept	septet (spectral)
S.M.	starting material
S_N	nucleophilic substitution
t	triplet (spectral)
T	temperature
t-Bu	*tert*-butyl
Tf	trifluoromethanesulfonyl
TFA	trifluoroacetic acid
TFE	2,2,2-trifluoroethanol
THF	tetrahydrofuran
THP	2-tetrahydropyranyl
TIPS	triisopropylsilyl
TLC	thin layer chromatography
TMS	trimethylsilyl
TOCSY	total correlation spectroscopy
TROESY	transverse rotating-frame overhauser enhancement spectroscopy
Ts	*p*-toluenesulfonyl
TsOH	*p*-toluenesulfonic acid
wt.	weight
δ	chemical shift

Chapter 1

The Interrupted Nazarov Reaction

1.1 The Nazarov Cyclization

5-Membered carbocycles are ubiquitous motifs in natural products and pharmaceutical drugs. Finding routes towards these moieties has been an attractive pursuit in synthetic organic chemistry. One of the most well-developed and efficient methods is the Nazarov cyclization.[1] The classic Nazarov reaction is an acid-catalyzed electrocyclization of cross-conjugated divinyl ketones into cyclopentenones.

The first reported example of the Nazarov reaction is the transformation of dibenzylideneacetone **1** to ketol **2** by Vorländer in 1903 (Scheme 1.1); however, the structure of **2** was originally misassigned.[2] The correct structure was later elucidated by Allen and co-workers using UV light absorption in 1955.[3]

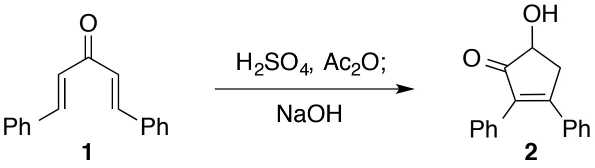

Scheme 1.1 Vorländer's Ketol.

In 1940s Ivan N. Nazarov transformed divinylacetylene **3** to cyclopentenone **4** (Scheme 1.2) via (i) aqueous acid mediated hydration, (ii) mercury salt mediated isomerization, and (iii) electrocyclic ring closure.[4] The notion of a pericyclic reaction was not established at that time. Rather, Nazarov proposed that the cyclization began with direct protonation of the enone followed by C-C bond formation (Scheme 1.3).[5]

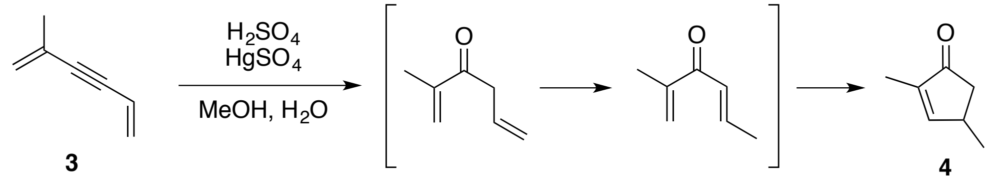

Scheme 1.2 Transformation of Divinylacetylene **3** to Cyclopentenone **4**.

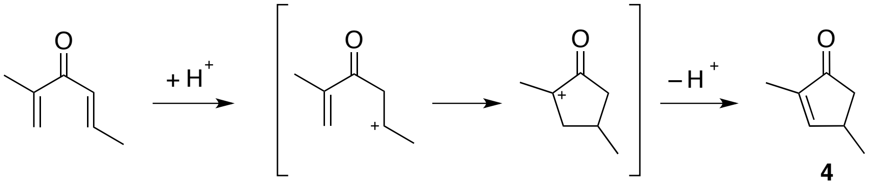

Scheme 1.3 Nazarov's Initial Proposed Mechanism to Cyclopentenone **4**.

After Woodward's seminal publication on conservation of orbital symmetry,[6] the mechanism for the Nazarov reaction was found to occur via a pericyclic reaction. When activated by protic or Lewis acid, cross-conjugated ketone **5** forms pentadienyl cation **6** (Scheme 1.4), which then undergoes thermal 4π conrotatory electrocyclization to oxyallyl cation intermediate **7**. The conrotatory motion of rotation was dictated by orbital symmetry of HOMO of the pentadienyl cation. At this stage, two stereogenic centers (β- and β'-positions) are set stereospecifically, but subsequent elimination of intermediate **7** removes one of these centers. Tautomerization of cyclopentadienol **8** affords the Nazarov cyclization product, cyclopentenone **9**.

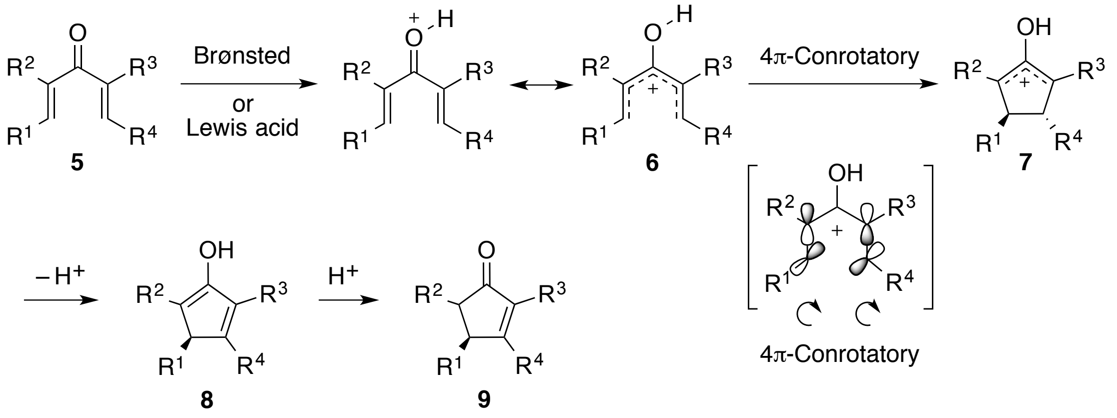

Scheme 1.4 Mechanism of the Nazarov Reaction.

1.2 The Interrupted Nazarov Reaction

There have been significant developments in the Nazarov reaction since Woodward's elucidation of the mechanism. One of the most fruitful areas of research involves introduction of additional bond forming events during the course of the reaction, diverging from the conventional path (proton elimination) at the reactive oxyallyl cation intermediate. For example, interception of oxidocyclopentenyl cation **7** inter- and intramolecularly with a variety of nucleophiles to furnish functionalized cyclopentanones **10** and polycyclic systems **11** has been extensively investigated. These variations have collectively been termed the "interrupted Nazarov reaction."[7] Vorländer's example has since been recognized as the first reaction of this nature. The notion of the interrupted Nazarov process can further include reactions of dienol or dienolate **8** with electrophiles.

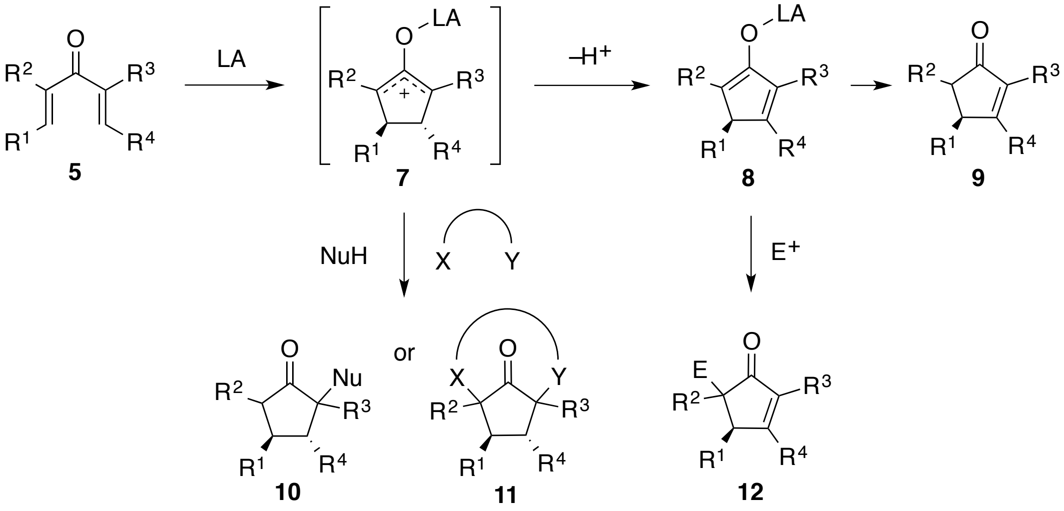
O
R2
R3
R1
R4
5
LA
O
LA
R2
R3
+
R1
R4
7
–H+
O
LA
R2
R3
R1
R4
8
O
R2
R3
R1
R4
9
NuH
X
Y
E+
O
Nu
R2
R3
R1
R4
10
or
X
O
Y
R2
R3
R1
R4
11
O
E
R2
R3
R1
R4
12

Scheme 1.5 The Interrupted Nazarov Reaction.

1.2.1 Interruption with Carbon Nucleophiles

1.2.1.1 Intramolecular Olefin Trapping

In 1998, West and co-workers demonstrated the first deliberate interrupted Nazarov reaction using a dienone tethered to an electron-rich alkene (Scheme 1.6).[8] In the presence of $BF_3•OEt_2$, trienone **13** underwent 4π electrocyclization to produce oxyallyl cation **14**. Nucleophilic addition of a pendent olefin to **14** led to a new tertiary cation in **15**, which could be quenched intramolecularly by the proximal enolate oxygen. Upon hydration, hemiketal **17** was formed as the isolated product.

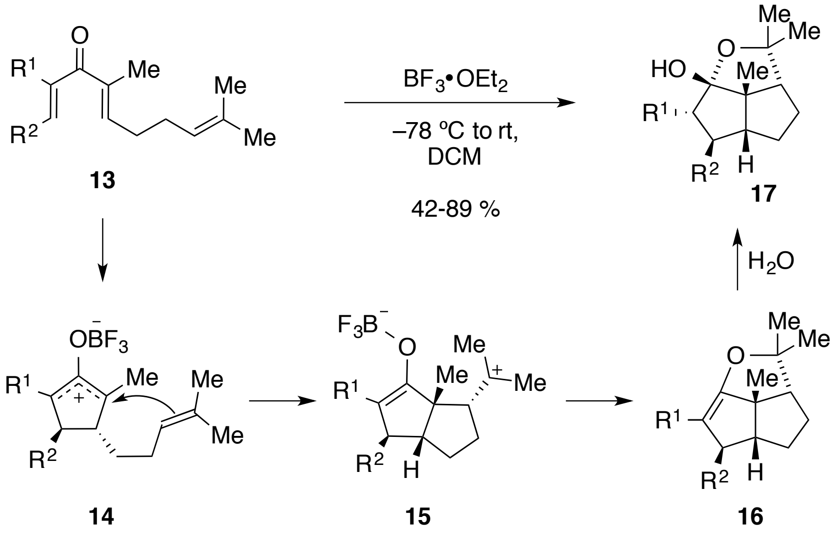

Scheme 1.6 Homologous Prins Type Interrupted Nazarov Reaction.

Participation of a remote olefin has also been seen in a rigid bicyclic Nazarov substrate **18** (Scheme 1.7).[9] Two different mechanisms were postulated to explain the formation of strained polycyclic cyclopropyl ketone **21**: (1) a direct ene-like mechanism from oxyallyl cation intermediate **19** to **21** and (2) a stepwise cation-olefin cyclization followed by hydride transfer to the resulting secondary cation on intermediate **20**.

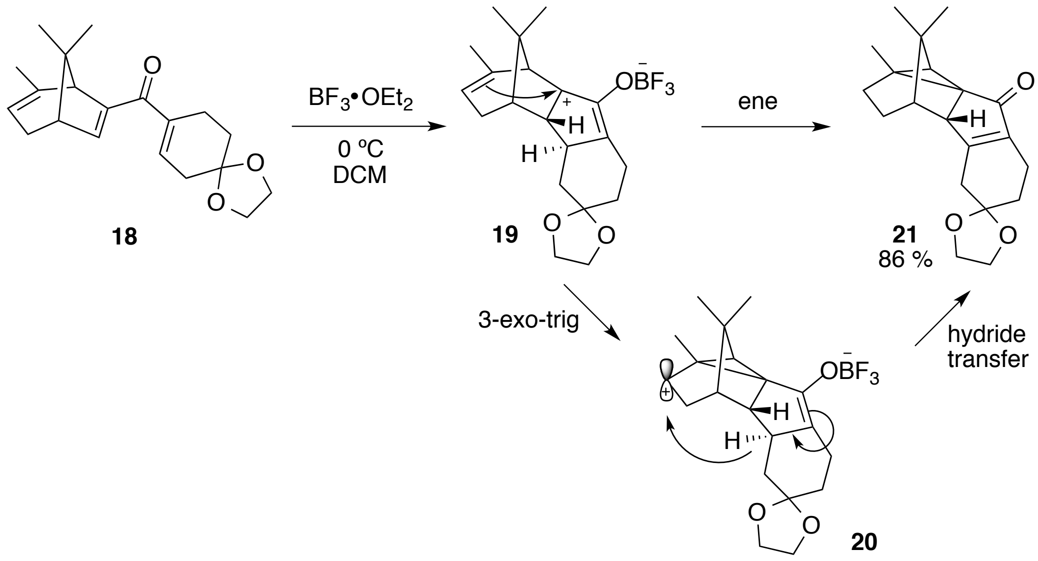
18
BF3•OEt2
0 ºC
DCM
19
ene
21
86 %
3-exo-trig
20
hydride
transfer

Scheme 1.7 Distal Olefin Participation in the Interrupted Nazarov Reaction.

Recently, West and co-workers attempted to construct angular triquinane skeletons via the intramolecular trapping strategy of the interrupted Nazarov reaction. They envisioned that the distal olefin on the cyclooctadiene moiety could intercept oxyallylcation **23** by a transannular homo-Prins reaction to furnish the core ring system in a single step (Scheme 1.8).[10] Unfortunately, the desired tricyclic product **24** was not formed with any of the Lewis and Brønsted acids used. Instead, bicyclic [6.3.0] product **25** was afforded in good yield via a regioselective elimination.

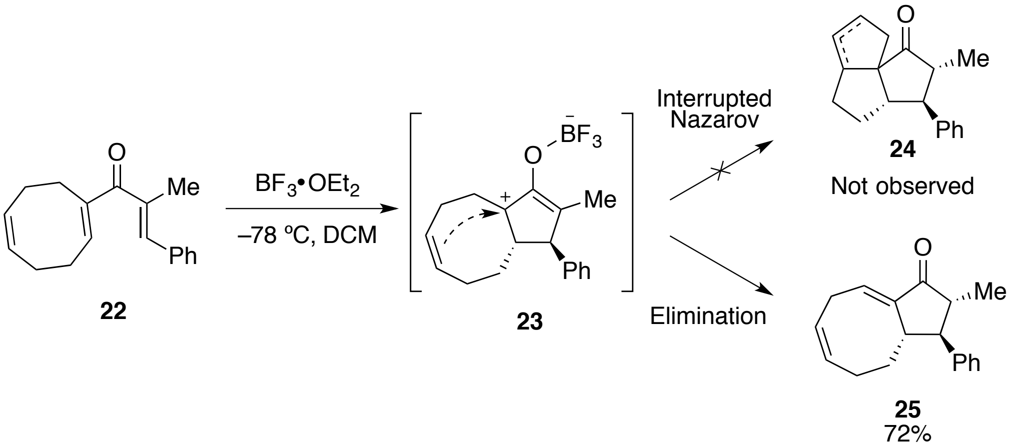
22
BF3•OEt2
–78 ºC, DCM
23
Interrupted
Nazarov
24
Not observed
Elimination
25
72%

Scheme 1.8 Attempted Synthesis of Angular Triquinane via the Interrupted Nazarov Reaction.

1.2.1.2 Intramolecular Arene Trapping

Inspired by the effective trapping of the oxyallyl cation with alkenes and conjugated dienes, West and co-workers conceived cascade polycyclization processes with the involvement of a tethered arene (Scheme 1.9).[11] When treated with $TiCl_4$, trienes **26** were successfully converted to polycyclic products **28** in good to excellent yields. Notably, this whole process furnished the steroid-like ring system as a single diastereomer with the construction of six contiguous stereocenters in a single step.

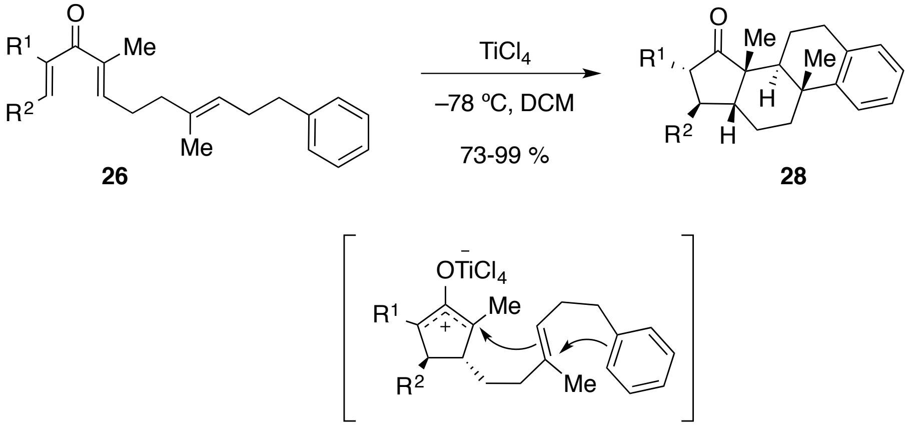

Scheme 1.9 Cascade Polycyclization.

Following the polycyclization cascade, West and co-workers examined a similar cyclization strategy using electron-rich tethered arenes to directly intercept the oxyallyl cation species (Scheme 1.10).[12] As an example, upon treatment with $TiCl_4$, aryl dienone **29** was converted to benzohydrindenone **30** in excellent yield. However, when phenyl-substituted dienone **31** was treated with Lewis acids ($TiCl_4$ and $BF_3{\bullet}OEt_2$), no desired arene trapping product was formed; only elimination product **32** was isolated. This is presumably due to insufficient nucleophilicity of the simple phenyl trap. The scope of this process included a furan-containing Nazarov substrate **33**. At a higher reaction temperature, **33** was converted to furohydrindenone **34** in moderate yield.

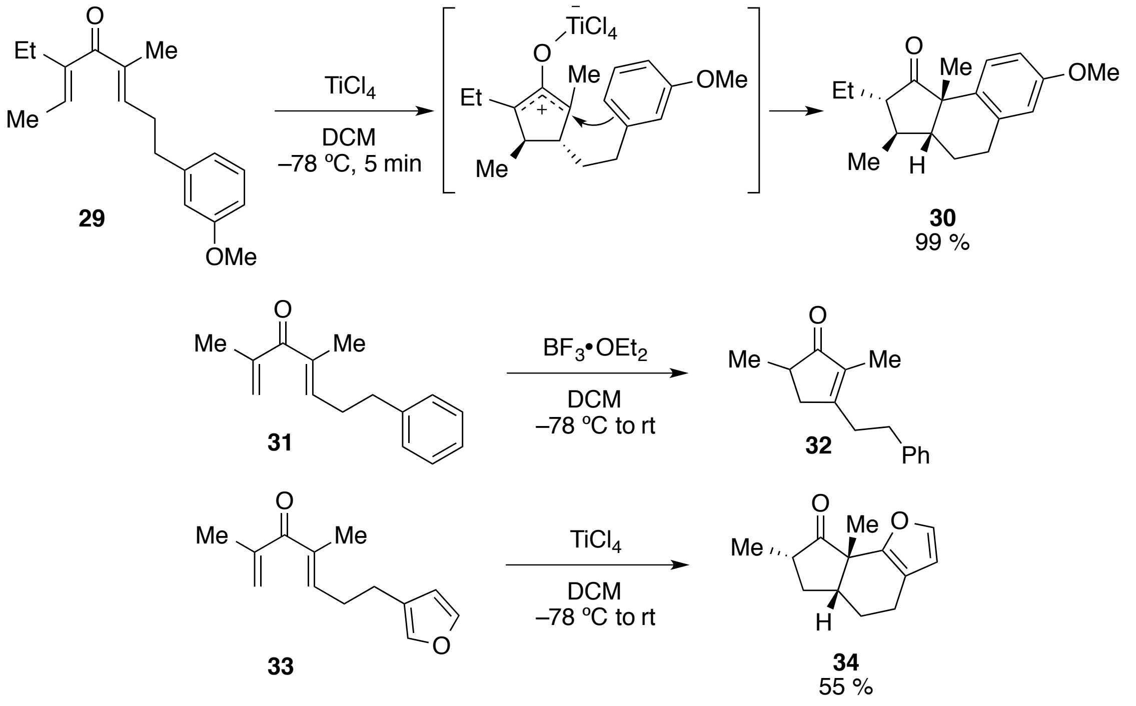

Scheme 1.10 Scope of Arene Traps in the Intramolecular Interrupted Nazarov Reaction.

In 2006, West and Grant showed that vinyl *gem*-dichlorocyclopropane species could serve as Nazarov reaction substrates via silver promoted electrocyclic ring opening.[13] Later, this methodology was extended to the interrupted Nazarov reaction. Vinyl dichlorocyclopropane with a tethered arene **35** underwent the 2π electrocyclic ring opening to pentadienyl cation intermediate **36** followed by 4π electrocyclization (Scheme 1.11).[14] Intramolecular arene trapping followed by the elimination of α-chlorocyclopentanones **37** furnished tricyclic cyclopentenones **38** in modest to good yield. Notably, the scope of arene groups encompassed electron-rich and electron-deficient substituents.

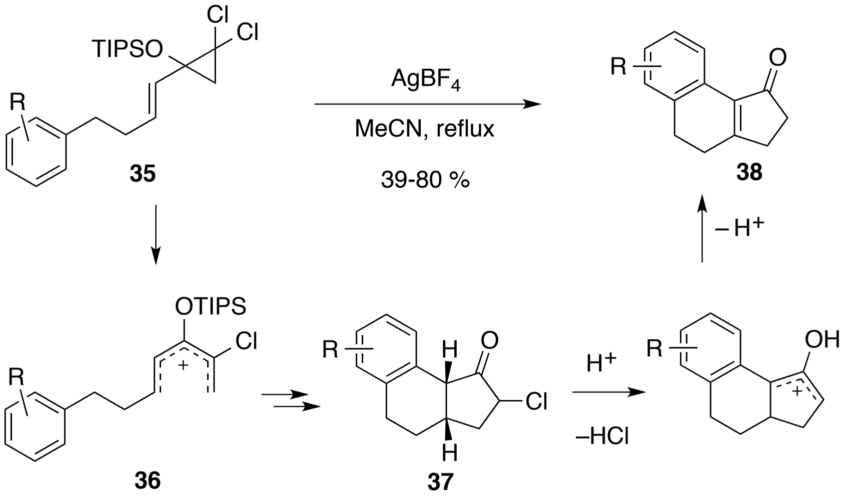
TIPSO
Cl
Cl
R
35
AgBF4
MeCN, reflux
39-80 %
R
O
38
– H+
OTIPS
Cl
R
+
36
R
H
O
Cl
H
37
H+
–HCl
R
OH
+

Scheme 1.11 Dichlorocyclopropane Substrates and Intramolecular Arene Trapping.

Recently, Flynn and co-workers used the intramolecular arene trapping process in their chiral auxiliary-induced asymmetric Nazarov cyclization. When treated with Cu(OTf)$_2$, α-oxazolidinyl dienone **39** underwent asymmetric Nazarov cyclization, followed by arene trapping of the resulting oxyallyl cation, affording a 4:1 mixture of diastereomers **40** and **41** in good yield (Scheme 1.12). [15]

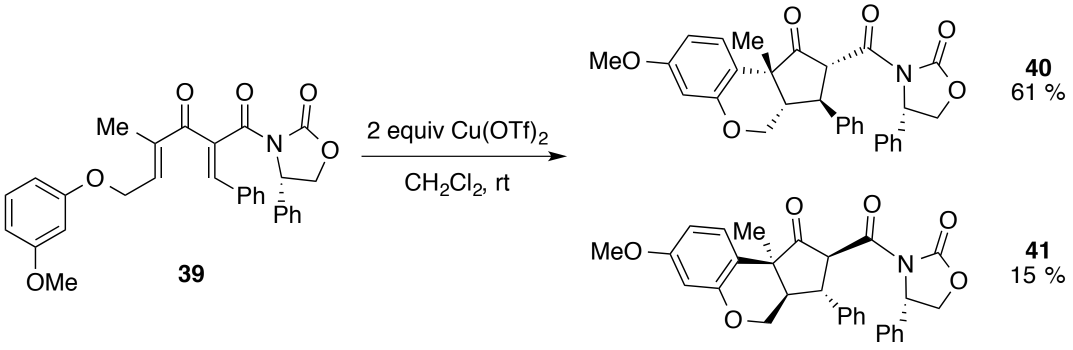
Me
O
O
O
N
O
Ph
Ph
O
OMe
39
2 equiv Cu(OTf)2
CH2Cl2, rt
MeO
Me
O
O
O
N
O
Ph
Ph
O
40
61 %
MeO
Me
O
O
O
N
O
Ph
Ph
O
41
15 %

Scheme 1.12 Enantioselective Intramolecular Arene Trapping.

A novel example of arene trapping has been found in a report by the Liu group.[16] They demonstrated the imino-Nazarov cyclization of 1-amino pentadienyl cation **43** derived from the condensation of aniline with dienal **42** in the presence of AgClO$_4$

(Scheme 1.13). Following 4π electrocyclic ring closure, allyl cation **45** was intercepted by a neighboring electron-rich arene to afford indoline-fused cyclopentanone **47**.

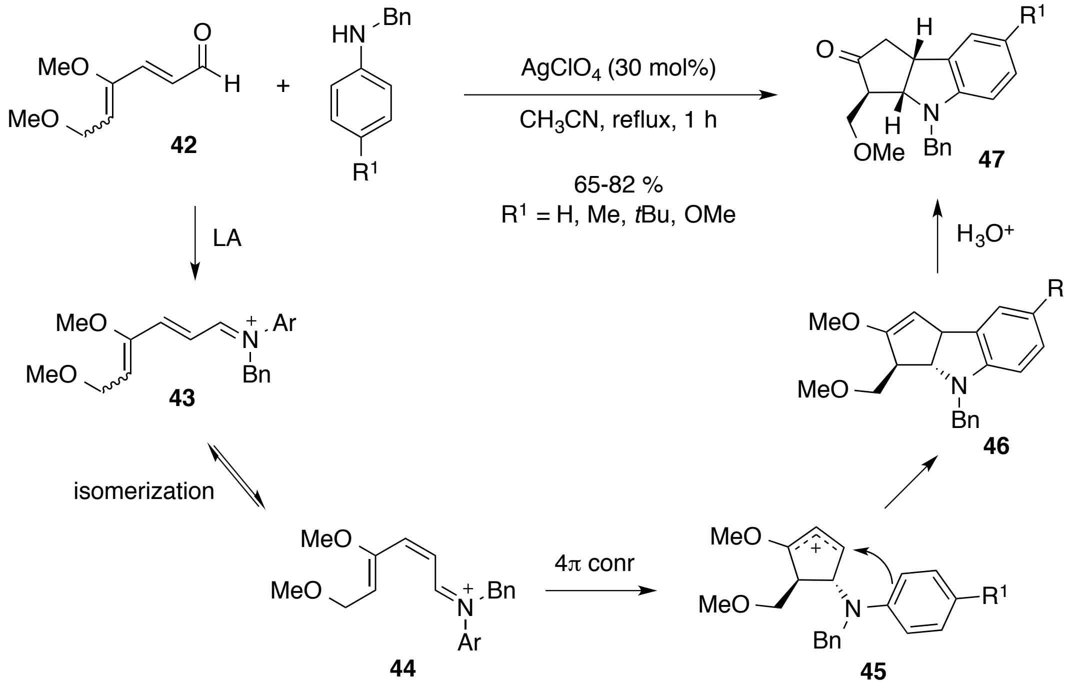

Scheme 1.13 Interrupted Imino-Nazarov Cyclization of 1-Aminopentadienyl Cation and Intramolecular Arene trapping.

Interestingly, when $Gd(OTf)_3$ was used as a Lewis acid, tetrahydroquinoline-fused cyclopentenone product **52** was formed (Scheme 1.14). The author noted that the mild nature and high oxophilicity of the acid is likely the reason for the formation of **52**. They hypothesized that the cascade transformation begins with the oxophilic Lewis acid catalyzed elimination of the methoxy group on **48**, generating cyclopentanone intermediate **49** with the *exo* olefin. Intermediate **49** then undergoes a retro-ene reaction to furnish cyclopentenone species **50** with an imine functional group. Upon deprotonation of the α proton, the resulting enolate **51** then adds to the imine via a half-chair-like transition state, affording tetrahydroquinoline-fused cyclopentenone **52** with high diastereoselectivity at the C-6 position.

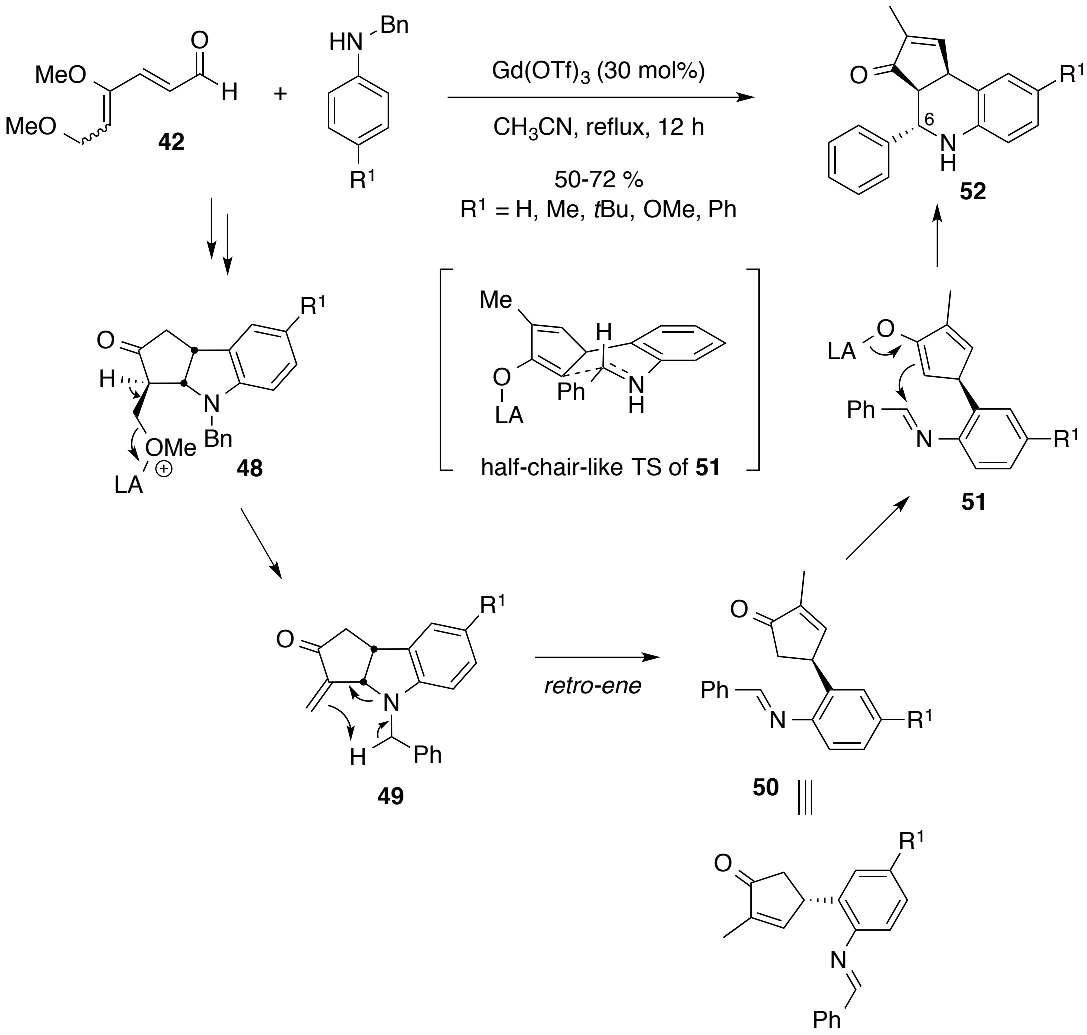

MeO
MeO
42
HN
Bn
R1
+
Gd(OTf)3 (30 mol%)
CH3CN, reflux, 12 h
50-72 %
R1 = H, Me, tBu, OMe, Ph
O
R1
6
N
H
52
R1
O
H
N
Bn
OMe
LA
48
Me
O
LA
H
Ph
N
H
half-chair-like TS of 51
LA
O
Ph
N
R1
51
R1
O
N
H
Ph
49
retro-ene
O
Ph
N
R1
50
R1
O
N
Ph

Scheme 1.14 Tetrahydroquinoline-Fused Cyclopentenone.

1.2.1.3 Intermolecular Arene Trapping

The first intermolecular arene trapping in the interrupted Nazarov reaction was reported in 2008 by West and co-workers. Electron-rich arene and heteroaromatics were proven to be effective trapping agents to afford α-arylated cyclopentanones **53** (Scheme 1.15).[17] However, the electrophilic aromatic substitution reaction did not work on an oxyallyl cation generated from acyclic dienones. Later, protected indoles were also found to be effective intermolecular arene traps.[18]

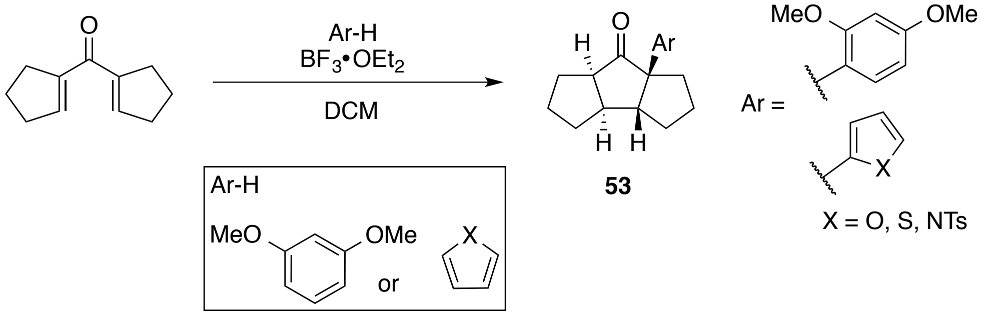
Ar-H
BF3•OEt2
DCM
Ar-H
MeO
OMe
or
X
H
Ar
H H
53
Ar =
MeO
OMe
X
X = O, S, NTs

Scheme 1.15 Intermolecular Arene Trapping.

The Tius group also demonstrated an intermolecular arene trapping using indoles. TMS enol ethers **54** served as alternative Nazarov substrates via *in situ* conversion to allenyl vinyl ketones **55** (Scheme 1.16).[19]

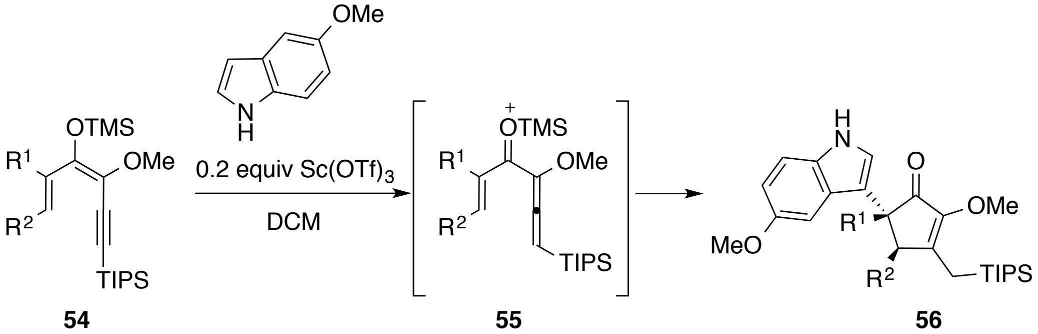
OMe
N
H
OTMS
R1
OMe
R2
TIPS
54
0.2 equiv Sc(OTf)3
DCM
+
OTMS
R1
OMe
R2
TIPS
55
H
N
O
OMe
MeO
R1
R2
TIPS
56

Scheme 1.16 Tius's Indole Interrupted Nazarov Reaction.

In 2011, Burnell and Marx directly used allenyl vinyl ketones **57** in the interrupted Nazarov reaction to react with a range of *N*-substituted pyrroles and indoles (Scheme 1.17).[20] Allenyl vinyl ketone **57** was converted to heterocycle-functionalized cyclopentenones **59** and **60**. In the case of the pyrrole trapping, high regioselectivity was obtained, favoring attachment at position ***a*** of oxyallyl cation **58**, but the overall reaction yield was moderate as Michael addition was found to be a competitive pathway. Notably, when pyrroles with electron-withdrawing groups on the nitrogen (Moc, Boc, Ms, Ts) were used in the reaction, the 1,4-adduct was not formed. Interrupted Nazarov reaction with indole traps took place in higher yield, albeit with poor regioselectivity (**59** vs **60**).

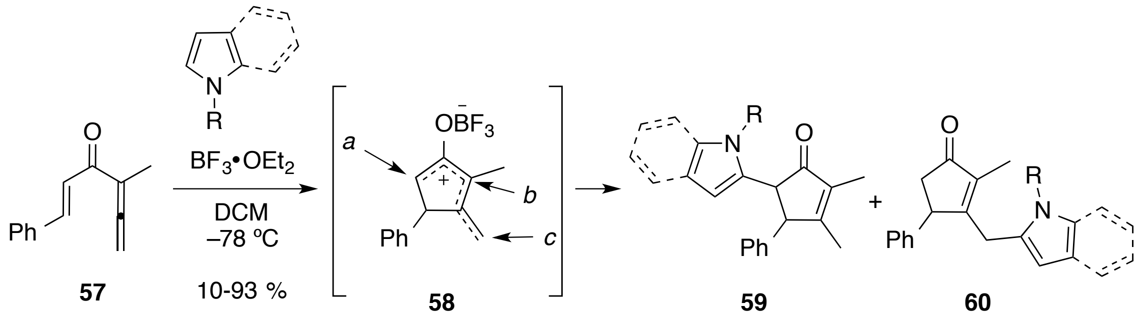

Scheme 1.17 Nazarov Cyclization of Allenyl Vinyl Ketones with Nitrogen Heterocycles.

Dienone **61** was already known to react with furan in the presence of BF$_3$•OEt$_2$ to afford [4+3] cycloaddition product **62** (Scheme 1.18),[21] but the Friedel-Crafts type reactivity of furan was not observed in the Nazarov reaction with an acyclic dienone. Recently, West and Wu discovered TMSOTf was an effective Lewis acid for the electrophilic substitution of heteroaromatics with acyclic dienone.[22] As an example, when acyclic dienone **61** was treated with TMSOTf and furan, α-arylated cyclopentanone **63** was furnished in good yield as a single diastereomer. It was noted that the facial selectivity of the furan addition was opposite to the indole interruption (see product **64**).

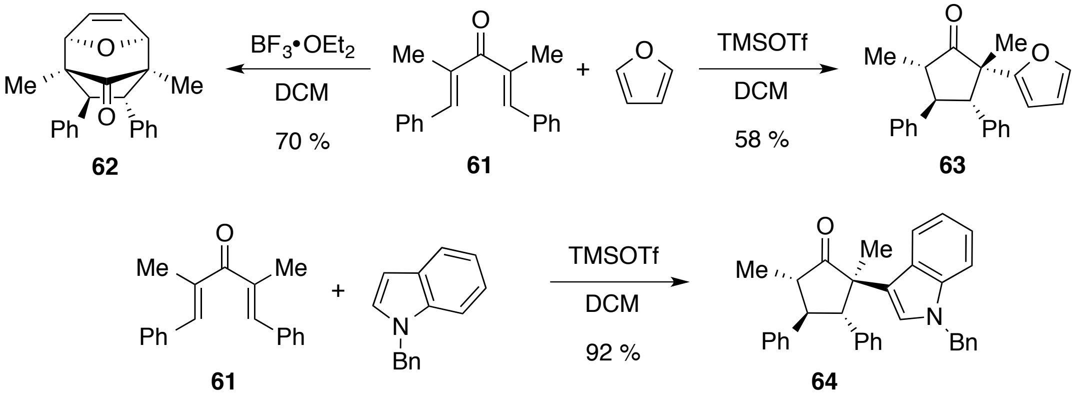

Scheme 1.18 Heteroarylation Pathway of Acyclic Dienone **61**.

1.2.1.4 Intermolecular Olefin Trapping

Prompted by the successful intramolecular olefin trapping, the West group investigated an intermolecular version of the olefin nucleophile prior to the study of intermolecular arene trapping described above. The first reported example employed allyltrimethylsilane as a trapping reagent (Scheme 1.19).[23] Dienone **61** was treated with BF_3•OEt_2 to afford a diastereomeric mixture of allylated products **65**/**66**/**67** and [3+2] cycloaddition product **68**.

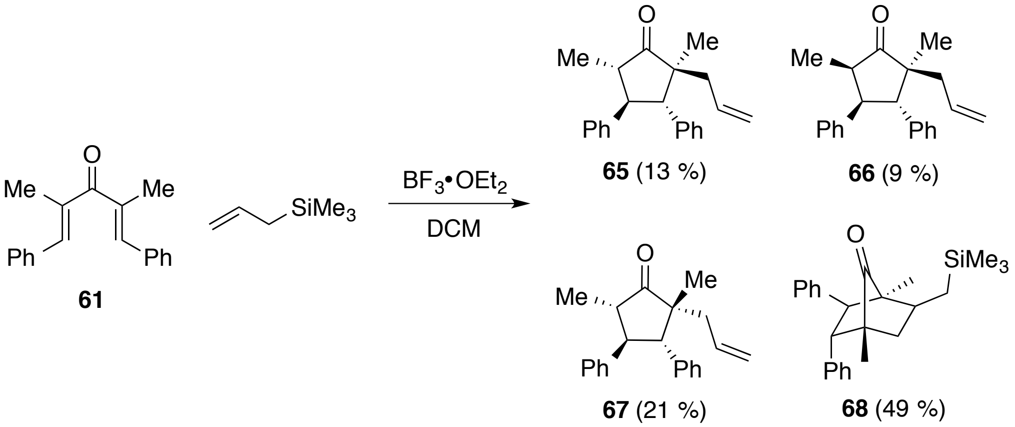

Scheme 1.19 Allyltrimethylsilane Trapping.

Interestingly, the use of a less labile allylsilane, allyltriisopropylsilane, in the interrupted Nazarov reaction exclusively afforded [3+2] cycloaddition products (Scheme 1.20). When BF_3•OEt_2 was used as a Lewis acid, unsymmetrical dienone **69** was converted to *exo* isomer **70** as a sole product. In case of $SnCl_4$, a mixture of isomers **71**/**70** was provided in favor of *endo* product **71**. Having bulky substituents on the silicon atom (allyltriiopropylsilane vs allyltrimethylsilane) was advantageous for the formation of bridged bicycles, presumably, slowing down the desilylation process of intermediate **72**.

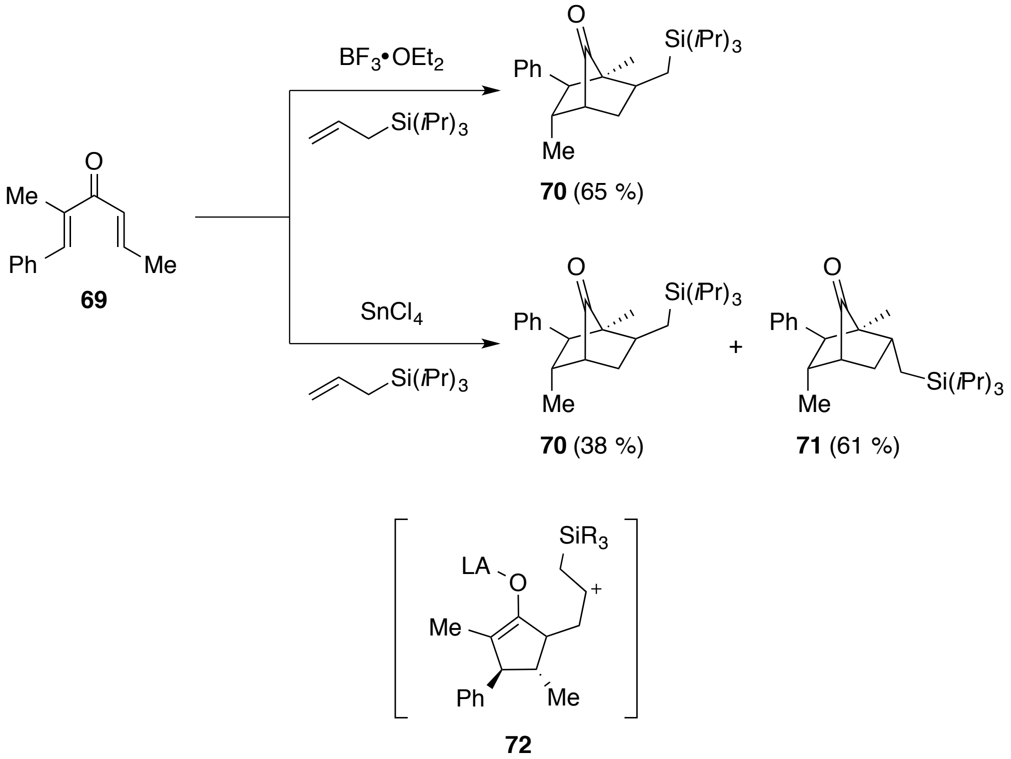
BF$_3$•OEt$_2$
Si(*i*Pr)$_3$
SnCl$_4$
Si(*i*Pr)$_3$
69
70 (65 %)
70 (38 %)
71 (61 %)
72
LA
SiR$_3$

Scheme 1.20 Allyltriisopropylsilane Trapping.

Following the original work, efforts were made by the same laboratory to facilitate the desilylation process as a termination step in order to selectively form 2-allylcyclopentanones, and a more extensive screen of Lewis acids as well as allyl donors was undertaken.[22] With respect to the selective formation of the allylation product, $TiCl_4$ was found to be the most effective Lewis acid, solely affording **65** and **67** with good diastereofacial control (Scheme 1.21). Use of allylstannane as an allyl donor also produced a diastereomeric mixture of **65** and **67**, but with reduced diastereoselectivity.

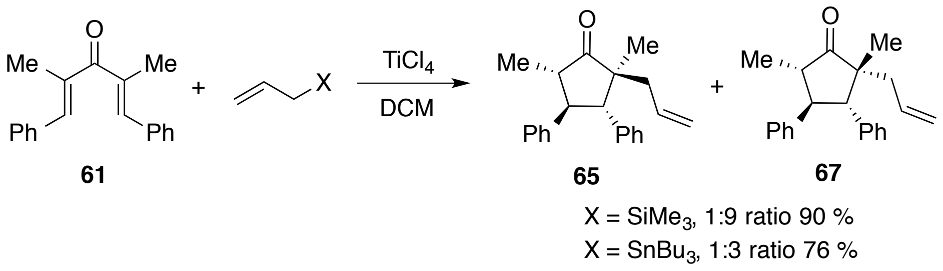
61
TiCl$_4$
DCM
65
67
X = SiMe$_3$, 1:9 ratio 90 %
X = SnBu$_3$, 1:3 ratio 76 %

Scheme 1.21 Efficient Lewis Acid $TiCl_4$ in the Allylation.

In addition to the [3+2] cycloaddition with allyltriiopropylsilane, West and Mahmoud observed the same trapping reactivity with vinyl sulfide. Sulfide-substituted bicyclo [2.2.1]heptanones **73** and **74** were afforded in good yield (Scheme 1.22).[24]

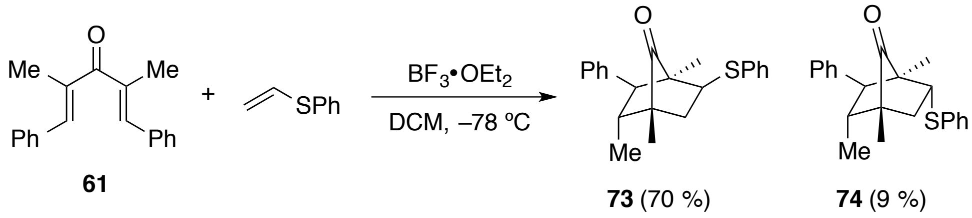

Me
O
Me
Ph
Ph
61
+
SPh
BF3•OEt2
DCM, –78 °C
O
Ph
SPh
Me
73 (70 %)
O
Ph
SPh
Me
74 (9 %)

Scheme 1.22 Vinyl Sulfide Trapping in the Interrupted Nazarov Reaction.

Electron-rich olefins have been used as trapping reagents in interrupted Nazarov reactions. Burnell and Marx demonstrated enol ether attack on a Nazarov intermediate during electrocyclization of an allenyl vinyl ketone **57** (Scheme 1.23).[25]

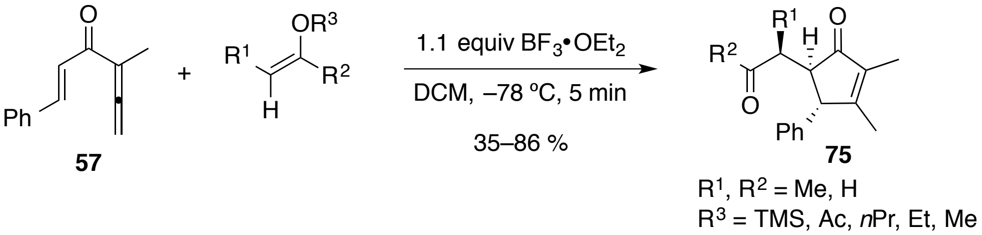

O
Ph
57
+
OR3
R1
R2
H
1.1 equiv BF3•OEt2
DCM, –78 °C, 5 min
35–86 %
R1
H
O
R2
O
Ph
75
R1, R2 = Me, H
R3 = TMS, Ac, nPr, Et, Me

Scheme 1.23 Nazarov Reactions of Allenyl Vinyl Ketone with Electron-Rich Alkenes.

Later, West and Wu generalized the use of electron-rich olefins on simple divinyl ketone substrates. Silyl enol ethers, silyl ketene acetals, and mixed ketene *S*,*O*-acetals successfully intercepted the Nazarov oxyallyl cation intermediate (Scheme 1.24).[26] The overall process provided highly substituted 1,4-diketones **76** with up to five contiguous stereocenters. Substrate scope was broadly tested. In case of the least reactive substrate dienone (lacking an α substituent), significant amounts of 1,4-adduct **77** were found to be the sole product.

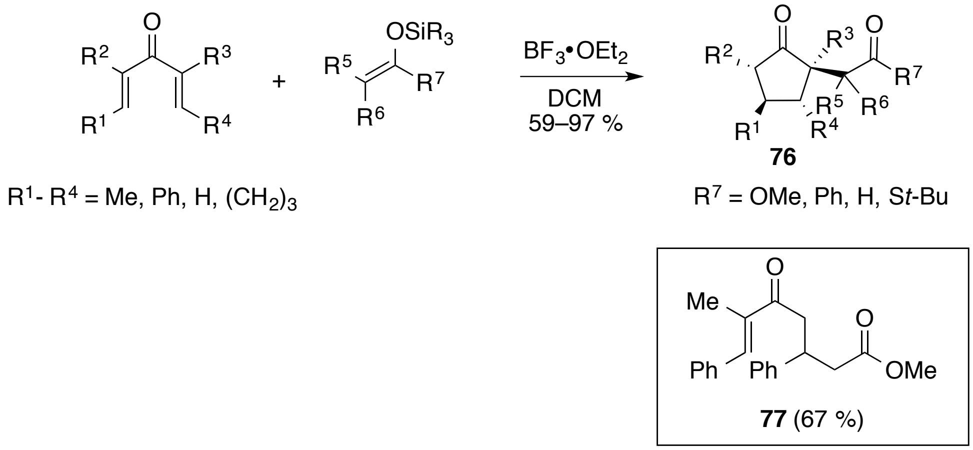
BF3•OEt2
DCM
59–97 %
76
R1- R4 = Me, Ph, H, (CH2)3
R7 = OMe, Ph, H, St-Bu
77 (67 %)

Scheme 1.24 Homologous Mukaiyama Reaction.

The 1,4-dicarbonyl systems are also accessible by the alkyne interrupted Nazarov reactions. In 2014, West and Wu demonstrated nucleophilic additions of electron rich alkynes to Nazarov intermediate **78** followed by intramolecular carboalkoxylation of intermediate **79** to build α-phenylacetyl cyclopentanones **80** (Scheme 1.25).[27] Competent alkynes possessed a methyl- or methoxy-substituted phenyl group. As an example, phenyl acetylene was found to be unreactive, presumably due to its inadequate nucleophilicity.

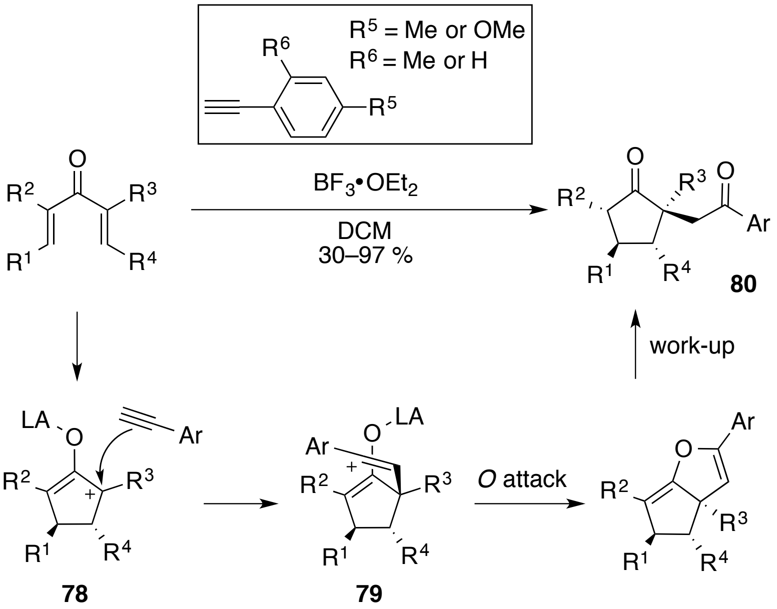
R5 = Me or OMe
R6 = Me or H
BF3•OEt2
DCM
30–97 %
80
work-up
O attack
78
79

Scheme 1.25 Formal Homologous Aldol Reactions: Electron Rich Arene Trapping.

1.2.1.5 [4+3] Cycloadditions

Interrupted Nazarov reactions have allowed facile access to keto-bridged 8-membered rings. West and co-workers demonstrated a series of intra- and intermolecular [4+3] cycloadditions in the interrupted Nazarov cyclization. The first example was the intramolecular case where oxyallyl intermediate **82**, generated from the treatment of divinyl ketone **81** with $FeCl_3$, was intercepted by the tethered 1,3-diene (Scheme 1.26).[28] Excellent diastereofacial selectivity was obtained: the tethered diene approached from the less hindered face of the oxyallyl cation.

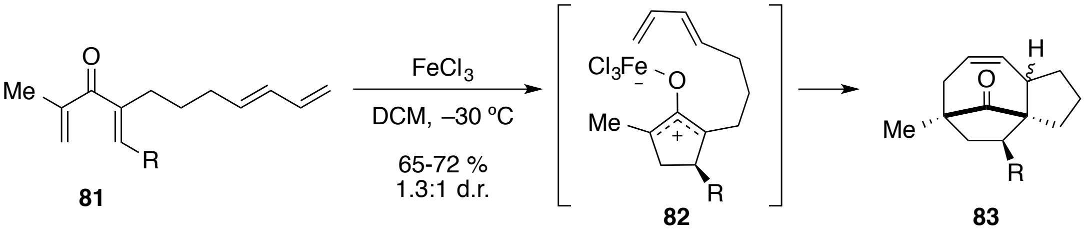
O
Me
R
81
FeCl3
DCM, –30 °C
65-72 %
1.3:1 d.r.
Cl3Fe
O
Me
+
R
82
H
O
Me
R
83

Scheme 1.26 Intramolecular [4+3] Cycloaddition.

In 2003, intermolecular [4+3] capture of the oxyallyl cation intermediate was reported. Treating dienones **84** with catalytic amounts of BF_3•OEt_2 in the presence of 1,3-dienes or furan furnished [4+3] cycloaddition product **85** or **86** in good to excellent yield (Scheme 1.27).[21] Later, Burnell and Marx showed analogous intermolecular processes with allenyl vinyl ketones.[25]

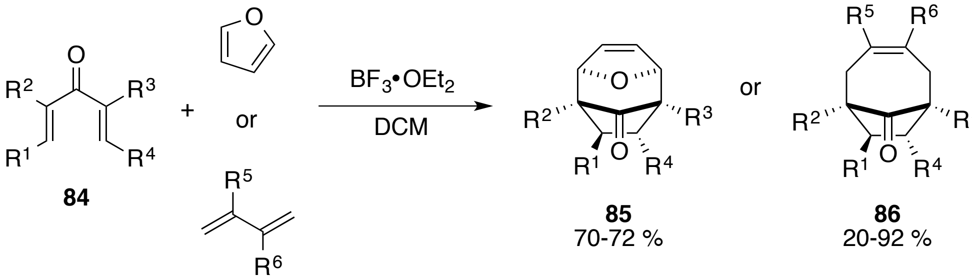
O
R2
R3
R1
R4
84
+
O
or
R5
R6
BF3•OEt2
DCM
O
R2
R3
R1
O
R4
85
70-72 %
or
R5
R6
R2
R3
R1
O
R4
86
20-92 %

Scheme 1.27 Domino Nazarov/Intermolecular [4+3] Cycloaddition Reactions.

1.2.2 Reductive Nazarov Reaction

In 1998, West and Giese performed a “reductive Nazarov reaction” wherein hydride intercepted the Nazarov intermediate (Scheme 1.28).[29] This process allowed retention of the two new stereocenters formed in the electrocyclization step. Triethylsilane was the hydride source and was tolerant of the Lewis acid used (BF_3•OEt_2 or TMSOTf). Notably, it was the first example of the use of catalytic Lewis acid to affect the Nazarov cyclization. The author noted that reduction in the amount of Lewis acid required might be attributed to catalysis by *in situ* generated Et_3Si-X species.

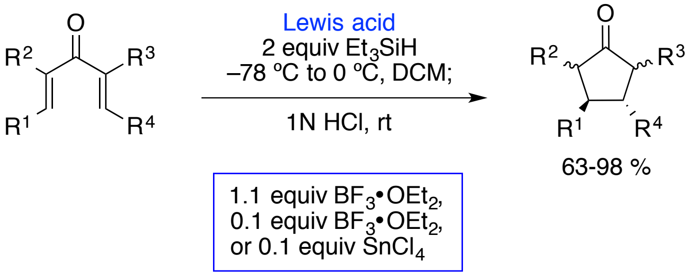

Scheme 1.28 The Reductive Nazarov Cyclization.

In 2000, West and Giese followed up with an in-depth study on the regioselectivity and stereoselectivity of this reaction.[30] It was not apparent whether the delivery of hydride was regioselective or stereoselective since a protonation step could also be responsible for the regio- and stereochemical outcome. Reductive Nazarov cyclization of unsymmetrical divinyl ketone **87** in the presence of Et_3SiD provided support for the idea that the delivery of hydride occurs regioselectively at the less substituted end of oxyallyl cation **88**. As a result, more substituted enolate **89** could be formed (Scheme 1.29). With respect to stereoselectivity, the hydride approached from the same face as the β substituent to give a *trans* relative stereochemistry (Scheme 1.30).

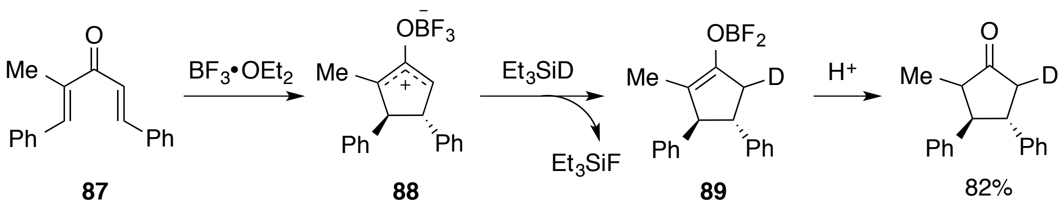

87
88
89
BF$_3$•OEt$_2$
Et$_3$SiD
Et$_3$SiF
H+
82%

Scheme 1.29 Reductive Cyclization of **87** in the Presence of Et$_3$SiD.

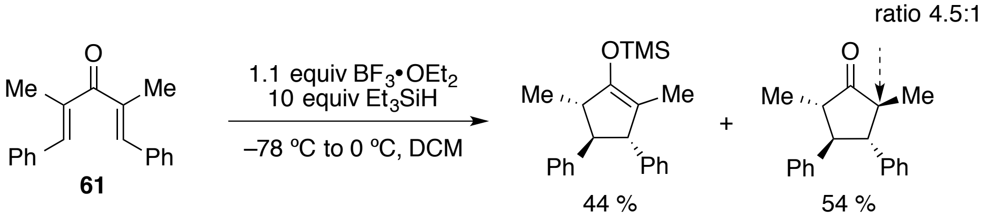

61
1.1 equiv BF$_3$•OEt$_2$
10 equiv Et$_3$SiH
–78 °C to 0 °C, DCM
44 %
54 %
ratio 4.5:1

Scheme 1.30 *trans* Relative Stereochemistry in the Silyl Enol Ether Product.

1.2.3 Heteroatoms

Unlike the fruitful study of carbon-based nucleophiles in the interrupted Nazarov reactions, the use of heteroatom-based nucleophiles has been relatively less well-studied. In 2002, Nair and co-workers observed an intramolecular oxygen trapping event of the Nazarov intermediate (Scheme 1.31).[31] Pentadienyl cation intermediate **91** was generated from Lewis acid promoted C-O bond cleavage of dihydrofuran substrate **90**. Subsequent Nazarov cyclization, recapture of the resulting oxyallyl cation **92** with orthoester borate oxygen, and hydrolysis led to bicyclic lactone product **93** in good yield.

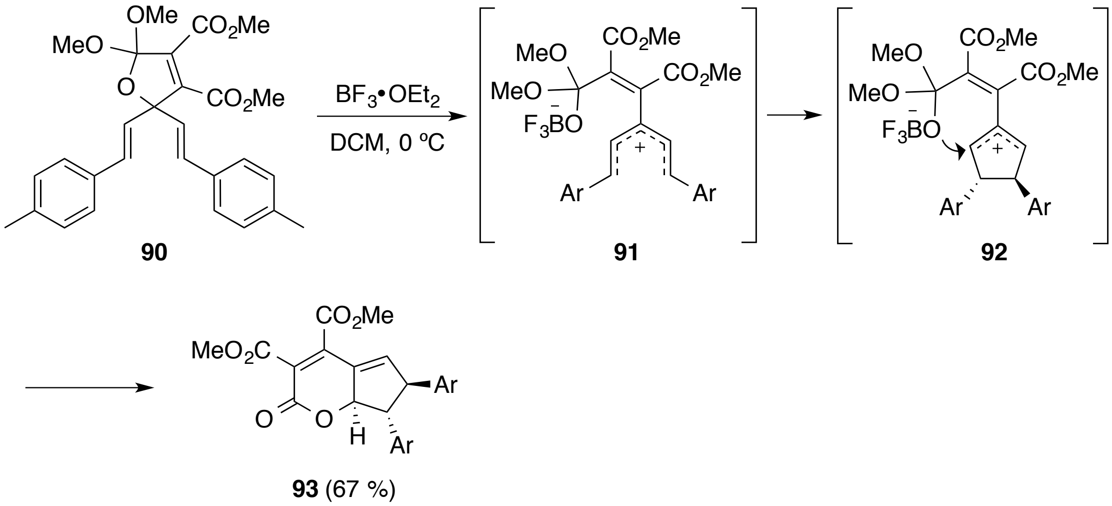

Scheme 1.31 Intramolecular Oxygen Trapping in the Interrupted Nazarov Reaction.

Examples of aliphatic alcohol trapping in the interrupted Nazarov reaction can be found in a report by Shindo and co-workers (Scheme 1.32).[32] In the presence of catalytic amounts of TfOH, the β-alkoxydienones **94** were converted to α-alkoxy cyclopentenones **95** in good yield via acid catalyzed Nazarov cyclization/intermolecular alcohol migration. A crossover experiment supported the intermolecular occurrence of the alcohol trapping event.

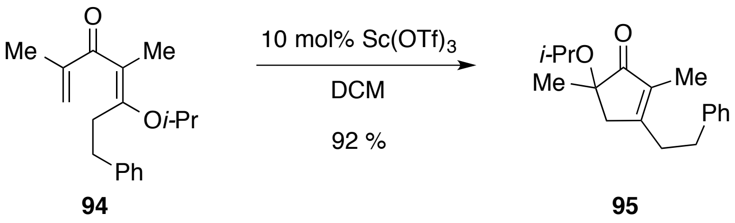

Scheme 1.32 Intermolecular Alcohol Trapping.

Burnell and Marx discovered a trifluoroacetate interrupted Nazarov reaction.[33] The trifluoroacetic acid functioned as a promoter for the Nazarov cyclization of allenyl vinyl ketone as well as a trapping reagent of the oxyallyl cation **96** (Scheme 1.33). Upon basic alumina mediated hydrolysis of the ester **97**, α-hydroxycyclopentenones **98** were afforded.

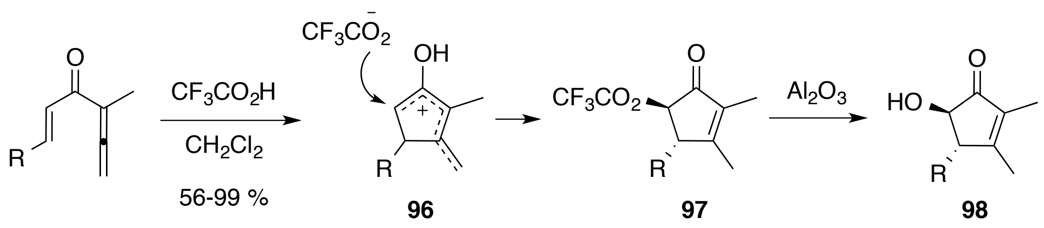
CF3CO2H
CH2Cl2
56-99 %
CF3CO2
OH
CF3CO2
Al2O3
HO
R
96
97
98

Scheme 1.33 Intermolecular Trapping with Trifluoroacetate.

Recently, Mischne and Riveira constructed a series of cyclopentadihydrofuran derivatives **102** using the iso-Nazarov reaction of π-conjugated 1,3-dicarbonyl compound **99** followed by intramolecular oxygen trapping of allyl cation intermediate **101** (Scheme 1.34).[34]

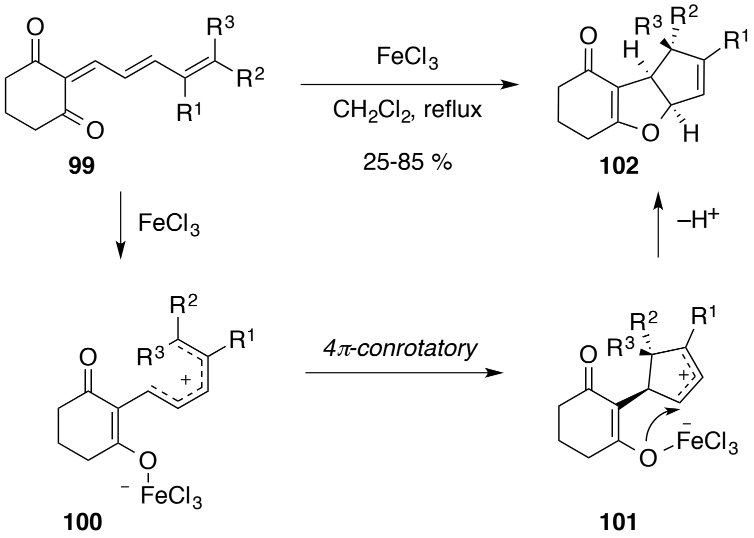
99
FeCl3
CH2Cl2, reflux
25-85 %
102
FeCl3
–H+
4π-conrotatory
100
101
R1
R2
R3
FeCl3

Scheme 1.34 Interrupted Vinylogous Iso-Nazarov Reaction.

The first nitrogen atom participation in the interrupted Nazarov reaction was reported by Tius and Dhoro in 2005 (Scheme 1.35).[35] Addition of a primary or secondary amine was responsible for the formation of allenyl vinyl ketones **104** and further allowed incorporation of amine functionality on the cyclopentenone product **105** following silica gel promoted electrocyclization. Later, the Tius group achieved an asymmetric variant by employing a camphor-based chiral auxiliary in place of the methyl ether, which controlled the torquoselectivity of the electrocyclization.[36]

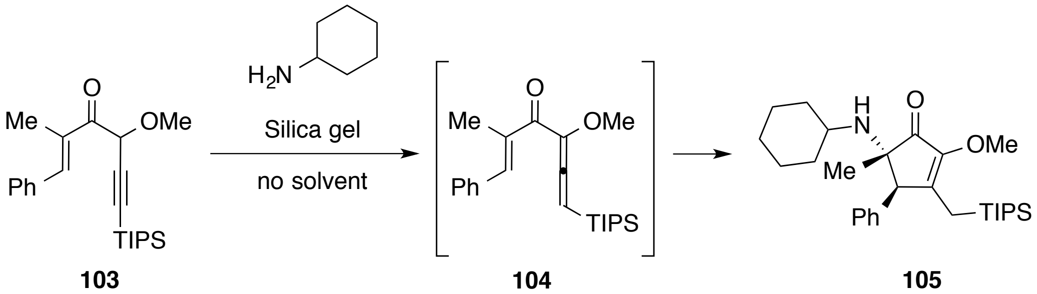

Scheme 1.35 Amine Interrupted Nazarov Reaction.

In 2007, West and co-workers demonstrated that organoazides could react with the Nazarov oxyallyl intermediate. These processes led to ring expansion products with new amide functionality. The first report focused on the intramolecular addition of the tethered azide (Scheme 1.36).[37] In this case, endoperoxides **109** and **110** were spontaneously formed; they could come from oxygen trapping on late stage intermediate **108** derived from Schmidt rearrangement. In the same year, intermolecular azide trapping of Nazarov intermediate **111**, generated from simple dienone, was achieved (Scheme 1.37).[38] The azide attack occurred at a less hindered position of the oxyallyl cation **111**, providing high regioselectivity. Dihydropyridone **112** was the sole product and peroxy-bridged products were not formed.

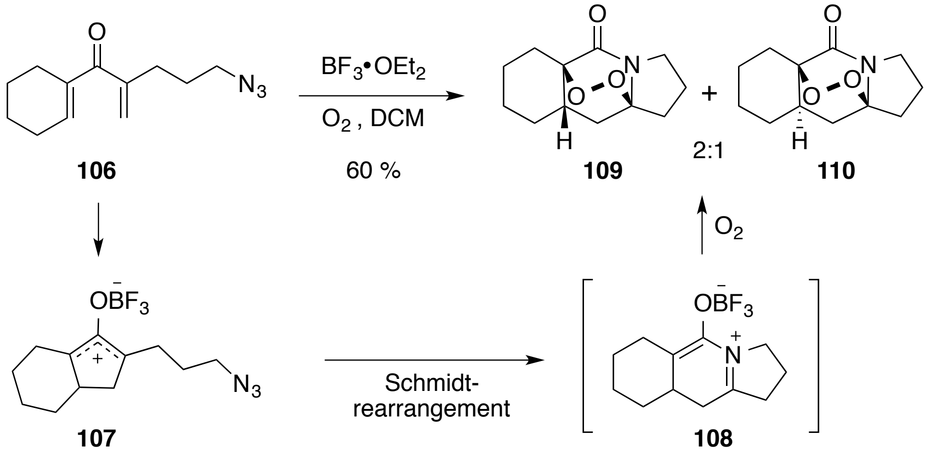

Scheme 1.36 Intramolecular Azide Trapping.

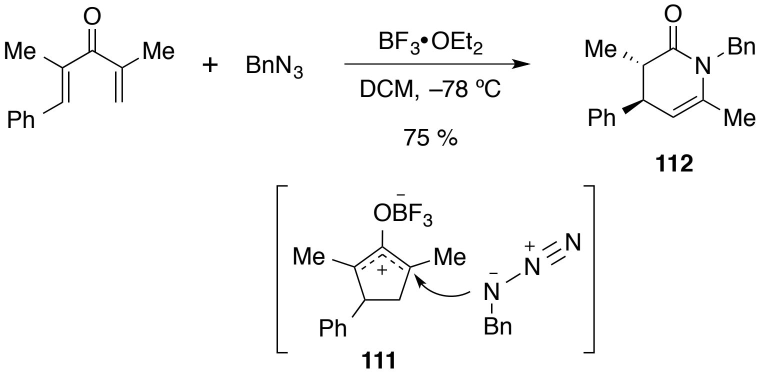

Scheme 1.37 Intermolecular Azide Trapping.

When simple dienone **61** was treated with trifluoromethanesulfonic acid in the presence of the organoazide, the subsequent Schmidt-type rearrangement did not take place. Instead, a [3+3]-adduct, bridged bicyclic triazine **113**, was produced in good yield (Scheme 1.38).[39]

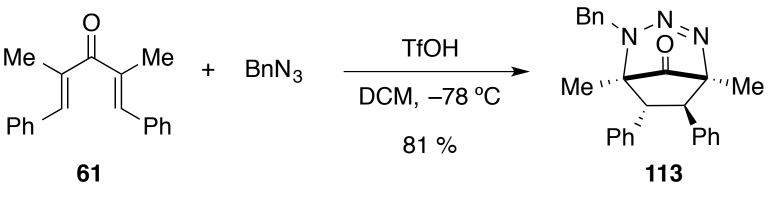

Scheme 1.38 Intermolecular Azide Capture via [3+3] Cycloaddition to Triazine **113**.

A halogen interrupted Nazarov reaction was initially reported by the West group using $TiCl_4$ on strained divinyl ketones.[40] The Burnell group expanded the Lewis acid mediated halogen migration to an oxyallyl cation intermediate generated from allenyl vinyl ketones.[41] Details of these reactions are covered in Section 5.2.2.

1.2.4 Skeletal Rearrangement

In the process of the Nazarov cyclization, unexpected cyclopentenones are often found with rearranged substituents.[42] The rearrangement takes place via sequential 1,2 shifts, or Wagner-Meerwein rearrangements, involving the oxyallyl cation intermediate. In 1991, Motoyoshiya and co-workers provided aspects of the mechanism for the formation of rearranged cyclopentenone **117** from trisubstituted dienone **114** in the presence of H_2SO_4 (Scheme 1.39).[43] The author proposed two different routes from the oxyallyl cation **115** to intermediate **116** via (1) a direct [1,2]-hydride shift and (2) a deprotonation and protonation sequence. The [1,2]-Wagner-Meerwein rearrangement takes place on the intermediate **116** to form rearranged product **117**.

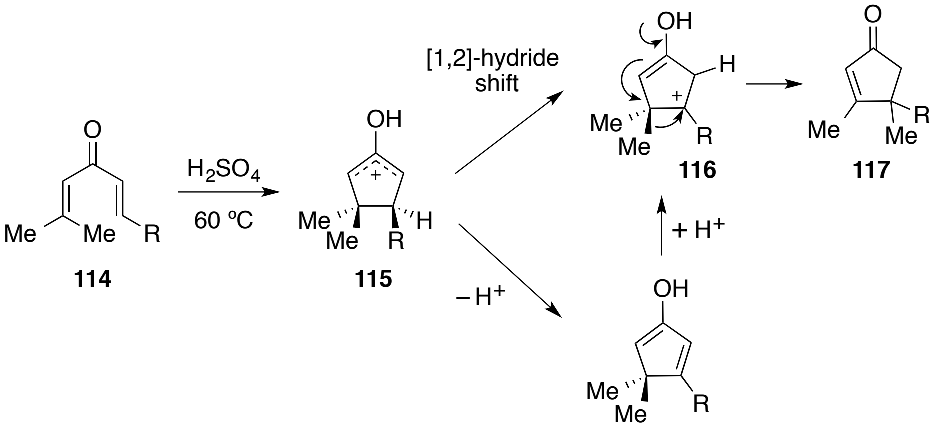

Scheme 1.39 Nazarov Cyclization/Wagner-Meerwein Sequence.

The Frontier group has extensively studied the Wagner-Meerwein rearrangement in the Nazarov reaction and provided insights towards chemoselectivity.[44,45] They initially reported that cyclic dienone **118**, bearing an electron-withdrawing substituent on an α-carbon, was efficiently converted to spirocycle **119** in the presence of a copper catalyst **120** (Scheme 1.40).[44] Later, acyclic dienones were subjected to similar reaction conditions to investigate the migratory aptitude of the substituents in comparison to the size of the substituents.[45] With respect to the migratory aptitude, 1,2 migration of an aromatic group was generally preferred over the migration of a methyl or a hydride. However, hydride migration was more favorable than migration of a bulky aromatic substituent such as 2,4,6-trimethoxyphenyl.

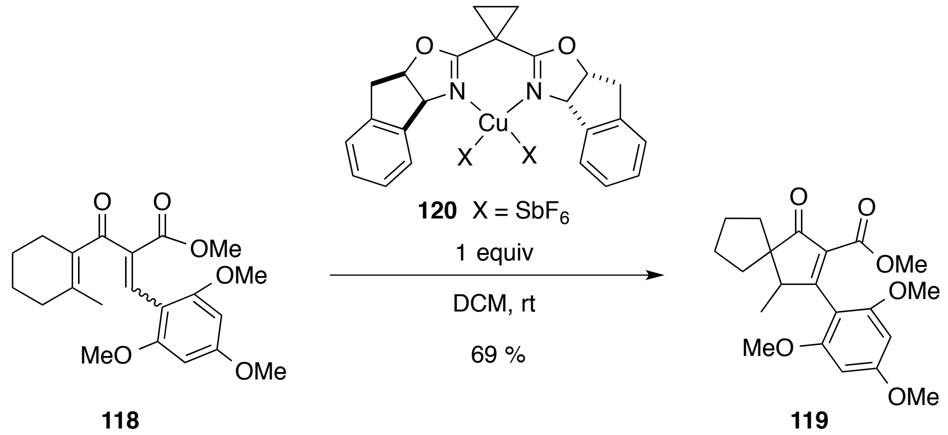

Scheme 1.40 Spirocycle Formation from Nazarov Substrate **118**.

1.2.5 Electrophilic Trapping

In the absence of an external nucleophile, the reactive Nazarov oxyallyl cation intermediate undergoes elimination to form a cyclopentadienol species, which is usually quenched by protonation. The enolate on the cyclopentadienol intermediate has been reacted with a selection of electrophiles such as Michael acceptors and electrophilic halogens.

Ma and co-workers demonstrated a catalytic Nazarov reaction followed by electrophilic fluorine capture on the enolate to construct fluorinated indanones **122** (Scheme 1.41).[46] *N*-Fluorobenzenesulfonimide (NFSI) was used as the electrophilic fluorine source. In this publication, an asymmetric variant of this work was also included using a chiral bis(oxazoline)copper(II) complex. Later, the Ma group extended this work, employing a β-ketoester as the starting material. Under the acidic conditions, Nazarov substrate **121** could be prepared *in situ* via Knoevenagel condensation.[47]

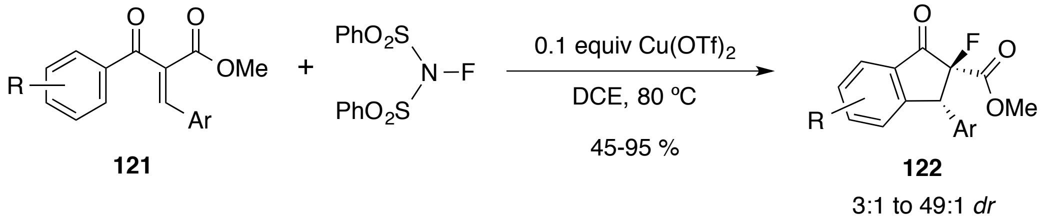
121
PhO_2S
N–F
PhO_2S
0.1 equiv $Cu(OTf)_2$
DCE, 80 °C
45-95 %
122
3:1 to 49:1 *dr*

Scheme 1.41 Nazarov Cyclization/Electrophilic Fluorination.

In 2011, Rueping and Ieawsuwan demonstrated a chiral Brønsted acid promoted asymmetric Nazarov cyclization followed by electrophilic bromine trapping (Scheme 1.42).[48] Treating polarized dienone **123** with a chiral bulky *N*-triflylphosphoramide in the presence of 2,4,4,6-tetrabromocyclohexa-2,5-dienone afforded a mixture of enantiomerically enriched α-bromocyclopentenones **124** and **125** in excellent yield and in high enantiomeric excess.

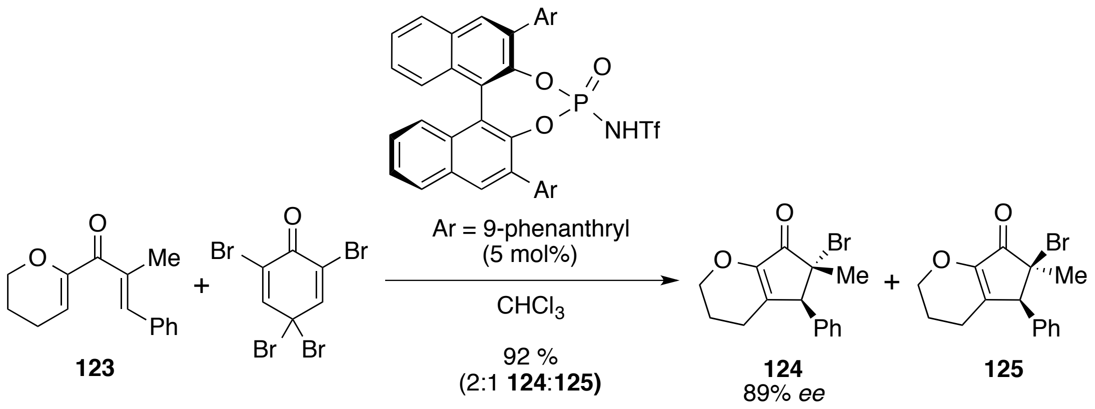
123
Ar = 9-phenanthryl
(5 mol%)
$CHCl_3$
92 %
(2:1 **124**:**125**)
124
89% *ee*
125

Scheme 1.42 Asymmetric Nazarov Cyclization/Bromination Sequence.

Michael acceptors have been reacted with the Nazarov enolate intermediate. The Frontier group reported the first example of using a Michael acceptor nitroalkene in the Nazarov reaction in 2006 (Scheme 1.43).[49] An iridium complex catalyzed the electrocyclization and also the 1,4-addition. This whole processes furnished three new adjacent stereocenters with high diastereoselectivity.

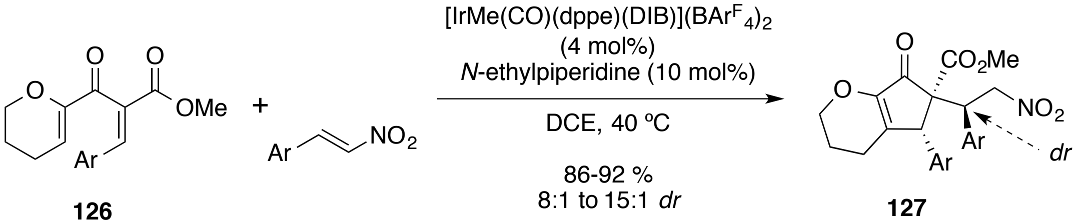

Scheme 1.43 Tandem Nazarov Cyclization/Michael Addition.

1.3 Conclusion

Adding value to the classical Nazarov reaction, interrupted Nazarov reactions have allowed us to preserve the stereospecific nature of electrocyclization and provide increased molecular complexity with enhanced step economy. The strategy of trapping Nazarov intermediates encompasses the use of heteroatom and π-nucleophiles such as allyl silanes, enol derivatives, and electron-rich arenes in both inter- and intramolecular variants.

These processes have been extensively investigated for the past 15 years; however, there are still no examples introducing simple alkyl groups in the interrupted Nazarov reaction. As well, beyond functionalizing 5-membered carbocycles, formation of 6-membered carbocycles, ring contraction, and cleavage of the Nazarov reaction intermediate have remained unexplored.

In the subsequent chapters, new modes of interrupted Nazarov reactions will be discussed. We started our journey to probe methods of using carbon-based σ-nucleophiles in the reaction, and details were reported in Chapter 2.

Chapter 2

Organoaluminum Mediated Nazarov Reactions: Interrupted to Oxidative Processes[50]

2.1 Introduction

Since the 1950s when Karl Ziegler, Nobel laureate, discovered the catalytic activity of $TiCl_3$ and triethylaluminum on polymerization,[51] organoaluminum reagents have been widely used throughout chemistry. Compared to other organometallic compounds (e.g., organolithium, organozinc, and organomagnesium), organoaluminum species show strong Lewis acidity arising from a low-lying empty p-orbital. Such acidic character attracts Lewis basic compounds to form acid-base adducts, allowing for high chemoselective reactivity. Organoaluminums can activate a variety of electrophiles, such as aldehydes, ketones, imines, and epoxides.[52] Furthermore, while coordinated, one of the ligands on the organoaluminum can be transferred to the electrophile to form new bonds.

2.1.1 Organoaluminum Reagents as Nucleophiles

Organoaluminum reagents have been used considerably as nucleophiles in both 1,2-additions and 1,4-additions (in the presence of Cu or Ni additives). More recently, asymmetric approaches of these reactions have been extensively investigated through the use of chiral ligands, covered in depth in a number of reviews.[52, 53]

Organoaluminum reagents have also been used in acetal cleavages[54] and similarly, epoxide openings. For example, Rainier and Cox demonstrated a one-pot glycal epoxidation and organoaluminum mediated C-1 carbon-carbon bond formation sequence (Scheme 2.1). The coordination of the organoaluminum to the C-2 alkoxide allowed for *syn* addition to the oxonium intermediate. Simple methyl, aryl, and vinyl substituents were incorporated to the C-glycoside in moderate to good yields.[55]

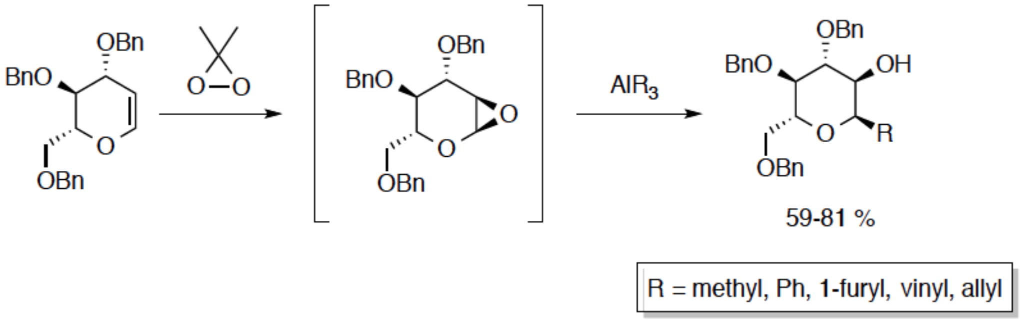
OBn
BnO
OBn
O
O—O
OBn
BnO
O
O
OBn
AlR$_3$
OBn
BnO
OH
O
R
OBn
59-81 %
R = methyl, Ph, 1-furyl, vinyl, allyl

Scheme 2.1 Organoaluminum-Mediated C-Glycoside Synthesis.

A more advanced example of epoxide opening by organoaluminums was found in a report from the Miyashita group.[56] Treatment of an epoxy alcohol with BuLi led to a lithium alkoxide, and following addition of an organoaluminum reagent generated an aluminum alkoxide intermediate (Scheme 2.2). This aluminum alkoxide intermediate was well suited for delivery of alkyl and alkynyl groups with concomitant opening of the epoxide. The sequential addition strategy allowed for regioselective alkyl and alkynyl additions to the epoxide with high stereoselectivity.

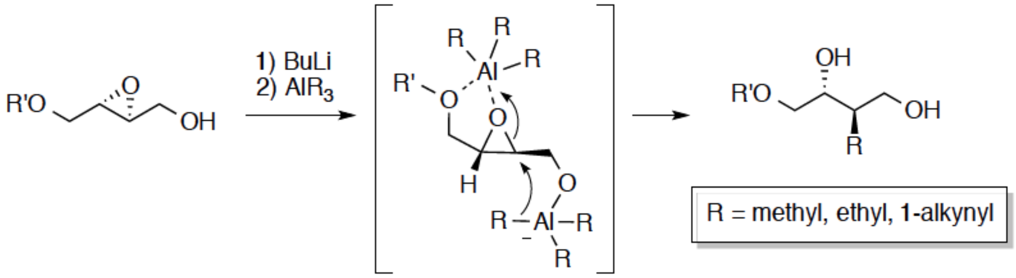
R'O
O
OH
1) BuLi
2) AlR$_3$
R
R
R
Al
R'
O
O
H
O
R
Al
R
R
R'O
OH
OH
R
R = methyl, ethyl, 1-alkynyl

Scheme 2.2 Organoaluminum Mediated Regioselective/Stereoselective Substitution Reaction of Epoxy Alcohol.

In addition, organoaluminum reagents have been used in a variety of nucleophilic substitution reactions. A novel example can be found in Yamamoto's report on trialkylaluminum mediated alkylative cyclization onto allyl phosphate esters (Scheme 2.3).[57] Treatment of geranyl diethyl phosphate with trimethylaluminum afforded a mixture of methyl substituted products via S_N1-like heterolysis of the phosphate ester.

When the *Z*-isomer, neryl diethyl phosphate, was treated with trimethylaluminum, the phosphate ester was displaced by the pendent olefin. A methyl group was then incorporated at the resulting tertiary cation to produce cyclized product **I**.

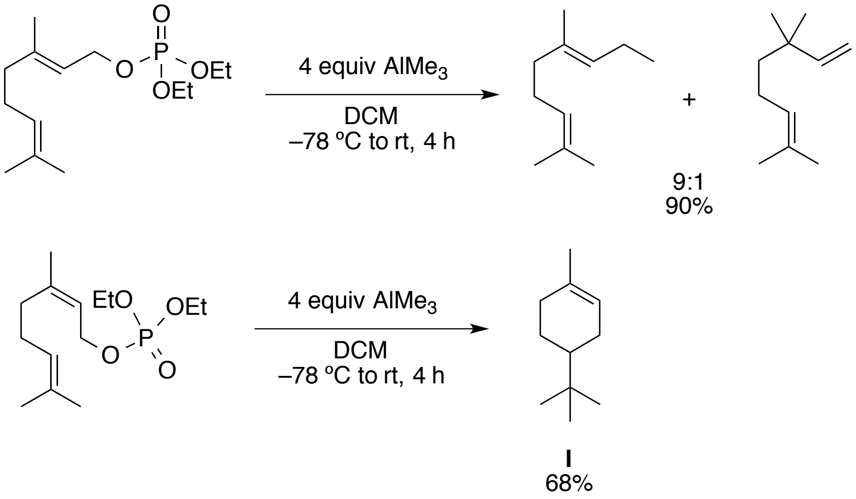
O
P
O
OEt
OEt
4 equiv AlMe3
DCM
–78 °C to rt, 4 h
+
9:1
90%
EtO
OEt
P
O
O
4 equiv AlMe3
DCM
–78 °C to rt, 4 h
I
68%

Scheme 2.3 Alkylative Displacement and Cyclization of Allyl Phosphate Esters.

The use of organoaluminum in the displacement reactions was extended by the Miyata group to alkylate ketones via umpolung reactivity.[58] By employing organoaluminum reagents with N-alkoxyenamines (Scheme 2.4), Miyata and co-workers were able to install alkyl and aryl substituents on the α-position of ketones, via an aluminum induced reversal in reactivity.

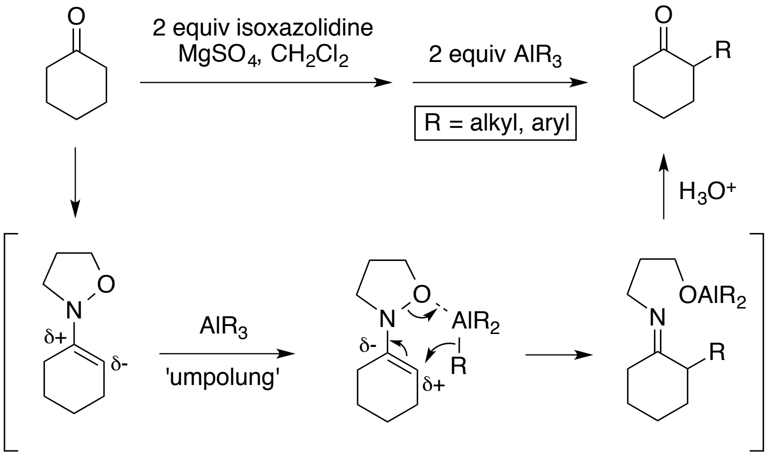
2 equiv isoxazolidine
$MgSO_4$, CH_2Cl_2
2 equiv AlR_3
R = alkyl, aryl
H_3O^+
δ+
δ-
AlR_3
'umpolung'
AlR_2
R
$OAlR_2$

Scheme 2.4 Organoaluminum Induced Umpolung Reactions of N-Alkoxyenamines.

2.1.2 Organoaluminum as a Medium for Redox Process

In addition to nucleophilic addition, organoaluminums have been widely used in redox processes. One of the most well known examples is the Oppenauer oxidation and its reverse reaction, the Meerwein-Ponndorf-Verley (MPV) reduction (Scheme 2.5). These reactions are in equilibrium, and the position of equilibrium relies on the oxidation potential of reactants. The stoichiometry of reagents can also affect the position of equilibrium (Le Chatelier's principle). One of the key features of these redox processes is high chemoselectivity: oxidation of secondary alcohols is faster than primary alcohols, and the reduction of aldehydes is more facile than the reduction of ketones. However, the classical Oppenauer oxidation and MPV reduction protocols both require superstoichiometric amounts of aluminum alkoxide and oxidant (hydride acceptor)/reductant (hydride donor) for reasonable yields.[59]

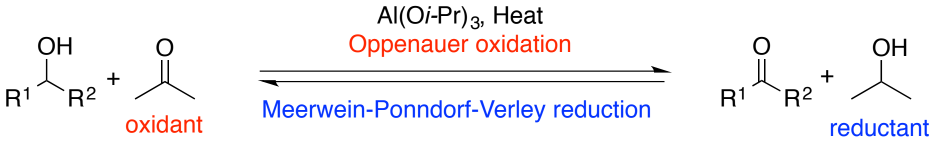
$Al(O\textit{i}\text{-}Pr)_3$, Heat
Oppenauer oxidation
Meerwein-Ponndorf-Verley reduction
OH
O
R^1
R^2
oxidant
reductant

Scheme 2.5 Oppenauer Oxidation and MPV Reduction.

In an effort to overcome the drawbacks of the Oppenauer oxidation/MPV reduction in lowering the loading of the aluminum Lewis acid, Nguyen and co-workers investigated the use of alkylaluminum reagents as catalysts in the reactions.[60] In the reduction of cyclohexanone in the presence of isopropanol, $AlMe_3$ and $ClAlMe_2$ both provided the reduced product, cyclohexanol, in satisfying yield within three hours (Table 2-1). When Al(*i*OPr)$_3$ was used, only 7 % yield was obtained in spite of a significantly longer reaction time. It has been postulated that aluminum alkoxide reagents would build higher degrees of aggregation[61] through bridging alkoxide ligands, making them less effective. The authors found that fresh aluminum alkoxide (in-house made) showed better reactivity than commercial Al(O*i*Pr)$_3$, supporting this hypothesis.

Table 2-1 Catalytic MPV Reduction by Alkylaluminum Reagents.

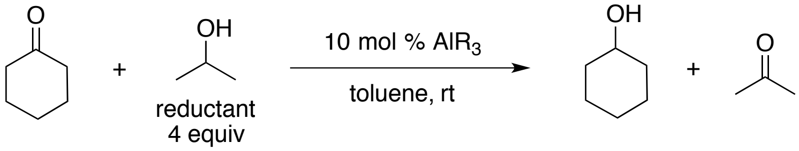

entry	catalyst	Yield (%)	Time (h)
1	$AlMe_3$	82	3
2	$ClAlMe_2$	96	2
3	Al(O*i*Pr)$_3$	7	12

Following the catalytic MPV reduction reaction, Nguyen's research group also demonstrated an improved Oppenauer oxidation protocol, utilizing not only catalytic amounts of trialkylaluminum, but also electron-deficient aldehydes as hydride acceptors to drive the equilibrium toward the oxidation product (Scheme 2.6).[62] From the optimization study on a series of aldehydes, aryl aldehydes bearing electron withdrawing groups – nitrobenzaldehyde, dichlorobenzaldehyde, and dinitrobenzaldehyde – were found to be the most suitable oxidant. 3-Nitrobenzaldehyde was chosen for the substrate scope study, since it is readily available, and inexpensive.

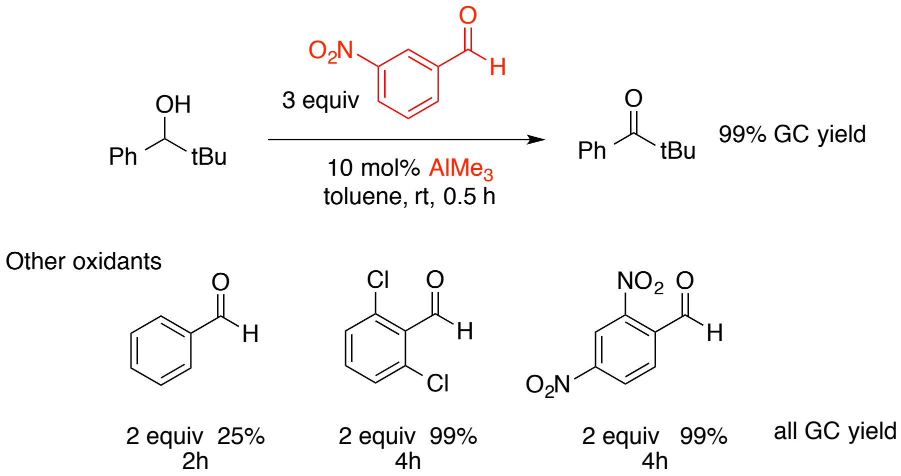
OH
Ph
tBu
O_2N
O
H
3 equiv
10 mol% $AlMe_3$
toluene, rt, 0.5 h
O
Ph
tBu
99% GC yield
Other oxidants
O
H
Cl
O
H
Cl
NO_2
O
H
O_2N
2 equiv 25%
2h
2 equiv 99%
4h
2 equiv 99%
4h
all GC yield

Scheme 2.6 Catalytic Oppenauer Oxidation with $AlMe_3$.

Endeavors to lower aluminum catalyst loading can be found in Maruoka's research as well. In 2001, his research group reported a new aluminum catalyst with a bidentate aluminum alkoxide ligand (Scheme 2.7).[63] The aluminum alkoxide was employed for the catalytic MPV reduction with *i*PrOH as the reducing reagent.

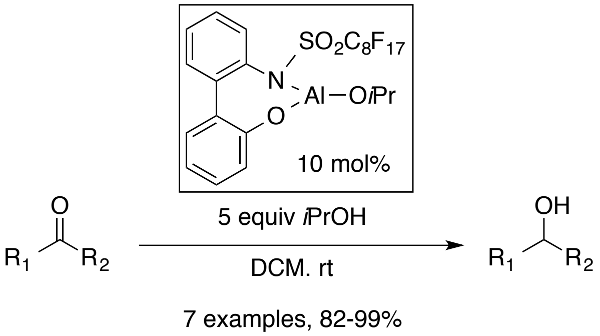
$SO_2C_8F_{17}$
N
O
Al—O*i*Pr
10 mol%
O
R_1
R_2
5 equiv *i*PrOH
DCM. rt
OH
R_1
R_2
7 examples, 82-99%

Scheme 2.7 Catalytic MPV Reduction with Aluminum Alkoxide.

Shortly after, the same research group showcased the efficient reactivity of the aluminum alkoxide in the Oppenauer oxidation. With pivaldehyde as a hydride acceptor, 1 mol% of aluminum catalyst was enough to oxidize carveol, generating carvone in excellent yield (Scheme 2.8).[64]

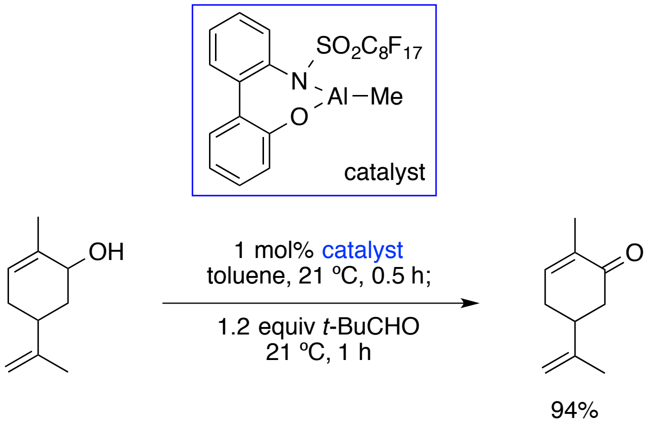

Scheme 2.8 Catalytic Oppenauer Oxidation by Aluminum Alkoxide.

The discovery of the catalytic reactivity of the aluminum alkoxide has opened the door for catalytic asymmetric MPV reductions. To this point, asymmetric MPV reduction protocols had been limited to using stoichiometric amounts of a chiral alcohol hydride donor.[65] In 2002, Nguyen and co-workers demonstrated the first catalytic (10 mol%), enantioselective MPV reduction, utilizing a chiral aluminum alkoxide derived from $AlMe_3$ and BINOL (Scheme 2.9).[66] High stereoselectivity, however, was observed only in halogen substituted acetophenones (80% ee). In case of the reduction on acetophenone, a drastic decrease in the enantiomeric excess (32 %) was observed. Controlling the enantioselectivity in the MPV reduction still has ample room for improvement.

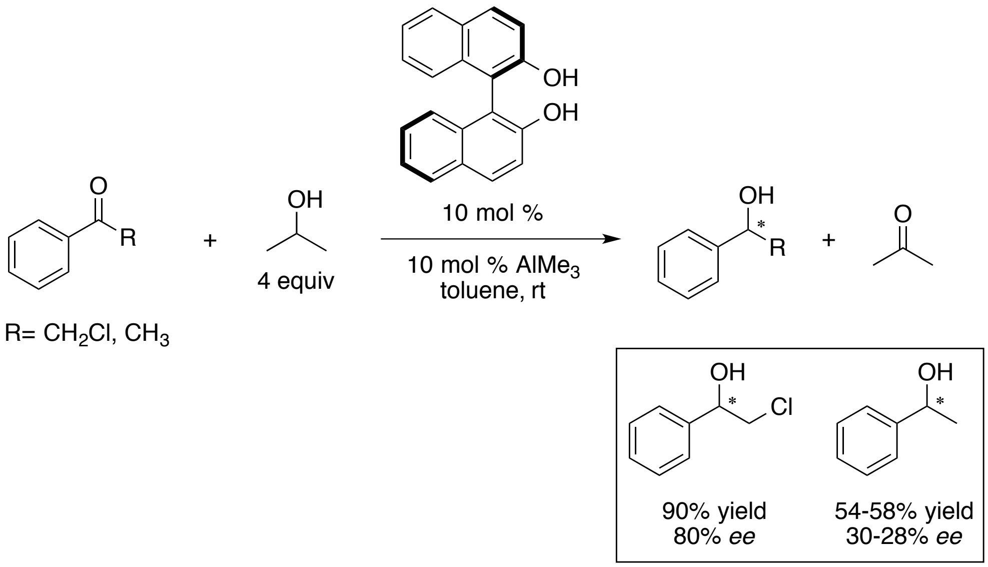

Scheme 2.9 Catalytic Asymmetric MPV Reduction.

2.2 Results and Discussion

2.2.1 Organoaluminum Mediated Interrupted Nazarov Reaction

Considering the fruitful use of trivalent organoaluminum reagents as Lewis acids and nucleophiles described above, we naturally conceived using them in the interrupted Nazarov reaction. From a literature search, the use of organoaluminums in the Nazarov reaction has been quite rare. The only organoaluminum reagents employed in the Nazarov reaction were alkyl aluminum halides, used simply as Lewis acids in the reaction.[67, 68] We wondered if trialkylaluminum reagents could replace the alkyl aluminum halides and if so, what the fate of the aluminum-carbonyl oxygen adduct would be.

This fundamental question led us to design a new type of interrupted Nazarov reaction employing triorganoaluminum reagents (Scheme 2.10). We envisioned, as long as the organoaluminum was sufficiently Lewis acidic to initiate the 4π electrocyclization process, one of the groups on aluminum could have a chance to migrate to a terminus of the cyclopentenyl cation **2** via metal-mediated delivery.[69] Upon protonation on the resulting aluminum enolate, substituted cyclopentanones **3** could be generated. Successful reactions could incorporate simple alkyl groups, a class of nucleophiles that to this point has been elusive in interrupted Nazarov reaction methodology.[1a, 7]

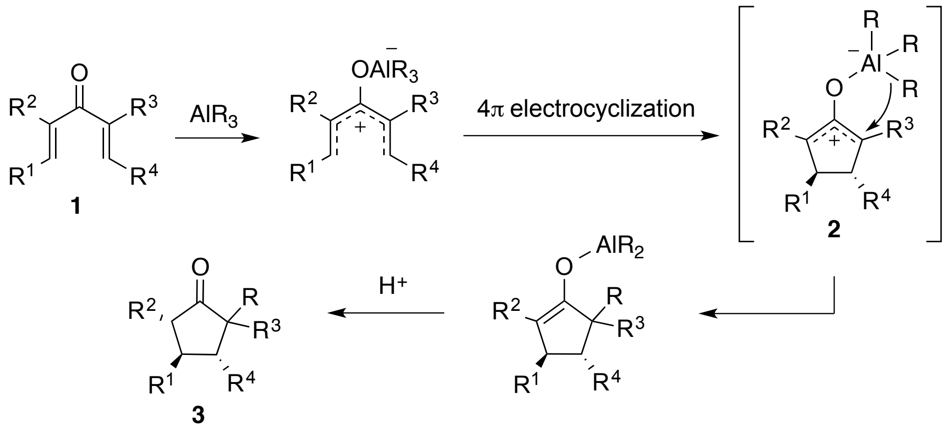

Scheme 2.10 Proposed Organoaluminum Based Nazarov Reaction.

We were uncertain as to whether triorganoaluminum reagents could initiate the Nazarov electrocyclization, as there was the possibility of premature methyl addition to the activated dienones in either 1,2- or 1,4-addition pathways. At the outset, we chose to examine the behavior of trimethylaluminum on a Nazarov substrate **1a** to test this idea (Table 2-2). The first attempt (entry 1) gratefully allowed us to find trace amount of methylated cyclopentanone **3a** in a complex mixture. It was the first example of a 4π electrocyclic process employing triorganoaluminum reagents. After the initial excitement, we proceeded with optimization of the reaction by changing the amount of $AlMe_3$, reaction temperatures, and solvents. Notably, in an ethereal solvent the trimethylaluminum reagent was inactive, and therefore **1a** was intact (entry 2). Eventually, we secured an optimal condition: 2.5 equivalents of $AlMe_3$ at low temperature in CH_2Cl_2 in the presence of 4 Å molecular sieves [70] (entry 7).

Table 2-2 Optimization of $AlMe_3$-Mediated Interrupted Nazarov Reaction.[a]

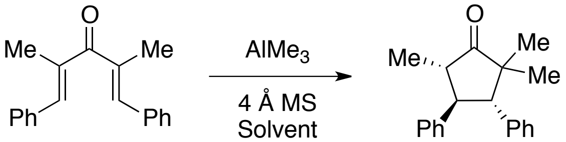

1a **3a**

Entry	Equiv $AlMe_3$	Solvent	Temperature (ºC)	Time	Yield[b] of **3a**
1	0.25	toluene	room temp.	20 min	< 10%
2	1.0	THF	−78 to 0	5 h	No reaction
3	1.5	toluene	−41	60 min	59%
4	1.5	CH_2Cl_2	−41	60 min	81%
5	2.0	toluene	−41	60 min	81%
6	2.0	CH_2Cl_2	−78	90 min	85%
7	**2.5**	**CH_2Cl_2**	**−78 to −41**	**30 min**	**92%**

[a] Addition of 4Å molecular sieves was noted to reduce variability in results. [b] Yields are based on isolated product after chromatography.

With the optimized conditions in hand, we moved to investigate the substrate scope of the trimethylaluminum mediated Nazarov reaction. In the case of symmetrical β, β'-aryl substituted 1,4-dien-3-ones, **1a-d** afforded methylated cyclopentanones **3a-d** in excellent yield (entries 1-4, Table 2-3). It is notable to mention that the products (**3a-d**) were obtained as single (all *trans*) diastereomers,[71] indicating complete stereoselectivity in the enolate protonation step.

Table 2-3 AlMe$_3$-Mediated Nazarov Cyclization.[a]

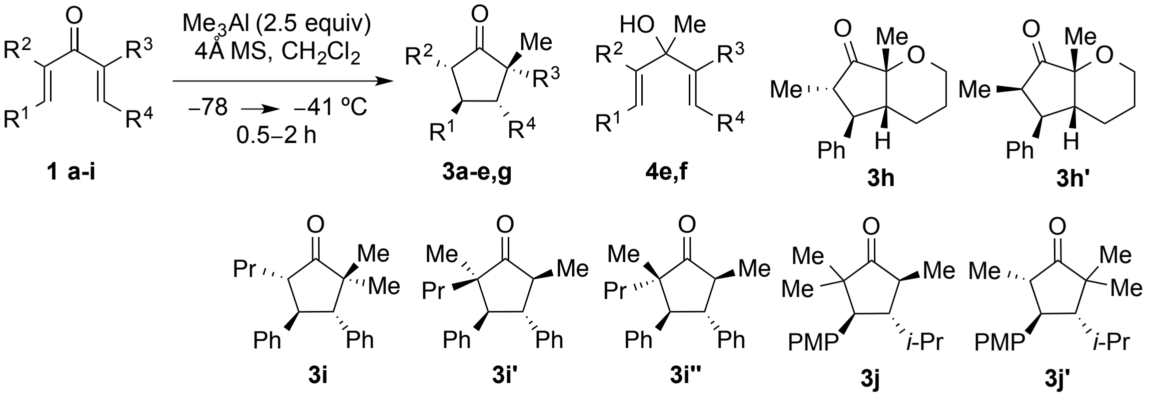

Entry	Substrate	R1	R2	R3	R4	Product(s)	Yield (%)[b]
1	**1a**	Ph	Me	Me	Ph	**3a**	92
2	**1b**	4-ClC$_6$H$_4$	Me	Me	4-ClC$_6$H$_4$	**3b**	92
3	**1c**	4-MeOC$_6$H$_4$	Me	Me	4-MeOC$_6$H$_4$	**3c**	82
4	**1d**	2-furyl	Me	Me	2-furyl	**3d**	94
5[c]	**1e**	*i*-Pr	Me	Me	*i*-Pr	**3e**[d]	54
6	**1f**	Ph	Me	H	Ph	**4f**	74
7	**1g**	Ph	Me	Me	H	**3g** (11:1)[e]	79
8	**1h**	Ph	Me	–O(CH$_2$)$_3$–		**3h/3h'** (2.3:1)[f]	79
9	**1i**	Ph	*n*-Pr	Me	Ph	**3i/3i'/3i''** (7.1:1.1:1.0)[g]	84
10	**1j**	4-MeOC$_6$H$_4$	Me	Me	*i*-Pr	**3j/3j'** (2:1)[h]	93

[a] Standard procedure: see experimental section [b] Yields are based on isolated product after chromatography. [c] The reaction was carried out at –25 ºC. [d] 1,2-Adduct **4e** was also obtained in ca. 23% yield. [e] Ratio of diastereomers (*trans*/*cis*), measured via integration of benzylic methine protons in ^{1}H NMR spectrum. [f] Ratio reflects isolated yields of **3h** and **3h'**. [g] Ratio of regioisomers/diastereomers determined by integration of benzylic methine protons in ^{1}H NMR spectrum. Only partial characterization of **3i''** was possible due to inseparable mixtures, so structural assignment is tentative. [h] Ratio of regioisomers, measured via integration of benzylic methine protons in ^{1}H NMR spectrum.

Compound **1e** gave a low yield of cyclopentanone **3e** (entry 5). We believe this is due to the higher temperature (–25 °C) required in the cyclization step, which allows the 1,2-addition of methyl to compete with cyclization to produce small amounts of alcohol **4e**. This undesired side-reaction completely outcompetes cyclization in the case of unsymmetrically substituted dienone **1f**, which lacks a substituent at C-4. In this case, dienol **4f** was the sole product obtained and with a high yield; we attribute this to slower electrocyclization in combination with greater accessibility of the carbonyl to attack by the relatively small methyl nucleophile.

Other unsymmetrically substituted dienones (**1g-j**) underwent the desired interrupted Nazarov reaction, allowing us to examine the regioselectivity in the methyl addition step (entries 7–9). Substrate **1g**, lacking an R^4 substituent, produced **3g** as an 11:1 *trans*/*cis* mixture via cyclization followed by methylation at the terminus adjacent to the unsubstituted carbon. Substrate **1h**, which contains a dihydropyran moiety, also gave bicyclic products **3h** and **3h'** in excellent yield. In this case, delivery of the methyl group was completely regio- and stereoselective, giving a *cis* ring-fusion, but a mixture of epimers (~ 2:1) was obtained at the site of the former enolate. Single crystal X-ray diffraction analysis was used to determine the relative configuration of the major epimer **3h** (Figure 2.1).[71]

Dienone **1i**, differing from **1a** only in the substitution of Me with *n*-Pr at C-2, afforded a mixture of three products in high yield; surprisingly, high regioselectivity for methylation on the methyl-substituted carbon in preference to the propyl-substituted position was observed for this substrate. Finally, dienone **1j** produced a mixture of regioisomers **3j** and **3j'** in excellent yield. Migration of the methyl group slightly favored the carbon adjacent to the 4-methoxyphenyl group (2:1 ratio, **3j**/**3j'**).

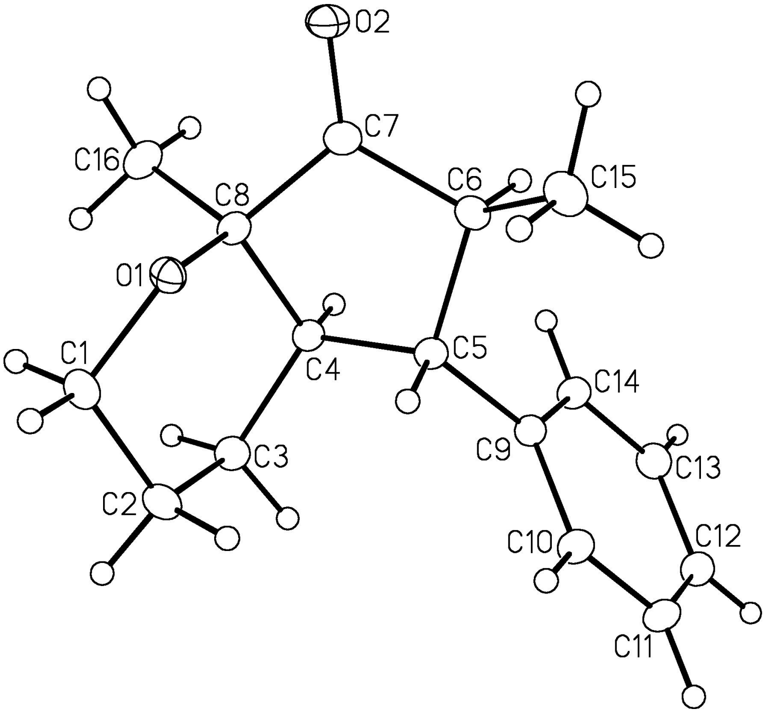

(Thermal ellipsoids shown at the 20 % probability level)

Figure 2.1 ORTEP Drawing of **3h**.

We were also interested to see if the β-aromatic substituents would have an electronic effect on the regioselectivity of the methylation (Scheme 2.11). Unsymmetrically substituted and sterically unbiased dienone **1k** was prepared via a two-step aldol condensation. Treatment of **1k** with $AlMe_3$ resulted in 2:1 mixture of inseparable regioisomers **3k**/**3k'**. The major product **3k** was found to have had nucleophilic methylation at the oxyallyl cation terminus adjacent to the *para*-methoxyphenyl group. The weak regioselectivity suggests that the electronic effect of the β-aryl group on the Nazarov intermediate by phenonium ion is not very dominant (Scheme 2.12).

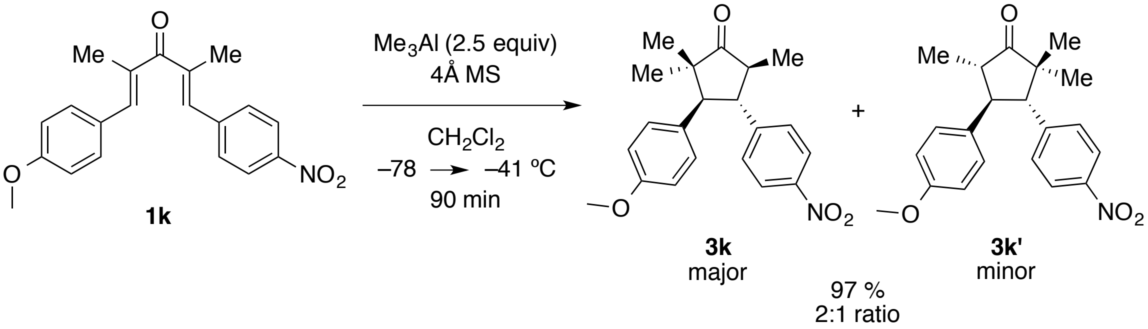
Me
Me
1k
NO2
Me3Al (2.5 equiv)
4Å MS
CH2Cl2
–78 → –41 °C
90 min
Me
Me
Me
NO2
3k
major
+
Me
Me
Me
NO2
3k'
minor
97 %
2:1 ratio

Scheme 2.11 Electronic Effect of Aromatic Substituents on the Regioselectivity.

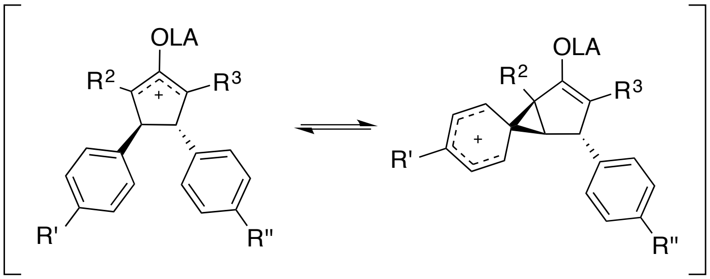
OLA
R2
R3
R'
R"
OLA
R2
R3
R'
R"

Scheme 2.12 Possible Formation of Phenonium Ion.

Since **3k** and **3k'** are not separable by flash chromatographic techniques, assignment of the regioisomers is worthy of discussion (Figure 2.2). In general, aromatic protons of PMP groups are more shielded than aromatic protons bearing a nitro group (inductive effect), allowing us to confidently assign the aromatic signals in the ^{1}H NMR spectrum. 2D NMR experiments (rOe and COSY) allowed us to designate $\mathbf{H_a}$ and $\mathbf{H_b}$ for **3k**. Finally, $\mathbf{H_b}$ has a rOe correlation to the most upfield methyl group (singlet). We were able to tell apart the two methyl groups (singlet) by using chemical shift differences, based on the trend (anisotropy effect) observed in previous reports.[30] Configuration of minor product **3k'** was confirmed in a similar way with the aromatic signals of the *para*-nitro phenyl group.

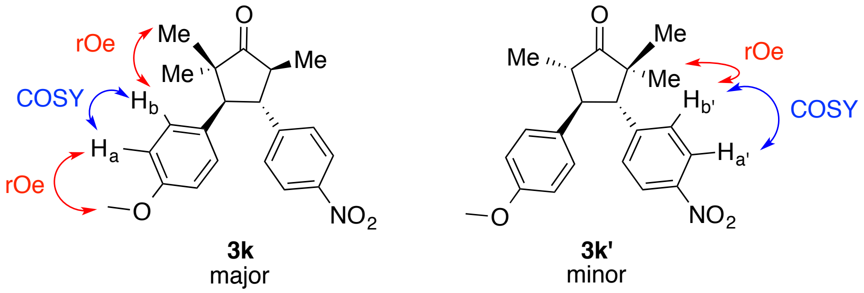
rOe
Me
Me
O
Me
COSY
Hb
Ha
rOe
O
NO2
3k
major
Me
O
Me
Me
rOe
Hb'
COSY
Ha'
O
NO2
3k'
minor

Figure 2.2 Assignment of **3k** and **3k'**.

Wanting to further investigate the regioselectivity of the trimethylaluminum interrupted Nazarov reaction, we looked to unsymmetrical dienone **1l** (Scheme 2.13). Even though both phenyl and naphthalene are planar, naphthalene has a slightly larger A-value due to its larger dimension. In this case, methylation occurred less selectively, providing a 1.8:1 mixture of regioisomers **3l** and **3l'**, curiously favouring the methylation adjacent to the bulkier naphthalene group.

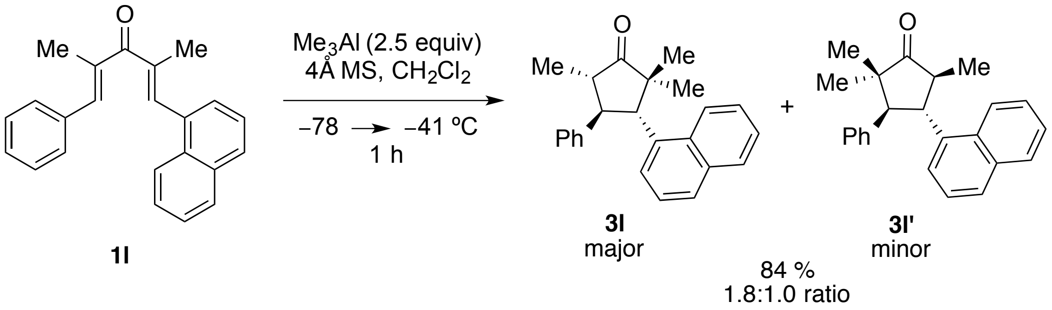
Me
O
Me
1l
Me3Al (2.5 equiv)
4Å MS, CH2Cl2
–78 → –41 °C
1 h
Me
O
Me
Me
Ph
3l
major
+
Me
Me
O
Me
Ph
3l'
minor
84 %
1.8:1.0 ratio

Scheme 2.13 Steric Effect of β-Substituents on the Regioselectivity.

In order to assign the regioisomers **3l**/**3l'** correctly, we needed to distinguish the phenyl and naphthyl signals in the ^{1}H NMR spectrum. Based on 1-methylnaphthalene having a signal at 7.97 ppm in $CDCl_3$ (its most downfield signal) that corresponded to $\mathbf{H_8}$ (Figure 2.3),[72] we assumed the most downfield signal for **3l** (8.24 ppm) was $\mathbf{H_a}$. This was further supported by a 1D-TOCSY experiment that showed a four proton correlation, beginning at $\mathbf{H_a}$. After confidently assigning $\mathbf{H_a}$, we examined the rOe correlations of $\mathbf{H_a}$.

Notable correlations were found to both H_b and a methyl singlet. This led us to conclude that **3l** was the regioisomer shown in Figure 2.3.

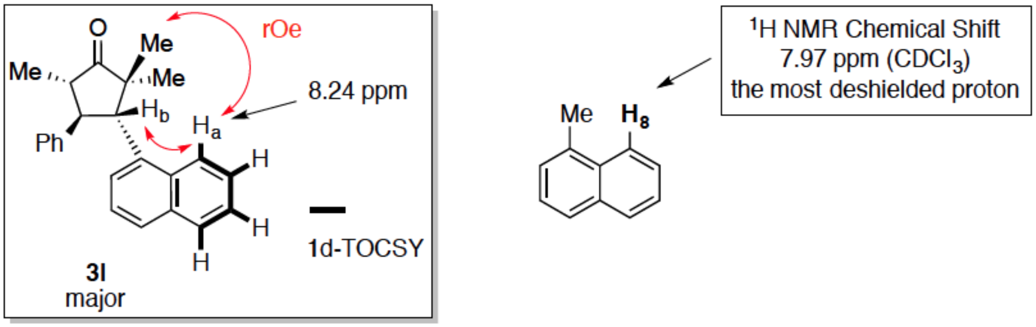

Figure 2.3 rOe Experiment for **3l** and Chemical Shift Comparison to 1-Methylnaphthalene.

From the two experiments (Scheme 2.11 and Scheme 2.13), we conclude that β-substituents of the Nazarov substrates have little influence on the regioselectivity of the methylation induced by trimethylaluminum.

Having established the generality of the $AlMe_3$ mediated reaction, we moved to study the range of organoaluminum reagents able to affect the 4π electrocyclization and transfer a substituent to the allyl terminus of the cyclized intermediate. Using dienone **1a**, we found that triisobutylaluminum produced a mixture of "reductive Nazarov" products[73] **5a** and **5a'** (Scheme 2.14), without the desired delivery of an *i*-Bu group. Reduced alcohol **6a** was also isolated as a minor product. Though we believed the hydride transfer happened through the isobutyl ligand of the aluminum, giving off isobutene, we did not rule out the possibility that these reduced products resulted from *in situ* generated diisobutylaluminum hydride (DIBAL-H), a known decomposition product of $(i\text{-Bu})_3Al$.[74] However, treatment of **1a** with DIBAL-H under the same conditions produced only **6a**, suggesting that the Nazarov cyclization and subsequent hydride transfer were mediated by $(i\text{-Bu})_3Al$, not DIBAL-H.

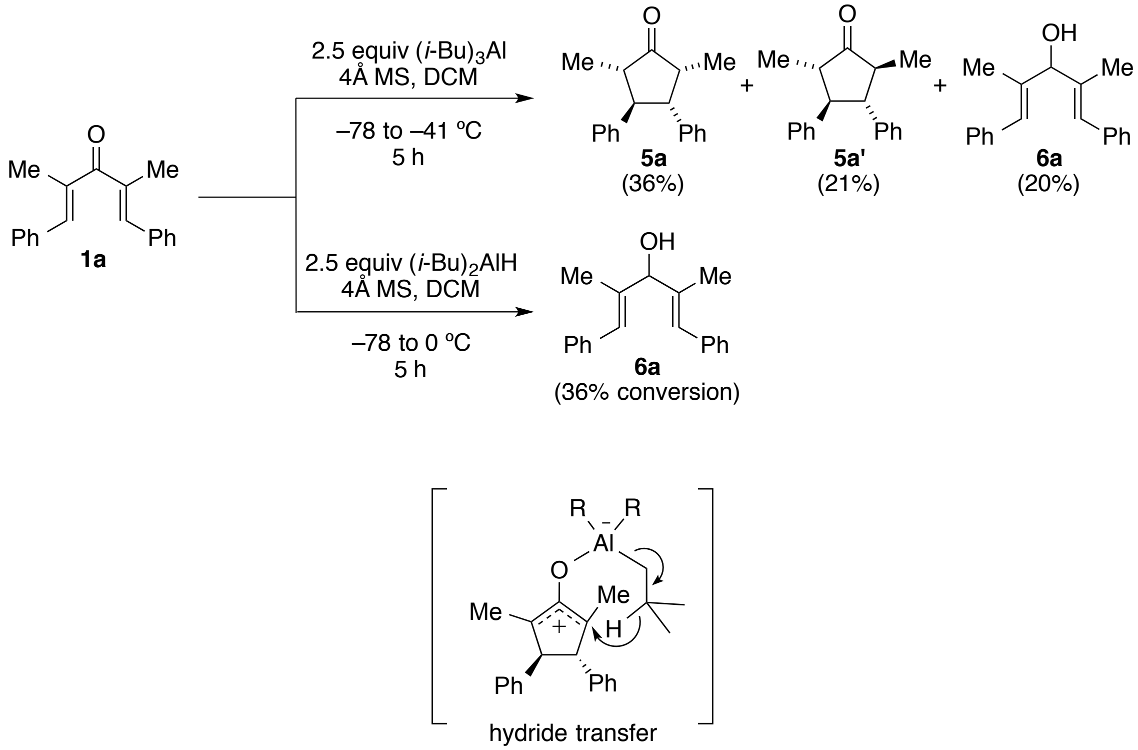
Me
Me
Ph
Ph
1a
2.5 equiv (i-Bu)3Al
4Å MS, DCM
–78 to –41 °C
5 h
5a
(36%)
5a'
(21%)
6a
(20%)
2.5 equiv (i-Bu)2AlH
4Å MS, DCM
–78 to 0 °C
5 h
6a
(36% conversion)
hydride transfer

Scheme 2.14 Al(*i*-Bu)$_3$ Mediated Reductive Nazarov Reaction.

Triethylaluminum also provided ethylated cyclopentanone **7a** in good yield (Scheme 2.15). The ethyl group was delivered exclusively on the opposite face to the adjacent phenyl substituent. Reductive Nazarov product **5a'** was also isolated as a minor product, indicating that the β-hydrogen atom of the ethyl ligands on the aluminum is transferable, similar to what was seen with (*i*-Bu)$_3$Al. The relative configuration of **7a** was confirmed via single crystal X-ray diffraction analysis (Figure 2.4).[71]

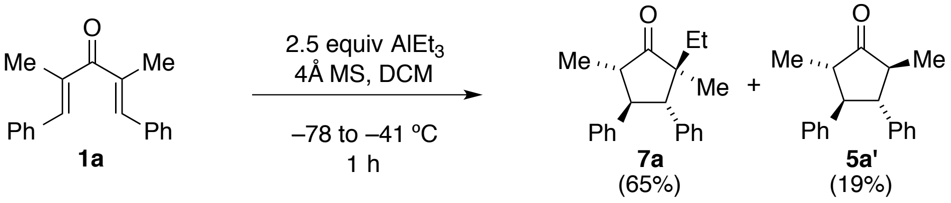
1a
2.5 equiv AlEt3
4Å MS, DCM
–78 to –41 °C
1 h
7a
(65%)
5a'
(19%)

Scheme 2.15 AlEt$_3$ Mediated Interrupted Nazarov Reaction.

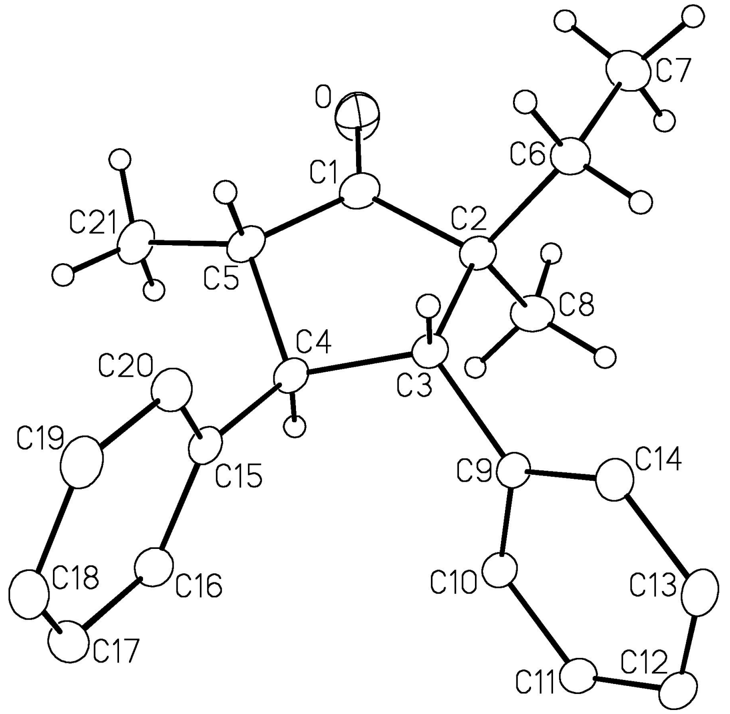

(Thermal ellipsoids shown at the 20 % probability level)

Figure 2.4 ORTEP Drawing of **7a**.

Diethylaluminum cyanide was also tested on dienone **1a**. While potentially capable of transferring either a cyano or ethyl group, this reagent allowed only the incorporation of cyanide to give stereoisomers **8a** and **8a'** in excellent yield, but as a nearly equal mixture (Scheme 2.16). Unlike previous examples (Me, Et), the addition of cyanide was unselective toward the β-aryl substituent. The relative configuration of **8a'** was assigned by single crystal X-ray diffraction analysis (Figure 2.5). Correlated to NMR data for other adducts (**3a** and **7a**) derived from **1a**, **8a** was assigned to have a *trans* relationship between the Ph and Me groups at C-4 and C-5; a *cis* relationship between the C-2 Me and C-3 Ph was apparent for **8a**.[30] Our assignments that these isomers did not differ in configuration at C-5 were also supported by the failure of DBU induced epimerization to interconvert **8a** and **8a'**.

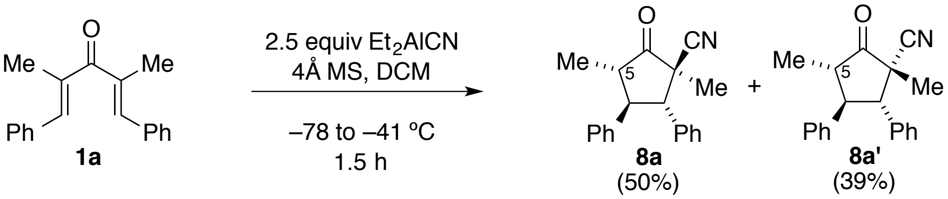
Me
Me
Ph
Ph
1a
2.5 equiv Et2AlCN
4Å MS, DCM
–78 to –41 °C
1.5 h
O
Me
CN
Me
5
Ph
Ph
8a
(50%)
+
O
Me
CN
Me
5
Ph
Ph
8a'
(39%)

Scheme 2.16 Et_2AlCN Mediated Interrupted Nazarov Reaction.

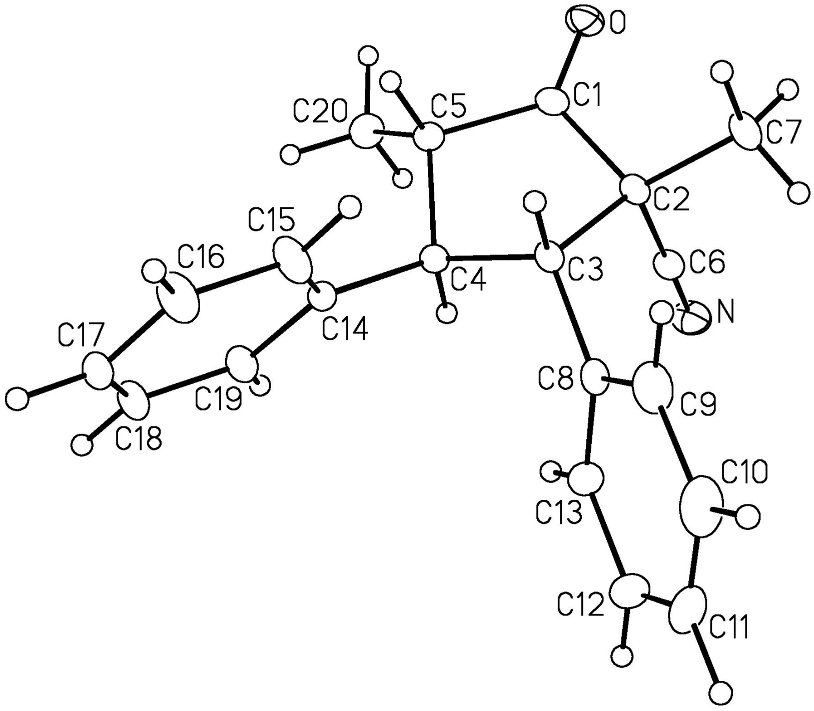
O
C1
C2
C3
C4
C5
C6
N
C7
C8
C9
C10
C11
C12
C13
C14
C15
C16
C17
C18
C19
C20

(Thermal ellipsoids shown at the 20 % probability level)

Figure 2.5 ORTEP Drawing of **8a'**.

Triphenylaluminum allowed phenylation at the α position, affording cyclopentanone **9a** in modest yield (Scheme 2.17). There have been precedents for intermolecular arylation by interrupted Nazarov reaction, but these examples have used electron-rich aromatic or heteroaromatic traps.[18, 19] To the best of our knowledge, this is the first case of trapping the Nazarov intermediate with a simple phenyl group. It is notable that longer reaction times and a higher reaction temperature (–30 °C) were required with $AlPh_3$. We also obtained substantial amounts of exocyclic elimination products **10a**, as an 11:1 mixture of epimers at C-5.

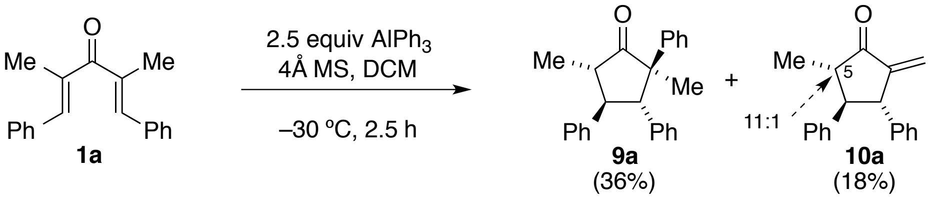

Scheme 2.17 $AlPh_3$ Mediated Interrupted Nazarov Reaction.

Organoazides have been used to react with oxyallyl cations in the [3+3] cycloadditions inter-[39] and intra-molecularly.[75] The synthetic value of the organoazides is apparent, and well presented in domino Nazarov cyclization/Schmidt rearrangement to form dihydropyridones[38] or peroxy bridged indolizidinones.[37] However, in none of these examples did the azide moiety remain intact. We wondered if organoaluminum azide would exhibit the same reactivity as the other organoaluminums, and insert an azide group on the cyclopentanone framework. Subjecting divinylketone **1a** to a solution of freshly prepared Me_2AlN_3[76] provided a 2:1 mixture of epimeric adducts **11a** and **11a'** in good yield (Scheme 2.18). To the best of our knowledge, this is the first instance of a reaction between azides and oxyallyl cations where the azide group remains intact.

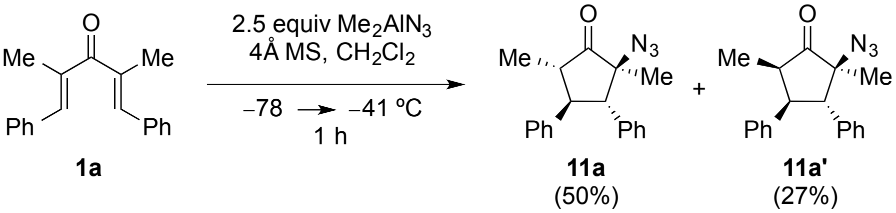

Scheme 2.18 Intramolecular Azide Trapping.

Single crystal X-ray diffraction analysis allowed for unambiguous assignment of the relative stereochemistry of major isomer **11a (**Figure 2.6).[71] To prove the structure of the minor isomer, catalytic amounts of DBU were added to an NMR tube containing **11a'** and the reaction was monitored via ^1H NMR over a period of 15 h (Scheme 2.19). During this time, a 40% conversion to **11a** was observed, confirming that they are epimeric at C-5.

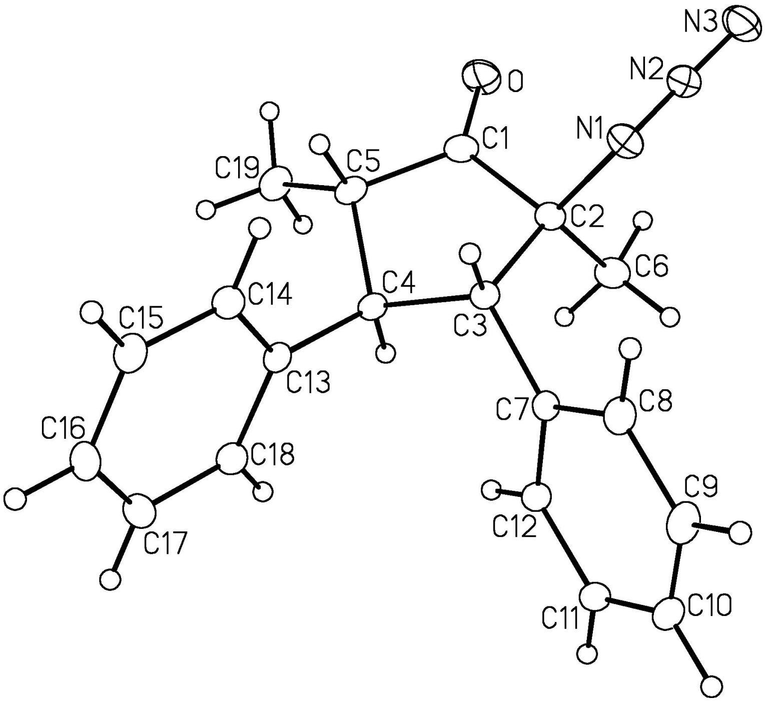
N3
N2
O
N1
C1
C19
C5
C2
C6
C14
C4
C15
C3
C13
C7
C8
C16
C18
C9
C12
C17
C11
C10

(Thermal ellipsoids shown at the 20 % probability level)

Figure 2.6 ORTEP Drawing of **11a'**

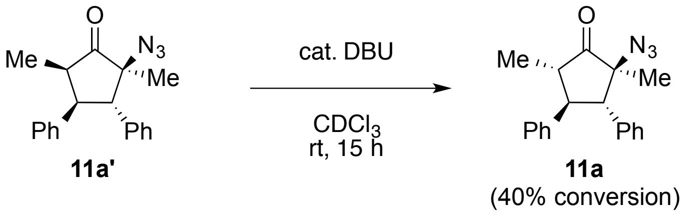
O
Me
N3
Me
Ph
Ph
11a'
cat. DBU
CDCl3
rt, 15 h
O
Me
N3
Me
Ph
Ph
11a
(40% conversion)

Scheme 2.19 Base-Induced Epimerization of **11a'**.

Our final goal of this project was to introduce a vinyl substituent on the Nazarov intermediate (Scheme 2.20) as the reactivity of a trivinylaluminum toward electrophilic sites is similar to previously handled organoaluminums,[77] and the vinyl group would provide a handle for further C-C bond forming reactions. Vinylaluminum reagents were prepared from known procedures: $AlCl_3$ with 3 equiv or Me_2AlCl with 1 equiv Grignard reagent.[55, 78] However, all attempted reactions with *in situ* made vinylaluminum reagents failed to provide positive results. Two factors may contribute to the lack of consumption of starting material: (1) magnesium salt byproduct from the *in situ* generation of the vinylaluminum reagent, (2) ethereal solvent wherein the commercial Grignard reagent is dissolved. When three equivalents of trivinylaluminum are applied to a divinylketone, there would be nine equivalents of ClMgBr salt generated in the reaction. I postulated that the salt would block carbonyls from reacting with the vinylaluminum. In addition, we noted in the earlier part of this chapter that $AlMe_3$ does not show any reactivity in THF for the Nazarov reaction (Table 2-2).

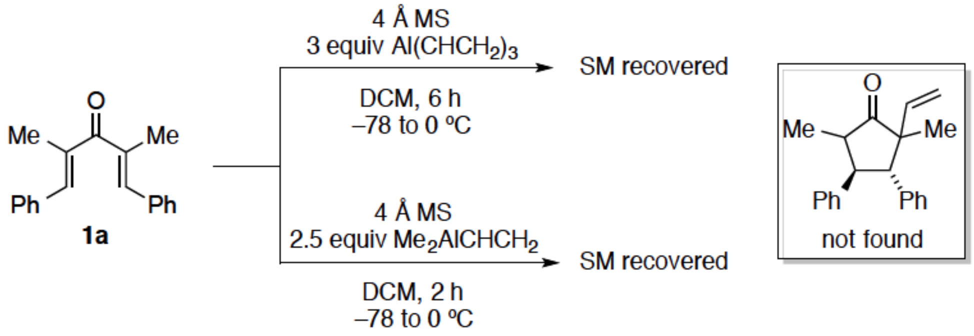

Scheme 2.20 Unsuccessful Vinylaluminum Reaction.

Having the trivinylaluminum results in mind, I focused on making a “salt free” alkynylaluminum reagent by using lithium acetylide ethylenediamine complex (Scheme 2.21). If the ethylenediamine can chelate to LiCl (byproduct from the formation of diethylalkynyl aluminum), a Nazarov substrate would be free to react with the organoaluminum. However, this approach also failed to make an alkynyl substituted cyclopentanone.

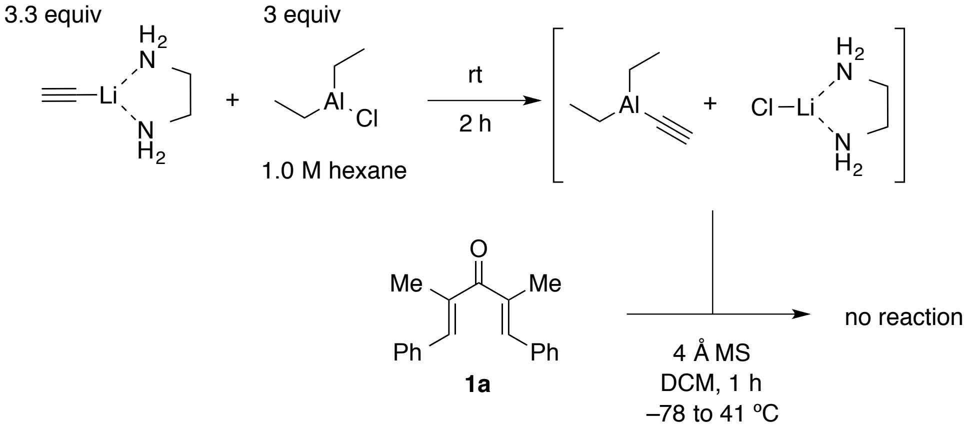
3.3 equiv
3 equiv
rt
2 h
1.0 M hexane
1a
4 Å MS
DCM, 1 h
–78 to 41 °C
no reaction

Scheme 2.21 Use of Ethylenediamine in Generation of Diethylalkynyl Aluminum.

2.2.2 Meerwein-Ponndorf-Verley Like Interrupted Nazarov Reaction

We continued our efforts towards installing vinyl and alkynyl functionality on the Nazarov intermediate by considering the Meerwein-Ponndorf-Verley (MPV) reaction. We were inspired by the work of Maruoka, where he demonstrated transfer of alkynyl groups to aldehydes using aluminum alkoxides (Scheme 2.22).[79] We hoped this methodology could be used with the Nazarov cyclization to add an alkynyl group to the oxyallyl cation with concomitant loss of acetone (Scheme 2.23).

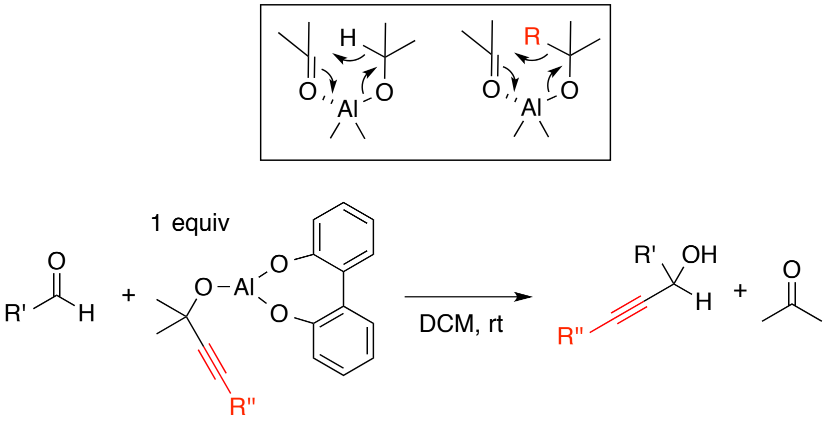
1 equiv
DCM, rt

Scheme 2.22 The MPV Alkynylation of Aldehydes.

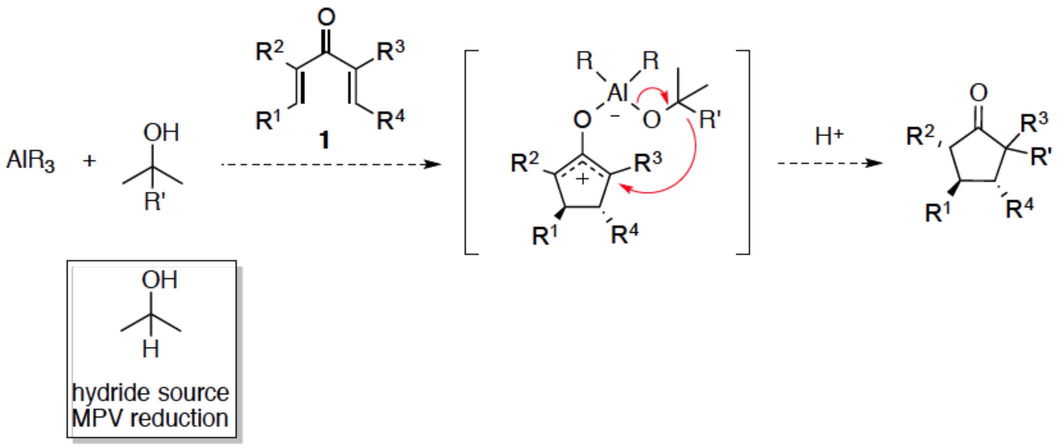
AlR3
+
OH
R'
R2
R3
R1
R4
1
R
R
Al
O
O
R'
H+
hydride source
MPV reduction

Scheme 2.23 Proposed MPV-Type Interrupted Nazarov Reaction.

Similar to Maruoka's work, we prepared an aluminum alkoxide and added it to a solution of substrate **1a** (Scheme 2.24). In 30 minutes at –41 °C **1a** was fully consumed in the presence of the aluminum Lewis acid, but the desired delivery of the alkynyl group did not take place based on the crude ^{1}H NMR spectrum. Instead, a complex mixture was produced.

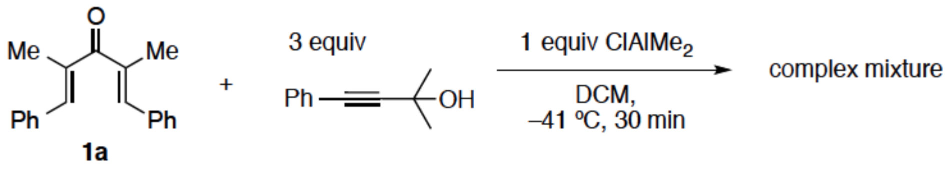
Me
Me
Ph
Ph
1a
+
3 equiv
Ph
OH
1 equiv ClAlMe2
DCM,
–41 °C, 30 min
complex mixture

Scheme 2.24 Unsuccessful Delivery of Alkynyl Functionality.

2.2.3 Organozinc Interrupted Nazarov Reaction

Having established the organoaluminum initiated Nazarov reaction, we hunted for other organometallic reagents capable of initiating the electrocyclization and delivering a substituent to the Nazarov intermediate. We were particularly interested in use of organozinc reagents as they are relatively mild reagents and are easily accessible. The pertinent question to ask was if they are as Lewis acidic as organoaluminums, and therefore able to trigger electrocyclization by themselves (Scheme 2.25).

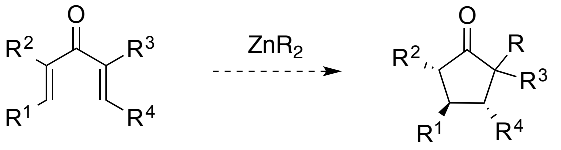

Scheme 2.25 Organozinc Interrupted Nazarov Reaction.

To answer the question above, 2.5 equivalents of diethylzinc were subjected to **1a** as a test substrate (Scheme 2.26). Opportunely, 1,2-adduct and 1,4-adduct were not found, even upon warming to room temperature and prolonged reaction time, leaving **1a** intact. From this result, we hypothesized that the organozinc interrupted Nazarov reaction could be feasible when an extra Lewis acid to initiate electrocyclization is present.

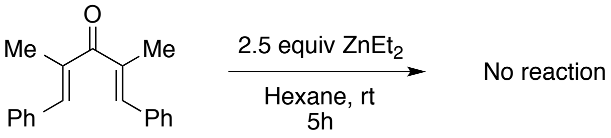

1a

Scheme 2.26 Reactivity of $ZnEt_2$ on a Nazarov Substrate.

Table 2-4 Optimization of $ZnEt_2$ Interrupted Nazarov Reaction.

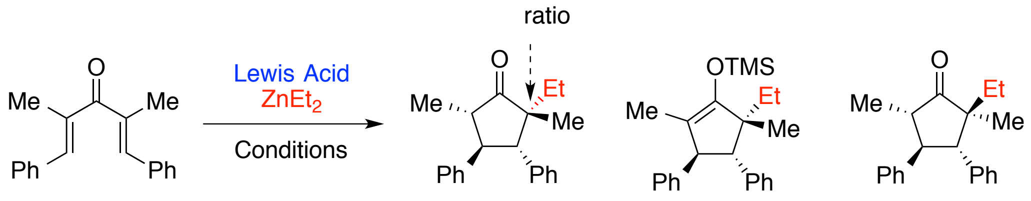

1a **7a'** **12a'** **7a**

Entry	Solvent	Lewis Acid	Et_2Zn (equiv)	Temp (ºC)	Time (min)	Product (Yield %)[a] [dr][b]
1	CH_2Cl_2	1.1 BF_3•OEt_2	2.0	–78	20	Complex mixture
2	hexane	1.1 TMSOTf	2.0	–41	30	**12a’** (95 %) [5:1]
3	hexane	1.1 Et_2AlCl	2.0	–41	60	**7a’** (75 %) [7.3:1]
4	CH_2Cl_2	1.2 Et_2AlCl	1.2	–78	40	Mostly S.M. + **7a’**
5	toluene	1.2 Et_2AlCl	1.2	–78	40	**7a’** (65 %) [20:1]
6	hexane	1.2 Et_2AlCl	1.5	–41	60	**7a’** (63 %) [10:1]
7	toluene	1.2 Et_2AlCl	1.5	–41	60	**7a’** (63 %) [12.5:1]
8	toluene	1.2 Et_2AlCl	1.5	–78	60	**7a’** (77 %) [20:1]
9	toluene	1.2 Et_2AlCl	2.0	–78	60	**7a’** (83 %) [14:1]
10	toluene	1.2 BF_3•OEt_2	2.0	–78	60	Mostly S.M.

[a] Yields are based on isolated product after chromatography. [b] Diastereomeric ratio **7a’**:**7a**

We continued our study by examining different Lewis acids (Table 2-4). BF_3•OEt_2 was not an efficient Lewis acid in this reaction (entry 1, 10). In the presence of TMSOTf and Et_2AlCl we observed ethyl group transfer from $ZnEt_2$ to the oxyallylcation (entry 2, 3). The respective major products, silyl enol ether **12a’** and cyclopentanone **7a’**, have an interesting stereochemical outcome as ethyl transfer occurs *syn* to the β-phenyl substituent, which is the opposite selectivity to that seen in the $AlEt_3$ mediated Nazarov reaction, e.g. **7a**. We hypothesize that a possible non-covalent interaction between zinc metal and π system of the β-aryl substituent is responsible for the stereochemical outcome. The relative configuration of **7a’** was determined by single crystal X-ray diffraction analysis (Figure 2.7). When treated with 2 M aq. HCl solution, **12a’** was converted to **7a'** without loss of diastereomeric ratio. Two experiments (entry 4 and 5) indicate toluene is better a solvent than dichloromethane. Though hexane and toluene worked about the same as a reaction solvent (entry 6 and 7), toluene was chosen for further optimization due to solubility of dienones. Use of 1.2 equiv Et_2AlCl and 2 equiv $ZnEt_2$ in toluene provided the highest yield and satisfying **7a'**/**7a** ratio (entry 9).

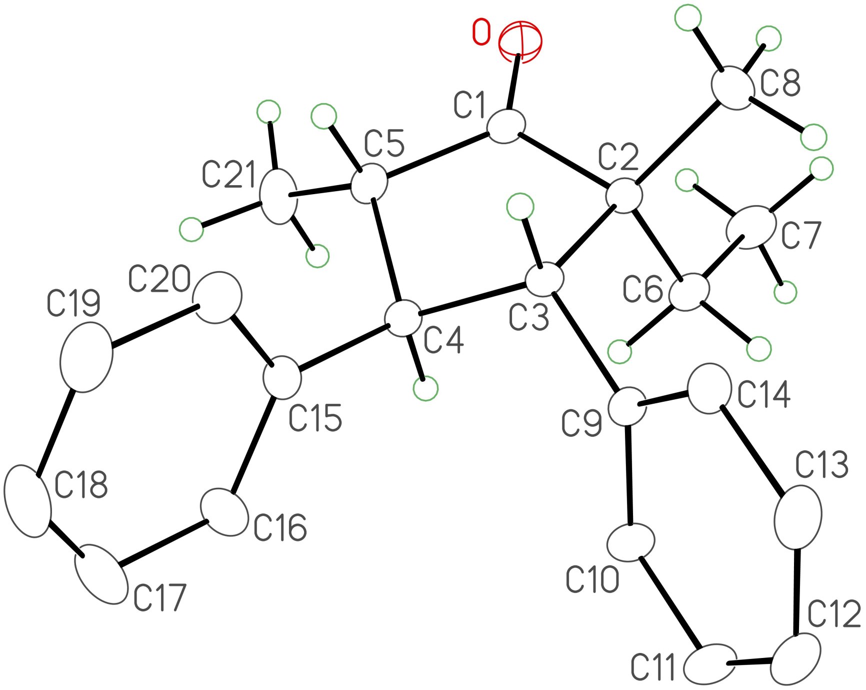

(Thermal ellipsoids shown at the 20 % probability level)

Figure 2.7 ORTEP Drawing of **7a'**.

Next, we investigated the reactivity of some of the symmetrical divinyl ketones discussed earlier (Table 2-5). Under the optimized conditions, dienones (**1a**-**1c**) were converted to ethyl substituted cyclopentanones **7a'**-**7c'** in good yield. Substrate **1d** required higher temperature (–25 ºC) and longer reaction time to be converted to **7d'**. Unfortunately, trisubstituted divinyl ketone **1g** did not cleanly undergo cyclization under the optimized conditions. As the formation of 1,4-addition product **13g** was dominant, it would be necessary to raise reaction temperature to facilitate the electrocyclization. Also, changing the order of addition could hinder the 1,4-addition pathway as well; if the Nazarov substrate is added to a solution of $ZnEt_2$ and Et_2AlCl, this may prevent $ZnEt_2$

from doing the 1,4-addition on the enone. Further studies involving the suppression of 1,4-addition and the diversification of this methodology to other organozinc reagents should be carried out in the future.

Table 2-5 $ZnEt_2$ Interrupted Nazarov Reaction.[a]

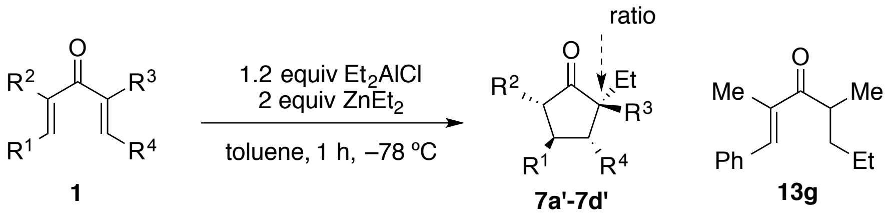

Entry	Substrate	R1	R2	R3	R4	Product	Yield (%)[c]
1	**1a**	Ph	Me	Me	Ph	**7a’:7a** (14:1)[b]	83
2	**1b**	4-ClC$_6$H$_4$	Me	Me	4-ClC$_6$H$_4$	**7b’:7b** (20:1)[b]	49
3	**1c**	4-MeOC$_6$H$_4$	Me	Me	4-MeOC$_6$H$_4$	**7c’** [d]	67
4[e]	**1d**	2-furyl	Me	Me	2-furyl	**7d’:7b** (6:1)[b]	57
5	**1g**	Ph	Me	Me	H	**13g**	44

[a] Standard procedure: see experimental section. [b] Ratio of diastereomers measured via integration of benzylic methine protons in ^{1}H NMR spectrum. [c] Yields are based on isolated product after chromatography. [d] Traces of diastereomer **7c** were found in the ^{1}H NMR spectrum. [e] The reaction was carried out at –25 ºC for 3 h.

2.2.4 Domino Oppenauer Oxidation/Electrocyclization

As shown in the introduction, Nguyen and coworkers demonstrated trimethylaluminum mediated Oppenauer oxidation (Scheme 2.27).[62] Substrate scope of the oxidation was quite broad: secondary alcohols, aliphatic primary alcohols, and allylic alcohols were converted to their corresponding ketones. However, the oxidation of divinylalcohols by an Oppenauer proctocol has not been investigated yet.

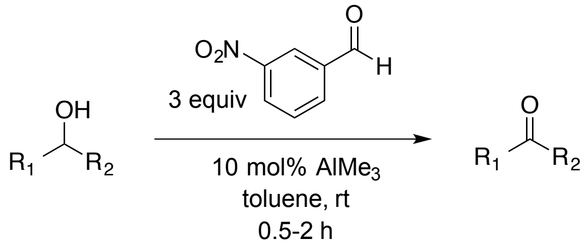

Scheme 2.27 $AlMe_3$-Catalyzed Alcohol Oxidation.

With the known use of $AlMe_3$ in the Oppenauer oxidation and our successful organoaluminum interrupted Nazarov reaction, we envisioned a domino Oppenauer oxidation and Nazarov cyclization reaction from divinylcarbinol **6** (Scheme 2.28). After the hydride of **6** is transferred to the hydride acceptor (nitrobenzaldehyde) via six-membered transition state **A**, the resulting pentadienylcation **B** could retain the lingering aluminum Lewis acid. If $AlMe_3$ is involved in the oxidation, the aluminum complex in **B** would have two methyl ligands and the reduced benzylic alkoxide. The question is whether the dialkylaluminum alkoxide could initiate the Nazarov cyclization or not. This oxidative process could be beneficial as Nazarov substrates are often prepared by the oxidation of divinylcarbinols.

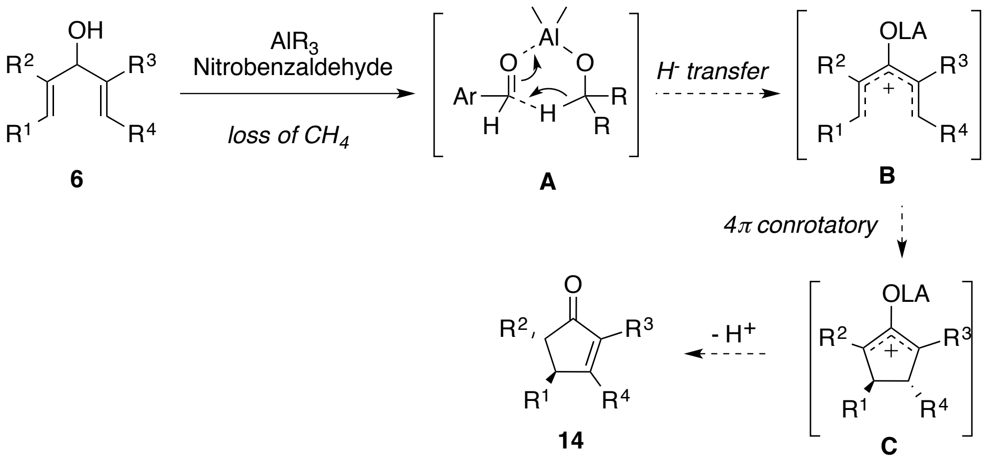

Scheme 2.28 Domino Oppenauer Oxidation/Nazarov Cyclization.

With this idea in mind, a series of aluminum Lewis acids were tested with divinyl alcohol **6a** and nitrobenzaldehyde (Table 2-6). Treatment of **6a** with catalytic amounts of Al(O*i*Pr)$_3$ and 3 equiv nitrobenzaldehyde afforded only trace amounts of Oppenauer oxidation product **1a** (entry 1). An increase of Al(O*i*Pr)$_3$ in the reaction condition gave a cyclized product, cyclopentanone **10a**, exclusively with exocyclic elimination (entry 2). Cyclopentenone **14a** was not formed in the reaction. Despite the poor yield (20 %), this example is believed to be the first case of an oxidative Nazarov reaction. Compared to the aluminum alkoxide, AlMe$_3$ proved to be more reactive, as starting material **6a** was fully consumed in 12 hours (entry 3). Lowering the amount of AlMe$_3$ and nitrobenzaldehyde provided a higher overall yield of **1a** and **10a**. Heating the reaction mixture shortened the reaction time and allowed full conversion of **1a** to **10a** (entry 9). Using 4-nitrobenzaldehyde in place of **16** did not increase yield noticeably (entry 10). When a stronger Lewis acid, ClAlMe$_2$, was used (entry 11), inseparable cyclopentadiene isomers **15a** and **15a'** were formed via cyclodehydration,[80] regardless of the presence of nitrobenzaldehyde. Isomerization of **15a** to **15a'** occurred in CDCl$_3$, presumably by the acidic medium in the NMR solvent.

Table 2-6 Screening Conditions for the Oxidative Nazarov Reaction.[a]

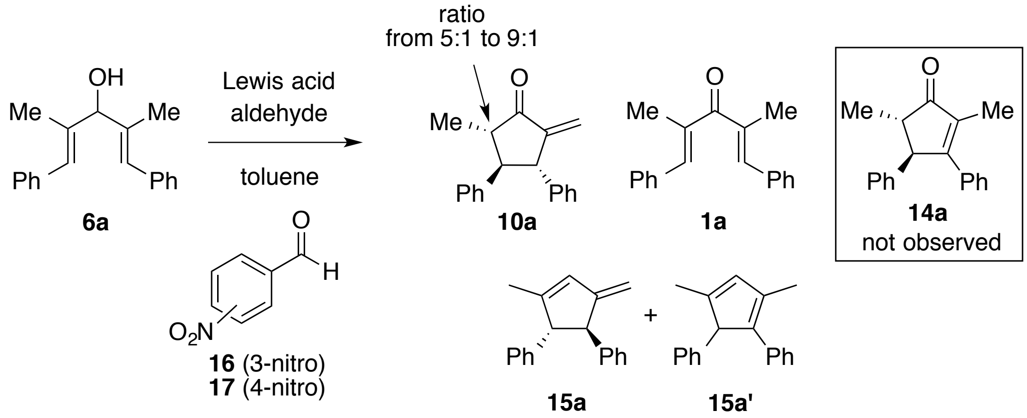
ratio
from 5:1 to 9:1
OH
Me
Me
Ph
Ph
6a
Lewis acid
aldehyde
toluene
O
H
O_2N
16 (3-nitro)
17 (4-nitro)
O
Me
Ph
Ph
10a
O
Me
Me
Ph
Ph
1a
O
Me
Me
Ph
Ph
14a
not observed
Ph
Ph
15a
+
Ph
Ph
15a'

Entry	AlR_3	Oxidant (equiv)	Additive	Temp (ºC)	Time	Product (yield %)[b]
1	0.1 Al(O*i*Pr)$_3$	**16** (3.0)	None	rt	2 d	**1a** (trace amount) + recovery of **6a**
2	1.2 Al(O*i*Pr)$_3$	**16** (3.0)	None	rt	2 d	**10a** (20)
3	1.2 AlMe$_3$	**16** (3.0)	None	rt	12 h	**10a** (12) + complex mixture
4	0.5 AlMe$_3$	**16** (3.0)	None	rt	2 d	**1a**(40)[c] + **10a**(23)[c]
5	0.5 AlMe$_3$	**16** (4.0)	None	rt	2 d	**1a**(52)[c] + **10a**(13)[c]
6	0.5 AlMe$_3$	**16** (1.0)	None	rt	2 d	**1a**(11)[c] + **10a**(48)[c]
7	0.25 AlMe$_3$	**16** (2.0)	None	rt	2 d	**1a**(62)[c] + **10a**(12)[c]
8	0.25 AlMe$_3$	**16** (1.2)	None	rt	2 d	**1a**(59)[c] + **10a**(16)[c]
9	0.25 AlMe$_3$	**16** (1.2)	4Å MS	110	1 h	**10a** (48)
10	0.25 AlMe$_3$	**17** (1.2)	4Å MS	110	1 h	**10a** (50)
11	0.25 ClAlMe$_2$	**16** (1.2)	None	rt	4 h	**15a** + **15a’** (96%, 0.9:1.0)[d]

[a] All reactions were carried out in 0.1 M toluene. [b] Yields are based on isolated product after chromatography. [c] **1a** and **10a** were isolated as a mixture, and individual yield was measured via integration of methyl protons. [d] **15a** and **15a’** were isolated as a mixture, and ratio was measured via integration of alkenyl protons.

With curiosity regarding which step – oxidation or electrocyclization – contributes to the low yield, we treated less reactive substrate **6m** with the optimized condition, resulting in the oxidation product **1m** in excellent yield (Scheme 2.29). Despite the longer reaction time (20 h) at high temperature, Nazarov cyclization products were not found. This experiment showed that the Oppenauer oxidation of Nazarov substrates could be a high-yielding reaction, and also revealed a potential limit of the substrate scope.

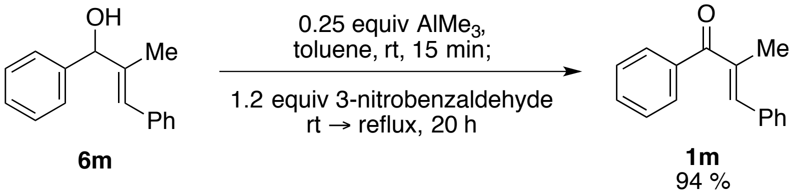

Scheme 2.29 Oxidation of **6m** with $AlMe_3$ and Nitrobenzaldehyde.

Although the planned domino reaction was conceptually novel, we decided not to carry it forward due to the low yields and the formation of cyclopentadiene with the stronger acid.

2.3 Conclusion

We have demonstrated the first example of a Nazarov reaction mediated by triorganoaluminum reagents. Though in some cases electrocyclization competes with a 1,2-addition pathway, this method generally leads to the formation of highly substituted cyclopentanones with good diastereoselectivity. Use of these organoaluminum compounds allowed incorporation of methyl, ethyl, and phenyl groups, as well as cyano and azido moieties. Triisobutylaluminum allowed reductive Nazarov cyclization via β-hydride transfer from an isobutyl ligand. Also, we saw the potential of using organozinc reagents in the interrupted Nazarov reaction. Interestingly, use of diethylzinc with an extra Lewis acid afforded the opposite stereochemical outcome to what triethylaluminum provided. Finally, domino Oppenauer oxidation/Nazarov cyclization reaction was explored, wherein divinyl alcohols served as Nazarov precursors.

2.4 Future Directions

When it comes to the organoaluminum interrupted Nazarov cyclization on the less reactive substrates, 1,2-addition is favoured over electrocyclization. To suppress the 1,2-addition, further studies involving additive effects should be carried out. While screening the $AlMe_3$ mediated Nazarov reaction (Table 2-2), $AlMe_3$ was found to be inactive in ethereal solvent. Addition of THF or diethyl ether, as a co-solvent or additive, would be helpful to slow down the reactivity of $AlMe_3$ in both 1,2-addition and Nazarov cyclization (Scheme 2.30). If there is an extra Lewis acid to initiate the electrocyclic ring closure, the “protected $AlMe_3$” might be able to intercept the oxyallyl cation intermediate, hopefully expanding the scope of substrates.

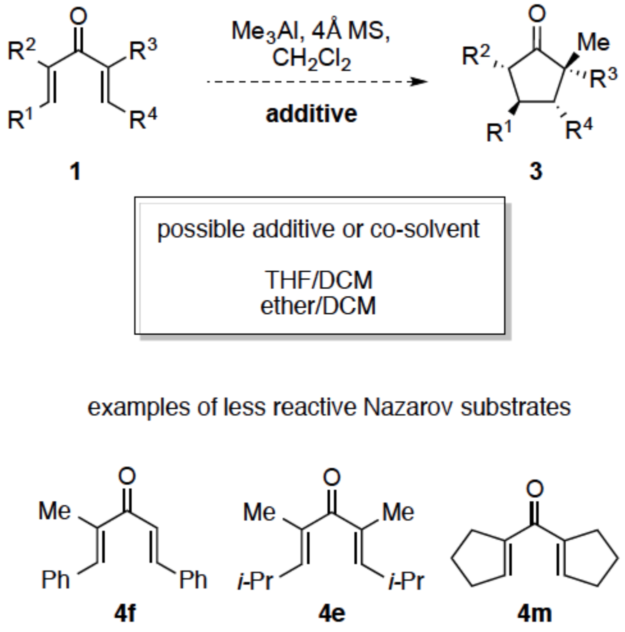
R2
R3
R1
R4
1
Me3Al, 4Å MS,
CH2Cl2
additive
R2
Me
R3
R1
R4
3
possible additive or co-solvent
THF/DCM
ether/DCM
examples of less reactive Nazarov substrates
Me
Ph
Ph
4f
Me
Me
i-Pr
i-Pr
4e
4m

Scheme 2.30 Additive Effect on the Suppression of 1,2-addition.

Regarding the organozinc interrupted Nazarov reaction, efforts will be made to expand the substrate scope of dienones and diversify this methodology to other organozinc reagents. Regioselectivity of ethyl migration on unsymmetrical divinyl ketone **1j** will be studied to support the hypothesis – non-covalent interaction between zinc and β-phenyl substituent – we made above. These experiments will be carried out with Et_2Zn and Et_3Al, individually, to compare the regioselectivity as well as stereoselectivity (Scheme 2.31).

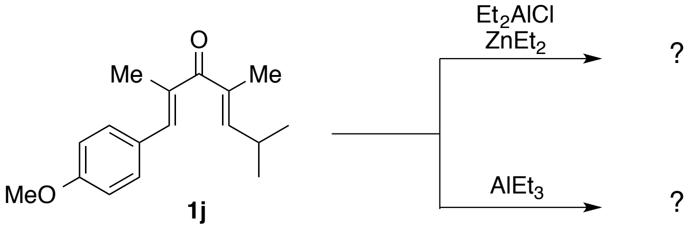

Scheme 2.31 Study of Ethyl Migration on Unsymmetrical Dienone **1j**.

2.5 Experimental

2.5.1 General Information

Reactions were carried out in flame-dried glassware under a positive argon atmosphere unless otherwise stated. Transfer of anhydrous solvents and reagents was accomplished with oven-dried syringes or cannulae. 4Å Molecular sieves were stored in an oven, and flame-dried before use. Solvents were distilled before use: methylene chloride from calcium hydride, tetrahydrofuran, and toluene from sodium/benzophenone ketyl. Thin layer chromatography was performed on glass plates precoated with 0.25 mm Kieselgel 60 F254 (Merck). Flash chromatography columns were packed with 230-400 mesh silica gel (Silicycle). Proton nuclear magnetic resonance spectra (^1H NMR) were recorded at 400 MHz or 500 MHz and coupling constants (J) are reported in Hertz (Hz). Standard notation was used to describe the multiplicity of signals observed in ^1H NMR spectra: broad (br), apparent (app), multiplet (m), singlet (s), doublet (d), triplet (t), etc. Carbon nuclear magnetic resonance spectra (^{13}C NMR) were recorded at 100 MHz or 125 MHz and are reported (ppm) relative to the center line of the triplet from chloroform-*d* (77.06 ppm). Infrared (IR) spectra were measured with a Mattson Galaxy Series FT-IR 3000 spectrophotometer. High-resolution mass spectrometry (HRMS) data (APPI/APCI/ESI technique) were recorded using an Agilent Technologies 6220 oaTOF instrument. HRMS data (EI technique) were recorded using a Kratos MS50 instrument. Dienones **1a**,[81] **1b**,[82] **1c**,[39] **1e**,[39] **1f**,[81] **1g**,[21] **1h**,[67a] and **1i**[39] were prepared via literature procedures.

2.5.2 Experimental Procedures and Characterization for the Organoaluminum Mediated Interrupted Nazarov Reaction

Preparation of Dienones 1d, 1j, 1k, and 1l

(1*E*,4*E*)-1,5-di(furan-2-yl)-2,4-dimethylpenta-1,4-dien-3-one (1d):

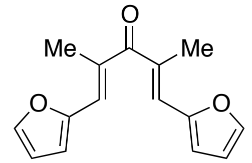

1d

A 250 mL round-bottom flask fitted with a reflux condenser and magnetic stir bar was charged with KOH (6.9 g, 122 mmol), H_2O (20 mL) and MeOH (40 mL) at room temperature. At this temperature a mixture of 3-pentanone (5.0 g, 58 mmol) and furfural (10.1 mL, 122 mmol) was added. The resulting solution was heated to reflux overnight. The reaction mixture was cooled to room temperature, and neutralized with 2M HCl solution. Organic compounds were extracted with DCM, rinsed with brine, and dried with $MgSO_4$. The crude mixture was partly purified by flash chromatography (hexanes/EtOAc 19:1) to give an oil which contained side products. Subsequent recrystalization with MeOH afforded **1d**, as a yellow solid (3.95 g, 28 %): R_f 0.46 (hexanes/EtOAc 9:1); mp 83-84 °C; IR (cast film) 3142, 3120, 2922, 1615, 1478, 1355, 1275 cm^{-1}; ^{1}H NMR (400 MHz, $CDCl_3$) δ 7.54 (dd, *J* = 1.8, 0.7 Hz, 2H), 6.95 (m, 2H), 6.61 (br. d *J* = 3.5 Hz, 2H), 6.52 (ddd, *J* = 3.5, 1.8, 0.5 Hz, 2H), 2.25 (d, *J* = 1.3 Hz, 6H); ^{13}C NMR (125 MHz, $CDCl_3$) δ 200.7, 151.9, 143.9, 133.7, 126.3, 114.2, 112.2, 15.2; HRMS (APPI) m/z calcd for $C_{15}H_{15}O_3$ ($[M+H]^+$) 243.1016, found: m/z 243.1019.

(1*E*,4*E*)-1-(4-methoxyphenyl)-2,4,6-trimethylhepta-1,4-dien-3-one (1j):

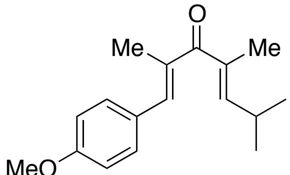

1j

Divinyl ketone **1j** was synthesized using a modification of the known procedure[39]: To a solution of a known starting material 1-penten-3-one, 1-(4-methoxyphenyl)-2-methyl[83] (1.9 g, 9.45 mmol) in DCM (30 mL) at –78 ºC, $TiCl_4$ (1.0 mL, 9.45 mmol, 1.0 equiv) was added dropwise, followed by *i*Pr_2NEt (2.0 mL, 11.3 mmol, 1.2 equiv) dropwise, turning the solution dark brown in color. After stirring at –78 ºC for 1 hour, isobutyraldehyde (1.3 mL, 14.2 mmol, 1.5 equiv) was added dropwise. The solution was stirred at -78 ºC for 2 hours, and then allowed to slowly warm to room temperature overnight. The reaction was then quenched with water (30 mL). Organic compounds were extracted with DCM, rinsed with brine, and dried with $MgSO_4$. The organic layer was filtered, concentrated by rotary evaporation and purified by flash column chromatography (silica gel, hexanes:EtOAc 5:1) to give a mixture of diastereomeric β-hydroxyketones (1.63 g), which were carried directly to the next step.

To a mixture of hydroxy ketones in DCM (29 mL) at 0 ºC was added TEA (1.22 mL, 8.76 mmol, 1.5 equiv), followed by methanesulfonyl chloride (0.59 mL, 7.60 mmol, 1.3 equiv) dropwise. The reaction mixure was stirred for 5 hours at a room temperature. DBU (4.4 mL, 29.2 mmol, 5.0 equiv) was added dropwise and the mixture was stirred overnight. The reaction was quenched with 1 M HCl (10 mL). The aqueous layer was extracted with DCM (2 × 20 mL). The organic layers were combined and washed with 1 M HCl (2 × 20 mL), water, and brine. The organic layer was then dried with $MgSO_4$, concentrated by rotary evaporation and purified by flash column chromatography (silica gel, hexanes:EtOAc 19:1 to 9:1) to yield **1j** (1.16 g, 48 %) as a colorless oil: R_f 0.29 (hexanes/EtOAc 9:1); IR (cast film) 3030, 2959, 2931, 1635, 1604, 1511, 1255 cm^{-1}; ^{1}H

NMR (500 MHz, $CDCl_3$) δ 7.39-7.36 (m, 2H), 7.05 (br s, 1H), 6.95-6.92 (m, 2H), 6.04 (dq, *J* = 9.5, 1.4 Hz, 1H), 3.84 (s, 3H), 2.72 (dsept, *J* = 9.5, 6.6 Hz, 1H), 2.13 (d, *J* = 1.4 Hz, 3H), 1.90 (d, *J* = 1.4 Hz, 3H), 1.04 (d, *J* = 6.6 Hz, 6H); ^{13}C NMR (100 MHz, $CDCl_3$) δ 202.0, 159.5, 148.8, 138.7, 135.0, 133.5, 131.2, 128.7, 113.9, 55.4, 28.2, 22.2, 14.9, 13.2; HRMS (EI, M^+) for $C_{17}H_{22}O_2$ calcd. 258.1620, found: m/z 258.1621.

(1*E*,4*E*)-1-(4-methoxyphenyl)-2,4-dimethyl-5-(4-nitrophenyl)penta-1,4-dien-3-one (1k):[*]

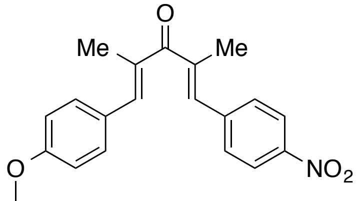

1k

The same procedure used for the synthesis of **1j** was applied to make **1k** from 1-penten-3-one, 1-(4-methoxyphenyl)-2-methyl (3.1 g, 15.3 mmol, 1.0 equiv) in DCM (100 mL) with 4-nitrobenzaldehyde (3.5 g, 23.0 mmol, 1.5 equiv).

The crude product was purified by flash column chromatography (silica gel, hexanes:EtOAc 19:1 to 8:2) to yield **1k** (3.1 g, 79 %) mixed with some impurities. The isolated product was further purified by recrystalization (ether) to provide pure **1k** (1.0 g, 21 %) as a light yellow solid: R_f 0.41 (hexanes/EtOAc 8:2); mp 73-75 °C; IR (cast film) 3076, 2958, 1635, 1600, 1512, 1343, 1254 cm^{-1}; ^1H NMR (500 MHz, $CDCl_3$) δ 8.29-8.27 (m, 2H), 7.59-7.56 (m, 2H), 7.47-7.44 (m, 2H), 7.31 (br s, 1H) 7.04 (br s, 1H), 6.99-6.96 (m, 2H), 3.87 (s, 3H), 2.24 (d, *J* = 1.3 Hz, 3H), 2.24 (d, *J* = 1.5 Hz, 3H); ^{13}C NMR (125 MHz, $CDCl_3$) δ 201.2, 160.1, 147.0, 142.7, 141.2, 140.9, 134.3, 133.6, 131.6, 130.0, 128.2, 123.7, 114.1, 55.4, 15.8, 14.3; HRMS (EI, M^+) for $C_{20}H_{19}NO_4$ calcd. 337.1314, found: m/z 337.1313.

---

[*] **1k** was synthesized by Mr. Carson Matier as a summer research assistant.

(1*E*,4*E*)-2,4-dimethyl-1-(naphthalen-1-yl)-5-phenylpenta-1,4-dien-3-one (1l):

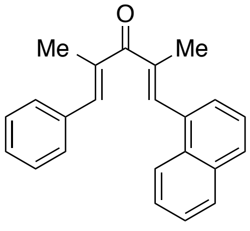

1l

Divinyl ketone **1l** was synthesized using a modification of the known procedure[39]: To a solution of a known starting material 2-methyl-1-phenyl-1-penten-3-one[83] (2.1 g, 12 mmol) in CH_2Cl_2 (60 mL) at –78 ºC was added $TiCl_4$ (1.3 mL, 12 mmol, 1.0 equiv) dropwise, followed by *i*Pr_2NEt (2.5 mL, 14.4 mmol, 1.2 equiv) dropwise. After stirring at –78 ºC for 1 hour, 1-naphthaldehyde (9.1 mL, 60 mmol, 5.0 equiv) was added dropwise. The solution was stirred at –78 ºC for 2 hours, and then allowed to slowly warm to room temperature overnight. The reaction was then quenched with water (30 mL). Organic compounds were extracted with CH_2Cl_2, rinsed with brine, and dried with $MgSO_4$. The organic layer was filtered, concentrated by rotary evaporation and purified by flash column chromatography (silica gel, hexanes:EtOAc 19:1) to give a mixture of diastereomeric β-hydroxyketones (2.2 g), which were carried directly to the next step.

To a mixture of hydroxy ketones (2.2 g, 6.7 mmol) in THF (34 mL) at 0 ºC was added Et_3N (1.4 mL, 10.0 mmol, 1.5 equiv), followed by methanesulfonyl chloride (0.57 mL, 7.3 mmol, 1.1 equiv) dropwise. The reaction mixure was stirred for 20 min at 0 ºC. DBU (5.0 mL, 33.3 mmol, 5.0 equiv) was then added and the mixture was stirred overnight at rt. The reaction was quenched with 1 M HCl (10 mL). The aqueous layer was extracted with ether (2 × 20 mL). The organic layers were combined and washed with 1 M HCl (2 × 20 mL), water, and brine. The organic layer was then dried with $MgSO_4$, concentrated by rotary evaporation and purified by flash column chromatography (silica gel, hexanes:EtOAc 19:1) to yield **1l** (2.0 g, 54 %) as a white solid: R_f 0.42 (hexanes/EtOAc 9:1); mp 79-81 °C; IR (cast film) 3057, 2956, 2920, 1637, 1446, 1247 cm^{-1}; ^1H NMR (500 MHz, $CDCl_3$) δ 7.95-7.90 (m, 2H), 7.89-7.87 (m, 1H), 7.73 (br s, 1H), 7.57-7.51 (m, 6H), 7.48-7.45 (m, 3H), 7.40-7.36 (m, 1H), 2.32 (d, J = 1.5 Hz, 3H), 2.12 (d, J = 1.5 Hz, 3H); ^{13}C NMR (125 MHz, $CDCl_3$) δ 201.8, 139.4, 139.0, 137.2, 136.8, 136.0, 133.6, 133.1, 131.5, 129.7, 128.7, 128.6, 128.6, 128.4, 126.7, 126.4, 126.1, 125.2, 124.5, 15.1, 14.9; HRMS (EI, M$^+$) for $C_{23}H_{20}O$ calcd. 312.1514, found: m/z 312.1514.

Representative Procedure of Organoaluminum Mediated Cyclization (3a)

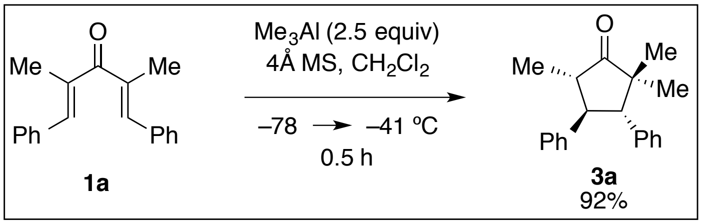

To a solution of **1a** (55 mg, 0.21 mmol) in CH_2Cl_2 (2.1 mL, 0.1 M) with activated 4Å MS (100 mg) was added 2.5 equivalents of $AlMe_3$ (0.26 mL, 2.0 M solution in toluene) at –78 ºC. The reaction mixture was then transferred into a –41 ºC bath, and stirred until complete consumption of **1a** was observed by TLC (30 min). The reaction was quenched with 2M aq. HCl (1 mL) and warmed to room temperature. After separation of the phases, the aqueous layer was extracted with CH_2Cl_2 (3 × 5 mL). The combined organic extracts were washed with brine, and dried over $MgSO_4$, filtered, and concentrated in vacuo. Purification by flash column chromatography (silica gel) provided the desired product **3a** (53 mg, 92 %).

Spectral Data of 3a-3e, 4e, 3g-3j, 4f, 6a, 7a, 8a, 8a′, 9a, 10a, 11a, 11a′

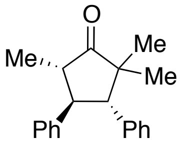

3a

Flash chromatography (20:1 hexane:EtOAc) gave **3a** (53 mg, 92 %) as a white solid.

***rac*-(3*S*,4*R*,5*S*)-2,2,5-trimethyl-3,4-diphenylcyclopentan-1-one (3a)**: R$_f$ 0.43 (hexanes/EtOAc 9:1); mp 134-136 °C; IR (cast film) 3027, 3003, 2927, 1726, 1601, 1498, 1455 cm^{-1}; ^{1}H NMR (500 MHz, CDCl$_3$) δ 7.26-7.22 (m, 6H), 7.18-7.12 (m, 4H), 3.34 (d, *J* = 12.3 Hz, 1H), 3.30 (dd, *J* = 12.3, 10.5 Hz, 1H), 2.42 (dq, *J* = 10.5, 7.0 Hz, 1H), 1.12 (s, 3H), 1.17 (d, *J* = 7.0 Hz, 3H), 0.74 (s, 3H); ^{13}C NMR (125 MHz, $CDCl_3$) δ 222.0, 140.7, 137.0, 129.1, 128.6, 128.0, 127.7, 126.8, 126.8, 58.4, 51.9, 50.7, 49.7, 24.0, 20.2, 13.5; HRMS (EI, M^+) for $C_{20}H_{22}O$ calcd. 278.1671, found: m/z 278.1670.

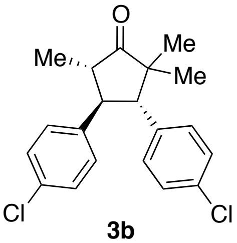

3b

Reaction performed under the standard procedure for 30 min. Flash chromatography (20:1 hexane:EtOAc) gave **3b** (61 mg, 92 %) as a white solid

***rac*-(3*S*,4*R*,5*S*)-3,4-bis(4-chlorophenyl)-2,2,5-trimethylcyclopentan-1-one (3b)**: R*f* 0.32 (hexanes/EtOAc 9:1); mp 123-125 °C; IR (cast film) 3030, 2966, 1735, 1494 cm^{-1}; ^{1}H NMR (500 MHz, $CDCl_3$) δ 7.23-7.21 (m, 4H), 7.16-7.15 (m, 2H), 7.08-7.07 (m, 2H), 3.24 (d, *J* = 12.2 Hz, 1H), 3.20 (dd, *J* = 12.2, 10.4 Hz, 1H), 2.36 (dq, *J* = 10.4, 7.0 Hz, 1H), 1.19 (s, 3H), 1.15 (d, *J* = 7.0 Hz, 3H), 0.72 (s, 3H); ^{13}C NMR (125 MHz, $CDCl_3$) δ 220.8, 138.8, 135.2, 132.8, 132.7, 130.2, 128.9, 128.9, 128.4, 58.1, 51.7, 50.3, 49.6, 23.9, 20.1, 13.4; HRMS (EI, M^+) for $C_{20}H_{20}OCl_2$ calcd. 346.0891, found: m/z 346.0887.

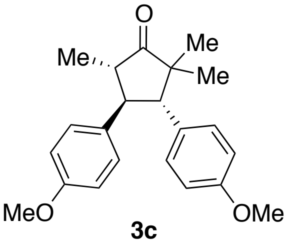

3c

Reaction performed under the standard procedure for 30 minutes. Flash chromatography (20:1 hexane:EtOAc) gave **3c** (44 mg, 82 %) as a white solid.

***rac*-(3*S*,4*R*,5*S*)-3,4-bis(4-methoxyphenyl)-2,2,5-trimethylcyclopentan-1-one (3c)**: R*f* 0.62 (hexanes/EtOAc 2:1); mp 155-157 °C; IR (cast film) 2963, 1735, 1515, 1250 cm^{-1}; ^{1}H NMR (500 MHz, $CDCl_3$) δ 7.15 (d, *J* = 8.5 Hz, 2H), 7.07 (d, *J* = 8.5 Hz, 2H), 6.78 (d, *J* = 8.5 Hz, 2H), 6. 77 (d, *J* = 8.5 Hz, 2H), 3.74 (s, 3H), 3.72 (s, 3H), 3.22 (d, *J* = 12.2 Hz, 1H), 3.18 (dd, *J* = 12.2, 10.5 Hz, 1H), 2.34 (dq, *J* = 10.5, 7.0 Hz, 1H), 1.18 (s, 3H), 1.15

(d, *J* = 7.0 Hz, 3H), 0.72 (s, 3H); ^{13}C NMR (125 MHz, CDCl$_3$) δ 222.4, 158.3, 158.3, 132.8, 130.0, 129.1, 128.6, 114.0, 113.5, 57.9, 55.1, 55.1, 51.9, 50.1, 49.7, 23.9, 20.1, 13.5; HRMS (EI, M$^+$) for $C_{22}H_{26}O_3$ calcd. 338.1882, found: m/z 338.1885.

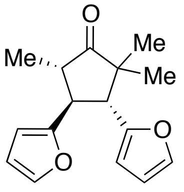

3d

Reaction performed under the standard procedure for 1 hour. Flash chromatography (39:1 to 19:1 hexane:EtOAc) gave **3d** (60 mg, 94 %) as a colorless oil.

***rac*-(3*R*,4*R*,5*S*)-3,4-di(furan-2-yl)-2,2,5-trimethylcyclopentan-1-one (3d)**: R$_f$ 0.39 (hexanes/EtOAc 9:1); mp 152-153 °C; IR (cast film) 3118, 2967, 1741, 1507 cm^{-1}; ^{1}H NMR (500 MHz, CDCl$_3$) δ 7.33 (ddd, *J* = 1.8, 0.8, 0.2 Hz, 1H), 7.29 (dd, *J* = 1.9, 0.8 Hz, 1H), 6.28 (dd, *J* = 3.2, 1.9 Hz, 1H), 6.25 (dd, *J* = 3.2, 1.9 Hz, 1H), 6.09 (app. dt, *J* = 3.2, 0.7 Hz, 1H), 6.07 (ddd, *J* = 3.2, 0.9, 0.5 Hz, 1H), 3.39 (d, *J* = 12.0 Hz, 1H), 3.34 (dd, *J* = 12.0, 10.6 Hz, 1H), 2.54 (dqd, *J* = 10.6, 7.0, 0.6 Hz, 1H), 1.25 (s, 3H), 1.22 (d, *J* = 7.0 Hz, 3H), 0.76 (s, 3H); ^{13}C NMR (125 MHz, CDCl$_3$) δ 221.0, 154.3, 152.8, 141.7, 141.6, 110.2, 110.1, 107.4, 106.4, 50.5, 49.7, 48.7. 43.6, 24.0, 20.3, 13.9; HRMS (EI, M$^+$) for $C_{16}H_{18}O_3$ calcd. 258.1256, found: m/z 258.1254.

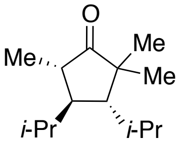

3e

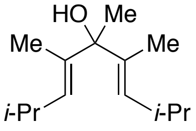

4e

Reaction performed under the standard procedure at –25 ºC for 1 hour.[84] Flash chromatography (49:1 hexane:EtOAc) gave **3e** (35 mg, 54 %) as a colorless oil, and **4e** (15 mg, 23 %) as a colorless oil.

***rac*-(3*R*,4*R*,5*S*)-3,4-diisopropyl-2,2,5-trimethylcyclopentan-1-one (3e)**: R$_f$ 0.67 (hexanes/EtOAc 9:1); IR (cast film) 2963, 2875, 1738 cm^{-1}; ^{1}H NMR (500 MHz, CDCl$_3$) δ 2.08 (dq, *J* = 9.1, 7.2 Hz, 1H), 1.97 (dsept, *J* = 4.5, 6.9 Hz, 1H), 1.90 (dsept, *J* = 2.3, 7.0 Hz, 1H), 1.62 (ddd, *J* = 9.2, 9.2, 4.5 Hz, 1H), 1.54 (dd, *J* = 9.2, 2.3 Hz, 1H), 1.17 (d, *J* =

7.1 Hz, 3H), 1.06 (s, 3H), 1.03 (d, *J* = 7.0 Hz, 3H), 1.01 (d, *J* = 7.2 Hz, 3H), 0.91 (s, 3H), 0.89 (d, *J* = 6.8 Hz, 3H), 0.89 (d, *J* = 7.0 Hz, 3H); ^{13}C NMR (125 MHz, CDCl$_3$) δ 225.2, 52.2, 49.4, 48.1, 43.5, 30.0, 26.8, 25.9, 23.8, 23.0, 19.9, 18.8, 17.3, 17.1; HRMS (EI, M$^+$) for $C_{14}H_{26}O$ calcd. 210.1984, found: m/z 210.1981.

(3*E*,6*E*)-2,4,5,6,8-pentamethylnona-3,6-dien-5-ol (4e): R$_f$ 0.54 (hexanes/EtOAc 9:1); IR (cast film) 3460, 2957, 2928, 2869, 1465, 1105 cm^{-1}; ^{1}H NMR (500 MHz, CDCl$_3$) δ 5.34 (dq, *J* = 9.1, 1.3 Hz, 2H), 2.50 (dsept, *J* = 9.1, 6.7 Hz, 2H), 1. 48 (d, *J* = 1.3 Hz, 6H), 1.46 (br, 1H), 1.37 (s, 3H), 0.95 (d, *J* = 6.7 Hz, 6H), 0.94 (d, *J* = 6.7 Hz, 6H); ^{13}C NMR (100 MHz, CDCl$_3$) δ 136.1, 132.0, 78.3, 27.3, 26.0, 23.0, 23.0, 12.3; HRMS (ESI, [M+Na]$^+$) for $C_{14}H_{26}NaO$ calcd. 233.1876, found: m/z 233.1879.

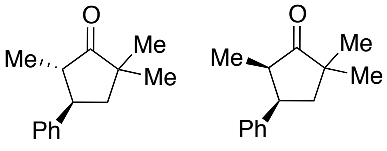

3g-*trans* **3g-*cis***

Reaction performed under the standard procedure. Flash chromatography (49:1 hexane:EtOAc) provided a mixture of **3g-*trans*** and **3g-*cis*** (60 mg, 79 %, 11 : 1). Subsequent flash chromatography (3:7 DCM:hexane) enabled the isolation of each diastereomer.

***rac*-(4*R*,5*S*)-2,2,5-trimethyl-4-phenylcyclopentan-1-one (3g-*trans*)**: colorless oil; R$_f$ 0.53 (hexanes/EtOAc 9:1); IR (film) 3029, 2962, 1738, 1455 cm^{-1}; ^{1}H NMR (500 MHz, CDCl$_3$) δ 7.36-7.32 (m, 2H), 7.27-7.23 (m, 3H), 2.87 (ddd, *J* = 12.2, 12.2, 6.2 Hz, 1H), 2.31 (dq, *J* = 12.1, 7.0 Hz, 1H), 2.12 (dd, *J* = 12.8, 6.2 Hz, 1H), 1.85 (app. t, *J* = 12.7 Hz, 1H), 1.18 (s, 3H), 1.09 (s, 3H), 1.06 (d, *J* = 7.0 Hz, 3H); ^{13}C NMR (125 MHz, CDCl$_3$) δ 223.3, 142.5, 128.7, 127.2, 126.8, 50.9, 47.3, 45.7, 45.5, 25.3, 24.6, 13.2; HRMS (EI, M$^+$) for $C_{14}H_{18}O$ calcd. 202.1358, found: m/z 202.1352.

***rac*-(4*R*,5*R*)-2,2,5-trimethyl-4-phenylcyclopentan-1-one (3g-*cis*)**: colorless oil; R$_f$ 0.53 (hexanes/EtOAc 9:1); IR (cast film) 3029, 2964, 1737, 1463 cm^{-1}; ^{1}H NMR (500 MHz, CDCl$_3$) δ 7.35-7.31 (m, 2H), 7.26-7.22 (m, 1H), 7.20-7.18 (m, 2H), 3.66 (m, 1H), 2.72 (dqdd, *J* = 7.8, 7.8, 1.3, 0.5 Hz, 1H), 2.22 (app. t, *J* = 12.6 Hz, 1H), 2.09 (ddd, *J* = 12.6, 6.2, 1.4 Hz, 1H), 1.22 (s, 3H), 1.17 (s, 3H), 0.73 (d, *J* = 7.8 Hz, 3H); ^{13}C NMR (125

MHz, $CDCl_3$) δ 224.9, 140.1, 128.3, 128.1, 126.4, 46.6, 45.5, 41.4, 39.9, 25.6, 25.1, 11.8; HRMS (EI, M^+) for $C_{14}H_{18}O$ calcd. 202.1358, found: m/z 202.1352.

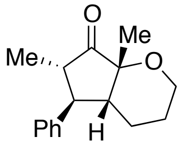

3h

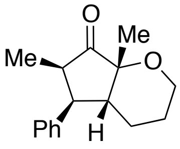

3h'

Reaction performed under the standard procedure for 1.5 hour. Flash chromatography (19:1 hexane:EtOAc) gave **3h** (45 mg, 55 %) as a white solid, and **3h′** (20 mg, 24 %) as a colorless oil.

***rac*-(4a*R*,5*R*,6*S*,7a*R*)-6,7a-dimethyl-5-phenylhexahydrocyclopenta[*b*]pyran-7(2*H*)-one (3h)**: R_f 0.42 (hexanes/EtOAc 8:2); mp 125-127 °C; IR (cast film) 2966, 2932, 2860, 1752, 1052 cm^{-1}; ^{1}H NMR (500 MHz, $CDCl_3$) δ 7.38-7.34 (m, 2H), 7.29-7.25 (m, 1H), 7.23-7.22 (m, 2H), 3.79 (ddddd, *J* = 11.6, 4.9, 1.8, 1.8, 0.8 Hz, 1H), 3.66 (ddd, *J* = 12.5, 11.7, 2.5 Hz, 1H), 3.16 (app. t, *J* = 11.6 Hz, 1H), 2.36 (dq, *J* = 11.6, 6.9 Hz, 1H), 1.96 (ddd, *J* = 11.8, 5.1, 2.1 Hz, 1H), 1.88 (ddddd, *J* = 13.3, 13.3, 13.3, 4.6, 4.6 Hz, 1H), 1.71 (dd app. t, *J* = 13.7, 13.7, 5.0 Hz, 1H), 1.57 (ddddd, *J* = 14.0, 4.4, 2.2, 2.2, 2.2 Hz, 1H), 1.40 (s, 3H), 1.38-1.33 (m, 1H), 1.12 (d, *J* = 6.9 Hz, 3H); ^{13}C NMR (125 MHz, $CDCl_3$) δ 214.8, 140.9, 128.8, 127.7, 127.1, 77.5, 61.8, 50.7, 49.1, 46.3, 20.6, 18.5, 16.4, 12.9; HRMS (EI, M^+) for $C_{16}H_{20}O_2$ calcd. 244.1463, found: m/z 244.1462.

***rac*-(4a*R*,5*R*,6*R*,7a*R*)-6,7a-dimethyl-5-phenylhexahydrocyclopenta[*b*]pyran-7(2*H*)-one (3h′)**: R_f 0.44 (hexanes/EtOAc 8:2); IR (cast film) 2967, 2935, 2861, 1750, 1052 cm^{-1}; ^{1}H NMR (500 MHz, $CDCl_3$) δ 7.36-7.32 (m, 2H), 7.27-7.23 (m, 1H), 7.18-7.15 (m, 2H), 3.96 (dd, *J* = 12.5, 8.6 Hz, 1H), 3.83-3.79 (m, 1H), 3.71-3.65 (m, 1H), 2.85 (dq, *J* = 8.0, 8.0 Hz, 1H), 2.35-2.32 (m, 1H), 1.88-1.80 (m, 2H), 1.74-1.66 (m, 1H), 1.41 (s, 3H), 1.38-1.31 (m, 1H), 0.72 (d, *J* = 7.9 Hz, 3H); ^{13}C NMR (125 MHz, $CDCl_3$) δ 216.5, 138.5, 128.9, 128.6, 126.8, 77.7, 61.7, 45.6, 43.7, 40.7, 20.2, 18.9, 16.5, 13.0; HRMS (APCI) m/z calcd for $C_{16}H_{21}O_2$ ($[M+H]^+$) 245.1536, found: m/z 245.1530.

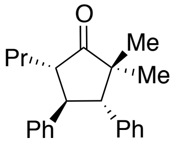

3i

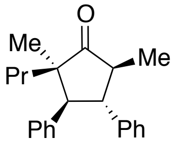

3i'

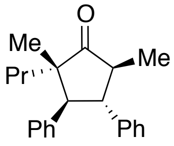

3i''

Reaction performed under the standard procedure for 1 hour. Flash chromatography (49:1 to 19:1 hexane:EtOAc) gave an inseparable mixture of **3i**, **3i′** and **3i′′** (49 mg, 84% 7.1: 1.1: 1.0). Further flash chromatography (20:80 to 30:70 DCM:hexane) allowed isolation of **3i′** for characterization.

***rac*-(3*S*,4*R*,5*S*)-2,2-dimethyl-3,4-diphenyl-5-propylcyclopentan-1-one (3i)**: R$_f$ 0.56 (hexanes/EtOAc 9:1); IR (cast film) 3029, 2961, 2930, 1735, 1465, 1453 cm^{-1}; ^{1}H NMR (500 MHz, $CDCl_3$) δ 7.25-7.19 (m, 6H), 7.17-7.10 (m, 4H), 3.46 (app. t, *J* = 11.8 Hz, 1H), 3.23 (d, *J* = 12.2 Hz, 1H), 2.49 (dt, *J* = 11.4, 5.7 Hz, 1H), 1.69-1.56 (m, 2H), 1.44-1.33 (ddqd, *J* = 18.9, 10.5, 7.3, 5.8 Hz, 1H), 1.24-1.15 (m, 1H), 1.17 (s, 3H), 0.82 (app. t, *J* = 7.3 Hz, 3H), 0.73 (s, 3H); ^{13}C NMR (125 MHz, $CDCl_3$) δ 222.0, 141.4, 137.0, 129.2, 128.5, 128.0, 127.8, 126.7, 126.7, 59.4, 56.3, 49.8, 48.3, 31.3, 23.7, 20.2, 19.7, 14.2; HRMS (EI, M$^+$) for $C_{22}H_{26}O$ calcd. 306.1984, found: m/z 306.1983.

***rac*-(2*R*,3*S*,4*R*,5*S*)-2,5-dimethyl-3,4-diphenyl-2-propylcyclopentan-1-one (3i′)**: colorless oil; R$_f$ 0.56 (hexanes/EtOAc 9:1); IR (cast film) 3029, 2961, 2929, 2872, 1734, 1453 cm^{-1}; ^{1}H NMR (500 MHz, $CDCl_3$) δ 7.25-7.11 (m, 10H), 3.42 (dd, *J* = 12.4, 10.5 Hz, 1H), 3.36 (d, *J* = 12.4 Hz, 1H), 2.33 (dq, *J* = 10.5, 7.0 Hz, 1H), 1.35-1.34 (m, 1H), 1.26-1.15 (m, 1H), 1.22 (s, 3H), 1.18 (d, *J* = 7.0 Hz, 3H), 1.02-0.89 (m, 2H), 0.73 (app. t, *J* = 7.2 Hz, 3H); ^{13}C NMR (125 MHz, $CDCl_3$) δ 221.3, 141.2, 136.9, 129.3, 128.6, 128.1, 127.7, 126.8 (2), 59.3, 53.0, 52.1, 50.3, 35.0, 21.5, 16.9, 14.7, 14.0; HRMS (EI, M$^+$) for $C_{22}H_{26}O$ calcd. 306.1984, found: m/z 306.1990.

***rac*-(2*S*,3*S*,4*R*,5*S*)-2,5-dimethyl-3,4-diphenyl-2-propylcyclopentan-1-one (3i′′)**, reported partially: ^{1}H NMR (500 MHz, $CDCl_3$) δ 3.63 (d, *J* = 12.2 Hz, 1H), 3.25 (app. t, *J* = 12.0 Hz, 1H), 2.31 (dq, *J* = 11.8, 6.9 Hz, 1H), 1.13 (d, *J* = 6.9 Hz, 3H), 0.98 (app. t, *J* = 7.0 Hz, 3H), 0.72 (s, 3H); ^{13}C NMR (125 MHz, $CDCl_3$) δ 221.9, 140.9, 137.5, 129.2, 128.6, 128.1, 127.7, 126.8, 126.6, 53.4, 53.4, 53.2, 50.5, 39.1, 20.6, 18.1, 14.7, 13.1

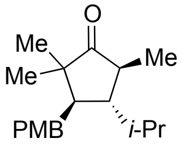

3j

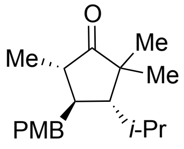

3j'

Reaction performed under the standard procedure for 1 hour. Flash chromatography (49:1 hexane:EtOAc) gave an inseparable mixture of **3j** and **3j′** (56 mg, 93% 2.0: 1.0). Further flash chromatography (1:4:35 Et_2O:DCM:hexane) allowed to isolate **3j** and **3j′** partially out.

***rac*-(3*S*,4*R*,5*S*)-4-isopropyl-3-(4-methoxyphenyl)-2,2,5-trimethylcyclopentan-1-one (3j)**: colorless oil; R_f 0.60 (hexane/EtOAc 8:2); IR (cast film) 2962, 2932, 1736, 1514, 1249 cm^{-1}; ^{1}H NMR (500 MHz, $CDCl_3$) δ 7.10-7.07 (m, 2H), 6.90-6.86 (m, 2H), 3.81 (s, 3H), 2.70 (d, *J* = 11.7 Hz, 1H), 2.18-2.07 (m, 2H), 1.80 (dsept, *J* = 2.7, 7.0 Hz, 1H), 1.27 (d, *J* = 6.7 Hz, 3H), 1.00 (s, 3H), 0.94 (d, *J* = 7.1 Hz, 3H), 0.77 (d, *J* = 7.0 Hz, 3H), 0.65 (s, 3H); ^{13}C NMR (100 MHz, $CDCl_3$) δ 223.9, 158.4, 130.4, 130.2, 113.5, 55.3, 54.8, 49.8, 49.4, 44.7, 27.8, 23.5, 22.0, 20.5, 18.1, 17.0; HRMS (EI, M^+) for $C_{18}H_{26}O_2$ calcd. 274.1933, found: m/z 274.1930.

***rac*-(3*R*,4*R*,5*S*)-3-isopropyl-4-(4-methoxyphenyl)-2,2,5-trimethylcyclopentan-1-one (3j′)**: colorless oil; R_f 0.60 (hexane/EtOAc 8:2); IR (cast film) 2963, 2932, 1736, 1514, 1251 cm^{-1}; ^{1}H NMR (500 MHz, $CDCl_3$) δ 7.21-7.18 (m, 2H), 6.91-6.88 (m, 2H), 3.83 (s, 3H), 2.67 (app. t, *J* = 11.7 Hz, 1H), 2.16 (dq, *J* = 11.5, 7.0 Hz, 1H), 2.01 (dd, *J* = 11.9, 3.8 Hz, 1H), 1.84 (dsept, *J* = 3.9, 7.0 Hz, 1H), 1.21 (s, 3H), 1.01 (d, *J* = 6.4 Hz, 3H), 1.00 (s, 3H), 0.86 (d, *J* = 6.9 Hz, 3H), 0.79 (d, *J* = 7.0 Hz, 3H); ^{13}C NMR (100 MHz, $CDCl_3$) δ 223.4, 158.2, 135.3, 128.8, 113.9, 57.0, 55.3, 52.9, 50.3, 49.6, 27.5, 25.5, 24.3, 20.9, 19.9, 13.2; HRMS (EI, M^+) for $C_{18}H_{26}O_2$ calcd. 274.1933, found: m/z 274.1933.

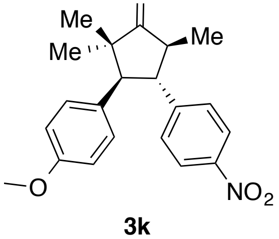

3k

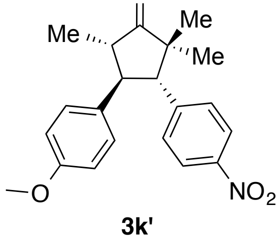

3k'

Reaction performed under the standard procedure for 90 min. Flash chromatography (9:1 to 17:3 hexane:EtOAc) gave **3k** and **3k′** (69 mg, 97 %, 2.0:1.0) an inseparable mixture: IR (cast film) 2966, 2931, 1737, 1516, 1348 cm^{-1}; HRMS (EI, M^{+}) for $C_{21}H_{23}O_4N$ calcd. 353.1627, found: m/z 353.1626.

3k; R_f 0.34 (hexane/EtOAc 8:2); ^{1}H NMR (500 MHz, $CDCl_3$) δ 8.13-8.11 (m, 2H), 7.44-7.41 (m, 2H), 7.09-7.06 (m, 2H), 6.81-6.79 (m, 2H), 3.75 (s, 3H), 3.39 (dd, *J* = 12.2, 11.4 Hz, 1H), 3.28 (d, *J* = 12.4 Hz, 1H), 2.44 (dq, *J* = 11.1, 7.0 Hz, 1H), 1.21 (s, 3H), 1.19 (d, *J* = 7.0 Hz, 3H), 0.78 (s, 3H); ^{13}C NMR (125 MHz, $CDCl_3$) δ 220.6, 158.7, 148.9, 146.9, 129.8, 128.5, 127.9, 123.9, 113.7, 58.0, 55.1, 51.7, 51.1, 49.7, 23.8, 20.1, 13.5.

3k'; R_f 0.34 (hexane/EtOAc 8:2); ^{1}H NMR (500 MHz, $CDCl_3$) δ 8.14-8.12 (m, 2H), 7.37-7.34 (m, 2H), 7.17-7.14 (m, 2H), 6.81-6.78 (m, 2H), 3.74 (s, 3H), 3.42 (d, *J* = 12.3 Hz, 1H), 3.26 (app. t, *J* = 11.9 Hz, 1H), 2.42 (dq, *J* = 11.6, 6.9 Hz, 1H), 1.25 (s, 3H), 1.19 (d, *J* = 7.0 Hz, 3H), 0.75 (s, 3H); ^{13}C NMR (125 MHz, $CDCl_3$) δ 220.5, 158.7, 147.0, 145.4, 131.5, 129.9, 128.4, 123.3, 114.3, 58.8, 55.2, 51.8, 50.0, 49.9, 24.0, 20.1, 13.3.

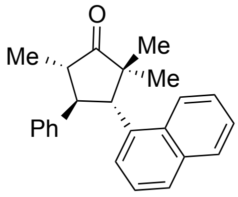

3l

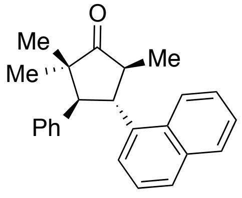

3l'

Reaction performed under the standard procedure for 1 hour. Flash chromatography (39:1 to 19:1 hexane:EtOAc) gave an inseparable mixture of **3l** and **3l′** (55 mg, 84 % 1.8: 1.0). Further flash chromatography (aluminum oxide ~150 mesh, 39:1 to 19:1 hexane:EtOAc) allowed partial isolation of **3l** for characterization.

3l (partial data); R_f 0.32 (hexane/EtOAc 9:1); IR (cast film) 3049, 2964, 2928, 2870, 1735, 1454 cm^{-1}; ^{1}H NMR (500 MHz, $CDCl_3$) δ 8.27 (d, *J* = 8.7 Hz, 1H), 7.83 (d, *J* = 8.1 Hz, 1H), 4.47 (d, *J* = 12.1 Hz, 1H), 3.52 (app. t, *J* = 11.8 Hz, 1H), 2.62 (dq, *J* = 11.6, 6.9 Hz, 1H), 1.30 (s, 3H), 1.28 (d, *J* = 7.0 Hz, 3H), 0.85 (s, 3H); ^{13}C NMR (125 MHz, $CDCl_3$) δ 221.9, 140.6, 134.1, 133.4, 133.3, 128.9, 128.5, 127.5, 127.3, 126.8, 126.0, 125.8, 125.3, 124.8, 123.6, 52.2, 51.8, 51.3, 50.5, 25.1, 20.8, 13.5; HRMS (EI, M^{+}) for $C_{24}H_{24}O$ calcd. 328.1827, found: m/z 328.1825.

3l’ (partial data): ^{1}H NMR (500 MHz, CDCl$_3$) δ 8.39 (d, *J* = 8.7 Hz, 1H), 7.86 (d, *J* = 8.1 Hz, 1H), 4.40 (app. t, *J* = 12.0 Hz, 1H), 3.72 (d, *J* = 12.2 Hz, 1H), 2.54 (br s, 1H), 1.35 (s, 3H), 1.19 (d, *J* = 7.0 Hz, 3H), 0.90 (s, 3H); ^{13}C NMR (125 MHz, CDCl$_3$) δ 221.9, 137.1, 133.9, 129.1, 128.8, 128.2, 128.0, 127.1, 126.7, 126.0, 125.7, 125.4, 122.6, 58.3, 50.0, 24.2, 20.2, 14.0 [Two quaternary carbon peaks and two tertiary carbon peaks were not reported due to presumed spectral overlap and broad signaling. However, correct numbers of carbon resonances, as a mixture of **3l** and **3l’**, were confirmed when ^{13}C NMR was obtained at 80 ºC in C$_6$D$_6$]

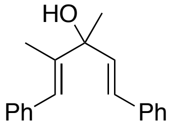

4f

Reaction performed under the standard procedure for 2 hours. Flash chromatography (19:1 to 9:1 hexane:EtOAc) gave **4f** (51 mg, 74 %) as a colorless oil

(1*E*,4*E*)-2,3-dimethyl-1,5-diphenylpenta-1,4-dien-3-ol (4f): R$_f$ 0.21 (hexanes/EtOAc 9:1); IR (cast film) 3374, 3024, 2979, 1494, 1447, 971 cm^{-1}; ^{1}H NMR (500 MHz, CDCl$_3$) δ 7.44-7.42 (m, 2H), 7.37-7.32 (m, 4H), 7.31-7.22 (m, 4H), 6.77(s, 1H), 6.68 (d, *J* = 16.1 Hz, 1H), 6.39 (d, *J* = 16.1 Hz, 1H) 1.93 (s, 3H), 1.81 (s, 3H), 1.64 (s, 3H) [OH proton was not observed]; ^{13}C NMR (125 MHz, CDCl$_3$) δ 142.3, 138.1, 136.9, 135.2, 129.1, 128.6, 128.3, 128.1, 127.6, 126.6, 126.4, 124.4, 76.3, 27.2, 14.6; HRMS (EI, M$^+$) for C$_{19}$H$_{20}$O calcd. 264.1514, found: m/z 264.1514.

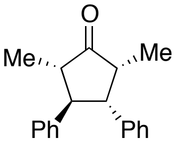

5a

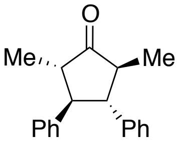

5a'

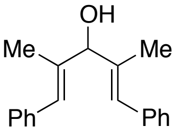

6a

Reaction performed under the standard procedure with neat Al(*i*-Bu)$_3$ for 5 hours. Flash chromatography (40:1 to 20:1 hexane:EtOAc) gave **5a** (22 mg, 36 %), **5a′** (13 mg, 21 %) and **6a** (white solid, 12 mg, 20 %).

5a and **5a′**: Spectral data are consistent with the reported values.[30]

(1*E*,4*E*)-2,4-dimethyl-1,5-diphenylpenta-1,4-dien-3-ol (6a): R_f 0.24 (hexanes/EtOAc 9:1); mp 69-71 °C; IR (cast film) 3368, 3023, 1491 cm^{-1}; ^{1}H NMR (500 MHz, $CDCl_3$) δ 7.37-7.31 (m, 8H), 7.25-7.22 (m, 2H), 6.72 (s, 2H), 4.72 (s, 1H), 1.87 (d, *J* = 3.1 Hz, 1H), 1.85 (d, *J* = 1.3 Hz, 6H); ^{13}C NMR (125 MHz, $CDCl_3$) δ 138.0, 137.7, 129.0, 128.2, 126.6, 126.6, 82.4, 14.1; HRMS (EI, M$^+$) for $C_{19}H_{20}O$ calcd. 264.1514, found: m/z 264.1514.

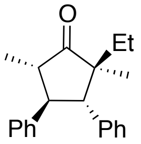

7a

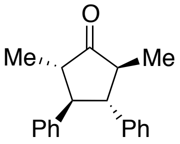

5a'

Reaction performed under the standard procedure with $AlEt_3$ (25 wt. % in toluene) for an hour. Flash chromatography (30:1 to 20:1 hexane:EtOAc) gave **7a** (white solid, 36 mg, 65 %) and **5a′** (9 mg, 19 %):

***rac*-(2*S*,3*S*,4*R*,5*S*)-2-ethyl-2,5-dimethyl-3,4-diphenylcyclopentan-1-one (7a)**: R_f 0.49 (hexanes/EtOAc 9:1); mp 101-103 °C; IR (cast film) 3030, 2965, 1727, 1452 cm^{-1}; ^{1}H NMR (500 MHz, $CDCl_3$) δ 7.30-7.23 (m, 6H), 7.20-7.16 (m, 4H), 3.67 (d, *J* = 12.2 Hz, 1H), 3.30 (app. t, *J* = 12.0 Hz, 1H), 2.33 (dq, *J* = 11.8, 6.9 Hz, 1H), 1.81 (dq, *J* = 15.0, 7.5 Hz, 1H), 1.47 (dq, *J* = 15.0, 7.5 Hz, 1H), 1.17 (d, *J* = 6.9 Hz, 3H), 1.07 (app. t, *J* = 7.5, 3H), 0.76 (s, 3H); ^{13}C NMR (125 MHz, $CDCl_3$) δ 221.8, 140.9, 137.4, 129.2, 128.6, 128.1, 127.7, 126.8, 126.6, 53.7, 53.4, 52.7, 50.5, 29.1, 20.4, 13.1, 9.2; HRMS (EI, M$^+$) for $C_{21}H_{24}O$ calcd. 292.1827, found: m/z 292.1829.

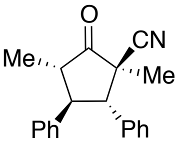

8a

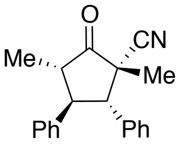

8a'

Reaction performed under the standard procedure with Et_2AlCN (1.0 M in toluene) for 90 minutes. Flash chromatography (40:1 to 20:1 hexane:EtOAc) gave a mixture of **8a** and **8a′** (54 mg, 89 %, 1.3 : 1). Subsequent flash chromatography (2:20:95 Et_2O:DCM:hexane) enabled the isolation of each diastereomer.

***rac*-(1*R*,3*S*,4*R*,5*S*)-1,3-dimethyl-2-oxo-4,5-diphenylcyclopentane-1-carbonitrile (8a)**, white solid: R$_f$ 0.29 (Et_2O:DCM:hexane 1:4:19); mp 105-107 °C; IR (cast film) 3031, 2984, 2238, 1752, 1453 cm^{-1}; ^{1}H NMR (500 MHz, $CDCl_3$) δ 7.32-7.18 (m, 10H), 4.09 (d, *J* = 12.4 Hz, 1H), 3.26 (app. t, *J* = 12.1 Hz, 1H), 2.65 (dq, *J* = 11.8, 6.9 Hz, 1H), 1.18 (d, *J* = 6.9 Hz, 3H), 1.12 (s, 3H); ^{13}C NMR (125 MHz, $CDCl_3$) δ 208.9, 138.4, 133.8, 129.1, 128.8 (2), 128.0, 127.7, 127.6, 120.3, 54.7, 52.3, 49.3, 48.6, 17.6, 13.2; HRMS (EI, M$^+$) for $C_{20}H_{19}ON$ calcd. 289.1467, found: m/z 289.1463.

***rac*-(1*S*,3*S*,4*R*,5*S*)-1,3-dimethyl-2-oxo-4,5-diphenylcyclopentane-1-carbonitrile (8a′)**, white solid: R$_f$ 0.35 (Et_2O:DCM:hexane 1:4:19); mp 142-143 °C; IR (cast film) 3031, 2982, 2934, 2232, 1757, 1454 cm^{-1}; ^{1}H NMR (500 MHz, $CDCl_3$) δ 7.33-7.28 (m, 4H), 7.26-7.22 (m, 3H), 7.22-7.14 (m, 3H), 3.53 (dd, *J* = 12.4, 11.4 Hz, 1H), 3.24 (d, *J* = 12.4 Hz, 1H), 2.55 (dq, *J* = 11.4, 7.1 Hz, 1H), 1.54 (s, 3H), 1.30 (d, *J* = 7.1 Hz, 3H); ^{13}C NMR (125 MHz, $CDCl_3$) δ 208.7, 138.2, 134.3, 128.9, 128.8, 128.7, 128.3, 127.5, 127.5, 117.2, 58.1, 51.9, 51.8, 51.7, 19.6, 14.2; HRMS (EI, M$^+$) for $C_{20}H_{19}ON$ calcd. 289.1467, found: m/z 289.1470.

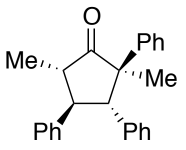

9a

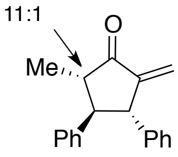

10a

Reaction performed under the standard procedure, but $AlPh_3$ (1.0 M in dibutyl ether) was added at –30 ºC and stirred for 2.5 hours.[84] Flash chromatography (49:1 to 29:1 hexane:EtOAc) gave **9a** (23 mg, 36 %) as a colorless oil, and **10a** (9 mg, 18 % 11:1).

***rac*-(2*R*,3*S*,4*R*,5*S*)-2,5-dimethyl-2,3,4-triphenylcyclopentan-1-one (9a)**: R$_f$ 0.42 (hexanes/EtOAc 9:1); IR (cast film) 3060, 3028, 2967, 1741, 1498, 1452 cm^{-1}; ^{1}H NMR (400 MHz, $CDCl_3$) δ 7.37-7.24 (m, 7H), 7.18-7.09 (m, 6H), 6.83-6.80 (m, 2H), 3.89 (d, *J* = 12.0 Hz, 1H), 3.42 (app. t, *J* = 12.0 Hz, 1H), 2.69 (dq, *J* = 12.0, 6.8 Hz, 1H), 1.26 (d, *J* = 6.8 Hz, 3H), 1.14 (s, 3H); ^{13}C NMR (100 MHz, $CDCl_3$) δ 220.2, 144.2, 140.5, 136.2, 129.1, 128.7, 128.5, 127.8, 127.7, 127.2, 127.0, 126.9, 126.8, 60.6, 58.0, 54.3, 50.4, 17.3, 13.4; HRMS (EI, M$^+$) for $C_{25}H_{24}O$ calcd. 340.1827, found: m/z 340.1834.

***rac*-(2*S*,3*R*,4*S*)-2-methyl-5-methylene-3,4-diphenylcyclopentan-1-one (10a)**: (Reported spectral data are of major epimer): R_f 0.45 (hexanes/EtOAc 9:1); IR (cast film) 3028, 2927, 1726, 1453 cm^{-1}; ^{1}H NMR (500 MHz, $CDCl_3$) δ 7.27-7.17 (m, 6H), 7.11-7.08 (m, 2H), 7.06-7.03 (m, 2H), 6.26 (dd, *J* = 3.4, 0.9 Hz, 1H), 5.05 (dd, *J* = 3.0, 0.9 Hz, 1H), 3.92 (d app. t, *J* = 11.4, 3.2 Hz, 1H), 2.86 (app. t, *J* = 12.0 Hz, 1H), 2.65 (dq, *J* = 12.2, 6.7 Hz, 1H), 1.15 (d, *J* = 6.7 Hz, 3H); ^{13}C NMR (125 MHz, $CDCl_3$) δ 206.0, 148.9, 140.4, 139.8, 128.7, 128.6, 128.5, 127.6, 127.1, 127.0, 119.8, 57.5, 54.9, 50.6, 12.2; HRMS (EI, M$^+$) for $C_{19}H_{18}O$ calcd. 262.1358, found: m/z 262.1358.

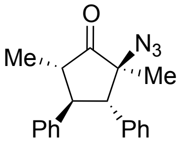

11a

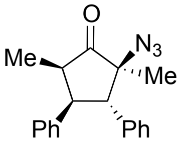

11a'

Me_2AlN_3 was generated *in situ*[76] : To a solution of sodium azide (0.148g, 2.28 mmol) in DCM (0.3 mL) was added Me_2AlCl (1.9 mL, 1.9 mmol, 1.0 M solution in hexane) at 0 °C. The reaction mixture was stirred at room temperature for 20 hours. The cloudy solution was then transferred to reaction vessels via syringe.

Reaction performed under the standard procedure with Me_2AlN_3 (1.0 M prepared *in situ*) for 30 minutes. The reaction was quenched with 1M aq. HCl (2 mL) and warmed to room temperature. After separation of the phases, the aqueous layer was extracted with CH_2Cl_2 (3 x 5 mL). The combined organic extracts were washed with brine, and dried over $MgSO_4$, filtered, and concentrated in vacuo. Flash chromatography (49:1 hexane:EtOAc) gave **11a** (white solid, 32 mg, 50 %), and **11a′** (white solid, 18 mg, 27 %).

***rac*-(2*S*,3*S*,4*R*,5*S*)-2-azido-2,5-dimethyl-3,4-diphenylcyclopentan-1-one** (**11a**): R_f 0.36 (hexanes/EtOAc 9:1); mp 142-145 °C; IR (cast film) 3031, 2967, 2096, 1746, 1453, 698 cm^{-1}; ^{1}H NMR (500 MHz, $CDCl_3$) δ 7.32-7.20 (m, 10H), 3.59 (d, *J* = 12.7 Hz, 1H), 3.19 (dd, *J* = 12.6, 11.5 Hz, 1H), 2.54 (dq, *J* = 11.5, 7.0 Hz, 1H), 1.20 (d, *J* = 7.0 Hz, 3H), 1.10 (s, 3H); ^{13}C NMR (125 MHz, $CDCl_3$) δ 215.5, 139.3, 135.1, 128.9, 128.8, 128.3, 127.6, 127.3, 127.2, 69.1, 55.5, 51.1, 48.9, 16.6, 13.3; HRMS (ESI, [M+Na]$^+$) for $C_{19}H_{19}N_3NaO$ calcd. 328.1420, found: m/z 328.1417.

***rac*-(2*S*,3*S*,4*R*,5*R*)-2-azido-2,5-dimethyl-3,4-diphenylcyclopentan-1-one (11a′)**: R*f* 0.31 (hexanes/EtOAc 9:1); mp 131-133 °C; IR (cast film) 3029, 2970, 2931, 2101, 1744, 1453, 698 cm^{-1}; ^{1}H NMR (500 MHz, CDCl$_3$) δ 7.28-7.14 (m, 10H), 3.43 (dd, *J* = 12.1, 11.0 Hz, 1H), 3.19 (d, *J* = 12.1 Hz, 1H), 2.46 (dq, *J* = 11.0, 7.0 Hz, 1H), 1.48 (s, 3H), 1.26 (d, *J* = 7.0 Hz, 3H); ^{13}C NMR (125 MHz, CDCl$_3$) δ 212.2, 139.4, 134.6, 129.7, 128.7, 128.0, 127.5, 127.5, 127.0, 68.7, 57.9, 51.0, 51.0, 17.2, 13.7; HRMS (ESI, [M+Na]$^+$) for $C_{19}H_{19}N_3NaO$ calcd. 328.1420, found: m/z 328.1421.

2.5.3 Experimental Procedures and Characterization for the Diethylzinc Interrupted Nazarov Reaction

Representative Procedure of Diethylzinc Interrupted Nazarov Reaction (7a')

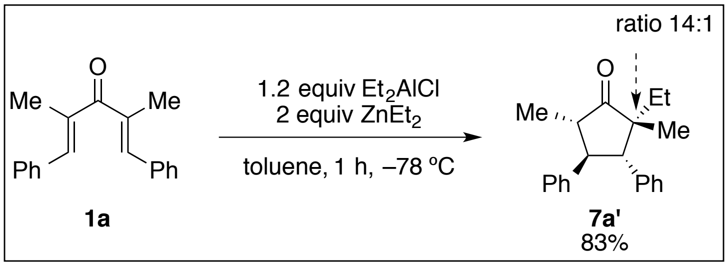

To a solution of **1a** (50 mg, 0.19 mmol) in toluene (1.9 mL, 0.1 M) was added 2 equivalents of ZnEt$_2$ (0.38 mL, 1 M solution in hexane) at –78 ºC. 1.2 equiv Et$_2$AlCl (0.11 mL, 25 wt. % in toluene) was then added dropwise to the reaction vessel. The mixture was stirred until complete consumption of **1a** was observed by TLC (1 h). The reaction was quenched with 1M aq. HCl (3 mL) and warmed to room temperature. After separation of the phases, the aqueous layer was extracted with CH$_2$Cl$_2$ (3 x 5 mL). The combined organic extracts were washed with brine, and dried over MgSO$_4$, filtered, and concentrated in vacuo. Purification by flash column chromatography (silica gel) provided two diastereomers **7a'** and **7a** (46 mg, 83 %, 14:1 ratio).

Spectral Data of 7a'-7d', **12a'**, and **13g**

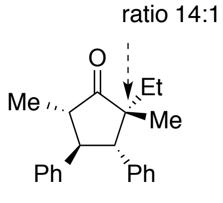

7a'

Flash chromatography (39:1 to 19:1 hexane:EtOAc) gave **7a'** (46 mg, 83 %) as a white solid: R*f* 0.43 (hexanes/EtOAc 9:1); mp 96-99 °C; IR (cast film) 3029, 2965, 1732, 1453 cm^{-1}; ^{1}H NMR (500 MHz, CDCl$_3$) δ 7.29-7.21 (m, 8H), 7.20-7.14 (m, 2H), 3.47-3.41 (m, 2H), 2.37 (dqd, *J* = 9.0, 7.1, 1.9 Hz, 1H), 1.50 (dq, *J* = 14.1, 7.5 Hz, 1H), 1.02 (dq, *J* = 14.1, 7.4 Hz, 1H), 1.24 (s, 3H), 1.22 (d, *J* = 7.1 Hz, 3H), 0.71 (app. t, *J* = 7.5, 3H); ^{13}C NMR (100 MHz, CDCl$_3$) δ 221.0, 141.1, 136.8, 129.3, 128.6, 128.0, 127.7, 126.7, 126.7, 59.3, 52.8, 52.0, 50.2, 25.3, 20.7, 14.0, 8.1; HRMS (EI, M$^+$) for $C_{21}H_{24}O$ calcd. 292.1827, found: m/z 292.1827.

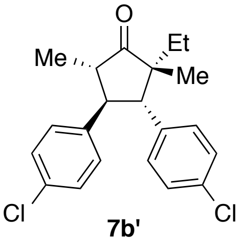

7b'

Reaction performed under the standard procedure for 1 hour. Flash chromatography (39:1 to 19:1 hexane:EtOAc) gave single diastereomer **7b'** (32 mg, 49 %) as a colorless oil: R*f* 0.35 (hexanes/EtOAc 9:1); IR (cast film) 3031, 2968, 2931, 1732, 1494, 1456 cm^{-1}; ^{1}H NMR (500 MHz, CDCl$_3$) δ 7.25-7.22 (m, 4H), 7.18-7.16 (m, 2H), 7.13-7.10 (m, 2H), 3.37-3.30 (m, 2H), 2.30 (dqd, *J* = 9.7, 7.1, 1.0 Hz, 1H), 1.45 (dq, *J* = 14.0, 7.3 Hz, 1H), 0.99 (dq, *J* = 14.1, 7.4 Hz, 1H), 1.20 (s, 3H), 1.19 (d, *J* = 7.1 Hz, 3H), 0.73 (app. t, *J* = 7.5, 3H); ^{13}C NMR (125 MHz, CDCl$_3$) δ 219.8, 139.2, 135.0, 132.8, 132.6, 130.4, 128.9, 128.9, 128.4, 58.9, 52.7, 51.8, 49.8, 25.3, 20.7, 13.8, 8.1; HRMS (EI, M$^+$) for $C_{21}H_{22}O^{35}Cl_2$ calcd. 360.1048, found: m/z 360.1049.

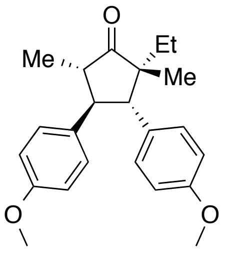
7c'

Reaction performed under the standard procedure for 1 hour. Flash chromatography (39:1 to 19:1 hexane:EtOAc) gave single diastereomer **7c'** (45 mg, 67 %) as a colorless oil: R$_f$ 0.40 (hexanes/EtOAc 8:2); IR (neat film) 3034, 2963, 2932, 1731, 1613, 1514, 1251 cm^{-1}; ^{1}H NMR (500 MHz, CDCl$_3$) δ 7.18-7.15 (m, 2H), 7.13-7.10 (m, 2H), 6.81-6.77 (m, 4H), 3.76 (s, 3H), 3.74 (s, 3H), 3.35-3.28 (m, 2H), 2.29 (dqd, *J* = 9.3, 7.0, 1.5 Hz, 1H), 1.46 (dq, *J* = 14.0, 7.5 Hz, 1H), 1.20 (s, 3H), 1.19 (d, *J* = 6.5 Hz, 3H), 1.05-0.98 (m, 1H), 0.72 (app. t, *J* = 7.4 Hz, 3H); ^{13}C NMR (125 MHz, CDCl$_3$) δ 221.3, 158.3, 158.3, 133.2, 130.1, 128.8, 128.5, 114.0, 113.4, 58.8, 55.1, 55.1, 52.7, 52.0, 49.6, 25.3, 20.7, 13.9, 8.1; HRMS (EI, M$^+$) for $C_{23}H_{28}O_3$ calcd. 352.2039, found: m/z 352.2037.

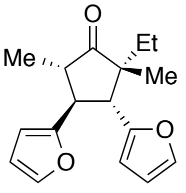
7d'

+

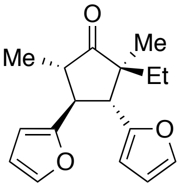
7d

ratio 6:1

Reaction performed at –25 ºC for 3 hours. Flash chromatography (99:1 to 39:1 hexane:EtOAc) gave an inseparable mixture of diastereomers **7d'** and **7d** (6:1 ratio, 34 mg, 57 %).

7d': R$_f$ 0.46 (hexanes/EtOAc 9:1); IR (neat film) 3117, 2967, 2932, 1739, 1506, 1457 cm^{-1}; ^{1}H NMR (500 MHz, CDCl$_3$) δ 7.36 (dd, *J* = 1.9, 0.8 Hz, 1H), 7.30 (dd, *J* = 1.9, 0.8 Hz, 1H), 6.30 (dd, *J* = 3.2, 1.9 Hz, 1H), 6.27 (dd, *J* = 3.2, 1.9 Hz, 1H), 6.12 (app. dt, *J* = 3.2, 0.7 Hz, 1H), 6.08 (ddd, *J* = 3.2, 0.9, 0.4 Hz, 1H), 3.48-3.41 (m, 2H), 2.51 (dqd, *J* = 9.6, 7.1, 1.4 Hz, 1H), 1.40 (dq, *J* = 14.2, 7.5 Hz, 1H), 1,25 (s, 3H), 1.25 (d, *J* = 7.0 Hz, 3H), 1.14 (dq, *J* = 14.2, 7.5 Hz, 1H), 0.70 (app. t, *J* = 7.5, 3H); ^{13}C NMR (125 MHz, CDCl$_3$) δ 220.4, 154.6, 152.6, 110.2, 110.1, 107.5, 106.2, 52.9, 51.1, 48.7, 43.5, 26.3, 21.2, 14.0, 8.3 [two aromatic carbon resonances not detected, due to presumed spectral overlap]; HRMS (EI, M^+) for $C_{17}H_{20}O_3$ calcd. 272.1412, found: m/z 272.1413.

7d (partial data): ^{1}H NMR (500 MHz, $CDCl_3$) δ 7.34 (dd, *J* = 1.8, 0.8 Hz, 1H), 7.32 (dd, *J* = 1.9, 0.8 Hz, 1H), 6.29 (dd, *J* = 3.2, 1.8 Hz, 1H), 6.28 (dd, *J* = 3.2, 1.8 Hz, 1H), 6.10-6.09 (m, 2H), 3.65 (d, *J* = 11.9 Hz, 1H), 3.34 (app. t, *J* = 11.9 Hz, 1H), 2.45 (dq, *J* = 11.8, 7.0 Hz, 1H), 1.80 (dq, *J* = 14.0, 7.4 Hz, 1H), 1.62 (s, 3H), 1.59 (dq, *J* = 14.0, 7.4 Hz, 1H), 1.22 (d, *J* = 7.0 Hz, 3H), 0.96 (app. t, *J* = 7.5, 3H); ^{13}C NMR (125 MHz, $CDCl_3$) δ 220.8, 154.3, 153.1, 110.0, 107.4, 106.5, 53.6, 50.0, 45.6, 43.5, 29.6, 20.0, 13.5, 8.9 [three aromatic carbon resonances not detected, due to presumed spectral overlap].

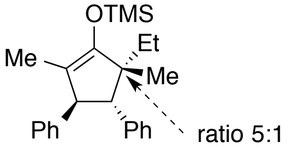

12a'

Reaction performed in hexane (1.5 mL, 0.1 M) at –41 ºC under the standard procedure with 1.1 equiv TMSOTf (0.031 mL, 0.17 mmol). Flash chromatography (49:1 hexane:EtOAc) gave an inseparable mixture of **12a'/12a** (52 mg, 95 %, 5:1 ratio) (partial characterization was made for the major product **12a'**): R_f 0.47 (hexanes/EtOAc 19:1); ^{1}H NMR (500 MHz, $CDCl_3$) δ 7.31-7.11 (m, 10H), 4.07 (dq, *J* = 9.6, 1.2 Hz, 1H), 3.00 (d, *J* = 9.6 Hz, 1H), 1.45 (d, *J* = 1.3 Hz, 3H), 1.34 (dq, *J* = 13.7, 7.5 Hz, 1H), 1.17 (s, 3H), 1.04 (dq, *J* = 13.7, 7.6 Hz, 1H), 0.64 (app. t, *J* = 7.5 Hz, 3H), 0.34 (s, 9H).

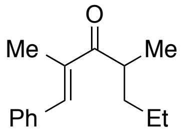

13g

Reaction performed under the standard procedure for 1 hour. Flash chromatography (49:1 hexane:diethyl ether) gave **13g** (30 mg, 44 %) as a colorless oil.

(*E*)-2,4-dimethyl-1-phenylhept-1-en-3-one (13g): R_f 0.58 (hexanes/EtOAc 9:1); IR (cast film) 3026, 2960, 1664, 1450 cm^{-1}; ^{1}H NMR (500 MHz, $CDCl_3$) δ 7.53-7.52 (m, 1H), 7.45-7.42 (m, 4H), 7.38-7.34 (m, 1H), 3.41 (app. sextet, *J* = 6.7 Hz, 1H), 2.09 (d, *J* = 1.4 Hz, 3H), 1.78-1.71 (m, 1H), 1.46-1.28 (m, 3H), 1.17 (d, *J* = 6.8 Hz, 3H), 0.94 (t, *J* = 7.3

Hz, 3H); ^{13}C NMR (125 MHz, $CDCl_3$) δ 206.9, 137.8, 137.3, 136.2, 129.7, 128.4, 128.4, 39.2, 36.5, 20.7, 17.8, 14.2, 13.5; HRMS (EI, M^+) for $C_{15}H_{20}O$ calcd. 216.1514, found: m/z 216.1513.

2.5.4 Experimental Procedures and Characterization for the Domino Oppenauer Oxidation/Electrocyclization

Preparation of Divinyl Alcohol (6a)

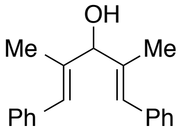

6a

To a solution of 2,4-dimethyl-1,5-diphenylpenta-1,4-dien-3-one **1a** (1.97 g, 7.5 mmol) and $CeCl_3 \cdot 7H_2O$ (2.80 g, 7.5 mmol) in MeOH (75 mL, 0.1 M) was added 1.6 equivalents of $NaBH_4$ (0.45 g, 12.0 mmol) at 0 ºC. The reaction mixture was stirred for 12 hours at room temperature and then quenched slowly with water (20 mL). The organic mixture was extracted with DCM (3 x 30 mL). The combined organic extracts were washed with brine, and dried over $MgSO_4$, filtered, and concentrated in vacuo. The crude dienol was purified by flash chromatography (9:1 hexane:EtOAc) to give 1.82 g (92 %) of **6a** as a white solid. Spectral data are reported in section 2.5.2 of this chapter.

Procedure for the Domino Oppenauer Oxidation/Electrocyclization (10a)

Note: For this reaction, dry toluene was injected to an argon-charged, flame-dried flask through anhydrous K_2CO_3 plug to remove water as much as possible.

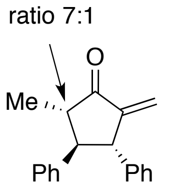

10a

To a solution of **6a** (40 mg, 0.15 mmol) in toluene (1.5 mL, 0.1 M) with activated 4 Å MS (about 60 mg) was added 0.25 equivalents of $AlMe_3$ (0.019 mL, 2.0 M solution in toluene) at room temperature. The solution was stirred for 15 minutes and then 1.2 equiv 3-nitrobenzaldehyde (27 mg, 0.18 mmol) was added. After stirring for 30 minutes, the fitted septum with the line of argon gas was taken off and an argon-charged, dry condenser was quickly attached to the flask. The reaction mixture was heated at reflux for 1 hour, cooled to room temperature and quenched with 1 M aq. HCl (1 mL). After separation of the phases, the aqueous layer was extracted with CH_2Cl_2 (3 x 5 mL). The combined organic extracts were washed with brine, and dried over $MgSO_4$, filtered, and concentrated in vacuo. Purification by flash column chromatography (19:1 hexane:EtOAc) provided the desired product **10a** (19.5 mg, 48 %). Spectral data are reported in Section 2.5.2 of this chapter.

Spectral Data of 1m and 15a/15a'

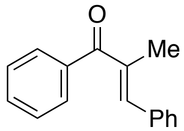

1m

Reaction performed under the standard procedure for 20 hours. Flash chromatography (19:1 to 9:1 hexane:EtOAc) gave **1m** (46 mg, 94 %). Spectral data are consistent with the reported values.[85]

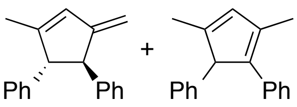

15a **15a'**

To a solution of divinyl alcohol **6a** (0.030 g, 0.11 mmol) in toluene (1.1 mL, 0.1 M) was added 0.25 equiv $ClAlMe_2$ (0.28 mL, 0.028 mmol, 1 M hexane solution). The reaction mixture was stirred at room temperature for 4 hours. The crude mixture was then filtered through neutral alumina pad (2 cm thickness) and rinsed with pentane (20 x 5 mL). The filtrate was concentrated in vacuo and products were found to be an inseparable mixture of **15a** and **15a'** (ratio 0.9:1.0, 26 mg, 96 %). **15a** was isomerized to **15a'** in $CDCl_3$ NMR solvent.

15a (partial ^{1}H NMR data due to spectral overlap): ^{1}H NMR (500 MHz, $CDCl_3$) δ 6.25-6.24 (m, 1H), 4.98-4.98 (m, 1H), 4.52-4.51 (m, 1H), 3.84-3.82 (m, 1H), 3.77-3.76 (m, 1H), 1.75-1.75 (m, 3H); ^{13}C NMR (125 MHz, $CDCl_3$) δ 157.5, 150.1, 145.2, 143.7, 130.9, 128.6, 128.5, 127.7, 127.6, 126.6, 126.2, 103.3, 65.3, 59.7, 15.8.

15a': R_f 0.93 (hexanes/EtOAc 9:1); IR (cast film) 3025, 2911, 2856, 1599, 1491, 1451 cm^{-1}; ^{1}H NMR (500 MHz, $CDCl_3$) δ 7.25-7.21 (m, 6H), 7.16-7.09 (m, 2H), 7.06-7.03 (m, 2H), 6.10-6.09 (m, 1H), 4.38-4.37 (m, 1H), 2.20 (d, J = 1.9 Hz, 3H), 1.87 (d, J = 1.5 Hz, 3H); ^{13}C NMR (125 MHz, $CDCl_3$) δ 149.2, 142.5, 139.1, 138.0, 136.8, 131.8, 128.5, 128.2, 128.1, 128.0, 126.3, 125.5, 63.4, 14.7, 14.7; HRMS (EI, M$^+$) for $C_{19}H_{18}$ calcd. 246.1409, found: m/z 246.1417.

Chapter 3

Synthesis of α-Hydroxycyclopentanones *via* One-Pot Oxidation of the Trimethylaluminum-Mediated Nazarov Reaction with Triplet Oxygen[86]

3.1 Introduction

There has been considerable interest in the Nazarov reaction for the past ten years, as described in many recent reviews.[1] One of the most developed areas in the Nazarov reaction has involved the exploration of domino/cascade processes: trapping the initially formed oxyallyl cation intermediate with various nucleophiles inter- and intramolecularly. This process has been termed the "interrupted Nazarov" reaction.[7] To date, the trapping strategies in the interrupted Nazarov reaction have largely been limited to π-nucleophiles such as electron rich arenes, allyl silanes and enol derivatives. Strong σ-nucleophiles have received minimal attention due to the risk of both 1,2 and 1,4-addition pathways to the divinyl ketone (see Chapter 1).

Recently, we expanded the scope of the interrupted Nazarov reaction to include simple σ-nucleophiles.[50] Organoaluminum species are found to be Lewis acidic enough to initiate Nazarov cyclization, as well as allow the delivery of simple alkyl, phenyl, cyano, and azido groups to the oxyallyl cation intermediate (Scheme 3.1). We proposed that an aluminium enolate was formed after the capture of the oxyallyl cation, which was presumably protonated during aqueous work-up. In this chapter, we will discuss the research conducted on a "second interruption" of the organoaluminum interrupted Nazarov reaction with molecular oxygen to build molecular complexity onto the cyclopentanone framework.

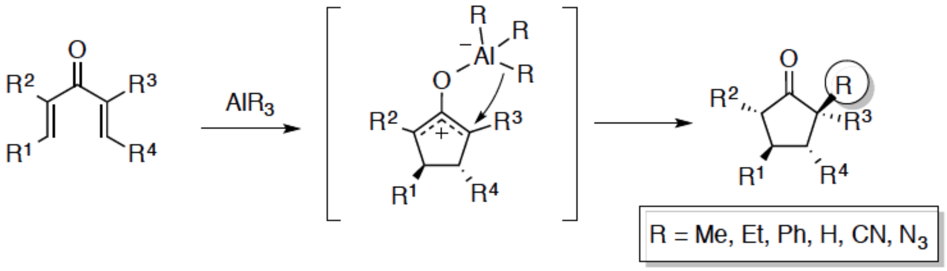

Scheme 3.1 Organoaluminum Mediated Interrupted Nazarov Reaction.

3.2 Results and Discussion

While performing one of the AlMe$_3$-mediated interrupted Nazarov reactions, the reaction flask was unintentionally exposed to the air for a few seconds, leading to the formation of a small amount (about 10 %) of new products (Scheme 3.2). Upon isolation and qualitative analysis, these new polar compounds were revealed to be a mixture of epimeric α-hydroxy cyclopentanones **4a**/**5a**. This raised an important question: where is the "OH cation" coming from?

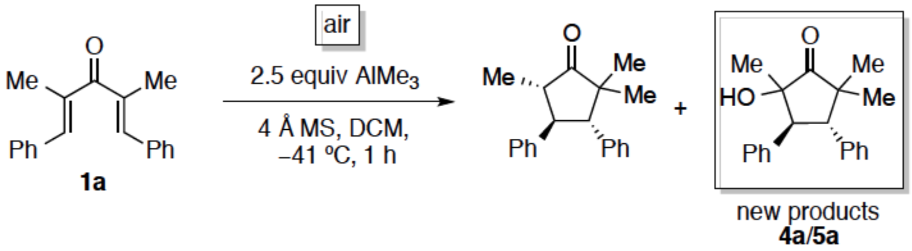

Scheme 3.2 Unexpected Finding: α-Hydroxycyclopentanones.

With these curious findings in hand, we searched the literature to find relevant examples of this reactivity. To the best of our knowledge, there is only one related example, reported by Rück and Kunz in 1991 (Scheme 3.3).[87] They reported, without proposing a mechanism, that the reaction of aluminum enolates with oxygen does indeed afford hydroxylated products. However, their enolic intermediate was formed by a photochemical process. Therefore, our finding is the first example whereby a thermally generated aluminum enolate produced an α-hydroxy ketone when exposed to molecular oxygen.

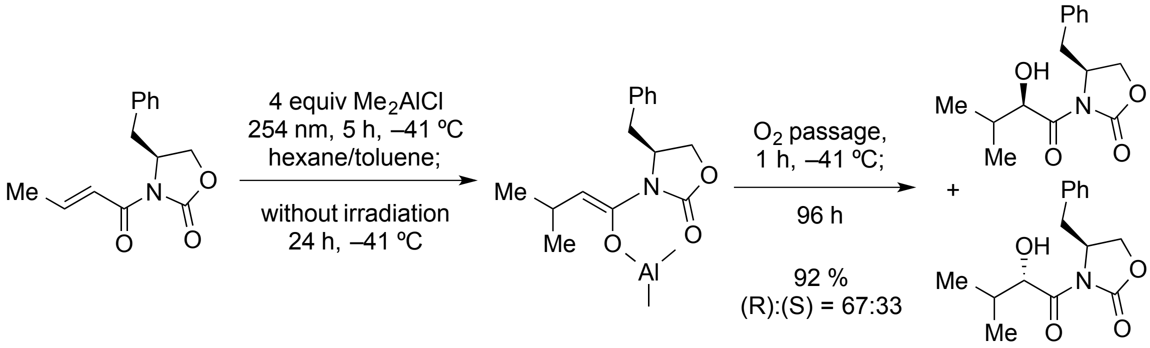

4 equiv Me$_2$AlCl
254 nm, 5 h, –41 °C
hexane/toluene;
without irradiation
24 h, –41 °C
O$_2$ passage,
1 h, –41 °C;
96 h
92 %
(R):(S) = 67:33

Scheme 3.3 Aluminum Enolate Reaction under Photochemical Condition and Autoxidation.

Wondering if our new finding could be synthetically useful in methodology oriented synthesis, I tried to find biologically important natural products bearing the α-*gem*-dimethyl and α'-hydroxy functionality. The α-*gem*-dimethyl and α'-hydroxy functionalized cyclopentanone framework are present in the cytotoxic norsesquiterpene redox congeners flammulinolide C and its reduced analogue flammulinolide B (Figure 3.1).[88]

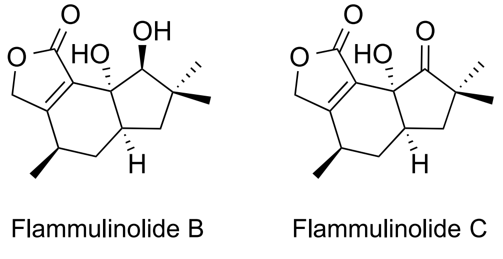

Flammulinolide B
Flammulinolide C

Figure 3.1 Natural Products Flammulinolide B and C.

With the presence of the framework in natural products and the intriguing unprecedented reactivity in mind, we decided to explore the formation of α-hydroxycyclopentanones by $AlMe_3$ mediated interrupted Nazarov cyclization and one-pot oxidation (Scheme 3.4).

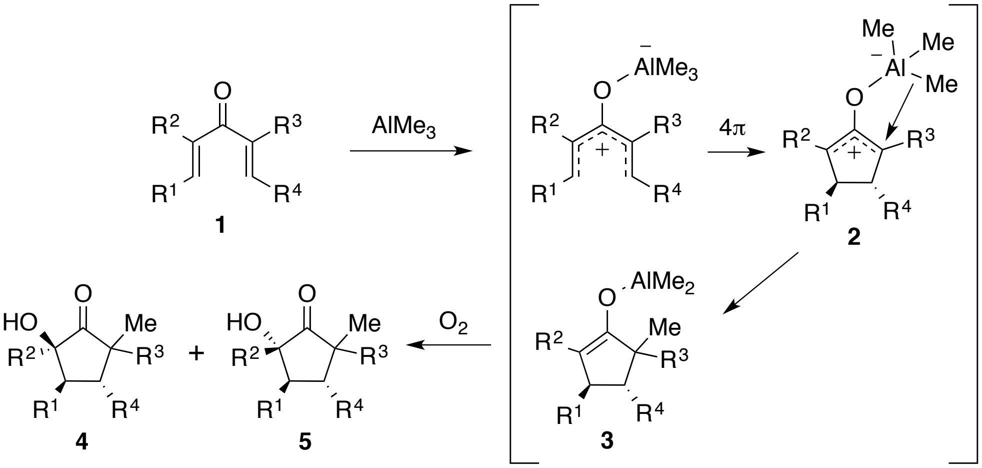

Scheme 3.4 One-Pot Interrupted Nazarov Reaction/Oxidation of the Aluminum Enolate.

Our attempts at optimization first focused on the timing of when to introduce oxygen to the reaction flask. Optimization study results showed that passage of O_2 gas* for 5 minutes after consumption of the starting 1,4-dien-3-one **1a** (as indicated by TLC analysis) was the most efficient means of obtaining the hydroxylated cyclopentanones **4a** and **5a** (79 %, 1.32:1 **4a**:**5a**). It should be noted that for safety reasons the reaction vessel was cooled to a lower reaction temperature prior to addition of oxygen to reduce the risk of vigorous reaction with residual $AlMe_3$. Also, purging the reaction vessel with O_2 gas prior to the addition of $AlMe_3$ at a lower temperature failed to give consistent levels of hydroxylated product **4a**/**5a**, and full conversion of **1a** was never observed.

---

* Extra dry oxygen (99.6%, H_2O < 10ppm) from Praxair was used for the oxidation.

Table 3-1 Trimethylaluminum Mediated Nazarov Cyclization and Oxidation of Resulting Aluminum Enolate.[a]

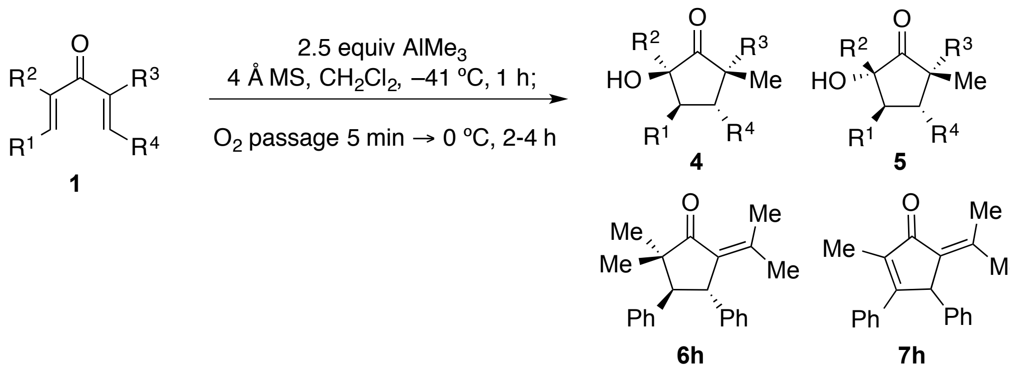
O
R2
R3
R1
R4
1
2.5 equiv AlMe3
4 Å MS, CH2Cl2, –41 °C, 1 h;
O2 passage 5 min → 0 °C, 2-4 h
O
R2
R3
HO
Me
R1
R4
4
O
R2
R3
HO
Me
R1
R4
5
O
Me
Me
Me
Me
Ph
Ph
6h
O
Me
Me
Me
Ph
Ph
7h

Entry	Dienone	R1	R2	R3	R4	Product (ratio)[b]	Yield (%)[c]
1	**1a**	Ph	Me	Me	Ph	**4a**/**5a** (1.32:1)	79
2	**1b**	4-ClC$_6$H$_4$	Me	Me	4-ClC$_6$H$_4$	**4b**/**5b** (1.23:1)	69
3	**1c**	4-MeOC$_6$H$_4$	Me	Me	4-MeOC$_6$H$_4$	**4c**/**5c** (1.14:1)	77
4	**1d**	2-furyl	Me	Me	2-furyl	**4d**/**5d** (1.29:1)	64
5[d]	**1e**	*i*-Pr	Me	Me	*i*-Pr	**4e**/**5e** (1:1.38)	33
6	**1f**	Ph	Me	Me	H	**4f**/**5f** (1:1.13)	68
7	**1g**	Ph	Me	–O(CH$_2$)$_3$–		**4g**/**5g** (1:1.72)	49
8[e]	**1h**	Ph	Me	C(OH)Me$_2$	Ph	**6h** (39%) + **7h** (22%)[f]	

[a]Standard procedure: To a solution of **1** with 4 Å MS in CH$_2$Cl$_2$ (0.1M) at –41 ºC was added 2.5 equiv AlMe$_3$ (2.0 M solution in toluene). The reaction mixture was stirred until complete consumption of starting material was observed by TLC. The solution was purged with O$_2$ gas for 5 min at –41ºC; then the solution was allowed to warm to 0 ºC under an oxygen atmosphere and stirred for 2-4 hrs. [b] Ratio determined from isolated yields. [c] Yields are based on isolated product after chromatography. [d] The reaction was carried out from –25 to 0 ºC. The Me$_3$Al 1,2-adduct was found as a side product. [e] The reaction was carried out from 0 ºC to a room temperature for 48 hours. [f] When 3.0 equivalents of AlMe$_3$ was used with no O$_2$ passage, **6h** was formed in 64% yield with no observed formation of **7h**.

Symmetrical β, β'-aryl substituted 1,4-dien-3-ones were the first substrates to be investigated (entries 2-4, Table 3-1). The α-hydroxylated cyclopentanones were formed in good yield; however, the oxygenation step proceeded with low facial selectivity, resulting in only a negligible preference for the *syn* product in each case. Single crystal X-ray diffraction analysis supported the assigned relative configuration of **4a** (Figure 3.2). The relative configurations of products **4b-d** and **5b-d** were assigned based on NMR comparisons to **4a** and **5a** respectively, relying on the observed trend – anisotropy effect – towards upfield ^{1}H NMR chemical shifts for α-methyl groups in a *cis* relationship to neighbouring β-aryl groups relative to their *trans* counterparts.[89]

In case of the symmetrical tetraalkyl 1,4-dien-3-one **1e,** the facial selectivity was reversed, slightly favouring the *anti* geometry; however, this reaction occurred with a significantly diminished yield (33 %). It was reported that Nazarov cyclization of **1e** could suffer from 1,2-addition of methyl to the carbonyl group to afford the tertiary bis(allylic) alcohol.[50] Due to the absence of β-aromatic substituents, correlating ^{1}H NMR chemical shifts of methyl groups was a valid way to assign the configuration of **4e** and **5e**; however, single crystal X-ray diffraction analysis allowed for unambiguous assignments of the relative stereochemistry of **4e** and **5e** (Figure 3.3).

Unsymmetrical dienones **1f** and **1g** (entries 6 and 7) were investigated next. When substrate **1f** was exposed to the reaction conditions, the methyl nucleophile reacted solely on the less substituted side of the oxyallyl cation, leading to the electrophilic oxygen to react on the more sterically demanding side of the molecule.

In case of dihydropyran-containing substrate **1g,** hydroxypentanones **4g** and **5g** were produced in moderate yield with the methyl nucleophile attacking the more electronically stabilized side of the oxyallyl cation. The relative configuration of the major epimer **5g** was determined by single crystal X-ray diffraction analysis.

We were curious to see if hydroxyalkyl-substituted dienone **1h**[90] could serve as a precursor to a 1,2-diol using this methodology. Unfortunately, subjecting **1h** to the reaction conditions did not provide the desired 1,2-diol, but instead, a mixture of alkylidene cyclopentanone **6h** and the corresponding cyclopentenone **7h** was obtained (entry 8). We believe this result is due to premature ejection of the exocyclic hydroxyl group by the aluminum enolate following either methyl trapping or elimination of the β-hydrogen of the oxyallyl cation.

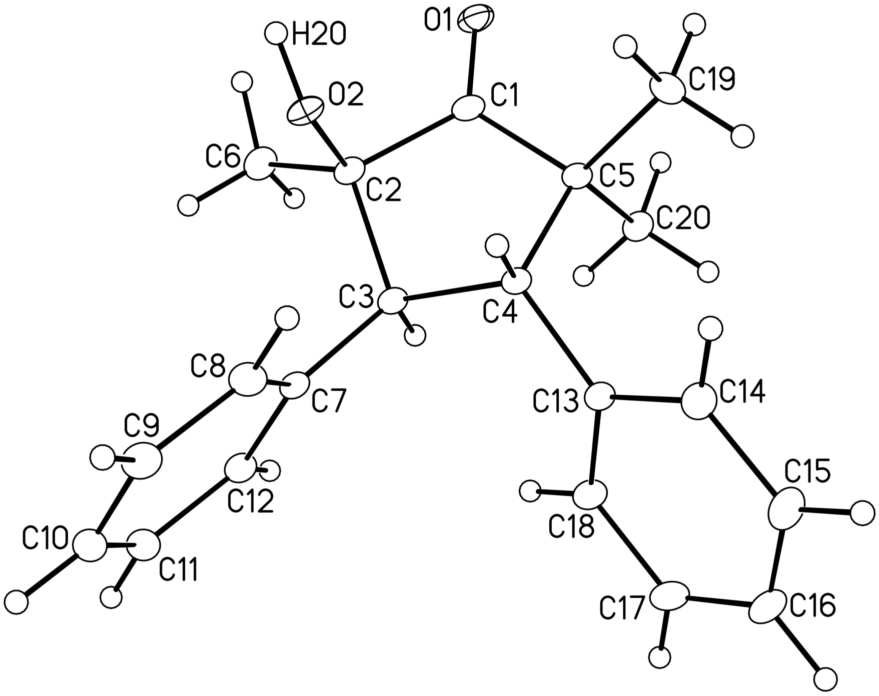
O1
H20
O2
C1
C19
C6
C2
C5
C20
C3
C4
C8
C7
C13
C14
C9
C15
C12
C18
C10
C11
C17
C16

(Thermal ellipsoids shown at the 20 % probability level)

Figure 3.2 ORTEP Drawing of **4a**.

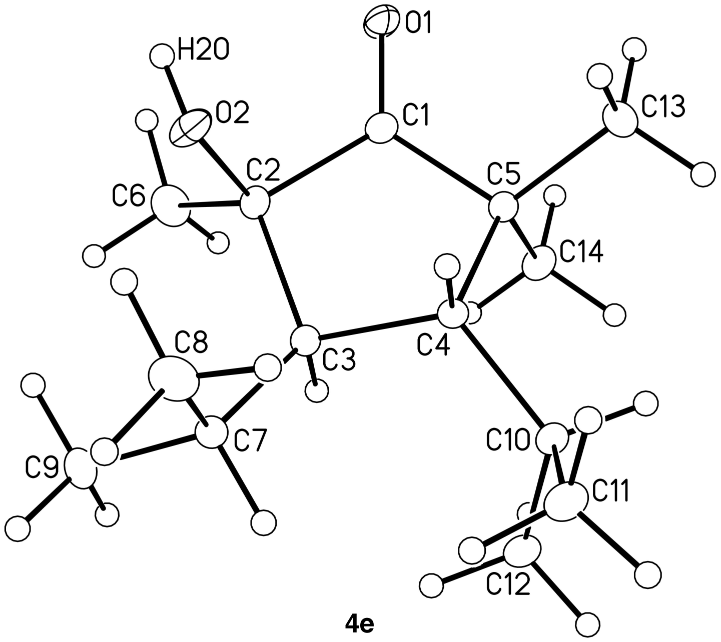
O1
H20
O2
C1
C13
C2
C6
C5
C14
C8
C3
C4
C7
C10
C9
C11
C12

4e

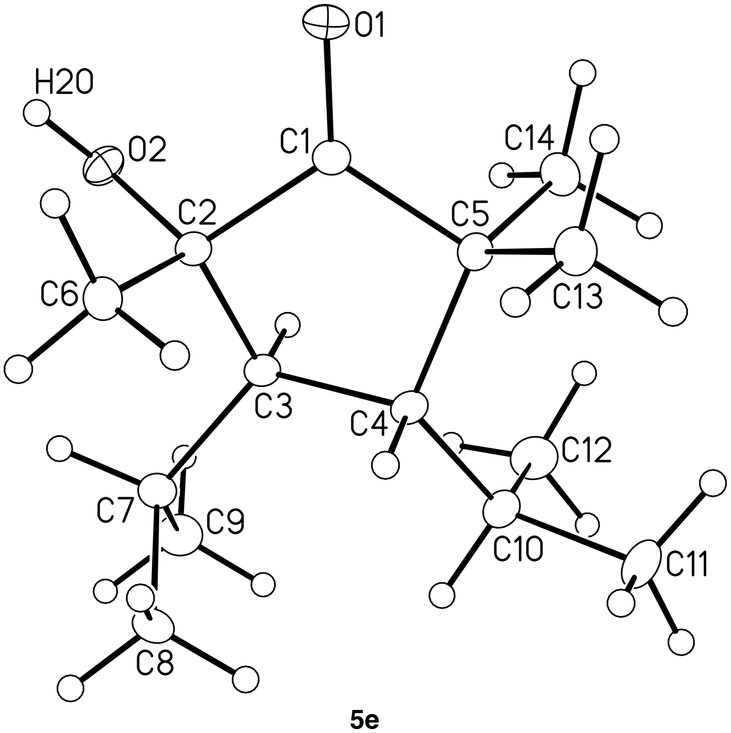
O1
H20
O2
C1
C14
C2
C5
C6
C13
C3
C4
C12
C7
C9
C10
C11
C8

5e

(Thermal ellipsoids shown at the 20 % probability level)

Figure 3.3 ORTEP Drawing of **4e** and **5e**.

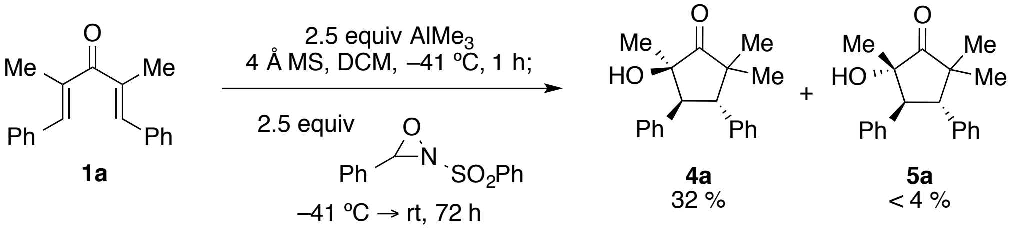

Scheme 3.5 Use of Davis Oxaziridine.

To compare the efficacy of the enolate capture with oxygen, we looked for other electrophilic oxygen sources. With this in mind, we investigated the use of Davis oxaziridine as our oxidizing agent (Scheme 3.5).[91] A solution of freshly prepared Davis oxaziridine in CH_2Cl_2 was added to the reaction vessel at –41 ºC via syringe following consumption of **1a** (TLC analysis). These conditions did produce **4a** and **5a**, but in a significantly reduced yield. Also, the reaction required higher temperature (room temperature versus 0 ºC) and longer reaction time (72 hours versus 2 hours). The diastereomeric ratio, however, was greater in favor of **4a** (8:1 **4a**:**5a**), presumably due to possible aromatic-aromatic interactions (π stacking) between the β-aryl substituent and the phenyl substituent of Davis oxaziridine. Furthermore, it was difficult to separate oxaziridine-derived by-products from **4a** and **5a**. Use of oxygen to afford α-hydroxy functionality is operationally simpler, more economical and higher yielding.

3.3 Mechanistic Proposal

The exact mechanism of hydroxyl introduction using oxygen as the oxidant remains unclear. In order to propose a plausible mechanism, we have to be able to answer what reaction component – $AlMe_3$ or the aluminium enolate – is involved in the oxidation step, as excess amounts (2.5 equivalents) of the $AlMe_3$ were used.

In 2000, Henderson and co-workers elucidated the structure of a dimethyl aluminium enolate **I** (Scheme 3.6).[92] Surprisingly, when subjected to 2,4,6-trimethylacetophenone, $AlMe_3$ favors enolization over 1,2-addition of methyl. The enolate compound **I**, a dimer with a central Al_2O_2 core, was isolated and characterized by X-ray crystallography. Henderson's work might provide valuable insight into the mechanism of our process. If the enolate **I** were to react with triplet oxygen without extra amounts of trimethylaluminum present to provide the corresponding α-hydroxyketone, we could propose direct aluminum enolate reaction with molecular oxygen.

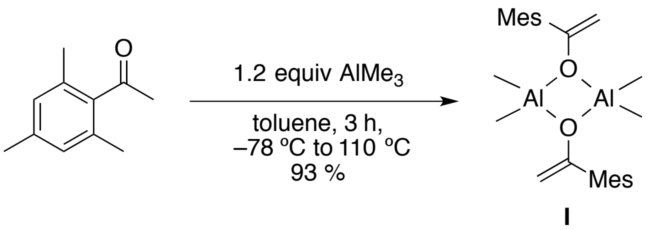

Scheme 3.6 The Formation of Aluminum Enolate.

In 1968, Davies and co-worker studied mechanisms of the autoxidation of trimethylaluminum (Scheme 3.7).[93] Based on the amount of absorbed oxygen (0.81–0.82 mol) by $AlMe_3$ in cyclohexane, they postulated $AlMe_3$ would undergo an insertion process to afford methylperoxyaluminum intermediate **A**, which was unstable, and underwent reorganization to aluminum alkoxides **B** and **C**.

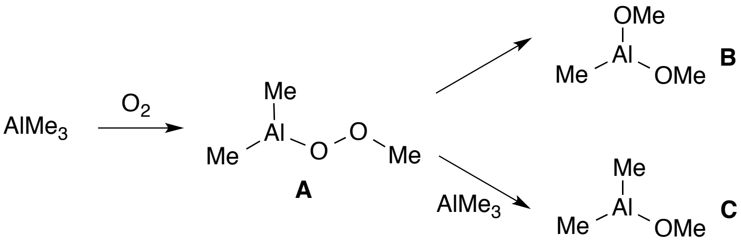

Scheme 3.7 Autoxidation of Trimethylaluminum.

The alkylperoxyaluminum intermediate also appeared in Nozaki and co-workers' report in 1980 (Scheme 3.8).[94] The proposed intermediate was involved in the oxidation of secondary alcohols to ketones with $AlMe_3$ and *t*-BuOOH. Addition of the peroxide to dimethylaluminum alkoxide could provide the peroxyaluminum species upon the release of methane. Oxidation then could occur by the loss of hydride, cleaving the O-O bond.

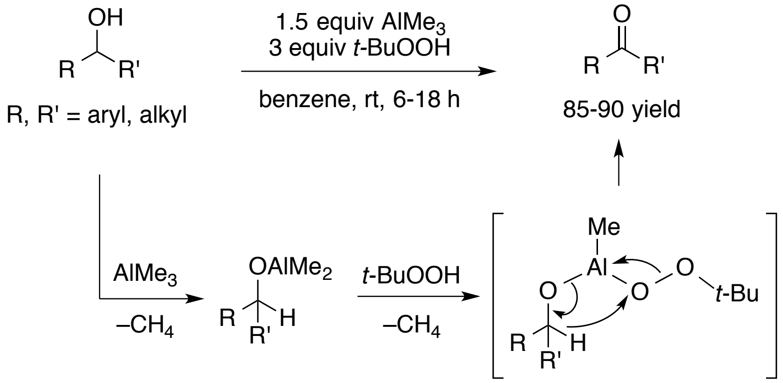
OH
R
R'
R, R' = aryl, alkyl
1.5 equiv AlMe3
3 equiv t-BuOOH
benzene, rt, 6-18 h
O
R
R'
85-90 yield
AlMe3
–CH4
OAlMe2
R
H
R'
t-BuOOH
–CH4
Me
Al
O
O
O
t-Bu
R
H
R'

Scheme 3.8 Alcohol Oxidation by *tert*-Butyl Hydroperoxide and $AlMe_3$.

With these studies in mind, I proposed a mechanism for the construction of α-hydroxy ketones (Scheme 3.9). After the methyl transfer to the Nazarov intermediate, triplet oxygen could be inserted into the aluminum enolate **II**. Similar to Nozaki's report, rearrangement of the peroxyaluminum intermediate **III** would lead to aluminum alkoxide species **IV**. Hydrolysis upon aqueous work-up would then afford the alcohol.

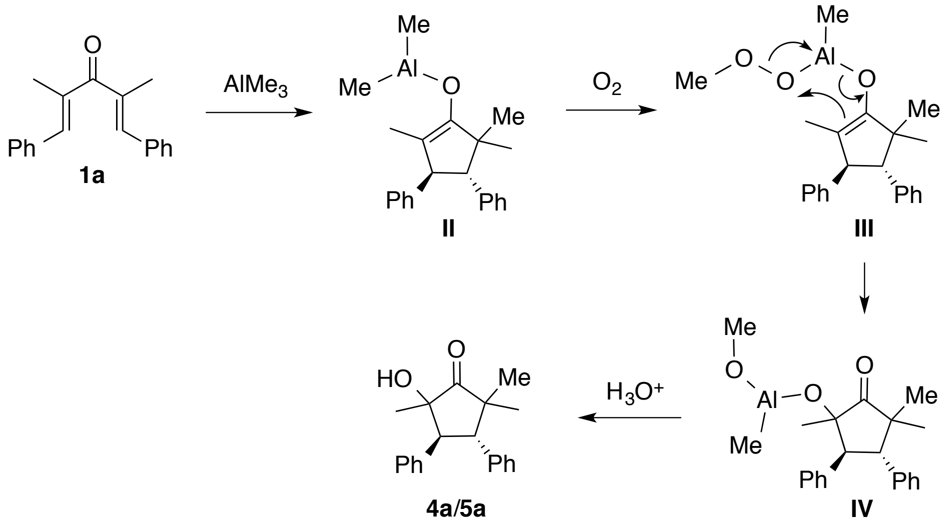

Scheme 3.9 Proposed Mechanism for the Aluminum Enolate Oxidation.

3.4 Conclusion

In summary, we have discovered a quick and convenient synthetic method to produce α-hydroxycyclopentanones via one-pot interrupted Nazarov cyclization/oxidation using trimethylaluminum and triplet oxygen. During the process, three new bonds were formed, two of which formed fully substituted α-carbons. The oxidation is cost-effective, operationally simple, and environmentally friendly. The mechanistic details of the unprecedented oxidation have not been fully investigated, but efforts will be made to elucidate them in the future.

3.5 Future Directions

The unique reactivity of the aluminum enolate with oxygen has rarely been studied except for our interrupted Nazarov reaction and Kunz's work[87]. This method could be more general and extended since there are other ways of generating aluminum enolates.

Organoaluminum reagents have been used with Cu(I) for 1,4-addition to α,β-unsaturated ketones. I am curious to see if the resulting enolate would react with triplet oxygen to introduce an α-hydroxy substituent (Scheme 3.10).

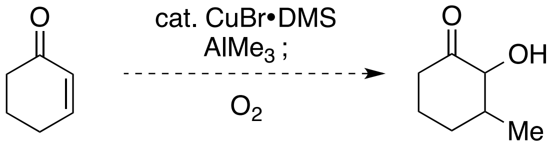

Scheme 3.10 Future Plan: One-Pot 1,4-Addition and Aluminum Enolate Oxidation.

In 1979, Nozaki and co-workers used an aluminum amide for crossed aldol reactions (Scheme 3.11).[95] The aluminum reagent was prepared by mixing diethylaluminum chloride with lithium tetramethylpiperidide.

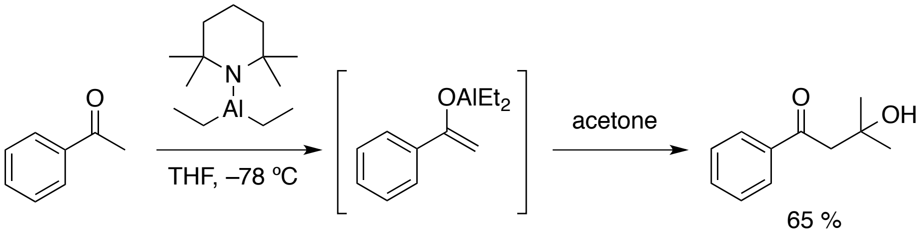

Scheme 3.11 Diethylaluminum 2,2,6,6-Tetramethylpiperidine Mediated Crossed Aldol Reaction.

Adopting the aluminum amide chemistry, I proposed a new synthetic route to make α-hydroxy ketones (Scheme 3.12). The aluminum enolate can be simply prepared from a ketone by using the aluminum amide. It would be interesting to see if the enolate could be oxidized to α-hydroxy ketones upon exposure to atmospheric oxygen. This method could be an alternative to other hydroxylation reactions such as the Rubottom oxidation[96] and MoOPH mediated oxidation.[97]

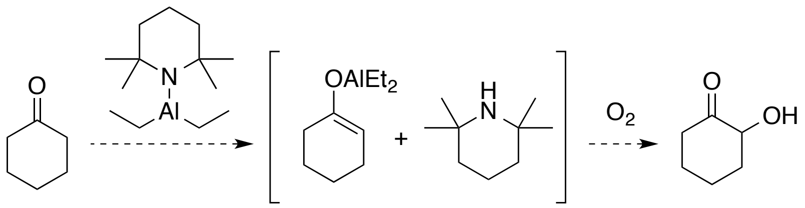

Scheme 3.12 Future Plan: Aluminum Amide and Triplet Oxygen.

The mechanism of the oxidation should be explored experimentally. If the excess amounts of $AlMe_3$ are responsible for the oxidation, not the aluminum enolate, it is conceivable that use of $AlMe_3$ and O_2 on silyl enol ethers could be an alternative method for the Rubottom oxidation (Scheme 3.13). This experiment may not be practical, but could at least provide some insights for the mechanism.

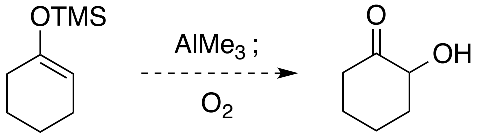

Scheme 3.13 Control Experiment: Rubottom Oxidation.

3.6 Experimental

3.6.1 General Information

Reactions were carried out in flame-dried glassware under a positive argon atmosphere unless otherwise stated. Transfer of anhydrous solvents and reagents was accomplished with oven-dried syringes or cannulae. 4 Å molecular sieves were stored in ovens, and flame-dried before use. Solvents were distilled before use: dichloromethane from calcium hydride, tetrahydrofuran and toluene from sodium/benzophenone ketyl. Thin layer chromatography was performed on glass plates precoated with 0.25 mm Kieselgel 60 F254 (Merck). Flash chromatography columns were packed with 230-400 mesh silica gel (Silicycle). Proton nuclear magnetic resonance spectra (^{1}H NMR) were recorded at 400 MHz or 500 MHz and coupling constants (*J*) are reported in Hertz (Hz). Standard notation is used to describe the multiplicity of signals observed in ^{1}H NMR spectra: broad (br), apparent (app), multiplet (m), singlet (s), doublet (d), triplet (t), etc. Carbon nuclear magnetic resonance spectra (^{13}C NMR) were recorded at 100 MHz or 125 MHz and are reported (ppm) relative to the center line of the triplet from chloroform-*d* (77.06 ppm). Infrared (IR) spectra were measured with a Mattson Galaxy Series FT-IR 3000 spectrophotometer. High-resolution mass spectrometry (HRMS) data (APPI/APCI/ESI technique) were recorded using an Agilent Technologies 6220 oaTOF instrument. HRMS data (EI technique) were recorded using a Kratos MS50 instrument. Extra dry oxygen (99.6 %, H_2O < 10 ppm) from Praxair was used for the oxidation.
Dienones **1a**,[81] **1b**,[82] **1c**,[39] **1d**,[50] **1e**,[39] **1f**,[21] **1g**,[67a] and **1h**,[90] were prepared via literature procedures.

3.6.2 Experimental Procedures and Characterization for the Synthesis of α-Hydroxycyclopentanones

Representative procedure for the construction of α-hydroxycyclopentanones (4a/5a)

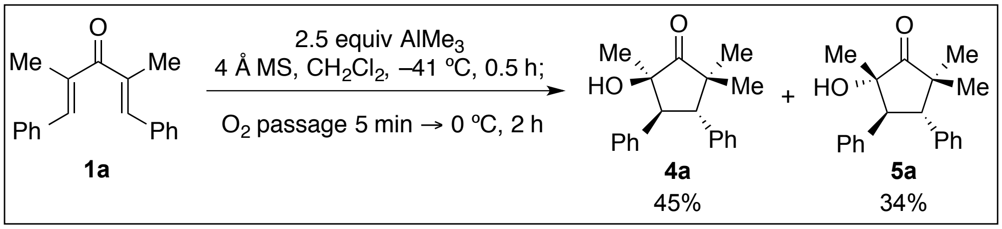

Activated 4Å molecular sieves (100 mg) were suspended in a solution of **1a** (50 mg, 0.19 mmol) in CH_2Cl_2 (1.9 mL, 0.1M). The mixture was cooled to –41 ºC and $AlMe_3$ (0.24 mL, 2.0 M solution in toluene) was added dropwise. The reaction mixture was stirred at –41 ºC until complete consumption of **1a** was observed by TLC (30 min). The solution was purged with O_2 gas for 5 min at –41 ºC, then the solution was allowed to warm to 0 ºC under a static oxygen atmosphere and stirred for 2 hrs. The reaction was quenched with 1M aq. HCl (3 mL) and warmed to room temperature. After separation of the phases, the aqueous layer was extracted with CH_2Cl_2 (3 x 10 mL). The combined organic extracts were washed with brine, and dried over $MgSO_4$, filtered, and concentrated in vacuo. Purification by flash column chromatography (silica gel) provided the desired products **4a** (25 mg, 45 %) and **5a** (19 mg, 34%).

Spectral Data of 4a/5a to 4g/5g, and 6h/7h

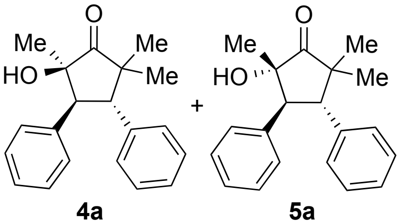

4a **5a**

Reaction was performed under the standard procedure. Flash chromatography (19:1 to 8:2 hexane:EtOAc) gave **4a** (25 mg, 45 %) and **5a** (19 mg, 34 %) as white solids.

4a: R_f 0.42 (hexanes/EtOAc 8:2); mp 188-190 °C; IR (cast film) 3442, 3026, 2982, 1737, 1449, 1394 cm^{-1}; ^1H NMR (500 MHz, $CDCl_3$) δ 7.32-7.13 (m, 10H), 3.89 (d, J = 13.2 Hz, 1H), 3.53 (d, J = 13.2 Hz, 1H), 1.57 (br, 1H), 1.37 (s, 3H), 1.33 (s, 3H), 0.75 (s, 3H); ^{13}C NMR (125 MHz, $CDCl_3$) δ 219.3 136.9, 135.3, 129.8, 129.0, 128.3, 128.1, 127.3, 126.8, 76.4, 53.1, 52.7, 48.5, 24.5, 22.4, 20.6; HRMS (EI, M$^+$) for $C_{20}H_{22}O_2$ calcd. 294.1620, found: m/z 294.1619.

5a: R$_f$ 0.33 (hexanes/EtOAc 8:2); mp 191-194 °C; IR (cast film) 3426, 3030, 2972, 1739, 1498, 1451 cm^{-1}; ^{1}H NMR (500 MHz, $CDCl_3$) δ 7.30-7.16 (m, 10H), 3.96 (d, *J* = 13.5 Hz, 1H), 3.54 (d, *J* = 13.5 Hz, 1H), 2.75 (s, 1H), 1.32 (s, 3H), 0.99 (s, 3H), 0.81 (s, 3H); ^{13}C NMR (125 MHz, $CDCl_3$) δ 223.1, 136.7, 136.3, 128.9, 128.9, 128.3, 128.2, 126.9, 126.9, 79.9, 51.4, 51.1, 47.3, 24.9, 21.5, 20.7; HRMS (EI, M$^+$) for $C_{20}H_{22}O_2$ calcd. 294.1620, found: m/z 294.1616.

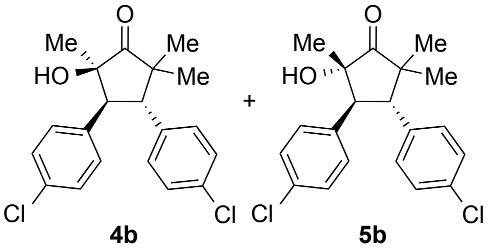

Dienone **1b** (53 mg, 0.16 mmol) was stirred with $AlMe_3$ for 1 h at –41 ºC, and then was stirred for 3 h at 0 ºC under O_2 atmosphere. Flash chromatography (19:1 to 8:2 hexane:EtOAc) gave **4b** (22 mg, 38 %) and **5b** (18 mg, 31 %) as white solids.

4b: R$_f$ 0.34 (hexanes/EtOAc 8:2); mp 152-154 °C; IR (cast film) 3462, 2969, 1741, 1494, 1092, 760 cm^{-1}; ^{1}H NMR (500 MHz, $CDCl_3$) δ 7.25-7.22 (m, 6H), 7.10-7.08 (m, 2H), 3.82 (d, *J* = 13.2 Hz, 1H), 3.42 (d, *J* = 13.2 Hz, 1H), 1.70 (s, 1H), 1.37 (s, 3H), 1.32 (s, 3H), 0.77 (s, 3H); ^{13}C NMR (125 MHz, $CDCl_3$) δ 218.7 135.1, 133.6, 133.3, 132.8, 131.0, 130.1, 128.5, 128.5, 76.2, 52.7, 52.6, 48.3, 24.5, 22.2, 20.4; HRMS (EI, M$^+$) for $C_{20}H_{20}O_2{}^{35}Cl_2$ calcd. 362.0841, found: m/z 362.0840.

5b: R$_f$ 0.23 (hexanes/EtOAc 8:2); mp 145-147 °C; IR (cast film) 3449, 2970, 1746, 1494, 1092, 756 cm^{-1}; ^{1}H NMR (500 MHz, $CDCl_3$) δ 7.28-7.23 (m, 4H), 7.20-7.18 (m, 2H), 7.14-7.11 (m, 2H), 3.86 (d, *J* = 13.5 Hz, 1H), 3.45 (d, *J* = 13.5 Hz, 1H), 2.77 (s, 1H), 1.30 (s, 3H), 0.97 (s, 3H), 0.80 (s, 3H); ^{13}C NMR (125 MHz, $CDCl_3$) δ 222.3, 134.9, 134.5, 133.1, 133.0, 130.2, 130.1, 128.8, 128.5, 79.7, 51.0, 50.7, 47.3, 24.8, 21.4, 20.6; HRMS (EI, M$^+$) for $C_{20}H_{20}O_2{}^{35}Cl_2$ calcd. 362.0841, found: m/z 362.0835.

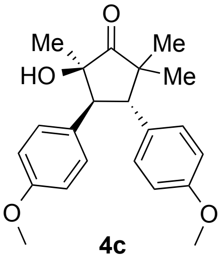
4c

+

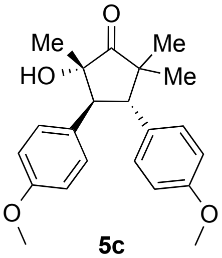
5c

Dienone **1c** (51 mg, 0.15 mmol) was stirred with $AlMe_3$ for 1 h at –41 ºC, and then was stirred for 2 h at 0 ºC under O_2 atmosphere. Flash chromatography (19:1 to 8:2 hexane:EtOAc) gave **4c** (22 mg, 41 %) as a white solid, and **5c** (19 mg, 36 %) as a colorless oil.

4c: R_f 0.47 (hexanes/EtOAc 2:1); mp 130-133 °C; IR (cast film) 3469, 2965, 2932, 2836, 1742, 1514, 1248 cm^{-1}; ^1H NMR (500 MHz, $CDCl_3$) δ 7.25-7.22 (m, 2H), 7.10-7.07 (m, 2H), 6.84-6.81 (m, 2H), 6.80-6.77 (m, 2H), 3.78 (d, J = 13.2 Hz, 1H), 3.76 (s, 3H), 3.75 (s, 3H), 3.45 (d, J = 13.2 Hz, 1H), 1.57 (s, 1H), 1.37 (s, 3H), 1.31 (s, 3H), 0.76 (s, 3H); ^{13}C NMR (125 MHz, $CDCl_3$) δ 219.7 158.8, 158.4, 130.7, 129.9, 129.0, 127.2, 113.8, 113.6, 76.3, 55.1, 55.1, 52.6, 52.2, 48.5, 24.5, 22.5, 20.5; HRMS (EI, M^+) for $C_{22}H_{26}O_4$ calcd. 354.1831, found: m/z 354.1832.

5c: R_f 0.35 (hexanes/EtOAc 2:1); IR (film) 3464, 2966, 1743, 1515, 1249 cm^{-1}; ^1H NMR (500 MHz, $CDCl_3$) δ 7.20-7.17 (m, 2H), 7.13-7.10 (m, 2H), 6.83-6.78 (m, 4H), 3.84 (d, J = 13.5 Hz, 1H), 3.77 (s, 3H), 3.75 (s, 3H), 3.43 (d, J = 13.4 Hz, 1H), 2.73 (s, 1H), 1.29 (s, 3H), 0.97 (s, 3H), 0.79 (s, 3H); ^{13}C NMR (125 MHz, $CDCl_3$) δ 223.5, 158.5, 158.4, 129.9, 129.8, 128.7, 128.4, 113.8, 113.7, 80.0, 55.2, 55.1, 51.0, 50.6, 47.3, 24.9, 21.4, 20.7; HRMS (EI, M^+) for $C_{22}H_{26}O_4$ calcd. 354.1831, found: m/z 354.1838.

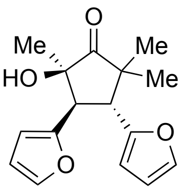
4d

+

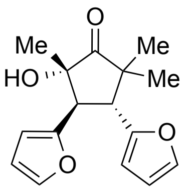
5d

Dienone **1d** (50 mg, 0.21 mmol) was stirred with $AlMe_3$ for 1 h at –41 ºC, and then was stirred for 3 h at 0 ºC under O_2 atmosphere. Flash chromatography (19:1 to 8:2 hexane:EtOAc) gave **4d** (21 mg, 36 %) and **5d** (16 mg, 28 %) as white solids.

4d: R$_f$ 0.34 (hexanes/EtOAc 8:2); mp 131-133 °C; IR (cast film) 3428, 2973, 2933, 1740, 1505, 1147, 1006, 724 cm^{-1}; ^{1}H NMR (500 MHz, CDCl$_3$) δ 7.39 (dd, *J* = 1.8, 0.8 Hz, 1H), 7.34 (dd, *J* = 1.9, 0.8 Hz, 1H), 6.34 (dd, *J* = 3.3, 1.9 Hz, 1H), 6.29 (dd, *J* = 3.2, 1.8 Hz, 1H), 6.21 (ddd, *J* = 3.3, 0.7, 0.7 Hz, 1H), 6.08 (ddd, *J* = 3.2, 0.7, 0.7 Hz, 1H), 3.78 (d, *J* = 12.8 Hz, 1H), 3.62 (d, *J* = 12.9 Hz, 1H), 1.92 (s, 1H), 1.46 (s, 3H), 1.38 (s, 3H), 0.82 (s, 3H); ^{13}C NMR (125 MHz, CDCl$_3$) δ 217.8 152.8, 150.9, 142.3, 141.8, 110.5, 110.1, 108.4, 107.4, 76.2, 48.4, 47.0, 47.0, 24.7, 22.3, 20.8; HRMS (EI, M$^+$) for $C_{16}H_{18}O_4$ calcd. 274.1205, found: m/z 274.1203.

5d: R$_f$ 0.20 (hexanes/EtOAc 8:2); mp 158-160 °C; IR (cast film) 3437, 2975, 1737, 1501, 1365, 1012, 742, 727 cm^{-1}; ^{1}H NMR (500 MHz, CDCl$_3$) δ 7.36 (dd, *J* = 1.9, 0.8 Hz, 1H), 7.32 (dd, *J* = 1.8, 0.8 Hz, 1H), 6.29 (dd, *J* = 3.3, 1.9 Hz, 1H), 6.27 (dd, *J* = 3.3, 1.8 Hz, 1H), 6.14 (ddd, *J* = 3.2, 0.8, 0.8 Hz, 1H), 6.06 (ddd, *J* = 3.2, 0.8, 0.8 Hz, 1H), 3.82 (d, *J* = 13.1 Hz, 1H), 3.51 (d, *J* = 13.1 Hz, 1H), 2.71 (s, 1H), 1.33 (s, 3H), 1.07 (s, 3H), 0.84 (s, 3H); ^{13}C NMR (125 MHz, CDCl$_3$) δ 221.7 152.4, 151.7, 142.1, 141.9, 110.2, 110.2, 108.0, 107.4, 79.8, 47.4, 46.7, 45.6, 25.1, 21.3, 21.1; HRMS (EI, M$^+$) for $C_{16}H_{18}O_4$ calcd. 274.1205, found: m/z 274.1204.

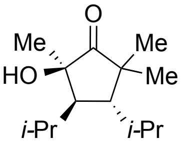

4e

+

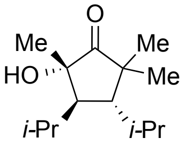

5e

Dienone **1e** (74 mg, 0.38 mmol) was stirred with AlMe$_3$ for 2 h at –25 ºC,[98] and then was stirred for 3 h at 0 ºC under O$_2$ atmosphere. Flash chromatography (49:1 to 9:1 hexane:EtOAc) gave **4e** (11 mg, 13 %) and **5e** (18 mg, 20 %) as white solids.

4e: R$_f$ 0.35 (hexanes/EtOAc 9:1); mp 106-108 °C; IR (cast film) 3458, 2964, 2891, 1744, 1385, 1372 cm^{-1}; ^{1}H NMR (500 MHz, CDCl$_3$) δ 2.06 ([X of ABXY] app sept of d, *J* = 7.1, 3.3 Hz, 1H), 1.97 ([Y of ABXY] app sept of d, *J* = 7.1, 3.0 Hz, 1H), 1.91-1.85 (AB portion of ABXY, J_{AB} = 10.6 Hz, $J_{AX} = J_{BY}$ = 3.3 Hz, 2H), 1.78 (s, 1H), 1.36 (s, 3H), 1.18 (s, 3H), 1.12 (d, *J* = 7.0 Hz, 3H), 1.06 (d, *J* = 7.0 Hz, 3H), 1.04 (d, *J* = 7.1 Hz, 3H), 1.01 (d, *J* = 7.0 Hz, 3H), 0.99 (s, 3H); ^{13}C NMR (125 MHz, CDCl$_3$) δ 224.2, 78.1, 50.1, 49.4, 47.9, 28.1, 27.5, 27.3, 26.0, 22.6, 21.6, 21.1, 20.2, 20.0; HRMS (EI, M$^+$) for $C_{14}H_{26}O_2$ calcd. 226.1933, found: m/z 226.1939.

5e: R*f* 0.20 (hexanes/EtOAc 9:1); mp 112-114 °C; IR (cast film) 3446, 2964, 2888, 1741, 1391, 1366 cm^{-1}; ^{1}H NMR (500 MHz, $CDCl_3$) δ 2.53 (s, 1H), 2.13 (app sept of d, *J* = 7.3, 3.9 Hz, 1H), 2.08 (app sept of d, *J* = 7.3, 3.3 Hz, 1H), 2.04 (dd, *J* = 12.9, 3.8 Hz, 1H), 1.81 (dd, *J* = 12.9, 3.3 Hz, 1H), 1.23 (s, 3H), 1.19 (s, 3H), 1.18 (d, *J* = 7.2 Hz, 3H), 1.12 (d, *J* = 7.2 Hz, 3H), 1.09 (d, *J* = 7.3 Hz, 3H), 1.08 (s, 3H), 1.06 (d, *J* = 7.3 Hz, 3H); ^{13}C NMR (125 MHz, $CDCl_3$) δ 225.9, 80.2, 49.8, 49.0, 46.8, 27.5, 27.1, 26.8, 22.1, 21.8, 20.9, 20.7, 20.7, 19.6; HRMS (EI, M$^+$) for $C_{14}H_{26}O_2$ calcd. 226.1933, found: m/z 226.1933.

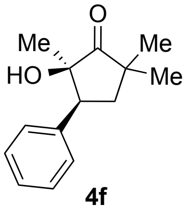

4f

+

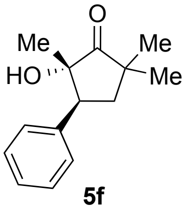

5f

Dienone **1f** (58 mg, 0.31 mmol) was stirred with $AlMe_3$ for 150 min at –41 ºC, and then was stirred for 3 h at 0 ºC under O_2 atmosphere. Flash chromatography (19:1 to 9:1 hexane:EtOAc) gave **4f** (22 mg, 32 %) and **5f** (24 mg, 36 %) as white solids.

4f: R*f* 0.45 (hexanes/EtOAc 8:2); mp 116-118 °C; IR (cast film) 3431, 3029, 2972, 1742, 1455, 706 cm^{-1}; ^{1}H NMR (500 MHz, $CDCl_3$) δ 7.41-7.36 (m, 4H), 7.35-7.32 (m, 1H), 3.08 (dd, *J* = 13.1, 6.4 Hz, 1H), 2.46 (app. t, *J* = 12.8 Hz, 1H), 1.99 (dd, *J* = 12.4, 6.4 Hz, 1H), 1.56 (s, 1H), 1.34 (s, 3H), 1.27 (s, 3H), 1.18 (s, 3H); ^{13}C NMR (125 MHz, $CDCl_3$) δ 220.2, 137.2, 129.5, 128.3, 127.4, 76.9, 50.0, 44.1, 40.4, 25.9, 25.3, 21.8; HRMS (EI, M$^+$) for $C_{14}H_{18}O_2$ calcd. 218.1307, found: m/z 218.1307.

5f: R*f* 0.32 (hexanes/EtOAc 8:2); mp 130-131 °C; IR (cast film) 3432, 3029, 2969, 1739, 1364 cm^{-1}; ^{1}H NMR (500 MHz, $CDCl_3$) δ 7.40-7.36 (m, 4H), 7.33-7.29 (m, 1H), 3.50-3.44 (m, 1H), 2.77 (s, 1H), 2.15-2.06 (m, 2H), 1.28 (s, 3H), 1.25 (s, 3H), 0.90 (s, 3H); ^{13}C NMR (125 MHz, $CDCl_3$) δ 224.3, 138.0, 128.3, 128.2, 127.0, 80.4, 48.1, 42.6, 37.7, 26.0, 26.0, 19.6; HRMS (EI, M$^+$) for $C_{14}H_{18}O_2$ calcd. 218.1307, found: m/z 218.1305.

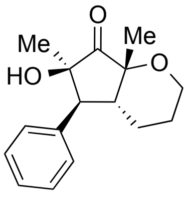
4g

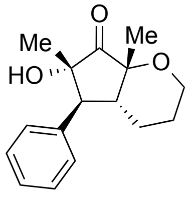
5g

Dienone **1g** (70 mg, 0.31 mmol) was stirred with AlMe$_3$ for 90 min at –41 ºC, and then was stirred for 4 h at 0 ºC under O$_2$ atmosphere. Flash chromatography (9:1 hexane:EtOAc) gave impure **4g**, and pure **5g** (25 mg, 31 %) as a white solid. Pure **4g** (colorless oil, 14mg, 18%) could be obtained after an additional flash chromatographic purification (1:4:19 to 2:6:16 to 2:3:5 Et$_2$O: DCM: Hex).

4g: R$_f$ 0.53 (hexanes/EtOAc 2:1); IR (film) 3488, 3027, 2933, 2861, 1759, 1453, 1374, 1054 cm^{-1}; ^{1}H NMR (500 MHz, CDCl$_3$) δ 7.42-7.38 (m, 2H), 7.36-7.32 (m, 3H), 3.83-3.79 (m, 1H), 3.72-3.67 (m, 1H), 3.43 (d, *J* = 12.9 Hz, 1H), 2.59-2.55 (m, 1H), 1.87-1.75 (m, 2H), 1.58-1.55 (m, 1H), 1.52 (br, 1H), 1.51 (s, 3H), 1.34 (s, 3H), 1.34-1.30 (m, 1H); ^{13}C NMR (125 MHz, CDCl$_3$) δ 211.9 135.7, 129.9, 128.5, 127.5, 76.9, 76.2, 61.9, 51.6, 40.5, 22.0, 20.0, 18.6, 16.6; HRMS (EI, M$^+$) for $C_{16}H_{20}O_3$ calcd. 260.1412, found: m/z 260.1413.

5g: R$_f$ 0.34 (hexanes/EtOAc 2:1); mp 176-178 °C; IR (cast film) 3449, 3030, 2942, 2859, 1753, 1370, 1057 cm^{-1}; ^{1}H NMR (500 MHz, CDCl$_3$) δ 7.42-7.38 (m, 2H), 7.34-7.27 (m, 3H), 3.86-3.82 (m, 1H), 3.77 (d, *J* = 13.2 Hz, 1H), 3.69 (ddd, *J* = 11.9, 11.9, 2.5 Hz, 1H), 2.57 (br, 1H), 2.32-2.28 (m, 1H), 1.93-1.75 (m, 3H), 1.48 (s, 3H), 1.37-1.32 (m, 1H), 0.91 (s, 3H); ^{13}C NMR (125 MHz, CDCl$_3$) δ 215.9, 136.1, 128.9, 128.6, 127.3, 79.6, 75.6, 61.9, 50.7, 38.2, 20.8, 20.2, 18.6, 17.3; HRMS (EI, M$^+$) for $C_{16}H_{20}O_3$ calcd. 260.1412, found: m/z 260.1415.

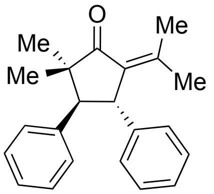
6h

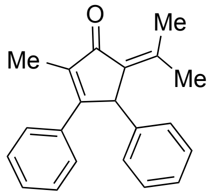
7h

To a solution of **1h** (50 mg, 0.16 mmol) in DCM was added 2.5 equiv of AlMe$_3$ at 0 ºC. The reaction mixture was warmed to rt and stirred for 26 h and then an additional 16 h under O_2 atmosphere. Flash chromatography (49:1 to 24:1 hexane:EtOAc) gave **6h** (19 mg, 39 %) as a colorless oil, and **7h** (10 mg, 22 %) as a white solid.

6h: R_f 0.43 (hexanes/EtOAc 9:1); IR (film) 3028, 2965, 2929, 1704, 1623, 705 cm^{-1}; ^{1}H NMR (500 MHz, $CDCl_3$) δ 7.11-7.03 (m, 6H), 6.89-6.85 (m, 2H), 6.63-6.60 (m, 2H), 4.53-4.51 (m, 1H), 3.37 (d, *J* = 8.6 Hz, 1H), 2.43 (d, *J* = 1.8 Hz, 3H), 1.62 (d, *J* = 1.0 Hz, 3H), 1.17 (s, 3H), 0.97 (s, 3H); ^{13}C NMR (125 MHz, $CDCl_3$) δ 211.3, 153.0, 141.3, 138.2, 132.5, 130.9, 129.6, 127.6, 127.3, 126.3, 126.0, 57.6, 50.5, 49.7, 26.6, 25.5, 22.3, 21.7; HRMS (EI, M$^+$) for $C_{22}H_{24}O$ calcd. 304.1827, found: m/z 304.1826.

7h: R_f 0.29 (hexanes/EtOAc 9:1); mp 138-141 °C; IR (cast film) 3026, 2919, 1679, 1623, 700 cm^{-1}; ^{1}H NMR (500 MHz, $CDCl_3$) δ 7.33-7.25 (m, 3H), 7.21-7.15 (m, 4H), 7.11-7.05 (m, 3H), 4.78 (br, 1H), 2.39 (d, *J* = 0.4 Hz, 3H), 1.98 (d, *J* = 1.8 Hz, 3H), 1.70 (s, 3H); ^{13}C NMR (125 MHz, $CDCl_3$) δ 197.5, 162.4, 147.3, 140.9, 139.4, 135.3, 134.5, 128.5, 128.4, 128.3, 128.2, 128.1, 126.4, 52.5, 24.0, 20.7, 9.9; HRMS (EI, M$^+$) for $C_{21}H_{20}O$ calcd. 288.1514, found: m/z 288.1515.

Chapter 4

Multi-Component Organoaluminum Interrupted Nazarov Cyclization

4.1 Introduction

Interruption of the Nazarov reaction has enabled facile access to a number of densely substituted cyclopentanone structures with new functionality.[1a, 7] The mode of the interruption can be sorted into three categories: (1) direct nucleophilic attack on one terminus of the oxyallyl cation,[50,99] (2) nucleophilic attack of the enol intermediate on an external electrophile,[100] and (3) cycloaddition of the oxyallyl cation with a π-system[101] (Scheme 4.1). However, sequential addition of a nucleophile and electrophile (not as a cycloaddition) to the Nazarov intermediate has not been achieved unless one counts protonation, perhaps due to spontaneous reaction between the two reagents.

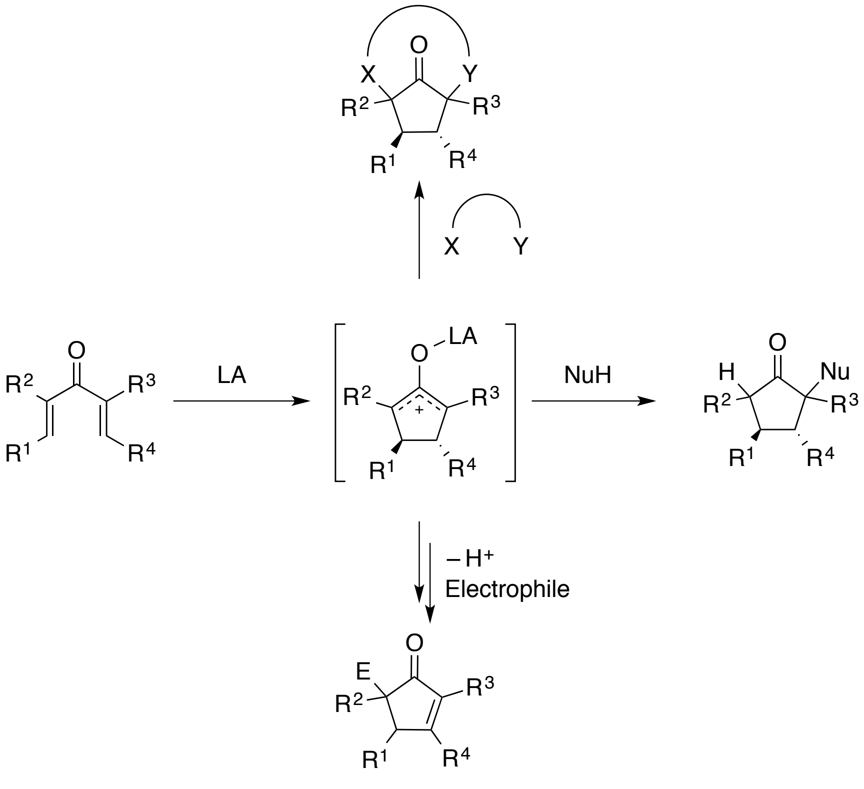

Scheme 4.1 Modes of Bond Formation in the Nazarov Reaction.

Recently, we reported a synthetic method to build α-hydroxycyclopentanones using trimethylaluminum and triplet oxygen.[86] The demonstration of a domino organoaluminum nucleophilic/molecular oxygen electrophilic dual interrupted Nazarov reaction (Scheme 4.2) led us to hypothesize that other double interrupted pathways for the development of diverse functionalization around the cyclopentanone core may be feasible.

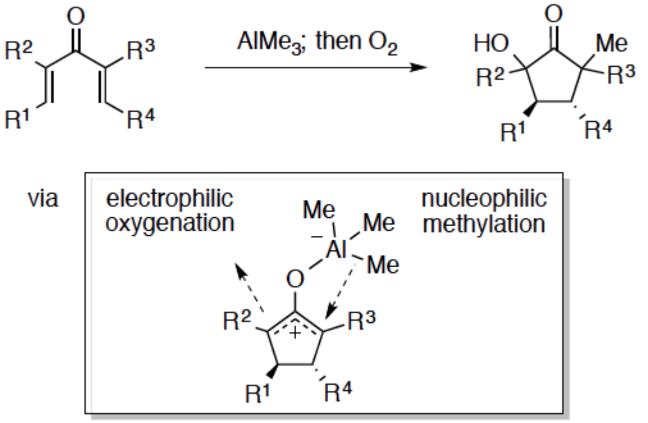

Scheme 4.2 One-Pot Oxidation of the Trimethylaluminum-Mediated Nazarov Reaction with Triplet Oxygen.

In this chapter, we will introduce the notion of intercepting the *in situ* generated aluminum enolate with electrophiles in one-pot and multi-component reactions, rather than simple protonation or oxidation by atmospheric oxygen.

4.2 Results and Discussion

4.2.1 Organoaluminum-Mediated Interrupted Nazarov Reaction and Electrophilic Trapping with Aldehydes

Since the early 1980s, organoaluminum reagents have been used in the Prins reaction: organoaluminum-catalyzed addition of alkenes to aldehydes and ketones, followed by nucleophilic addition onto the resulting carbocation. As an example, trimethylaluminum was used with formaldehyde to achieve sequential hydroxymethylation and vicinal methylation with alkenes[102] and enol ethers.[103]

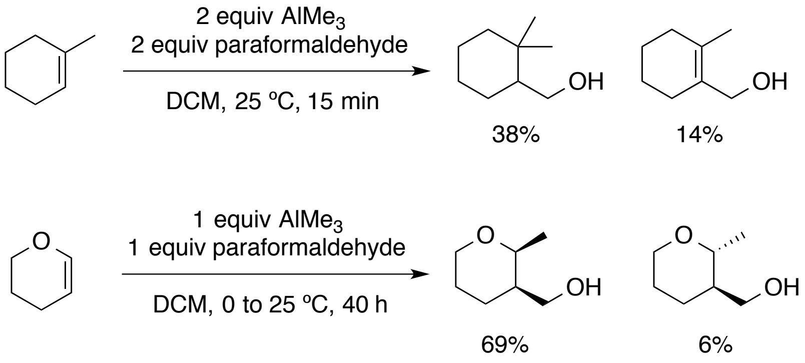
2 equiv AlMe3
2 equiv paraformaldehyde
DCM, 25 °C, 15 min
OH
OH
38%
14%
1 equiv AlMe3
1 equiv paraformaldehyde
DCM, 0 to 25 °C, 40 h
O
O
O
OH
OH
69%
6%

Scheme 4.3 Domino Prins Reaction/Organoaluminum Carbocation Capture.

The Prins reaction is believed to begin with the nucleophilic addition onto the activated carbonyl by the alkene, followed by either trapping of the carbocation or proton elimination. I speculatively considered the alkene as a platform where electrophilic and nucleophilic additions can harmonize. Consequently, I was curious to see if we could apply the symbiosis of the electrophile and nucleophile to the Nazarov oxyallyl cation intermedate (Figure 4.1) despite the fact that sequence of nucleophilic and electrophilic additions in the Prins reaction are opposite to what would need to occur in a doubly interrupted Nazarov reaction.

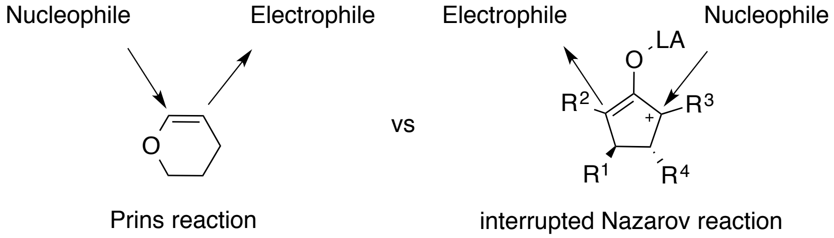
Nucleophile
Electrophile
O
Prins reaction
vs
Electrophile
Nucleophile
O
LA
R2
R3
+
R1
R4
interrupted Nazarov reaction

Figure 4.1 Comparison of the Prins Reaction to the Interrupted Nazarov Reaction.

With this idea in mind, I designed a double interrupted Nazarov reaction in a one-pot and multi-component fashion (Scheme 4.4). As reported in Section 2.2.1, organoaluminum reagents behave as Lewis acids to initiate electrocyclization and as sources of alkyl nucleophiles.[50] In the presence of the organoaluminum, paraformaldehyde would be unmasked, so that the aluminum enolate **2** following the Nazarov cyclization and transfer of an aluminum ligand could attack the activated formaldehyde. This reaction would allow for access to a highly substituted cyclopentanone with three new C-C bonds and four contiguous stereocenters.

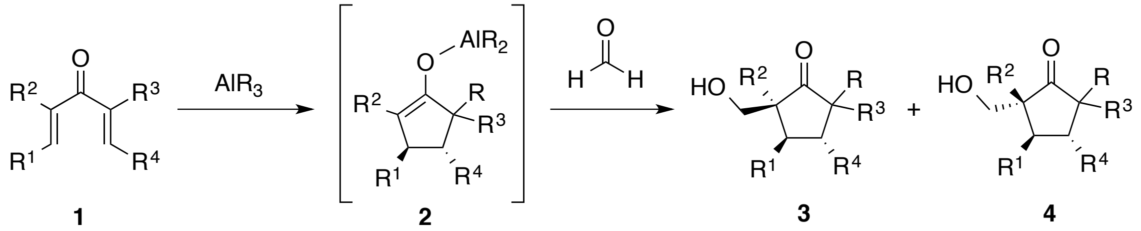
R2
O
R3
R1
R4
1
AlR3
AlR2
O
R2
R
R3
R1
R4
2
O
H
H
HO
R2
O
R
R3
R1
R4
3
+
HO
R2
O
R
R3
R1
R4
4

Scheme 4.4 Double Interrupted Nazarov Reaction.

Table 4-1 $AlMe_3$ Mediated Interrupted Nazarov Reaction and Electrophilic Addition of Formaldehyde.[a]

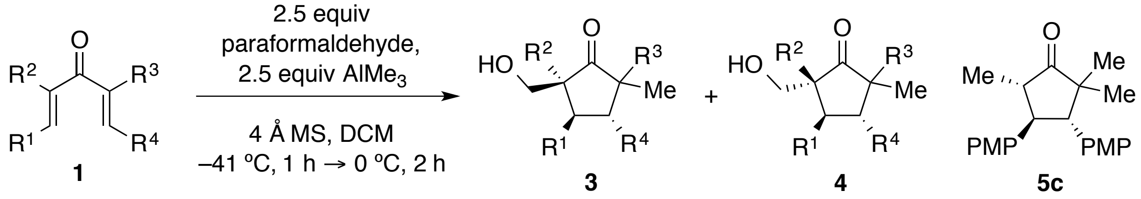

Entry	Substrate	R^1	R^2, R^3	R^4	Products (Yield %)[b]
1	**1a**	Ph	Me	Ph	**3a** (76%), **4a** (6%)
2	**1b**	4-ClC_6H_4	Me	4-ClC_6H_4	**3b** (81%)
3	**1c**	4-$MeOC_6H_4$	Me	4-$MeOC_6H_4$	**3c** (34%), **4c** (4%), **5c** (43%)
4	**1d**	2-furyl	Me	2-furyl	**3d** (71%)
5[c]	**1e**	*i*-Pr	Me	*i*-Pr	No reaction
6[d]	**1f**	Ph	Me	H	**3f** (47%), **4f** (20%)

[a]Standard procedure: see experimental section [b] Yields are based on isolated product after chromatography. [c] The reaction was carried out from –25 to 0 ºC. [d] 4 equivalents of $AlMe_3$ were used. After the addition of $AlMe_3$, the reaction mixture was stirred for 2 h at –41 ºC and 2 h at 0 ºC.

We began our study with symmetrical Nazarov substrates **1a**-**1e** (Table 4-1). Dienone **1a** afforded the desired products **3a** and **4a** in great yield with high dr (13:1) (entry 1). Single crystal X-ray diffraction analysis was used to determine the relative configuration of minor product **4a** (Figure 4.2). The reaction conditions (stoichiometry and use of the molecular sieves) were taken from the reported organoaluminum-mediated interrupted Nazarov chemistry. 2.5 Equivalents of paraformaldehyde (2.5:1.0 ratio of formaldehyde to dienone) were set as the previous Prins reaction used a 1:1 ratio of aldehyde to organoaluminum. Under the same condition, paramethoxyphenyl (PMP) substituted divinyl ketone **1c** was converted to **3c** and **4c** in only 38 % overall yield (entry 3). Based on the amount of mono-interrupted Nazarov product **5c**, the enolate addition to the activated formaldehyde was not as effective. In the case of **1b** and **1d** (entry 2, 4), aluminum enolate addition to formaldehyde occurred in a more selective manner since signals of minor diastereomers were not detected in ^{1}H NMR spectra, nor was any of the minor isomer detected during purification. The stereoselectivity dropped noticeably when trisubstituted dienone **1f** was subjected to the reaction conditions, affording **3f** and **4f** in 2.4:1.0 ratio (entry 6). The relative configuration of **3f** was determined by single crystal X-ray diffraction analysis (Figure 4.3). Unfortunately, we found a limitation of this multi-component reaction. Tetraalkyl substituted substrate **1e** was intact at –25 to 0 ºC (entry 5). In the earlier report, **1e** was converted to methylated cyclopentanone **5e** in moderate yield (Scheme 4.5).[99] Failure to consume **1e** may result from competitive Lewis acid-base interaction of $AlMe_3$ and paraformaldehyde.

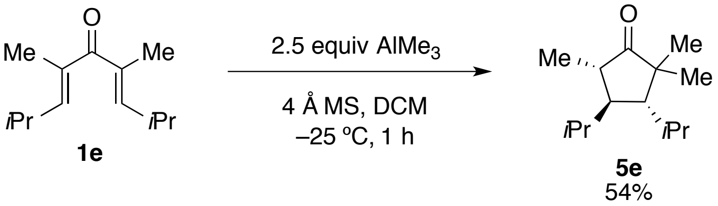

Scheme 4.5 $AlMe_3$-Mediated Interrupted Nazarov Reaction of **1e**.

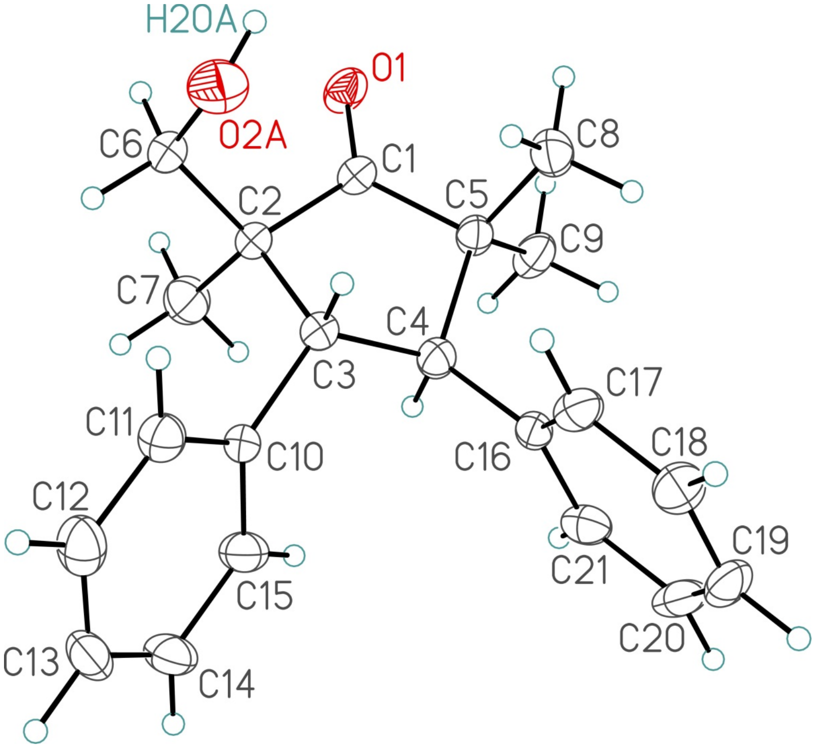
H2OA
O1
O2A
C6
C1
C8
C2
C5
C9
C7
C4
C3
C17
C11
C10
C16
C18
C12
C19
C15
C21
C20
C13
C14

(Thermal ellipsoids shown at the 30 % probability level)

Figure 4.2 ORTEP Drawing of **4a**.

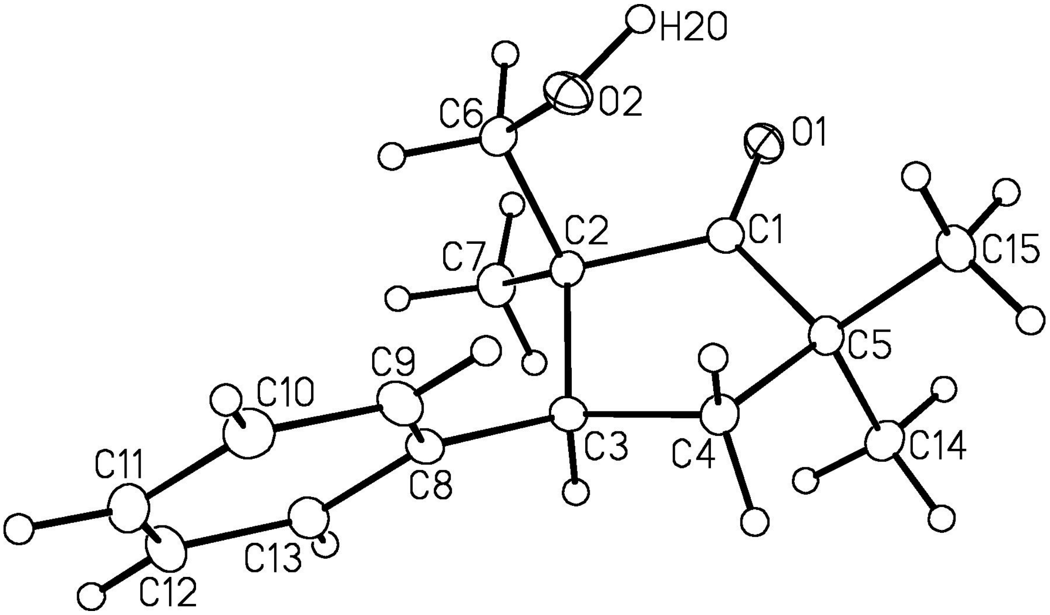
H2O
C6
O2
O1
C2
C1
C7
C15
C9
C5
C10
C11
C8
C3
C4
C14
C13
C12

(Thermal ellipsoids shown at the 20 % probability level)

Figure 4.3 ORTEP Drawing of **3f**.

Next, we studied the reactivity of dienone **1a** in the presence of paraformaldehyde and $AlEt_3$ (Scheme 4.6). Dienone **1a** afforded a mixture of three diastereomers **6a**, **6a'**, and **7a** in 59 % overall yield.

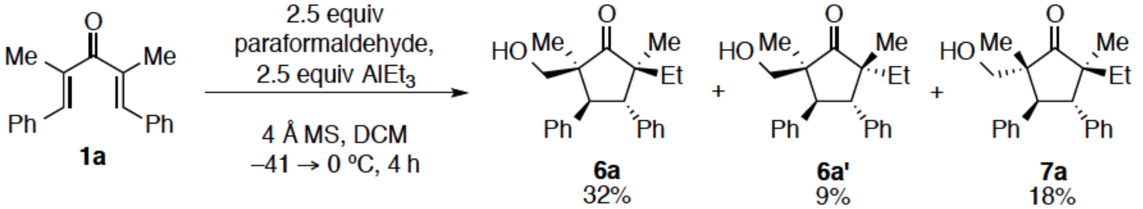

Me
Me
O
Ph
Ph
1a
2.5 equiv paraformaldehyde, 2.5 equiv AlEt3
4 Å MS, DCM
–41 → 0 °C, 4 h
HO
Me
O
Me
Et
Ph
Ph
6a
32%
+
6a'
9%
+
7a
18%

Scheme 4.6 $AlEt_3$ Mediated Interrupted Nazarov Reaction in Paraformaldehyde.

As **6a** and **6a'** were isolated as an inseparable mixture, the geometry was tentatively assigned by using ^1H NMR chemical shift correlations (Figure 4.4). Upfield ^1H NMR chemical shifts for the alcohol methylene protons in a *syn* relationship to β-aryl groups were observed in **6a** and **6a'**. In addition, product **6a** displays a methyl singlet at 0.83 ppm, which is more shielded relative to its *trans* counterparts (~1.35-1.24 ppm). Following this trend, the configuration of **7a** was also assigned.

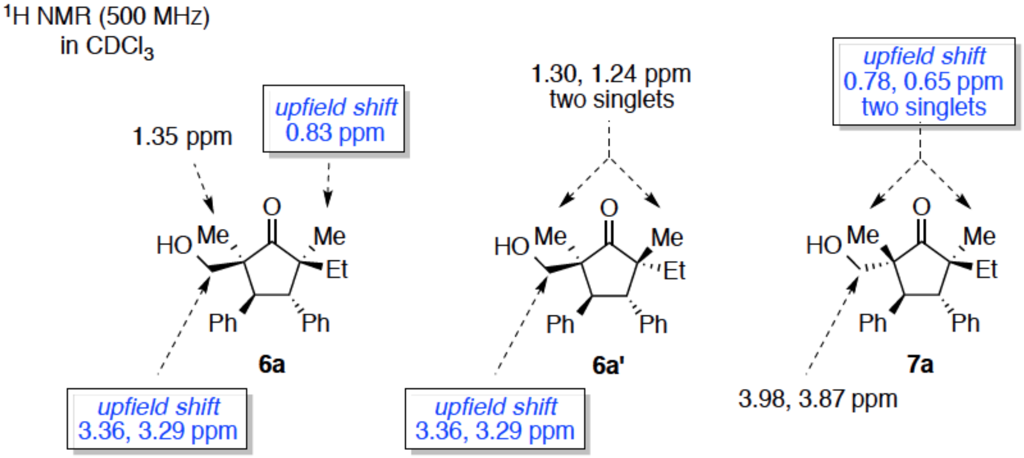

1H NMR (500 MHz) in CDCl3
1.35 ppm
upfield shift 0.83 ppm
1.30, 1.24 ppm two singlets
upfield shift 0.78, 0.65 ppm two singlets
HO
Me
O
Me
Et
Ph
Ph
6a
6a'
7a
upfield shift 3.36, 3.29 ppm
upfield shift 3.36, 3.29 ppm
3.98, 3.87 ppm

Figure 4.4 ^1H NMR Chemical Shift Correlations of **6a**, **6a'**, and **7a**.

The multi-component approach with paraformaldehyde was extended to the reductive Nazarov reaction.[29,30] In the presence of Et_2AlCl, Et_3SiH and paraformaldehyde, **1a** was converted to an equimolar quantity of **8a** and **9a** (Scheme 4.7). The hydride transfer occurred stereoselectively to the same face as β-phenyl group. This trend was seen previously in the reductive Nazarov papers. Unfortunately, the enolate addition to formaldehyde was not selective, unlike the trimethylaluminum cases (see **3a** and **4a**). However, the use of Et_2AlCl has potential for introducing other nucleophiles and expanding the substrate scope as premature 1,2 addition is not a concern in this case.

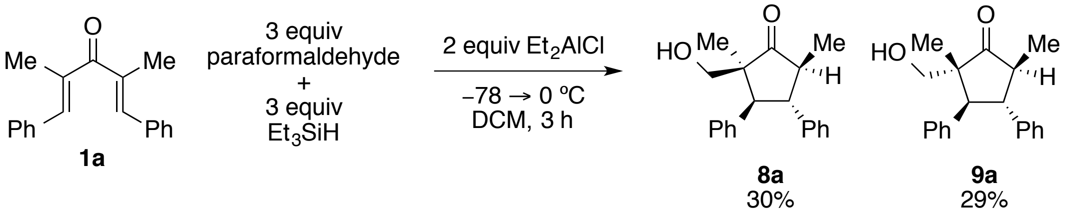
Me
Me
Ph
Ph
O
1a
3 equiv paraformaldehyde
+
3 equiv
Et3SiH
2 equiv Et2AlCl
−78 → 0 °C
DCM, 3 h
HO
Me
O
Me
H
Ph
Ph
8a
30%
HO
Me
O
Me
H
Ph
Ph
9a
29%

Scheme 4.7 Reductive Nazarov Reaction in Paraformaldehyde.

We assigned the configuration of products **8a** and **9a** by ^{1}H NMR using the differences in chemical shifts (Figure 4.5). The assignment was further confirmed by two X-ray crystallographic analyses (Figure 4.6).

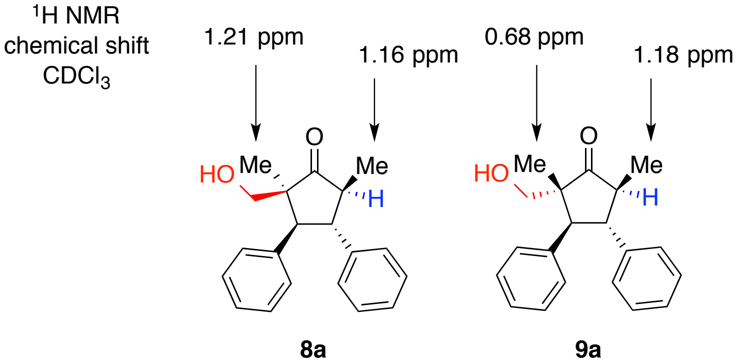
1H NMR
chemical shift
CDCl3
1.21 ppm
1.16 ppm
0.68 ppm
1.18 ppm
HO
Me
O
Me
H
HO
Me
O
Me
H
8a
9a

Figure 4.5 ^{1}H NMR Chemical Shift Correlations for **8a** and **9a**.

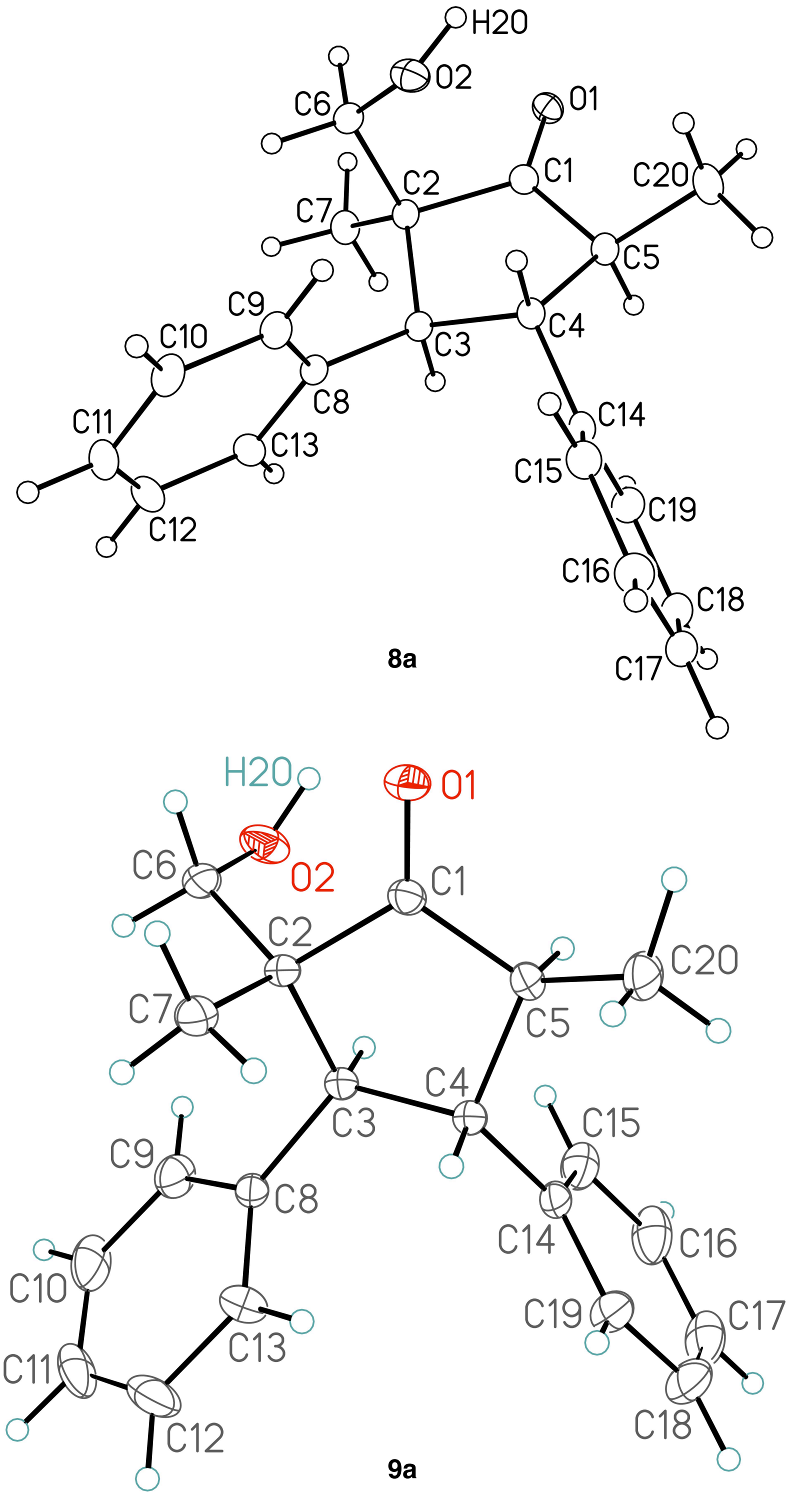
H20
O2
O1
C6
C1
C20
C2
C7
C5
C4
C9
C10
C3
C8
C14
C11
C13
C15
C19
C12
C16
C18
C17
H20
O1
O2
C6
C1
C2
C20
C7
C5
C4
C3
C15
C9
C8
C16
C14
C10
C19
C17
C13
C11
C12
C18

8a

9a

(Thermal ellipsoids shown at the 20 % probability level for **8a**)

(Thermal ellipsoids shown at the 30 % probability level for **9a**)

Figure 4.6 ORTEP Drawing of **8a** and **9a**.

Curious as to whether nucleophilic attack of the enolate onto acetaldehyde could be made in the interrupted Nazarov reaction, 0.83 equivalents of paraldehyde – the trimer of acetaldehyde – were used under the standard conditions with **1a** in place of paraformaldehyde (Scheme 4.8). The reaction produced almost equimolar quantities of **10a** and **11a** in low yield. Considerable amounts of **5a** (ca. 35 %) were also found in the crude ^{1}H NMR spectrum.

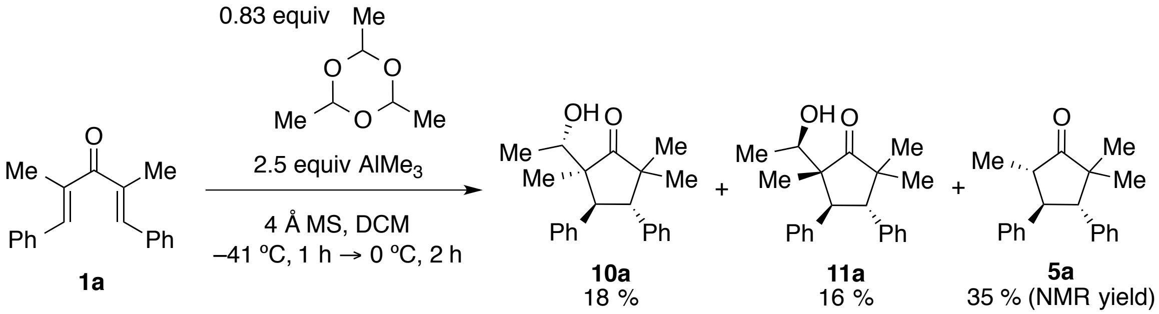

Scheme 4.8 Double Interrupted Nazarov Reaction with $AlMe_3$ and Paraldehyde.

The configuration of **10a** and **11a** was assigned tentatively. First, ^{1}H NMR chemical shifts of the alcoholic methine protons were compared in order to propose the stereochemistry at C-2 positions (Figure 4.7). An upfield shift was observed on the proton *syn* to β-phenyl group (**10a**). The configuration at the secondary alcohol centre has not been assigned rigorously; however, the indicated relative stereochemistry is proposed, based upon aldol addition of the aluminum enolate to acetaldehyde via a chair-like Zimmerman-Traxler transition state.

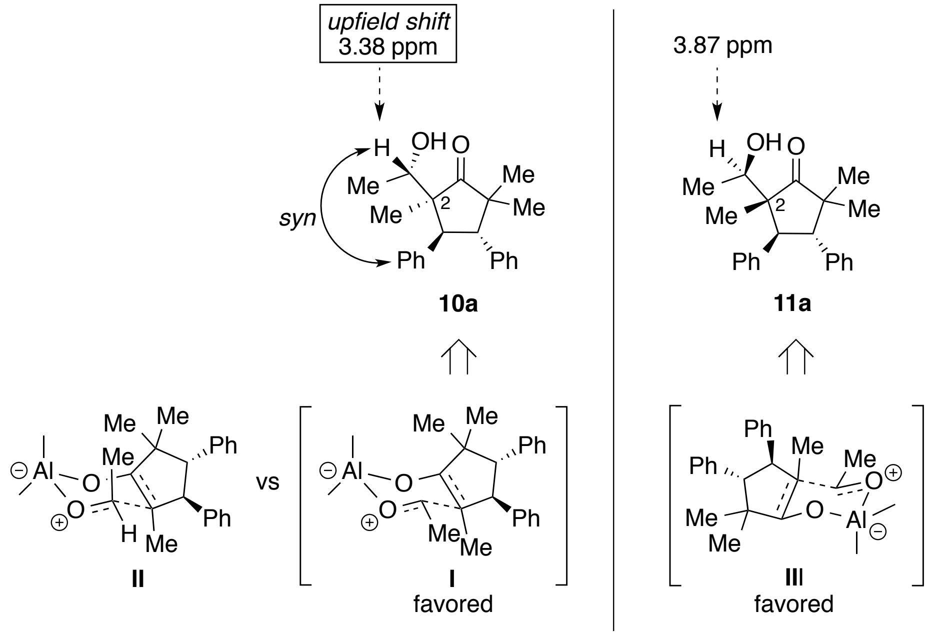

Figure 4.7 ^{1}H NMR Chemical Shift Correlations for **10a** and **11a** and 6-Membered Transition State.

4.2.2 Ring Expansion Strategy: Interrupted Nazarov Reaction and Simmons-Smith Type Cyclopropanation

Use of organoaluminum reagents can be found in cyclopropanation reactions. The history of organoaluminum-mediated cyclopropanation may begin with the research on diisobutylaluminum chloride. Triisobutylaluminum is known to react with carbon tetrachloride, providing the diisobutylaluminum chloride as well as isobutyl chloride byproduct. To explain the formation of diisobutylaluminum chloride and isobutyl chloride, Collette[104] proposed a carbene intermediate in the reaction, although no carbene-trapping experiments were carried out.

Corresponding to the Collette's proposal, Miller (reported in 1964) [105] experimentally carried out carbene-trapping reactions and studied the reactivity of both triethylaluminum and polyhalomethanes. Treating cyclohexene with 1.5 equivalents of $AlEt_3$ and 1 equivalent of CH_2I_2 afforded norcarane in 20 % yield (Scheme 4.9). It was the first example of an organoaluminum-mediated cyclopropanation. In the report, a noncarbene mechanism, involving an organoaluminum carbenoid Et_2AlCH_2I, was also proposed for the formation of the cyclopropane.

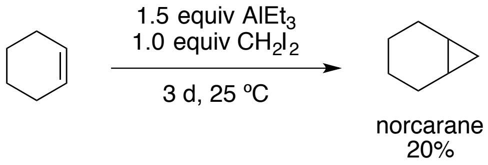
1.5 equiv $AlEt_3$
1.0 equiv CH_2I_2
3 d, 25 ºC
norcarane
20%

Scheme 4.9 First Organoaluminum-Mediated Cyclopropanation.

Following Miller's original report, in 1985 Yamamoto and co-workers established a reliable method to generate cyclopropane rings using trialkylaluminum reagents and CH_2I_2 (Scheme 4.10).[106] It was imperative to use equimolar amounts of the organoaluminum and CH_2I_2 to obtain the optimum yield as the dialkylaluminum iodide intermediate could undergo decomposition when excess amounts of trialkylaluminum reagents were available (Miller's case, 1.5:1.0 $AlEt_3$:CH_2I_2). Under the optimized conditions, all trialkylaluminum reagents (e.g., $AlMe_3$, $AlEt_3$, Al*i*Bu_3) provided cyclopropanated products in excellent yield. Two different solvents, DCM and hexane, were used in the cyclopropanation reactions.

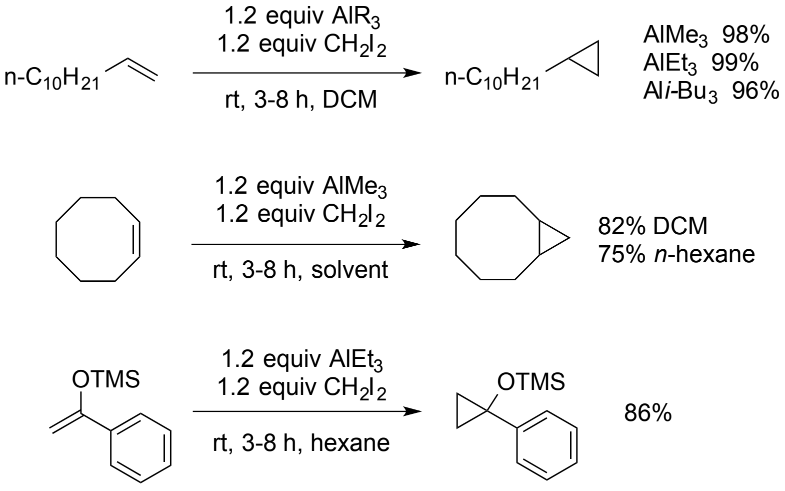
n-$C_{10}H_{21}$
1.2 equiv AlR_3
1.2 equiv CH_2I_2
rt, 3-8 h, DCM
n-$C_{10}H_{21}$
$AlMe_3$ 98%
$AlEt_3$ 99%
Al*i*-Bu_3 96%
1.2 equiv $AlMe_3$
1.2 equiv CH_2I_2
rt, 3-8 h, solvent
82% DCM
75% *n*-hexane
OTMS
1.2 equiv $AlEt_3$
1.2 equiv CH_2I_2
rt, 3-8 h, hexane
OTMS
86%

12

Scheme 4.10 Organoaluminum Mediated Cyclopropanation.

I was particularly interested in one of the examples in Yamamoto's report, namely the cyclopropanation of a silyl enol ether. Silyl enol ether **12** was converted to a cyclopropyl carbinol upon treatment with $AlEt_3$ and CH_2I_2. Digressing from the main subject, I saw a structural similarity of the substrate **12** and the aluminum enolate intermediate **2** (Figure 4.8).

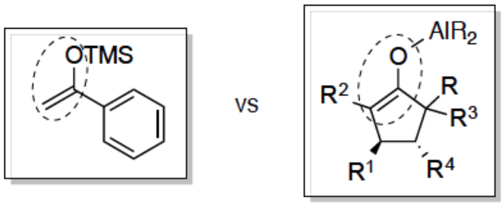
OTMS
vs
AlR2
O
R2
R
R3
R1
R4

12 **2**

Figure 4.8 Structural Similarity of TMS Enol Ether **12** and Aluminum Enolate **2**.

In the organoaluminum mediated interrupted Nazarov reaction, the aluminum enolates are protonated during acidic workup, providing highly substituted cyclopentanones. I wondered if the aluminum enolate **2** could be cyclopropanated by trialkylaluminum-alkylidene iodide to generate bicycloalkanols **13** (Scheme 4.11).

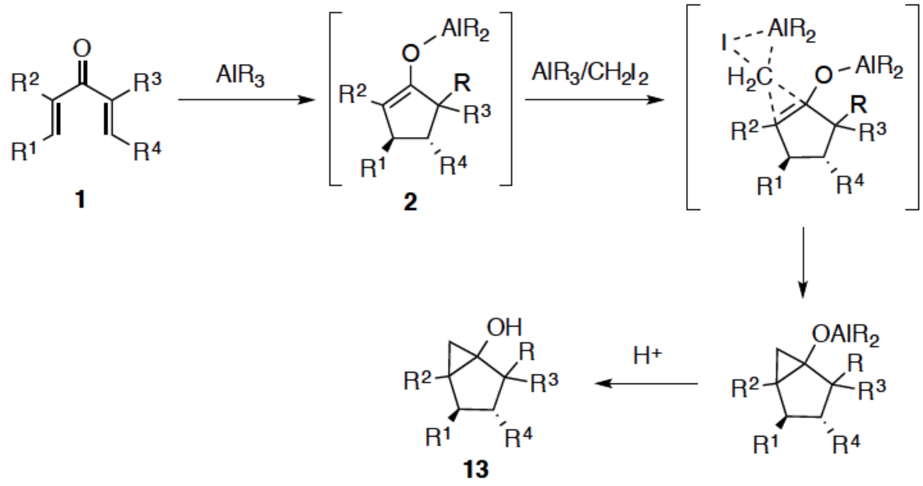
O
R2
R3
R1
R4
1
AlR3
AlR2
O
R2
R
R3
R1
R4
2
AlR3/CH2I2
I
AlR2
H2C
O
AlR2
R
R2
R3
R1
R4
OAlR2
R
R2
R3
R1
R4
H+
OH
R
R2
R3
R1
R4
13

Scheme 4.11 Domino Interrupted Nazarov Reaction/Cyclopropanation.

Dienone **1a** was chosen as a test substrate to evaluate possible reaction conditions to form the desired bicyclohexanol **13a** (Table 4-2). We began our investigation with standard reaction conditions from the trimethylaluminum interrupted Nazarov reaction discussed in Chapter 2: 2.5 equivalents of $AlMe_3$ in dichloromethane, with 2.5 equivalents of CH_2I_2. Unfortunately, only methyl interrupted Nazarov product **5a** was found (entry 1). Next, we looked at changing the solvent to hexanes. In this case, we found 2.5 equivalents of $AlMe_3$ and CH_2I_2 led to a small quantity of **13a** after 3 days (entry 2). After further optimization, we found that 3 equivalents of $AlMe_3$ and CH_2I_2 led to the highest yield of **13a** (65 %, entry 8).

Table 4-2 $AlMe_3$ /CH_2I_2 Mediated Interrupted Nazarov Reaction and Cyclopropanation.

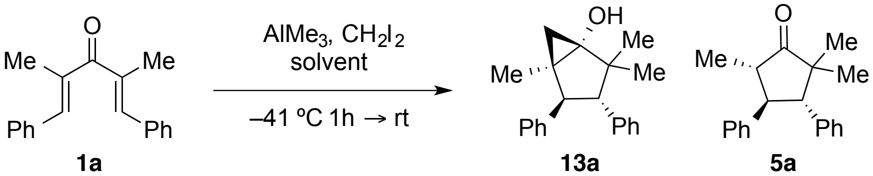

entry	$AlMe_3$ equiv	CH_2I_2 equiv	Solvent	Time	Product Yield (%)[a]
1	2.5 (2.0 M in toluene)	2.5	DCM	2 d	**5a** + complex mixture
2	2.5 (2.0 M in toluene)	2.5	hexane	3 d	**13a** (25%)[b]
3	4.0 (2.0 M in toluene)	2.5	toluene	2 d	**5a** + complex mixture
4	2.5 (2.0 M in toluene)	4.0	hexane	7 d	**13a** (11%) + **5a** (68%)
5	3.0 (2.0 M in hexane)	2.0	hexane	7 d	**13a** (40%) + **5a** (51%)
6	3.0 (2.0 M in hexane)	3.0	hexane	7 d	**13a** (61%)
7	3.0 (2.0 M in hexane)	4.0	hexane	7 d	**13a** (60%)
8	3.0 (2.0 M in hexane)	3.0	hexane	8 d	**13a** (65%)

[a] Yields are based on isolated product after chromatography. [b] **1a** was fully consumed, and **5a** was also found in the crude NMR.

The methodology was further probed with dienones **1b** and **1d** (Scheme 4.12). Under the optimized conditions, **1b** was converted to a mixture of **13b** and methylation product **5b**. In the case of furyl-substituted **1d**, TLC indicated the presence of methylated product **5d**, but as time went on, the reaction underwent decomposition, rather than forming **13d**.

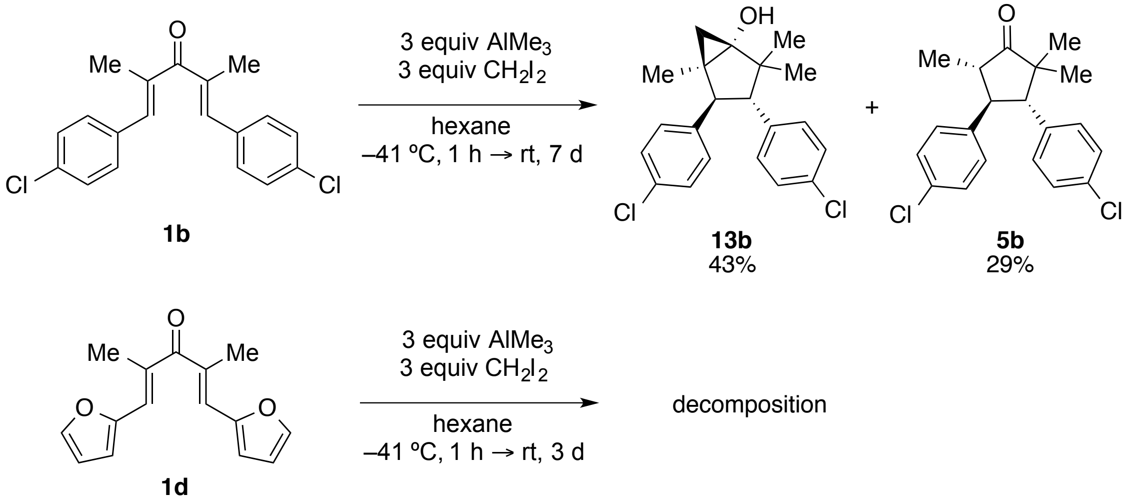

1b
3 equiv AlMe3
3 equiv CH2I2
hexane
–41 °C, 1 h → rt, 7 d
13b
43%
+
5b
29%
1d
3 equiv AlMe3
3 equiv CH2I2
hexane
–41 °C, 1 h → rt, 3 d
decomposition

Scheme 4.12 Test Substrates **1b** and **1d**.

A provisional structural assignment of **13a** was made using 2D NMR studies, indicating the carbenoid reacted with high stereoselectivity – *syn* to the adjacent β-phenyl substituent (Figure 4.9). The two benzylic methine protons $\mathbf{H_a}$ and $\mathbf{H_b}$ were assigned by a HMBC experiment: heteronuclear correlation between proton $\mathbf{H_a}$ and the -CH_2 carbon was detected. The two geminal protons were also differentiated, correlating with the benzylic methine protons by nOe experiment.

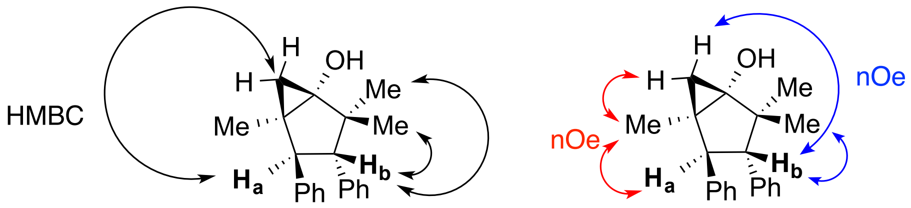
HMBC
H
H
OH
Me
Me
Me
Ha
Hb
Ph
Ph
nOe
nOe

key HMBC correlations

key nOe correlations

Figure 4.9 Diagnostic 2D NMR Correlations of **13a**

We found that upon storage **13a** began to decompose to a mixture of two new products that had incorporated two additional oxygen atoms into their respective molecular formula. Careful analysis of the spectral data led us to assign the new compounds as auto-oxidized peroxides **14a** and **15a** (Scheme 4.13). This autoxidation enabled us to make densely functionalized cyclohexanones with 4 stereocenters, which had not been accessible by Nazarov cyclization. The relative configuration of **14a** was determined by X-ray crystallography (Figure 4.10). Regarding the geometry of **14a**, placing bulky phenyl substituents on the equatorial positions of the chair conformation makes the peroxide substituent to be axial, which could attack a neighbouring carbonyl group. On the other hand, the peroxide of **15a** would be on the equatorial position, staying away from the carbonyl group.

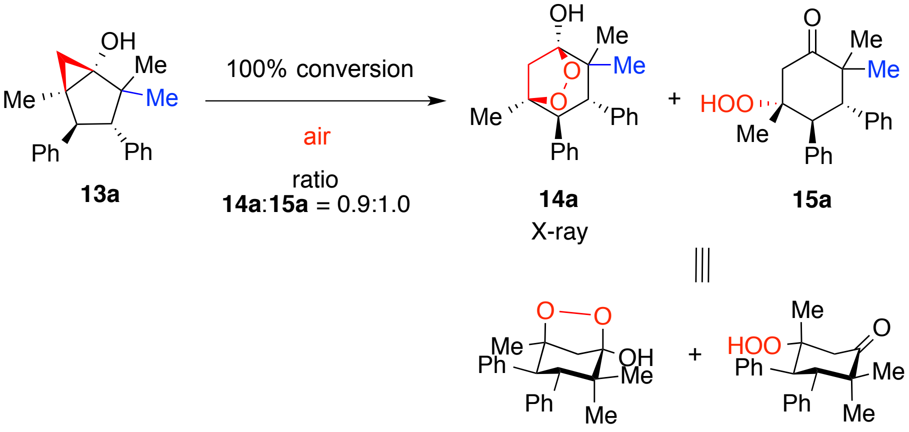
OH
Me
Me
Me
Ph
Ph
13a
100% conversion
air
ratio
14a:15a = 0.9:1.0
OH
Me
Me
O
O
Me
Ph
Ph
14a
X-ray
+
O
Me
Me
HOO
Me
Ph
Ph
15a
O
O
Me
Ph
OH
Me
Ph
Me
+
Me
HOO
Ph
O
Me
Ph
Me

Scheme 4.13 Autoxidation Product **14a** and **15a** and Rationale for Formation of a Peroxyacetal in the Case of **14a**.

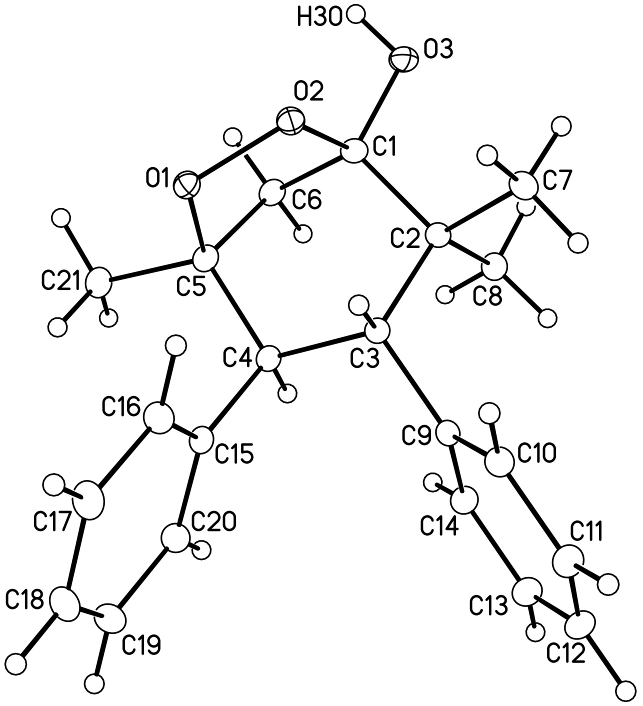
H3O
O3
O2
C1
O1
C6
C7
C2
C21
C5
C8
C4
C3
C16
C15
C9
C10
C17
C20
C14
C11
C18
C19
C13
C12

(Thermal ellipsoids shown at the 20 % probability level)

Figure 4.10 ORTEP Drawing of **14a**.

Considering the possibility that autoxidized products are one isomer in equilibrium, such as **14a** and **16a** (Scheme 4.14), I wanted to confirm that **14a** and **15a** were epimers and not tautomers.

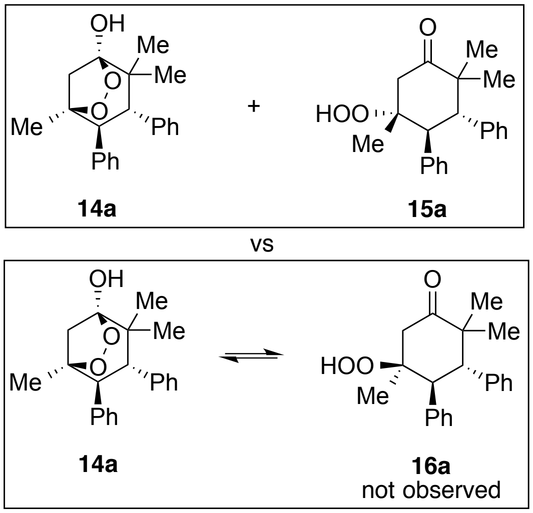
OH
Me
Me
O
O
Me
Ph
Ph
14a
+
O
Me
Me
HOO
Me
Ph
Ph
15a
vs
14a
16a
not observed

Scheme 4.14 Potential Equilibrium of Peroxides.

The following derivatization experiment confirmed the presence of epimers **14a** and **15a**. Treatment of the mixture of **14a** and **15a** with PPh_3 for one hour provided an equimolar quantity of β-hydroxy-cyclohexanones **17a** and **18a** (Scheme 4.15). If it were a mixture of **14a** and **16a**, the product must have been only **17a**.

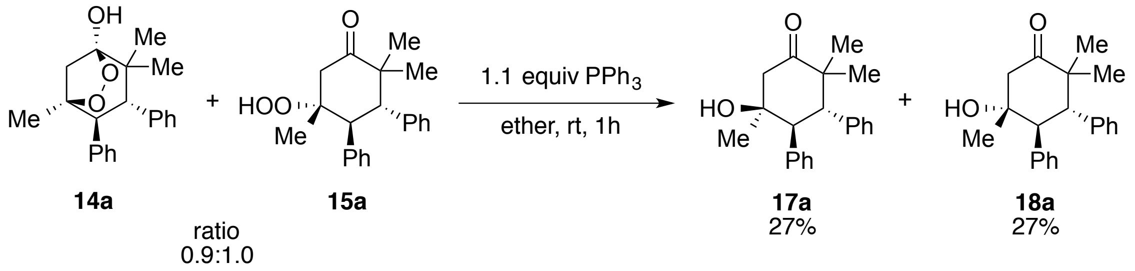
OH
Me
Me
O
O
Me
Ph
Ph
+
O
Me
Me
HOO
Me
Ph
Ph
1.1 equiv PPh3
ether, rt, 1h
O
Me
Me
HO
Me
Ph
Ph
+
O
Me
Me
HO
Me
Ph
Ph
14a
15a
ratio
0.9:1.0
17a
27%
18a
27%

Scheme 4.15 Derivatization of Peroxides to β-Hydroxy-Cyclohexanones.

A similar oxidation reaction was found in a report by the Blanco group.[107] Bicyclo[3.1.0]alkan-1-ols were oxidatively rearranged to hydroperoxycyclohexanones and peroxyhemiketals in the presence of atmospheric oxygen, catalytic amounts of $Cu(acac)_2$, and light (daylight or 100 W domestic light bulb at 30 cm) (Scheme 4.16). Notably, when $Cu(acac)_2$ or light was omitted, the oxidative reaction took significantly longer (3.5 h vs 48 h) and yield of the peroxidated products decreased (Scheme 4.17).

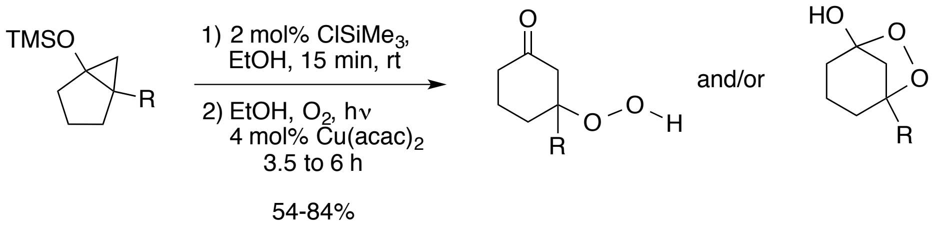
TMSO
R
1) 2 mol% ClSiMe3,
EtOH, 15 min, rt
2) EtOH, O2, hν
4 mol% Cu(acac)2
3.5 to 6 h
54-84%
O
R
O
O
H
and/or
HO
O
O
R

Scheme 4.16 Oxidative Rearrangement of Bicyclo[3.1.0]alkan-1-ols.

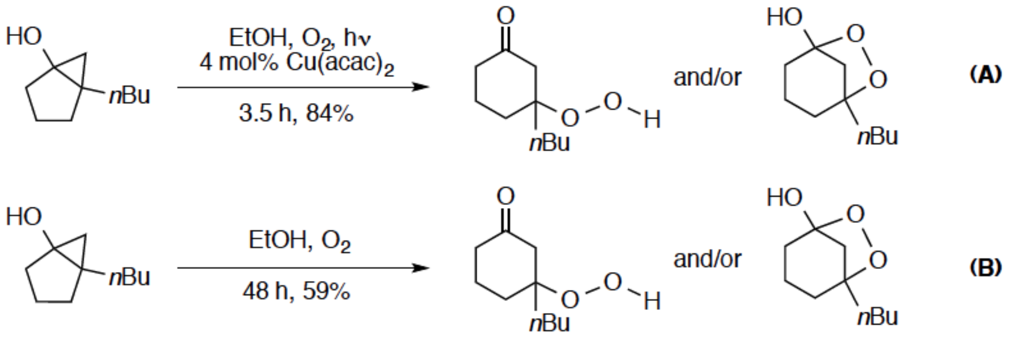
HO
nBu
EtOH, O2, hν
4 mol% Cu(acac)2
3.5 h, 84%
O
O
O
H
nBu
and/or
HO
O
O
nBu
(A)
HO
nBu
EtOH, O2
48 h, 59%
O
O
O
H
nBu
and/or
HO
O
O
nBu
(B)

Scheme 4.17 Blanco's Control Experiment.

The mechanism for the formation of **14a** and **15a** likely begins with abstraction of a hydrogen atom on the free alcohol by triplet oxygen (Scheme 4.18). Following a homolytic bond cleavage, addition of the peroxide radical to the resulting tertiary radical produces the two peroxides, one of which closes to make **14a**.

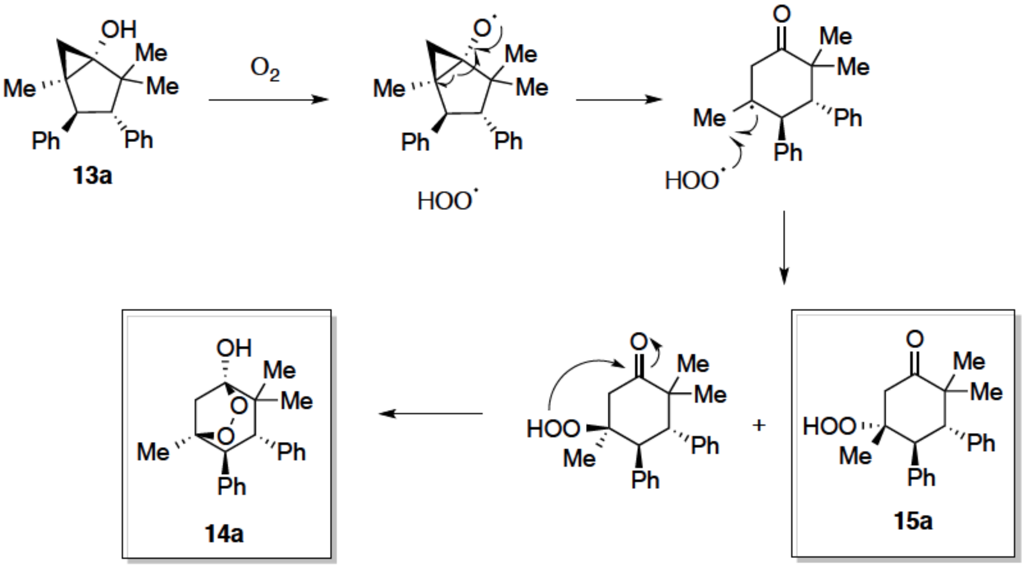
OH
Me
Me
Me
Ph
Ph
13a
O2
O
Me
Me
Me
Ph
Ph
HOO
O
Me
Me
Me
Ph
Ph
HOO
OH
Me
Me
O
O
Me
Ph
Ph
14a
O
Me
Me
HOO
Me
Ph
Ph
+
O
Me
Me
HOO
Me
Ph
Ph
15a

Scheme 4.18 Proposed Mechanism for the Autoxidation of **13a**.

The mechanistic proposal is supported by the findings by DePuy and Gibson. Cyclopropanone methyl hemiketal was reported to react with atmospheric oxygen to afford ring opened β-hydroperoxy ester (Scheme 4.19).[108] The proposed radical intermediate was also found to be intercepted by the bromine radical from bromotrichloromethane.

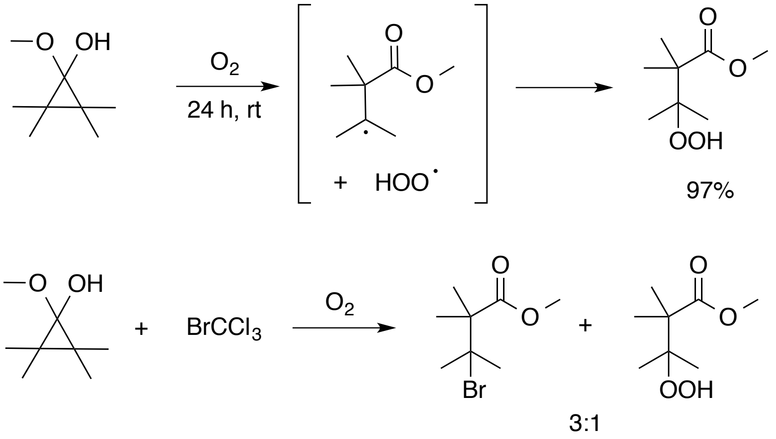

Scheme 4.19 Free Radical Reactions of Cyclopropanol.

4.3 Conclusion

In this chapter, we described multiple one-pot and multi-component reactions applied to the Nazarov cyclization to introduce molecular complexity. The electrophilic quenching of the enolate with masked aldehydes afforded highly substituted cyclopentanones with four contiguous stereocenters (two quaternary), and a new pendant hydroxyl group.

We also demonstrated the first cyclopropanation reactions on the aluminum enolate. Use of $AlMe_3$ with diiodomethane in the Nazarov reaction enabled us to construct bicyclohexanols with five contiguous stereocenters. The cyclopropanated products are quickly auto-oxidized to a mixture of peroxides. β-Hydroxy-cyclohexanone frameworks were easily prepared by treating these peroxides with PPh_3.

4.4 Future Plans

We have seen that the Nazarov cyclization can suffer from 1,2 addition when less reactive Nazarov substrates are treated with trimethylaluminum. To broaden the scope of the one-pot Nazarov reaction/cyclopropanation, we should find a stronger Lewis acid, which can promote both electrocyclization and cyclopropanation.

Along those lines, dialkylaluminum halides might be appropriate, as it is known to generate cyclopropane rings in the presence of CH_2I_2.[106] In this case, trapping the Nazarov intermediate can be done intermolecularly by π-nucleophiles or triethylsilane (Scheme 4.20).

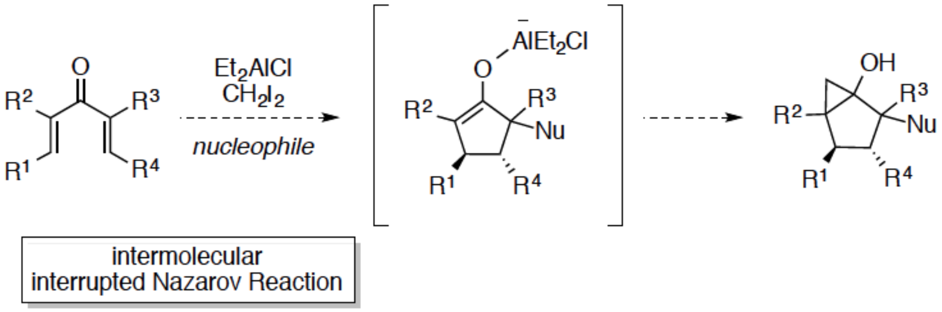

Scheme 4.20 Interrupted Nazarov Reaction/Cyclopropanation with Et_2AlCl and CH_2I_2.

Similarly, TMSOTf could lead to useful products. The replacement of $AlMe_3$ with TMSOTf (Scheme 4.21) could have several advantages: (1) expansion of substrate scope, (2) diversifying nucleophiles, and more importantly, (3) controlling the formation of autoxidized products.

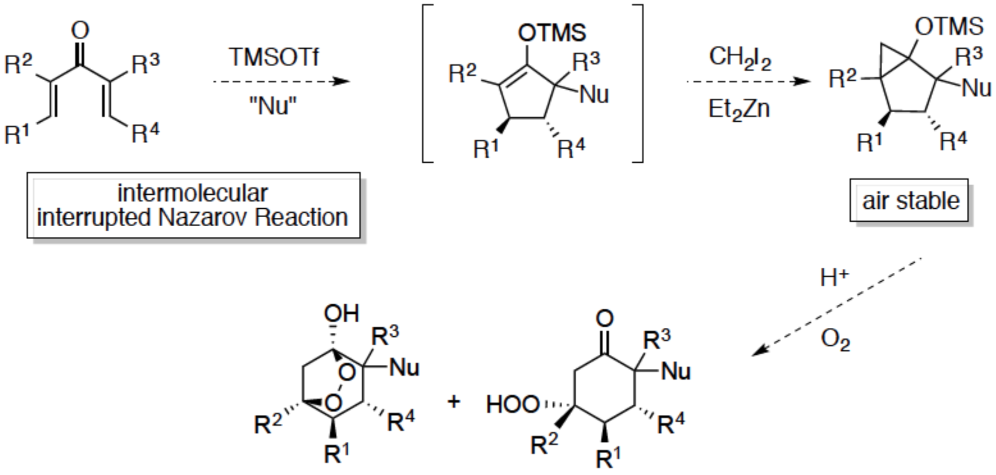
TMSOTf
"Nu"
intermolecular
interrupted Nazarov Reaction
OTMS
Nu
CH_2I_2
Et_2Zn
air stable
H^+
O_2
OH
HOO

Scheme 4.21 Intermolecular Interrupted Nazarov Reaction and Carbenoid Quenching.

4.5 Experimental

4.5.1 General Information

Reactions were carried out in flame-dried glassware under a positive argon atmosphere unless otherwise stated. Transfer of anhydrous solvents and reagents was accomplished with oven-dried syringes or cannulae. 4 Å molecular sieves were stored in oven, and flame-dried before use. Solvents were distilled before use: methylene chloride from calcium hydride, hexane from sodium, and tetrahydrofuran and toluene from sodium/benzophenone ketyl. Thin layer chromatography was performed on glass plates precoated with 0.25 mm Kieselgel 60 F254 (Merck). Flash chromatography column were packed with 230-400 mesh silica gel (Silicycle). Proton nuclear magnetic resonance spectra (^{1}H NMR) were recorded at 400 MHz or 500 MHz and coupling constants (*J*) are reported in Hertz (Hz). Standard notation was used to describe the multiplicity of signals observed in ^{1}H NMR spectra: broad (br), apparent (app), multiplet (m), singlet (s), doublet (d), triplet (t), etc. Carbon nuclear magnetic resonance spectra (^{13}C NMR) were recorded at 100 MHz or 125 MHz and are reported (ppm) relative to the center line of the triplet from chloroform-*d* (77.06 ppm). Infrared (IR) spectra were measured with a Mattson Galaxy Series FT-IR 3000 spectrophotometer. High-resolution mass spectrometry (HRMS) data (APPI/APCI/ESI technique) were recorded using an Agilent Technologies 6220 oaTOF instrument. HRMS data (EI technique) were recorded using a Kratos MS50 instrument.

Synthesis of dienones: please refer to Chapter 2.

4.5.2 Experimental Procedures and Characterization for One-Pot Organoaluminum Mediated Interrupted Nazarov Reaction and Electrophilic Quenching with Aldehydes.

Representative Procedure of the $AlMe_3$ Mediated Interrupted Nazarov Reaction in Paraformaldehyde (3a/4a)

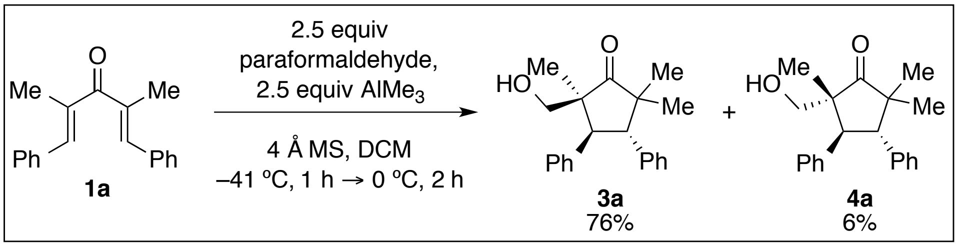

O
Me
Me
Ph
Ph
1a
2.5 equiv
paraformaldehyde,
2.5 equiv AlMe3
4 Å MS, DCM
–41 °C, 1 h → 0 °C, 2 h
HO
Me
O
Me
Me
Ph
Ph
3a
76%
+
HO
Me
O
Me
Me
Ph
Ph
4a
6%

To a solution of **1a** (55 mg, 0.21 mmol) and activated 4 Å molecular sieves (100 mg) in CH_2Cl_2 (2.1 mL, 0.1 M) was added 2.5 equivalents of paraformaldehyde (16 mg, 0.52 mmol) under argon atmosphere. The mixture was cooled to –41 ºC and 2.5 equiv $AlMe_3$ (0.26 mL, 2.0 M solution in toluene) was added dropwise. After complete consumption of **1a** was observed by TLC (1 hour), the solution was warmed to 0 ºC. After 2 hours, the reaction was carefully quenched with 1 M aq. HCl (2 mL) and warmed to room temperature. After separation of the phases, the aqueous layer was extracted with CH_2Cl_2 (3 × 10 mL). The combined organic extracts were washed with H_2O (10 mL), brine, and dried over $MgSO_4$, filtered, and concentrated in vacuo. Purification by flash column chromatography (silica gel) provided the desired products **3a** (49 mg, 76 %) and **4a** (4 mg, 6 %).

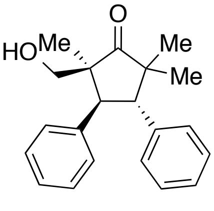

3a

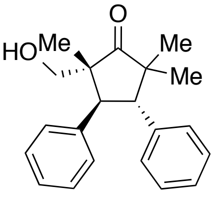

4a

Reaction was performed under the standard procedure. Flash chromatography (9:1 to 8:2 hexane:EtOAc) gave **3a** (49 mg, 76 %) and **4a** (4 mg, 6 %) as white solids.

3a: R_f 0.31 (hexanes/EtOAc 8:2); mp 163-165 °C; IR (cast film) 3440, 3026, 2968, 1732, 1453 cm^{-1}; ^1H NMR (500 MHz, $CDCl_3$) δ 7.33-7.31 (m, 2H), 7.26-7.12 (m, 8H), 3.97 (d, J = 13.4 Hz, 1H), 3.79 (d, J = 13.3 Hz, 1H), 3.38 (d, J = 10.5 Hz, 1H), 3.23 (d, J = 10.6

Hz, 1H), 1.65 (br s, 1H), 1.27 (s, 3H), 1.23 (s, 3H), 0.79 (s, 3H); ^{13}C NMR (125 MHz, $CDCl_3$) δ 225.7, 137.5, 137.1, 128.9, 128.9, 128.4, 128.1, 126.9, 126.6, 66.4, 53.8, 53.3, 52.3, 49.9, 22.8, 21.5, 20.5; HRMS (ESI, $[M+Na]^+$) for $C_{21}H_{24}NaO_2$ calcd. 331.1669, found: m/z 331.1664.

4a: R_f 0.23 (hexanes/EtOAc 8:2); mp 172-175 °C; IR (cast film) 3443, 3026, 2967, 2928, 1730, 1465 cm^{-1}; ^{1}H NMR (500 MHz, $CDCl_3$) δ 7.27-7.21 (m, 8H), 7.19-7.14 (m, 2H), 4.25 (d, *J* = 13.3 Hz, 1H), 3.87 (dd, *J* = 11.1, 5.5 Hz, 1H), 3.71 (d, *J* = 13.2 Hz, 1H), 3.48 (dd, *J* = 11.1, 5.9 Hz, 1H), 1.94 (app. t, *J* = 5.9 Hz, 1H), 1.29 (s, 3H), 0.76 (s, 3H), 0.70 (s, 3H); ^{13}C NMR (125 MHz, $CDCl_3$) δ 225.2, 137.2, 137.1, 129.2, 129.1, 128.2, 128.1, 126.7, 126.6, 64.9, 55.2, 52.2, 49.2, 44.9, 24.7, 19.6, 15.9; HRMS (APCI) m/z calcd for $C_{21}H_{25}O_2$ ($[M+H]^+$) 309.1849, found: m/z 309.1849.

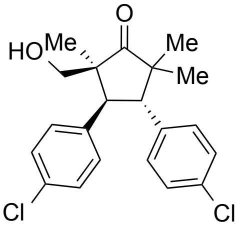

3b

Reaction was performed under the standard procedure. Flash chromatography (9:1 to 8:2 hexane:EtOAc) gave **3b** (46 mg, 81 %) as a colorless oil.

3b: R_f 0.60 (hexanes/EtOAc 2:1); IR (cast film) 3490, 3050, 2967, 2930, 1734, 1494, 1093 cm^{-1}; ^{1}H NMR (500 MHz, $CDCl_3$) δ 7.30-7.27 (m, 2H), 7.26-7.22 (m, 4H), 7.13-7.10 (m, 2H), 3.97 (d, *J* = 13.3 Hz, 1H), 3.68 (d, *J* = 13.3 Hz, 1H), 3.47 (d, *J* = 10.4 Hz, 1H), 3.17 (d, *J* = 10.4 Hz, 1H), 1.65 (br s, 1H), 1.21 (s, 6H, 2 overlapping CH_3 groups), 0.78 (s, 3H); ^{13}C NMR (125 MHz, $CDCl_3$) δ 225.0, 136.0, 135.4, 132.9, 132.6, 130.4, 130.1, 128.7, 128.4, 66.7, 53.9, 53.1, 52.3, 49.8, 22.6, 21.4, 20.4; HRMS (EI, M^+) for $C_{21}H_{22}O_2{}^{35}Cl_2$ calcd. 376.0997, found: m/z 376.0994.

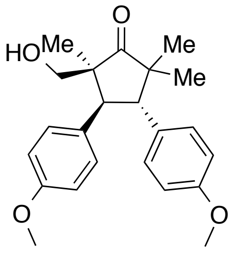
3c

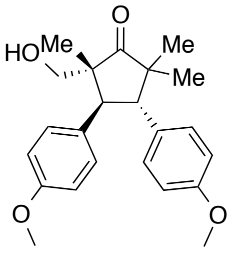
4c

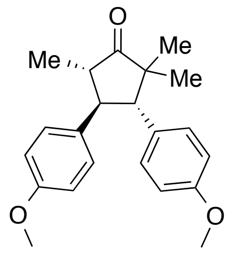
5c

Reaction was performed under the standard procedure. The reaction mixture was stirred at –41 ºC for 1.5 hours and at 0 ºC for 2 hours. Flash chromatography (9:1 to 6:4 hexane:EtOAc) gave **3c** (19 mg, 34 %) and **4c** (2 mg, 4 %) as a colorless oil. **5c** (22 mg, 43 %) was also isolated as a colorless oil.

3c: R*f* 0.16 (hexanes/EtOAc 8:2); IR (cast film) 3502, 3035, 2964, 2932, 1733, 1515, 1249 cm^{-1}; ^{1}H NMR (500 MHz, $CDCl_3$) δ 7.24-7.21 (m, 2H), 7.12-7.08 (m, 2H), 6.81-6.77 (m, 4H), 3.83 (d, *J* = 13.4 Hz, 1H), 3.75 (s, 3H), 3.75 (s, 3H), 3.67 (d, *J* = 13.4 Hz, 1H), 3.38 (dd, *J* = 10.7, 6.5 Hz, 1H), 3.25 (dd, *J* = 10.7, 4.7 Hz, 1H), 1.54 (dd, *J* = 6.4, 4.7 Hz, 1H), 1.26 (s, 3H), 1.20 (s, 3H), 0.78 (s, 3H); ^{13}C NMR (125 MHz, $CDCl_3$) δ 226.1, 158.5, 158.3, 129.8, 129.8, 129.5, 129.0, 113.9, 113.6, 66.4, 55.1, 55.1, 53.7, 52.9, 51.8, 49.9, 22.9, 21.5, 20.5; HRMS (EI, M$^+$) for $C_{23}H_{28}O_4$ calcd. 368.1988, found: m/z 368.1998.

4c: R*f* 0.09 (hexanes/EtOAc 8:2); IR (cast film) 3498, 2965, 2932, 1733, 1515, 1250 cm^{-1}; ^{1}H NMR (500 MHz, $CDCl_3$) δ 7.13-7.09 (m, 4H), 6.80-6.75 (m, 4H), 4.09 (d, *J* = 13.4 Hz, 1H), 3.82 (dd, *J* = 11.1, 5.7 Hz, 1H), 3.73 (s, 3H), 3.73 (s, 3H), 3.57 (d, *J* = 13.3 Hz, 1H), 3.43 (dd, *J* = 11.1, 6.1 Hz, 1H), 1.91 (app. t, *J* = 6.0 Hz, 1H), 1.24 (s, 3H), 0.72 (s, 3H), 0.67 (s, 3H); ^{13}C NMR (125 MHz, $CDCl_3$) δ 225.6, 158.3, 158.3, 130.1, 130.0, 129.3, 129.1, 113.7, 113.6, 65.1, 55.2, 55.1 (2), 51.8, 49.2, 44.5, 24.7, 19.6, 15.9; HRMS (ESI, [M+Na]$^+$) for $C_{23}H_{28}NaO_4$ calcd. 391.1880, found: m/z 391.1882.

5c: Spectral data are consistent with the reported values.[99]

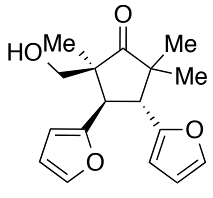

3d

Reaction was performed with **1d** (50 mg, 0.21 mmol) under the standard procedure. Flash chromatography (9:1 to 8:2 hexane:EtOAc) gave **3d** (43 mg, 71 %) as a white solid: R*f* 0.25 (hexanes/EtOAc 8:2); mp 118-120 °C; IR (cast film) 3420, 3149, 3113, 2966, 2927, 2875, 1724, 1464, 1028 cm^{-1}; ^{1}H NMR (500 MHz, CDCl$_3$) δ 7.37 (dd, *J* = 1.9, 0.8 Hz, 1H), 7.34 (dd, *J* = 1.9, 0.8 Hz, 1H), 6.32 (dd, *J* = 3.2, 1.9 Hz, 1H), 6.29 (dd, *J* = 3.2, 1.9 Hz, 1H), 6.19 (app. dt, *J* = 3.2, 0.7 Hz, 1H), 6.07 (app. dt, *J* = 3.2, 0.8 Hz, 1H), 3.84, 3.76 (ABq, J_{AB} = 13.0 Hz, 2H), 3.49 (dd, *J* = 11.1, 7.4 Hz, 1H), 3.27 (dd, *J* = 11.1, 3.8 Hz, 1H), 1.98 (br. dd, *J* = 7.5, 4.6 Hz, 1H) 1.28 (s, 3H), 1.23 (s, 3H), 0.82 (s, 3H); ^{13}C NMR (125 MHz, CDCl$_3$) δ 224.3, 153.1, 152.9, 141.8, 141.6, 110.4, 110.0, 107.6, 107.1, 67.5, 54.2, 50.0, 48.0, 46.0, 22.8, 21.3, 21.0; HRMS (EI, M$^+$) for $C_{17}H_{20}O_4$ calcd. 288.1362, found: m/z 288.1364.

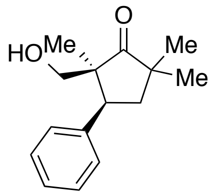

3f

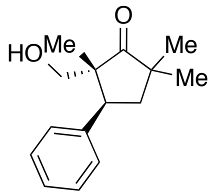

4f

Reaction was performed under the standard procedure. The reaction mixture was stirred at –41 ºC for 2 hours, and 0 ºC for 2 hours. Flash chromatography (19:1 to 9:1 hexane:EtOAc) gave **3f** (24 mg, 47 %) as a white solid and **4f** (10 mg, 20 %) as a colorless oil.

3f: R*f* 0.15 (hexanes/EtOAc 9:1); mp 90-91 °C; IR (cast film) 3481, 3029, 2964, 2932, 1730, 1454 cm^{-1}; ^{1}H NMR (400 MHz, CDCl$_3$) δ 7.40-7.35 (m, 4H), 7.33-7.28 (m, 1H), 3.35 (dd, *J* = 13.5, 6.5 Hz, 1H), 3.27 (A of ABX, J_{AB} = 10.7 Hz, J_{AX} = 6.7 Hz, 1H), 3.23 (B of ABX, J_{AB} = 10.7 Hz, J_{BX} = 4.4 Hz, 1H), 2.49 (app. t, *J* = 12.8 Hz, 1H), 2.01 (dd, *J* = 12.5, 6.5 Hz, 1H), 1.49 (X of ABX, J_{AX} = 6.5 Hz, J_{BX} = 4.6 Hz, 1H), 1.25 (s, 3H), 1.18 (s, 3H), 1.17 (s, 3H); ^{13}C NMR (100 MHz, CDCl$_3$) δ 226.4, 138.7, 128.5, 128.4, 127.1, 65.9, 54.1, 49.2, 45.8, 40.7, 25.2, 24.2, 20.9; HRMS (EI, M^+) for $C_{15}H_{20}O_2$ calcd. 232.1463, found: m/z 232.1466.

4f: R$_f$ 0.09 (hexanes/EtOAc 9:1); IR (cast film) 3464, 3030, 2965, 2937, 1736, 1465, 1031 cm^{-1}; ^{1}H NMR (500 MHz, $CDCl_3$) δ 7.38-7.35 (m, 2H), 7.31-7.27 (m, 3H), 3.78-3.72 (m, 2H), 3.40 (dd, *J* = 11.2, 6.2 Hz, 1H), 2.32 (app. t, *J* = 13.0 Hz, 1H), 2.05-1.99 (m, 2H), 1.28 (s, 3H), 1.16 (s, 3H), 0.61 (s, 3H); ^{13}C NMR (125 MHz, $CDCl_3$) δ 226.4, 138.7, 128.8, 128.3, 126.9, 64.8, 55.4, 45.0, 42.0, 39.0, 25.9, 24.2, 14.8; HRMS (EI, M^+) for $C_{15}H_{20}O_2$ calcd. 232.1463, found: m/z 232.1464.

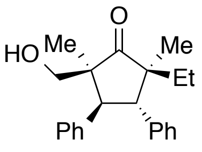

6a

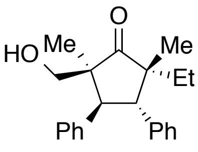

6a'

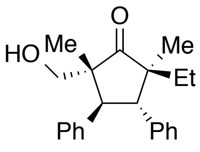

7a

Reaction performed under the standard procedure with 2.5 equivalents of $AlEt_3$ (0.22 mL, 0.48 mmol, 25 wt. % in toluene). Flash chromatography (19:1 to 8:2 hexane:EtOAc) gave **6a** and **6a′** as an inseparable mixture (25 mg, 40 %, 3.7:1.0 ratio) and **7a** (11 mg, 18 %) as a colorless oil.

6a: R$_f$ 0.30 (hexanes/EtOAc 8:2); IR (film) 3445, 3059, 2969, 1723, 1452, 1076 cm^{-1}; ^{1}H NMR (500 MHz, $CDCl_3$) δ 7.33-7.31 (m, 2H), 7.28-7.15 (m, 8H), 4.17 (d, *J* = 13.2 Hz, 1H), 3.83 (d, *J* = 13.2 Hz, 1H), 3.36, 3.29 (ABq, J_{AB} = 11.0 Hz, 2H), 1.83 (dq, *J* = 14.3, 7.6 Hz, 1H), 1.57 (br s, 1H), 1.49 (dq, *J* = 14.4, 7.4 Hz, 1H), 1.35 (s, 3H), 1.06 (app. t, *J* = 7.5 Hz, 3H), 0.83 (s, 3H); ^{13}C NMR (125 MHz, $CDCl_3$) δ 225.3, 137.4, 136.9, 129.0, 128.7, 128.5, 128.1, 127.0, 126.7, 65.3, 54.0, 53.4, 51.9, 47.5, 28.2, 21.5, 20.6, 9.3; HRMS (APCI) m/z calcd for $C_{22}H_{27}O_2$ ($[M+H]^+$) 323.2006, found: m/z 323.2007.

6a′(partial data): R$_f$ 0.30 (hexanes/EtOAc 8:2); ^{1}H NMR (500 MHz, $CDCl_3$) δ 3.98, 3.92 (ABq, J_{AB} = 13.4 Hz, 2H), 3.36 (d, *J* = 10.8 Hz, 1H), 3.23 (d, *J* = 10.8 Hz, 1H), 1.30 (s, 3H), 1.24 (s, 3H), 0.98 (dq, *J* = 14.3, 7.5 Hz, 1H), 0.74 (app. t, *J* = 7.5 Hz, 3H); ^{13}C NMR (125 MHz, $CDCl_3$) δ 224.1, 137.3, 137.3, 129.1, 128.7, 128.5, 128.1, 126.9, 66.6, 54.3, 53.5, 53.0, 51.6, 25.7, 21.4, 19.7, 8.2.

7a: R$_f$ 0.24 (hexanes/EtOAc 8:2); IR (cast film) 3466, 3029, 2967, 2933, 1732, 1453, 1043 cm^{-1}; ^{1}H NMR (500 MHz, $CDCl_3$) δ 7.27-7.20 (m, 8H), 7.18-7.14 (m, 2H), 4.27 (d, *J* = 13.2 Hz, 1H), 3.98 (d, *J* = 13.2 Hz, 1H), 3.87 (dd, *J* = 11.1, 5.6 Hz, 1H), 3.48 (dd, *J* = 11.0, 6.1 Hz, 1H), 2.01 (app. t, *J* = 5.9 Hz, 1H), 1.82 (dq, *J* = 14.3, 7.5 Hz, 1H), 1.49 (dq, *J* = 14.4, 7.5 Hz, 1H), 1.07 (app. t, *J* = 7.5 Hz, 3H), 0.78 (s, 3H), 0.65 (s, 3H); ^{13}C NMR (125 MHz, $CDCl_3$) δ 225.0, 137.4, 137.3, 129.2, 129.2, 128.2, 128.1, 126.6, 126.5, 64.9, 55.1, 53.9, 46.0, 44.6, 28.5, 19.9, 14.9, 9.6; HRMS (APCI) m/z calcd for $C_{22}H_{27}O_2$ ($[M+H]^+$) 323.2006, found: m/z 323.2006.

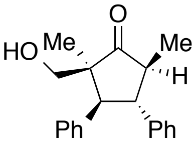

8a

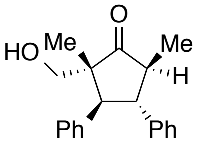

9a

To a solution of dienone **1a** (50 mg, 0.19 mmol), 3 equivalents of paraformaldehyde (18 mg, 0.57 mmol), and Et_3SiH (0.091 mL, 0.57 mmol) in CH_2Cl_2 (1.9 mL, 0.1 M) was added 2 equivalents of Et_2AlCl (0.18 mL, 0.38 mmol, 25 wt. % in toluene) at – 78 ºC. The mixture was stirred for 1 hour, and then warmed to 0 ºC. After 2 hours, the reaction was carefully quenched with 1 M aq. HCl (3 mL) at 0 ºC. Flash chromatography (9:1 to 8:2 hexane:EtOAc) gave **8a** (17 mg, 30 %) and **9a** (16 mg, 29 %) as white solids.

8a: R_f 0.34 (hexanes/EtOAc 8:2); mp 165-167 °C; IR (cast film) 3502, 3028, 2964, 2931, 1728, 1456 cm^{-1}; ^{1}H NMR (500 MHz, $CDCl_3$) δ 7.34-7.32 (m, 2H), 7.30-7.23 (m, 6H), 7.22-7.14 (m, 2H), 3.65 (app. t, *J* = 12.1 Hz, 1H), 3.45 (d, *J* = 12.4 Hz, 1H), 3.43 (dd, *J* = 10.6, 6.1 Hz, 1H), 3.28 (dd, *J* = 10.7, 4.3 Hz, 1H), 2.52 (dq, *J* = 11.8, 6.8 Hz, 1H), 1.61-1.59 (m, 1H), 1.23 (s, 3H), 1.16 (d, *J* = 6.8 Hz, 3H); ^{13}C NMR (125 MHz, $CDCl_3$) δ 222.8, 141.0, 136.8, 129.0, 128.6, 128.4, 127.6, 127.1, 126.8, 66.3, 58.5, 54.3, 52.2, 51.5, 20.6, 11.9; HRMS (EI, M^+) for $C_{20}H_{22}O_2$ calcd. 294.1620, found: m/z 294.1619.

9a: R_f 0.19 (hexanes/EtOAc 8:2); mp 140-142 °C; IR (cast film) 3454, 3029, 2967, 2930, 1736, 1453 cm^{-1}; ^{1}H NMR (500 MHz, $CDCl_3$) δ 7.32-7.30 (m, 2H), 7.27-7.21 (m, 6H), 7.19-7.15 (m, 2H), 4.00 (d, *J* = 12.6 Hz, 1H), 3.85 (dd, *J* = 10.9, 5.3 Hz, 1H), 3.48 (dd, *J* = 10.8, 5.2 Hz, 1H), 3.34 (app. t, *J* = 12.0 Hz, 1H), 2.14 (dq, *J* = 11.6, 7.0 Hz, 1H), 2.04 (br. t, *J* = 5.3 Hz, 1H), 1.18 (d, *J* = 7.1 Hz, 3H), 0.68 (s, 3H); ^{13}C NMR (125 MHz, $CDCl_3$) δ 222.2, 140.6, 136.9, 129.3, 128.6, 128.2, 127.8, 126.9, 126.8, 65.4, 55.3, 53.2, 50.6, 50.2, 15.7, 13.2; HRMS (EI, M$^+$) for $C_{20}H_{22}O_2$ calcd. 294.1620, found: m/z 294.1619.

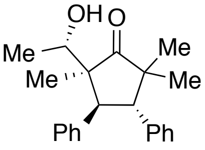
10a

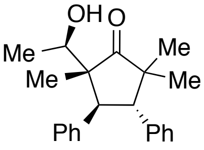
11a

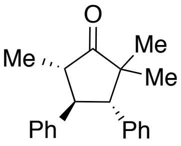
5a

Reaction was performed with 0.83 equivalents of paraldehyde (2.5 equivalents of acetaldehyde unit) under the standard procedure. Flash chromatography (19:1 to 9:1 hexane:EtOAc) gave **10a** (11 mg, 18 %) and **11a** (10 mg, 16 %) as white solids. **5a** was also found in the crude ^{1}H NMR spectrum and the yield was calculated to be 35 %. With respect to the calculation for **5a**, the isolated yield of **10a** was used as a standard and comparing integration of benzylic methine protons of **5a** and **10a** led to the calculated yield (35 %).

10a: R_f 0.18 (hexanes/EtOAc 9:1); mp 128-129 °C; IR (cast film) 3512, 3028, 2967, 2931, 1726, 1451 cm^{-1}; ^{1}H NMR (500 MHz, $CDCl_3$) δ 7.39-7.37 (m, 2H), 7.28-7.13 (m, 8H), 4.26 (d, J = 13.4 Hz, 1H), 3.79 (d, J = 13.4 Hz, 1H), 3.38 (q, J = 6.4 Hz, 1H), 1.29 (s, 3H), 1.24 (s, 3H), 1,18 (d, J = 6.4 Hz, 3H), 0.73 (s, 3H), OH peak not observed; ^{13}C NMR (100 MHz, $CDCl_3$) δ 224.8, 138.1, 137.3, 128.9, 128.5, 127.8, 127.5, 126.3, 125.9, 70.8, 55.2, 54.3, 52.8, 49.4, 22.7, 22.3, 21.0, 19.6; HRMS (EI, M$^+$) for $C_{22}H_{26}O_2$ calcd. 322.1933, found: m/z 322.1927.

11a: R_f 0.12 (hexanes/EtOAc 9:1); mp 177-181 °C; IR (cast film) 3527, 3028, 2970, 2931, 1729, 1451 cm^{-1}; ^{1}H NMR (400 MHz, $CDCl_3$) δ 7.26-7.11 (m, 10H), 4.24 (d, J = 13.3 Hz, 1H), 3.87 (q, J = 6.5 Hz, 1H), 3.58 (d, J = 13.3 Hz, 1H), 1,36 (d, J = 6.5 Hz, 3H), 1.22 (s, 3H), 0.89 (s, 3H), 0.77 (s, 3H), OH peak not observed; ^{13}C NMR (100 MHz, $CDCl_3$) δ 225.6, 137.6, 137.2, 129.8, 129.2, 128.1, 128.0, 126.7, 126.7, 71.1, 56.4, 53.5, 49.5, 47.3, 24.8, 19.6, 18.6, 16.0; HRMS (EI, M$^+$) for $C_{22}H_{26}O_2$ calcd. 322.1933, found: m/z 322.1923.

5a: Spectral data are consistent with the reported values.[99]

4.5.3 Experimental Procedures and Characterization for the Domino Interrupted Nazarov Reaction/Cyclopropanation

Representative procedure for the Interrupted Nazarov Reaction and Cyclopropanation (13a)

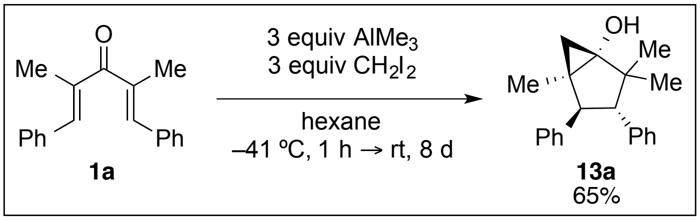

To a solution of **1a** (50 mg, 0.19 mmol) and 3 equivalents of CH_2I_2 (0.046 mL, 0.57 mmol) in hexane (1.9 mL, 0.1 M) was added 3 equivalents of $AlMe_3$ (0.29 mL, 0.57 mmol, 2.0 M hexane) at –41 ºC. The reaction mixture was stirred for 1 hour and then warmed to room temperature. The argon line was detached from the reaction vessel and the septum was thoroughly sealed with electrical tape to prevent solvent loss. After 8 days, the solution was cooled to 0 ºC and then carefully quenched with 1 M aq. HCl (3 mL). After separation of the phases, the aqueous layer was extracted with CH_2Cl_2 (3 × 10 mL). The combined organic extracts were washed with brine, and dried over $MgSO_4$, filtered, and concentrated in vacuo. Purification by flash column chromatography (silica gel) provided the desired product **13a** (36 mg, 65 %). To slow the auto-oxidation process and collect clean spectral data, the NMR sample was prepared under argon gas.

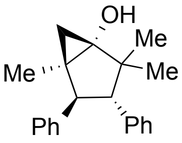

13a

Reaction was performed under the standard procedure. Flash chromatography (19:1 to 8:2 hexane:EtOAc) gave **13a** (36 mg, 65 %) as a colorless oil.

13a: R$_f$ 0.14 (hexanes/EtOAc 9:1); IR (cast film) 3411, 3028, 2963, 2926, 1450, 1146 cm^{-1}; ^{1}H NMR (500 MHz, CDCl$_3$) δ 7.29-7.25 (m, 2H), 7.23-7.17 (m, 6H), 7.15-7.12 (m, 2H), 3.59 (d, *J* = 11.7 Hz, 1H), 2.58 (d, *J* = 11.7 Hz, 1H), 2.03 (br s, 1H), 1.39 (d, *J* = 6.0 Hz, 1H), 1.32 (s, 3H), 1.12 (s, 3H), 0.85 (s, 3H), 0.56 (d, *J* = 6.1, Hz, 1H); ^{13}C NMR (125 MHz, CDCl$_3$) δ 141.3, 137.9, 129.8, 128.1, 127.8, 127.7, 126.4, 126.3, 69.8, 56.8, 50.9, 44.8, 32.4, 22.3, 19.3, 18.4, 16.2; HRMS (EI, M$^+$) for $C_{21}H_{24}O$ calcd. 292.1827, found: m/z 292.1825.

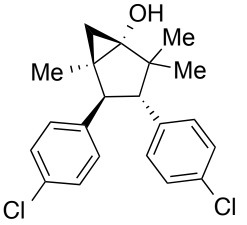

13b

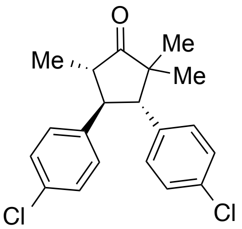

5b

Reaction was performed under the standard procedure. Flash chromatography (19:1 to 8:2 hexane:EtOAc) gave **13b** (28 mg, 43 %) as a colorless oil and **5b** (18 mg, 29 %).

13b: R$_f$ 0.67 (hexanes/EtOAc 2:1); IR (cast film) 3388, 2964, 2927, 1493, 1092cm^{-1}; ^{1}H NMR (500 MHz, CDCl$_3$) δ 7.25-7.22 (m, 2H), 7.18-7.15 (m, 2H), 7.12-7.07 (m, 4H), 3.47 (d, *J* = 11.8 Hz, 1H), 2.45 (d, *J* = 11.8 Hz, 1H), 1.98 (br s, 1H), 1.33 (d, *J* = 6.2 Hz, 1H), 1.28 (s, 3H), 1.08 (s, 3H), 0.83 (s, 3H), 0.56 (d, *J* = 6.1, Hz, 1H); ^{13}C NMR (125 MHz, CDCl$_3$) δ 139.5, 136.1, 132.5, 132.2, 130.9, 129.0, 128.4, 128.1, 69.5, 56.6, 50.6, 44.8, 32.2, 22.3, 19.2, 18.3, 16.0; HRMS (EI, M$^+$) for $C_{21}H_{22}O^{35}Cl_2$ calcd. 360.1048, found: m/z 360.1047.

5b: Spectral data are consistent with the reported values.[99]

Autoxidation of 13a to 14a and 15a

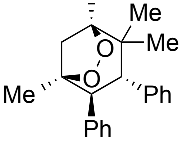

14a

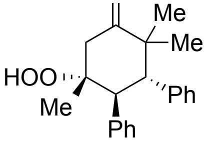

15a

Freshly isolated **13a** (36 mg) was left in a 100 mL round-bottom flask. Upon exposure to air, **13a** (oil) began to solidify into a white solid. After 5 hours, the solid was collected for spectroscopic studies, and found to be a mixture of **14a** and **15a** (1.0:1.1 ratio). **15a** (white solid) was partially isolated by flash chromatography (9:1 to 7:3 hexane:EtOAc).

14a (partial data): R$_f$ 0.26 (hexanes/EtOAc 8:2); ^{1}H NMR (500 MHz, CDCl$_3$) δ 3.68 (d, *J* = 12.3 Hz, 1H), 3.17 (d, *J* = 12.3 Hz, 1H), 2.90 (d, *J* = 11.6 Hz, 1H), 2.72 (s, 1H), 2.47 (d, *J* = 11.7 Hz, 1H), 1.04 (s, 6H, 2 overlapping CH$_3$ groups), 1.01 (s, 3H); ^{13}C NMR (125 MHz, CDCl$_3$) δ 140.1, 138.4, 127.3, 126.4, 126.2, 110.7, 87.3, 54.6, 54.4, 50.2, 43.4, 21.5, 20.6, 20.5 (3 aromatic carbon resonances not detected, due to presumed spectral overlap);

15a, white solid: R$_f$ 0.24 (hexanes/EtOAc 8:2); mp 171-174 °C; IR (cast film) 3369, 3030, 2976, 1712, 1691, 1452, 1288 cm^{-1}; ^{1}H NMR (500 MHz, CDCl$_3$) δ 7.61 (s, 1H), 7.15-7.01 (m, 10H), 4.31 (d, *J* = 13.2 Hz, 1H), 3.68 (dq, *J* = 12.8, 1.0 Hz, 1H), 3.22 (d, *J* = 13.2 Hz, 1H), 2.63 (d, *J* = 12.8 Hz, 1H), 1.20 (s, 3H), 1.09 (d, *J* = 0.9 Hz, 3H), 1.02 (s, 3H); ^{13}C NMR (125 MHz, CDCl$_3$) δ 212.8, 137.9, 137.4, 127.5, 127.4, 126.4, 126.4, 85.7, 52.3, 48.9, 48.1, 47.6, 23.4, 21.4, 18.8 (2 aromatic carbon resonances not detected, due to presumed spectral overlap); HRMS (ESI, [M+Na]$^+$) for C$_{21}$H$_{24}$NaO$_3$ calcd. 347.1618, found: m/z 347.1613.

Reduction of 14a and 15a to β-hydroxyketones 17a and 18a

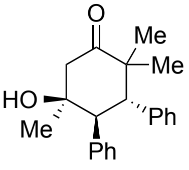

17a

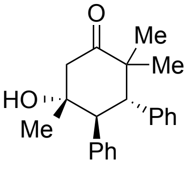

18a

To a solution of **14a/15a** (84 mg, 0.26 mmol, 1.0:1.1 ratio) in Et$_2$O (5.2 mL, 0.05 M) was added 1.1 equivalents of PPh$_3$ (76 mg, 0.29 mmol) at room temperature. The reaction mixture was stirred for 1 hour and concentrated in vacuo. Flash chromatography (silica gel, 8:2 to 7:3 hexane:EtOAc) provided **17a** (22 mg, 27 %) and **18a** (22 mg, 27 %) as white solids.

17a: R*f* 0.45 (hexanes/EtOAc 2:1); mp 222-225 °C; IR (cast film) 3410, 2972, 1700, 1454 cm^{-1}; ^{1}H NMR (500 MHz, $CDCl_3$) δ 7.23-7.21 (m, 1H), 7.14- 6.99 (m, 9H), 3.71 (d, *J* = 12.7 Hz, 1H), 3.59 (d, *J* = 12.7 Hz, 1H), 3.08 (d, *J* = 13.9 Hz, 1H), 2.58 (d, *J* = 14.0 Hz, 1H) 1.55 (s, 1H), 1.17 (s, 3H), 1.13 (d, *J* = 1.0 Hz, 3H), 1.01 (s, 3H); ^{13}C NMR (125 MHz, $CDCl_3$) δ 212.9, 138.9, 138.2, 132.4, 128.2, 127.6, 127.3, 126.6, 126.2, 74.5, 52.9, 52.8, 51.3, 48.7, 30.3, 22.9, 21.2; HRMS (EI, M$^+$) for $C_{21}H_{24}O_2$ calcd. 308.1776, found: m/z 308.1777.

18a: R*f* 0.29 (hexanes/EtOAc 2:1); mp 168-170 °C; IR (cast film) 3459, 3030, 2972, 1708, 1452 cm^{-1}; ^{1}H NMR (500 MHz, $CDCl_3$) δ 7.16-7.02 (m, 10H), 3.87 (d, *J* = 13.2 Hz, 1H), 3.25 (dq, *J* = 13.0, 1.1 Hz, 1H), 3.19 (d, *J* = 13.2 Hz, 1H), 2.64 (d, *J* = 13.0 Hz, 1H) 1.75 (br s, 1H), 1.17 (s, 3H), 1.13 (d, *J* = 1.0 Hz, 3H), 1.03 (s, 3H); ^{13}C NMR (125 MHz, $CDCl_3$) δ 212.3, 137.6, 137.4, 132.4 (br, confirmed with HSQC experiment),* 128.5, 127.9, 127.4, 126.8, 126.4, 73.6, 54.4, 52.6, 52.2, 49.0, 23.2, 23.2, 21.6; HRMS (EI, M$^+$) for $C_{21}H_{24}O_2$ calcd. 308.1776, found: m/z 308.1775.

---

* As it was uncertain if this small/broad carbon peak at 132.4 ppm was a real resonance, an HSQC experiment was carried out to observe its correlation with one of aromatic protons.

Chapter 5

Synthesis of 1,4-Diketones: Potassium Permanganate Interrupted Nazarov Reactions

5.1 Introduction

5.1.1 Oxidative Cleavage of Olefins

The oxidative cleavage of olefins is an important reaction in organic chemistry. Ozonolysis (Scheme 5.1) is one of the most robust oxidative cleavage methods traditionally used to cleave alkenes and enones. Different products can be obtained depending on whether the workup procedure is reductive or oxidative. For example, cleavage of alkenes can produce aldehydes or ketones and cleavage of enones can generate carboxylic acids.[109]

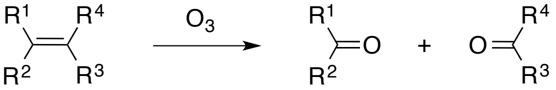

Scheme 5.1 Ozonolysis.

To date, there are a few alternatives to the ozonolysis. The advent of the Lemieux-Johnson reaction[110] (an OsO_4 catalyzed periodate oxidation of olefinic bonds) in 1956 was a breakthrough. As an example, *trans*-stilbene can be oxidized to benzaldehyde in good yield in the presence of 1 mole% of OsO_4 and 2.1 equivalents of $NaIO_4$, (Scheme 5.2). The oxidation reaction stopped at the aldehyde product, and no carboxylic acid product was formed. Aqueous dioxane (75 %) was used as the reaction solvent. It was noted that the presence of water was essential to the reaction, and was required for the hydrolysis of osmate ester.

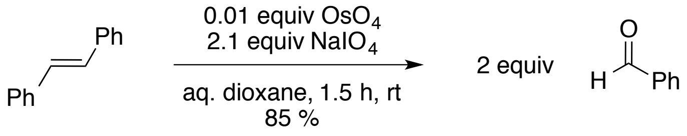
Ph
Ph
0.01 equiv OsO4
2.1 equiv NaIO4
aq. dioxane, 1.5 h, rt
85 %
2 equiv
O
H
Ph

Scheme 5.2 Lemieux-Johnson Oxidation of *trans*-Stilbene to Benzaldehyde.

The combination of OsO_4 and $NaIO_4$ has also been used in the oxidative cleavage of allylic alcohols. An early example of the OsO_4 promoted cleavage of allylic alcohols can be found in Zurflüh's report in 1970.[111] Under their conditions, the allylic alcohol was transformed into the keto acid in moderate yield (Scheme 5.3). The product was confirmed to be the carboxylic acid product, rather than the aldehyde, based on the IR data (OH peak at 3400-2500 cm^{-1}) and the ^1H NMR data (OH at 9.40 ppm). Although the IR data corresponded with the acid product, the ^1H NMR data showed a peak at 9.40 ppm, which could suggest the presence of an aldehyde functional group.

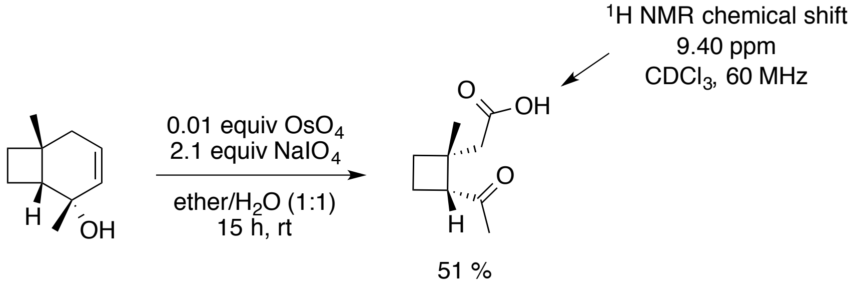
¹H NMR chemical shift
9.40 ppm
CDCl3, 60 MHz
H
OH
0.01 equiv OsO4
2.1 equiv NaIO4
ether/H2O (1:1)
15 h, rt
O
OH
O
H
51 %

Scheme 5.3 OsO_4/$NaIO_4$ Promoted Oxidative Cleavage of Allylic Alcohol.

In 2004 Jin and co-workers further investigated the OsO_4 and $NaIO_4$ protocol and reported that the addition of 2,6-lutidine improved the yield of the Lemieux-Johnson oxidation product **I** by suppressing the side reaction that produces α-hydroxy ketone product **II** (Scheme 5.4).[112] The addition of pyridine in lieu of 2,6-lutidine also reduced the amount of the side product, but epimerization at the α-position of the aldehyde was observed.

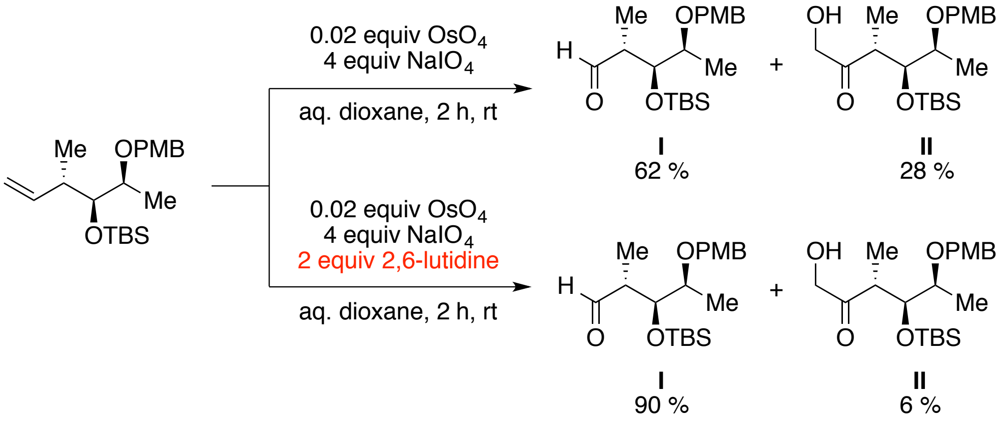
0.02 equiv OsO4
4 equiv NaIO4
aq. dioxane, 2 h, rt
0.02 equiv OsO4
4 equiv NaIO4
2 equiv 2,6-lutidine
aq. dioxane, 2 h, rt
Me
OPMB
Me
OTBS
H
O
+
OH
I
62 %
II
28 %
I
90 %
II
6 %

Scheme 5.4 Effect of 2,6-lutidine on the Lemieux-Johnson Oxidation.

In 2001, Borhan and co-workers used catalytic amounts of OsO_4 and 4 equivalents of Oxone (potassium peroxymonosulfate), as a replacement for periodate, to cleave olefins (Scheme 5.5).[113] Alkenes and enones were oxidatively cleaved to the corresponding ketones and carboxylic acids in good yields. Notably, aldehyde products were not found under these conditions.

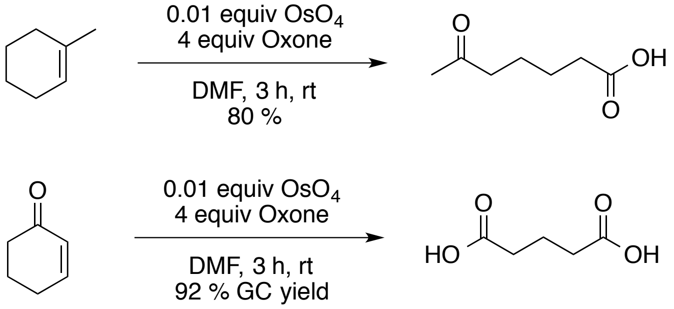
0.01 equiv OsO4
4 equiv Oxone
DMF, 3 h, rt
80 %
0.01 equiv OsO4
4 equiv Oxone
DMF, 3 h, rt
92 % GC yield
O
OH
HO

Scheme 5.5 Oxidative Cleavage of Olefins Using OsO_4 and Oxone.

Other groups also reported the replacement of OsO_4 with other oxidants. For instance, Silverstein and co-workers employed a catalytic amount of $RuCl_3$ and stoichiometric amounts of $NaIO_4$ in the oxidative cleavage of allylic alcohols (Scheme 5.6).[114] Lower valence forms of ruthenium are oxidized to RuO_4, which is the active oxidant.

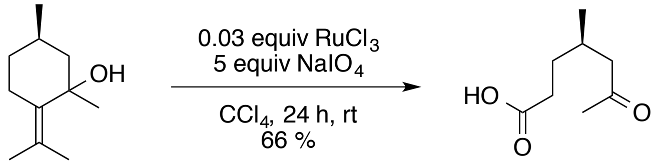

Scheme 5.6 Oxidative Cleavage of Allylic Alcohols Using $RuCl_3$ and $NaIO_4$.

Potassium permanganate ($KMnO_4$) has been also used for the oxidative cleavage reaction of alkenes. $KMnO_4$ is often used in aqueous solution due to its low solubility in most organic solvents, and under these conditions, the oxidation products are ketones or carboxylic acids, depending on the number of substituents on the alkene. Controlling the oxidation reaction to obtain aldehyde products was found to be challenging. Water, solvent or co-solvent, generated the cleaved product in the hydrate form, which was susceptible to over-oxidation to the carboxylic acid. However, use of phase transfer catalysis (PTC) in a non-aqueous solvent (e.g. CH_2Cl_2) made it possible to obtain aldehydes by increasing the solubility of permanganate in non-aqueous media (Scheme 5.7).[115]

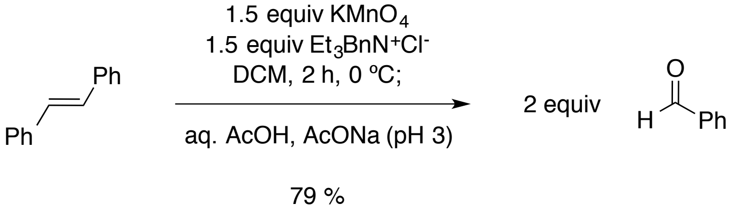

Scheme 5.7 Homogeneous Permanganate Oxidation of *trans*-Stilbene to Benzaldehyde.

The transformation of olefins to ketones and aldehydes can be accomplished in a two-step manner via intermediate 1,2-diol products. A number of oxidants such as $Pb(OAc)_4$, MnO_2, $VO(acac)_2$, PCC, etc., have been proven to cleave 1,2-diols oxidatively.[109a]

As described above, both electron-rich and electron-deficient olefins have been oxidatively cleaved by ozonolysis or commonly used oxidizing agents to introduce new functional groups. In this chapter, we will discuss application of the oxidative cleavage reaction to an oxyallyl cation as a novel extension of the “interrupted Nazarov” concept.[1a, 7]

5.2 Results and Discussion

5.2.1 Potassium Permanganate Interrupted Nazarov Reaction

Potassium permanganate is a powerful oxidant, and its versatility has been proven in many oxidation reactions involving alcohols, aldehydes, alkenes, alkynes, amines, and sulfides, etc.[116] However, oxidation on electron deficient oxyallyl cations has not yet been studied. Considering the high oxidation state of the permanganate anion, we were curious to see if permanganate could react with the Nazarov intermediate **2** via a [3+3] cycloaddition following 4π electrocyclization (Scheme 5.8). We envisioned the formation of diols on the cyclopentanone ring or further oxidation to the decarbonylated 1,4-diketone product **3**. We were particularly interested in the potential formation of the 1,4-diketones **3** because they are widely used as synthetic building blocks to construct heterocyclic 5-membered rings.

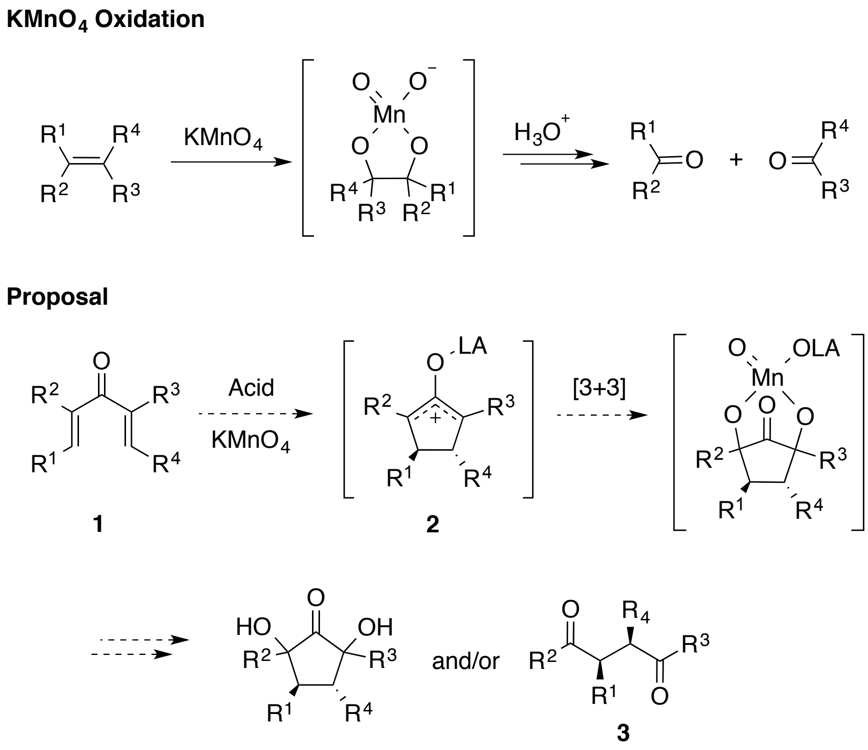

Scheme 5.8 Proposed Permanganate Interrupted Nazarov Reaction.

With a goal of probing the proposed reactivity of permanganate in the Nazarov reaction, we embarked on screening reaction conditions. As a control experiment, Nazarov substrate **1a** was treated with $KMnO_4$, and stirred for 18 hours in dichloromethane. Direct oxidation onto dienone **1a** was not observed in this case and **1a** was fully recovered (entry 1, Table 5-1). This result established the feasibility of this project by demonstrating that premature oxidation of the starting dienone could be avoided. As we planned to use crude (as purchased) solvents, moisture sensitive Lewis acids were excluded from the screening conditions. Initial attempts at using $FeCl_3•6H_2O$ resulted in the formation of *syn*-2,3-disubstituted 1,4 diketone **3a** with an 11 % isolated yield (entry 2). To the best of our knowledge, this type of transformation to the decarbonylation product is highly unprecedented. The relative configuration of **3a** was determined by single crystal X-ray diffraction analysis (Figure 5.1).[117]

Efforts to increase the solubility of permanganate and promote higher yields produced two conditions that were investigated further due to similar yields of **3a** (entry 7 and 9). When methanol was used as the solvent (entry 7), side products incorporating a methoxide group were observed by ^{1}H NMR. Therefore, we decided to further investigate conditions involving dichloromethane, $FeCl_3$•$6H_2O$, and a phase transfer catalyst, $BnNEt_3Cl$. However, the addition of substoichiometric amounts of $BnNEt_3Cl$ resulted in a reduced yield of **3a** despite full consumption of the starting material **1a** (entry 10). A tedious screening process was then used to determine if a two-solvent system would be more effective. It was found that treating **1a** with 1.5 equiv $FeCl_3$•$6H_2O$ and 2.5 equiv $KMnO_4$ in a 2:1 mixture of CH_2Cl_2/CH_3CN at low temperature (entry 14) furnished a 71 % yield of **3a**. Additionally, it was discovered that when 18-crown-6 was used as the additive, the solubility of $KMnO_4$ increased in dichloromethane, but only trace amounts of **3a** were observed (entry 15).

Table 5-1 Screening Conditions for the $KMnO_4$ Interrupted Nazarov Reaction. [a]

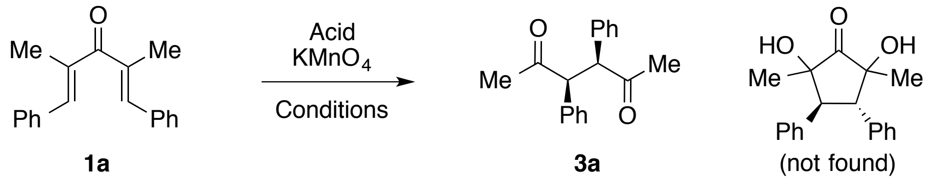

Entry	Acid (equiv)	$KMnO_4$ (equiv)	Solvent	Temp (ºC)	Yield of **3a** (%)[b]
1	none	2	CH_2Cl_2	rt [c]	No rxn
2	1.2 $FeCl_3$•$6H_2O$	2	CH_2Cl_2	rt [d]	11 %
3	1.2 $FeCl_3$•$6H_2O$	2	MeOH	rt	No rxn
4	0.2 $Sc(OTf)_3$	2	MeOH	rt	No rxn
5	xs. HCl	2	CH_2Cl_2	rt	NA[e]
6	xs. HCl	2	CH_3CN	rt [j]	NA[e]
7	xs. HCl	2	MeOH	rt	28 %
8	H_2SO_4	2	CH_2Cl_2	rt	NA[e]
9	1.2 $FeCl_3$•$6H_2O$	3	CH_2Cl_2/additive[f]	rt	31 %
10	1.2 $FeCl_3$•$6H_2O$	3	CH_2Cl_2/additive[g]	rt	22 %
11	1.2 $FeCl_3$	3	CH_2Cl_2/additive[f]	rt	NA[e]
12	1.2 $FeCl_3$•$6H_2O$	3	CH_3CN	rt [c]	trace [h]
13	1.2 $FeCl_3$•$6H_2O$	3	CH_2Cl_2/CH_3CN[i]	rt	49 %
14	1.5 $FeCl_3$•$6H_2O$	2.5	CH_2Cl_2/CH_3CN[i]	-15 to rt	**71 %**
15	1.5 $FeCl_3$•$6H_2O$	2.5	CH_2Cl_2/additive[k]	-15 to rt	trace [h]

[a] The standard reaction time was 4 h unless otherwise noted. [b] Isolated yield [c] The reaction mixture was stirred for 18 h. [d] The reaction mixture was stirred for 14 h. [e] **1a** was fully consumed, but **3a** was not found in a complex mixture. [f] 0.2 equiv $BnNEt_3Cl$ was added to dissolve $KMnO_4$. [g] 0.4 equiv $BnNEt_3Cl$ was added. [h] Starting material was present with a trace amount of **3a**. [i] 2:1 v/v ratio [j] The reaction time was 30 min. [k] 0.2 equiv 18-crown-6 was added.

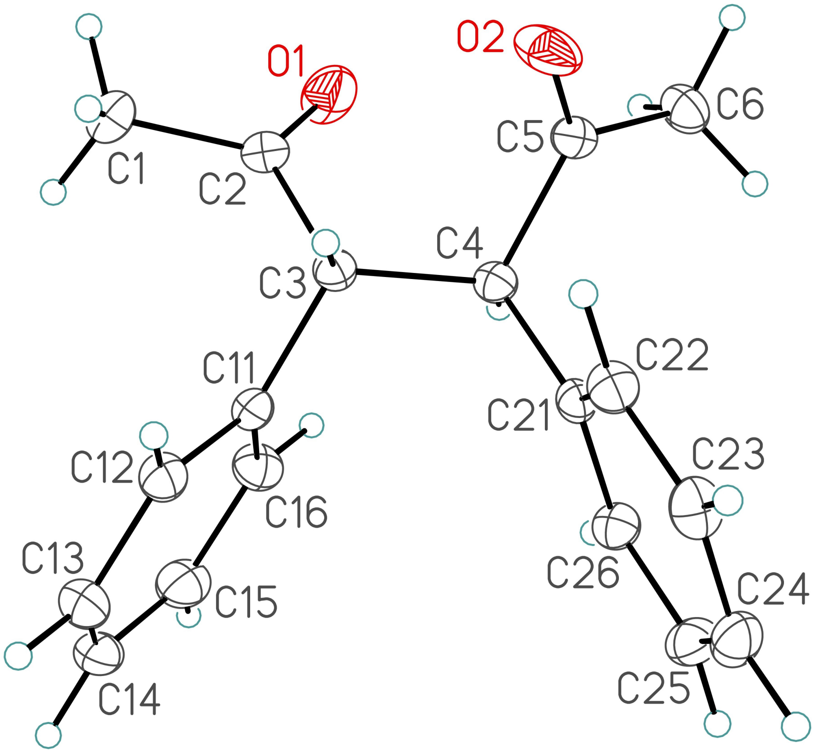
O2
O1
C6
C5
C1
C2
C4
C3
C22
C11
C21
C23
C12
C16
C13
C26
C24
C15
C25
C14

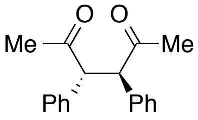
O
O
Me
Me
Ph
Ph

3a

(Thermal ellipsoids shown at the 30 % probability level)

Figure 5.1 ORTEP Drawing of **3a**.

Table 5-2 Synthesis of 1,4-Diketones via $KMnO_4$ Interruptions of the Nazarov Intermediates.[a] 118

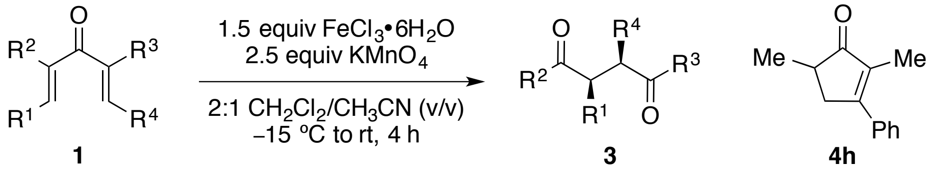

Entry	Dienone	R1	R2	R3	R4	Products (yield%)[b]
1	**1a**	Ph	Me	Me	Ph	**3a** (71 %)
2	**1b**	4-Cl-C_6H_4	Me	Me	4-Cl-C_6H_4	**3b** (60 %)
3[c]	**1c**	4-MeO-C_6H_4	Me	Me	4-MeO-C_6H_4	**3c** (45 %)
4[d]	**1d**	2-furyl	Me	Me	2-furyl	**3d** (17 %)
5	**1e**	*i*-Pr	Me	Me	*i*-Pr	**NA**[e]
6	**1f**	Ph	Me	Me	1-Naph	**3f** (52 %)[f]
7	**1g**	Ph	Me	*n*-Pr	Ph	**3g** (66 %)
8	**1h**	H	Me	Me	Ph	**3h** (45 %), **4h** (16 %)
9	**1i**	*i*-Pr	Me	Me	Ph	**3i** (55 %)
10	**1j**	*i*-Pr	Me	Me	4-MeO-C_6H_4	**3j** (36 %)

[a] Standard procedure: $KMnO_4$ was dissolved in a 2:1 mixture of CH_2Cl_2 and CH_3CN for 30 min. To a solution of $KMnO_4$, $FeCl_3•6H_2O$ was added and stirred for 10 min, and then the temperature was lowered to –15 ºC. The ketone was added at –15 ºC and stirred for 3 h, followed by additional stirring at room temperature for 1h. [b] Yields are based on isolated product after chromatography. [c] The reaction mixture was stirred at –15 ºC for 4 h and filtered through silica. [d] 2.0 equiv $FeCl_3•6H_2O$ was used. The reaction mixture was stirred for an hour at –15 ºC and additional 4 hours at 0 ºC. [e] Starting material was recovered with intractable minor mixtures. [f] A mixture of rotamers.

To investigate the substrate scope of this reaction, Nazarov precursors were prepared in one step from 3-pentanone or two steps from the corresponding enones via aldol condensations. First, symmetrical divinyl ketones were tested using the optimal conditions discovered during the initial screening process (Table 5-2). Dienone **1b** afforded 1,4-diketone **3b** in good yield (60 %). Under these oxidizing conditions, we observed that **1c**, bearing an electron rich arene, was converted to **3c** with a reduced yield (26 %). Keeping the reaction temperature at –15 ºC was necessary to obtain a higher yield (45 %) in this case. Compound **1d** containing heteroaromatic substituents was converted to **3d** in low yield (17 %). These reaction conditions were not applicable to substrate **1e**, containing aliphatic substituents, and desired product was not formed. Use of different acids, such as TMSOTf, $TiCl_4$, and HCl, as well as exposure to room temperature were not successful in achieving conversion to **3e**.[119]

Unsymmetrically substituted dienones (**1f-1j**) did undergo the permanganate interrupted Nazarov reaction. Adding a larger substituent at the C-5 position of dienone **1f** resulted in **3f** being isolated as a mixture of rotamers, due to the higher rotational energy barrier. Substrate **1g**, differing from **1a** in the substitution of the methyl group with a propyl group at C-4, provided **3g** in good yield (66 %). Substrate **1h**, lacking a substituent at the C-1 position, was transformed into an α-substituted 1,4-diketone **3h** in modest yield (44 %). In this case, cyclopentenone **4h** was isolated as a side product in 16 % yield. It was discovered that electron rich arenes were less compatible with $KMnO_4$ as seen in the comparison of reactions using dienone **1i** and **1j** (Table 5-2, Entry 9 and 10).

We next attempted to postulate reaction mechanisms. Although there are no relevant mechanistic details for this type of transformation, we have proposed two plausible mechanisms using two equivalents of $KMnO_4$. We suggest a nucleophilic trapping of the oxyallyl cation intermediate with a permanganate anion after the 4π electrocyclization (**Mechanism A**, Scheme 5.9). The resulting enolate could then be oxidized by another molecule of permanganate to cleave a carbon-carbon bond, resulting in the loss of Mn(III) [120] to generate a carboxylate and a ketone. Carboxylate addition into the permanganate (VII) species in equilibrium followed by loss of manganese (V) and carbon dioxide would afford a decarbonylated 1,4-diketone. The by-product Mn(III) could then disproportionate to Mn(II) and Mn(IV), or the Mn(III) and Mn(V) could make two Mn(IV) species.[120]

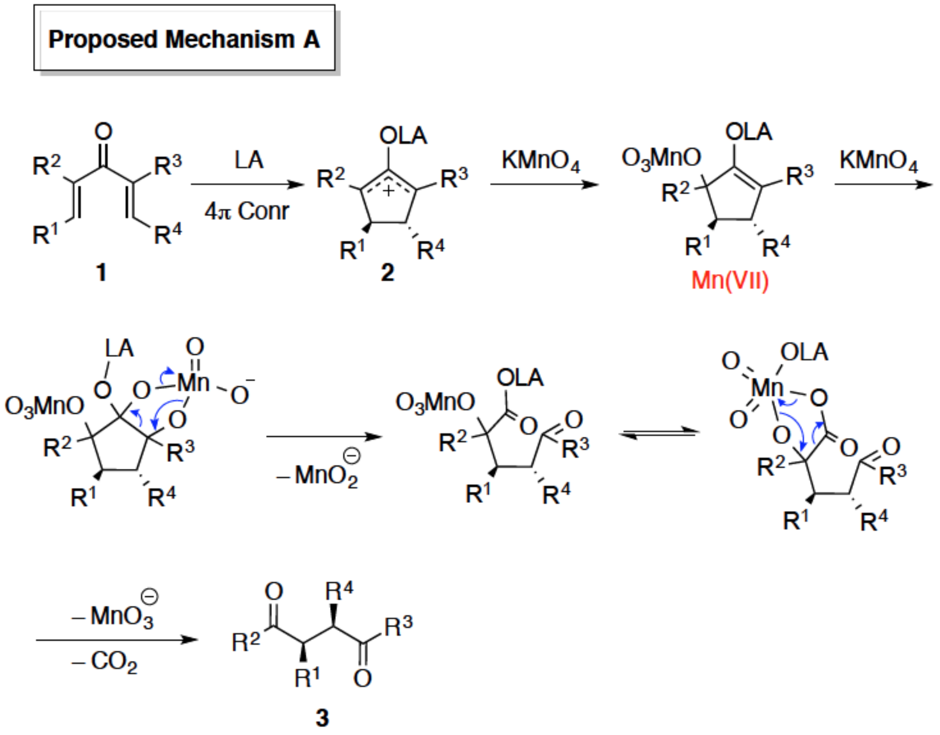

Scheme 5.9 Proposed **Mechanism A** for the $KMnO_4$ Interrupted Nazarov Reaction.

On the other hand, the oxyallyl cation could undergo a concerted or stepwise [3+3] cycloaddition with permanganate to produce a hypomanganate ester (V) (**Mechanism B**, Scheme 5.10). Through equilibrium of the Mn(V) complexes, the α-oxyanion could react with an additional Mn(VII), affording tricyclic manganese complex **A**. Considering the initial [3+3] cycloaddition provides *syn*-α,α' substituents, the tricyclic complex **A** would be a *cis,trans*-angular structure bearing higher strain than the *cis,cis*-tricycles. In both mechanisms, we postulated discharge of carbon dioxide rather than carbon monoxide, but further mechanistic studies are required to verify this.

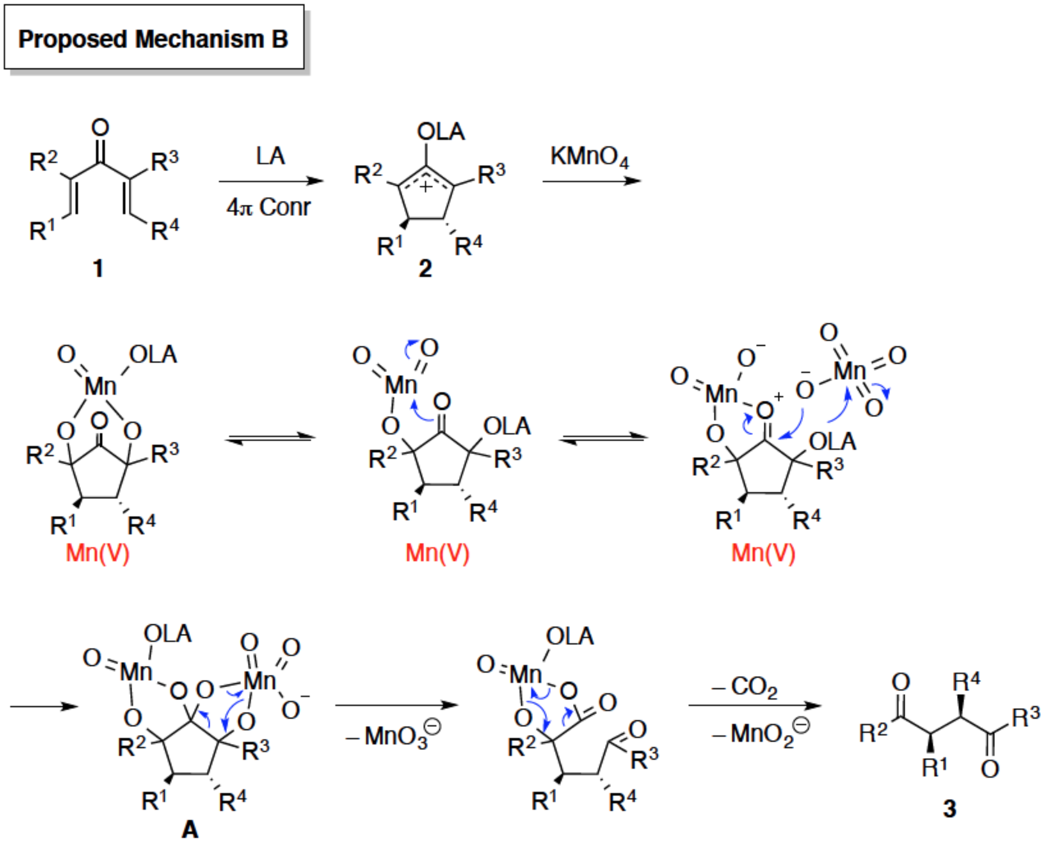

Scheme 5.10 Proposed **Mechanism B** for the $KMnO_4$ Interrupted Nazarov Reaction.

5.2.2 Halogen Interrupted Nazarov Reactions

Halogen interrupted Nazarov reactions were initially studied by the West group, using $TiCl_4$ on bridged bicyclic dienone substrates (Scheme 5.11).[40] The chloride trapping was only effective on the bridged bicyclic oxyallyl cation species. Later, Burnell and co-workers applied the halide interruption to a Nazarov intermediate derived from allenyl vinyl ketones.[41] Unlike the two examples, a diatomic halogenation process on the oxyallyl cation has not been reported to date.

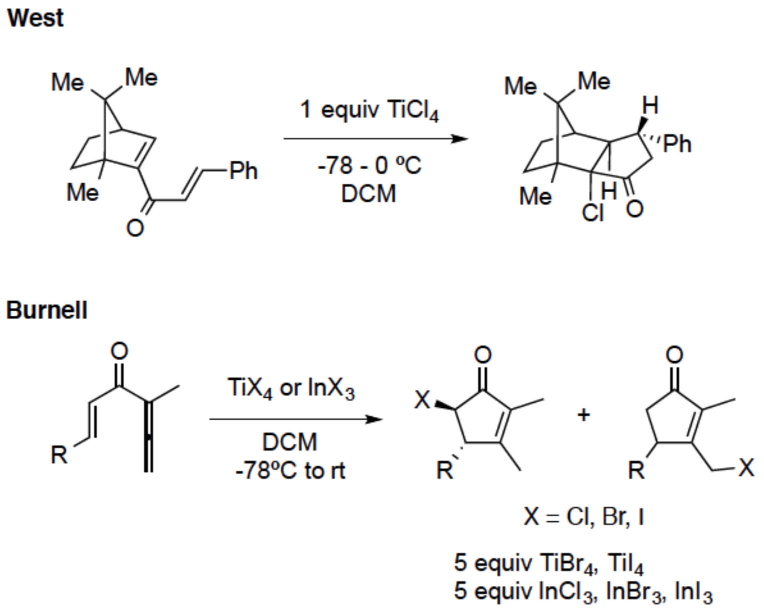
West

Burnell

Me
Me
Me
O
Ph
1 equiv TiCl4
-78 - 0 ºC
DCM
Me
Me
H
Ph
Me
H
Cl
O
O
R
TiX4 or InX3
DCM
-78ºC to rt
X
O
R
+
O
R
X
X = Cl, Br, I
5 equiv TiBr4, TiI4
5 equiv InCl3, InBr3, InI3

Scheme 5.11 Examples of Halide Interrupted Nazarov Cyclizations from West and Burnell.

Diatomic halogenation reactions typically take place on alkenes and enones and provide useful handles for further functionalization. This led us to question whether or not it was possible to halogenate the Nazarov intermediate to access these synthetic tools. Considering the opposite polarity at the two termini of the oxyallyl cation, the addition of two halogen atoms seemed feasible, but has never been explored.

Use of $KMnO_4$ in the Nazarov reaction allowed for unprecedented dihalogenation of the oxyallyl cation intermediate. For screening conditions to prepare 1,4-diketones, HCl was being studied as a Nazarov acid that would be compatible with the aqueous conditions favoured by $KMnO_4$. In the course of screening conditions with HCl, unexpected dichlorinated cyclopentanone products **5a**/**6a** were formed (Scheme 5.12).

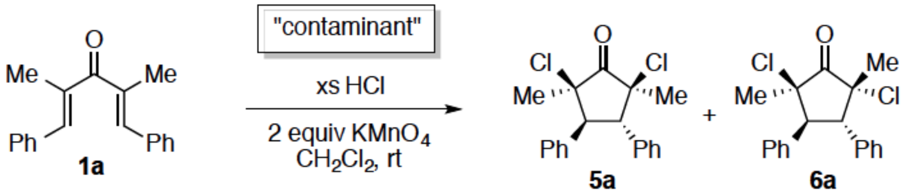
O
Me
Me
Ph
Ph
1a
"contaminant"
xs HCl
2 equiv KMnO4
CH2Cl2, rt
Cl
O
Cl
Me
Me
Ph
Ph
5a
+
Cl
O
Me
Me
Cl
Ph
Ph
6a

Scheme 5.12 A Fortuitous Finding: Chlorine Interrupted Nazarov Reaction.

However, this reaction was irreproducible under the same conditions: HCl and $KMnO_4$ in CH_2Cl_2. In light of the capriciousness of this reaction, it was necessary to scrutinize all aspects of the conditions to determine what factors allowed the formation of **5a** and **6a**, specifically, whether a critical contaminant was necessary. After ruling out any impurities in the starting materials, reagents and solvents, we ultimately took note of the needle used for addition of HCl, which was old and seemed to have some patches of rust. We wondered whether iron-based contaminants might be promoting this unexpected transformation.

In the event, we found that **5a**/**6a** could be produced in very good overall yield under the previously stated conditions by adding a catalytic amount of Fe(0) powder, as a substitute for the suspected rusty needle (Scheme 5.13). Iron contamination from the needle played an important role as the reaction without Fe(0) resulted in 8 spots on a TLC wherein **5a/6a** were not observed. We propose that an iron halide salt (II or III), oxidized via the permanganate, was the active catalyst for initiating the electrocyclization step. The incorporation of two chlorine atoms in products **5a** and **6a** could arise from diatomic chlorine being generated *in situ* by mixing HCl with $KMnO_4$, as previously reported by Venable and Jackson (eq. 1).[121] Additionally, a similar method was found in Davy's report in 1811 where chlorine gas was produced by mixing HCl and MnO_2.[122]

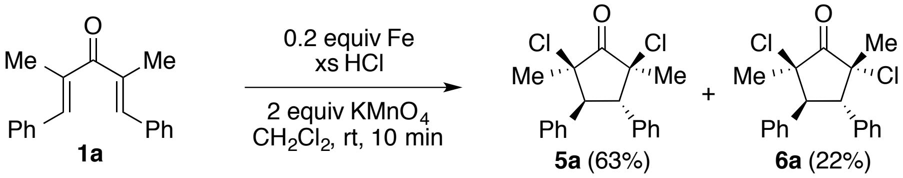

Scheme 5.13 Chlorine Interrupted Nazarov Reaction.

$$2KMnO_4 + 8HCl \longrightarrow 2KCl + 2MnO_2 + 4H_2O + 3Cl_2 \qquad \textbf{(1)}$$

The stereochemistry of **5a** was confirmed using X-ray crystallography (Figure 5.2). In case of product **6a**, there are half numbers of ^{1}H NMR resonances observed, compared to **5a**. This indicated that there is a C_2 axis of symmetry within **6a**. ^{1}H NMR correlation studies were used to assign the relative configuration of **6a** between two possibilities: (1) two methyl substituents *syn* to β-phenyl substituents or (2) *anti* to the β-phenyl substituents (Figure 5.3). We have consistently observed that α-methyl substituents *syn* to β-phenyl groups have an upfield shift in the ^{1}H NMR relative to their *anti* counterparts (anisotropy effect).[30]

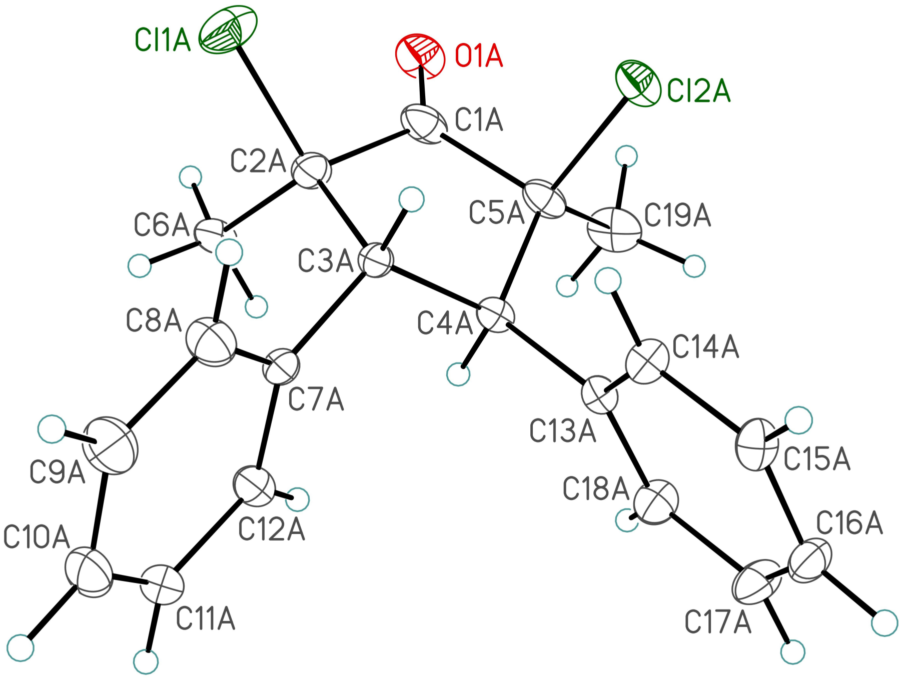
Cl1A
O1A
Cl2A
C1A
C2A
C5A
C19A
C6A
C3A
C8A
C4A
C14A
C7A
C13A
C15A
C9A
C18A
C16A
C12A
C10A
C17A
C11A

(Thermal ellipsoids shown at the 30 % probability level)

Figure 5.2 ORTEP Drawing of **5a**.

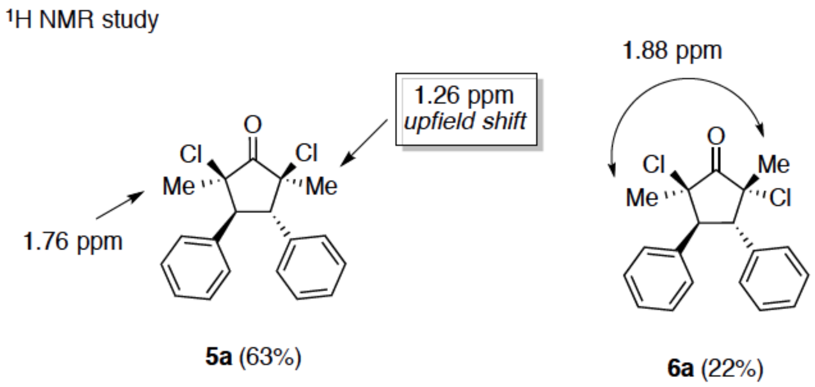

¹H NMR study
1.88 ppm
1.26 ppm
upfield shift
O
Cl
Cl
Me
Me
1.76 ppm
O
Cl
Me
Me
Cl
5a (63%)
6a (22%)

Figure 5.3 ^{1}H NMR study of **5a** and **6a**.

Following this result, our attention was focused on to other halogenation reactions. A reaction with HBr furnished a mixture of brominated compounds **7a** and **8a** in excellent yield (Scheme 5.14). The configuration of **7a**, lacking a C2 axis, was readily assigned, as there were two sets of methine and methyl proton resonances present in the ^{1}H NMR spectrum. Product **8a** was assigned by ^{1}H NMR studies, as in the case of the chlorination example.

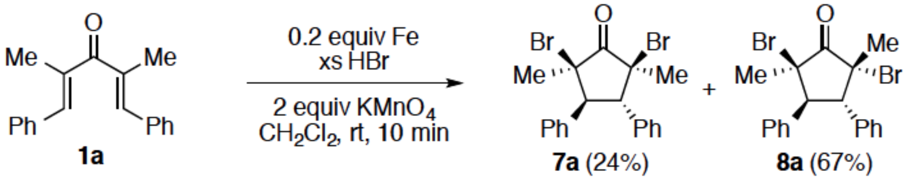

O
Me
Me
Ph
Ph
1a
0.2 equiv Fe
xs HBr
2 equiv KMnO4
CH2Cl2, rt, 10 min
O
Br
Br
Me
Me
Ph
Ph
7a (24%)
+
O
Br
Me
Me
Br
Ph
Ph
8a (67%)

Scheme 5.14 Bromine Interrupted Nazarov Reaction.

Interestingly, the diastereoselectivity of the bromination reaction was opposite to the chlorination reaction in that **8a** (having a C_2 axis) was the major product, presumably resulting from a stepwise addition to the oxyallyl cation via a possible bromonium ion (Scheme 5.15). The bromonium ion intermediate could illustrate the absence of **9a**. This unobserved product might be disfavoured as the addition of bromide via **path B** would increase vicinal Me-Ph eclipsing interactions.

However, diatomic bromine has never been proposed as a nucleophile, and the only way to form the bromonium ion intermediate is via nucleophilic addition of bromine to the oxyallyl cation. The proposal of the bromonium ion intermediate remains unproven and further studies are needed to focus on why bromide attacks *syn* to the β aryl substituent to afford the major product **8a**.

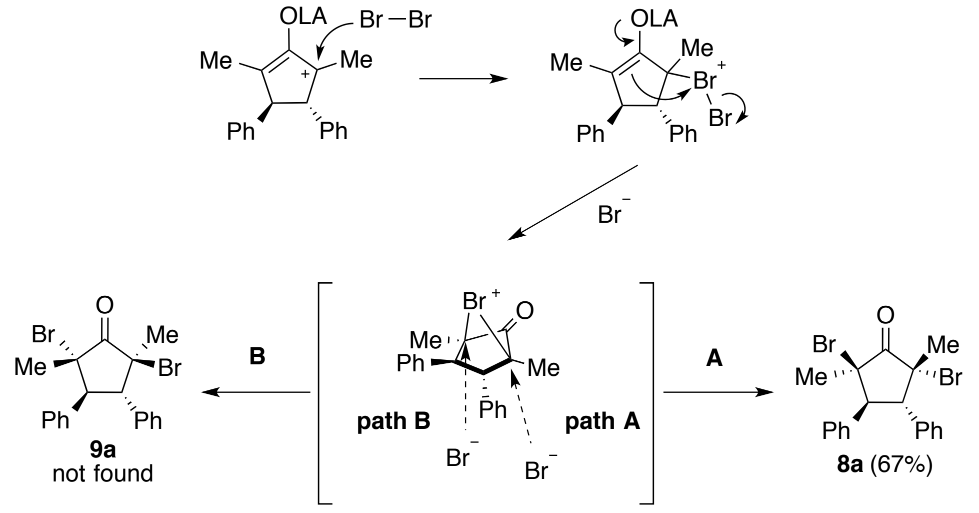
OLA
Br−Br
Me
Me
Ph
Ph
OLA
Me
Me
Br
Br
Ph
Ph
Br⁻
B
A
path B
path A
Br⁻
Br⁻
Me
Ph
Me
Ph
O
Br
Br
Me
Me
Br
Ph
Ph
not found
Br
Me
Me
Br
Ph
Ph
(67%)

9a

8a

Scheme 5.15 Proposed Mechanism of Formation of the Bromonium Ion.

In a separate reaction, hydrogen fluoride was used in order to install fluorine onto the cyclopentanone motif. Unfortunately, all attempts failed to afford the formation of the desired products. Instead, signals associated with chlorinated products **5a** and **6a** as well as cyclopentenone **4a** were found in the crude ^{1}H NMR spectrum (Scheme 5.16). This result was particularly interesting in that there was no obvious chlorine source other than dichloromethane solvent. Under these conditions, HCl could be generated from a fluoride-chloride exchange, and the permanganate could oxidize *in situ* formed HCl to Cl_2.

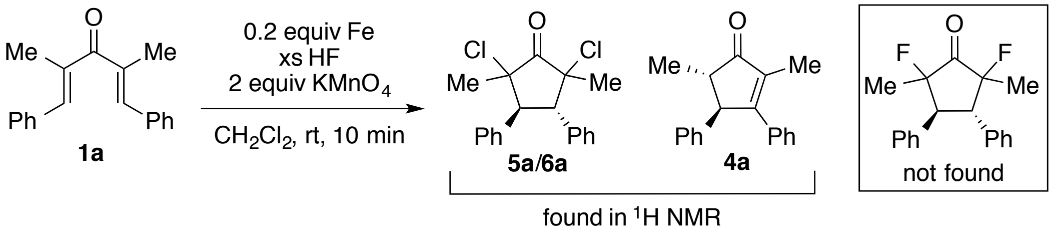
O
Me
Me
Ph
Ph
0.2 equiv Fe
xs HF
2 equiv KMnO4
CH2Cl2, rt, 10 min
Cl
Cl
Me
Me
Ph
Ph
Me
Me
Ph
Ph
F
F
Me
Me
Ph
Ph
not found
found in 1H NMR

1a

5a/6a

4a

Scheme 5.16 Use of Hydrogen Fluoride with $KMnO_4$ in the Nazarov Reaction.

5.2.3 Alternative Routes to Nazarov Intermediates and Oxidative Cleavage

To broaden the generality of our methodology – the oxidative cleavage of oxyallyl cations – and support the assumption that 1,4-diketone products are formed via oxyallyl cation intermediates, efforts were made to find alternative chemical pathways to form the Nazarov oxyallyl intermediate, and observe whether the same oxidative cleavage was observed. Oxyallyl cation intermediates can be prepared by reducing α,α'-dihaloketone with iron carbonyls[123] or Zn-Cu couple[124] and treating the α-haloketone with a base[125] upon discharge of a leaving group (Scheme 5.17).

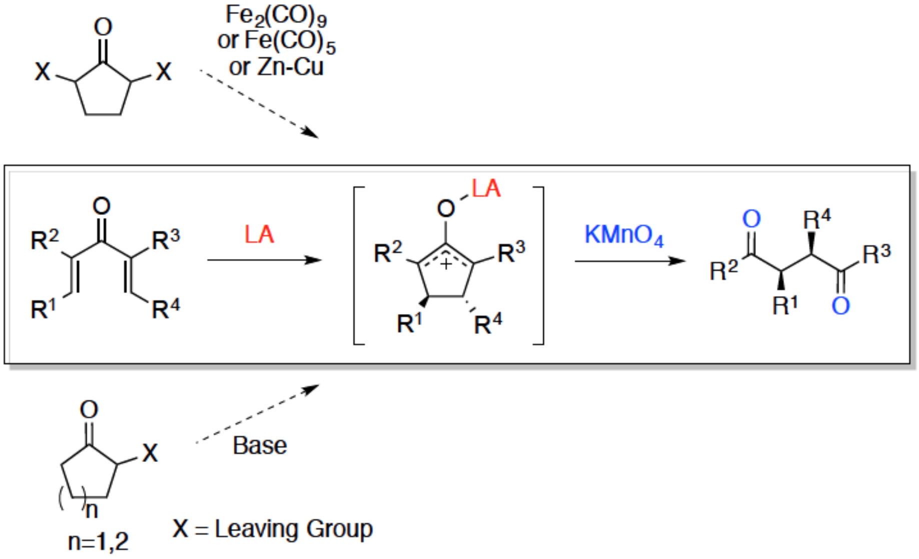

Scheme 5.17 Alternative Routes to the Oxyallyl Cation.

In 1982 Föhlisch and co-workers demonstrated [4+3] cycloadditions on base-induced generation of oxyallyl cations from α-haloketones, utilizing 2,2,2-trifluoroethanol (TFE) and sodium trifluoroethoxide, often known as *Föhlisch conditions* (Scheme 5.18).[125] The Föhlisch conditions have two key features: (1) weak nucleophilicity of the solvent due to an inductive effect and (2) its high ionizing power to facilitate the departure of a leaving group.

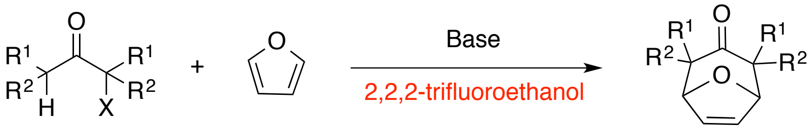
Base
2,2,2-trifluoroethanol
R1
R2
H
X
O
+

Scheme 5.18 [4+3] Cycloaddition using Föhlisch Conditions.

Considering the fact that the Favorskii rearrangement pathway could be a competing reaction (Scheme 5.19), weakening the nucleophilicity of the solvent is important to achieve the desired oxidative cleavage. However, the Föhlisch conditions employ an oxidizable solvent, making it incompatible with the strong oxidant $KMnO_4$.

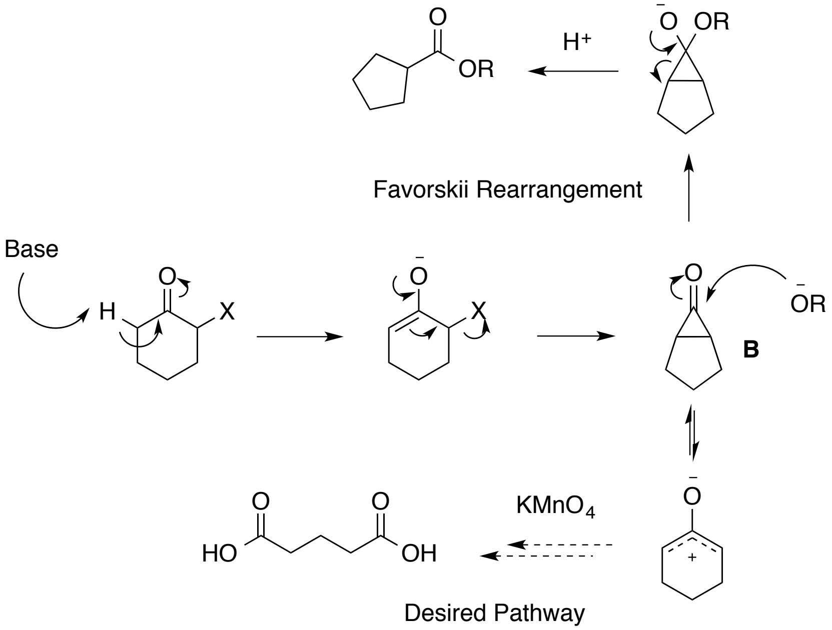
H+
OR
Favorskii Rearrangement
Base
H
X
B
KMnO4
HO
OH
Desired Pathway

Scheme 5.19 Competing Favorskii Rearrangement.

Because of the reason described above, a new solvent system was required that met the following criteria: (1) capable of dissolving the oxidant, (2) capable of ionizing the leaving group, and (3) less likely to react with the electrophilic cyclopropanone **B**

(Scheme 5.19). Among polar solvents, alcohols were ruled out due to low compatibility with the oxidant, while nitromethane would be a good option if it did not have an acidic proton.

With the limited selection of bases and solvents, *t*BuOK and $KMnO_4$ in CH_3CN were chosen and applied to an α-bromoketone, providing a mixture of adipic acid and glutaric acid in a 2:1 ratio (Scheme 5.20). The major product would come from the more substituted enolate followed by oxidation. Changing the order of addition and lowering the temperature to favor the formation of the kinetic enolate were unsuccessful. Also, addition of silver salts did not influence the ratio of the mixture. This preliminary study showed a limitation: the oxidant could readily react with the more substituted enolate prior to the formation of the oxyallyl cation intermediate. To avoid this, two substituents could be installed at the α,α' positions of the ketone to allow for incorporation of an enolizable proton only in the desired position (Scheme 5.21).

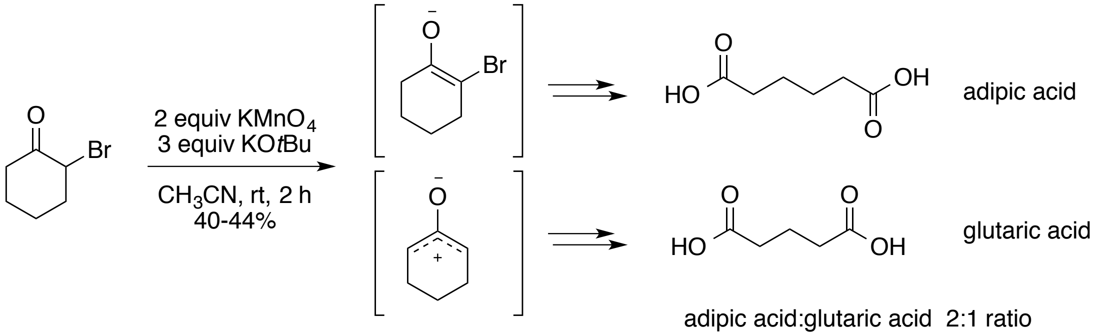

2 equiv KMnO4
3 equiv KOtBu
CH3CN, rt, 2 h
40-44%
Br
HO
OH
adipic acid
glutaric acid
adipic acid:glutaric acid 2:1 ratio

Scheme 5.20 Oxidative Cleavage of the Base-Induced Oxyallyl Cation.

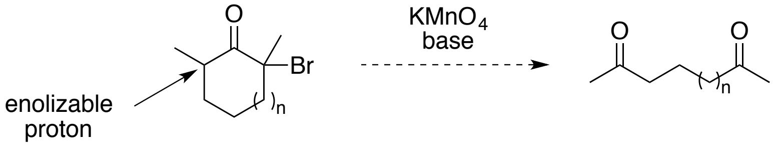

enolizable proton
Br
KMnO4
base
n

Scheme 5.21 Control of Enolization Using a α,α'-Substituted Ketone.

In the 1970's, Noyori and co-workers generated oxyallyl cation intermediates from both cyclic and linear α,α'-dibromoketones in the presence of $Fe_2(CO)_9$ or $Fe(CO)_5$, and demonstrated that a [4+3] cycloaddition of the allyl cation species with furan was possible (Scheme 5.22).[123]

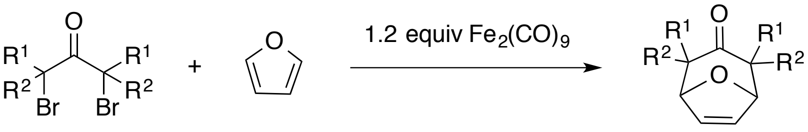

Scheme 5.22 Noyori Reaction Conditions.

With the Noyori conditions in mind, we examined the possibility of oxidative cleavage of dihaloketones via the formation of oxyallyl cation intermediates. The compatibility of iron carbonyls and strong oxidants is limited and the choice of solvent is very important. Iron carbonyls are soluble in benzene, but potassium permanganate is not. After solubility tests, it was believed that using benzene as a solvent could slow the oxidation by $KMnO_4$, and allow the reducing reagent to generate the oxyallyl cation species. Treating dibromoketone **8a** with 2.5 equivalents of both $Fe(CO)_5$ and $KMnO_4$ in benzene afforded 1,4-diketones **3a** in low yield (Scheme 5.23). Since 68 % of the starting material was recovered from the reaction, extra $Fe(CO)_5$ was added to the reaction vessel in an attempt to push the reaction to completion and consume **8a**. Upon full consumption of **8a**, however, the reaction provided a complex mixture of products. When $Fe_2(CO)_9$ was used instead of $Fe(CO)_5$, only trace amounts of **3a** was observed within a complex mixture.

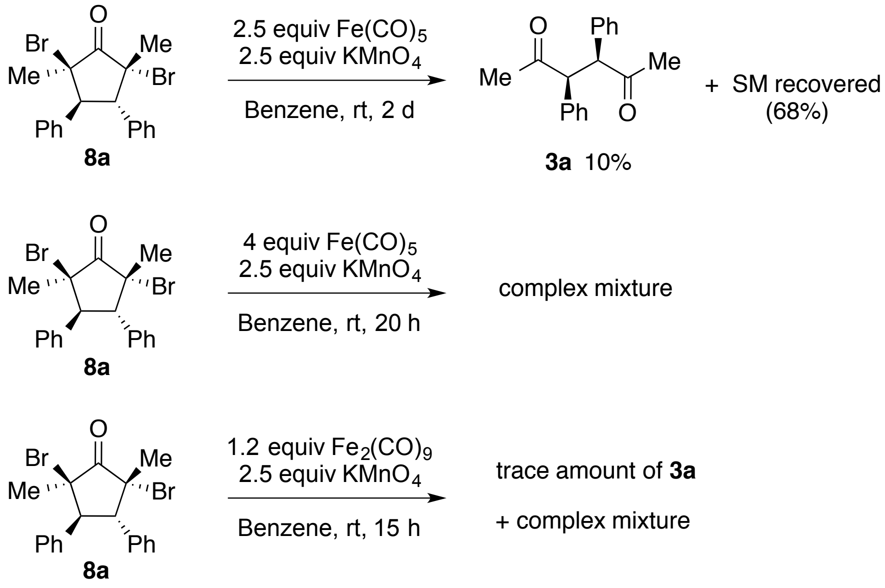
8a
2.5 equiv $Fe(CO)_5$
2.5 equiv $KMnO_4$
Benzene, rt, 2 d
3a 10%
+ SM recovered (68%)
8a
4 equiv $Fe(CO)_5$
2.5 equiv $KMnO_4$
Benzene, rt, 20 h
complex mixture
8a
1.2 equiv $Fe_2(CO)_9$
2.5 equiv $KMnO_4$
Benzene, rt, 15 h
trace amount of 3a
+ complex mixture

Scheme 5.23 Oxidative Cleavage of the Iron-Carbonyl-Induced Oxyallyl Cation.

It is apparent from these preliminary studies that oxyallyl cations, formed from routes that do not involve Nazarov electrocyclization, potentially can be trapped oxidatively with $KMnO_4$, but the search for solvents and oxyallyl generation conditions that are compatible with $KMnO_4$ is a work in progress.

5.3 Conclusion

In summary, we have demonstrated the first oxidative cleavage of oxyallyl cation species derived from the Nazarov reaction. The potassium permanganate interrupted Nazarov reactions afforded *syn*-2,3-disubstituted 1,4-diketones in moderate yield. This new methodology allows the formation of two C-O bonds and one C-C bond, and the cleavage of two C-C bonds.

In the course of investigating the permanganate interrupted Nazarov reaction, we also discovered that diatomic halogens could intercept oxyallyl cations to provide two handles on the cyclopentanones, which could then be further functionalized. Installing chlorine and bromine on Nazarov intermediates to produce α,α'-dihalogenated cyclopentanones is now feasible.

5.4 Future Directions

In regards to the oxidative cleavage of the base-induced oxyallyl cation, we need to determine mild oxidation conditions that are compatible with the Föhlisch reaction conditions. To the best of our knowledge, $NaIO_4$ and OsO_4 are not known to oxidize alcohols. For future studies, we hope to replace $KMnO_4$ with $NaIO_4$ and catalytic amounts of OsO_4 and subject the base-induced oxyallyl cation to both these conditions and the Föhlisch conditions (Scheme 5.24). This type of reaction should be carried out in anhydrous conditions; however, $NaIO_4$ is soluble in mostly aqueous solvents. Addition of a phase transfer catalyst could increase the solubility of $NaIO_4$ under the anhydrous conditions. It would be interesting to discover if the oxidation ceases at the aldehyde formation stage, as seen in the Lemieux-Johnson oxidation.

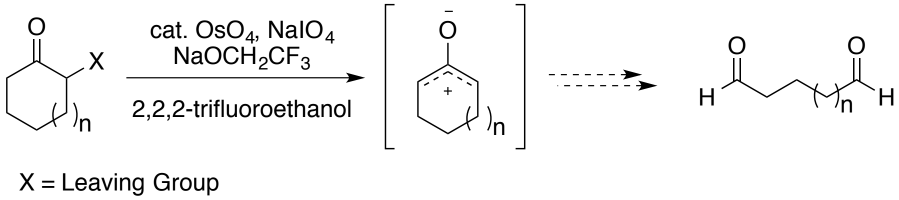

Scheme 5.24 Future Work on Screening Oxidants.

The preliminary result of the halogen interrupted Nazarov reaction has guaranteed the feasibility of this project. Efforts will be made to increase the facial selectivity of the halogenation, expand the substrate scope, and screen for optimal reaction conditions. With regards to expanding the substrate scope, it will be necessary to use a stronger acid to allow less reactive Nazarov substrates to favor electrocyclization, as direct halogenation of enones could be a competing reaction (Scheme 5.25).[126]

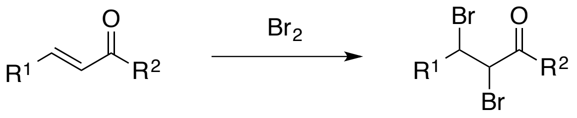

Scheme 5.25 Bromination of Enones.

5.5 Experimental

5.5.1 General Information

Reactions were carried out in flame-dried glassware under a positive argon atmosphere unless otherwise stated. Transfer of anhydrous solvents and reagents was accomplished with oven-dried syringes or cannulae. Solvents were distilled before use in the synthesis of dienones: dichloromethane from calcium hydride, tetrahydrofuran sodium/benzophenone ketyl. Thin layer chromatography was performed on glass plates precoated with 0.25 mm Kieselgel 60 F254 (Merck). Flash chromatography columns were packed with 230-400 mesh silica gel (Silicycle). Proton nuclear magnetic resonance spectra (^{1}H NMR) were recorded at 400 MHz or 500 MHz and coupling constants (*J*) are reported in Hertz (Hz). Standard notation is used to describe the multiplicity of signals observed in ^{1}H NMR spectra: broad (br), apparent (app), multiplet (m), singlet (s), doublet (d), triplet (t), etc. Carbon nuclear magnetic resonance spectra (^{13}C NMR) were recorded at 100 MHz or 125 MHz and are reported (ppm) relative to the center line of the triplet from chloroform-*d* (77.06 ppm). Infrared (IR) spectra were measured with a Mattson Galaxy Series FT-IR 3000 spectrophotometer. High-resolution mass spectrometry (HRMS) data (APPI/APCI/ESI technique) were recorded using an Agilent Technologies 6220 oaTOF instrument. HRMS data (EI technique) were recorded using a Kratos MS50 instrument. $KMnO_4$ reagent (≥99.0 %, Caledon lab chemicals) was used for reactions.

Dienones **1a**,[81] **1b**,[82] **1c**,[39] **1d**,[50] **1e**,[39] **1g**,[39] **1h**,[21] and **1j**[50] were prepared via literature procedures.

5.5.2 Experimental Procedures and Characterization for Potassium Permanganate Interrupted Nazarov Reaction

Preparation of Dienones 1f and 1i

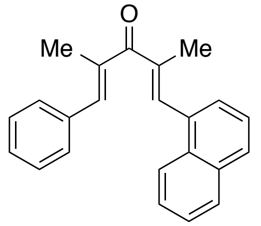

1f

Divinyl ketone **1f** was synthesized using a modification of the known procedure[39]: To a solution of a known starting material 2-methyl-1-phenyl-1-penten-3-one[83] (2.1 g, 12 mmol) in CH_2Cl_2 (60 mL) at –78 ºC was added $TiCl_4$ (1.3 mL, 12 mmol, 1.0 equiv) dropwise, followed by *i*Pr_2NEt (2.5 mL, 14 mmol, 1.2 equiv) dropwise. After stirring at –78 ºC for 1 h, 1-naphthaldehyde (9.1 mL, 60 mmol, 5.0 equiv) was added dropwise. The solution was stirred at –78 ºC for 2 h, and then allowed to slowly warm to room temperature overnight. The reaction was then quenched with water (30 mL). Organic compounds were extracted with CH_2Cl_2, rinsed with brine, and dried with $MgSO_4$. The organic layer was filtered, concentrated by rotary evaporation and purified by flash column chromatography (silica gel, hexanes:EtOAc 19:1) to give a mixture of diastereomeric β-hydroxyketones (2.2 g), which were carried directly to the next step.

To a mixture of hydroxy ketones (2.2 g, 6.7 mmol) in THF (34 mL) at 0 ºC was added Et_3N (1.4 mL, 10.0 mmol, 1.5 equiv), followed by methanesulfonyl chloride (0.57 mL, 7.3 mmol, 1.1 equiv) dropwise. The reaction mixure was stirred for 20 min at 0 ºC. DBU (5.0 mL, 33.3 mmol, 5.0 equiv) was then added and the mixture was stirred overnight at rt. The reaction was quenched with 1 M HCl (10 mL). The aqueous layer was extracted with ether (2 × 20 mL). The organic layers were combined and washed with 1 M HCl (2 x 20 mL), water, and brine. The organic layer was then dried ($MgSO_4$), concentrated by rotary evaporation and purified by flash column chromatography (silica gel, hexanes:EtOAc 19:1) to yield **1f** (2.01 g, 54 %) as a white solid: R_f 0.42 (hexanes/EtOAc 9:1); mp 79-81 °C; IR (cast film) 3057, 2956, 2920, 1637, 1446, 1247 cm^{-1}; ^1H NMR (500 MHz, $CDCl_3$) δ 7.95-7.90 (m, 2H), 7.89-7.87 (m, 1H), 7.73 (br s, 1H), 7.57-7.51 (m, 6H), 7.48-7.45 (m, 3H), 7.40-7.36 (m, 1H), 2.32 (d, J = 1.5 Hz, 3H), 2.12 (d, J = 1.5 Hz, 3H); ^{13}C NMR (125 MHz, $CDCl_3$) δ 201.8, 139.4, 139.0, 137.2, 136.8, 136.0, 133.6, 133.1, 131.5, 129.7, 128.7, 128.6, 128.6, 128.4, 126.7, 126.4, 126.1, 125.2, 124.5, 15.1, 14.9; HRMS (EI, M^+) for $C_{23}H_{20}O$ calcd. 312.1514, found: m/z 312.1514.

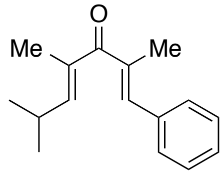

1i

Divinyl ketone **1i** was synthesized using a modification of the known procedure[39]: To a solution of 2-methyl-1-phenyl-1-penten-3-one[83] (2.1 g, 12 mmol) in CH_2Cl_2 (60 mL, 0.2 M) at –78 °C was added $TiCl_4$ (1.3 mL, 12 mmol, 1.0 equiv) dropwise, followed by *i*Pr_2NEt (2.5 mL, 14 mmol, 1.2 equiv) dropwise. The dark red solution was stirred for 1 h at –78 °C before adding isobutyraldehyde (5.48 mL, 60 mmol, 5 equiv) dropwise. The solution was stirred for 1 h at –78 °C before being brought to room temperature to stir overnight. The reaction was quenched with H_2O (30 mL). The aqueous layer was extracted with CH_2Cl_2 (2 x 30 mL) and the organic layers were combined, washed with H_2O (2 x 30 mL) and brine (1 x 30 mL), and dried ($MgSO_4$). The organic layer was filtered, concentrated by rotary evaporation and purified by column chromatography (silica gel, hexanes:EtOAc column volumes of 19:1 to 18:2 to 17:3) to give a mixture of diastereomeric β-hydroxyketones, which were carried directly to the next step.

To a solution of hydroxy ketones (1.8 g, 7.3 mmol) in THF (37 mL, 0.2 M) at 0 °C was added Et_3N (1.5 mL, 11 mmol, 1.5 equiv) followed by MsCl (0.62 mL, 8.1 mmol, 1.1 equiv) drop wise, and DBU (5.5 mL, 37 mmol, 5.0 equiv). The reaction was brought to room temperature and allowed to stir overnight. The reaction was quenched with 1 M HCl solution (10 mL). The aqueous layer was extracted with ether (2 x 20 mL). The organic layers were combined, washed with 1 M HCl (2 x 20 mL), H_2O (1 x 20 mL) and brine (1 x 20 mL), and dried ($MgSO_4$). The organic layer was filtered, concentrated by rotary evaporation and purified by column chromatography (silica gel, hexanes:EtOAc 19:1) to yield **1i** (0.92 g, 34 %) as a pale yellow oil: R_f 0.76 (hexanes:EtOAc 9:1); IR (cast film) 3025, 2960, 1637, 1448 cm^{-1}; ^1H NMR (500 MHz, $CDCl_3$) δ 7.42-7.38 (m, 4H), 7.35-7.30 (m, 1H), 7.04 (q, J = 1.4 Hz, 1H), 6.13 (dq, J = 9.5, 1.4 Hz, 1H), 2.74 (dsept, J = 9.5, 6.6 Hz, 1H), 2.13 (d, J = 1.5 Hz, 3H), 1.92 (d, J = 1.4 Hz, 3H), 1.06 (d, J = 6.6 Hz, 6H); ^{13}C NMR (125 MHz, $CDCl_3$) δ 202.1, 150.0, 138.3, 137.2, 136.3, 133.7, 129.6, 128.6, 128.2, 28.3, 22.2, 15.0, 12.9; HRMS (EI, M^+) for $C_{16}H_{20}O$ calcd. 228.1514, found: m/z 228.1513.

Representative Procedure for the Potassium Permanganate Interrupted Nazarov Reaction (3a)

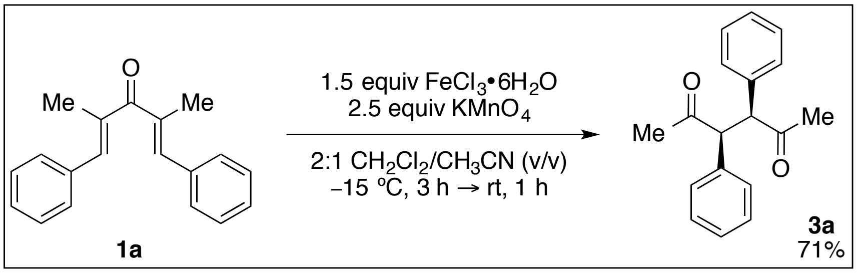

Solvents, dichloromethane and acetonitrile, were taken directly from fresh bottles without further purification/drying processes. The reaction was carried out in an open flask. 2.5 equiv $KMnO_4$ (0.076 g, 0.48 mmol) was dissolved in a mixture of CH_2Cl_2:CH_3CN (2:1 ratio, 3 mL) and stirred for 30 min at room temperature. 1.5 equiv $FeCl_3$•$6H_2O$ (0.077 g, 0.29 mmol) was then added and stirred for 10 min. The reaction temperature was lowered to –15 ºC and **1a** (solid, 0.050 g, 0.19 mmol) was added in one portion. The temperature was maintained for 3 h, and raised to room temperature. After 1 hour, the solution was filtered through a silica plug (2 cm thickness) and rinsed with 50 mL ethyl acetate. The organic filtrate was concentrated by a rotary evaporator. Purification by flash column chromatography (silica gel) provided the desired product **3a** (0.036 g, 71 %) as a white crystalline solid.

Spectral Data of 3a-3j

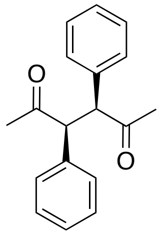

3a

Dienone **1a** (0.050 g, 0.19 mmol) was subjected to the standard condition. Flash chromatography (19:1 to 9:1 hexane:EtOAc) gave **3a** (0.036 g, 71 %) as a white solid.

3a: R*f* 0.24 (hexanes/EtOAc 9:1); mp 105-107 °C; IR (cast film) 3029, 2930, 1708, 1495, 1454 cm^{-1}; ^{1}H NMR (400 MHz, CDCl$_3$) δ 7.16-7.09 (m, 6H), 6.97-6.92 (m, 4H), 4.40 (s, 2H), 2.15 (s, 6H); ^{13}C NMR (125 MHz, CDCl$_3$) δ 208.0, 135.5, 128.7, 128.6, 127.3, 62.0, 29.3; HRMS (EI, M$^+$) for $C_{18}H_{18}O_2$ calcd. 266.1307, found: m/z 266.1307.

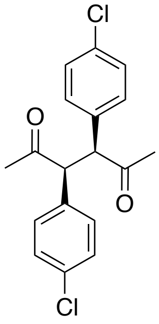

3b

Dienone **1b** (0.063 g, 0.19 mmol) was subjected to the standard condition. Flash chromatography (19:1 to 17:3 hexane:EtOAc) gave **3b** (0.038 g, 60 %) as a white solid.

3b: R*f* 0.47 (hexanes/EtOAc 8:2); mp 138-140 °C; IR (cast film) 3029, 2930, 1711, 1491, 1356 cm^{-1}; ^{1}H NMR (500 MHz, CDCl$_3$) δ 7.16-7.14 (m, 4H), 6.91-6.88 (m, 4H), 4.35 (s, 2H), 2.15 (s, 6H); ^{13}C NMR (125 MHz, CDCl$_3$) δ 207.2, 133.7, 133.6, 129.9, 129.1, 61.2, 29.3; HRMS (EI, M$^+$) for $C_{18}H_{16}O_2{}^{35}Cl_2$ calcd. 334.0527, found: m/z 334.0528.

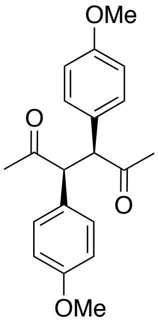

3c

Dienone **1c** (0.061 g, 0.19 mmol) was subjected to the standard condition. The reaction temperature was kept at –15 ºC for 4 h and filtered through a silica plug. Flash chromatography (19:1 to 8:2 hexane:EtOAc) gave **3c** (0.028 g, 45 %) as a white solid.

3c: R*f* 0.30 (hexanes/EtOAc 8:2); mp 139-142 °C; IR (cast film) 3002, 2959, 1707, 1512, 1254 cm^{-1}; ^{1}H NMR (400 MHz, CDCl$_3$) δ 6.89-6.85 (m, 4H), 6.70-6.67 (m, 4H), 4.31 (s, 2H), 3.72 (s, 6H), 2.14 (s, 6H); ^{13}C NMR (100 MHz, CDCl$_3$) δ 208.4, 158.7, 129.7, 127.6, 114.1, 61.1, 55.1, 29.2; HRMS (EI, M$^+$) for $C_{20}H_{22}O_4$ calcd. 326.1518, found: m/z 326.1517.

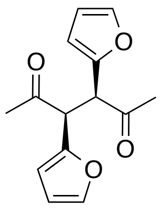

3d

Dienone **1d** (0.048 g, 0.20 mmol) was subjected to the standard condition with 2 equiv $FeCl_3 \cdot 6H_2O$ (0.108 g, 0.40 mmol). After the reaction temperature was raised to 0 ºC, the solution was stirred for 4 hours. Flash chromatography (19:1 to 9:1 hexane:EtOAc) gave **3d** (0.009 g, 18 %) as a white solid: R*f* 0.45 (hexanes/EtOAc 8:2); mp 79-81 °C; IR (cast film) 3130, 2949, 1719, 1502, 1200 cm^{-1}; ^{1}H NMR (500 MHz, CDCl$_3$) δ 7.28 (dd, *J* = 1.9, 0.8 Hz, 2H), 6.23 (dd, *J* = 3.3, 1.9 Hz, 2H), 6. 06 (dd, *J* = 3.2, 0.8 Hz, 2H), 4.70 (s, 2H), 2.21 (s, 6H); ^{13}C NMR (125 MHz, CDCl$_3$) δ 204.1, 148.9, 142.7, 110.6, 108.8, 52.9, 28.7; HRMS (EI, M$^+$) for $C_{14}H_{14}O_4$ calcd. 246.0892, found: m/z 246.0896.

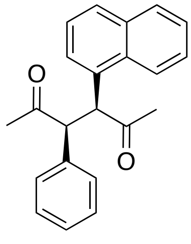

3f

Dienone **1f** (0.062 g, 0.20 mmol) was subjected to the standard condition. Flash chromatography (17:2:1 hexane:CH_2Cl_2:EtOAc) gave **3f** (colorless oil, 0.033 g, 52 %) as a mixture of rotamers: R_f 0.19 (hexanes/EtOAc 9:1); IR (cast film) 3061, 2926, 1709, 1354 cm^{-1}; HRMS (EI, M^+) for $C_{22}H_{20}O_2$ calcd. 316.1463, found: m/z 316.1464.

^1H and ^{13}C NMR spectra were obtained at a high temperature in C_6D_6 and at 26.4 ºC in $CDCl_3$.

^1H NMR (400 MHz, acquired at 84.7 ºC, C_6D_6) δ 7.96 (br s, 1H), 7.43 (d, *J* = 8.1 Hz, 1H), 7.35 (d, *J* = 8.1 Hz, 1H), 7.26-7.03 (m, 4H), 6.86-6.83 (m, 2H), 6.69-6.64 (m, 2H), 6.62-6.58 (m, 1H), 5.37 (br s, 1H), 4.69 (br s, 1H), 2.03 (s, 3H), 1.83 (s, 3H); ^{13}C NMR (100 MHz, acquired at 66.1 ºC, C_6D_6) δ 206.4 (br), 136.1, 134.6, 133.1, 132.8, 129.2, 129.0, 128.4, 127.2, 126.4, 125.7, 125.4, 123.5 (br), 62.7 (br), 55.3 (br), 29.1, 28.6 [One carbonyl and two aromatic resonances were not observed due to spectral overlap and/or peak broadening];

Major rotamer: ^1H NMR (500 MHz, acquired at 26.4 ºC, $CDCl_3$) δ 8.02 (br d, *J* = 7.6 Hz, 1H), 7.72 (br d, *J* = 7.0 Hz, 1H), 7.67 (br d, *J* = 7.4 Hz, 1H), 7.42-7.37 (m, 4H), 6.96-6.90 (m, 5H), 5.47 (d, *J* = 11.1 Hz, 1H), 4.61 (d, *J* = 11.0 Hz, 1H), 2.24 (s, 3H), 2.09 (s, 3H); ^{13}C NMR (125 MHz, acquired at 26.4 ºC, $CDCl_3$) δ 208.2, 207.5, 134.9, 134.0, 132.1, 132.0, 128.7, 128.6, 128.3, 128.1, 127.2, 126.2, 125.6, 125.5, 125.2, 122.8, 62.3, 54.6, 29.4, 29.2.

Minor rotamer (partially reported): ^1H NMR (500 MHz, acquired at 26.4 ºC, $CDCl_3$) δ 4.91 (br s, 1H), 4.86 (br s, 1H), 2.33 (s, 3H), 2.05 (s, 3H); ^{13}C NMR (125 MHz, acquired at 26.4 ºC, $CDCl_3$) δ 127.8, 127.6, 64.9, 58.6, 29.8, 28.8.

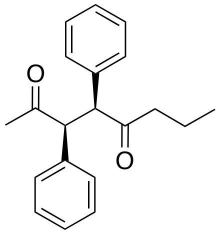

3g

Dienone **1g** (0.055 g, 0.19 mmol) was subjected to the standard condition.

Flash chromatography (39:1 to 19:1 hexane:EtOAc) gave **3g** (0.037 g, 66 %) as a white solid: R_f 0.33 (hexanes/EtOAc 9:1); mp 92-94 °C; IR (cast film) 3029, 2963, 1709, 1494, 1356 cm^{-1}; ^{1}H NMR (500 MHz, $CDCl_3$) δ 7.16-7.09 (m, 6H), 6.99-6.93 (m, 4H), 4.42 (ABq, $\Delta\nu_{AB}$ = 20.2 Hz, J_{AB} = 11.3 Hz, 2H), 2.54 (ddd, J = 17.1, 8.1, 6.1 Hz, 1H), 2.37 (ddd, J = 17.1, 8.1, 6.8 Hz, 1H), 2.16 (s, 3H), 1.65-1.47 (m, 2H), 0.81 (t, J = 7.4 Hz, 3H); ^{13}C NMR (125 MHz, $CDCl_3$) δ 210.1, 208.0, 135.7, 135.6, 128.8, 128.7, 128.6, 128.6, 127.3, 127.2, 62.0, 61.5, 43.8, 29.4, 17.1, 13.5; HRMS (EI, M$^+$) for $C_{20}H_{22}O_2$ calcd. 294.1620, found: m/z 294.1624.

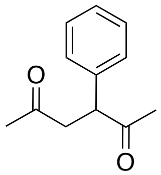

3h

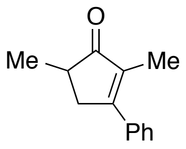

4h

Dienone **1h** (oil, 0.037 g, 0.20 mmol) dissolved in 0.2 mL CH_2Cl_2 was subjected to the standard condition. Flash chromatography (19:1 to 18:2 to 17:3 hexane:EtOAc) gave **3h** (0.017 g, 45 %) as a colorless oil and **4h** (0.006 g, 16 %) as a colorless oil.

3h: R_f 0.15 (hexanes/EtOAc 9:1); IR (cast film) 3029, 2922, 1712, 1494, 1356 cm^{-1}; ^{1}H NMR (400 MHz, $CDCl_3$) δ 7.35-7.30 (m, 2H), 7.29-7.25 (m, 1H), 7.21-7.18 (m, 2H), 4.22 (dd, J = 10.2, 3.9 Hz, 1H), 3.43 (dd, J =18.0, 10.2 Hz, 1H), 2.56 (dd, J = 18.0, 3.9 Hz, 1H), 2.16 (s, 3H), 2.11 (s, 3H); ^{13}C NMR (125 MHz, $CDCl_3$) δ 207.2, 206.9, 138.0, 129.3, 128.3, 127.7, 54.1, 46.6, 30.1, 29.1; HRMS (EI, M$^+$) for $C_{12}H_{14}O_2$ calcd. 190.0994, found: m/z 190.0997.

4h: Spectral data are consistent with the reported values.[127]

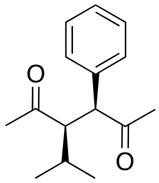

3i

Dienone **1i** (oil, 0.046 g, 0.20 mmol) dissolved in 0.2 mL CH_2Cl_2 was subjected to the standard condition. Flash chromatography (19:1 to 9:1 hexane:EtOAc) gave **3i** (0.026 g, 55 %) as a yellow oil: R_f 0.36 (hexanes/EtOAc 9:1); IR (cast film) 3028, 2964, 1706, 1353 cm^{-1}; ^1H NMR (500 MHz, $CDCl_3$) δ 7.38-7.34 (m, 2H), 7.32-7.29 (m, 1H), 7.25-7.22 (m, 2H), 4.22 (d, *J* = 11.4 Hz, 1H), 3.39 (dd, *J* = 11.4, 3.2 Hz, 1H), 2.34 (s, 3H), 2.00 (s, 3H), 1.51 (sept d, *J* = 7.0, 3.2 Hz, 1H), 0.98 (d, *J* = 7.2 Hz, 3H), 0.75 (d, *J* = 6.9 Hz, 3H); ^{13}C NMR (125 MHz, $CDCl_3$) δ 212.1, 208.3, 136.5, 129.2, 128.9, 127.7, 60.3, 58.5, 33.2, 29.1, 26.9, 22.2, 17.2; HRMS (EI, M^+) calcd for $C_{15}H_{20}O_2$ 232.1463; found m/z 232.1467.

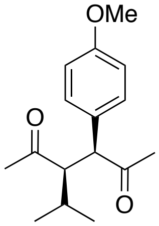

3j

Dienone **1j** (oil, 0.052 g, 0.20 mmol) dissolved in 0.2 mL CH_2Cl_2 was subjected to the standard condition. Flash chromatography (19:1 to 17:3 hexane:EtOAc) gave **3j** (0.019 g, 36 %) as a white solid: R_f 0.43 (hexanes/EtOAc 8:2); mp 76-78 °C; IR (cast film) 2963, 2935, 1706, 1512. 1255 cm^{-1}; ^1H NMR (500 MHz, $CDCl_3$) δ 7.16-7.13 (m, 2H), 6.91-6.88 (m, 2H), 4.16 (d, *J* = 11.4 Hz, 1H), 3.82 (s, 3H), 3.34 (dd, *J* = 11.5, 3.2 Hz, 1H), 2.33 (s, 3H), 1.99 (s, 3H), 1.53 (sept d, *J* = 7.1, 3.2 Hz, 1H), 0.98 (d, *J* = 7.2 Hz, 3H), 0.75 (d, *J* = 6.9 Hz, 3H); ^{13}C NMR (125 MHz, $CDCl_3$) δ 212.3, 208.6, 159.2, 129.9, 128.4, 114.6, 59.4, 58.5, 55.3, 33.2, 29.0, 26.9, 22.2, 17.2; HRMS (EI, M^+) for $C_{16}H_{22}O_3$ calcd. 262.1569, found: m/z 262.1566.

5.5.3 Experimental Procedures and Characterization for Halogen Interrupted Nazarov Reaction

Chlorine Interrupted Nazarov Cyclization (5a and 6a)

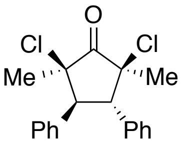
5a

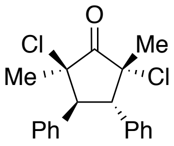
6a

To an open flask charged with concentrated HCl (37 %, 0.38 mL) was added Fe granules (10-40 mesh, 0.040 mmol, 0.0020 g), and stirred for 10 min at room temperature. CH_2Cl_2 (0.1 M, 1.9 mL) and 2 equiv $KMnO_4$ (0.38 mmol, 0.060 g) were then added to the solution, and stirred for 10 min. **1a** (0.019 mmol, 0.050 g) was added in one portion to the reaction vessel and stirred for 10 min. The reaction mixture was diluted with distilled water (2 mL) and carefully quenched with saturated $NaHCO_3$ solution (10 mL). The aqueous layer was extracted with CH_2Cl_2 (2 x 20 mL). The organic layers were combined and rinsed with brine and dried with $MgSO_4$. The filtered organic solution was concentrated by rotary evaporation and purified by flash column chromatography (silica gel, hexanes:EtOAc 39:1 to 19:1) to yield **5a** (0.040 g, 63 %) as a white solid and **6a** (0.014 g, 22 %) as a white solid.

5a: R_f 0.28 (hexanes/EtOAc 9:1); mp 170-172 °C; IR (cast film) 3033, 2976, 1766, 1500, 1452 cm^{-1}; ^1H NMR (400 MHz, $CDCl_3$) δ 7.34-7.21 (m, 10H), 4.60 (d, *J* = 13.3 Hz, 1H), 3.56 (d, *J* = 13.3 Hz, 1H), 1.76 (s, 3H), 1.26 (s, 3H); ^{13}C NMR (100 MHz, $CDCl_3$) δ 205.6, 133.8, 133.2, 129.7, 129.0, 128.5, 128.3, 128.0, 127.7, 69.9, 68.4, 54.3, 53.2, 23.4, 23.4; HRMS (EI, M^+) for $C_{19}H_{18}O^{35}Cl_2$ calcd. 332.0735, found: m/z 332.0734.

6a: R_f 0.47 (hexanes/EtOAc 9:1); mp 184-187 ºC; IR (cast film) 3031, 2972, 2924, 1764, 1448 cm^{-1}; ^1H NMR (500 MHz, $CDCl_3$) δ 7.33-7.23 (m, 10H), 4.03 (s, 2H), 1.88 (s, 6H); ^{13}C NMR (125 MHz, $CDCl_3$) δ 203.5, 133.7, 129.9, 128.1, 127.8, 71.2, 53.5, 24.6; HRMS (EI, M^+) for $C_{19}H_{18}O^{35}Cl_2$ calcd. 332.0735, found: m/z 332.0736.

Bromine Interrupted Nazarov Cyclization (7a and 8a)

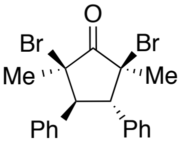
7a

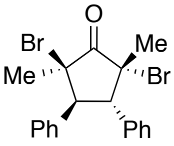
8a

To an open flask charged with concentrated HBr (48 wt. % in H_2O, 0.38 mL) was added Fe granules (10-40 mesh, 0.04 mmol, 0.002 g), and stirred for 10 min at room temperature. CH_2Cl_2 (0.10 M, 1.9 mL) and 2 equiv $KMnO_4$ (0.38 mmol, 0.060 g) were then added to the solution, and stirred for 10 min. **1a** (0.019 mmol, 0.050 g) was added in one portion to the reaction vessel and stirred for 10 min. The reaction mixture was diluted with distilled water (2 mL) and carefully quenched with saturated $NaHCO_3$ solution (10 mL). The aqueous layer was extracted with CH_2Cl_2 (2 × 20 mL). The organic layers were combined and rinsed with brine and dried with $MgSO_4$. The filtered organic solution was concentrated by rotary evaporation and purified by flash column chromatography (silica gel, hexanes/EtOAc 19:1) to yield **7a** (0.019 g, 24 %) as a white solid and **8a** (0.054 g, 67 %) as a white solid.

7a: R_f 0.29 (hexanes/EtOAc 9:1); mp 140-141 °C; IR (cast film) 3089, 3030, 2964, 2917, 1756, 1451, 1443 cm^{-1}; ^1H NMR (500 MHz, $CDCl_3$) δ 7.35-7.23 (m, 10H), 4.80 (d, *J* = 13.0 Hz, 1H), 3.25 (d, *J* = 13.0 Hz, 1H), 1.94 (s, 3H), 1.39 (s, 3H); ^{13}C NMR (125 MHz, $CDCl_3$) δ 206.0, 133.9, 133.8, 129.5, 129.1, 128.5, 128.2, 128.0, 127.8, 65.5, 59.8, 55.4, 53.9, 24.6, 24.5; HRMS (EI, M^+) for $C_{19}H_{18}O^{81}Br_2$ calcd. 423.9684, found: m/z 423.9677.

8a: R_f 0.47 (hexanes/EtOAc 9:1); mp 145-146 °C; IR (cast film) 3089, 3030, 2912, 1753, 1451 cm^{-1}; ^1H NMR (500 MHz, $CDCl_3$) δ 7.31-7.24 (m, 10H), 3.78 (s, 2H), 2.11 (s, 6H); ^{13}C NMR (125 MHz, $CDCl_3$) δ 203.0, 134.6, 129.8, 128.1, 127.8, 68.4, 54.1, 26.0; HRMS (EI, M^+) for $C_{19}H_{18}O^{81}Br_2$ calcd. 423.9684, found: m/z 423.9677.

References

---

(1) Book Chapter: a) F. G. West, O. Scadeng, Y.-K. Wu, R. J. Fradette and S. Joy, in *Comprehensive Organic Synthesis, 2nd Edition*, Vol. 5 (Eds: G. A. Molander, P. Knochel), Elsevier: Oxford, **2014**, pp. 827–866. Recent reviews: b) D. R. Wenz, J. Read de Alaniz, *Eur. J. Org. Chem*. **2015**, *2015*, 23–37; c) M. A. Tius, *Chem. Soc. Rev*. **2014**, *43*, 2979–3002; d) W. Nakanishi, F. G. West, *Curr. Opin. Drug Discov.* **2009**, *12*, 732–751; e) H. Pellisier, *Tetrahedron* **2005**, *61*, 6479–6517; f) M. A. Tius, *Eur. J. Org. Chem*. **2005**, 2193–2206; g) A. J. Frontier and C. Collison, *Tetrahedron* **2005**, *61*, 7577–7606.

(2) D. Vorländer, G. Schroedter, *Ber. Dtsch. Chem. Ges*. **1903**, *36*, 1490

(3) C. F. H. Allen, J. A. Van Allan, J. F. Tinker *J. Org. Chem*. **1955**, *20*, 1387–1391.

(4) I. N. Nazarov, I. I. Zaretskaya, *Bull. Acad. Sci. USSR*, *Div. chem. Sci*. **1944**, 65.

(5) I. N. Nazarov, I. I. Zaretskaya. *J. Gen. Chem. USSR* (*Engl. Transl.*), **1957**, *27*, 693–713.

(6) R. B. Woodward, R. Hoffmann, *Angew. Chem. Int. Ed*. **1969**, *8*, 781–932.

(7) Review: T. N. Grant, C. J. Rieder, F. G. West, *Chem. Commun*. **2009**, 5676–5688.

(8) J. A. Bender, A. E. Blize, C. C. Browder, S. Giese, F. G. West, *J. Org. Chem*, **1998**, *63*, 2430–2431.

(9) S. Giese, R. D. Mazzola, Jr., C. M. Amann, A. M. Arif, F. G. West, *Angew. Chem. Int. Ed.* **2005**, *44*, 6546–6549.

(10) C. D. Matier, Y. Kwon, F. G. West, *Can J. Chem*. **2014**, *92*, 58–61.

(11) J. A. Bender, A. M. Arif, F. G. West, *J. Am. Chem. Soc*. **1999**, *121*, 7443–7444.

(12) C. C. Browder, F. P. Marmsäter, F. G. West, *Org. Lett*, **2001**, *3*, 3033–3035.

(13) T. N. Grant, F. G. West, *J. Am. Chem. Soc*. **2006**, *128*, 9348–9349.

(14) T. N. Grant, F. G. West, *Org. Lett*. **2007**, *9*, 3789–3792.

(15) J. H. Chaplin, K. Jackson, J. M. White, B. L. Flynn *J. Org. Chem.*, **2014**, *79*, 3659–3664.

(16) R. William, S. Wang, F. Ding, E. N. Arviana, X.-W. Liu, *Angew. Chem. Int. Ed.* **2014**, *53*, 10742 –10746.

---

(17) C. J. Rieder, R. F. Fradette, F. G. West, *Chem. Commun.* **2008**, 1572–1574.

(18) C. J. Rieder, R. F. Fradette, F. G. West, *Heterocycles* **2010**, *80*, 1413–1427.

(19) A. K. Basak, M. A. Tius, *Org. Lett.* **2008**, *10*, 4073–4076.

(20) V. M. Marx, F. M. LeFort, D. J. Burnell, *Adv. Synth. Catal.* **2011**, *353*, 64–68.

(21) Y. Wang, B. D. Schill, A. M. Arif, F. G. West, *Org. Lett.* **2003**, *5*, 2747–2750.

(22) Y.-K. Wu, C. R. Dunbar, R. McDonald, M. J. Ferguson, F. G. West, *J. Am. Chem. Soc.* **2014**, *136*, 14903-14911.

(23) S. Giese, L. Kastrup, D. Stiens, F. G. West, *Angew. Chem. Int. Ed.* **2000**, *39*, 1970–1973.

(24) B. Mahmoud, F. G. West, *Tetrahedron Lett.* **2007**, *48*, 5091–5094.

(25) V. M. Marx, D. J. Burnell, *J. Am. Chem. Soc.* **2010**, *132*, 1685–1689.

(26) Y.-K. Wu, R. McDonald, F. G. West, *Org. Lett.* **2011**, *13*, 3584–3587.

(27) Y.-K. Wu, F. G. West, *Org. Lett.* **2014**, *16*, 2534–2537.

(28) Y. Wang, A. M. Arif, F. G. West, *J. Am. Chem. Soc.* **1999**, *121*, 876–877.

(29) S, Giese, F. G. West, *Tetrahedron Lett.* **1998**, *39*, 8393–8396.

(30) S. Giese, F. G. West, *Tetrahedron* **2000**, *56*, 10221–10228.

(31) V. Nair, S. Bindu, V. Sreekumar, A. Chiaroni, *Org. Lett.* **2002**, *4*, 2821–2823.

(32) M. Shindo, K. Yaji, T. Kita, K. Shishido, *Synlett* **2007**, 1096–1100.

(33) V. M. Marx, D. J. Burnell, *Org. Lett.* **2009**, *11*, 1229–1231.

(34) M. J. Riveira, M. P. Mischne, *J. Org. Chem.* **2014**, *79*, 8244–8254.

(35) F. Dhoro, M. A. Tius, *J. Am. Chem. Soc.* **2005**, *127*, 12472–12473.

(36) F. Dhoro, T. E. Kristensen, V. Stockmann, G. P. A. Yap, M. A. Tius, *J. Am. Chem. Soc.* **2007**, *129*, 7256–7257.

(37) A. Rostami, Y. Wang, A. M. Arif, R. McDonald, F. G. West, *Org. Lett.* **2007**, *9*, 703–706.

(38) D. Song, A. Rostami, F. G. West, *J. Am. Chem. Soc.* **2007**, *129*, 12019–12022.

(39) O. Scadeng, M. Ferguson, F. G. West, *Org. Lett.* **2011**, *13*, 114–117.

(40) T. D. White, F. G. West, *Tetrahedron Lett.* **2005**, *46*, 5629–5632.

(41) V. M. Marx, T. S. Cameron, D. J. Burnell, *Tetrahedron Lett.* **2009**, *50*, 7213–7216.

---

(42) a) S. E. Denmark, G. A. Hite, *Helv. Chim. Acta* **1988**, *71*,195–208; b) C. Kuroda, H. Koshio, A. Koito, H. Sumiya, A. Murase, Y. Hirono, *Tetrahedron* **2000**, *56*, 6441–6455.

(43) J. Motoyoshiya, T. Yazaki, S. Hayashi, *J. Org. Chem*. **1991**, *56*, 735–740.

(44) a) J. Huang, A. J. Frontier, *J. Am. Chem. Soc*. **2007**, *129*, 8086–8061; b) J. Huang, D. Leboeuf, A. J. Frontier, *J. Am. Chem. Soc*. **2011**, *133*, 6307–6317.

(45) D. Leboeuf, J. Huang, V. Gandon, A. J. Frontier, *Angew. Chem. Int. Ed*. **2011**, *50*, 10981–10985.

(46) J. Nie, H.-W. Zhu, H.-F. Cui, M.-Q. Hua, J.-A. Ma, *Org. Lett*. **2007**, *9*, 3053–3056.

(47) H.-F. Cui, K.-Y. Dong, G.-W. Zhang, L. Wang, J.-A. Ma, *Chem. Commun*. **2007**, 2284–2286.

(48) M. Rueping, W. Ieawsuwan, *Chem. Commun*. **2011**, *47*, 11450–11452.

(49) M. Janka, W. He, I. E. Haedicke, F. R. Fronczek, A. J. Frontier, R. Eisenberg, *J. Am. Chem. Soc*. **2006**, *128*, 5312–5313.

(50) A portion of this chapter has been published: Y. Kwon, R. McDonald, F. G. West, *Angew. Chem. Int. Ed.*, **2013**, *52*, 8616–8619.

(51) a) K. Ziegler, Brennst.-Chem. **1952**, *33*, 193–200; b) G. Natta, G. Dall' Asta, G. Mazzanti, I. Pasquon, A. Valvassori, A. Zambelli, *J. Am. Chem. Soc*. **1961**, *83*, 3343–3344.

(52) Y. Naganawa, K. Maruoka, *Top. Organomet. Chem*. **2013**, *41*, 187–214.

(53) W. D. Wulff, in *Lewis Acids in Organic Synthesis*, Vol. 1 (Ed: H. Yamamoto), WILEY-VCH: Weinheim, Germany, **2000**, pp. 283–354.

(54) K. Ishihara, N. Hanaki, H. Yamamoto, *J. Am. Chem. Soc*. **1993**, *115*, 10695–10704.

(55) J. D. Rainier, J. M. Cox, *Org. Lett*. **2000**, *2*, 2707–2709.

(56) M. Sasaki, K. Tanino, M. Miyashita, *Org. Lett*. **2001**, *3*, 1765–1767.

(57) Y. Kitagawa, S. Hashimoto, S. Iemura, H. Yamamoto, H. Nozaki, *J. Am. Chem. Soc*. **1976**, *98*, 5030–5031.

(58) T. Miyoshi, T. Miyakawa, M. Ueda, O. Miyata, *Angew. Chem. Int. Ed*. **2011**, *50*, 928 –931.

---

(59) K. Flack, K. Kitagawa, P. Pollet, C. A. Eckert, K. Richman, J. Stringer, W. Dubay, C. L. Liotta, *Org. Process Res. Dev*. **2012**, *16*, 1301−1306.

(60) E. J. Campbell, H. Zhou, S. T. Nguyen, *Org. Lett*, **2001**, *3*, 2391–2393.

(61) R. Kow, R. Nygren, M. W. Rathke, *J. Org. Chem.* **1977**, *42*, 826–827.

(62) C. R. Graves, B.-S. Zeng, S. T. Nguyen, *J. Am. Chem. Soc.* **2006**, *128*, 12596–12597.

(63) T. Ooi, H. Ichikawa, K. Maruoka, *Angew. Chem. Int. Ed*. **2001**, *40*, 3610–3612.

(64) T. Ooi, H. Otsuka, T. Miura, H. Ichikawa, K. Maruoka, *Org. Lett*. **2002**, *4*, 2669–2672.

(65) T. Ooi, T. Miura, K. Maruoka, *Angew. Chem. Int. Ed*. **1998**, *37*, 2347–2349.

(66) E. J. Campbell, H. Zhou, S. T. Nguyen, *Angew. Chem. Int. Ed*. **2002**, 41, 1020–1022.

(67) Use of $EtAlCl_2$ as Lewis acid in Nazarov reaction: a) G. Liang, S. N. Gradl, D. Trauner, *Org. Lett*. **2003**, *5*, 4931–4934; b) S.-H. Kim, J. K. Cha, *Synthesis* **2000**, 2113–2116; c) For a recent example of R_3Al-initiated Nazarov cyclization followed by trapping with a pendent phosphine, see: J. Boudreau, M.-A. Courtemanche, V. M. Marx, D. J. Burnell, F.-G. Fontaine, *Chem. Commun.* **2012**, *48*, 11250-11252.

(68) Use of Me_2AlCl in 6π electrocyclization: L. M. Bishop, J. E. Barbarow, R. G. Bergman, D. Trauner, *Angew. Chem. Int. Ed*. **2008**, *47*, 8100–8103.

(69) Halide trapping of the Nazarov intermediate has been postulated to occur via Ti(IV)-mediated delivery of halogen ligands. See: reference (40) and (41)

(70) Triorganoaluminum reagents are highly sensitive to traces of water, and inclusion of molecular sieves in the reaction mixture was found to improve reproducibility.

(71) CCDC 915117 (**3a**), 915118 (**3h**), 915119 (**7a**), 915120 (**8a'**) and 915121 (**11a**) contain the supplementary crystallographic data for this chapter. These data may be obtained free of charge from the Cambridge Crystallographic Data Centre via www.ccdc.cam.ac.uk/data_request/cif.

(72) L. Ernst, P. Schulz, *Magn. Reson. Chem*. **1992**, *30*, 73–76.

(73) For an alternative approach to the "reductive Nazarov" reaction, see: reference (29) and (30)

(74) K. Ziegler, H. Martin, F. Krupp, *Justus Liebigs Ann. Chem*. **1960**, *629*, 14–19.

---

(75) A. G. Schultz, M. Macielag, M. Plummer, *J. Org. Chem*. **1988**, *53*, 391–395.

(76) V. Aureggi, G. Sedelmeier, *Angew, Chem. Int. Ed*. **2007**, *46*, 8440–8444.

(77) See examples: a) H. Suzuki, N. Yamazaki, C. Kibayashi, *Tetrahedron Lett.* **2001**, *42*, 3013–3015.

(78) K. Haraguchi, Y. Kubota, and H. Tanaka, *J. Org. Chem*. **2004**, *69*, 1831–1836.

(79) T. Ooi, T. Miura, K. Maruoka, *J. Am. Chem. Soc*. **1998**, *120*, 10790–10791.

(80) C. D. Smith, G. Rosocha, L. Mui, R. A. Batey, *J. Org. Chem.* **2010**, *75*, 4716–4727.

(81) A. Arnold, M. Markert, R. Mahrwald, *Synthesis* **2006**, *7*, 1099–1102.

(82) C. J. Rieder, K. J. Winberg, F. G. West, *J. Org. Chem.* **2011**, *76*, 50–56.

(83) R. G. Kelleher, M. A. McKervey, P. Vibuljan, *J. Chem. Soc., Chem. Commun.* **1980**, 486–488.

(84) Ethylene glycol/ethanol bath with dry ice was used to set –25 ºC and –30 ºC. See: D. W. Lee, C. M. Jensen, *J. Chem. Educ*. **2000**, *77*, 629.

(85) A. Saito, M. Umakoshi, N. Yagyu, and Y. Hanzawa, *Org. Lett*. **2008**, *10*, 1783–1785.

(86) A portion of this chapter has been published: Y. Kwon, O. Scadeng, R. McDonald, F. G. West, *Chem. Commun.* **2014***, 50*, 5558–5560.

(87) K. Rück, H. Kunz, *Angew. Chem. Int. Ed.*, **1991**, *30*, 694–696.

(88) Y. Wang, L. Bao, D. Liu, X. Yang, S. Li, H. Gao, X. Yao, H. Wen, H. Liu, *Tetrahedron*, **2012**, *68*, 3012–3018.

(89) For an example, see: reference (30).

(90) O. Scadeng, F. G. West, *Eur. J. Org. Chem*. **2014**, 1860–1865.

(91) For the preparation of oxaziridine, see: F. A. Davis, S. Chattopadhyay, J. C. Towson, S. Lal, T. Reddy, *J. Org. Chem.* **1988**, *53*, 2087–2089.

(92) J. F. Allan, W. Clegg, M. R. J. Elsegood, K. W. Henderson, A. E. McKeown, P. H. Moran, I. M. Rakov, *J. Organomet. Chem*. **2000**, *602*, 15–23.

(93) A. G. Davies and B. P. Roberts, *J. Chem. Soc. (B)*, **1968**, 1074–1078.

(94) K. Takai, K. Oshima, H. Nozaki, *Tetrahedron Lett*. **1980**, *21*, 1657–1660.

(95) H. Nozaki, K. Oshima, K. Takai, S. Ozawa, *Chem. Lett*. **1979**, 379–380.

---

(96) a) G. M. Rubottom, R. Marrero *J. Org. Chem.* **1975**, *40*, 3783–3784; b) G. M. Rubottom, J. M. Gruber *J. Org. Chem.* **1978**, *43*, 1599–1602; c) G. M. Rubottom, H. D. Juve, Jr., *J. Org. Chem.*, **1983**, *48*, 422–425.

(97) E. Vedejs, D. A. Engler, J. E. Telschow, *J. Org. Chem*. **1978**, *43*, 188–196.

(98) Ethylene glycol/ethanol bath with dry ice was used to obtain a stable bath temperature of –25 ºC. See: D. W. Lee, C. M. Jensen, *J. Chem. Educ*. **2000**, *77*, 629.

(99) For recent examples, see: reference (16), (26), and (27)

(100) For examples, see: reference (46) and (48); J. L. Brooks, P. A. Caruana, A. J. Frontier, *J. Am. Chem. Soc*. **2011**, *133*, 12454–12457.

(101) For examples, see: reference (21), (28), and (39)

(102) a) B. B. Snider, R. Cordova, R. T. Price, *J. Org. Chem*. **1982**, *47*, 3643–3646; b) B. B. Snider, D. J. Rodini, M. Karras, T. C. Kirk, E. A. Deutach, R. Cordova, R. T. Price, *Tetrahedron* **1981**, 3927.

(103) B. B. Snider, G. B. Phillips, *J. Org. Chem*. **1983**, *48*, 2789–2792.

(104) J. W. Collette, *J. Org. Chem.* **1963**, *28*, 2489–2490.

(105) D. B. Miller, *Tetrahedron Lett*. **1964**, *5*, 989–993.

(106) K. Maruoka, Y. Fukutani, H. Yamamoto, *J. Org. Chem*. **1985**, *50*, 4412–4414.

(107) J.-P. Barnier, V. Morisson, L. Blanco, *Synth. Commun*. **2001**, *31*, 349–357.

(108) D. H. Gibson, C. H. DePuy, *Tetrahedron Lett*. **1969**, *10*, 2203–2206.

(109) Book Chapter: a) D. G. Lee, T. Chen, in *Comprehensive Organic Synthesis*, Vol. 7 (Eds: B. M. Trost, I. Fleming), Pergamon Press: Oxford, **1991**, pp. 541–591; For a mechanism, see: b) R. Criegee, *Angew. Chem. Int. Ed*. **1975**, *14*, 745–752.

(110) R. Pappo, D. S. Allen, R. U. Lemieux, Jr., W. S. Johnson, *J. Org. Chem.* **1956**, *21*, 478–479.

(111) R, Zurflüh, L. L Dunham, V. L. Spain, J. B. Siddall, *J. Am. Chem. Soc.* **1970**. *92*. 425–417.

(112) W. Yu, Y. Mei, Y. Kang, Z. Hua, Z. Jin, *Org. Lett*. **2004**, *6*, 3217–3219.

(113) B. R. Travis, R. S. Narayan, B. Borhan, *J. Am. Chem. Soc*, **2002**, *124*, 3824–3825.

(114) F. X. Webster, J. Rivas-Enterrios, R. M. Silverstein, *J. Org. Chem*. **1987**, *52*, 689–691.

---

(115) T. Ogino, K. Mochizuki, *Chem. Lett.* **1979**, *8*, 443–446.

(116) A. J. Fatiadi, *Synthesis* **1987**, *1987*, 85–127.

(117) The *syn* relative configurations of the other diketone products were assigned by analogy to this one.

(118) As an undergraduate CHEM401 project, Mr. Devon Schatz contributed to the synthesis of divinyl ketones **1e**, **1g**, and **1i** as well as repeating some of the reactions.

(119) Mr. Devon Schatz carried out this particular work as a CHEM401 project.

(120) For a review, see: S. Dash, S. Patel, B. K. Mishra, *Tetrahedron* **2009**, *65*, 707-739.

(121) a) F. P. Venable, D. H. Jackson, *J. Am. Chem. Soc.* **1920**, *42*, 237–239; b) H. N. Alyea *J. Chem. Educ.* **1969**, *46*, A218.

(122) H. Davy, *Phil. Trans. R. Soc. Lond.* **1811**, *101*, 155–162.

(123) R. Noyori, Y. Taba, S. Makino, H. Takaya, *Tetrahedron Lett.* **1973**, *14*, 1741.

(124) a) H. M. R. Hoffmann, K. E. Clemens, R. H. Smithers, *J. Am. Chem. Soc.* **1972**, *94*, 3940; b) N. N. Joshi, H. M. R. Hoffmann, *Tetrahedron Lett.* **1986**, *27*, 687–690.

(125) B. Föhlisch, E. Gehrlach, R. Herter, *Angew. Chem. Int. Ed. Engl.* **1982**, *21*, 137.

(126) a) H. Ohno, K. Miyamura, T. Tanaka *J. Org. Chem.* **2002**, *67*, 1359–1367; b) S. Adimurthy, S. Ghosh, P. U. Patoliya, G. Ramachandraiah, M. Agrawal, M. R. Gandhi, S. C. Upadhyay, P. K. Ghosh, B. C. Ranu, *Green Chem.* **2008**, *10*, 232–237.

(127) A. D. Jenkins, A. Herath, M. Song, J. Montgomery, *J. Am. Chem. Soc.* **2011**, *133*, 14460–14466.

Appendix I: Selected NMR Spectra

(Chapter 2)

Yong 5 20 col
498.122 MHz H1 1D in cdcl3 (ref. to CDCl3 @ 7.26 ppm), temp 27.2 C -> actual temp = 27.0 C, autoxdb probe
date: Mar 28 2012 sweep width: 6001Hz acq.time: 5.0s relax.time: 0.1s # scans: 16   dig.res.: 0.1 Hz/pt hz/mm:19.7 Pulse Sequence: s2pul
spectrometer:d300   file:/mnt/d600/home13/westnmr/nmrdata/YONGHOON/Book5/2012.03.28.i5_Yong-5-20-col_H1_1D

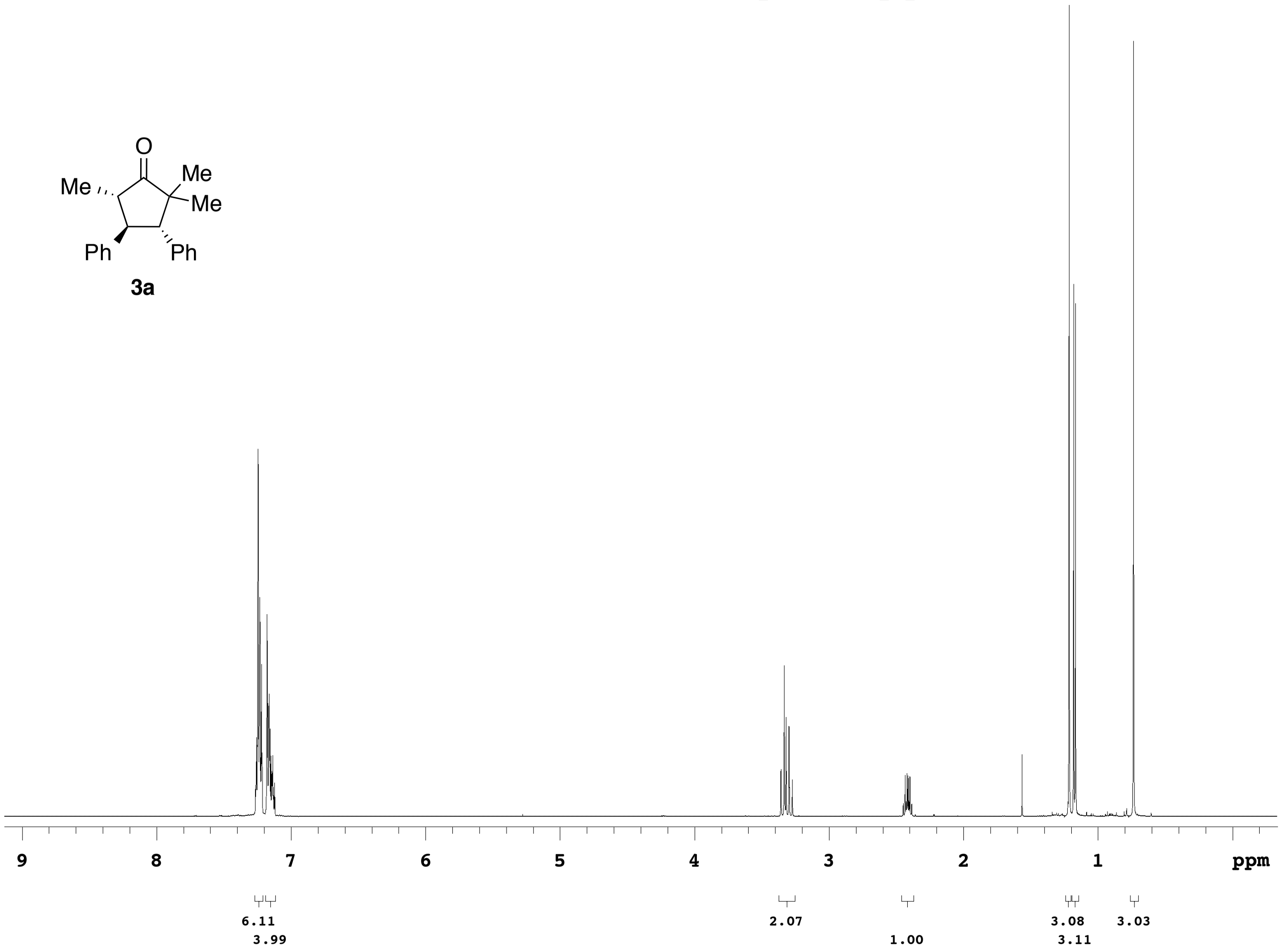

125.267 MHz C13[H1] APT_ad in cdcl3 (ref. to CDCl3 @ 77.06 ppm), temp 27.2 C -> actual temp = 27.0 C, autoxdb probe
date: Mar 28 2012, sweep width: 33827Hz acq.time: 2.5s relax.time: 0.1s # scans: 96 dig.res.: 0.3 Hz/pt hz/mm:140.9
C & CH2 same, CH & CH3 opposite side of solvent signal
spectrometer:d300 file:/mnt/d600/home13/westnmr/nmrdata/YONGHOON/Book5/2012.03.28.i5_Yong-5-20-col_C13_APT_ad
Pulse Sequence: APT_ad

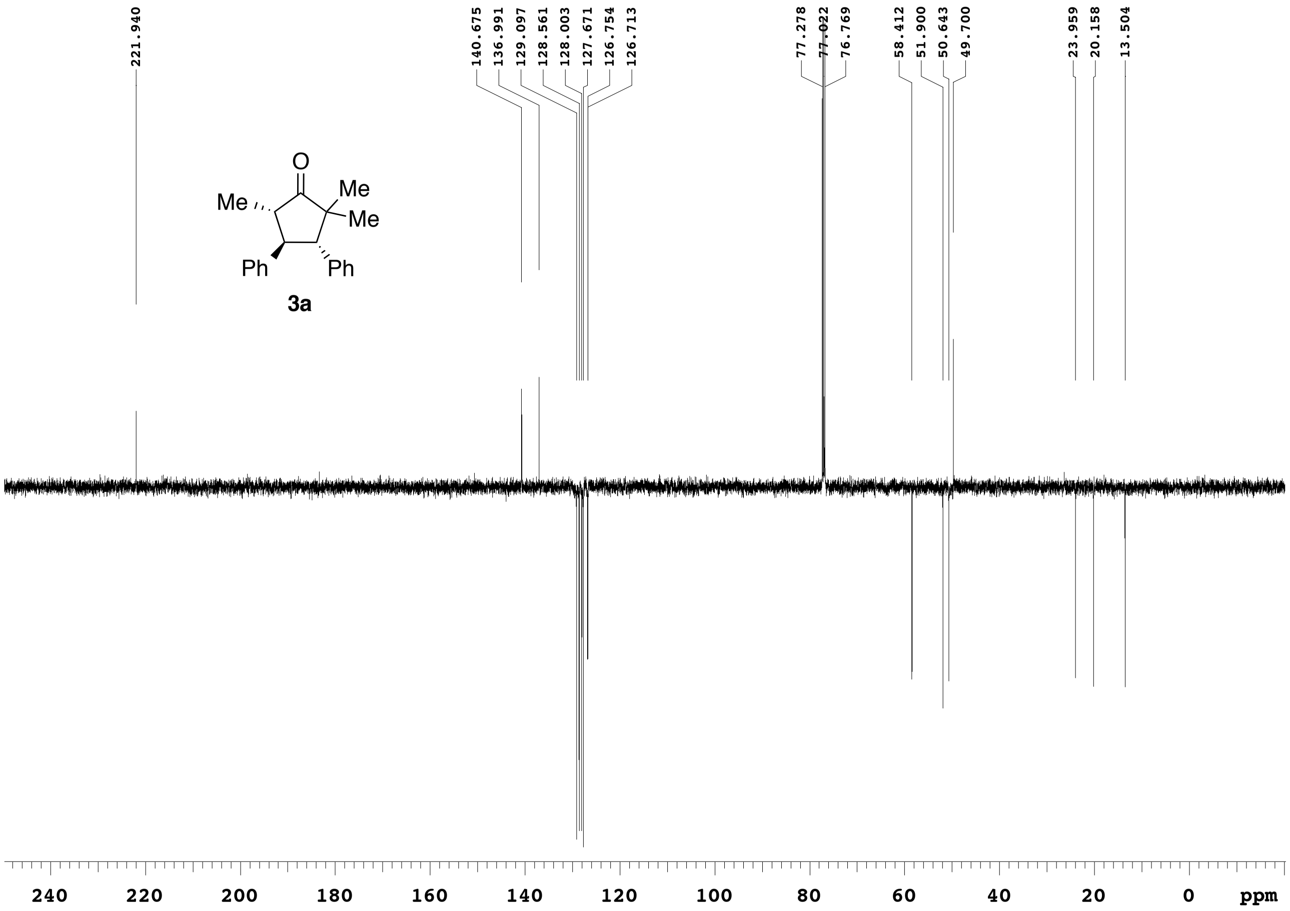

Yong-6-66-col
498.118 MHz H1 1D in cdcl3 (ref. to CDCl3 @ 7.26 ppm), temp 27.2 C -> actual temp = 27.0 C, autoxdb probe

Pulse Sequence: s2pul

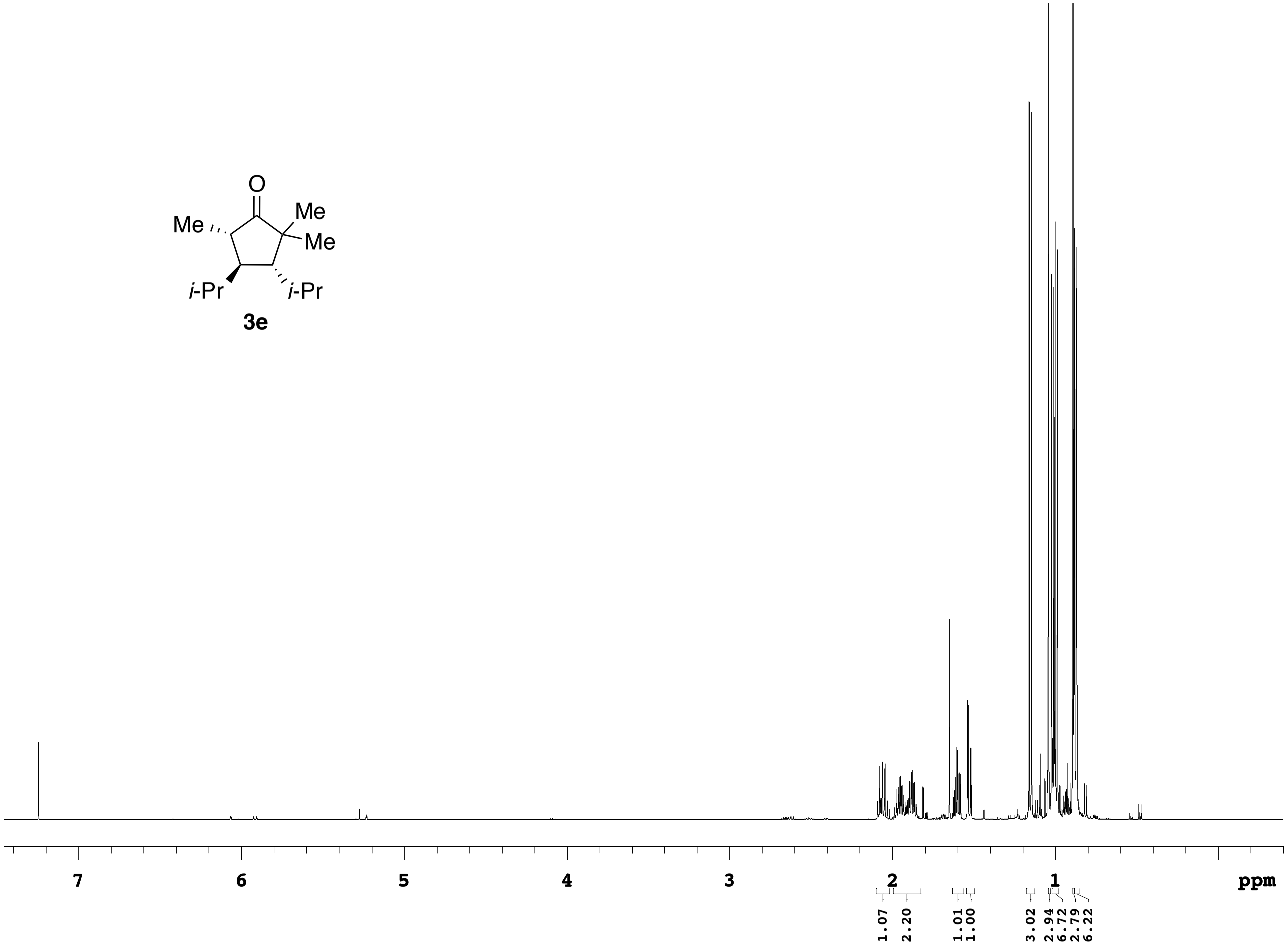

3e

Yong 6 66 col
125.266 MHz C13[H1] APT_ad in cdcl3 (ref. to CDCl3 @ 77.06 ppm), temp 27.2 C -> actual temp = 27.0 C, autoxdb probe
date: Aug 7 2012, sweep width: 33827Hz acq.time: 2.5s relax.time: 0.1s # scans: 100 dig.res.: 0.3 Hz/pt hz/mm:140.9
C & CH2 same, CH & CH3 opposite side of solvent signal
spectrometer:d300 file:/mnt/d600/home13/westnmr/nmrdata/YONGHOON/Book6/2012.08.07.i5_Yong-6-66-col_C13_APT_ad
Pulse Sequence: APT_ad

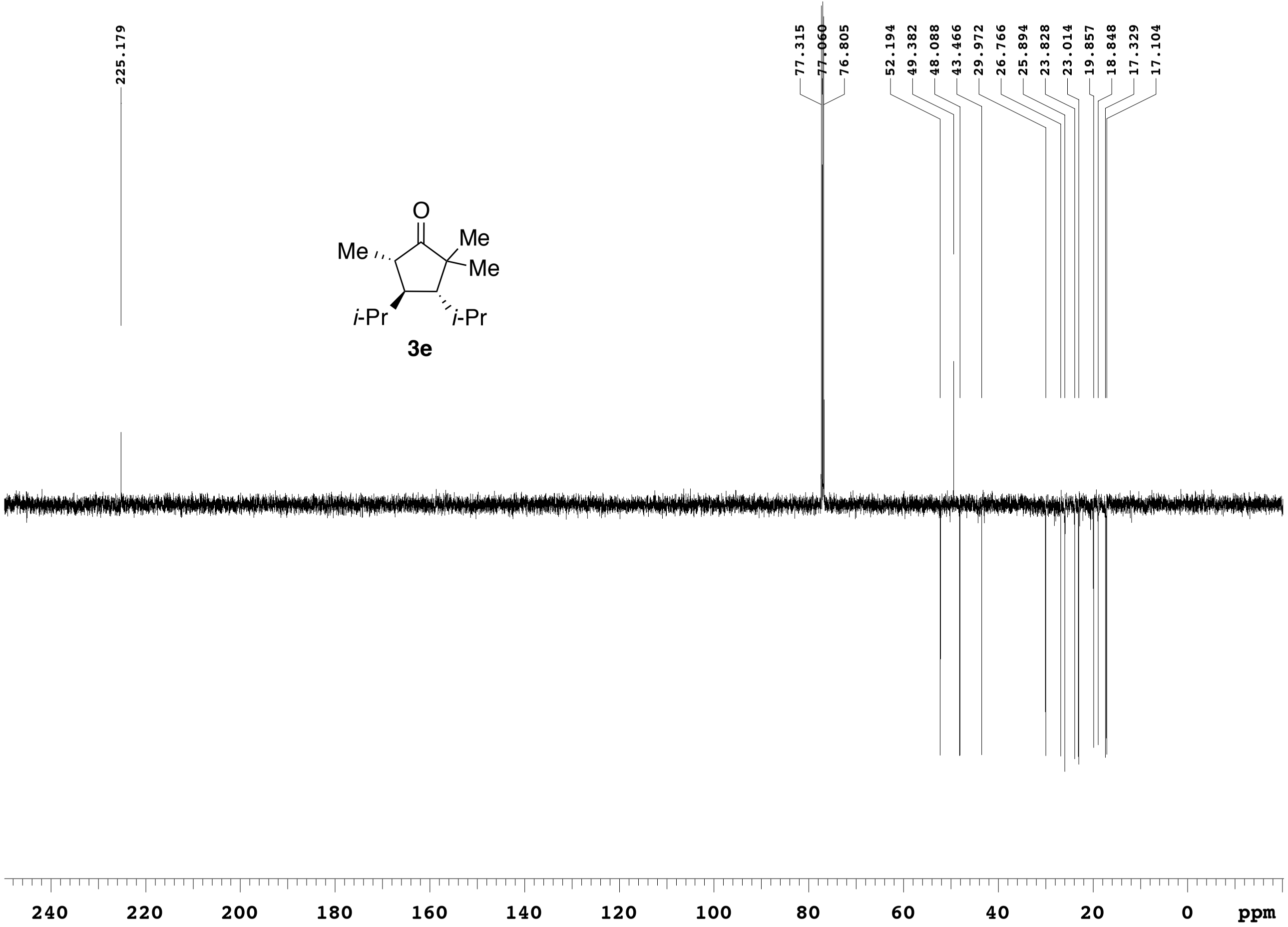

Yong-5-150-col-major
498.122 MHz H1 1D in cdcl3 (ref. to CDCl3 @ 7.26 ppm), temp 27.2 C -> actual temp = 27.0 C, autoxdb probe

Pulse Sequence: s2pul

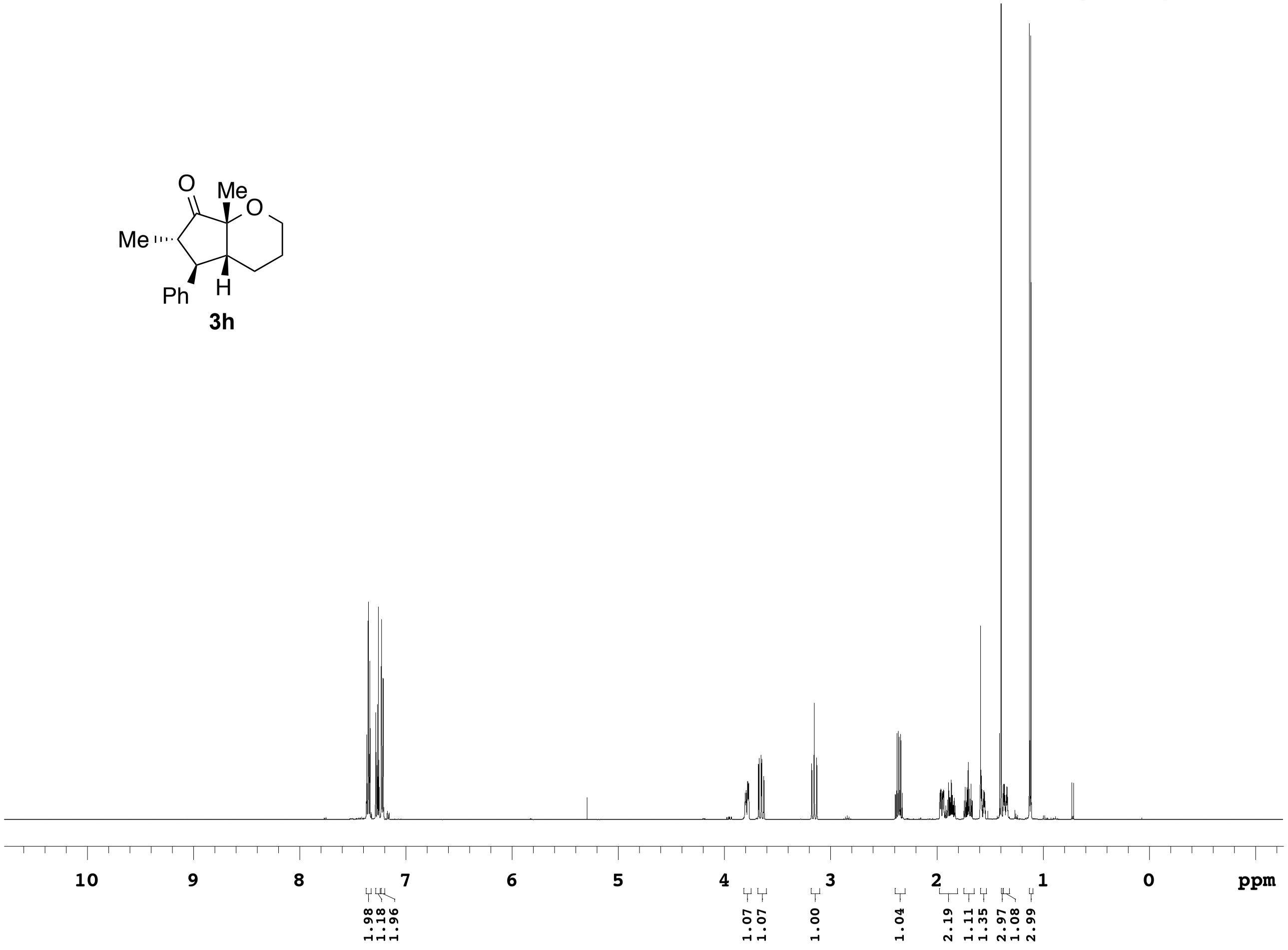

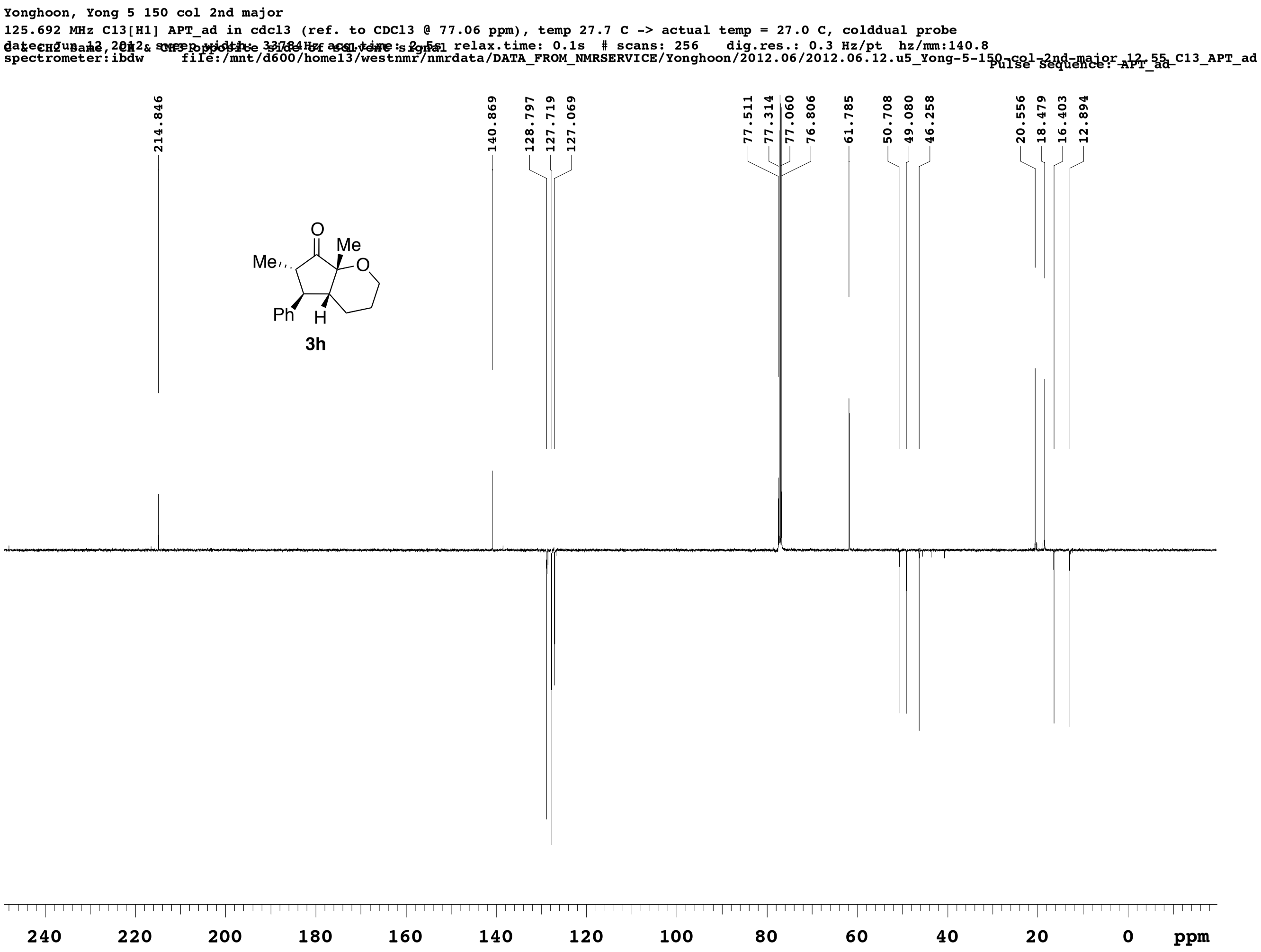
Yonghoon, Yong 5 150 col 2nd major
125.692 MHz C13[H1] APT_ad in cdcl3 (ref. to CDCl3 @ 77.06 ppm), temp 27.7 C -> actual temp = 27.0 C, colddual probe
date: Jun 12 2012 sweep width: 33784Hz acq.time: 2.5s relax.time: 0.1s # scans: 256 dig.res.: 0.3 Hz/pt hz/mm:140.8
C & CH2 same, CH & CH3 opposite side of solvent signal
spectrometer:ibdw file:/mnt/d600/home13/westnmr/nmrdata/DATA_FROM_NMRSERVICE/Yonghoon/2012.06/2012.06.12.u5_Yong-5-150-col-2nd-major_12_55_C13_APT_ad
Pulse Sequence: APT_ad
214.846
140.869
128.797
127.719
127.069
77.511
77.314
77.060
76.806
61.785
50.708
49.080
46.258
20.556
18.479
16.403
12.894
O
Me
Me
O
Ph
H
3h
240
220
200
180
160
140
120
100
80
60
40
20
0
ppm

Yong 5 150 col 1stspot minor
498.122 MHz H1 1D in cdcl3 (ref. to CDCl3 @ 7.26 ppm), temp 27.2 C -> actual temp = 27.0 C, autoxdb probe
date: Jun 12 2012 sweep width: 6001Hz acq.time: 5.0s relax.time: 0.1s # scans: 32 dig.res.: 0.1 Hz/pt hz/mm:20.5 Pulse Sequence: s2pul
spectrometer:d300 file:/mnt/d600/home13/westnmr/nmrdata/YONGHOON/Book5/2012.06.12.i5_Yong-5-150-col-1stspot-minor_H1_1D

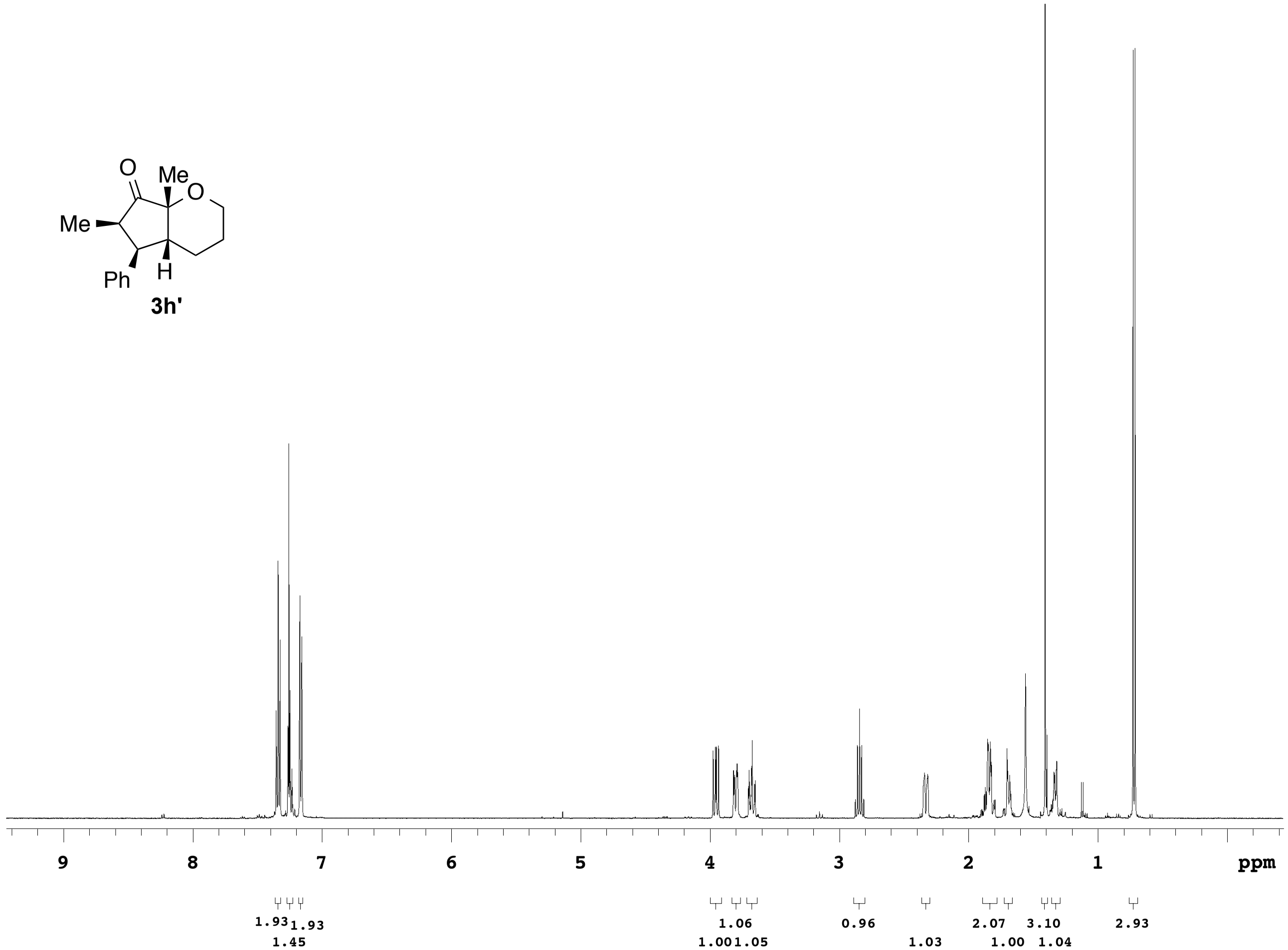
3h'

Yong 5 150 col 1stspot minor
125.267 MHz C13[H1] APT_ad in cdcl3 (ref. to CDCl3 @ 77.06 ppm), temp 27.2 C -> actual temp = 27.0 C, autoxdb probe
date: Jun 12 2012, sweep width: 33827Hz acq.time: 2.5s relax.time: 0.1s # scans: 772 dig.res.: 0.3 Hz/pt hz/mm:140.9
C & CH2 same, CH & CH3 opposite side of solvent signal
spectrometer:ibdw file:/mnt/d600/home13/westnmr/nmrdata/YONGHOON/Book5/2012.06.12.i5_Yong-5-150-col-1stspot-minor_C13_APT_ad
Pulse Sequence: APT_ad

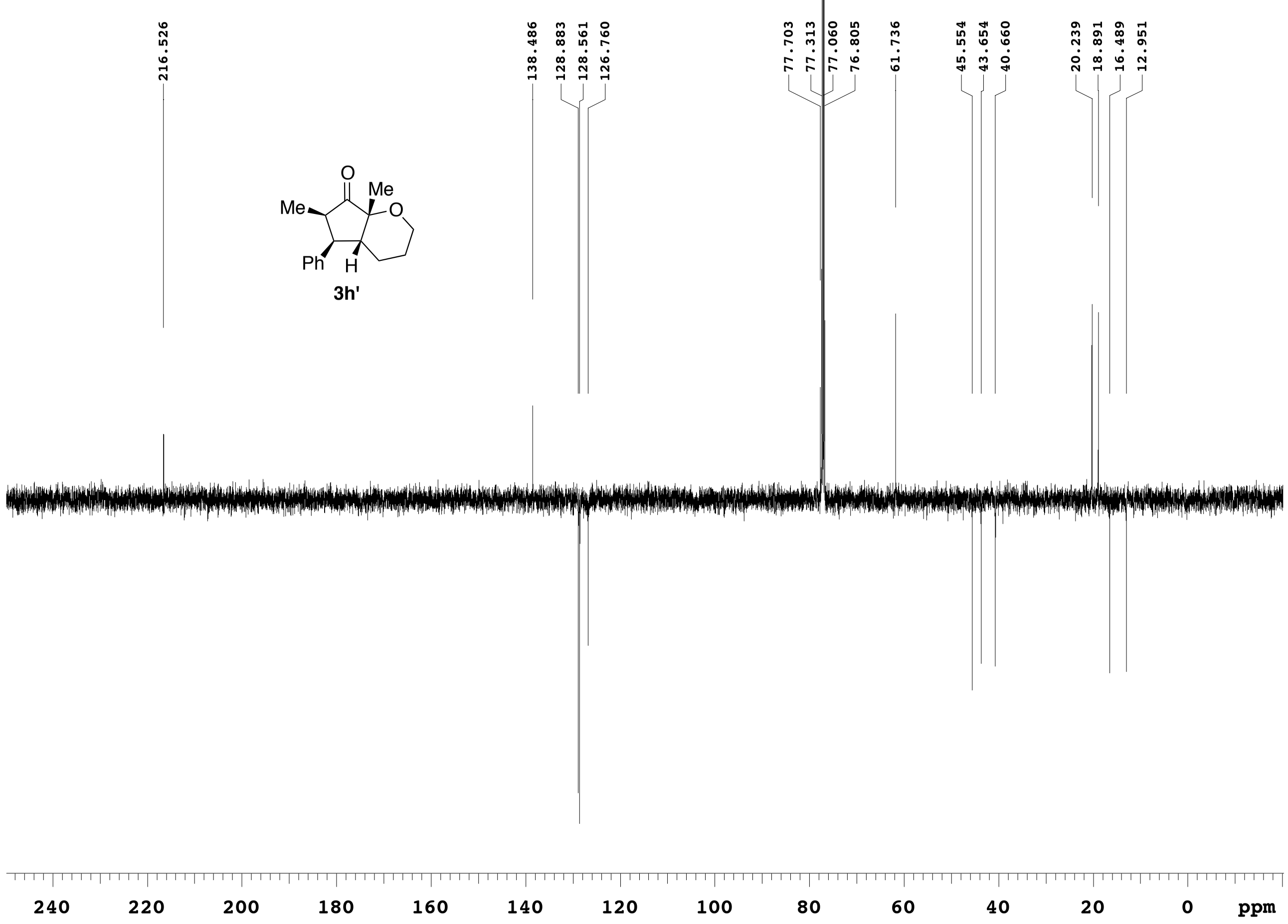

3h'

```
Yong-11-36-col-EA removed
498.118 MHz H1 1D in cdcl3 (ref. to CDCl3 @ 7.26 ppm), temp 26.4 C -> actual temp = 27.0 C, autoxdb probe

date: Jul 14 2014  sweep width: 6001Hz  acq.time: 5.0s  relax.time: 0.1s  # scans:  16   dig.res.: 0.1 Hz/pt  hz/mm:18.4
spectrometer:d300     file:/mnt/d600/home13/westnmr/nmrdata/YONGHOON/Book11/2014.07.14.i5_Yong-11-36-col-EA_removed_H1_1D
```

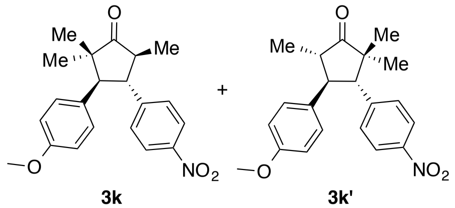

3k major

3k' minor

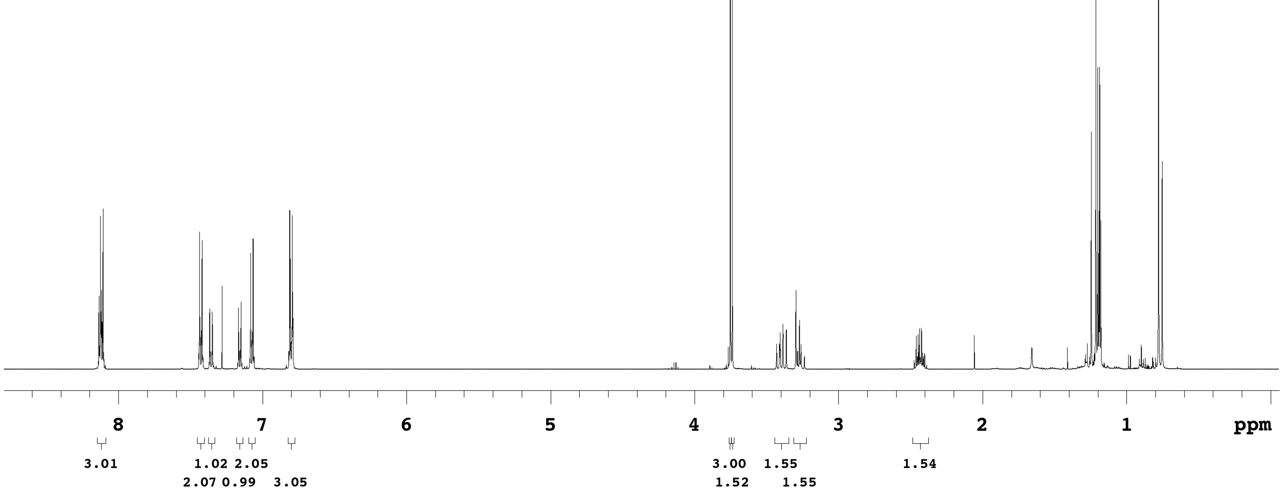

Pulse Sequence: s2pul

```
Yong-11-36-col-EA-removed
125.266 MHz C13[H1] APT_ad in cdcl3 (ref. to CDCl3 @ 77.06 ppm), temp 26.4 C -> actual temp = 27.0 C, autoxdb probe
C & CH2 same, CH & CH3 opposite side of solvent signal

date: Jul 15 2014  sweep width: 33827Hz acq.time: 2.5s  relax.time: 0.1s  # scans: 1036   dig.res.: 0.3 Hz/pt  hz/mm:140.9
spectrometer:d300     file:/mnt/d600/home13/westnmr/nmrdata/YONGHOON/Book11/2014.07.15.i5_Yong-11-36-col-EA-removed_19.32_C13_APT_ad
```

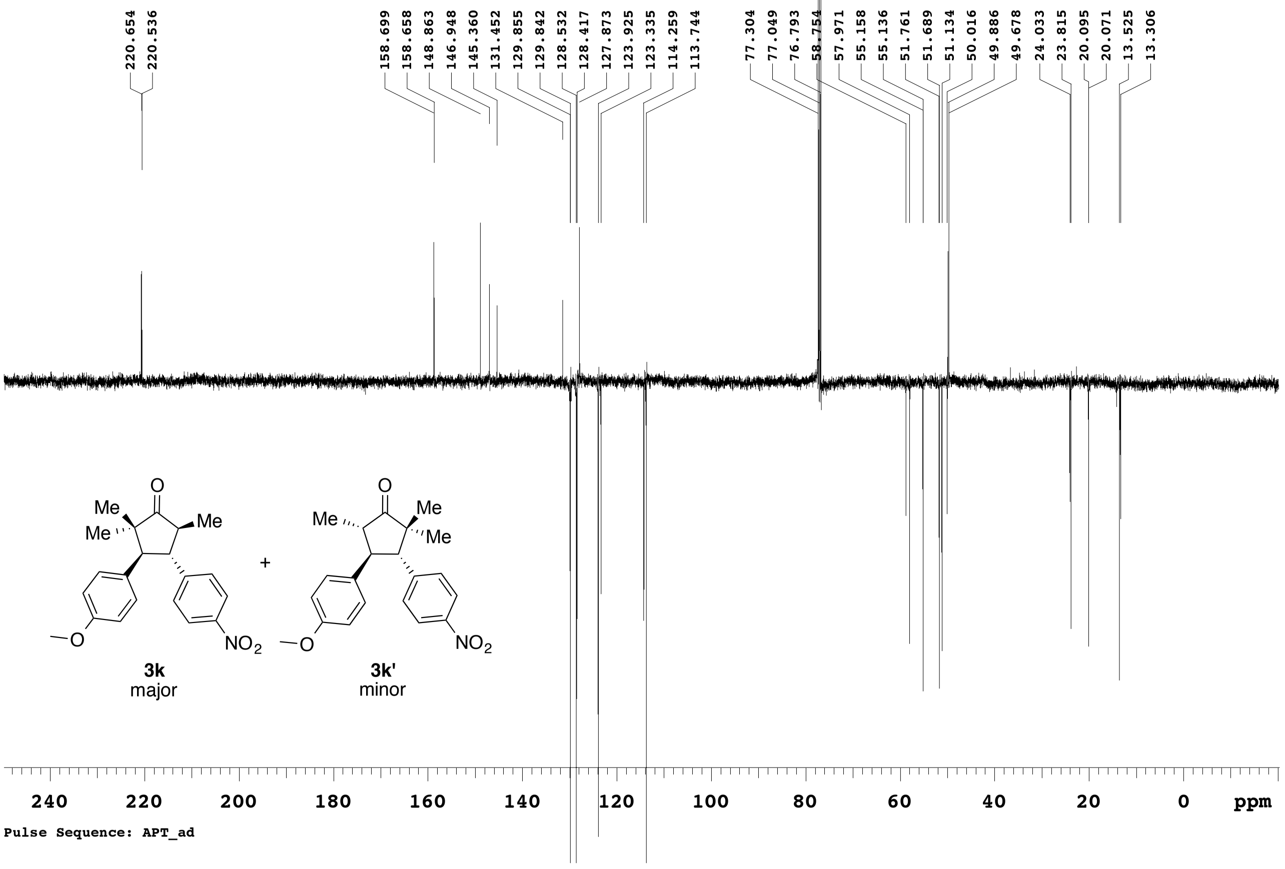

Yonghoon, Yong-11-36-col-Ea removed
399.951 MHz H1 bashdROESY in cdcl3
temp 25.5C --> actual temp = 26.9, sw400 probe

Temp. 25.5 C / 298.6 K
Operator: nmrlab

Relax. delay 1.000 sec
Acq. time 1.000 sec
Width 4801.9 Hz
2D Width 39.5 Hz
8 repetitions
2 x 32 increments
OBSERVE H1, 399.9486687 MHz
DATA PROCESSING
Sq. sine bell 0.364 sec
Shifted by -0.359 sec
F1 DATA PROCESSING
Sq. sine bell 0.785 sec
Shifted by -0.785 sec
FT size 8192 x 1024
Total time 26 min

Pulse Sequence: bashdROESY

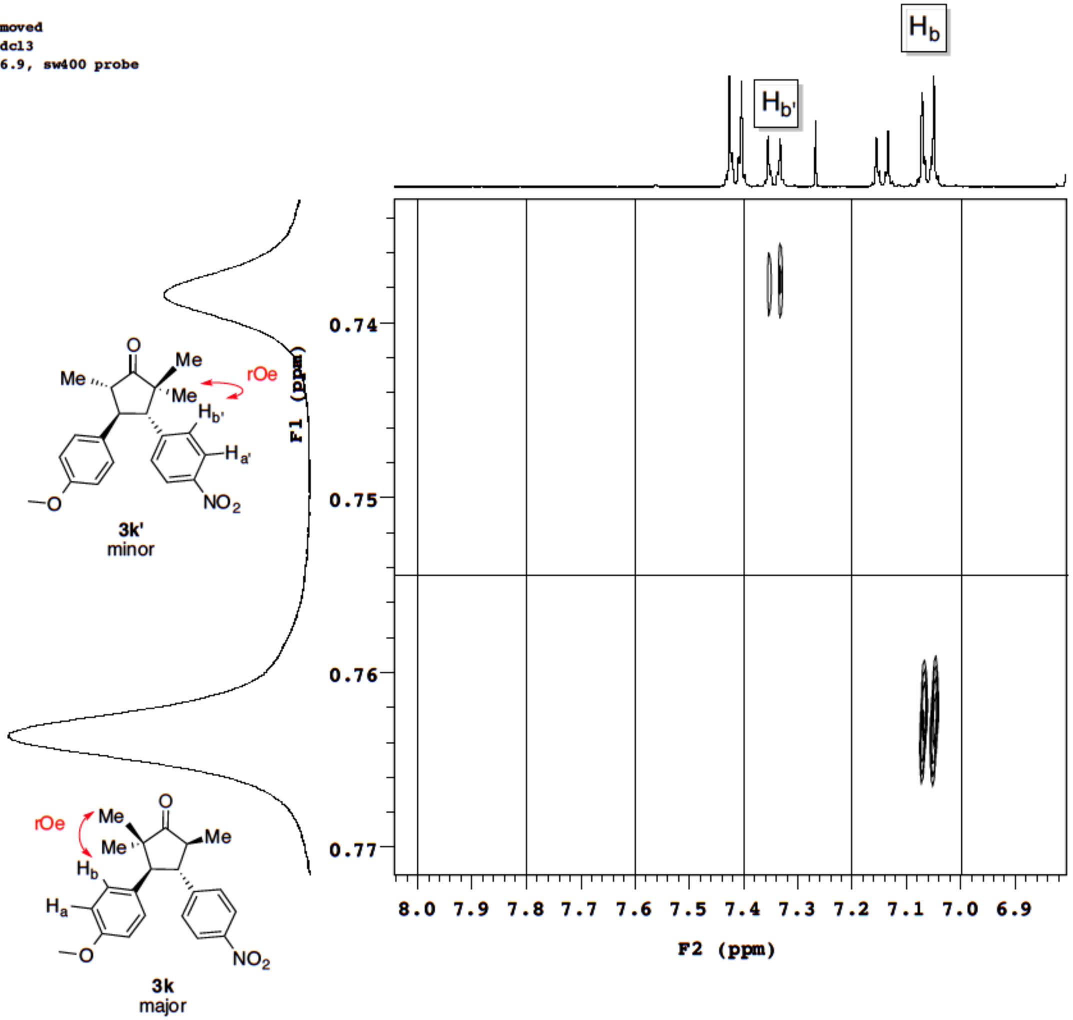

```
Yong-11-40-col
498.118 MHz H1 1D in cdcl3 (ref. to CDCl3 @ 7.26 ppm), temp 26.4 C -> actual temp = 27.0 C, autoxdb probe

date: Jul  6 2014  sweep width: 6001Hz  acq.time: 5.0s  relax.time: 0.1s  # scans:  16   dig.res.: 0.1 Hz/pt  hz/mm:25.0
spectrometer:d300     file:/mnt/d600/home13/westnmr/nmrdata/YONGHOON/Book11/2014.07.06.i5_Yong-11-40-col_H1_1D
```

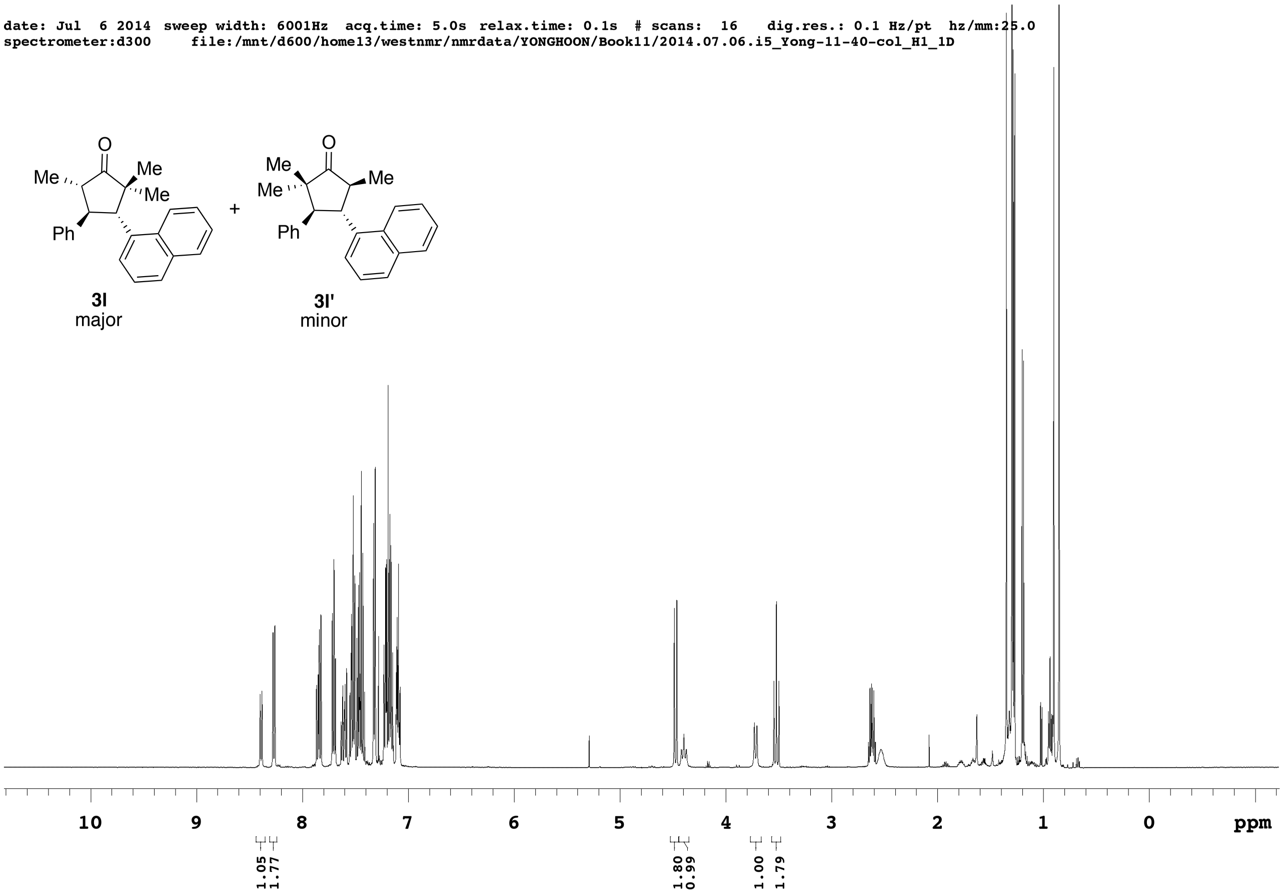

3l
major

+

3l'
minor

```
Pulse Sequence: s2pul
```

Yong-11-40-col
125.266 MHz C13[H1] APT_ad in cdcl3 (ref. to CDCl3 @ 77.06 ppm), temp 26.4 C -> actual temp = 27.0 C, autoxdb probe
C & CH2 same, CH & CH3 opposite side of solvent signal

date: Jul 6 2014 sweep width: 33827Hz acq.time: 2.5s relax.time: 0.1s # scans: 13748 dig.res.: 0.3 Hz/pt hz/mm:140.9
spectrometer:d300   file:/mnt/d600/home13/westnmr/nmrdata/YONGHOON/Book11/2014.07.06.i5_Yong-11-40-col_21.20_C13_APT_ad

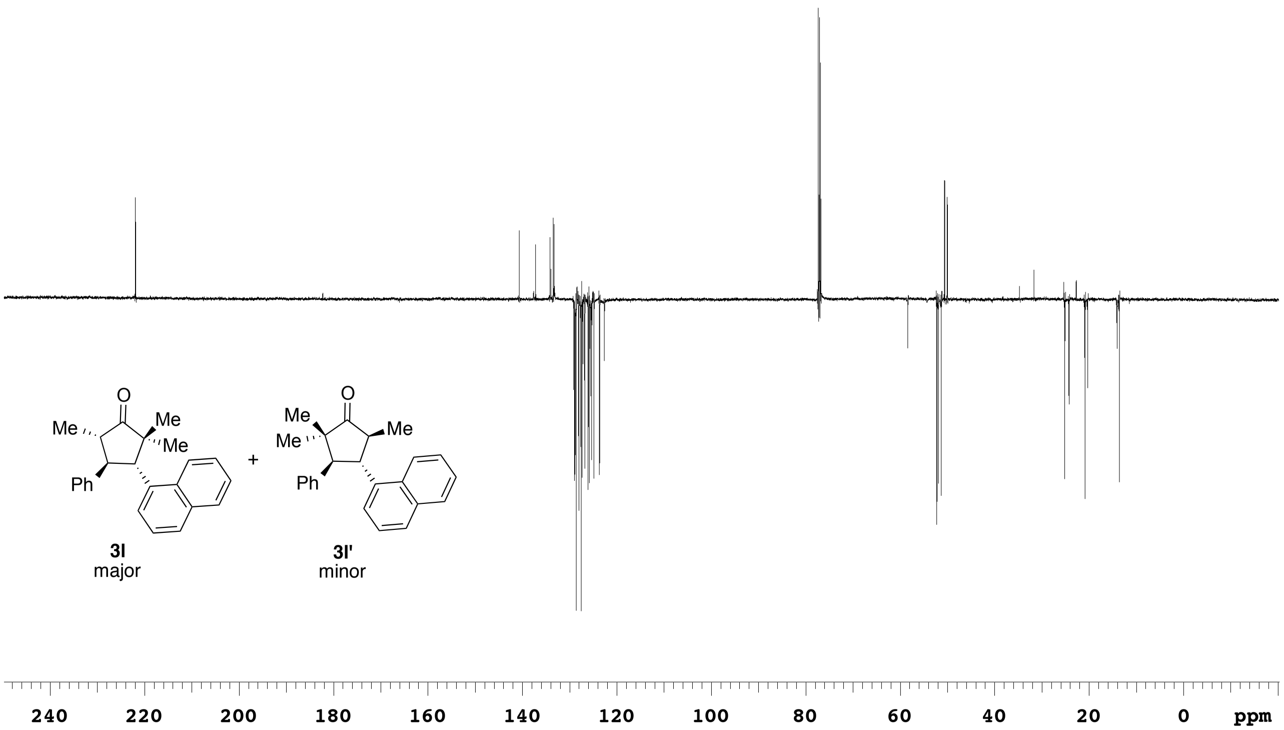

Pulse Sequence: APT_ad

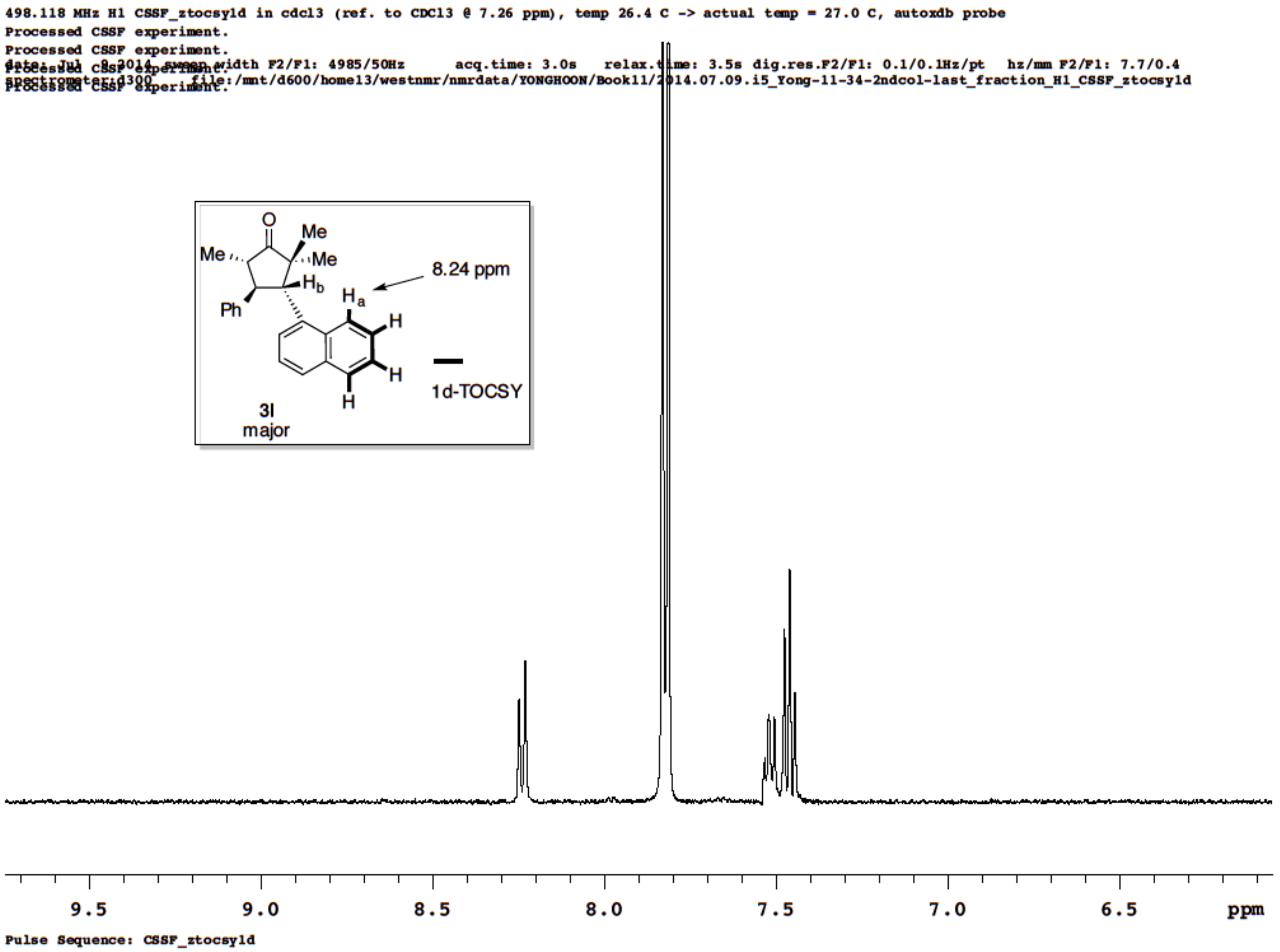
498.118 MHz H1 CSSF_ztocsy1d in cdcl3 (ref. to CDCl3 @ 7.26 ppm), temp 26.4 C -> actual temp = 27.0 C, autoxdb probe
Processed CSSF experiment.
Processed CSSF experiment.
Processed CSSF experiment.
Processed CSSF experiment.
date: Jul 9 2014 sweep width F2/F1: 4985/50Hz acq.time: 3.0s relax.time: 3.5s dig.res.F2/F1: 0.1/0.1Hz/pt hz/mm F2/F1: 7.7/0.4
spectrometer:d300 file:/mnt/d600/home13/westnmr/nmrdata/YONGHOON/Book11/2014.07.09.i5_Yong-11-34-2ndcol-last_fraction_H1_CSSF_ztocsy1d
O
Me
Me
Me
H_b
H_a
8.24 ppm
Ph
H
H
H
1d-TOCSY
3l
major
9.5
9.0
8.5
8.0
7.5
7.0
6.5
ppm
Pulse Sequence: CSSF_ztocsy1d

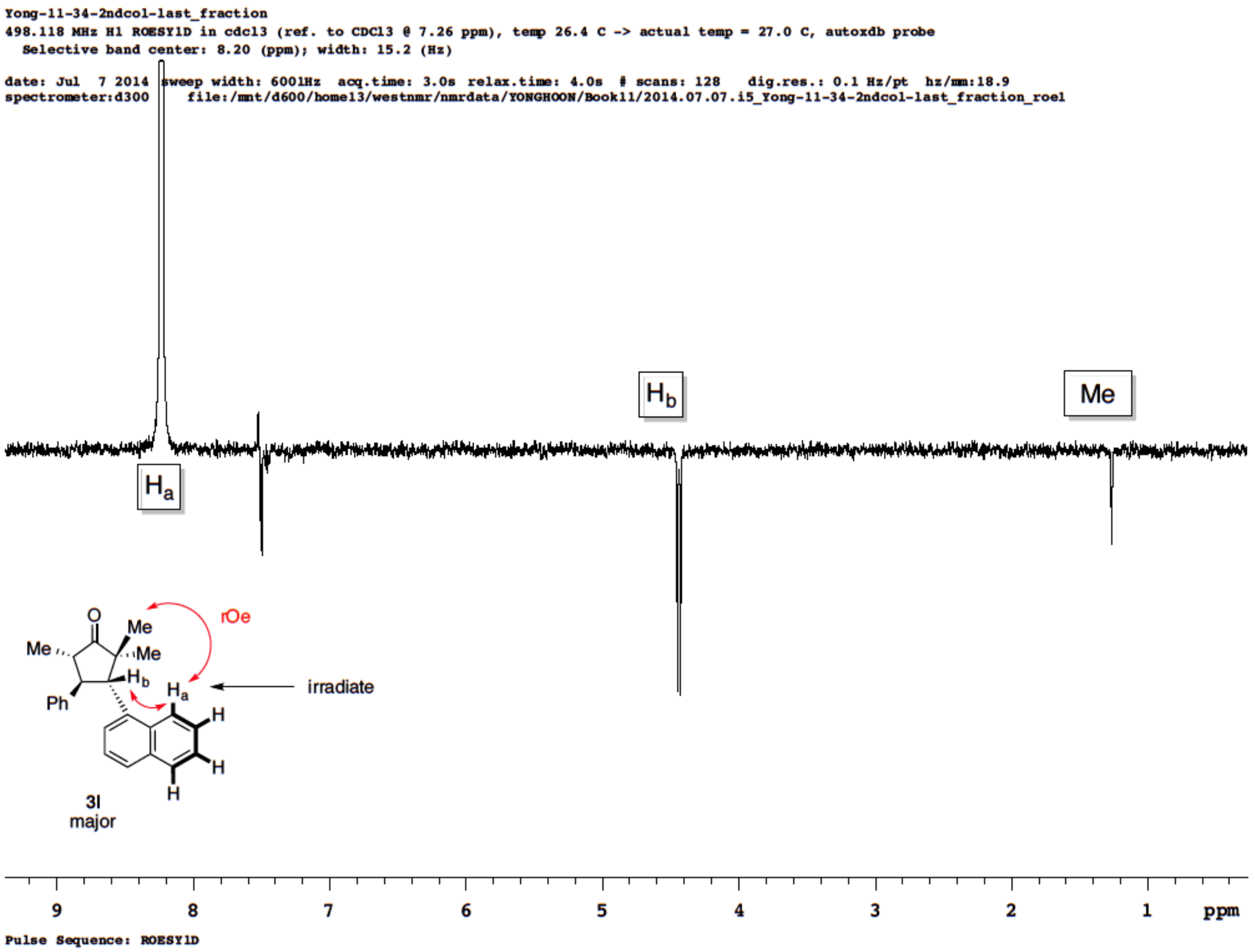

```
Yong-11-34-2ndcol-last_fraction
498.118 MHz H1 ROESY1D in cdcl3 (ref. to CDCl3 @ 7.26 ppm), temp 26.4 C -> actual temp = 27.0 C, autoxdb probe
  Selective band center: 8.20 (ppm); width: 15.2 (Hz)

date: Jul  7 2014  sweep width: 6001Hz  acq.time: 3.0s  relax.time: 4.0s  # scans: 128   dig.res.: 0.1 Hz/pt  hz/mm:18.9
spectrometer:d300     file:/mnt/d600/home13/westnmr/nmrdata/YONGHOON/Book11/2014.07.07.i5_Yong-11-34-2ndcol-last_fraction_roe1
```

H$_a$
H$_b$
Me
O
Me
Me
Me
Ph
H$_b$
H$_a$
rOe
irradiate
H
H
H
3l
major
9
8
7
6
5
4
3
2
1
ppm

Pulse Sequence: ROESY1D

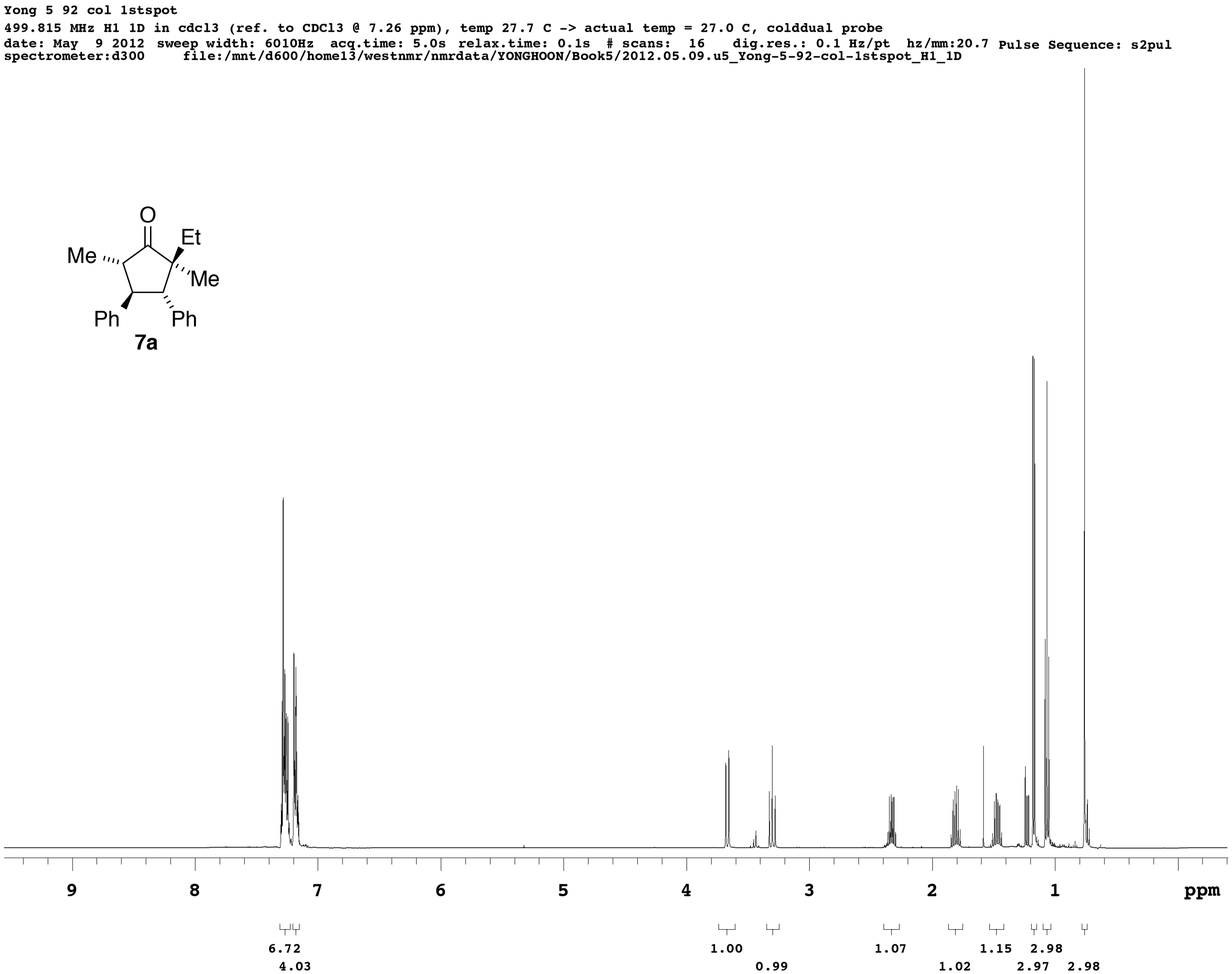

7a

Yong 5 92 col 1stspot
499.815 MHz H1 1D in cdcl3 (ref. to CDCl3 @ 7.26 ppm), temp 27.7 C -> actual temp = 27.0 C, colddual probe
date: May 9 2012 sweep width: 6010Hz acq.time: 5.0s relax.time: 0.1s # scans: 16 dig.res.: 0.1 Hz/pt hz/mm:20.7 Pulse Sequence: s2pul
spectrometer:d300 file:/mnt/d600/home13/westnmr/nmrdata/YONGHOON/Book5/2012.05.09.u5_Yong-5-92-col-1stspot_H1_1D
O
Et
Me
Me
Ph
Ph
9
8
7
6
5
4
3
2
1
ppm
6.72
4.03
1.00
0.99
1.07
1.02
1.15
2.97
2.98
2.98

Yong 5 92 col 1stspot
125.692 MHz C13[H1] 1D in cdcl3 (ref. to CDCl3 @ 77.06 ppm), temp 27.7 C -> actual temp = 27.0 C, colddual probe
date: May 9 2012 sweep width: 33784Hz acq.time: 2.5s relax.time: 0.1s # scans: 60 dig.res.: 0.3 Hz/pt hz/mm:140.8 Pulse Sequence: s2pul
spectrometer:d300 file:/mnt/d600/home13/westnmr/nmrdata/YONGHOON/Book5/2012.05.09.u5_Yong-5-92-col-1stspot_C13_1D

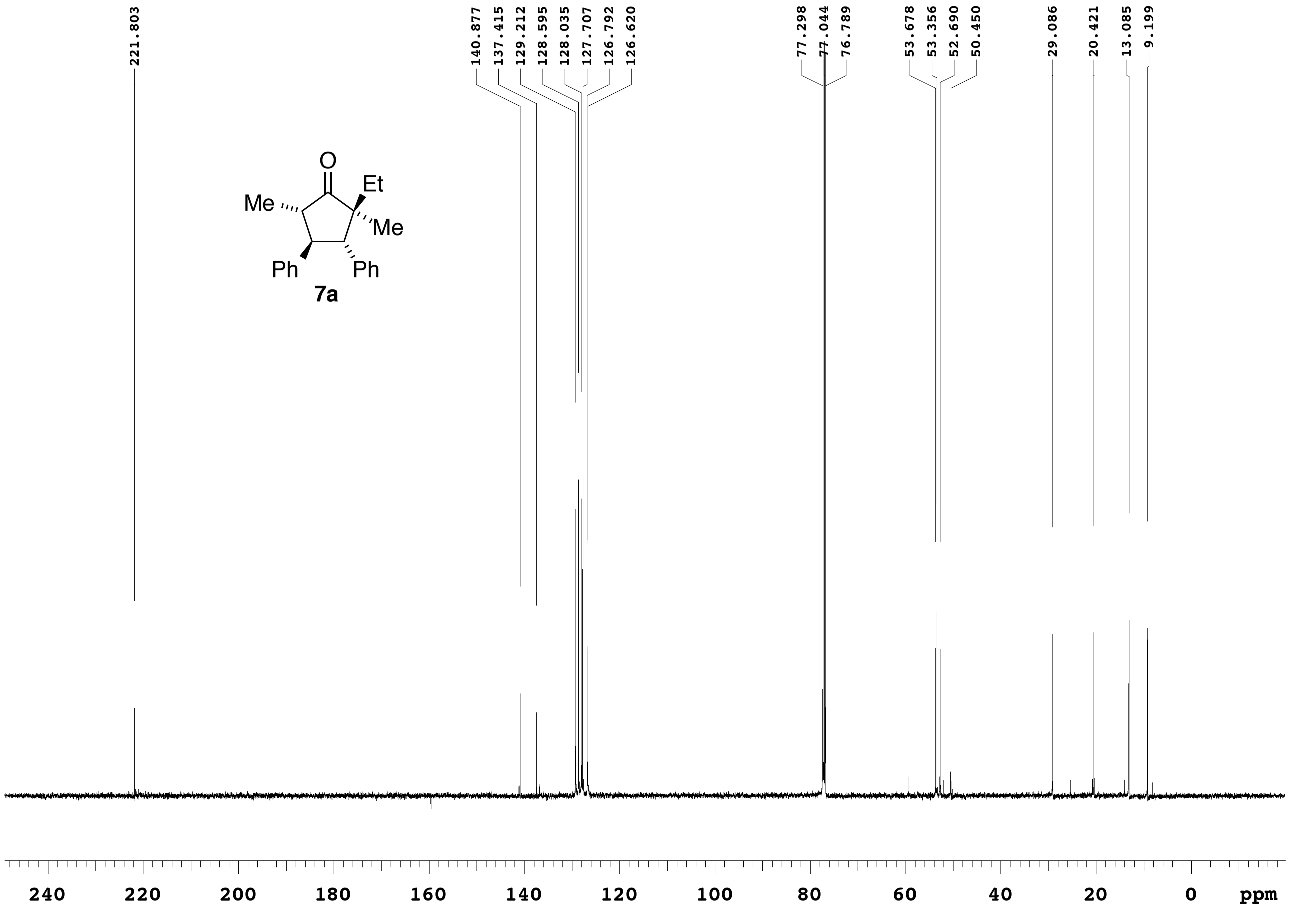

```
Yong 6 144 col 1st
498.118 MHz H1 1D in cdcl3 (ref. to CDCl3 @ 7.26 ppm), temp 27.2 C -> actual temp = 27.0 C, autoxdb probe
date: Nov 12 2012  sweep width: 6010Hz  acq.time: 5.0s  relax.time: 0.1s  # scans:  16   dig.res.: 0.1 Hz/pt  hz/mm:25.0 Pulse Sequence: s2pul
spectrometer:d300     file:/mnt/d600/home13/westnmr/nmrdata/YONGHOON/Book6/2012.11.12.i5_Yong-6-144-col-1st_H1_1D
```

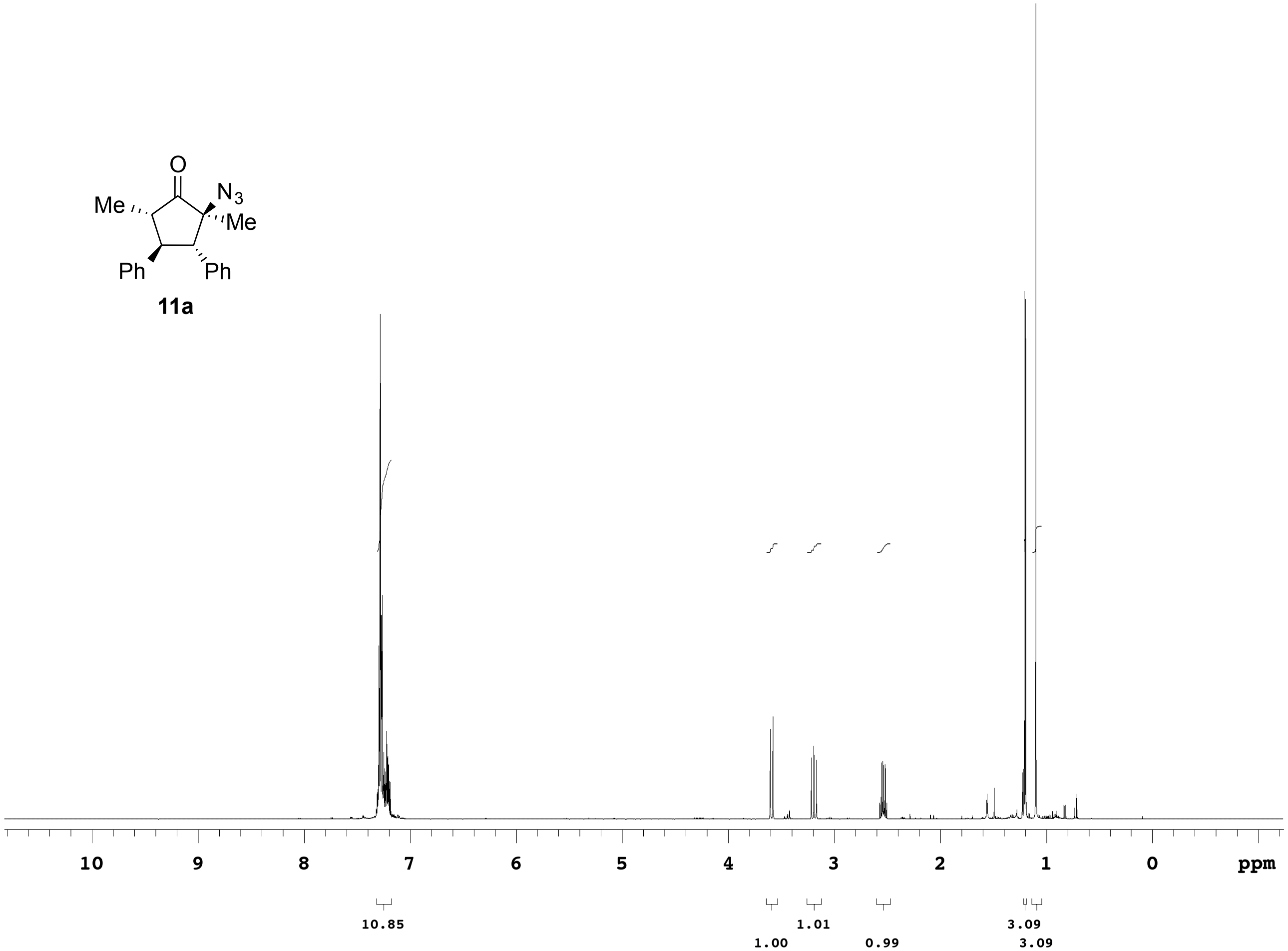

11a

Yong 6 144 col 1st
125.266 MHz C13[H1] 1D in cdcl3 (ref. to CDCl3 @ 77.06 ppm), temp 27.2 C -> actual temp = 27.0 C, autoxdb probe
date: Nov 12 2012 sweep width: 33784Hz acq.time: 2.5s relax.time: 0.1s # scans: 16936 dig.res.: 0.3 Hz/pt hz/mm:140.8 Pulse Sequence: s2pul
spectrometer:d300   file:/mnt/d600/home13/westnmr/nmrdata/YONGHOON/Book6/2012.11.12.i5_Yong-6-144-col-1st_C13_1D

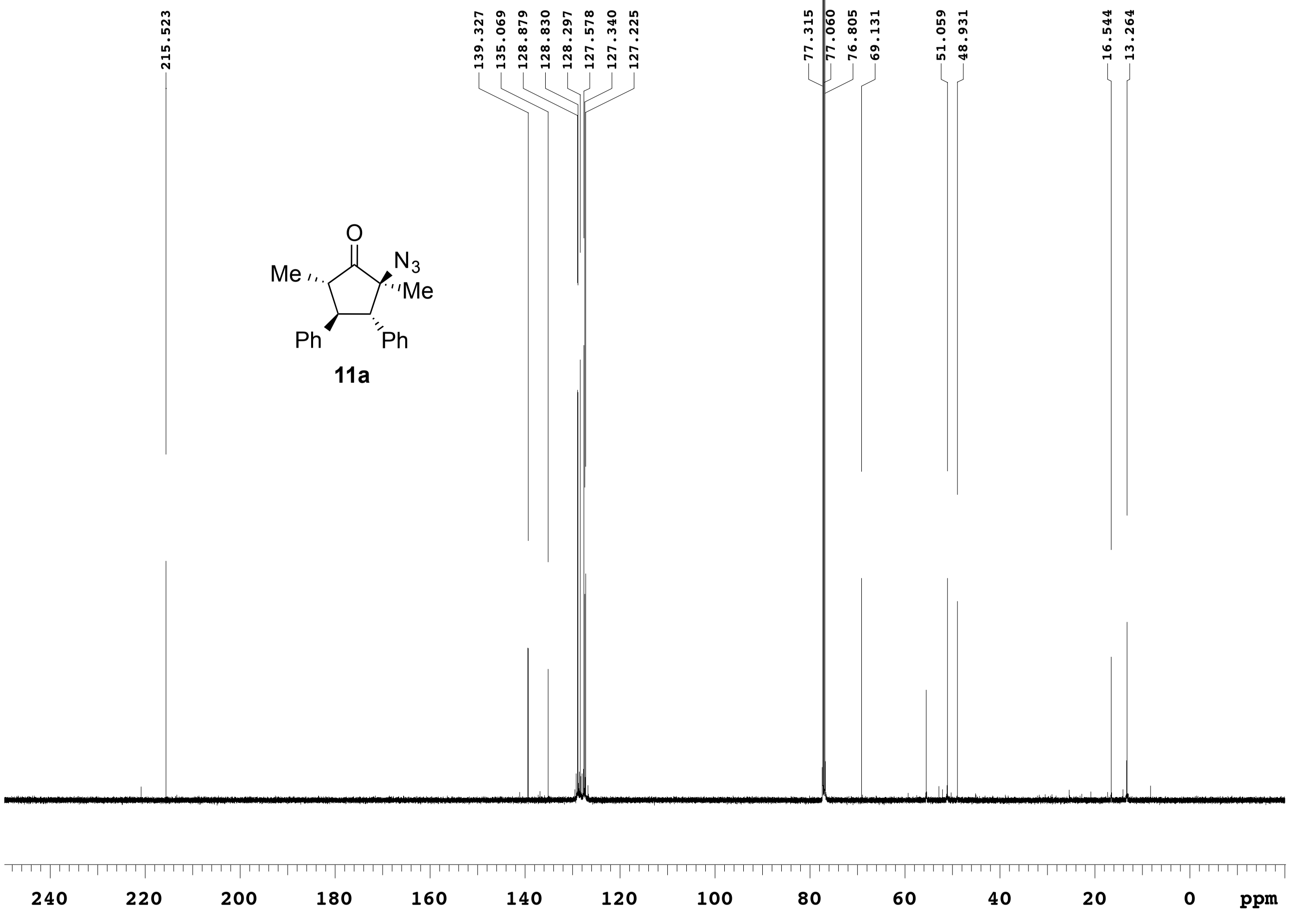

```
Yong 6 144 col 2nd
498.118 MHz H1 1D in cdcl3 (ref. to CDCl3 @ 7.26 ppm), temp 27.2 C -> actual temp = 27.0 C, autoxdb probe
date: Nov 12 2012  sweep width: 6010Hz  acq.time: 5.0s  relax.time: 0.1s  # scans:  16   dig.res.: 0.1 Hz/pt  hz/mm:25.0 Pulse Sequence: s2pul
spectrometer:d300     file:/mnt/d600/home13/westnmr/nmrdata/YONGHOON/Book6/2012.11.12.i5_Yong-6-144-col-2nd_H1_1D
```

11a'

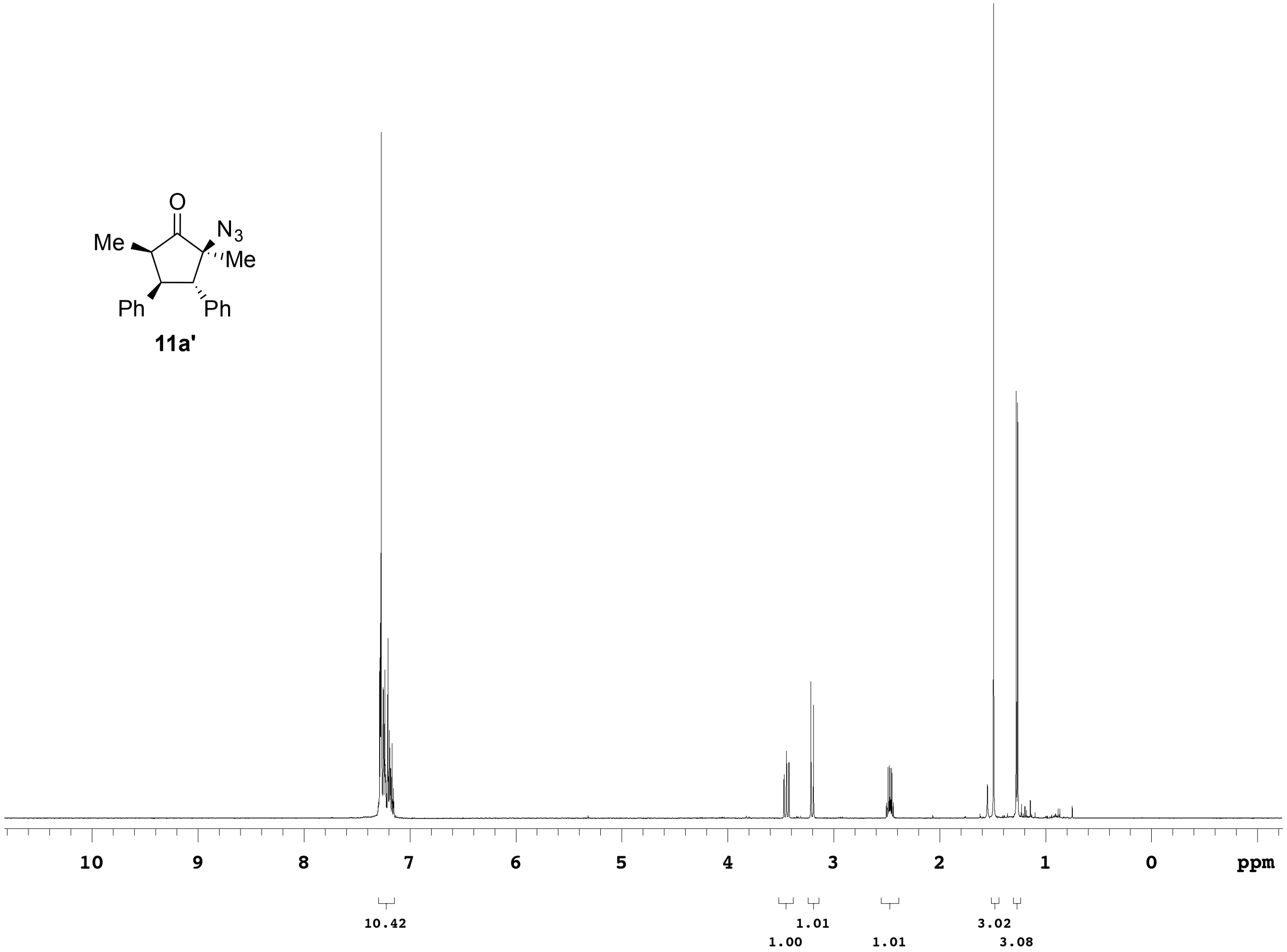

Yong 6 144 col 2nd
125.266 MHz C13[H1] 1D in cdcl3 (ref. to CDCl3 @ 77.06 ppm), temp 27.2 C -> actual temp = 27.0 C, autoxdb probe
date: Nov 12 2012 sweep width: 33784Hz acq.time: 2.5s relax.time: 0.1s # scans: 588 dig.res.: 0.3 Hz/pt hz/mm:140.8Pulse Sequence: s2pul
spectrometer:d300 file:/mnt/d600/home13/westnmr/nmrdata/YONGHOON/Book6/2012.11.12.i5_Yong-6-144-col-2nd_C13_1D

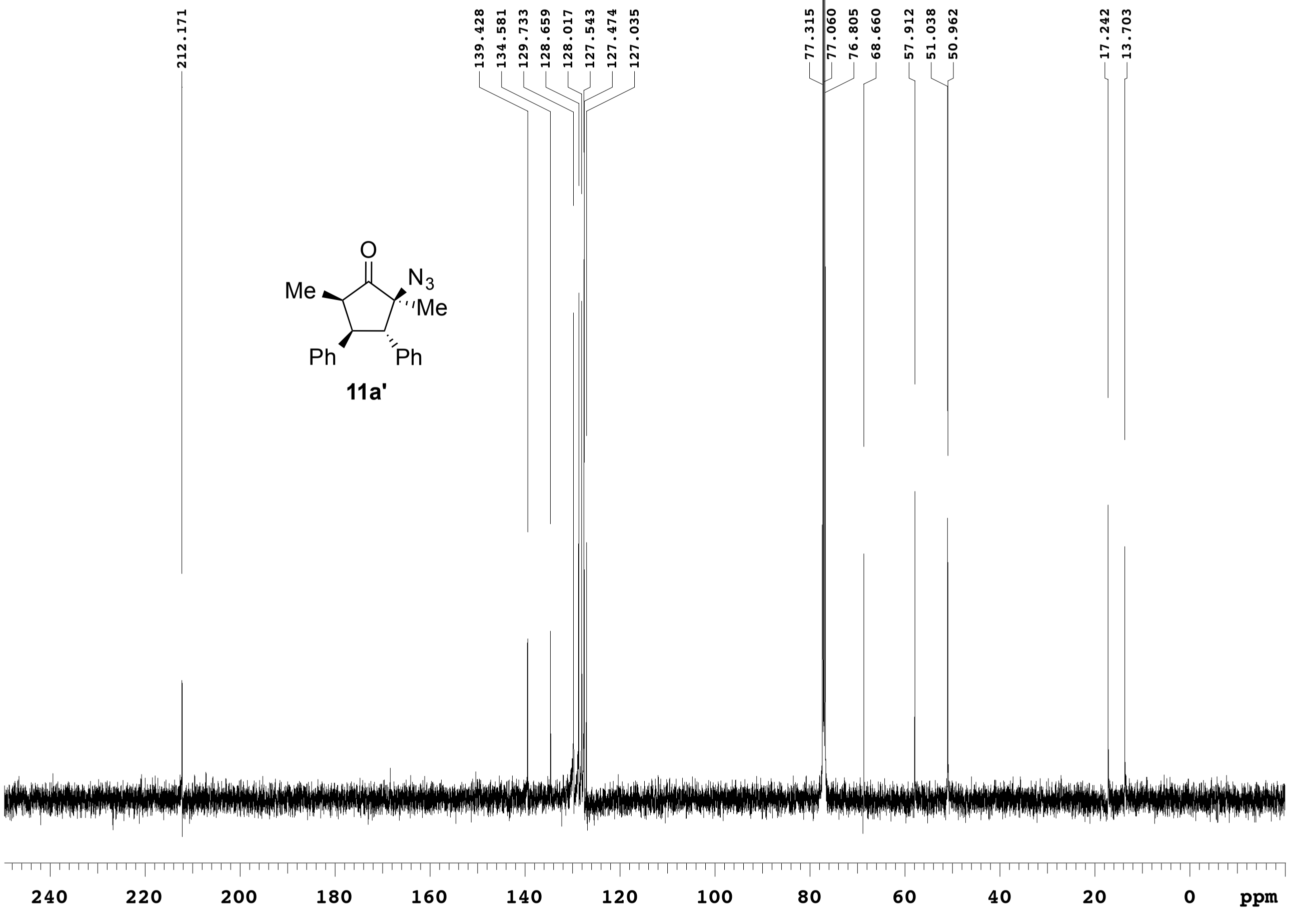

Yong-8-126-col
498.118 MHz H1 1D in cdcl3 (ref. to CDCl3 @ 7.26 ppm), temp 26.4 C -> actual temp = 27.0 C, autoxdb probe

date: Jul 31 2013 sweep width: 6001Hz acq.time: 5.0s relax.time: 0.1s # scans: 16 dig.res.: 0.1 Hz/pt hz/mm:25.0
spectrometer:d300 file:/mnt/d600/home13/westnmr/nmrdata/YONGHOON/Book8/2013.07.31.i5_Yong-8-126-col_H1_1D

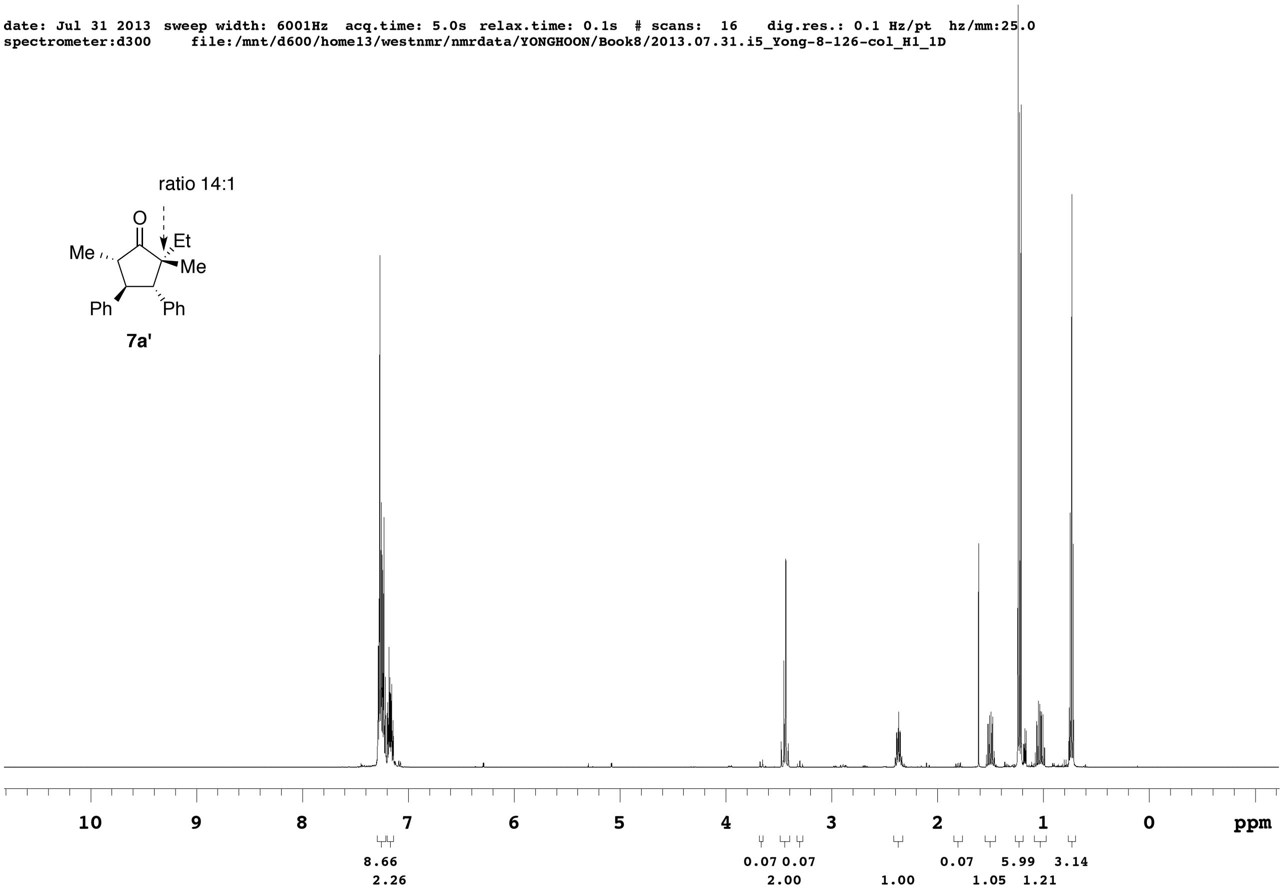

Pulse Sequence: s2pul

```
Yong-8-119-col
100.539 MHz C13[H1] 1D in cdcl3 (ref. to CDCl3 @ 77.06 ppm), temp 26.5 C -> actual temp = 27.0 C, autoxdb probe

date: Jul 25 2013  sweep width: 26954Hz acq.time: 2.5s  relax.time: 0.1s  # scans: 1236  dig.res.: 0.2 Hz/pt  hz/mm:112.3
spectrometer:d300     file:/mnt/d600/home13/westnmr/nmrdata/YONGHOON/Book8/2013.07.25.i4_Yong-8-119-col_C13_1D
```

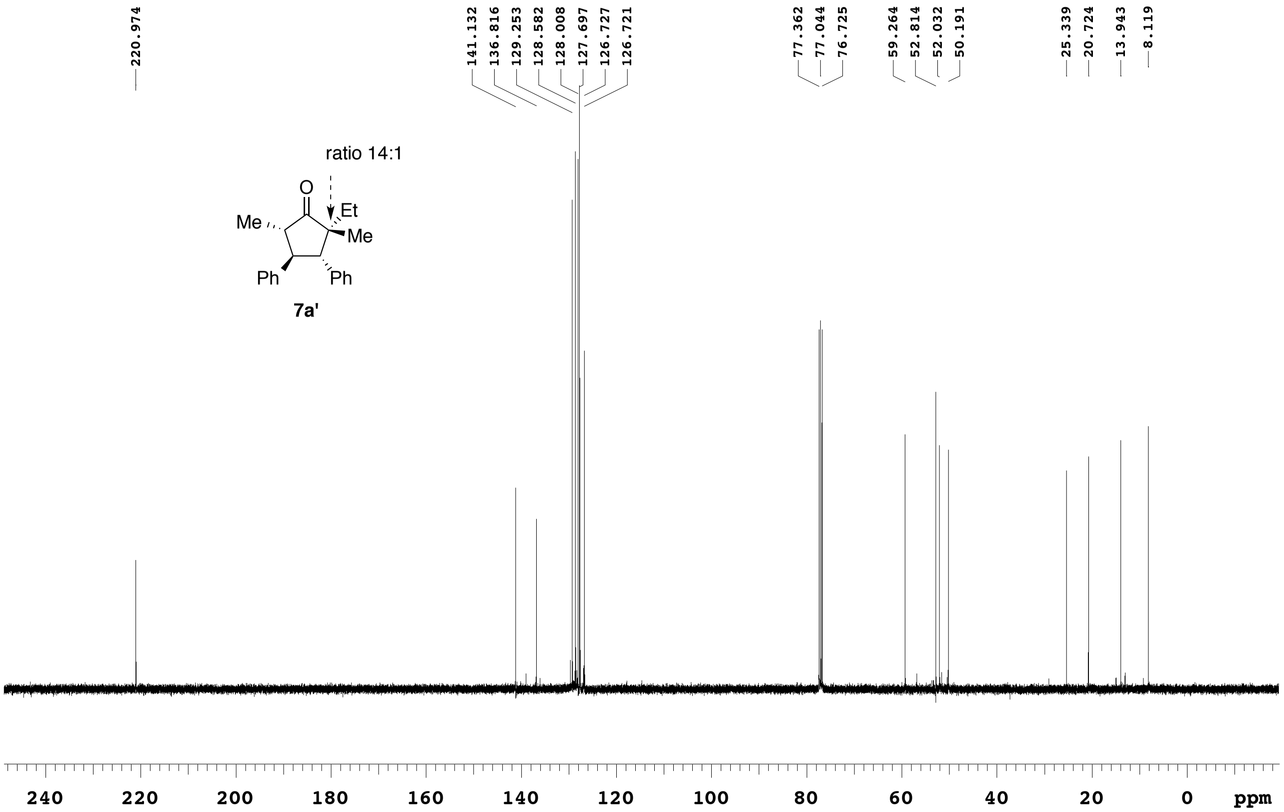

7a'

```
Pulse Sequence: s2pul
```

```
Yong-8-140-col-1stspot
498.118 MHz H1 1D in cdcl3 (ref. to CDCl3 @ 7.26 ppm), temp 26.4 C -> actual temp = 27.0 C, autoxdb probe

date: Aug  7 2013  sweep width: 6001Hz  acq.time: 5.0s  relax.time: 0.1s  # scans:  16   dig.res.: 0.1 Hz/pt  hz/mm:18.9
spectrometer:d300     file:/mnt/d600/home13/westnmr/nmrdata/YONGHOON/Book8/2013.08.07.i5_Yong-8-140-col-1stspot_H1_1D
```

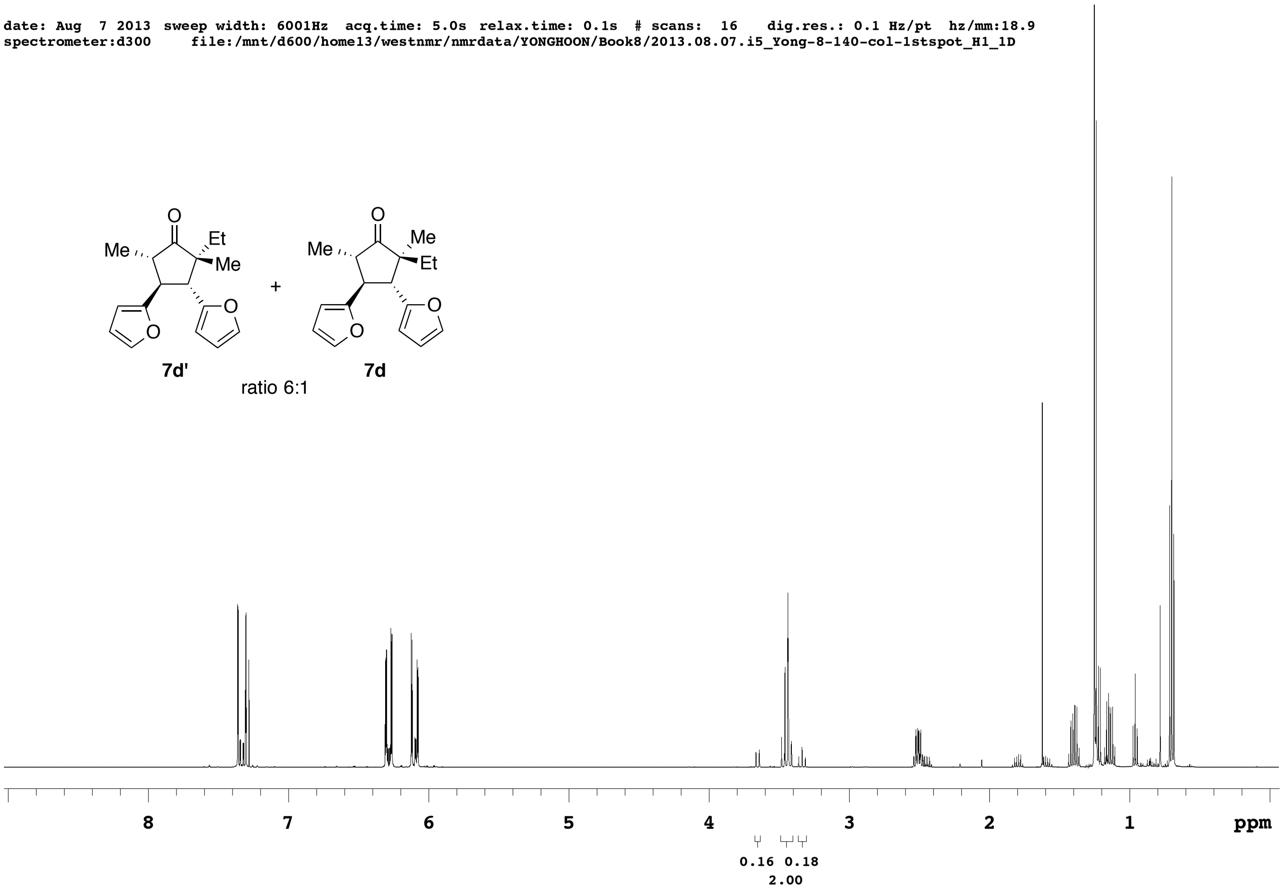

7d' ratio 6:1 **7d**

```
Pulse Sequence: s2pul
```

```
Yong-8-140-col-1stspot
125.266 MHz C13[H1] APT_ad in cdcl3 (ref. to CDCl3 @ 77.06 ppm), temp 26.4 C -> actual temp = 27.0 C, autoxdb probe
C & CH2 same, CH & CH3 opposite side of solvent signal

date: Aug  7 2013  sweep width: 33827Hz acq.time: 2.5s  relax.time: 0.1s  # scans: 424    dig.res.: 0.3 Hz/pt  hz/mm:140.9
spectrometer:d300     file:/mnt/d600/home13/westnmr/nmrdata/YONGHOON/Book8/2013.08.07.i5_Yong-8-140-col-1stspot_C13_APT_ad
```

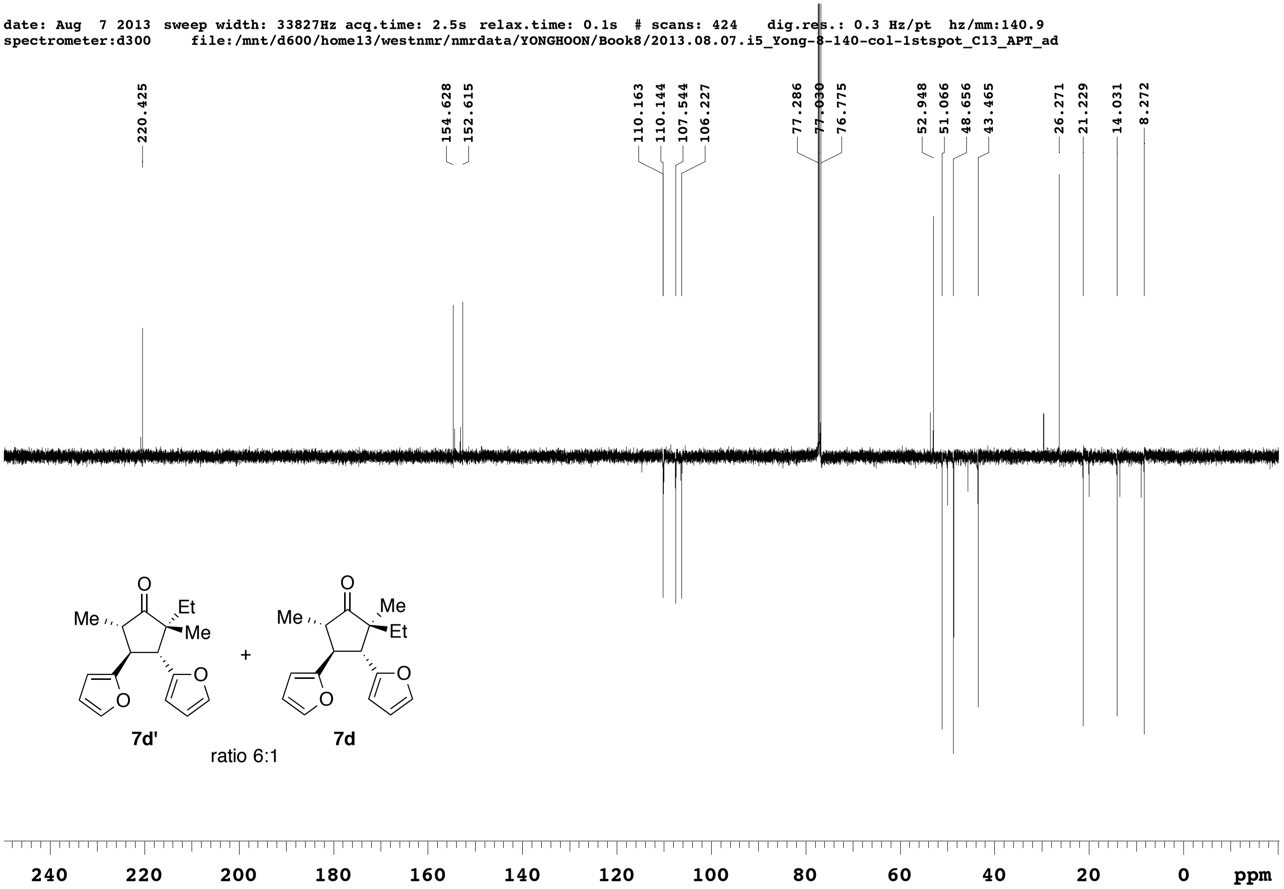

Pulse Sequence: APT_ad

```
Yong-3-84-columned
498.122 MHz H1 1D in cdcl3 (ref. to CDCl3 @ 7.26 ppm), temp 27.2 C -> actual temp = 27.0 C, autoxdb probe

date: Jul 25 2011  sweep width: 6001Hz  acq.time: 5.0s  relax.time: 0.1s  # scans:  16   dig.res.: 0.1 Hz/pt  hz/mm:25.0
spectrometer:d300     file:/mnt/d600/home13/westnmr/nmrdata/YONGHOON/Book3/2011.07.25.i5_Yong-3-84-columned_H1_1D
```

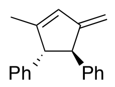

15a

+

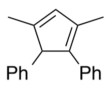

15a'

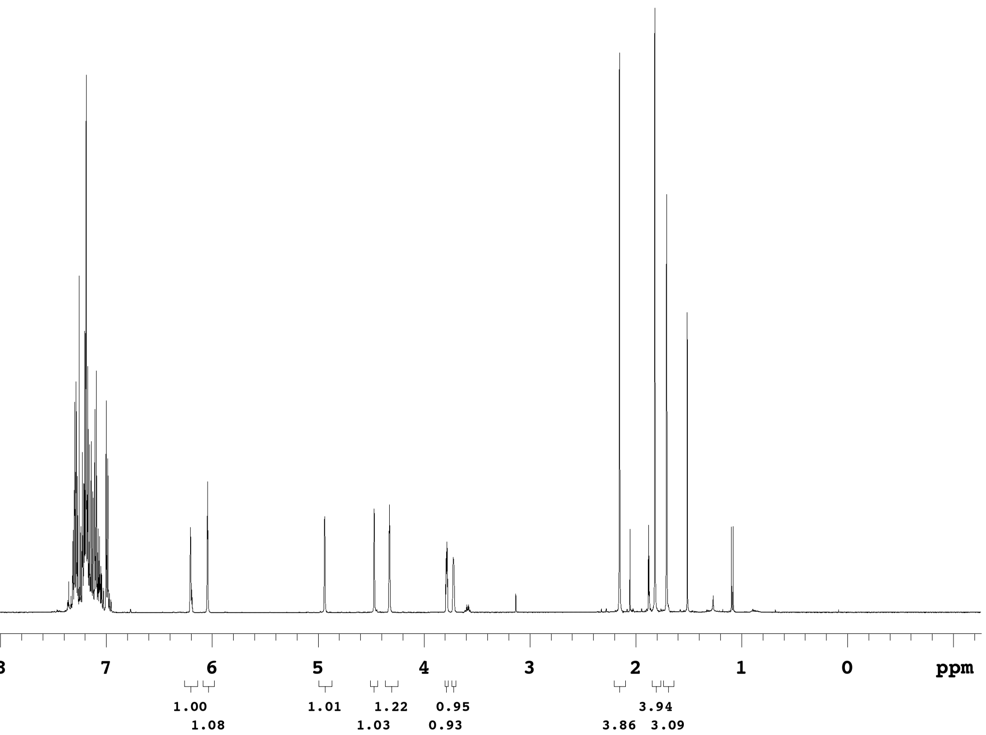

```
Pulse Sequence: s2pul
```

Yong-3-84-columned
125.692 MHz C13[H1] APT_ad in cdcl3 (ref. to CDCl3 @ 77.06 ppm), temp 27.7 C -> actual temp = 27.0 C, colddual probe
C & CH2 same, CH & CH3 opposite side of solvent signal

date: Jul 25 2011 sweep width: 33784Hz acq.time: 2.5s relax.time: 0.1s # scans: 328   dig.res.: 0.3 Hz/pt hz/mm:90.0
spectrometer:d300   file:/mnt/d600/home13/westnmr/nmrdata/YONGHOON/Book3/2011.07.25.u5_Yong-3-84-columned_C13_APT_ad

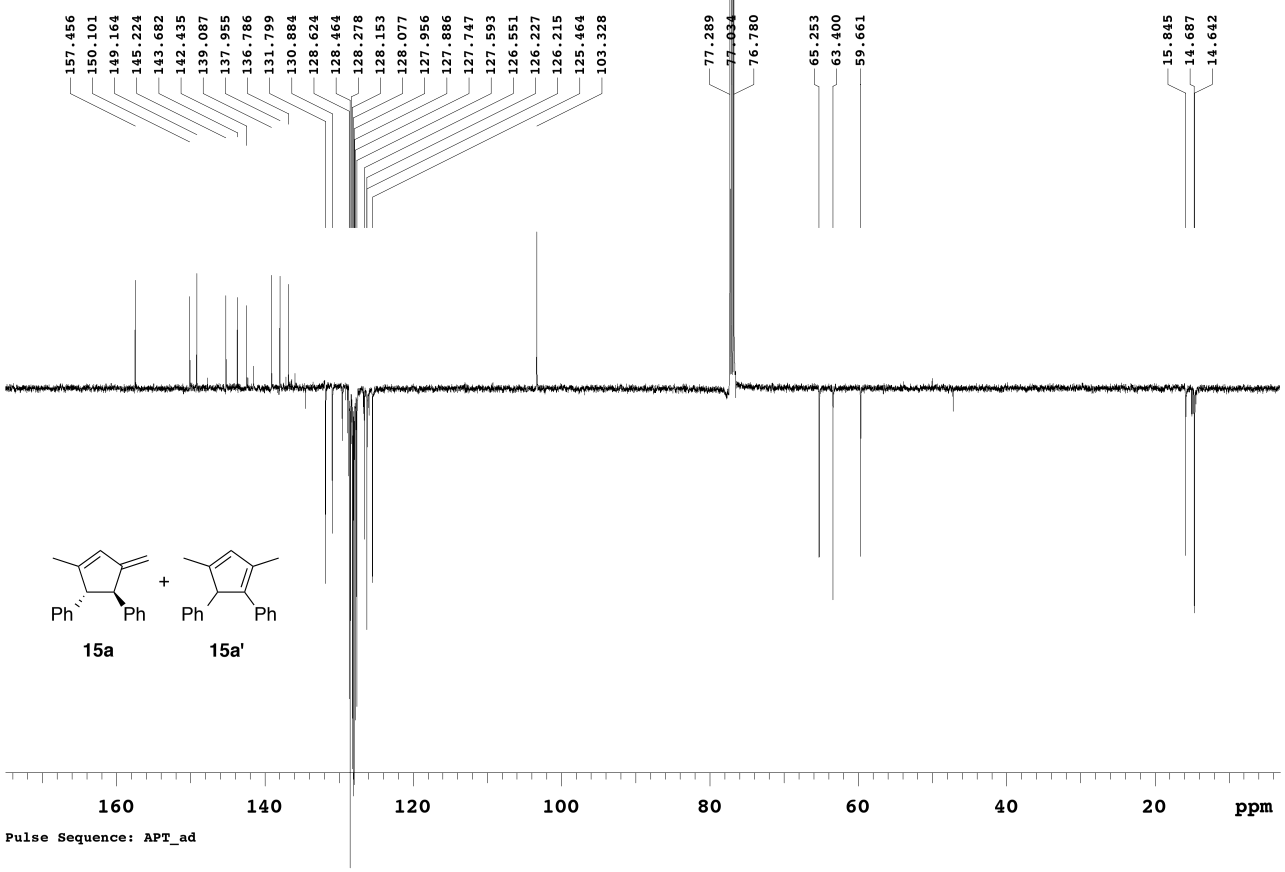

Pulse Sequence: APT_ad

```
Yong-3-96-crude
499.815 MHz H1 1D in cdcl3 (ref. to CDCl3 @ 7.26 ppm), temp 27.7 C -> actual temp = 27.0 C, colddual probe

date: Jul 30 2011  sweep width: 6010Hz  acq.time: 5.0s  relax.time: 0.1s  # scans:  16   dig.res.: 0.1 Hz/pt  hz/mm:17.7
spectrometer:d300     file:/mnt/d600/home13/westnmr/nmrdata/YONGHOON/Book3/2011.07.30.u5_Yong-3-96-crude_H1_1D
```

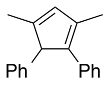

15a'

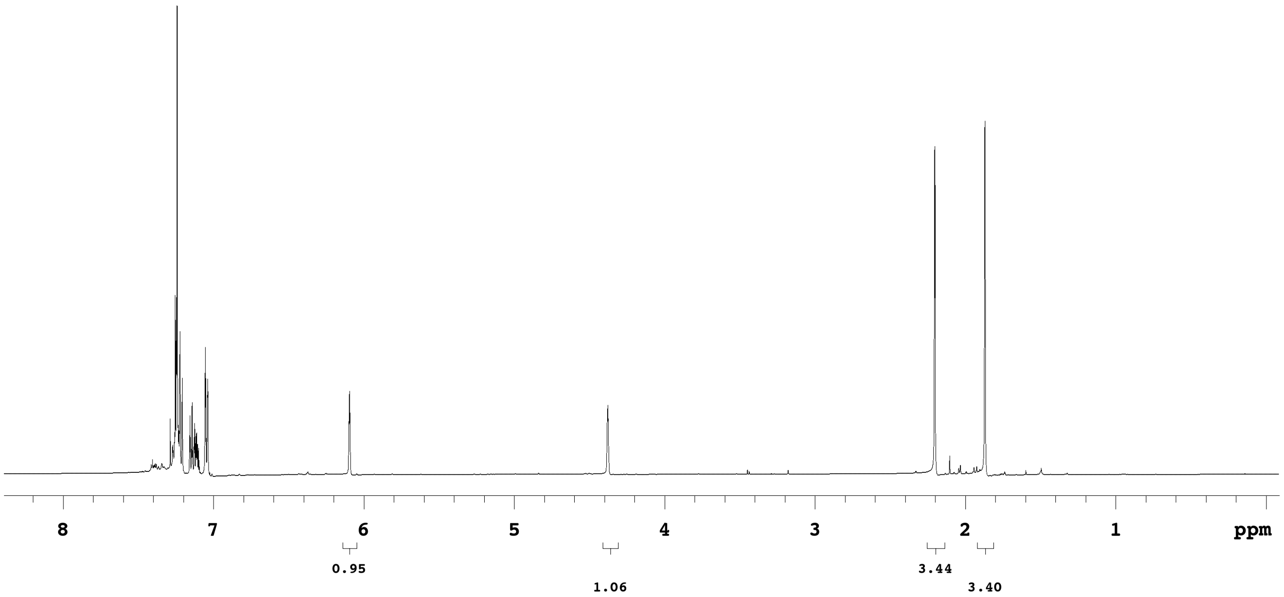

```
Pulse Sequence: s2pul
```

125.267 MHz C13[H1] APT_ad in cdcl3 (ref. to CDCl3 @ 77.06 ppm), temp 27.2 C -> actual temp = 27.0 C, autoxdb probe
C & CH2 same, CH & CH3 opposite side of solvent signal

date: May 30 2011 sweep width: 33827Hz acq.time: 2.5s relax.time: 0.1s # scans: 328   dig.res.: 0.3 Hz/pt hz/mm:95.3
spectrometer:d300   file:/mnt/d600/home13/westnmr/nmrdata/YONGHOON/Book2/2011.05.30.i5_Yong2-141-alumina-plugged_C13_APT_ad

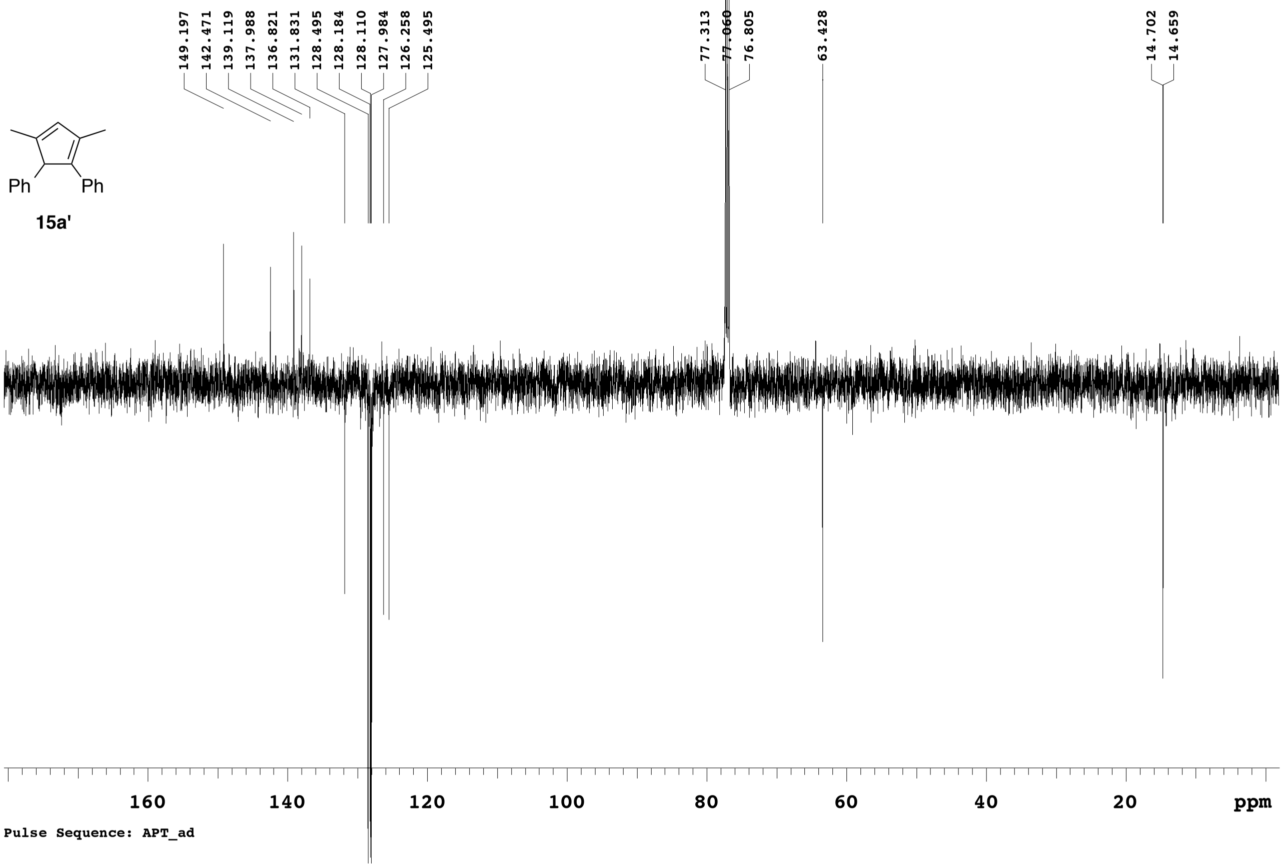

Pulse Sequence: APT_ad

Appendix II: Selected NMR Spectra

(Chapter 3)

```
Yong 5 134 col 2ndspot
498.122 MHz H1 1D in cdcl3 (ref. to CDCl3 @ 7.26 ppm), temp 27.2 C -> actual temp = 27.0 C, autoxdb probe
date: Jun  5 2012  sweep width: 6001Hz  acq.time: 5.0s  relax.time: 0.1s  # scans:  16   dig.res.: 0.1 Hz/pt  hz/mm:20.3 Pulse Sequence: s2pul
spectrometer:d300     file:/mnt/d600/home13/westnmr/nmrdata/YONGHOON/Book5/2012.06.05.i5_Yong-5-134-col-2ndspot_H1_1D
```

4a

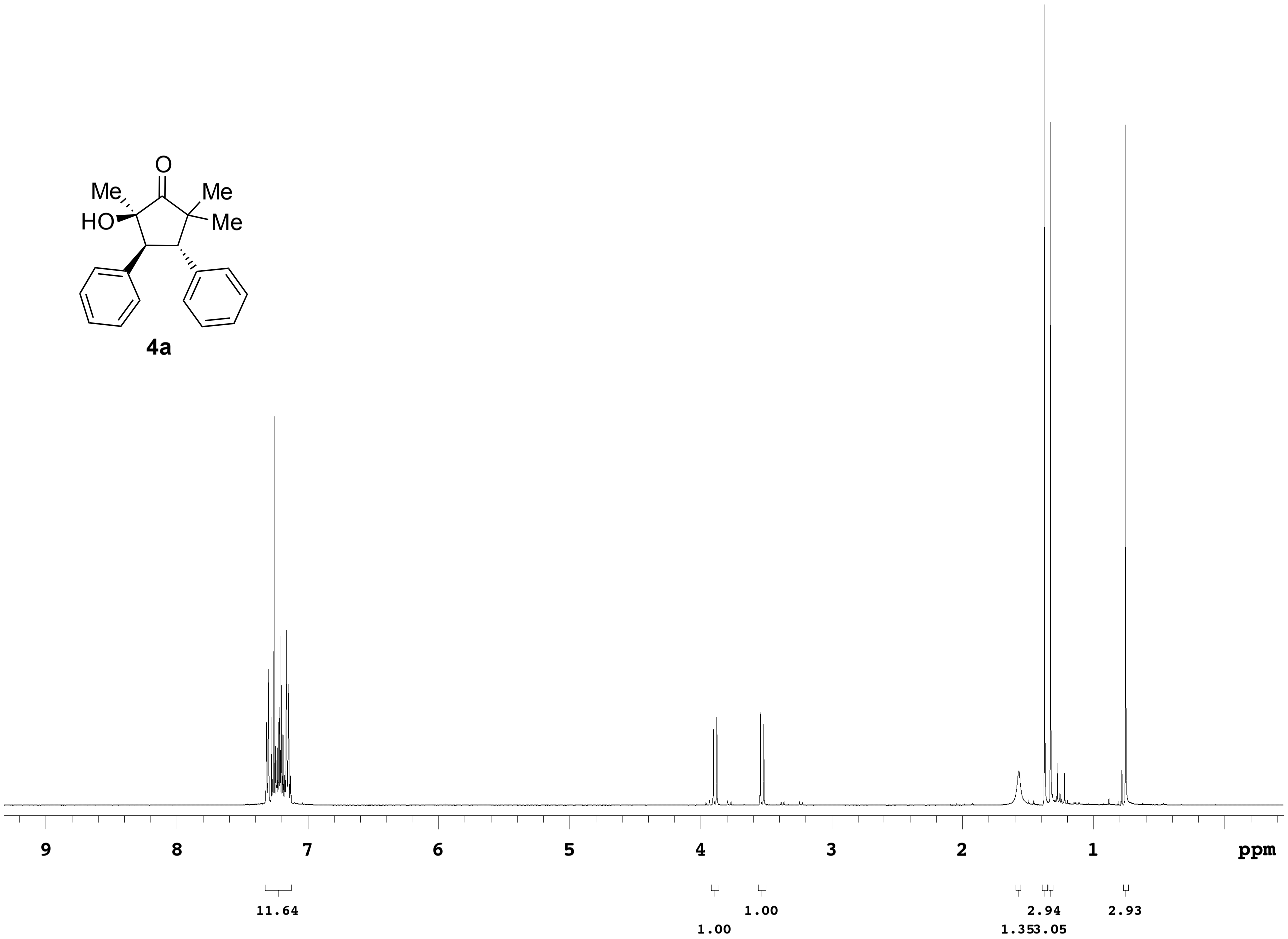

```
Yong 7 68 col major
125.266 MHz C13[H1] 1D in cdcl3 (ref. to CDCl3 @ 77.06 ppm), temp 27.2 C -> actual temp = 27.0 C, autoxdb probe
date: Feb  1 2013  sweep width: 33827Hz acq.time: 2.5s  relax.time: 0.1s  # scans: 172   dig.res.: 0.3 Hz/pt  hz/mm:140.9Pulse Sequence: s2pul
spectrometer:d300     file:/mnt/d600/home13/westnmr/nmrdata/YONGHOON/Book7/2013.02.01.i5_Yong-7-68-col-major_C13_1D
```

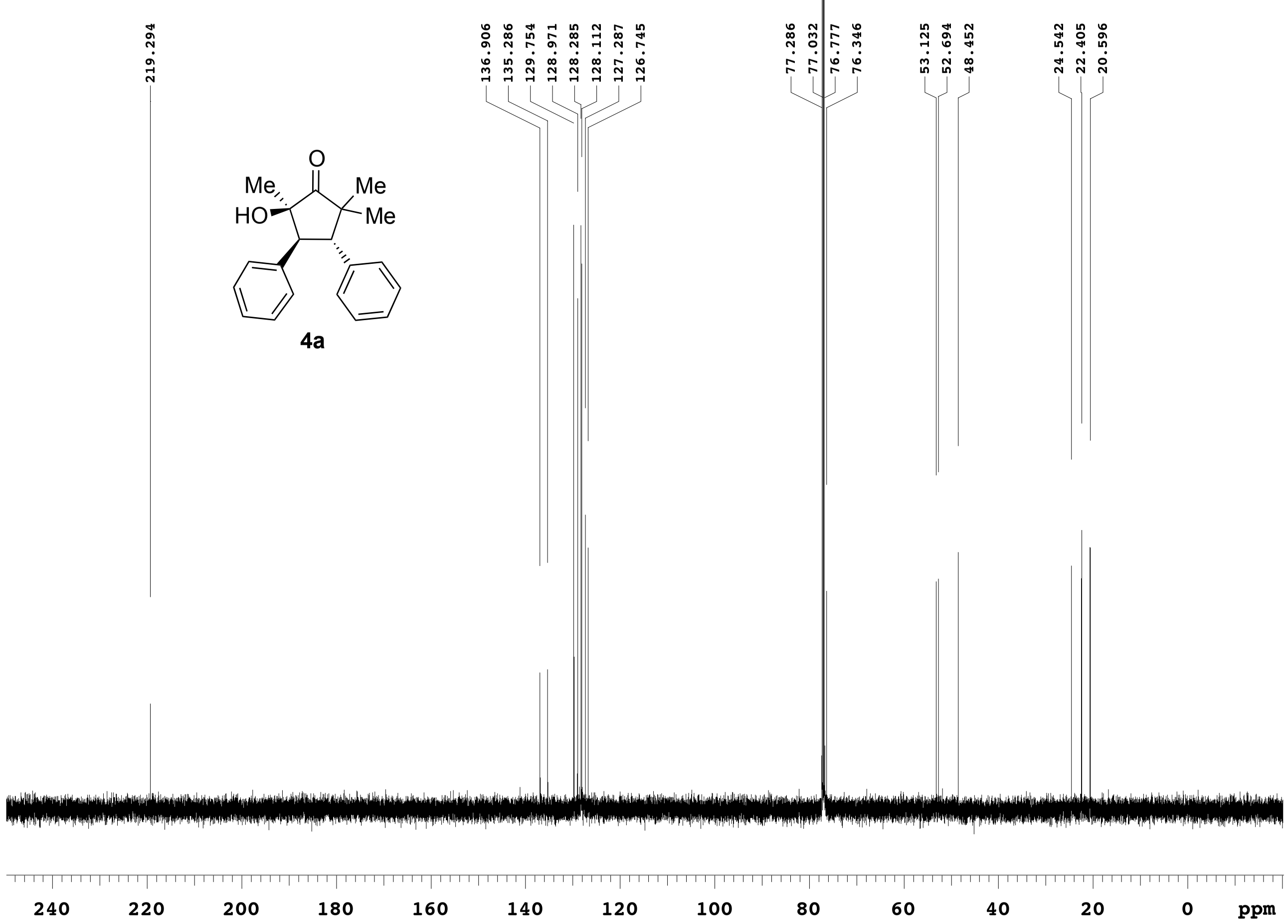

```
Yong 7 68 col minor solvent removed
399.794 MHz H1 1D in cdcl3 (ref. to CDCl3 @ 7.26 ppm), temp 27.0 C -> actual temp = 27.0 C, autoxdb probe
date: Apr  2 2013  sweep width: 4802Hz  acq.time: 5.0s  relax.time: 0.1s  # scans:  16   dig.res.: 0.1 Hz/pt  hz/mm:15.9 Pulse Sequence: s2pul
spectrometer:d300     file:/mnt/d600/home13/westnmr/nmrdata/YONGHOON/Book7/2013.04.02.i4_Yong-7-68-col-minor-solvent_removed_H1_1D
```

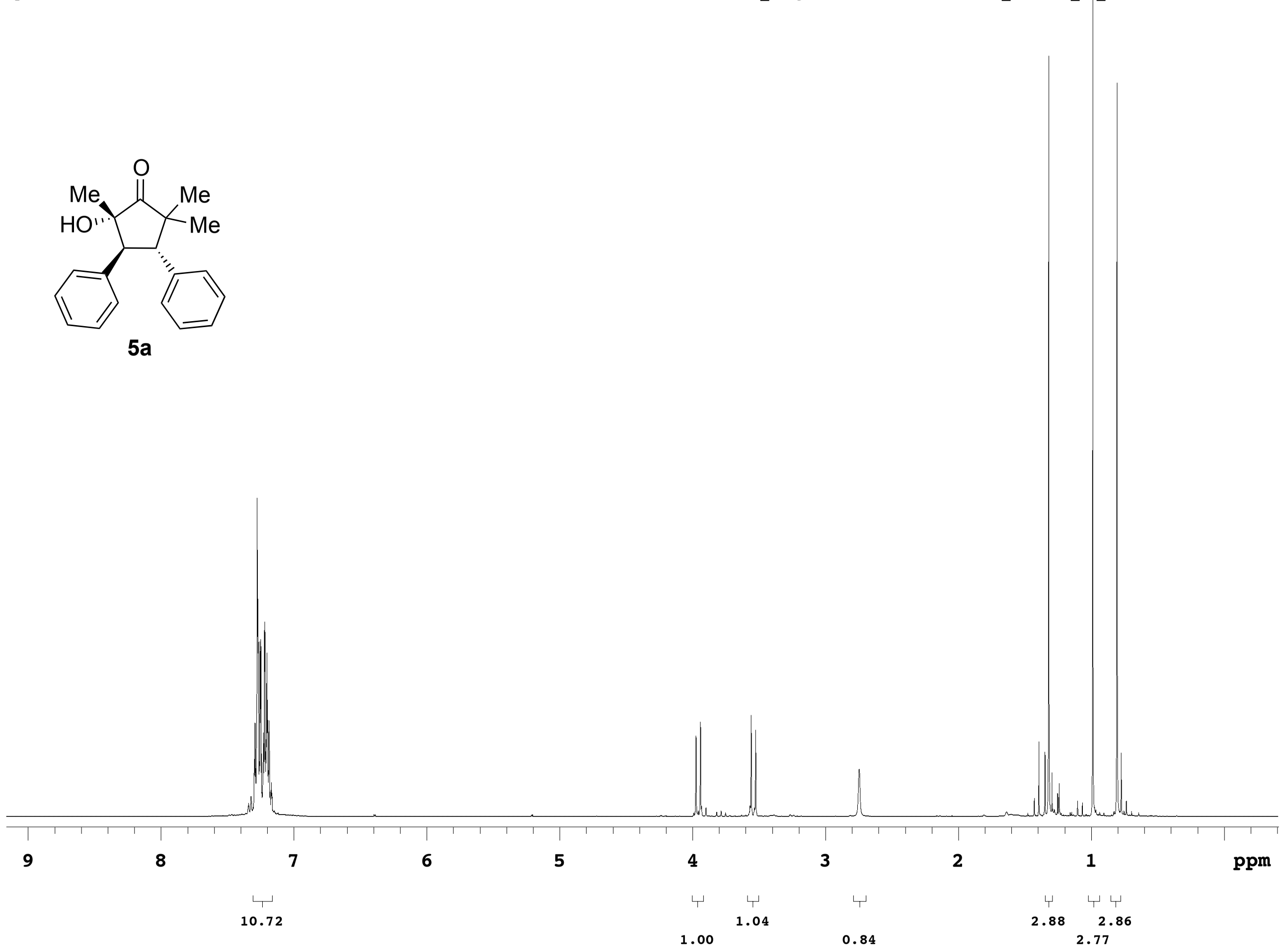

Yong 7 68 col minor
125.266 MHz C13[H1] 1D in cdcl3 (ref. to CDCl3 @ 77.06 ppm), temp 27.2 C -> actual temp = 27.0 C, autoxdb probe
date: Feb 1 2013 sweep width: 33827Hz acq.time: 2.5s relax.time: 0.1s # scans: 204 dig.res.: 0.3 Hz/pt hz/mm:140.9 Pulse Sequence: s2pul
spectrometer:d300 file:/mnt/d600/home13/westnmr/nmrdata/YONGHOON/Book7/2013.02.01.i5_Yong-7-68-col-minor_C13_1D

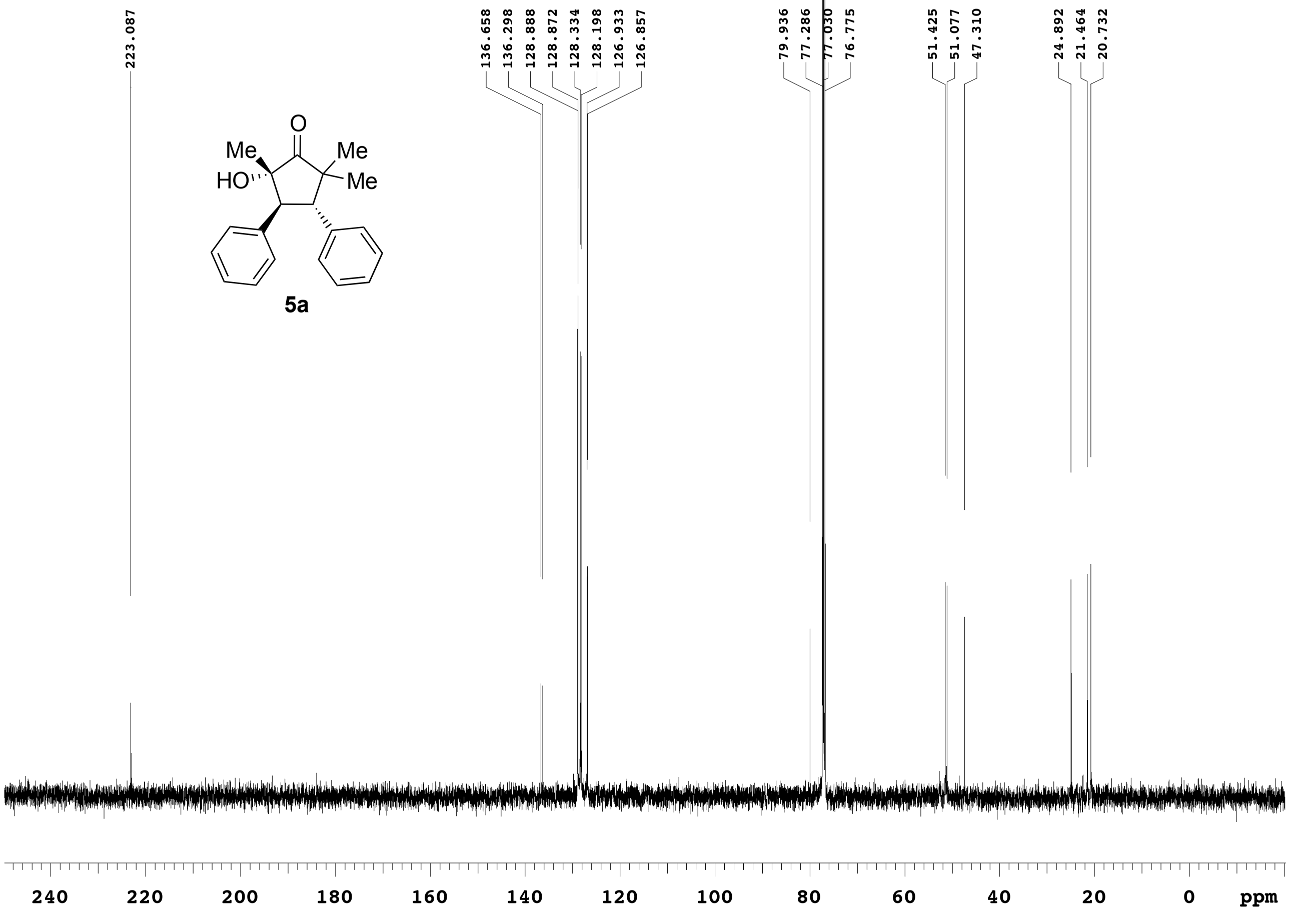

Yong 7 98 col 1stspot EAremoved
498.118 MHz H1 1D in cdcl3 (ref. to CDCl3 @ 7.26 ppm), temp 27.2 C -> actual temp = 27.0 C, autoxdb probe
date: Feb 19 2013 sweep width: 6001Hz acq.time: 5.0s relax.time: 0.1s # scans: 16   dig.res.: 0.1 Hz/pt hz/mm:25.0 Pulse Sequence: s2pul
spectrometer:d300   file:/mnt/d600/home13/westnmr/nmrdata/YONGHOON/Book7/2013.02.19.i5_Yong-7-98-col-1stspot-EAremoved_H1_1D

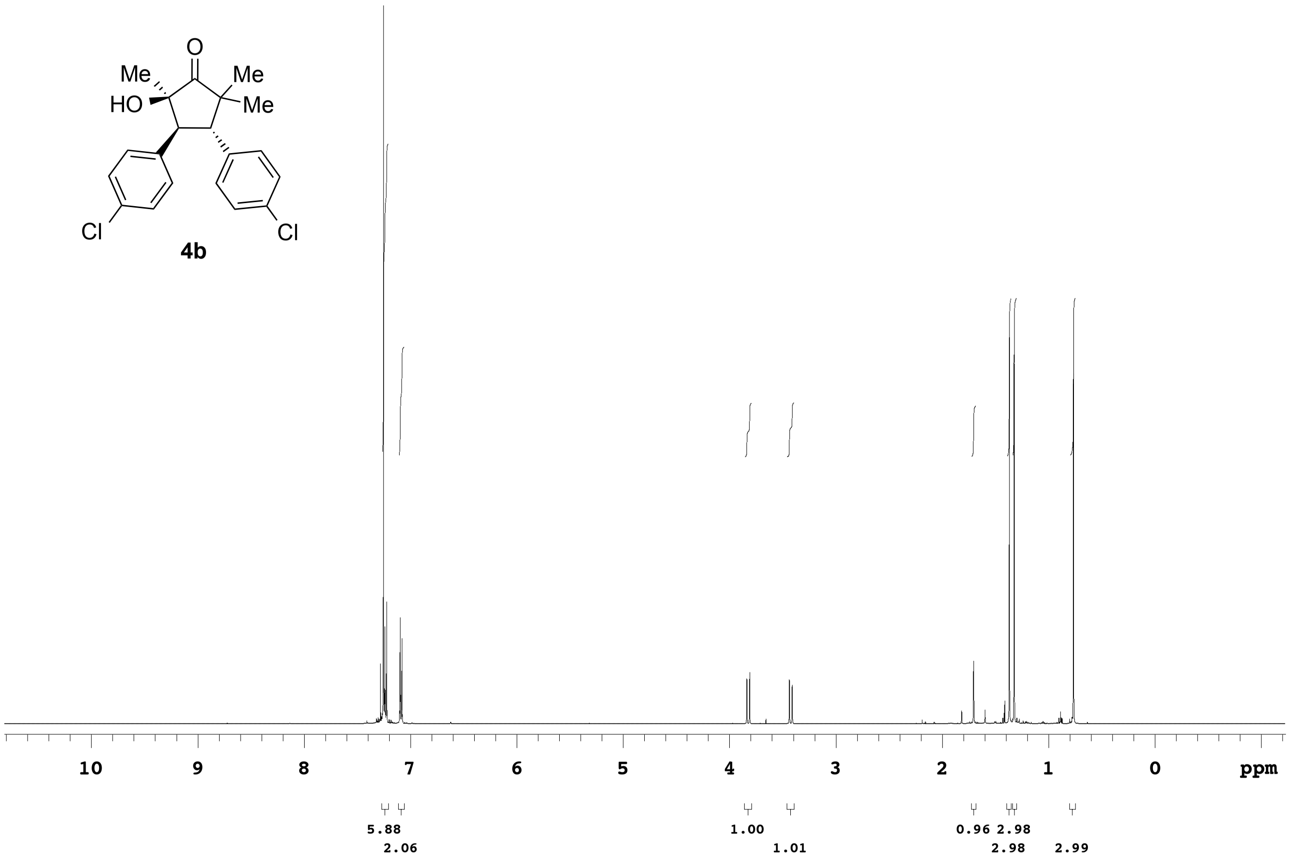

Yong 7 98 col 1stspot EAremoved
125.266 MHz C13[H1] 1D in cdcl3 (ref. to CDCl3 @ 77.06 ppm), temp 27.2 C -> actual temp = 27.0 C, autoxdb probe
date: Feb 19 2013 sweep width: 33827Hz acq.time: 2.5s relax.time: 0.1s # scans: 348 dig.res.: 0.3 Hz/pt hz/mm:140.9 Pulse Sequence: s2pul
spectrometer:d300 file:/mnt/d600/home13/westnmr/nmrdata/YONGHOON/Book7/2013.02.19.i5_Yong-7-98-col-1stspot-EAremoved_C13_1D

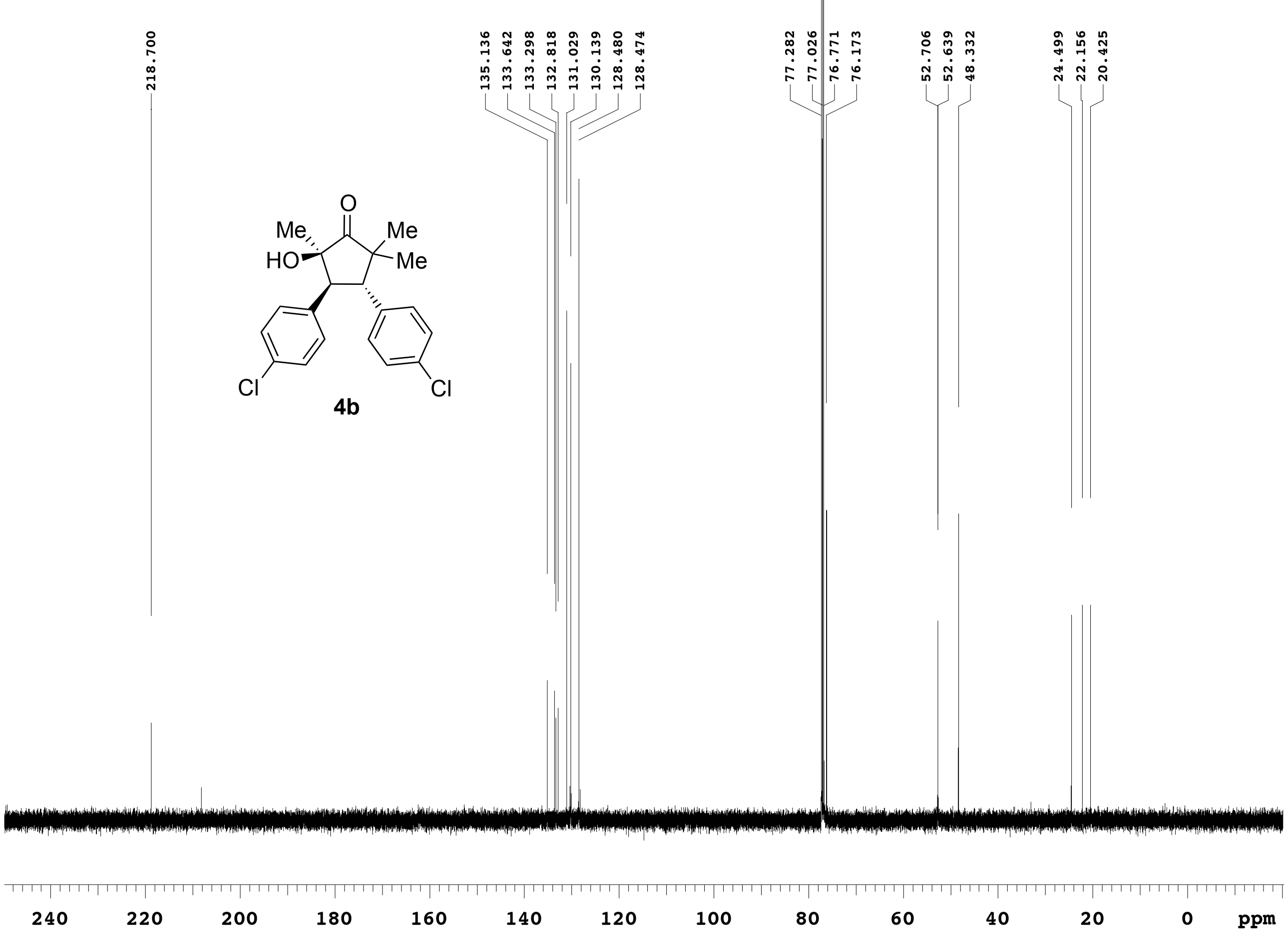

```
Yong-7-158-col-2ndspot
498.118 MHz H1 1D in cdcl3 (ref. to CDCl3 @ 7.26 ppm), temp 26.4 C -> actual temp = 27.0 C, autoxdb probe
```

```
Pulse Sequence: s2pul
```

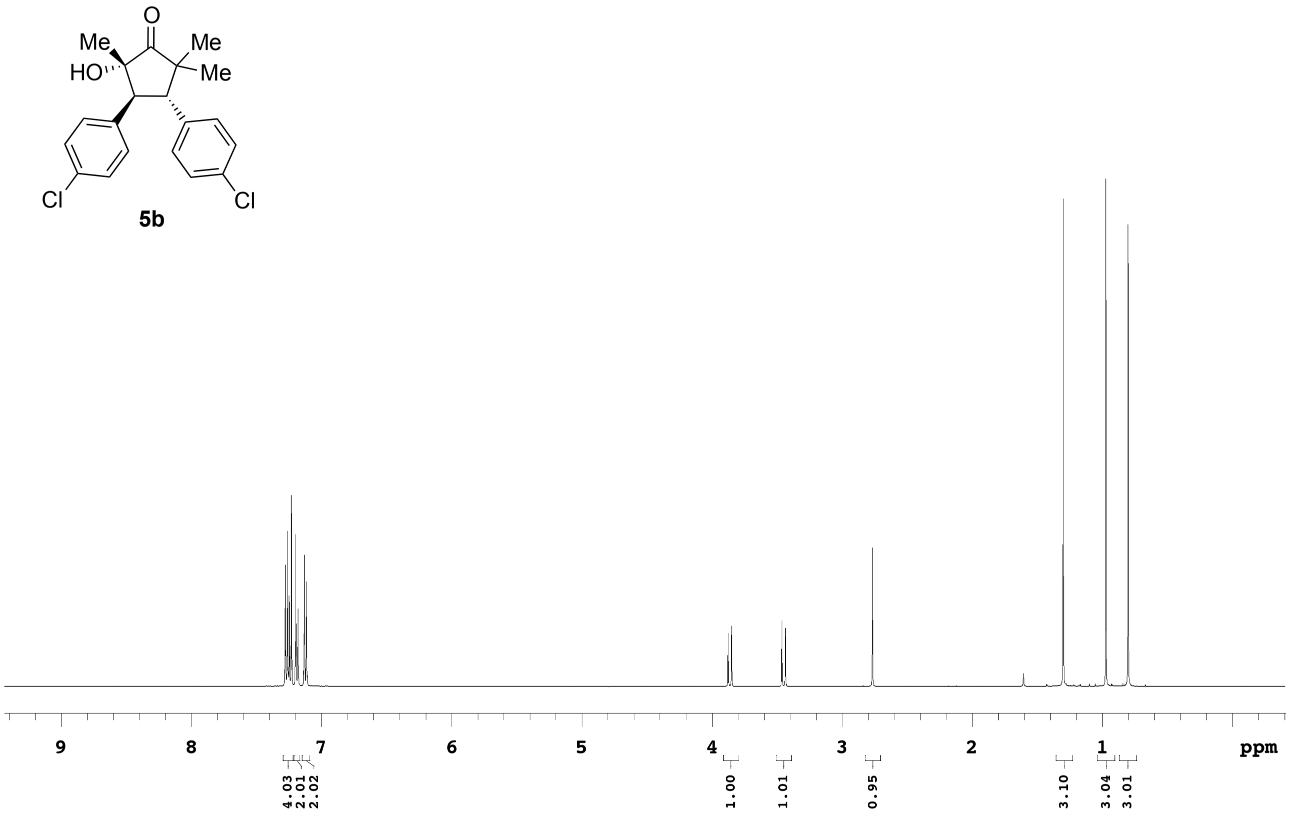

Yong 7 98 col 2ndspot
125.266 MHz C13[H1] 1D in cdcl3 (ref. to CDCl3 @ 77.06 ppm), temp 27.2 C -> actual temp = 27.0 C, autoxdb probe
date: Feb 18 2013 sweep width: 33827Hz acq.time: 2.5s relax.time: 0.1s # scans: 208   dig.res.: 0.3 Hz/pt hz/mm:140.9Pulse Sequence: s2pul
spectrometer:d300   file:/mnt/d600/home13/westnmr/nmrdata/YONGHOON/Book7/2013.02.18.i5_Yong-7-98-col-2ndspot_C13_1D

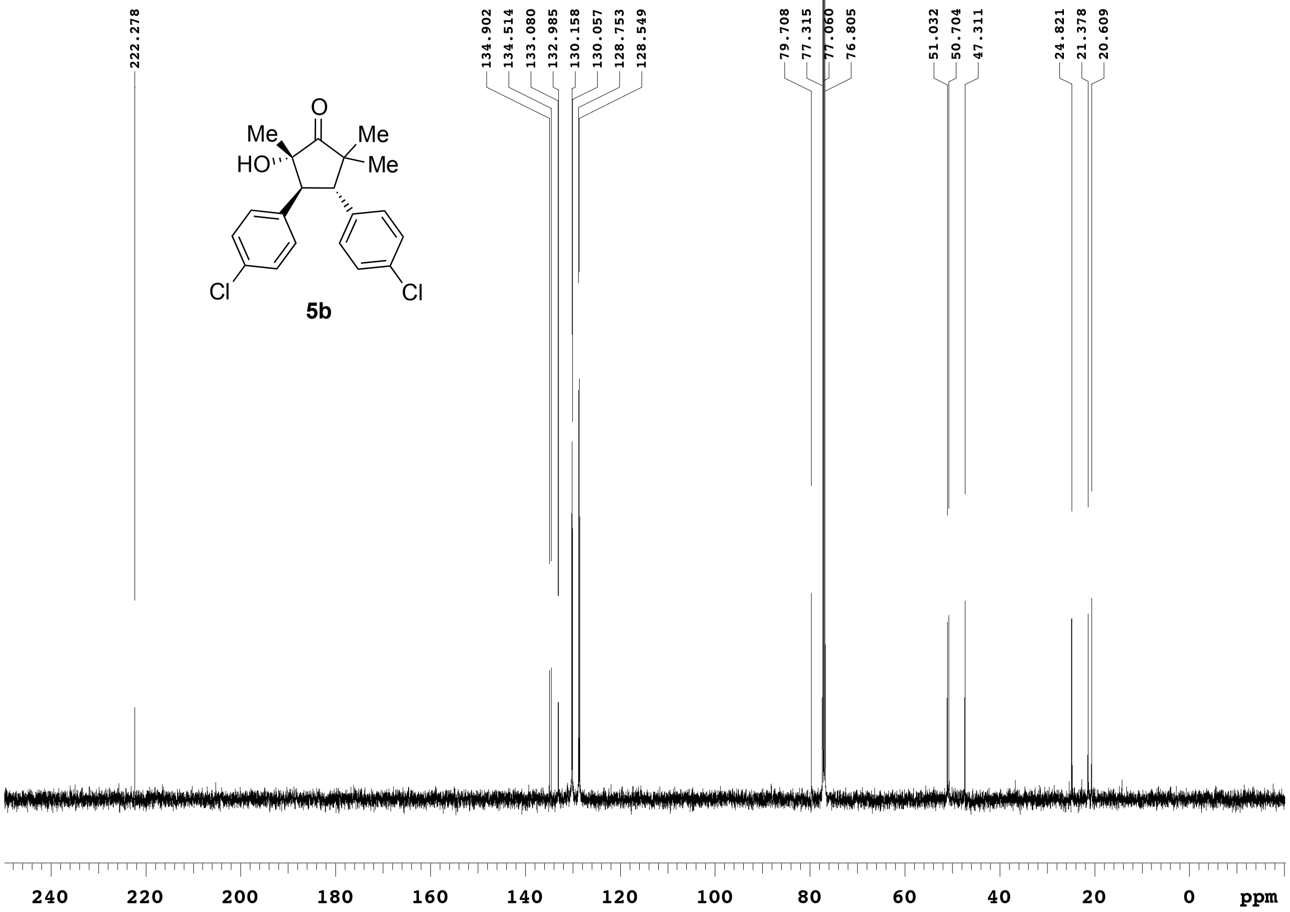

Yong 7 92 col 1stspot
498.118 MHz H1 1D in cdcl3 (ref. to CDCl3 @ 7.26 ppm), temp 27.2 C -> actual temp = 27.0 C, autoxdb probe
date: Feb 12 2013 sweep width: 6001Hz acq.time: 5.0s relax.time: 0.1s # scans: 16 dig.res.: 0.1 Hz/pt hz/mm:20.4 Pulse Sequence: s2pul
spectrometer:d300 file:/mnt/d600/home13/westnmr/nmrdata/YONGHOON/Book7/2013.02.12.i5_Yong-7-92-col-1stspot_H1_1D

4c

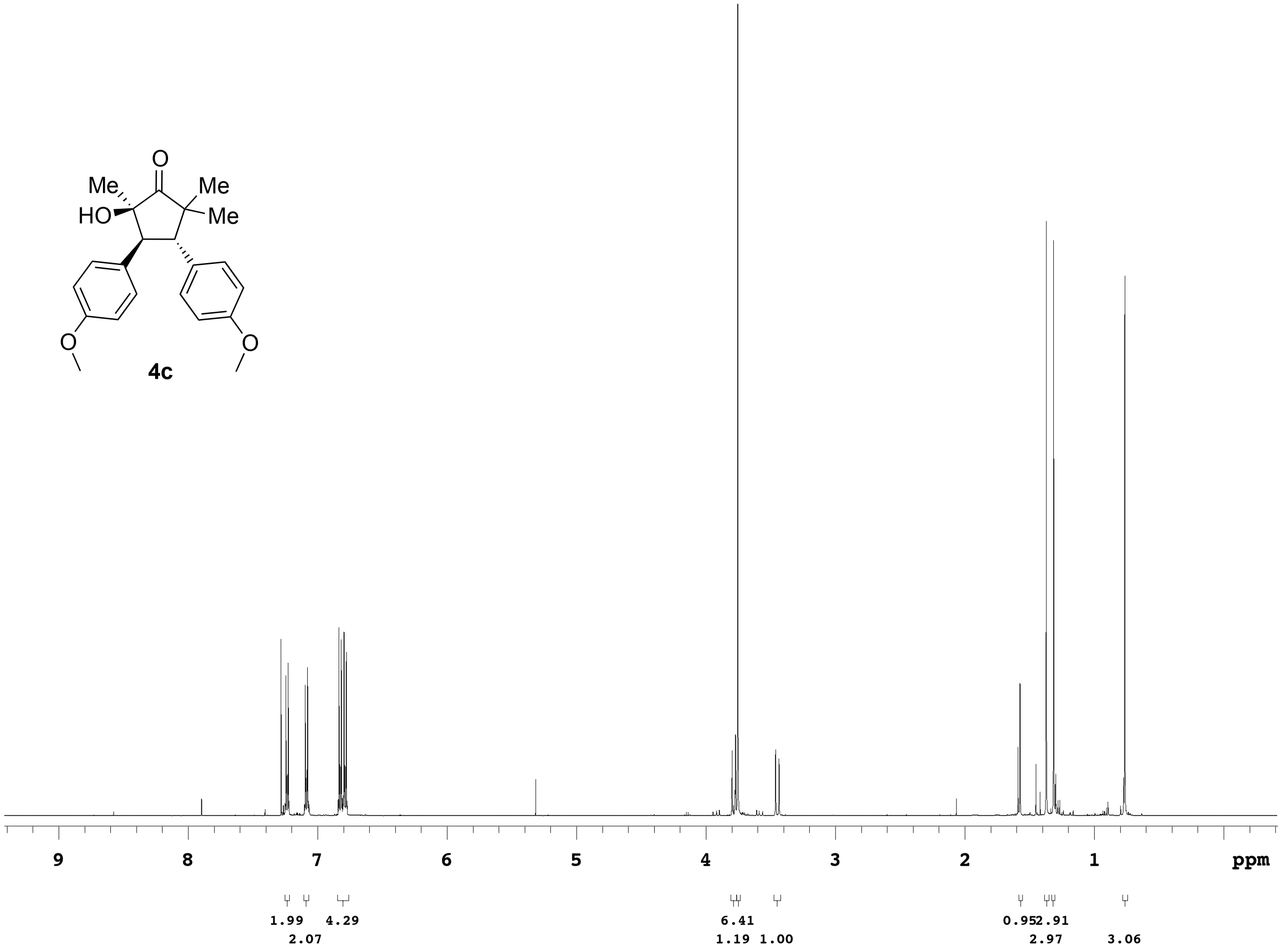

Yong 7 92 col 1stspot
125.266 MHz C13[H1] 1D in cdcl3 (ref. to CDCl3 @ 77.06 ppm), temp 27.2 C -> actual temp = 27.0 C, autoxdb probe
date: Feb 12 2013 sweep width: 33827Hz acq.time: 2.5s relax.time: 0.1s # scans: 1392 dig.res.: 0.3 Hz/pt hz/mm:140.9Pulse Sequence: s2pul
spectrometer:d300 file:/mnt/d600/home13/westnmr/nmrdata/YONGHOON/Book7/2013.02.12.i5_Yong-7-92-col-1stspot_C13_1D

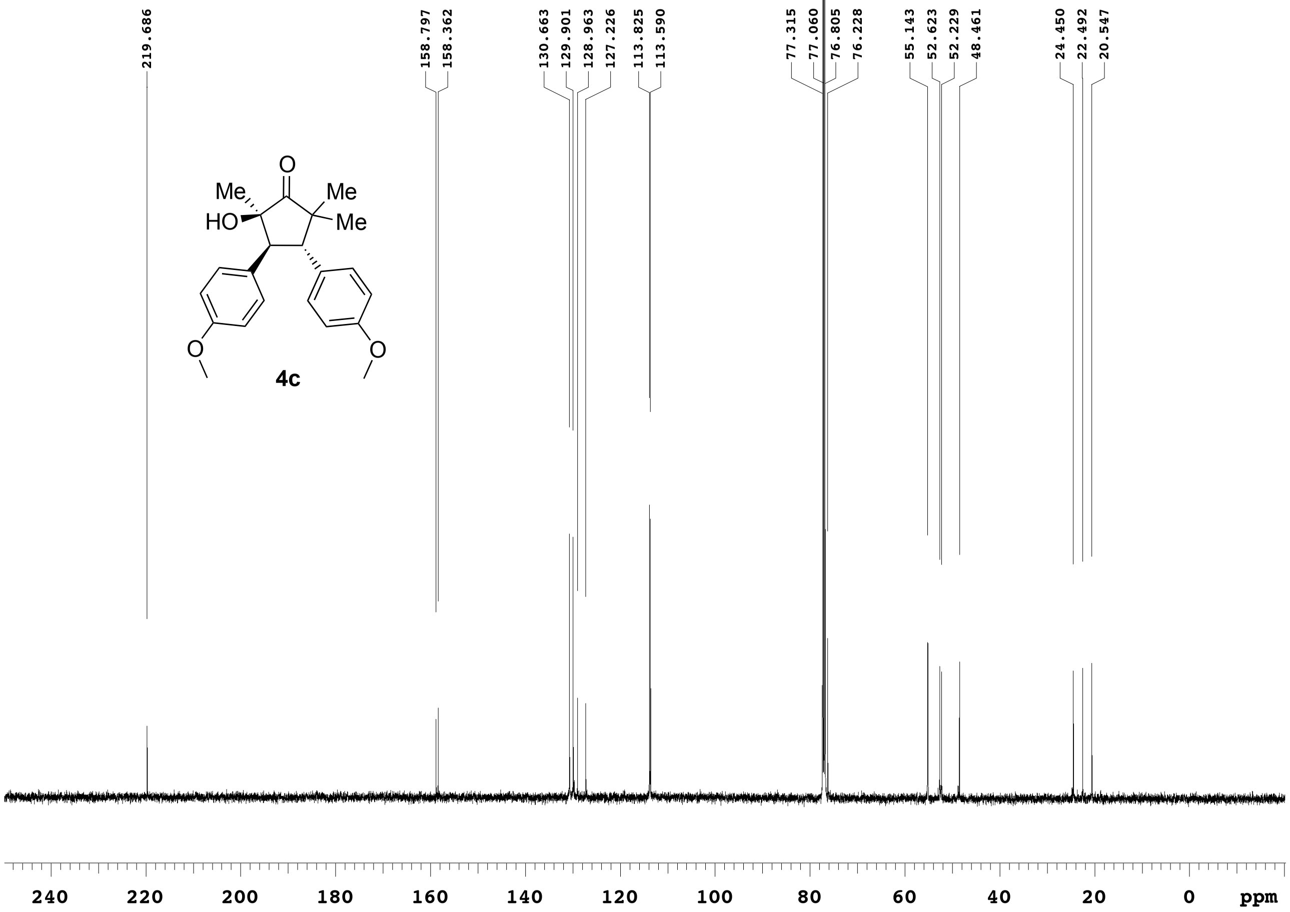

Yong-7-92-col-2ndspot
498.118 MHz H1 1D in cdcl3 (ref. to CDCl3 @ 7.26 ppm), temp 27.2 C -> actual temp = 27.0 C, autoxdb probe

Pulse Sequence: s2pul

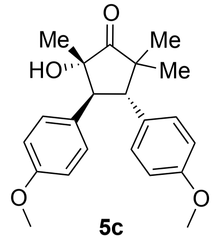

5c

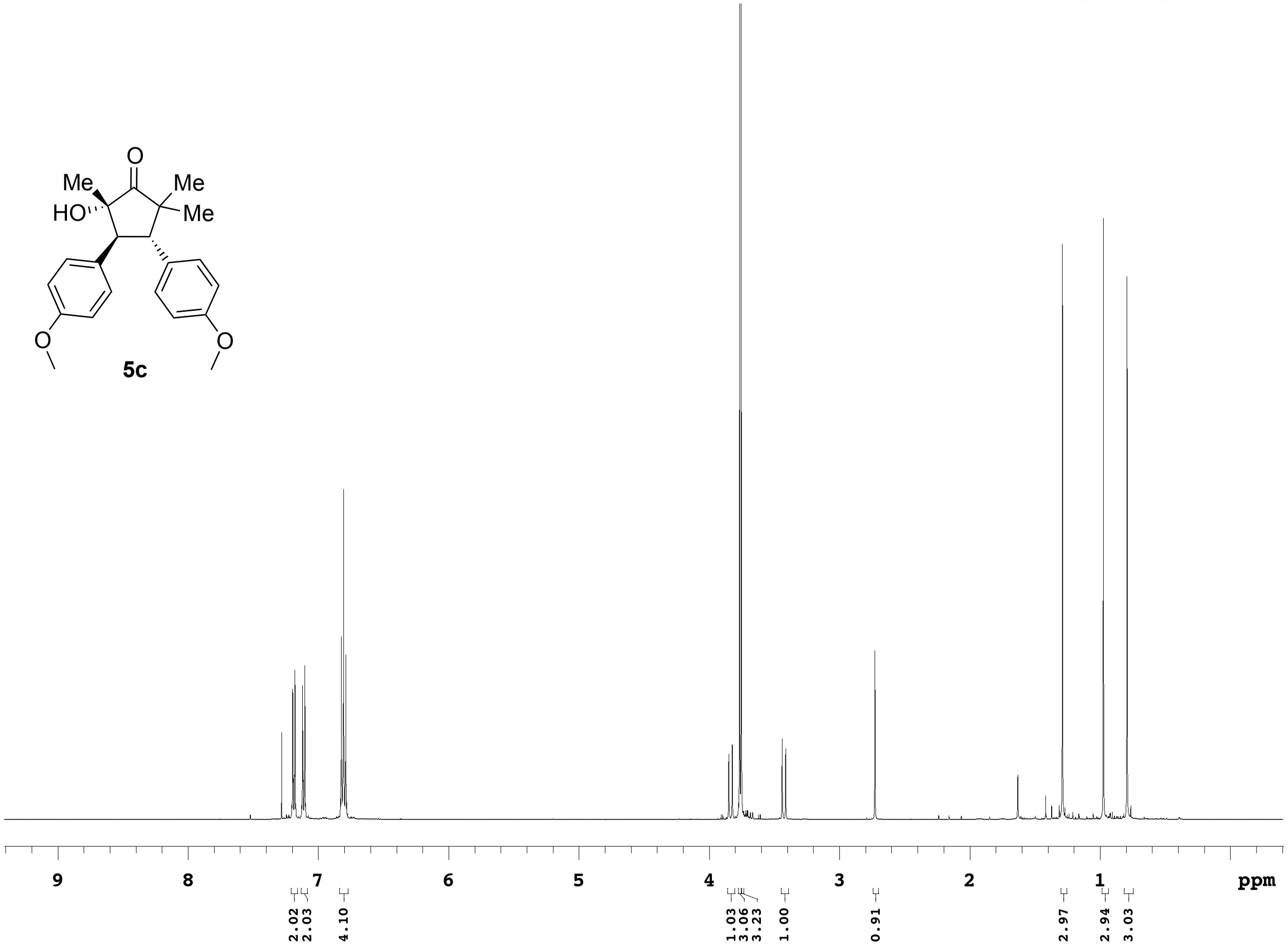

Yong 7 92 col 2ndspot
125.266 MHz C13[H1] 1D in cdcl3 (ref. to CDCl3 @ 77.06 ppm), temp 27.2 C -> actual temp = 27.0 C, autoxdb probe
date: Feb 13 2013 sweep width: 33827Hz acq.time: 2.5s relax.time: 0.1s # scans: 192 dig.res.: 0.3 Hz/pt hz/mm:140.9 Pulse Sequence: s2pul
spectrometer:d300 file:/mnt/d600/home13/westnmr/nmrdata/YONGHOON/Book7/2013.02.13.i5_Yong-7-92-col-2ndspot_C13_1D

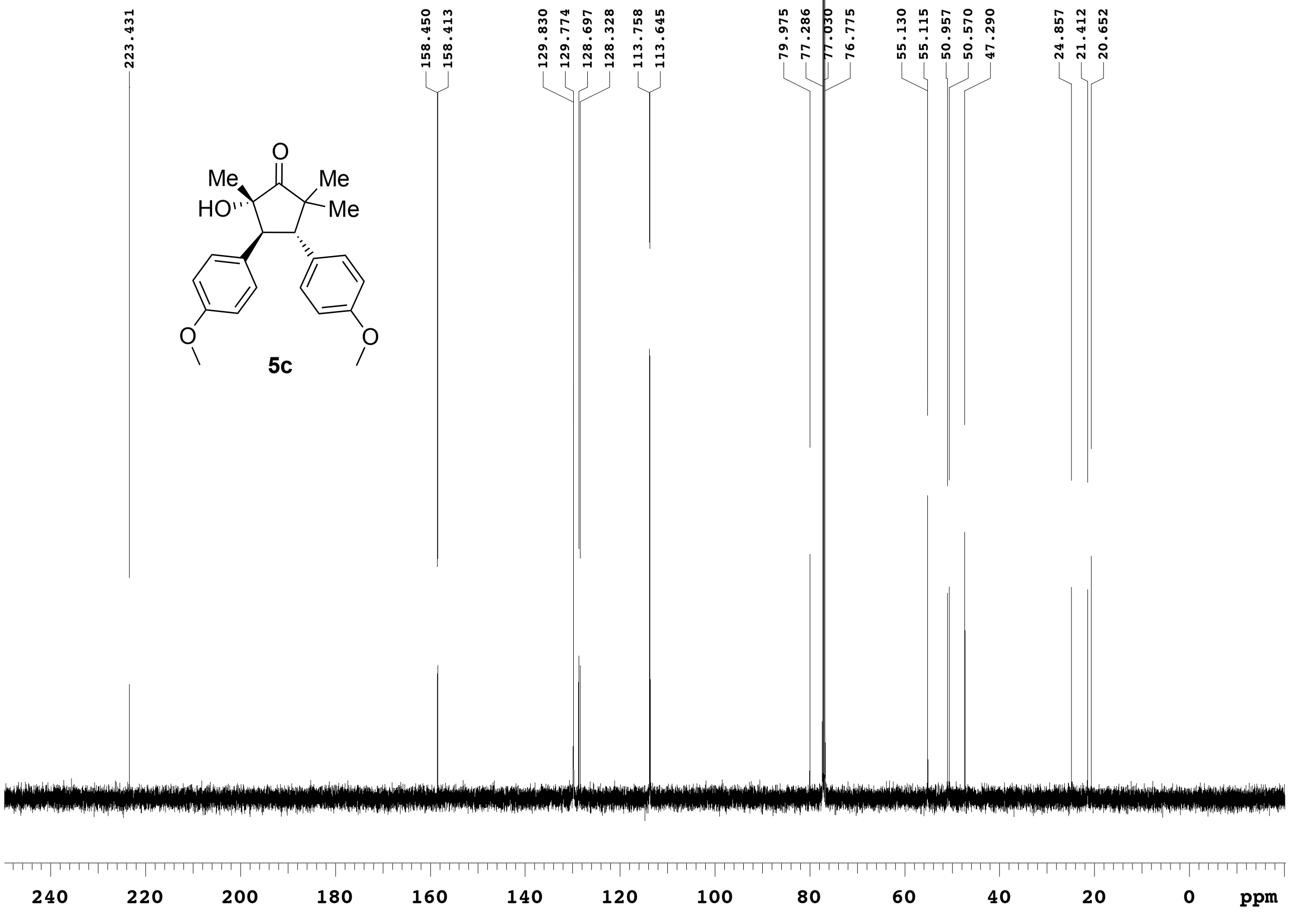

5c

Yong-7-120-col-2ndspot
498.118 MHz H1 1D in cdcl3 (ref. to CDCl3 @ 7.26 ppm), temp 27.2 C -> actual temp = 27.0 C, autoxdb probe

Pulse Sequence: s2pul

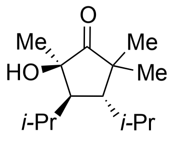
O
Me
HO
Me
Me
i-Pr
i-Pr

4e

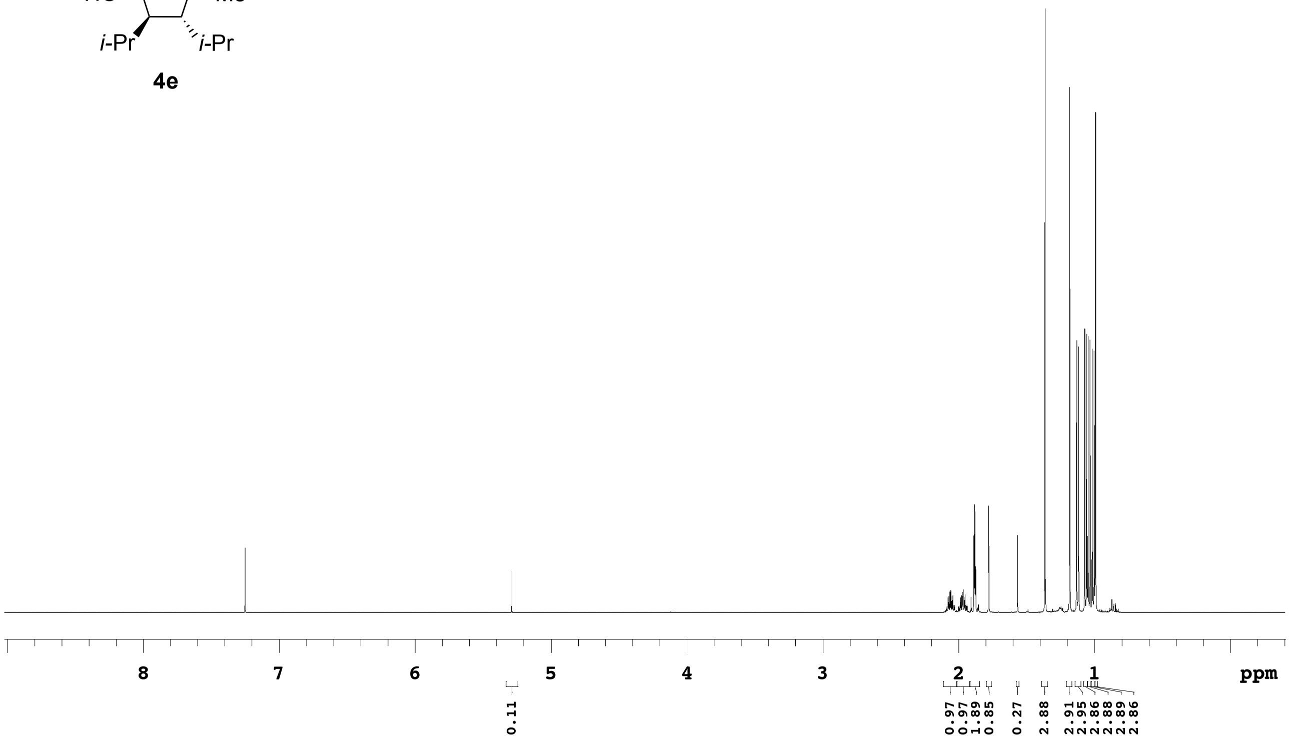

Yong 7 120 col 2ndspot
125.266 MHz C13[H1] 1D in cdcl3 (ref. to CDCl3 @ 77.06 ppm), temp 27.2 C -> actual temp = 27.0 C, autoxdb probe
date: Mar 1 2013 sweep width: 33827Hz acq.time: 2.5s relax.time: 0.1s # scans: 280 dig.res.: 0.3 Hz/pt hz/mm:140.9Pulse Sequence: s2pul
spectrometer:d300 file:/mnt/d600/home13/westnmr/nmrdata/YONGHOON/Book7/2013.03.01.i5_Yong-7-120-col-2ndspot_C13_1D

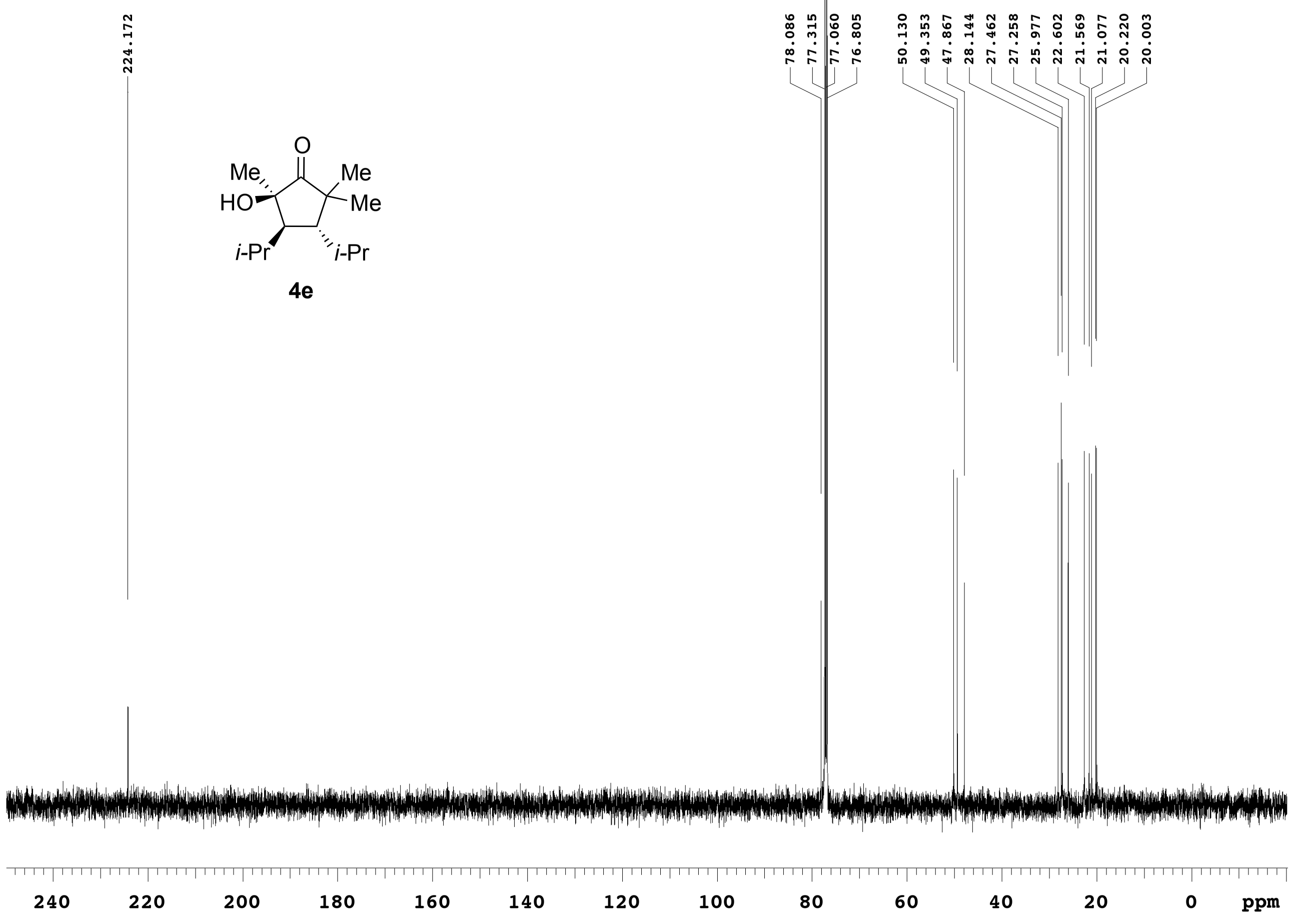

4e

Yong-7-120-col-3rdspot
498.118 MHz H1 1D in cdcl3 (ref. to CDCl3 @ 7.26 ppm), temp 27.2 C -> actual temp = 27.0 C, autoxdb probe

Pulse Sequence: s2pul

O
Me
Me
Me
HO
i-Pr
i-Pr

5e

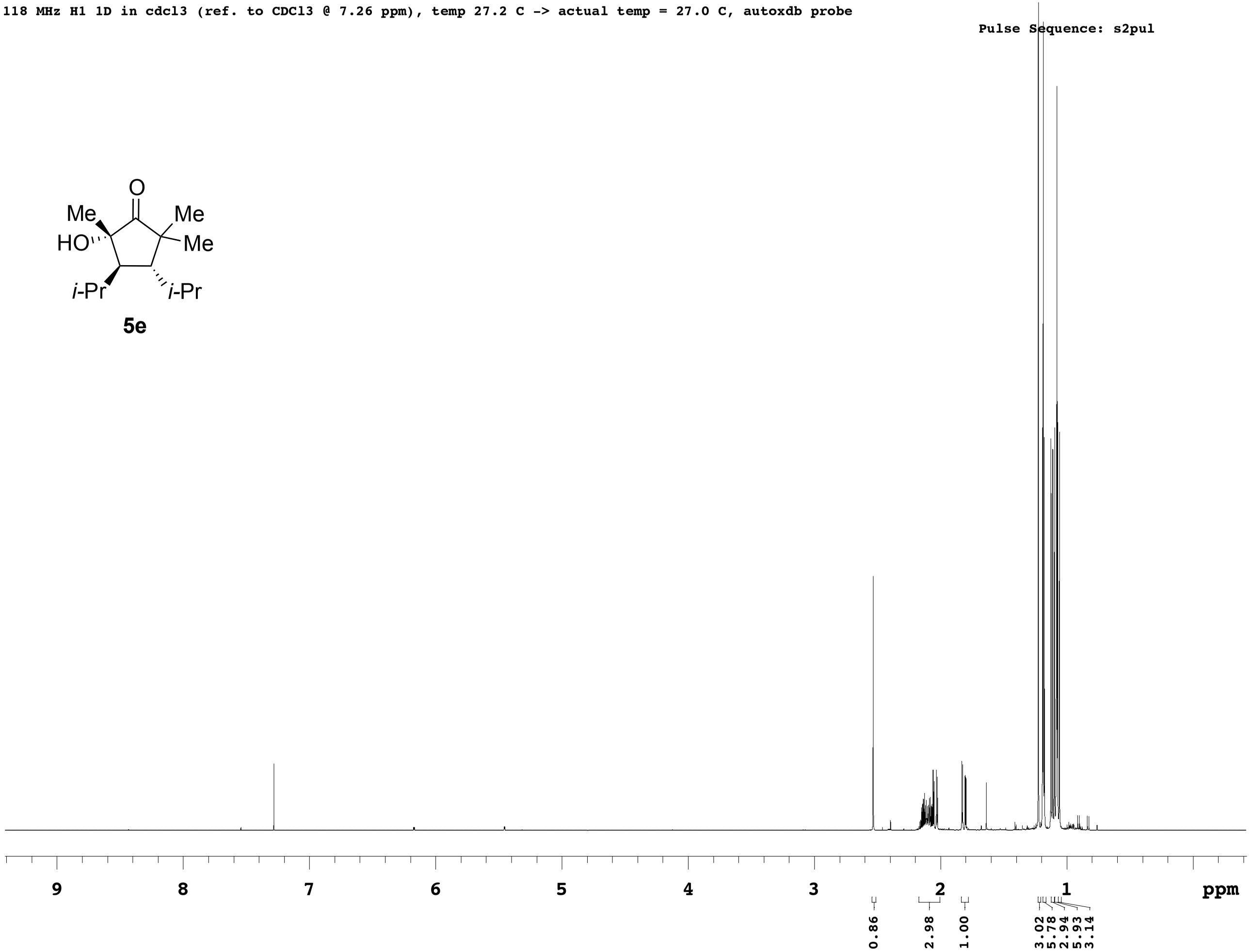

Yong 7 120 col 3rdspot
125.266 MHz C13[H1] 1D in cdcl3 (ref. to CDCl3 @ 77.06 ppm), temp 27.2 C -> actual temp = 27.0 C, autoxdb probe
date: Feb 26 2013 sweep width: 33827Hz acq.time: 2.5s relax.time: 0.1s # scans: 344 dig.res.: 0.3 Hz/pt hz/mm:140.9 Pulse Sequence: s2pul
spectrometer:d300 file:/mnt/d600/home13/westnmr/nmrdata/YONGHOON/Book7/2013.02.26.i5_Yong-7-120-col-3rdspot_C13_1D

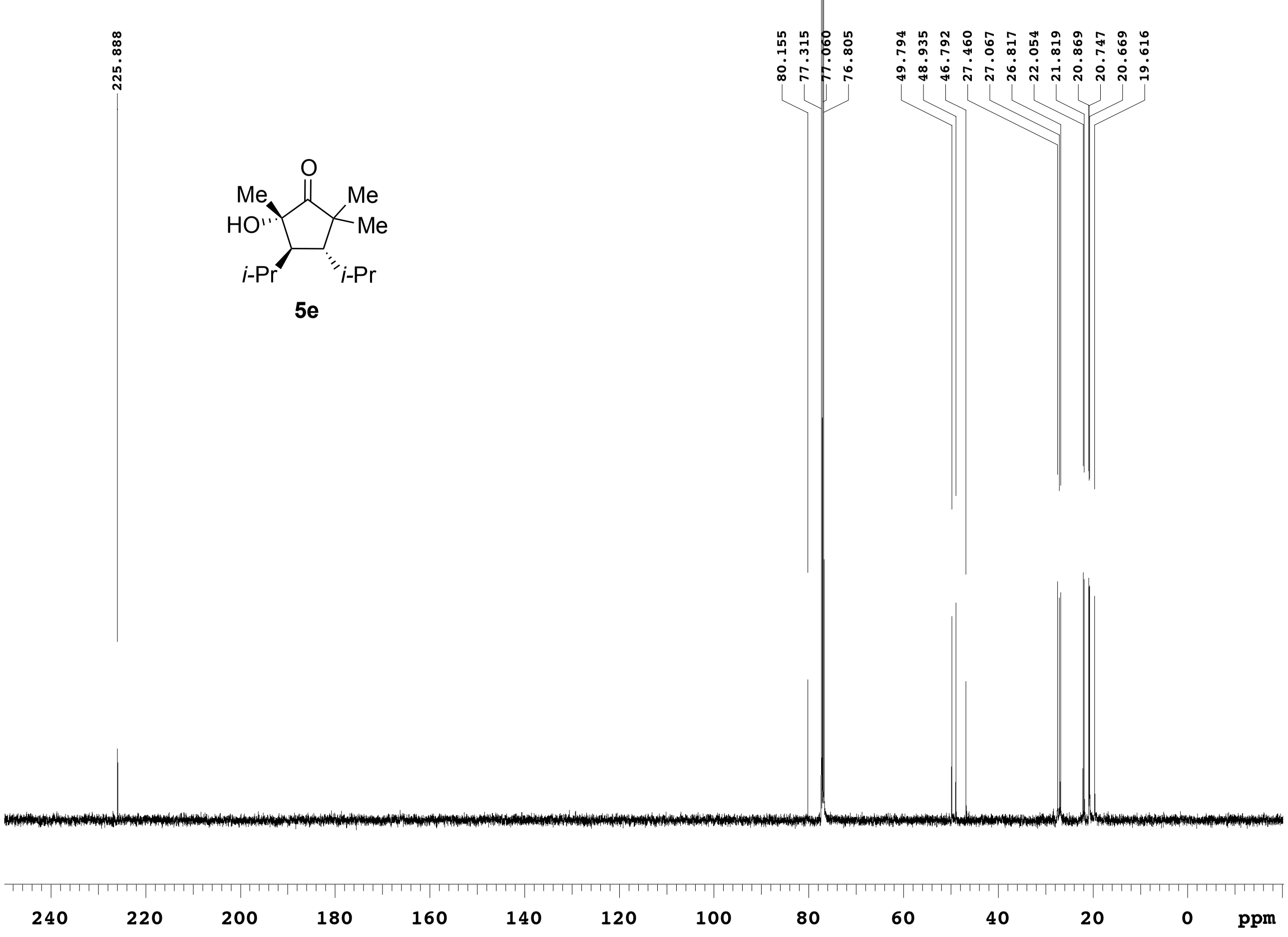

Yong-7-86-col-1stspot-recolumned
498.118 MHz H1 1D in cdcl3 (ref. to CDCl3 @ 7.26 ppm), temp 27.2 C -> actual temp = 27.0 C, autoxdb probe

Pulse Sequence: s2pul

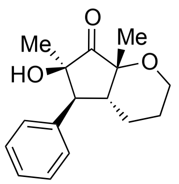

4g

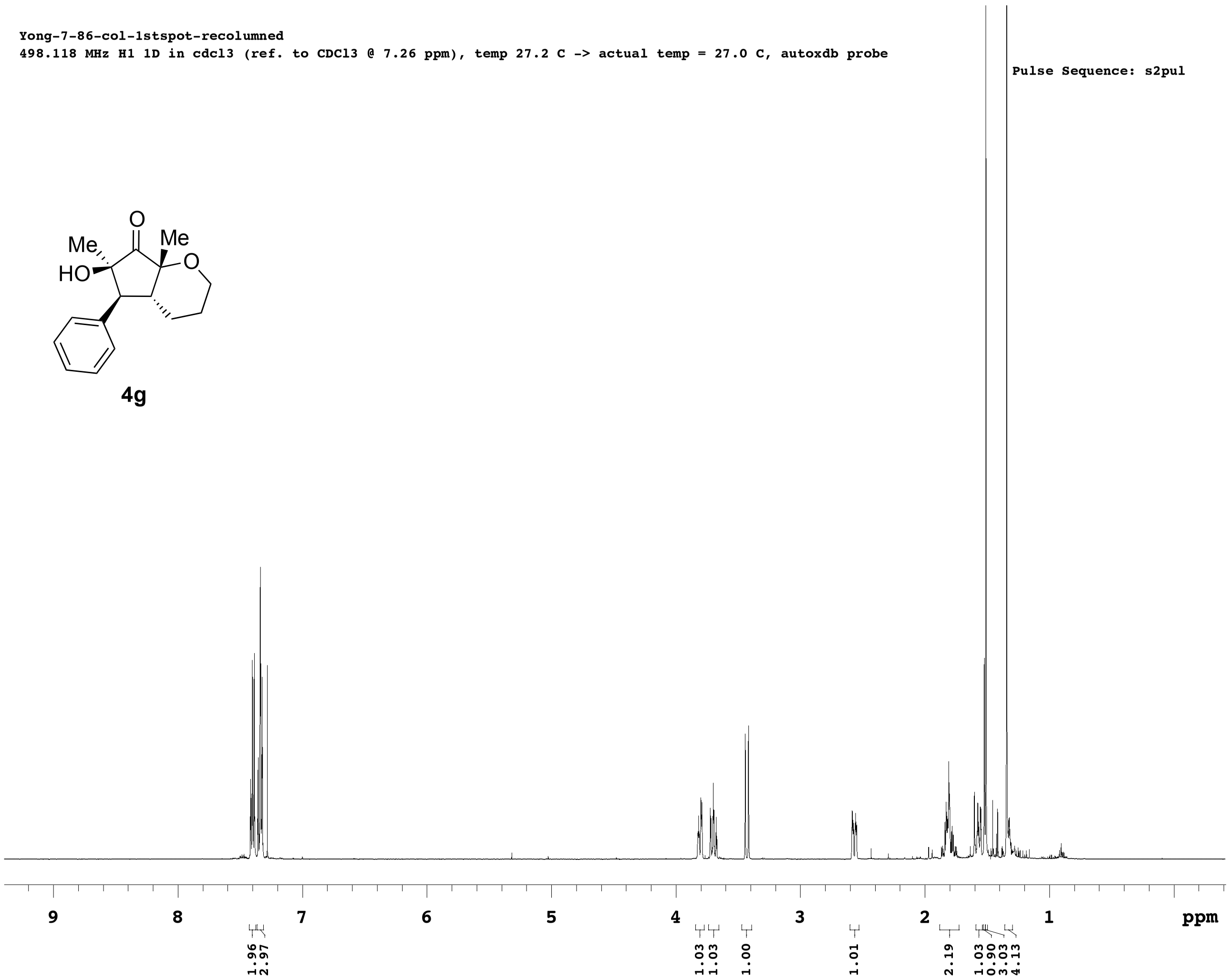

Yong 7 86 col 1stspot recolumned
125.266 MHz C13[H1] APT_ad in cdcl3 (ref. to CDCl3 @ 77.06 ppm), temp 27.2 C -> actual temp = 27.0 C, autoxdb probe
date: Mar 2 2013, sweep width: 33827Hz acq.time: 2.5s relax.time: 0.1s # scans: 25236 dig.res.: 0.3 Hz/pt hz/mm:140.9
C & CH2 same, CH & CH3 opposite side of solvent signal
spectrometer:d300 file:/mnt/d600/home13/westnmr/nmrdata/YONGHOON/Book7/2013.03.02.i5_Yong-7-86-col-1stspot-recolumned_C13_APT_ad
Pulse Sequence: APT_ad

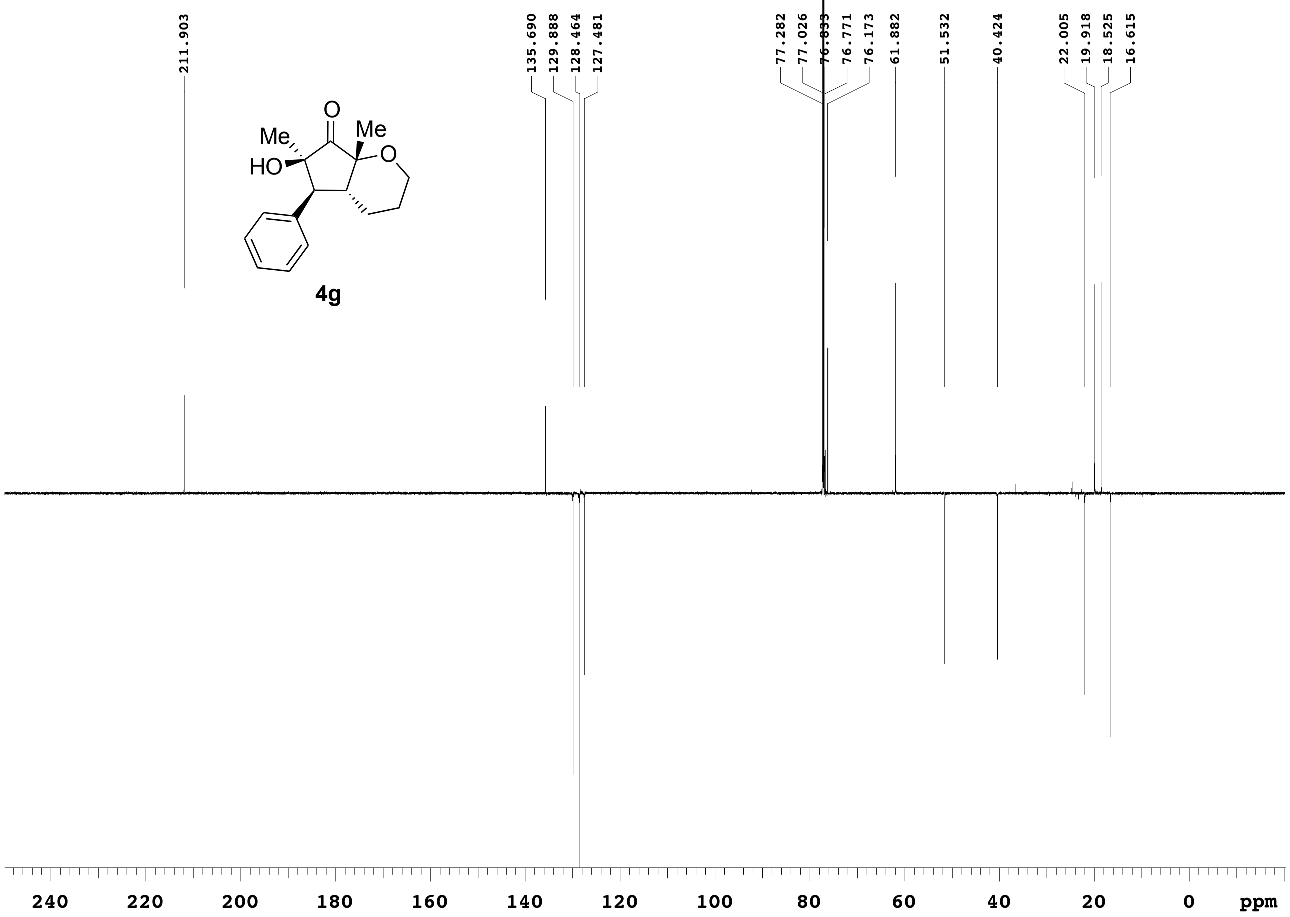

4g

Yong-7-86-col-2ndspot-EAremoved
498.118 MHz H1 1D in cdcl3 (ref. to CDCl3 @ 7.26 ppm), temp 27.2 C -> actual temp = 27.0 C, autoxdb probe

Pulse Sequence: s2pul

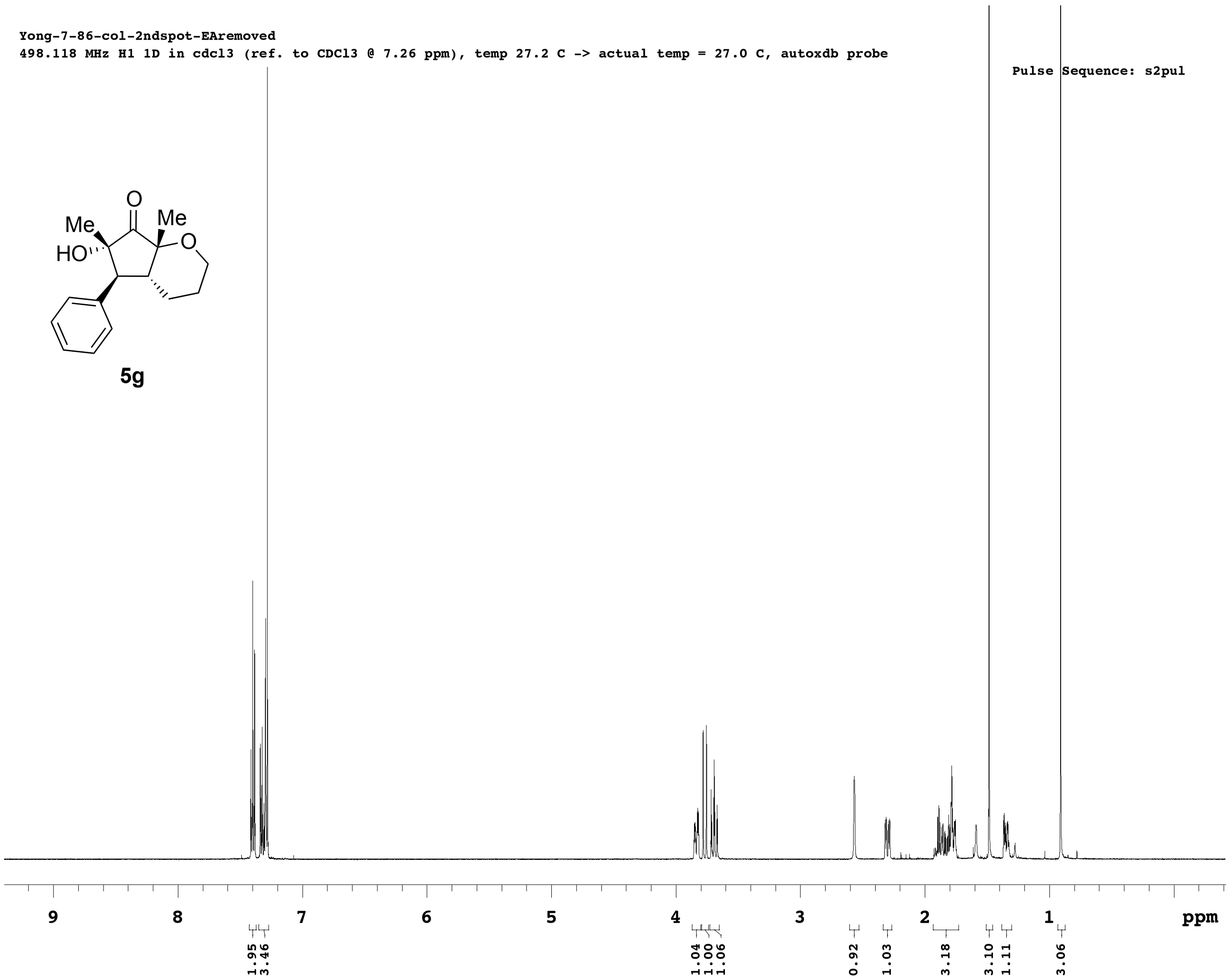

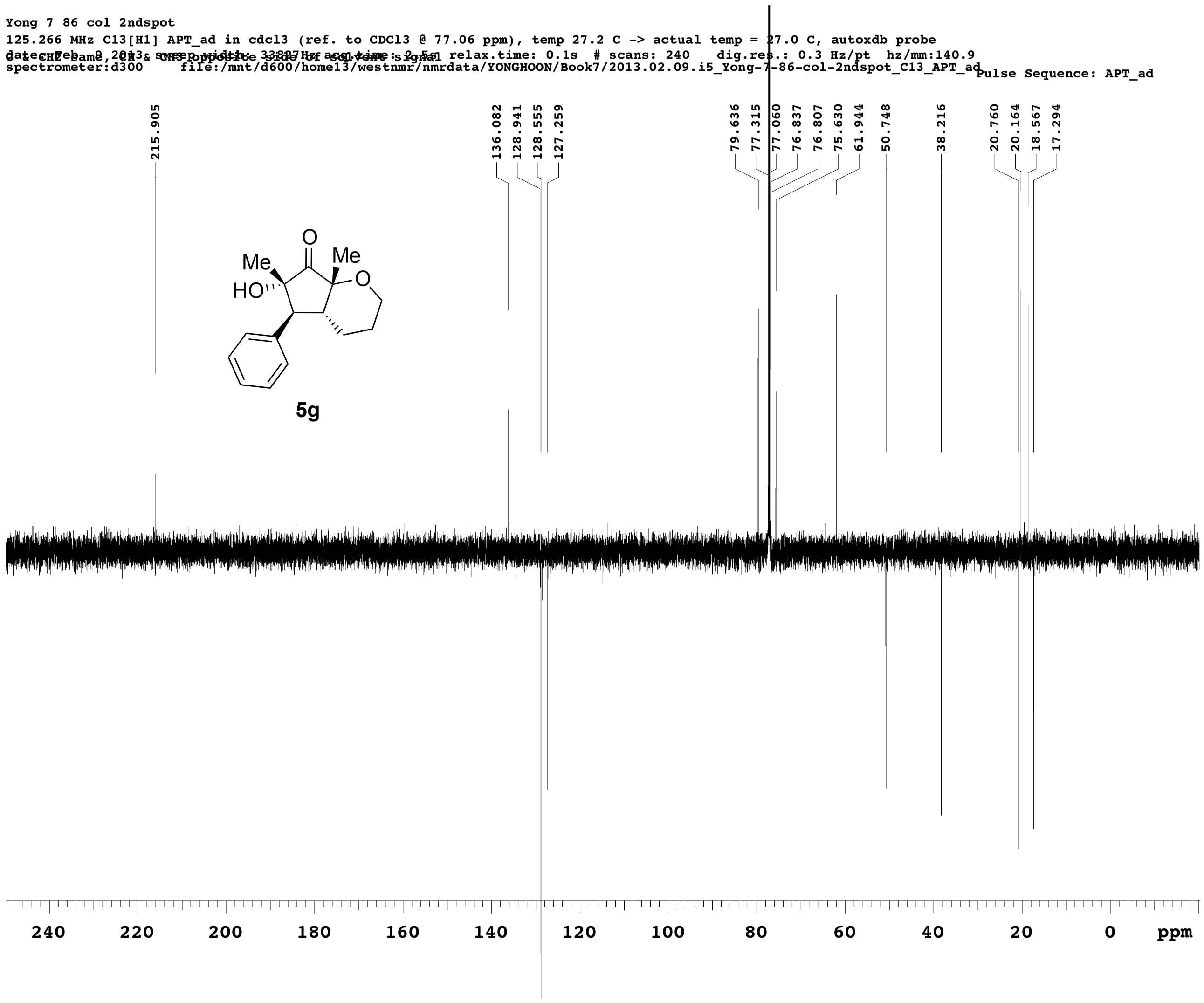
Yong 7 86 col 2ndspot
125.266 MHz C13[H1] APT_ad in cdcl3 (ref. to CDCl3 @ 77.06 ppm), temp 27.2 C -> actual temp = 27.0 C, autoxdb probe
date: Feb 9 2013, sweep width: 33827Hz acq.time: 2.5s relax.time: 0.1s # scans: 240 dig.res.: 0.3 Hz/pt hz/mm:140.9
C & CH2 same, CH & CH3 opposite side of solvent signal
spectrometer:d300 file:/mnt/d600/home13/westnmr/nmrdata/YONGHOON/Book7/2013.02.09.i5_Yong-7-86-col-2ndspot_C13_APT_ad
Pulse Sequence: APT_ad
215.905
136.082
128.941
128.555
127.259
79.636
77.315
77.060
76.837
76.807
75.630
61.944
50.748
38.216
20.760
20.164
18.567
17.294
Me
HO
O
Me
O
240
220
200
180
160
140
120
100
80
60
40
20
0
ppm

5g

Appendix III: Selected NMR Spectra

(Chapter 4)

Yong-5-140-col-2ndspot
498.122 MHz H1 1D in cdcl3 (ref. to CDCl3 @ 7.26 ppm), temp 27.2 C -> actual temp = 27.0 C, autoxdb probe

date: Jun 7 2012 sweep width: 6001Hz acq.time: 5.0s relax.time: 0.1s # scans: 16   dig.res.: 0.1 Hz/pt hz/mm:18.6
spectrometer:d300   file:/mnt/d600/home13/westnmr/nmrdata/YONGHOON/Book5/2012.06.07.i5_Yong-5-140-col-2ndspot_H1_1D

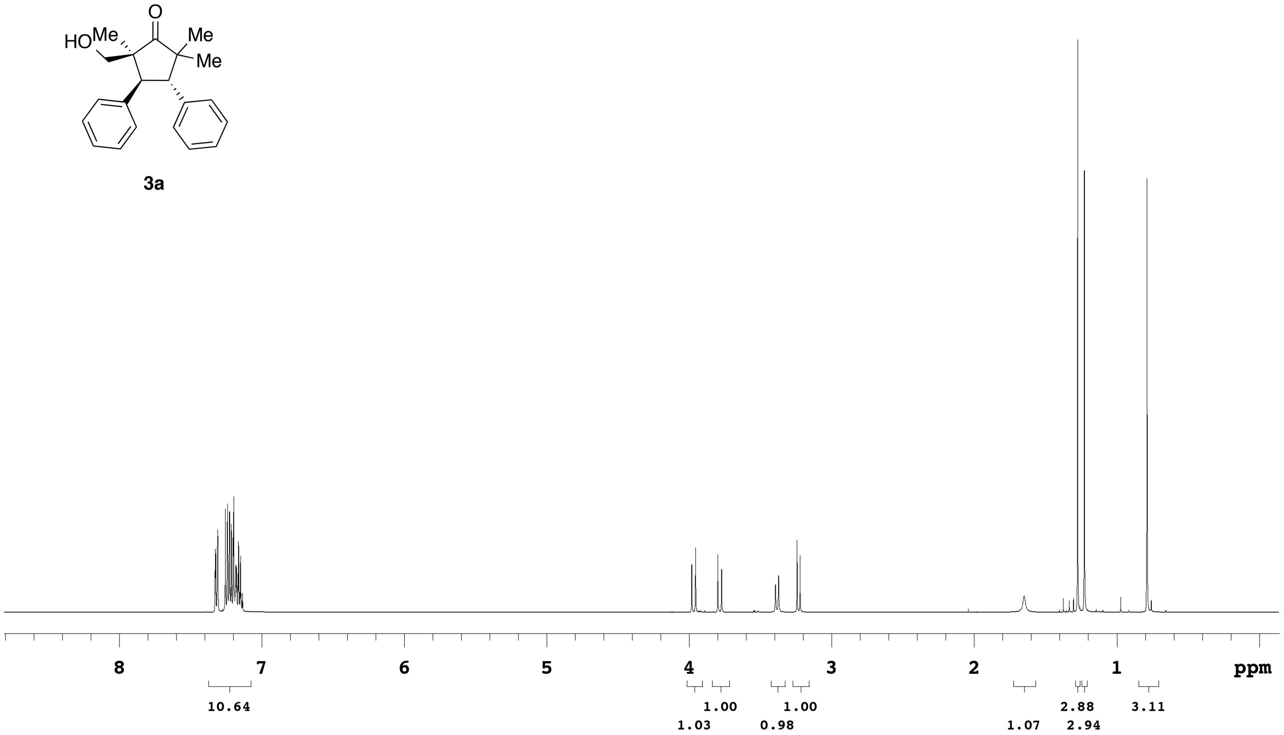

3a

Pulse Sequence: s2pul

125.267 MHz C13[H1] 1D in cdcl3 (ref. to CDCl3 @ 77.06 ppm), temp 27.2 C -> actual temp = 27.0 C, autoxdb probe

date: Jun 6 2012 sweep width: 33827Hz acq.time: 2.5s relax.time: 0.1s # scans: 220   dig.res.: 0.3 Hz/pt hz/mm:140.9
spectrometer:d300   file:/mnt/d600/home13/westnmr/nmrdata/YONGHOON/Book5/2012.06.06.i5_Yong-5-140-col-2ndspot_C13_1D

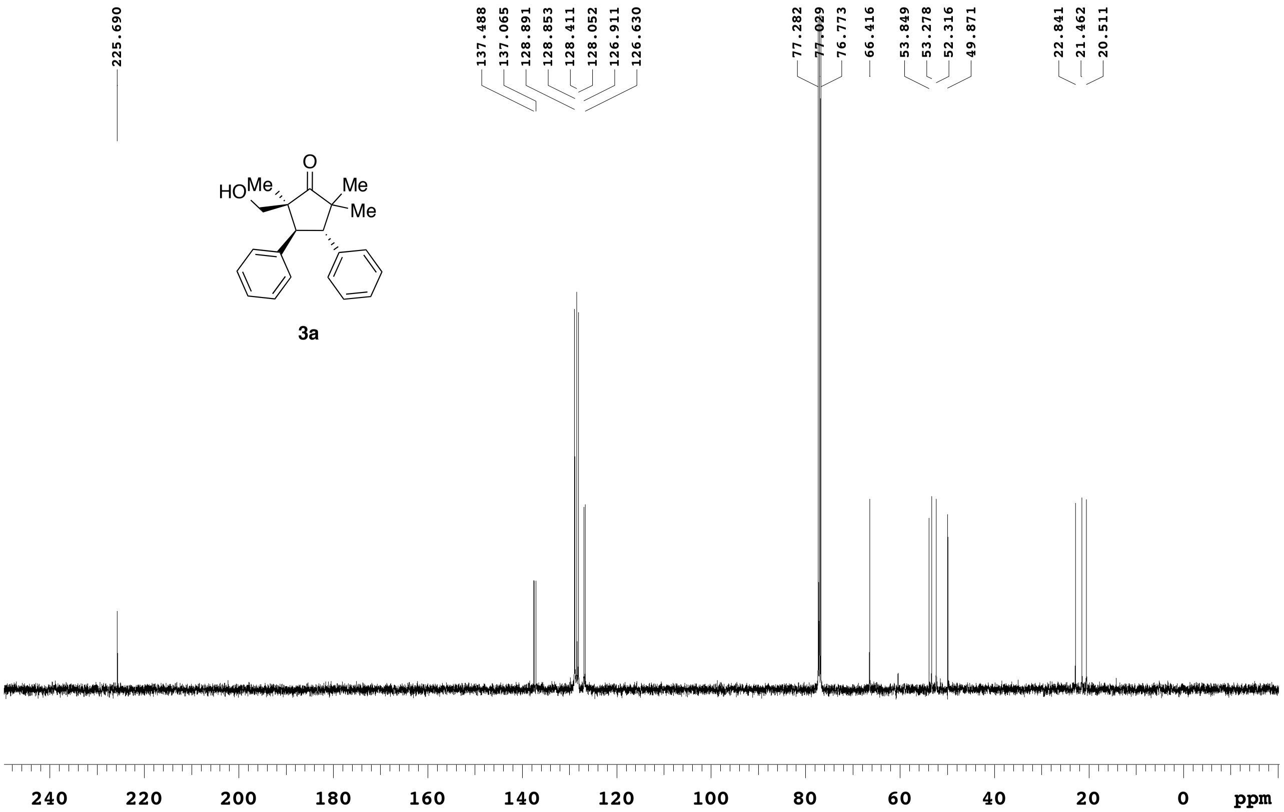

3a

Pulse Sequence: s2pul

Yong-6-80-col-minor
498.118 MHz H1 1D in cdcl3 (ref. to CDCl3 @ 7.26 ppm), temp 27.2 C -> actual temp = 27.0 C, autoxdb probe

date: Sep 19 2012 sweep width: 6010Hz acq.time: 5.0s relax.time: 0.1s # scans: 16   dig.res.: 0.1 Hz/pt hz/mm:17.1
spectrometer:d300   file:/mnt/d600/home13/westnmr/nmrdata/YONGHOON/Book6/2012.09.19.i5_Yong-6-80-col-minor_H1_1D

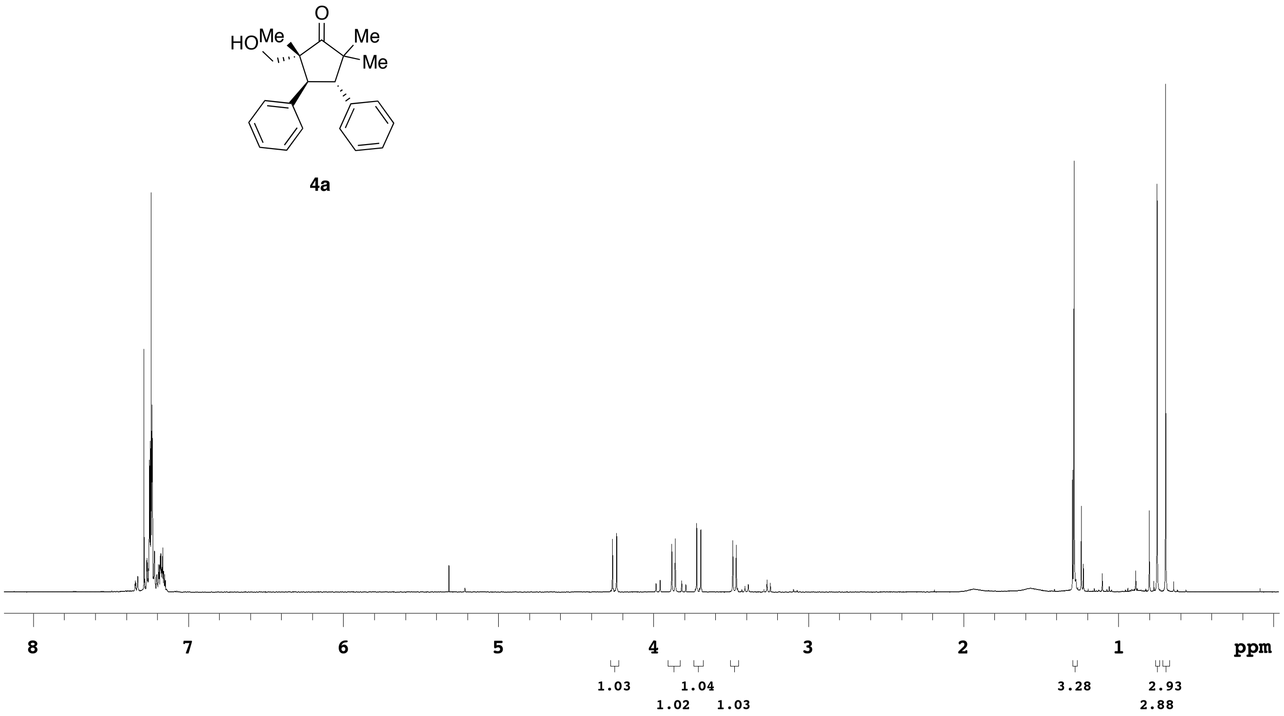

4a

Pulse Sequence: s2pul

Yong-6-80-col-minor
125.266 MHz C13[H1] 1D in cdcl3 (ref. to CDCl3 @ 77.06 ppm), temp 26.4 C -> actual temp = 27.0 C, autoxdb probe

date: Nov 2 2014 sweep width: 33827Hz acq.time: 2.5s relax.time: 0.1s # scans: 200 dig.res.: 0.3 Hz/pt hz/mm:140.9
spectrometer:d300 file:/mnt/d600/home13/westnmr/nmrdata/YONGHOON/Book6/2014.11.02.i5_Yong-6-80-col-minor_21.12_C13_1D

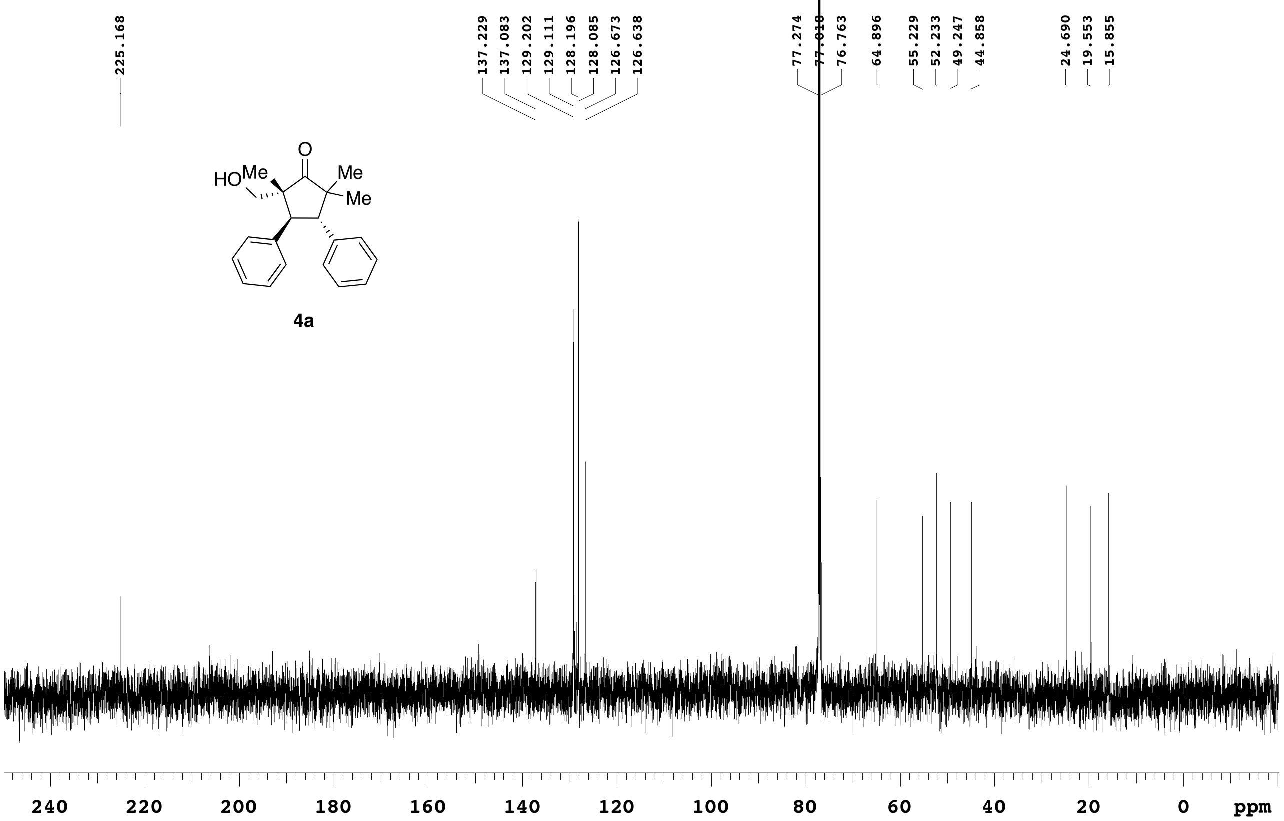

4a

Pulse Sequence: s2pul

Yong-6-190-col-1st
399.794 MHz H1 1D in cdcl3 (ref. to CDCl3 @ 7.26 ppm), temp 27.0 C -> actual temp = 27.0 C, autoxdb probe

date: Dec 6 2012 sweep width: 4808Hz acq.time: 5.0s relax.time: 0.1s # scans: 16 dig.res.: 0.1 Hz/pt hz/mm:14.6
spectrometer:d300 file:/mnt/d600/home13/westnmr/nmrdata/YONGHOON/Book6/2012.12.06.i4_Yong-6-190-col-1st_H1_1D

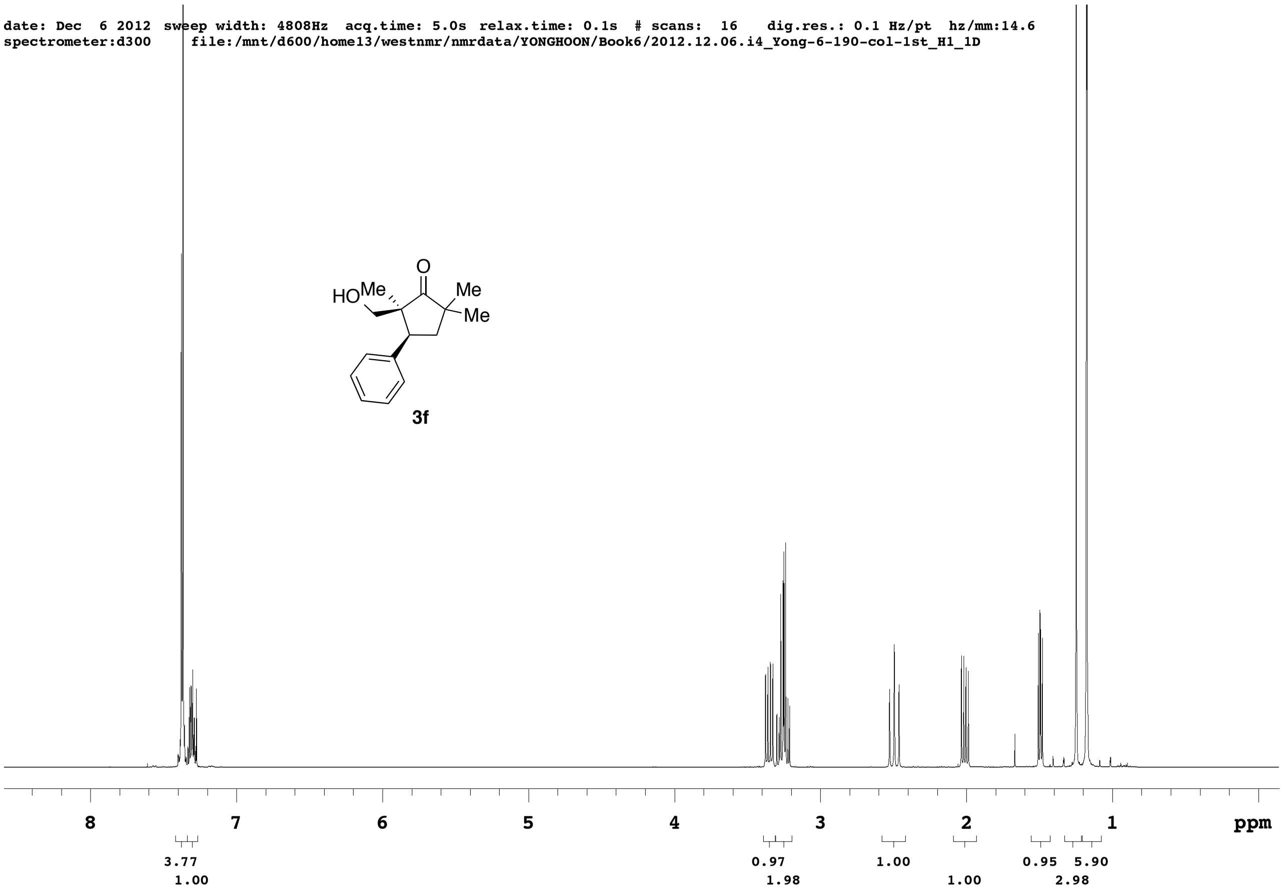

Pulse Sequence: s2pul

Yong-6-190-col-1st
100.539 MHz C13[H1] 1D in cdcl3 (ref. to CDCl3 @ 77.06 ppm), temp 27.0 C -> actual temp = 27.0 C, autoxdb probe

date: Dec 6 2012 sweep width: 27174Hz acq.time: 2.5s relax.time: 0.1s # scans: 132   dig.res.: 0.2 Hz/pt hz/mm:113.2
spectrometer:d300   file:/mnt/d600/home13/westnmr/nmrdata/YONGHOON/Book6/2012.12.06.i4_Yong-6-190-col-1st_C13_1D

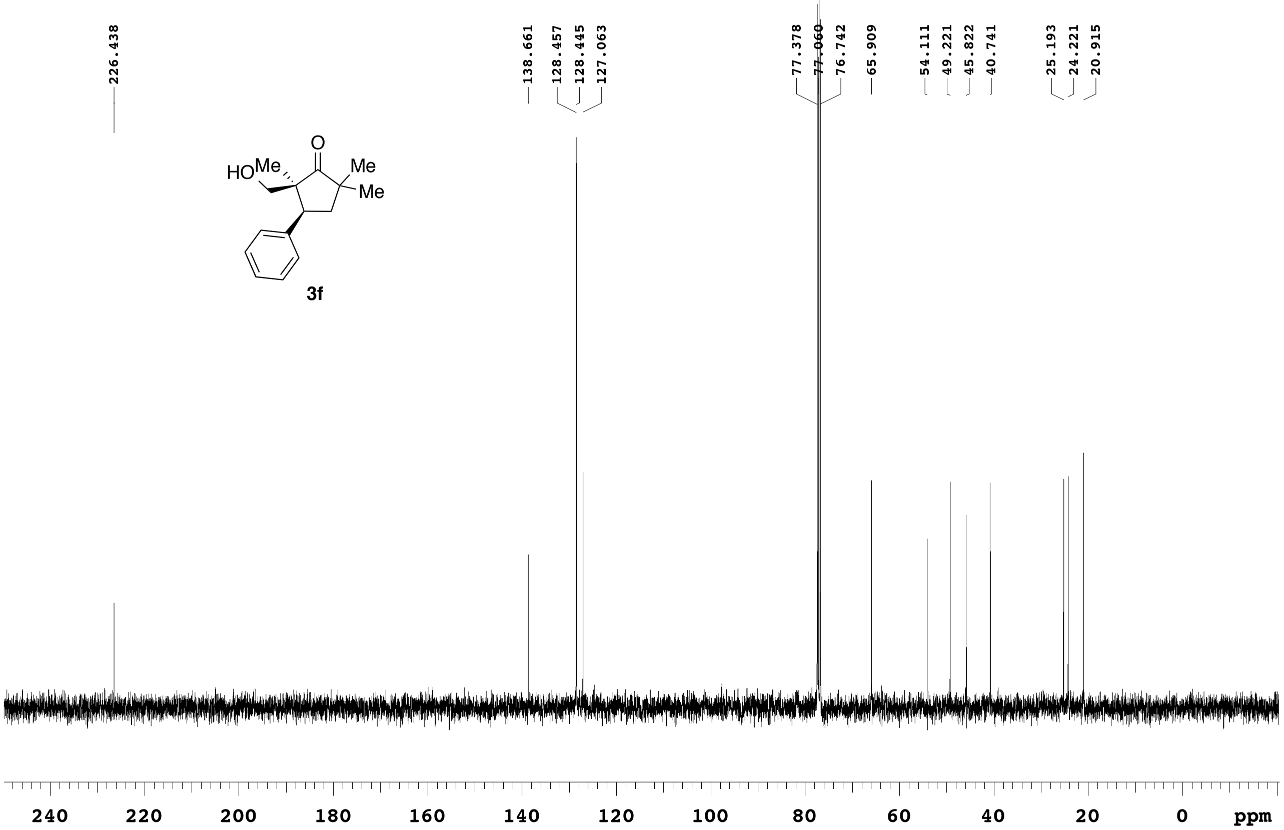

Pulse Sequence: s2pul

Yong-6-190-col-2ndspot
498.118 MHz H1 1D in cdcl3 (ref. to CDCl3 @ 7.26 ppm), temp 27.2 C -> actual temp = 27.0 C, autoxdb probe

date: Dec 6 2012 sweep width: 6001Hz acq.time: 5.0s relax.time: 0.1s # scans: 16   dig.res.: 0.1 Hz/pt hz/mm:17.7
spectrometer:d300   file:/mnt/d600/home13/westnmr/nmrdata/YONGHOON/Book6/2012.12.06.i5_Yong-6-190-col-2ndspot_H1_1D

4f

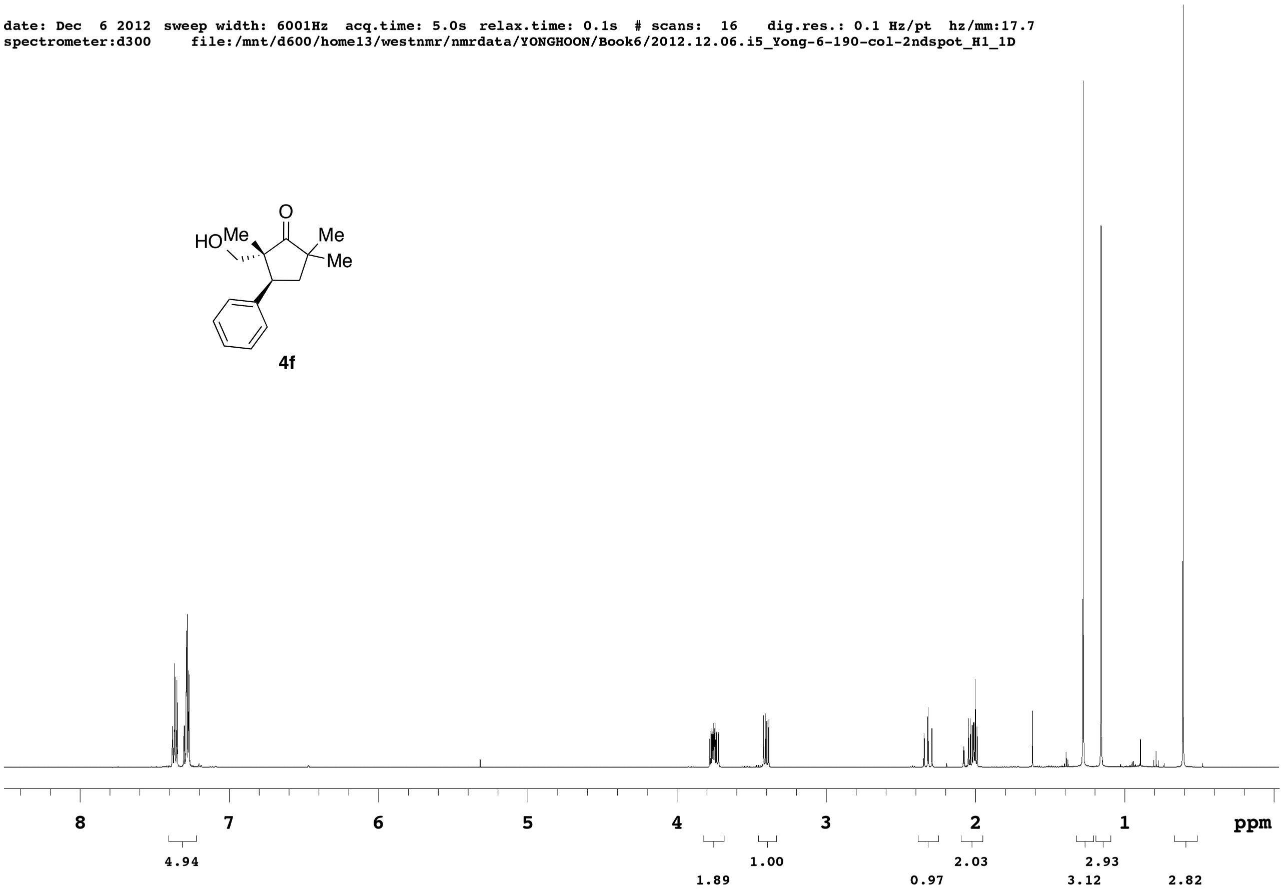

Pulse Sequence: s2pul

Yong-6-190-col-2ndspot
125.266 MHz C13[H1] 1D in cdcl3 (ref. to CDCl3 @ 77.06 ppm), temp 26.4 C -> actual temp = 27.0 C, autoxdb probe

date: Nov 2 2014 sweep width: 33827Hz acq.time: 2.5s relax.time: 0.1s # scans: 424   dig.res.: 0.3 Hz/pt hz/mm:140.9
spectrometer:d300   file:/mnt/d600/home13/westnmr/nmrdata/YONGHOON/Book6/2014.11.02.i5_Yong-6-190-col-2ndspot_21.45_C13_1D

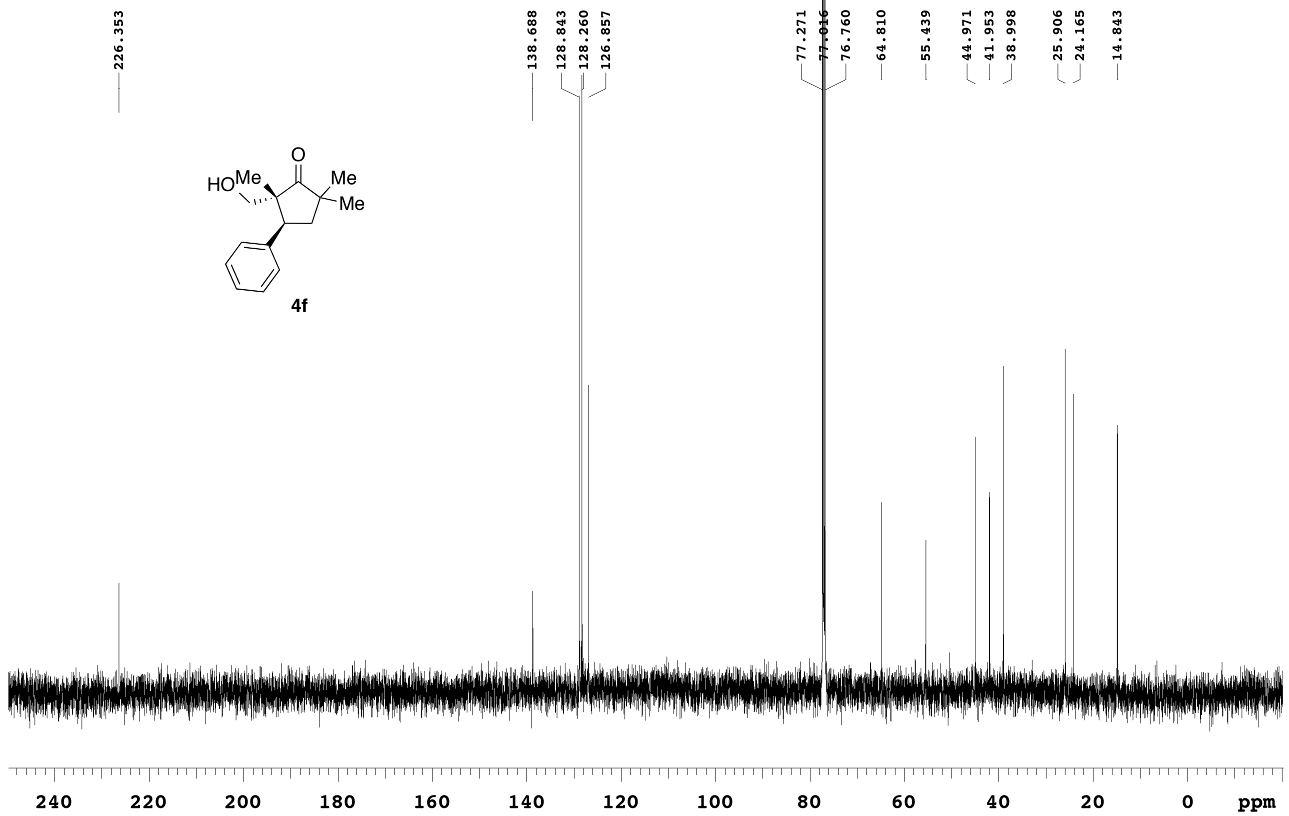

Pulse Sequence: s2pul

Yong-6-194-purification-3rdspot
498.118 MHz H1 1D in cdcl3 (ref. to CDCl3 @ 7.26 ppm), temp 26.4 C -> actual temp = 27.0 C, autoxdb probe

date: May 16 2013 sweep width: 6001Hz acq.time: 5.0s relax.time: 0.1s # scans: 16 dig.res.: 0.1 Hz/pt hz/mm:18.7
spectrometer:d300 file:/mnt/d600/home13/westnmr/nmrdata/YONGHOON/Book6/2013.05.16.i5_Yong-6-194-purification-3rdspot_H1_1D

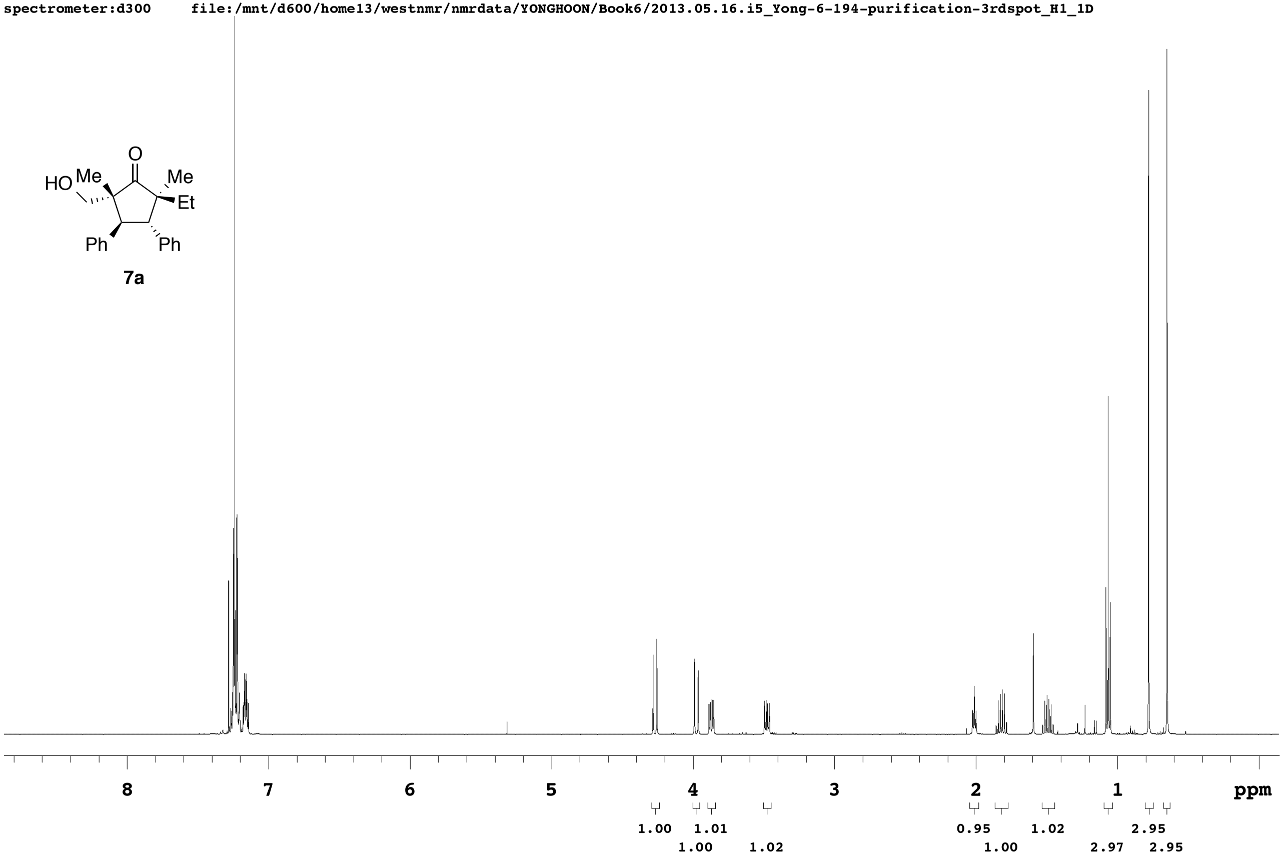

Pulse Sequence: s2pul

Yong-6-194-purification-3rdspot
125.266 MHz C13[H1] APT_ad in cdcl3 (ref. to CDCl3 @ 77.06 ppm), temp 26.4 C -> actual temp = 27.0 C, autoxdb probe
C & CH2 same, CH & CH3 opposite side of solvent signal

date: May 16 2013 sweep width: 33827Hz acq.time: 2.5s relax.time: 0.1s # scans: 504   dig.res.: 0.3 Hz/pt hz/mm:140.9
spectrometer:d300   file:/mnt/d600/home13/westnmr/nmrdata/YONGHOON/Book6/2013.05.16.i5_Yong-6-194-purification-3rdspot_C13_APT_ad

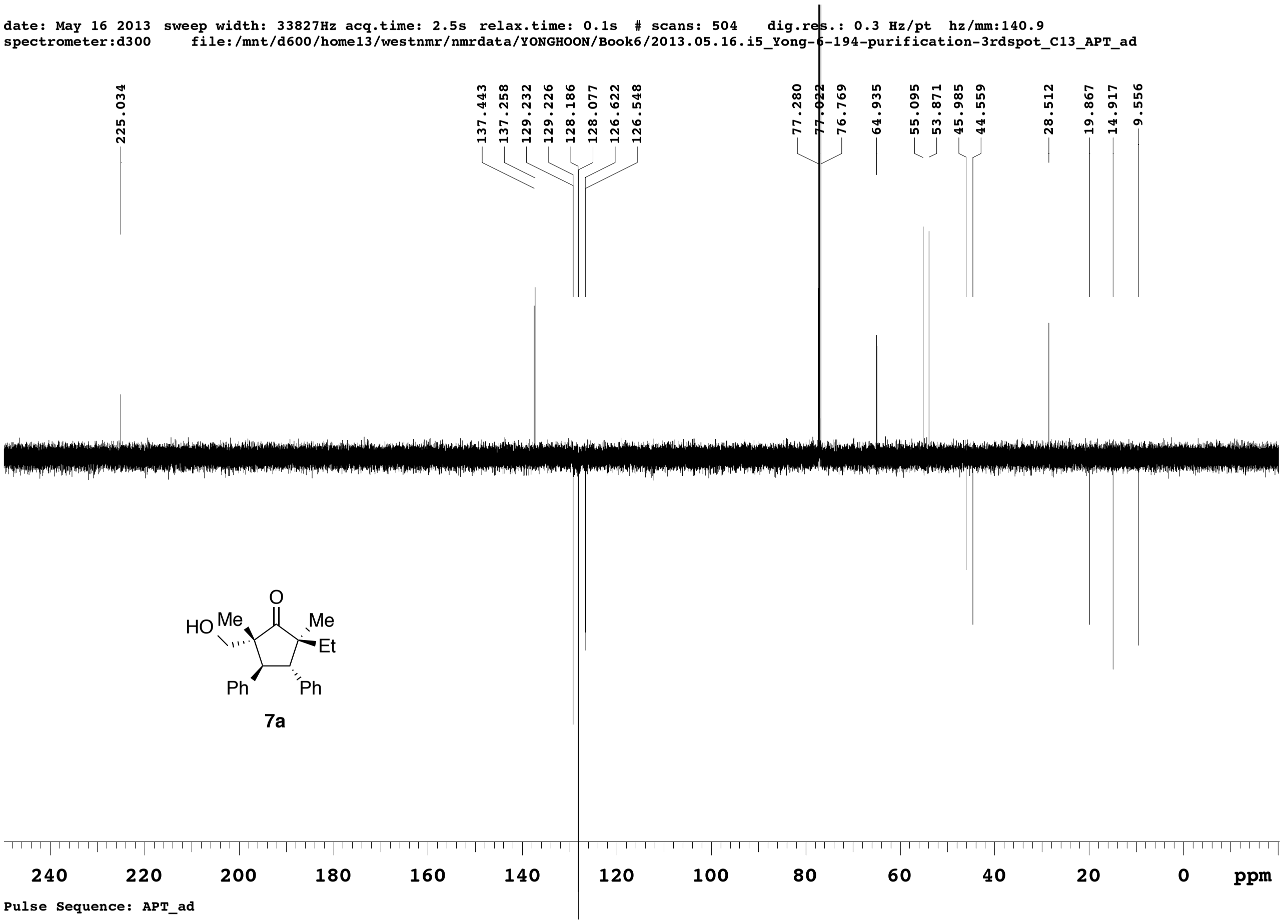

Pulse Sequence: APT_ad

Yong-6-117-col-2nd
498.118 MHz H1 1D in cdcl3 (ref. to CDCl3 @ 7.26 ppm), temp 27.2 C -> actual temp = 27.0 C, autoxdb probe

date: Oct 30 2012 sweep width: 6010Hz acq.time: 5.0s relax.time: 0.1s # scans: 16   dig.res.: 0.1 Hz/pt hz/mm:17.2
spectrometer:d300   file:/mnt/d600/home13/westnmr/nmrdata/YONGHOON/Book6/2012.10.30.i5_Yong-6-117-col-2nd_H1_1D

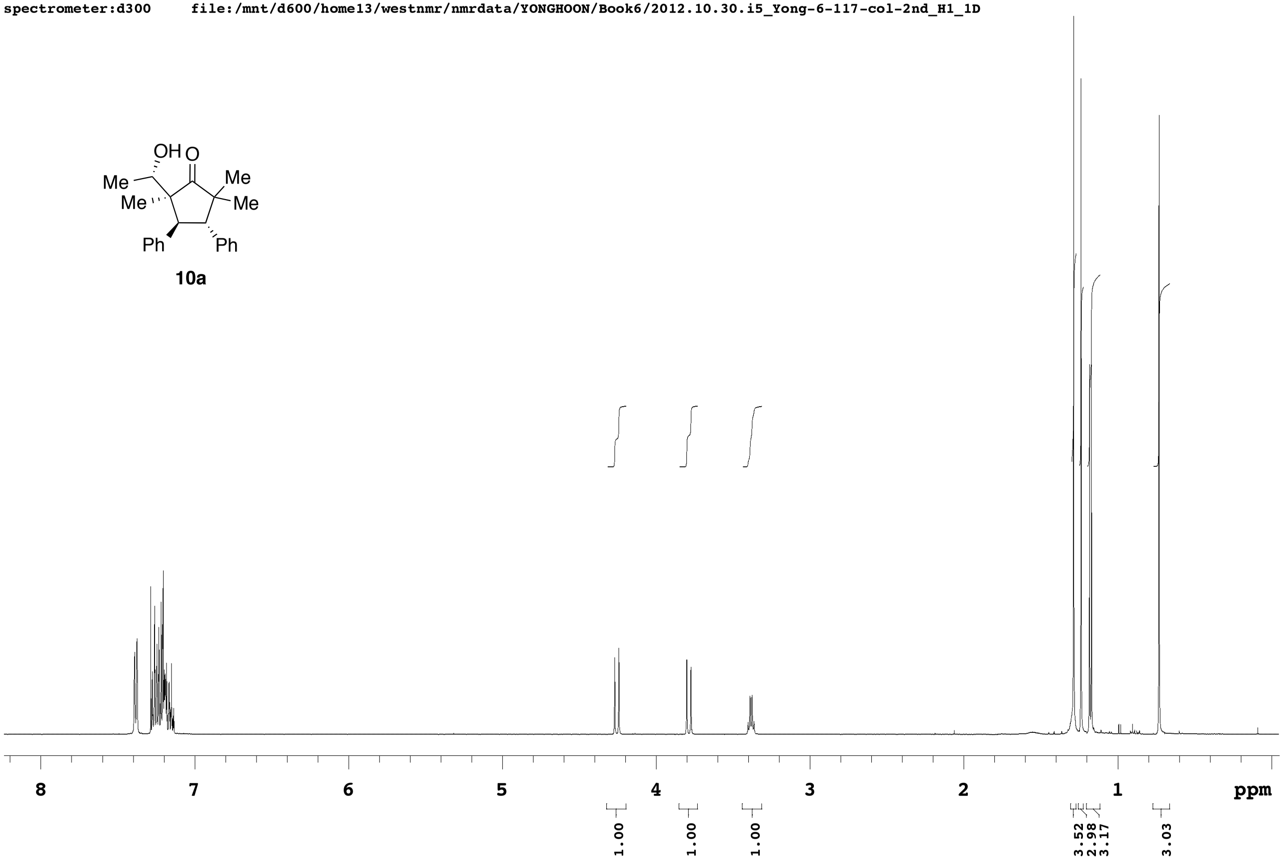

10a

Pulse Sequence: s2pul

Yong-6-117-col-2nd
100.539 MHz C13[H1] 1D in cdcl3 (ref. to CDCl3 @ 77.06 ppm), temp 27.0 C -> actual temp = 27.0 C, autoxdb probe

date: Nov 1 2012 sweep width: 26954Hz acq.time: 2.5s relax.time: 0.1s # scans: 15080 dig.res.: 0.2 Hz/pt hz/mm:112.3
spectrometer:d300   file:/mnt/d600/home13/westnmr/nmrdata/YONGHOON/Book6/2012.11.01.i4_Yong-6-117-col-2nd_C13_1D

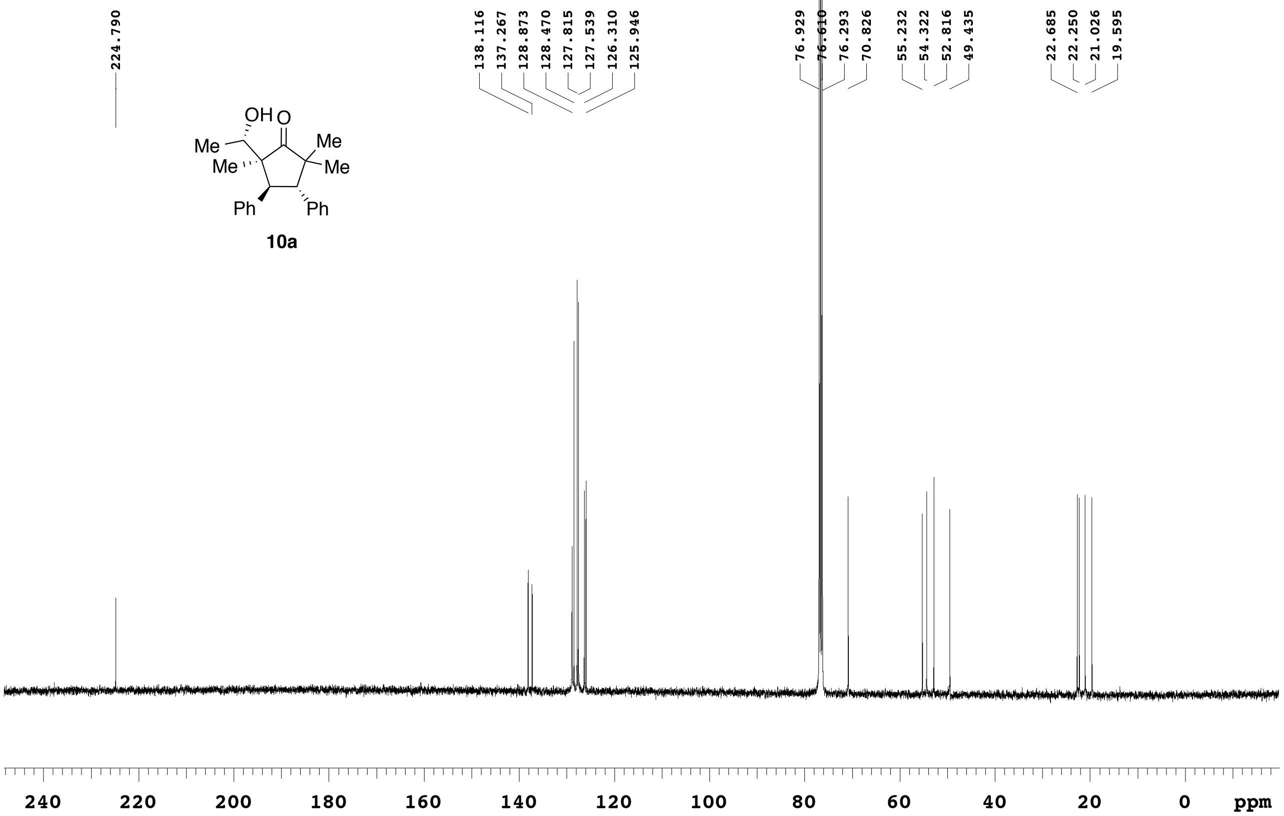

Pulse Sequence: s2pul

399.794 MHz H1 1D in cdcl3 (ref. to CDCl3 @ 7.26 ppm), temp 27.0 C -> actual temp = 27.0 C, autoxdb probe

date: Nov 6 2012 sweep width: 4802Hz acq.time: 5.0s relax.time: 0.1s # scans: 16   dig.res.: 0.1 Hz/pt hz/mm:14.2
spectrometer:d300   file:/mnt/d600/home13/westnmr/nmrdata/YONGHOON/Book6/2012.11.06.i4_Yong-6-117-col-4th_H1_1D

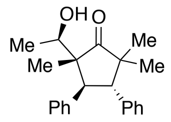

11a

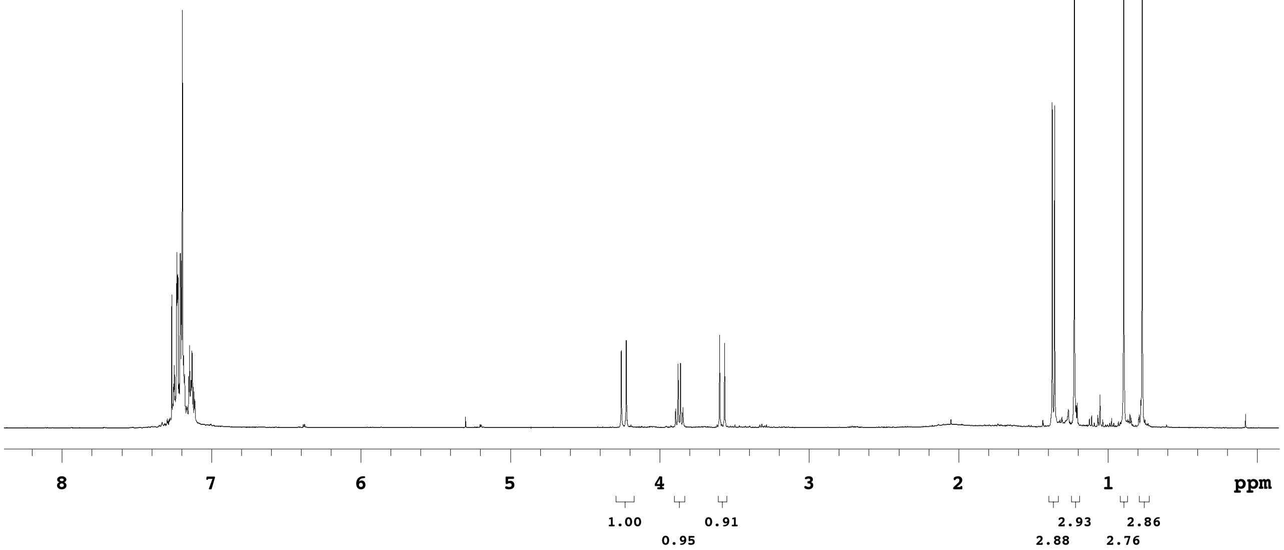

Pulse Sequence: s2pul

Yong-6-117-col-4th
100.539 MHz C13[H1] 1D in cdcl3 (ref. to CDCl3 @ 77.06 ppm), temp 27.0 C -> actual temp = 27.0 C, autoxdb probe

date: Nov 6 2012 sweep width: 26954Hz acq.time: 2.5s relax.time: 0.1s # scans: 18632 dig.res.: 0.2 Hz/pt hz/mm:112.3
spectrometer:d300 file:/mnt/d600/home13/westnmr/nmrdata/YONGHOON/Book6/2012.11.06.i4_Yong-6-117-col-4th_C13_1D

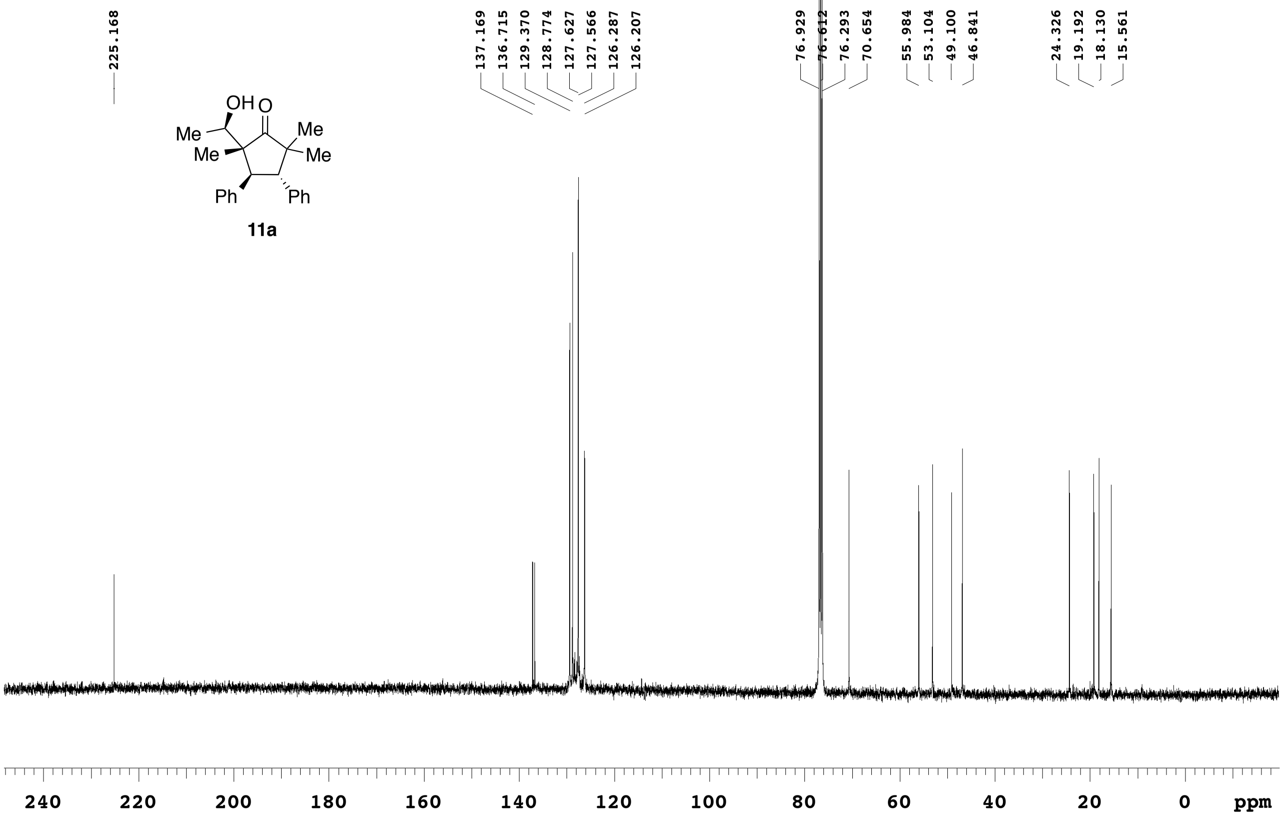

11a

Pulse Sequence: s2pul

Yong-8-50-col
498.118 MHz H1 1D in cdcl3 (ref. to CDCl3 @ 7.26 ppm), temp 26.4 C -> actual temp = 27.0 C, autoxdb probe

date: Jun 19 2013 sweep width: 6001Hz acq.time: 5.0s relax.time: 0.1s # scans: 16 dig.res.: 0.1 Hz/pt hz/mm:15.3
spectrometer:d300 file:/mnt/d600/home13/westnmr/nmrdata/YONGHOON/Book8/2013.06.19.i5_Yong-8-50-col_H1_1D

13a

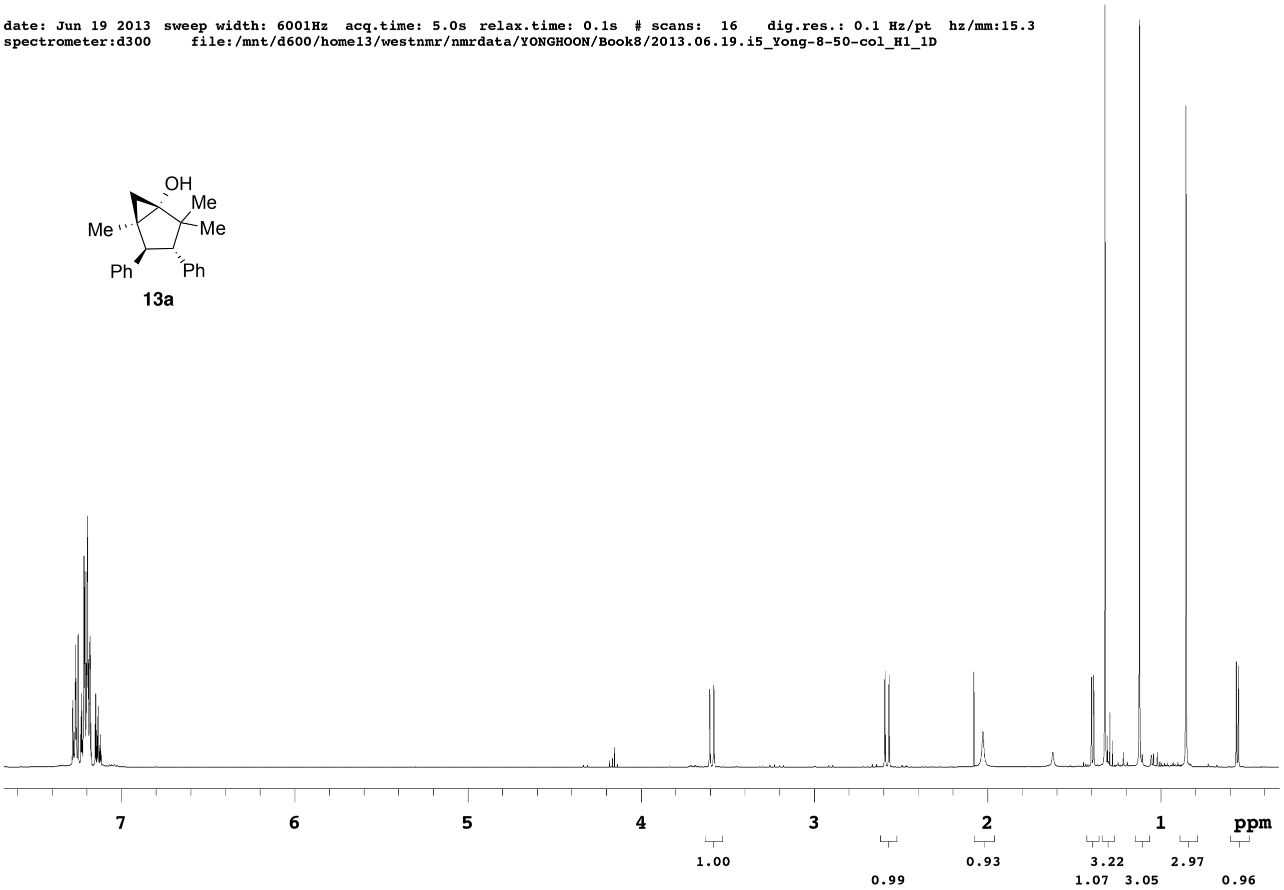

Pulse Sequence: s2pul

125.266 MHz C13[H1] APT_ad in cdcl3 (ref. to CDCl3 @ 77.06 ppm), temp 27.2 C -> actual temp = 27.0 C, autoxdb probe
C & CH2 same, CH & CH3 opposite side of solvent signal

date: Feb 22 2013 sweep width: 33827Hz acq.time: 2.5s relax.time: 0.1s # scans: 400   dig.res.: 0.3 Hz/pt hz/mm:83.8
spectrometer:d300   file:/mnt/d600/home13/westnmr/nmrdata/YONGHOON/Book7/2013.02.22.i5_Yong-7-110-col_C13_APT_ad

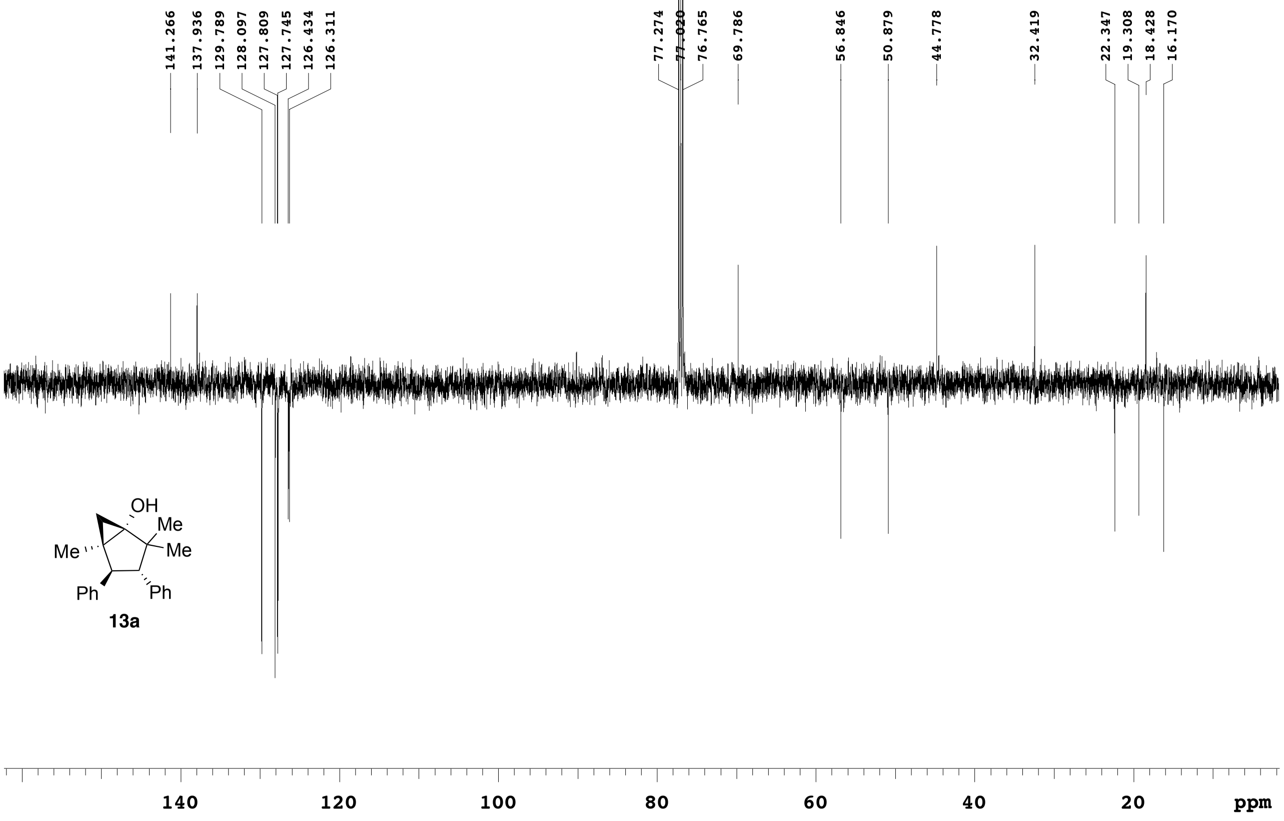

13a

Pulse Sequence: APT_ad

Yong-8-68-col-spot A
498.118 MHz H1 1D in cdcl3 (ref. to CDCl3 @ 7.26 ppm), temp 26.4 C -> actual temp = 27.0 C, autoxdb probe

date: Jun 21 2013 sweep width: 6001Hz acq.time: 5.0s relax.time: 0.1s # scans: 16   dig.res.: 0.1 Hz/pt hz/mm:16.4
spectrometer:d300   file:/mnt/d600/home13/westnmr/nmrdata/YONGHOON/Book8/2013.06.21.i5_Yong-8-68-col-spot_A_H1_1D

17a

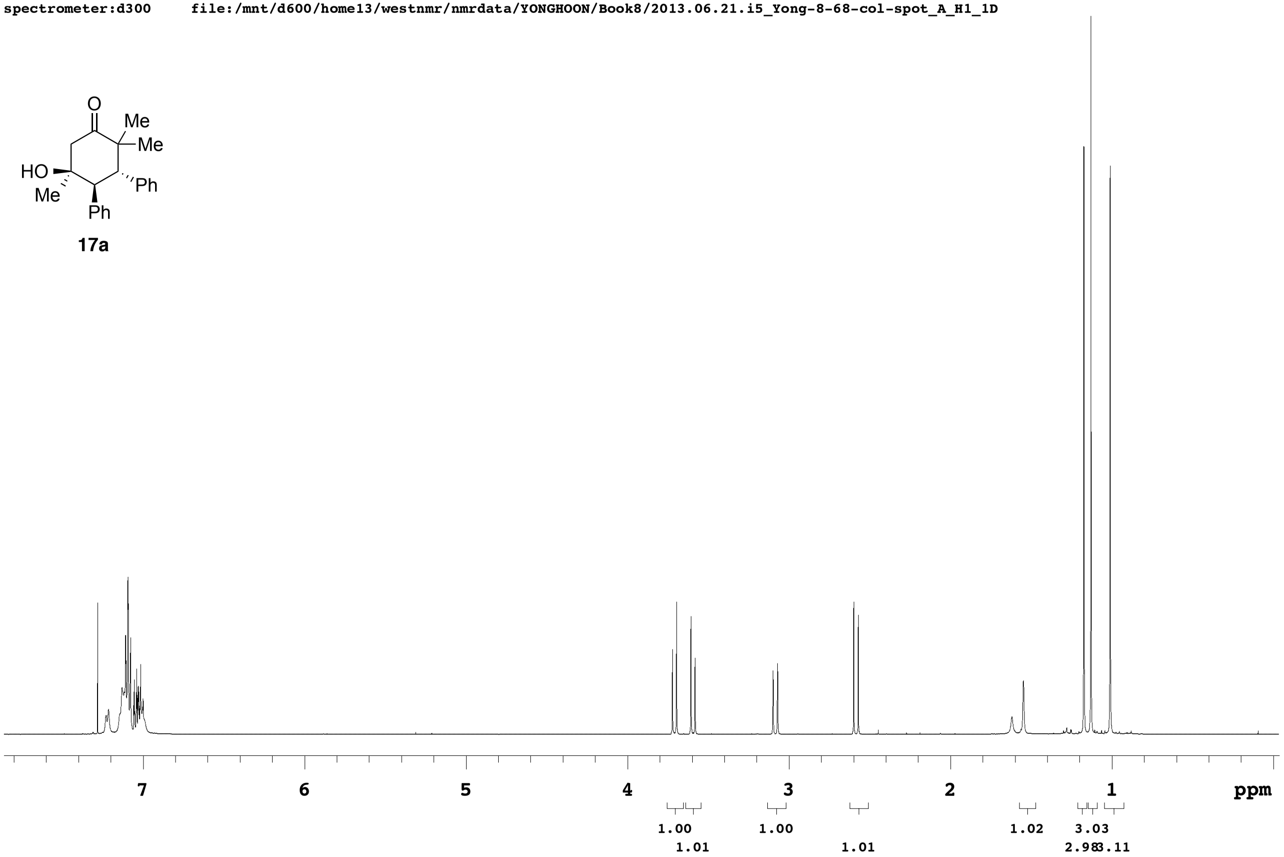

Pulse Sequence: s2pul

Yong-8-68-col-spot A
125.266 MHz C13[H1] 1D in cdcl3 (ref. to CDCl3 @ 77.06 ppm), temp 26.4 C -> actual temp = 27.0 C, autoxdb probe

date: Jun 21 2013 sweep width: 33827Hz acq.time: 2.5s relax.time: 0.1s # scans: 416   dig.res.: 0.3 Hz/pt hz/mm:140.9
spectrometer:d300   file:/mnt/d600/home13/westnmr/nmrdata/YONGHOON/Book8/2013.06.21.i5_Yong-8-68-col-spot_A_C13_1D

17a

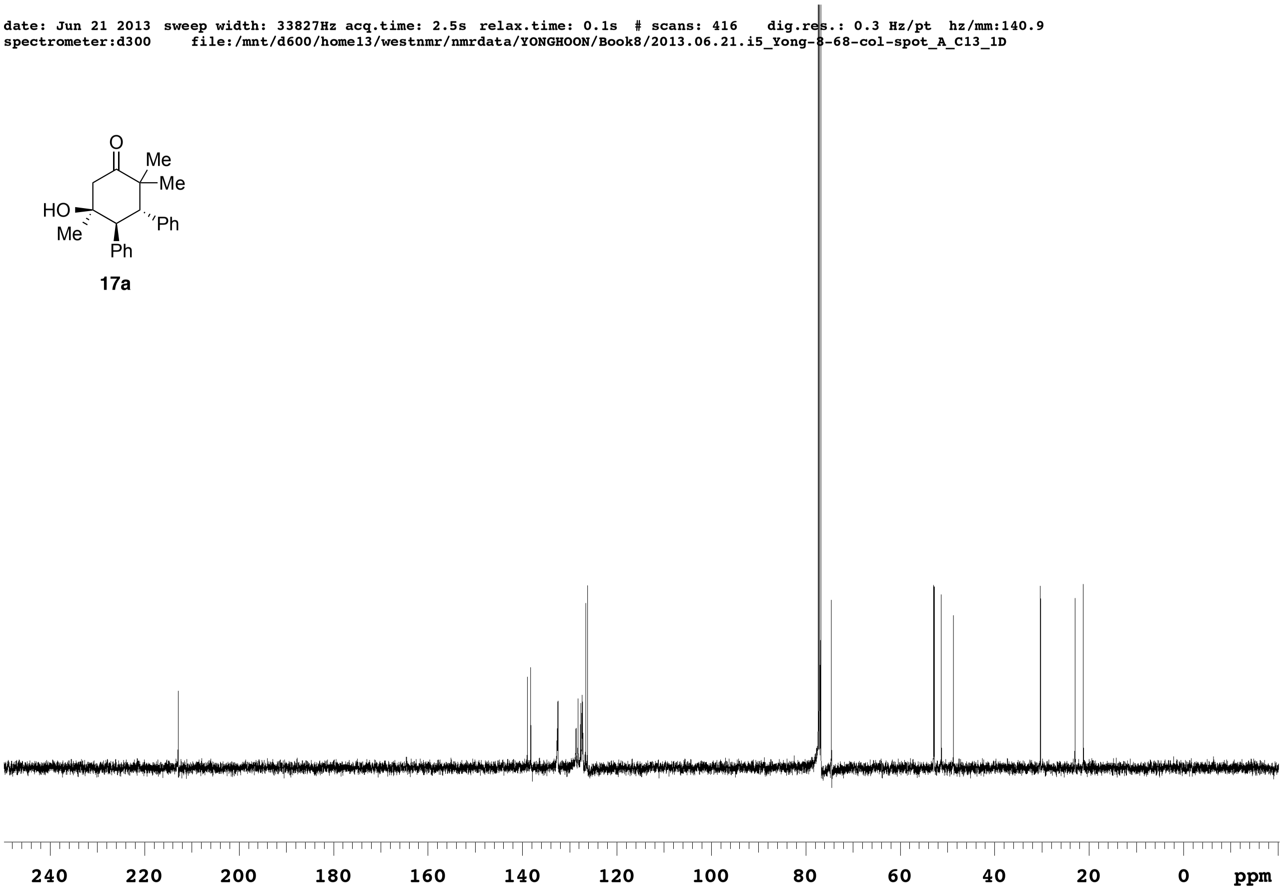

Pulse Sequence: s2pul

Yong-8-68-col-spot B
498.118 MHz H1 1D in cdcl3 (ref. to CDCl3 @ 7.26 ppm), temp 26.4 C -> actual temp = 27.0 C, autoxdb probe

date: Jun 21 2013 sweep width: 6001Hz acq.time: 5.0s relax.time: 0.1s # scans: 16   dig.res.: 0.1 Hz/pt hz/mm:16.9
spectrometer:d300   file:/mnt/d600/home13/westnmr/nmrdata/YONGHOON/Book8/2013.06.21.i5_Yong-8-68-col-spot_B_H1_1D

18a

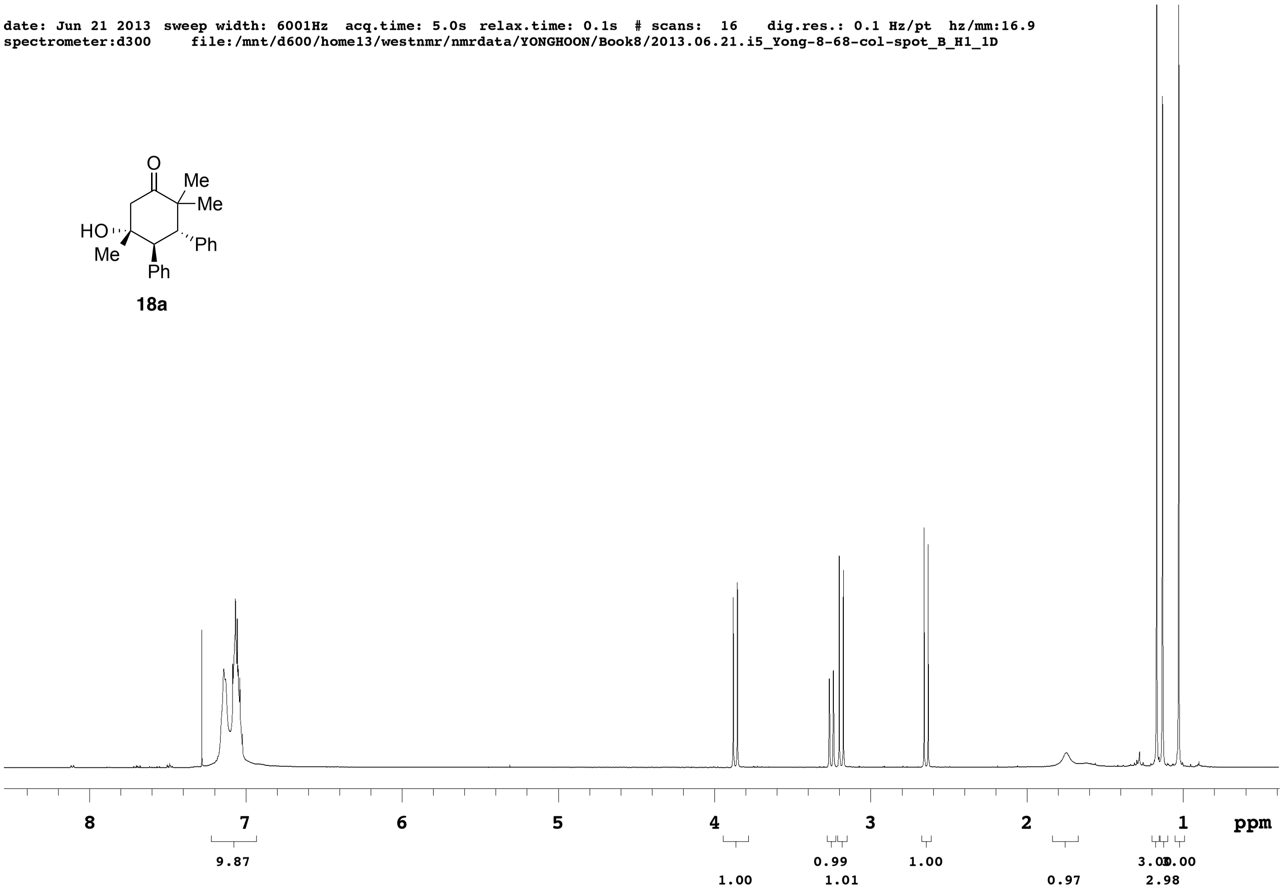

Pulse Sequence: s2pul

```
125.266 MHz C13[H1] APT_ad in cdcl3 (ref. to CDCl3 @ 77.06 ppm), temp 26.4 C -> actual temp = 27.0 C, autoxdb probe
C & CH2 same, CH & CH3 opposite side of solvent signal

date: Jun 21 2013  sweep width: 33827Hz acq.time: 2.5s  relax.time: 0.1s  # scans: 228    dig.res.: 0.3 Hz/pt  hz/mm:111.2
spectrometer:d300     file:/mnt/d600/home13/westnmr/nmrdata/YONGHOON/Book8/2013.06.21.i5_Yong-8-68-col-spot_B_C13_APT_ad
```

18a

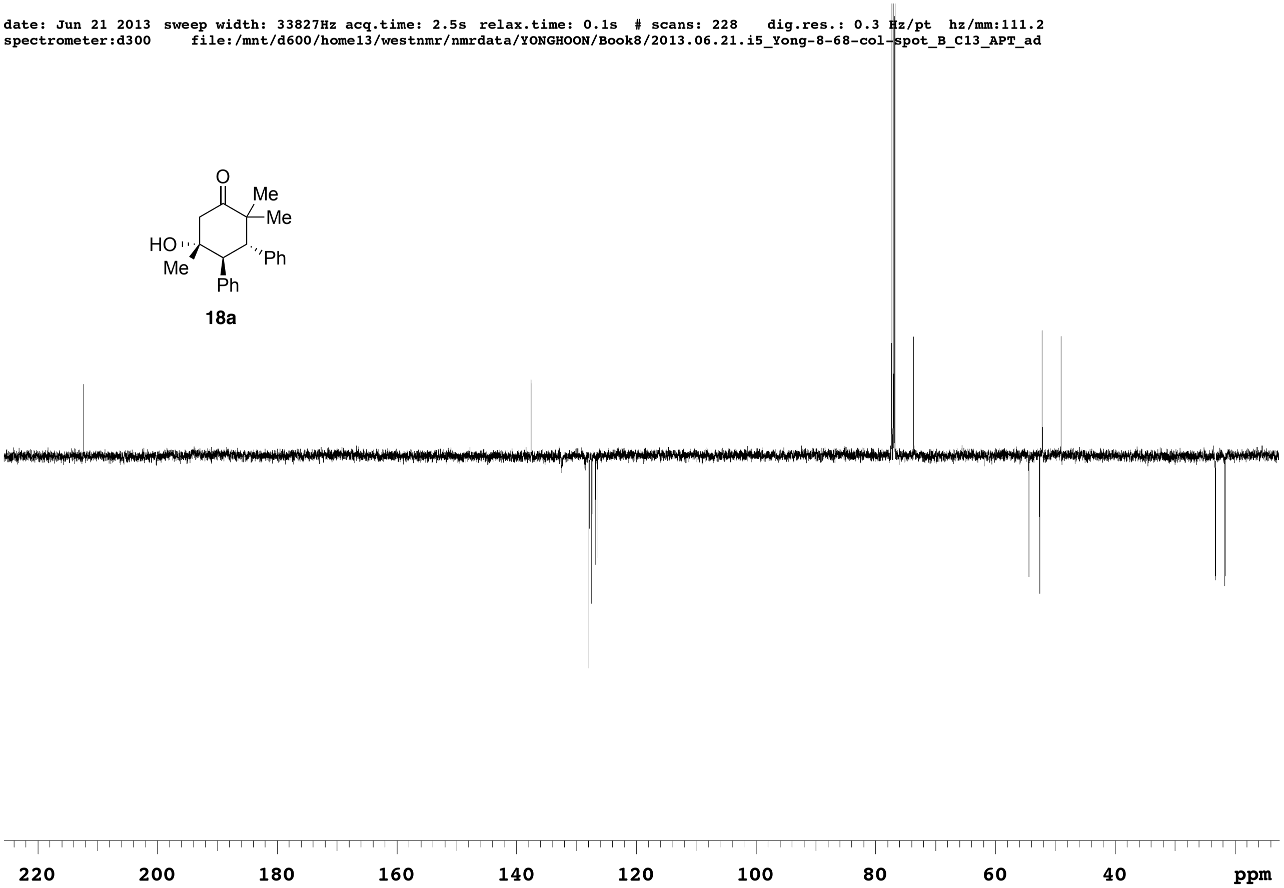

Pulse Sequence: APT_ad

Appendix IV: Selected NMR Spectra

(Chapter 5)

Yong-9-20-col
399.984 MHz H1 1D in cdcl3 (ref. to CDCl3 @ 7.26 ppm), temp 25.9 C -> actual temp = 27.0 C, onenmr probe

date: Oct 1 2013 sweep width: 4808Hz acq.time: 5.0s relax.time: 0.1s # scans: 16 dig.res.: 0.1 Hz/pt hz/mm:20.0
spectrometer:d300 file:/mnt/d600/home13/westnmr/nmrdata/YONGHOON/Book9/2013.10.01.mr4_Yong-9-20-col_H1_1D

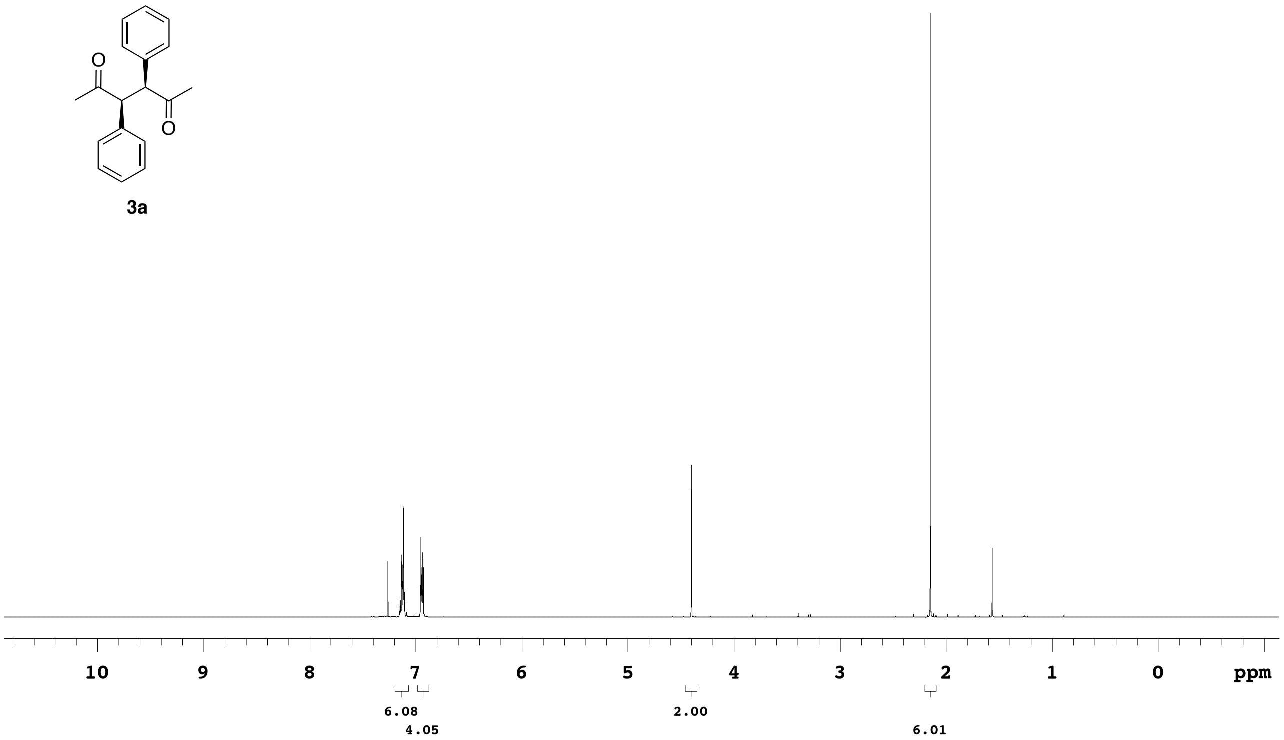
3a

Pulse Sequence: s2pul

Yong-8-200-col
125.266 MHz C13[H1] APT_ad in cdcl3 (ref. to CDCl3 @ 77.06 ppm), temp 26.4 C -> actual temp = 27.0 C, autoxdb probe
C & CH2 same, CH & CH3 opposite side of solvent signal

date: Sep 16 2013 sweep width: 33827Hz acq.time: 2.5s relax.time: 0.1s # scans: 13848 dig.res.: 0.3 Hz/pt hz/mm:140.9
spectrometer:d300 file:/mnt/d600/home13/westnmr/nmrdata/YONGHOON/Book8/2013.09.16.i5_Yong-8-200-col_C13_APT_ad

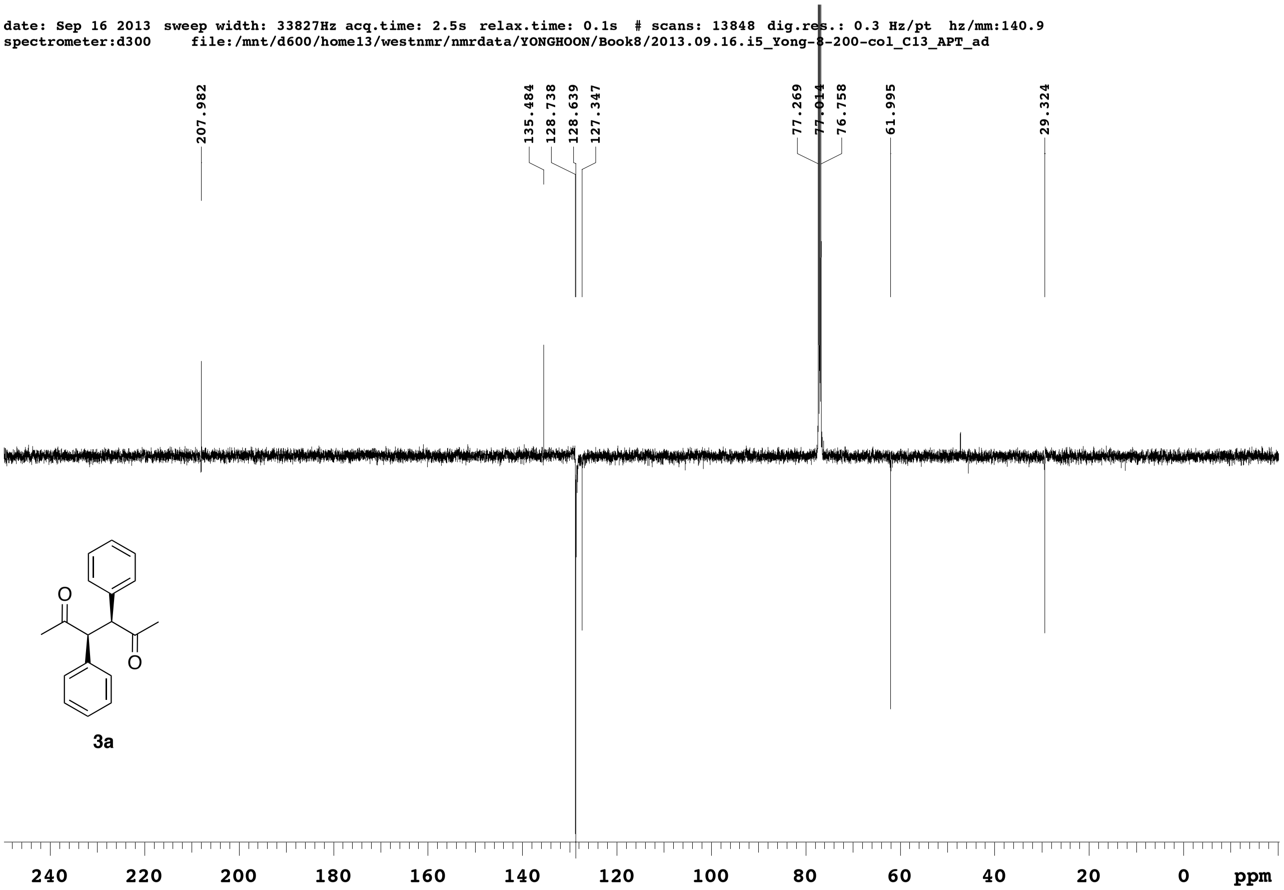

Pulse Sequence: APT_ad

Yong-10-174-col
498.118 MHz H1 1D in cdcl3 (ref. to CDCl3 @ 7.26 ppm), temp 26.4 C -> actual temp = 27.0 C, autoxdb probe

date: Apr 25 2014 sweep width: 6001Hz acq.time: 5.0s relax.time: 0.1s # scans: 16 dig.res.: 0.1 Hz/pt hz/mm:19.0
spectrometer:d300 file:/mnt/d600/home13/westnmr/nmrdata/YONGHOON/Book10/2014.04.25.i5_Yong-10-174-col_H1_1D

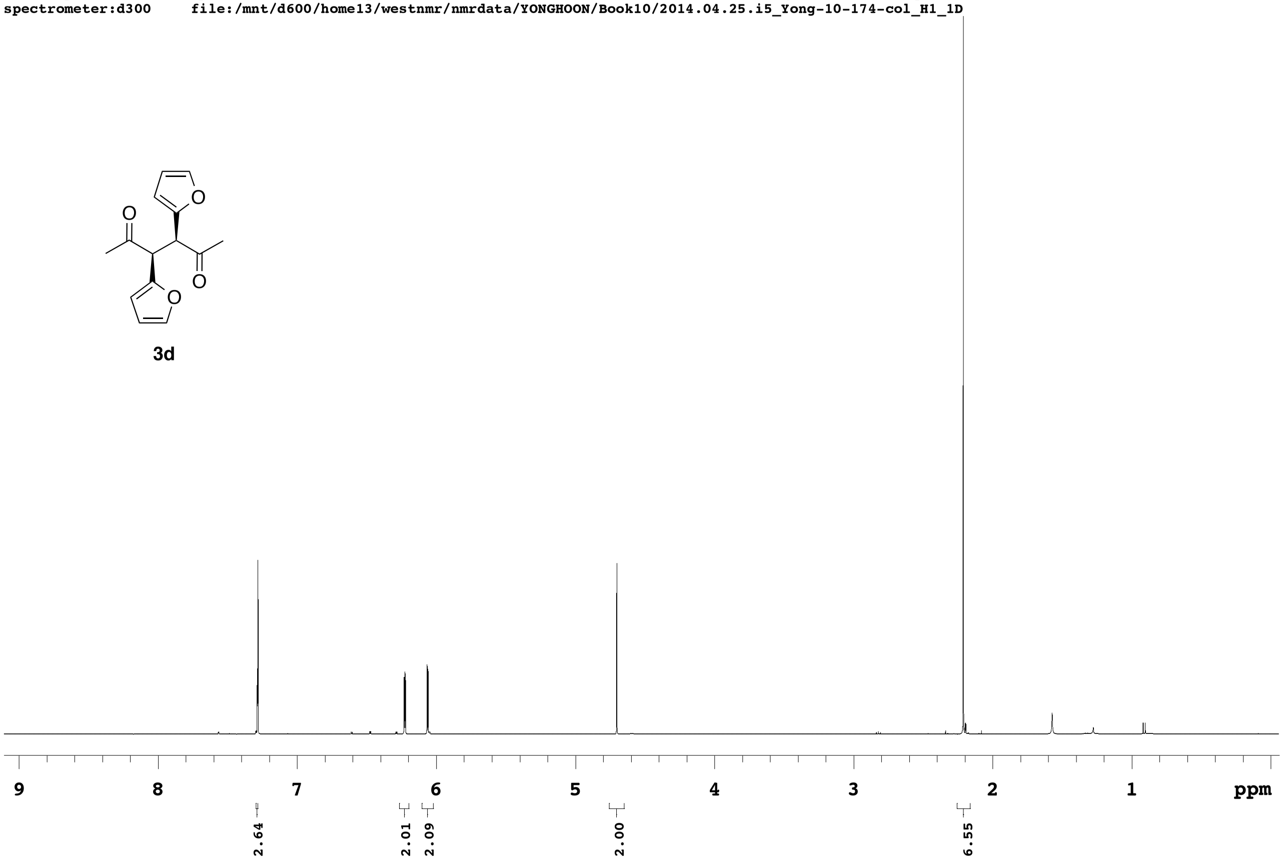

3d

Pulse Sequence: s2pul

Yong-10-174-col
125.266 MHz C13[H1] 1D in cdcl3 (ref. to CDCl3 @ 77.06 ppm), temp 26.4 C -> actual temp = 27.0 C, autoxdb probe

date: Apr 25 2014 sweep width: 33827Hz acq.time: 2.5s relax.time: 0.1s # scans: 272   dig.res.: 0.3 Hz/pt hz/mm:140.9
spectrometer:d300   file:/mnt/d600/home13/westnmr/nmrdata/YONGHOON/Book10/2014.04.25.i5_Yong-10-174-col_C13_1D

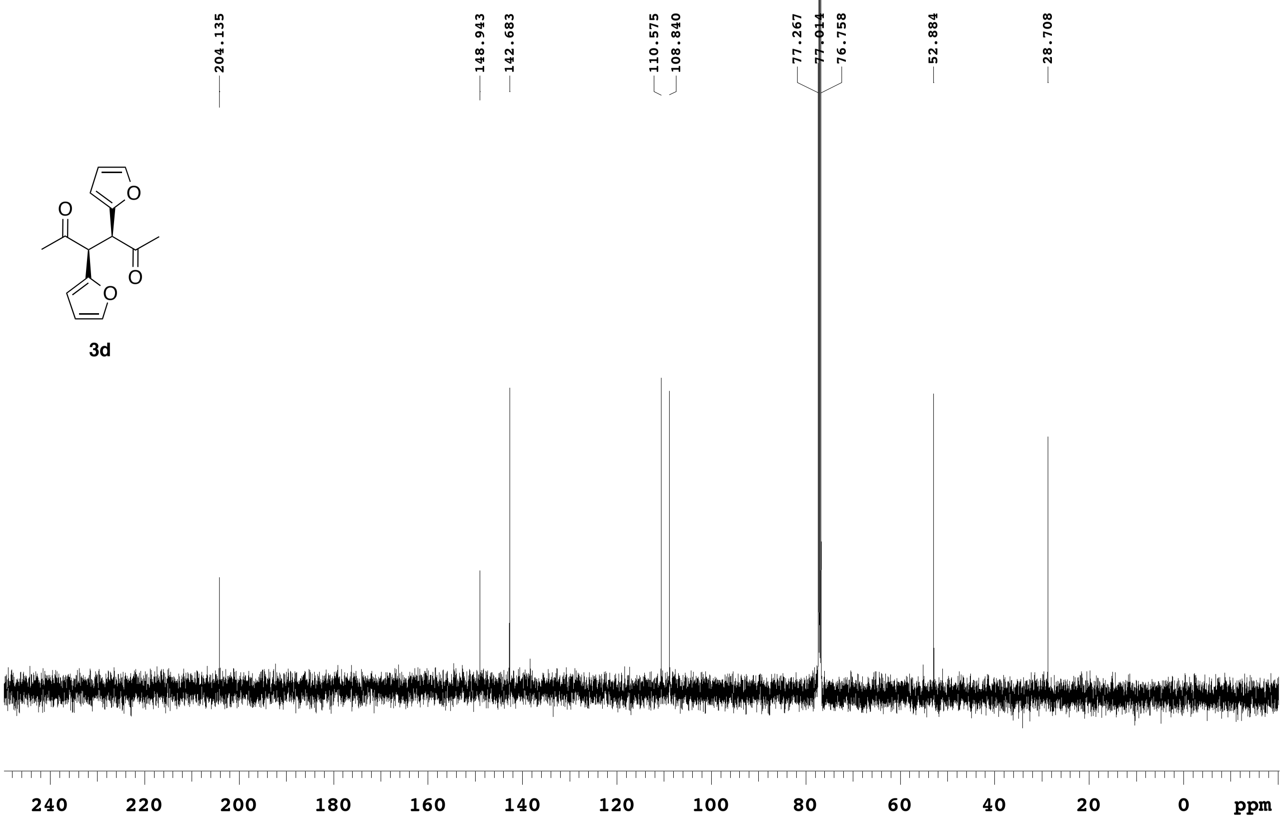

3d

Pulse Sequence: s2pul

Yong-10-66-col
498.118 MHz H1 1D in cdcl3 (ref. to CDCl3 @ 7.26 ppm), temp 26.4 C -> actual temp = 27.0 C, autoxdb probe

date: Feb 6 2014 sweep width: 6001Hz acq.time: 5.0s relax.time: 0.1s # scans: 16 dig.res.: 0.1 Hz/pt hz/mm:17.7
spectrometer:d300 file:/mnt/d600/home13/westnmr/nmrdata/YONGHOON/Book10/2014.02.06.i5_Yong-10-66-col_H1_1D

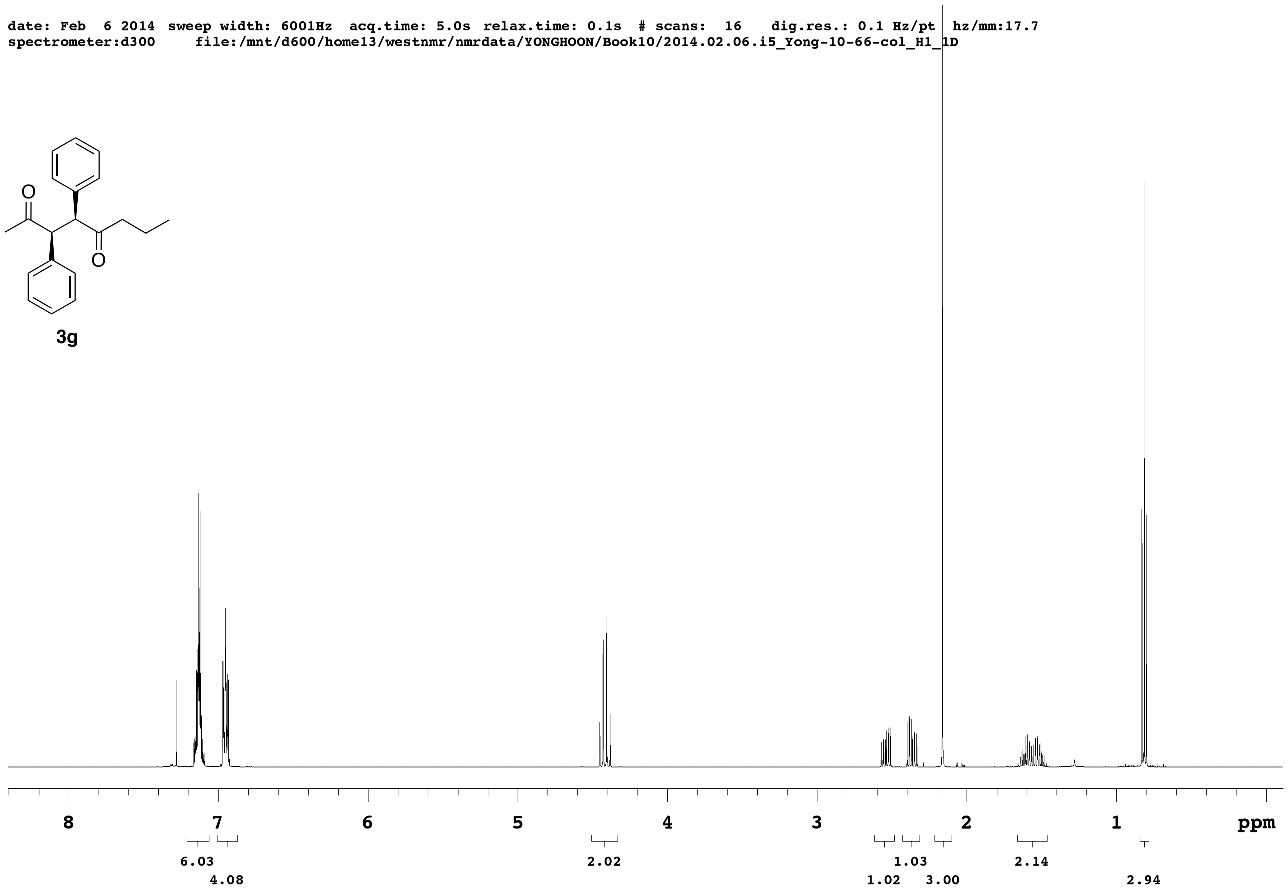

Pulse Sequence: s2pul

Yong-10-66-col
125.266 MHz C13[H1] 1D in cdcl3 (ref. to CDCl3 @ 77.06 ppm), temp 26.4 C -> actual temp = 27.0 C, autoxdb probe

date: Feb 6 2014 sweep width: 33827Hz acq.time: 2.5s relax.time: 0.1s # scans: 168 dig.res.: 0.3 Hz/pt hz/mm:140.9
spectrometer:d300 file:/mnt/d600/home13/westnmr/nmrdata/YONGHOON/Book10/2014.02.06.i5_Yong-10-66-col_C13_1D

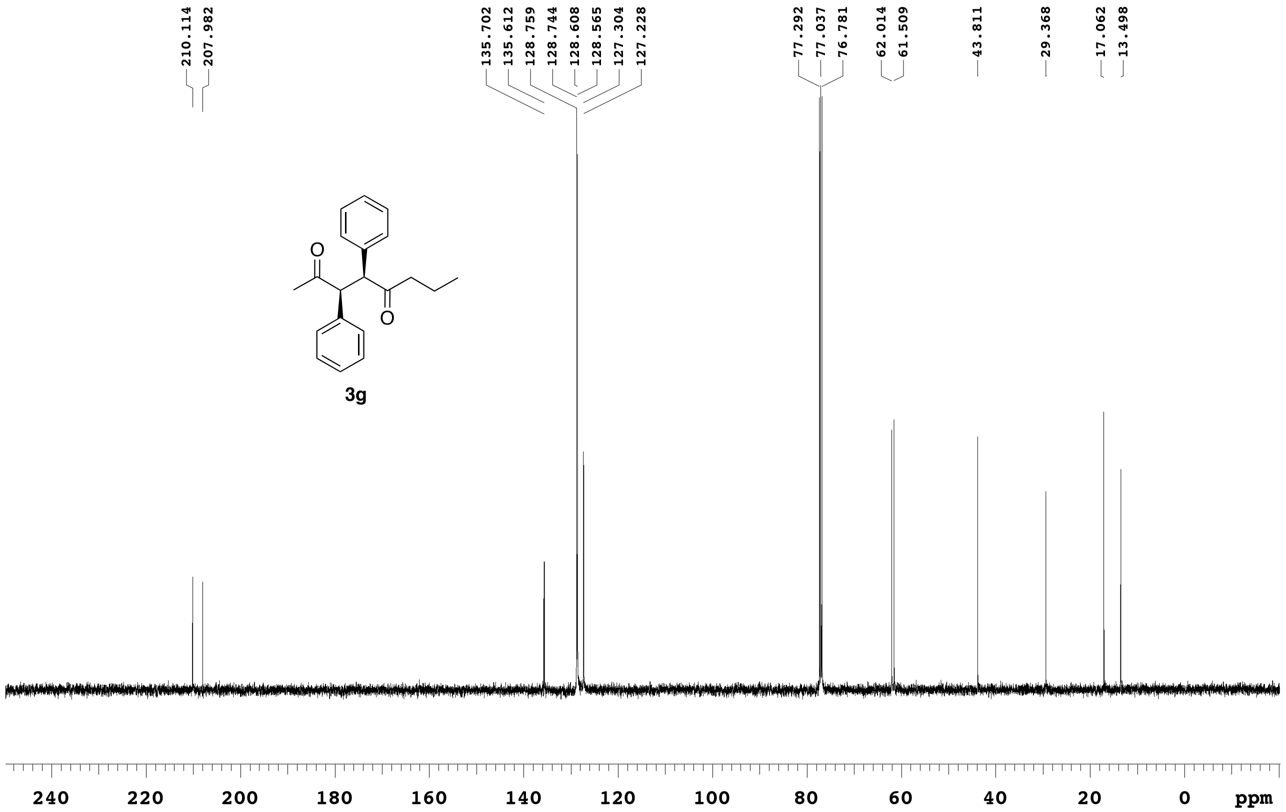

Pulse Sequence: s2pul

Yong-10-50-col
498.118 MHz H1 1D in cdcl3 (ref. to CDCl3 @ 7.26 ppm), temp 26.4 C -> actual temp = 27.0 C, autoxdb probe

date: Jan 22 2014 sweep width: 6001Hz acq.time: 5.0s relax.time: 0.1s # scans: 16   dig.res.: 0.1 Hz/pt hz/mm:18.3
spectrometer:d300   file:/mnt/d600/home13/westnmr/nmrdata/YONGHOON/Book10/2014.01.22.i5_Yong-10-50-col_H1_1D

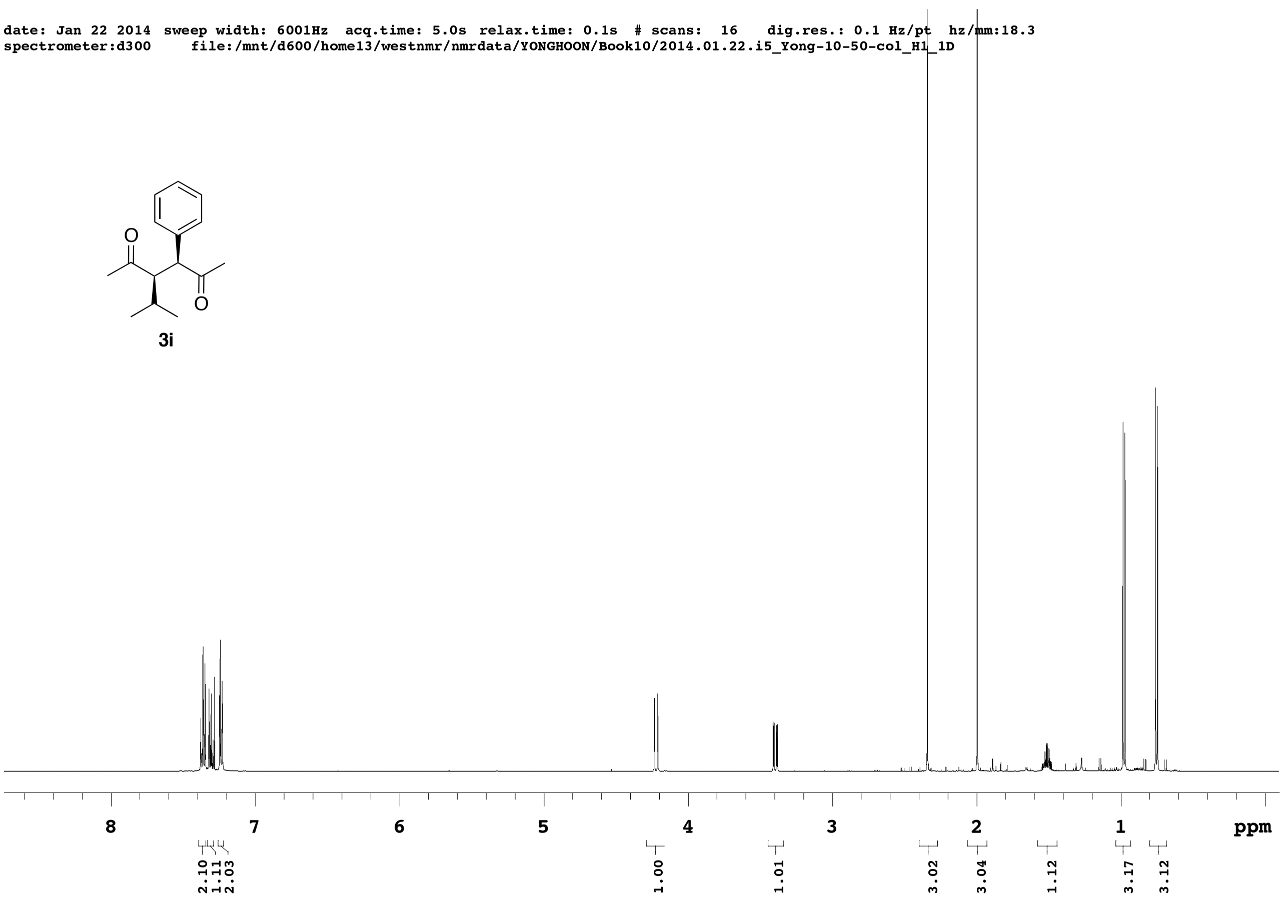

3i

Pulse Sequence: s2pul

Yong-10-50-col
125.266 MHz C13[H1] 1D in cdcl3 (ref. to CDCl3 @ 77.06 ppm), temp 26.4 C -> actual temp = 27.0 C, autoxdb probe

date: Jan 22 2014 sweep width: 33827Hz acq.time: 2.5s relax.time: 0.1s # scans: 244   dig.res.: 0.3 Hz/pt hz/mm:140.9
spectrometer:d300   file:/mnt/d600/home13/westnmr/nmrdata/YONGHOON/Book10/2014.01.22.i5_Yong-10-50-col_C13_1D

3i

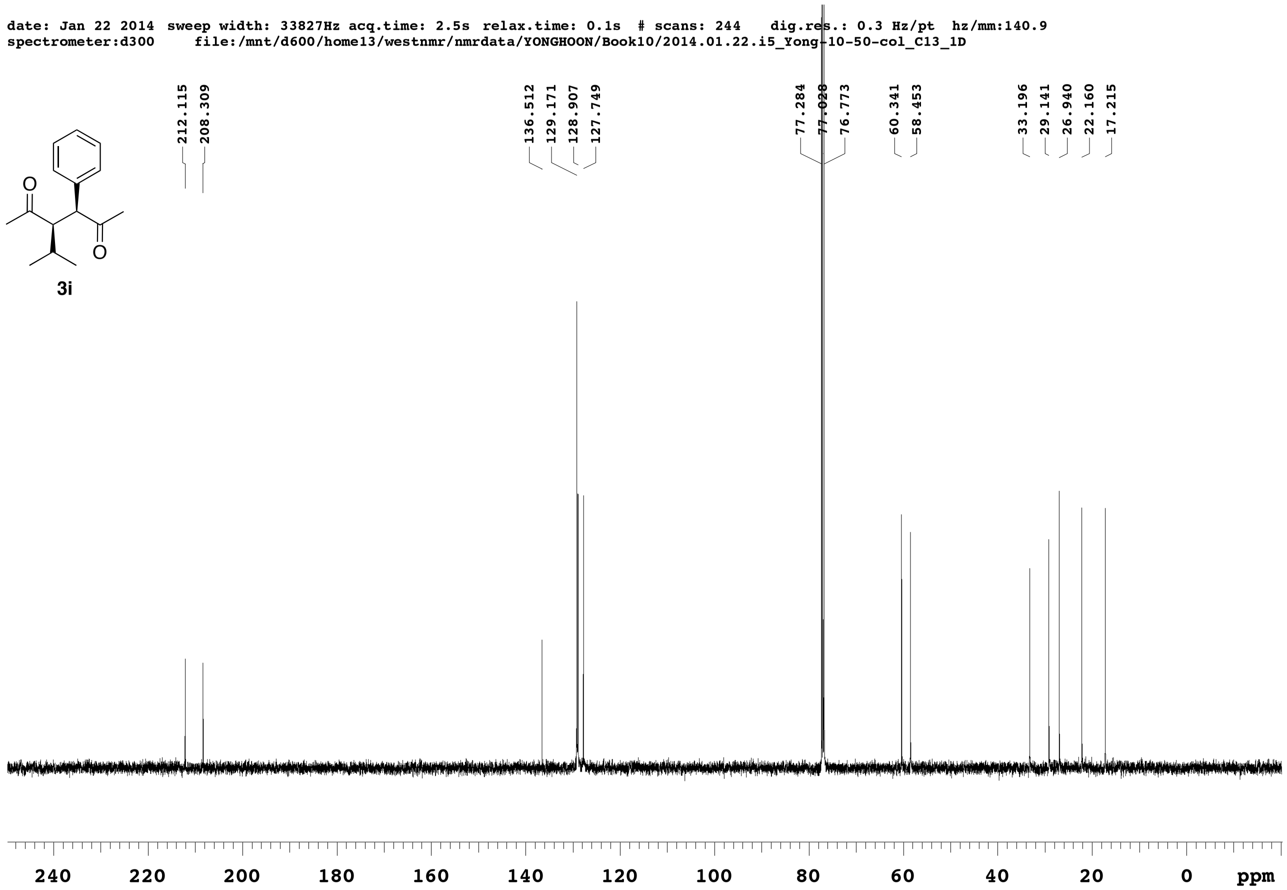

Pulse Sequence: s2pul

Yong-9-108-col-2ndspot
498.118 MHz H1 1D in cdcl3 (ref. to CDCl3 @ 7.26 ppm), temp 26.4 C -> actual temp = 27.0 C, autoxdb probe

date: Oct 31 2013 sweep width: 6001Hz acq.time: 5.0s relax.time: 0.1s # scans: 16   dig.res.: 0.1 Hz/pt hz/mm:18.8
spectrometer:d300   file:/mnt/d600/home13/westnmr/nmrdata/YONGHOON/Book9/2013.10.31.i5_Yong-9-108-col-2ndspot_H1_1D

7a

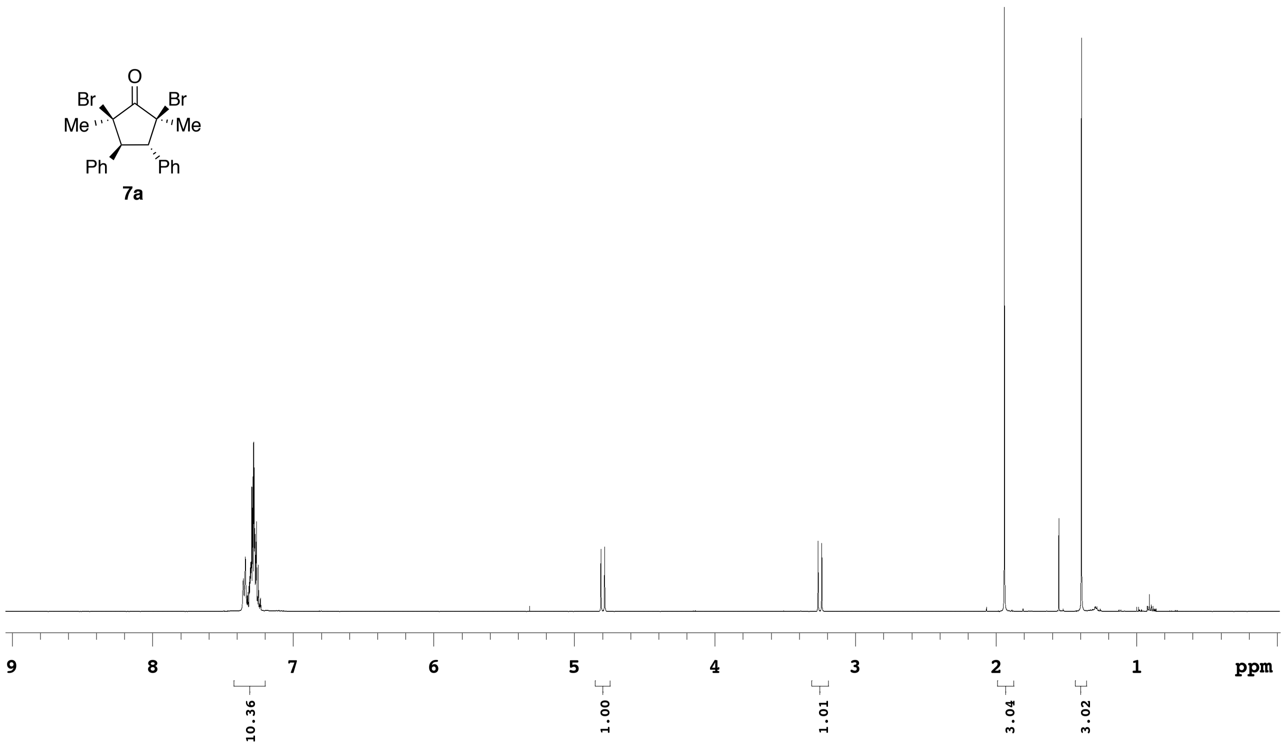

Pulse Sequence: s2pul

Yong-9-108-col-2ndspot
125.266 MHz C13[H1] 1D in cdcl3 (ref. to CDCl3 @ 77.06 ppm), temp 26.4 C -> actual temp = 27.0 C, autoxdb probe

date: Oct 31 2013 sweep width: 33827Hz acq.time: 2.5s relax.time: 0.1s # scans: 372   dig.res.: 0.3 Hz/pt hz/mm:140.9
spectrometer:d300   file:/mnt/d600/home13/westnmr/nmrdata/YONGHOON/Book9/2013.10.31.i5_Yong-9-108-col-2ndspot_C13_1D

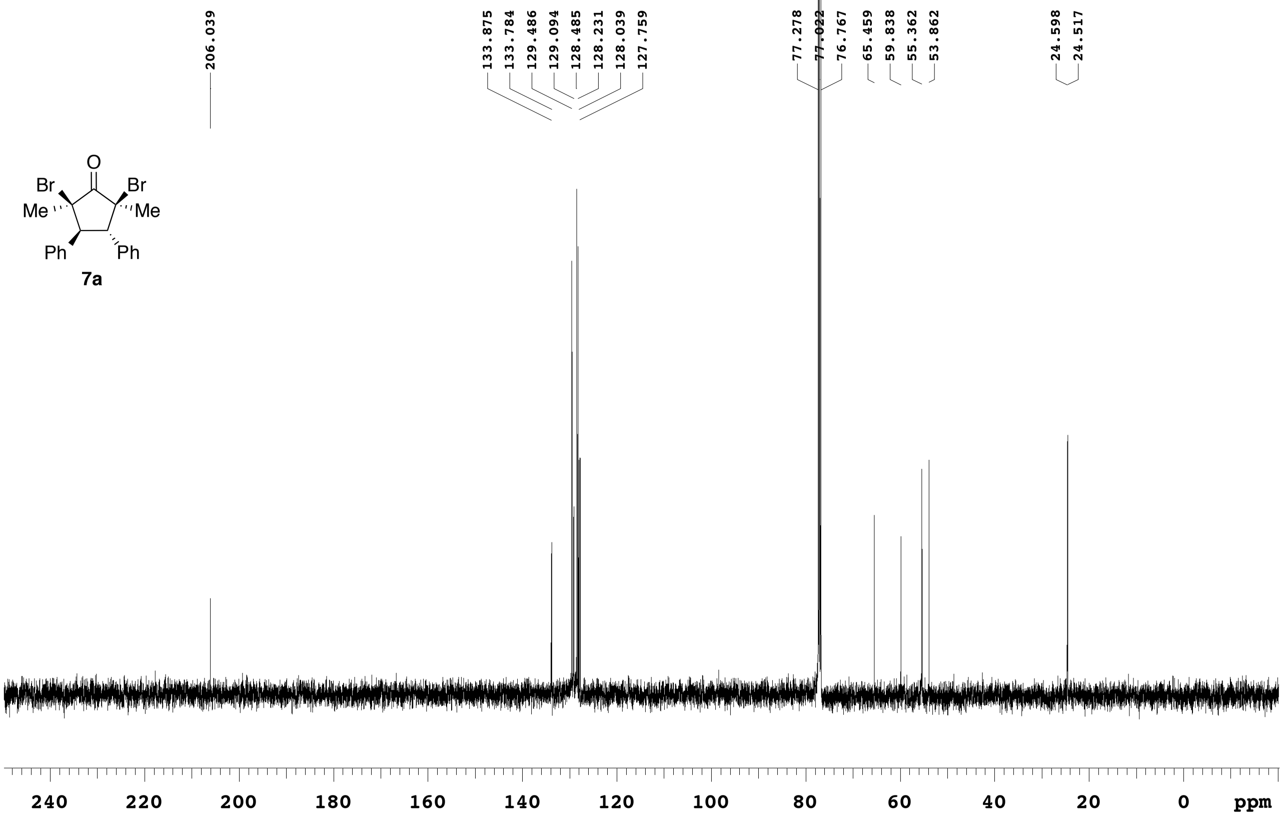

Pulse Sequence: s2pul

Yong-9-108-col-1stspot
498.118 MHz H1 1D in cdcl3 (ref. to CDCl3 @ 7.26 ppm), temp 26.4 C -> actual temp = 27.0 C, autoxdb probe

date: Oct 31 2013 sweep width: 6001Hz acq.time: 5.0s relax.time: 0.1s # scans: 16   dig.res.: 0.1 Hz/pt hz/mm:19.4
spectrometer:d300   file:/mnt/d600/home13/westnmr/nmrdata/YONGHOON/Book9/2013.10.31.i5_Yong-9-108-col-1stspot_H1_1D

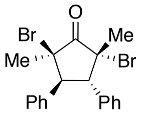

8a

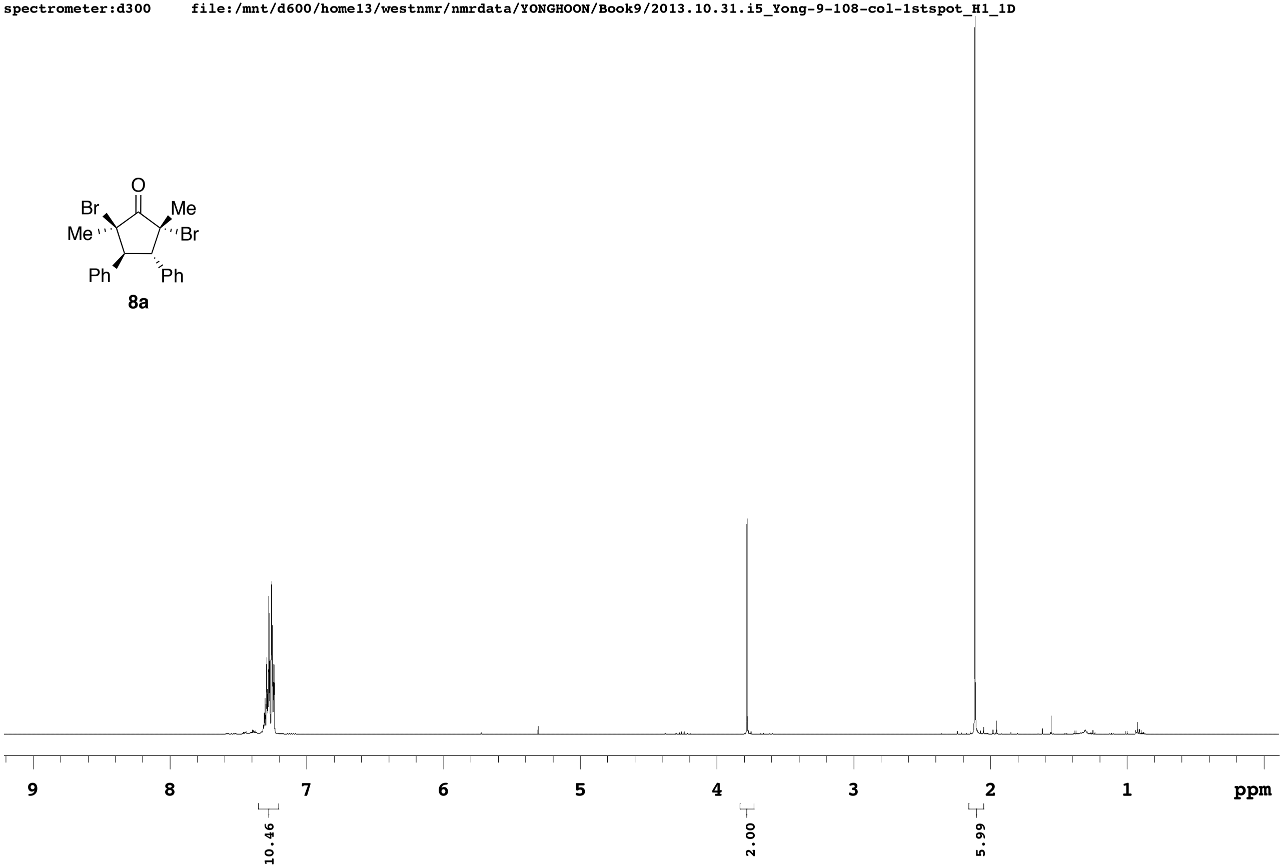

Pulse Sequence: s2pul

Yong-9-108-col-1stspot
125.266 MHz C13[H1] 1D in cdcl3 (ref. to CDCl3 @ 77.06 ppm), temp 26.4 C -> actual temp = 27.0 C, autoxdb probe

date: Oct 31 2013 sweep width: 33827Hz acq.time: 2.5s relax.time: 0.1s # scans: 468 dig.res.: 0.3 Hz/pt hz/mm:140.9
spectrometer:d300 file:/mnt/d600/home13/westnmr/nmrdata/YONGHOON/Book9/2013.10.31.i5_Yong-9-108-col-1stspot_C13_1D

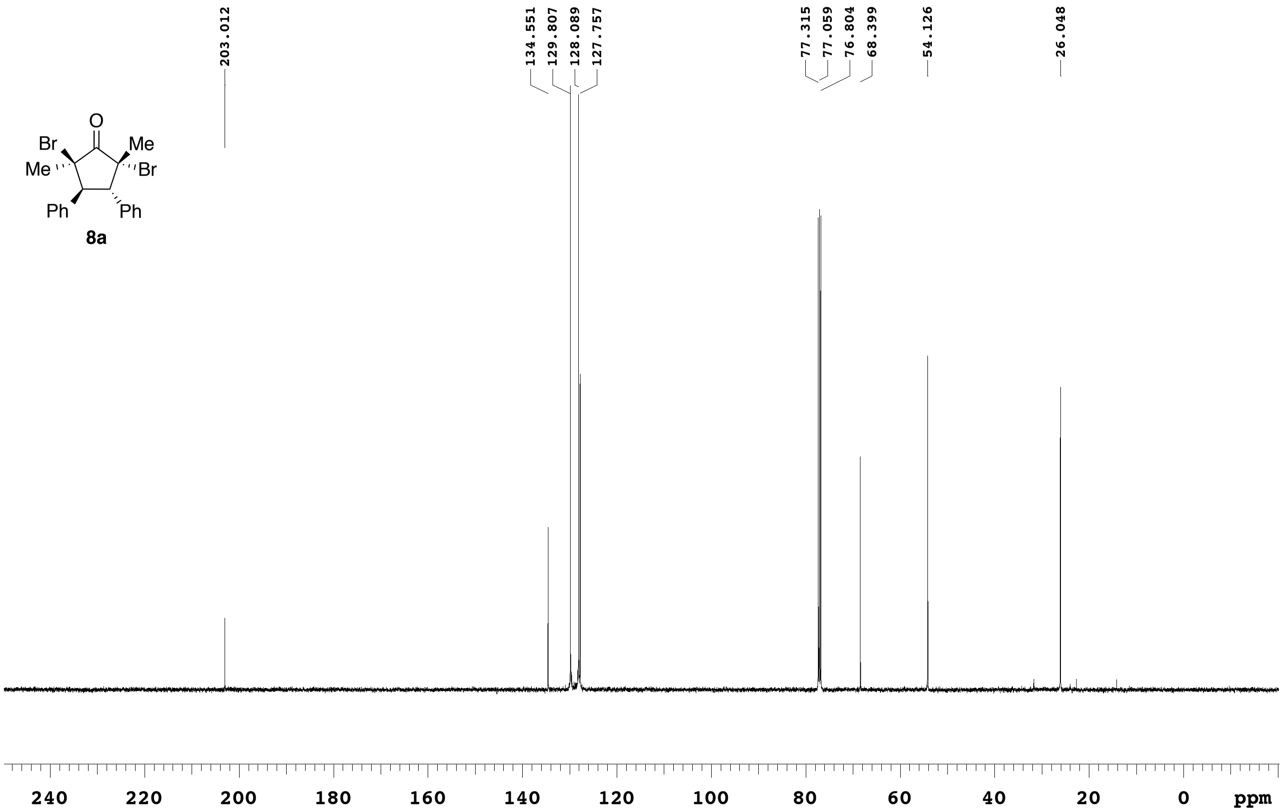

Pulse Sequence: s2pul

Appendix V: X-ray Crystallographic Data for Compound 3a

(Chapter 2)

STRUCTURE REPORT

XCL Code: FGW1206 **Date:** 8 August 2012

Compound: 2,2,5-Trimethyl-3,4-diphenylcyclopentanone
Formula: $C_{20}H_{22}O$

Supervisor: F. G. West

Crystallographer: R. McDonald

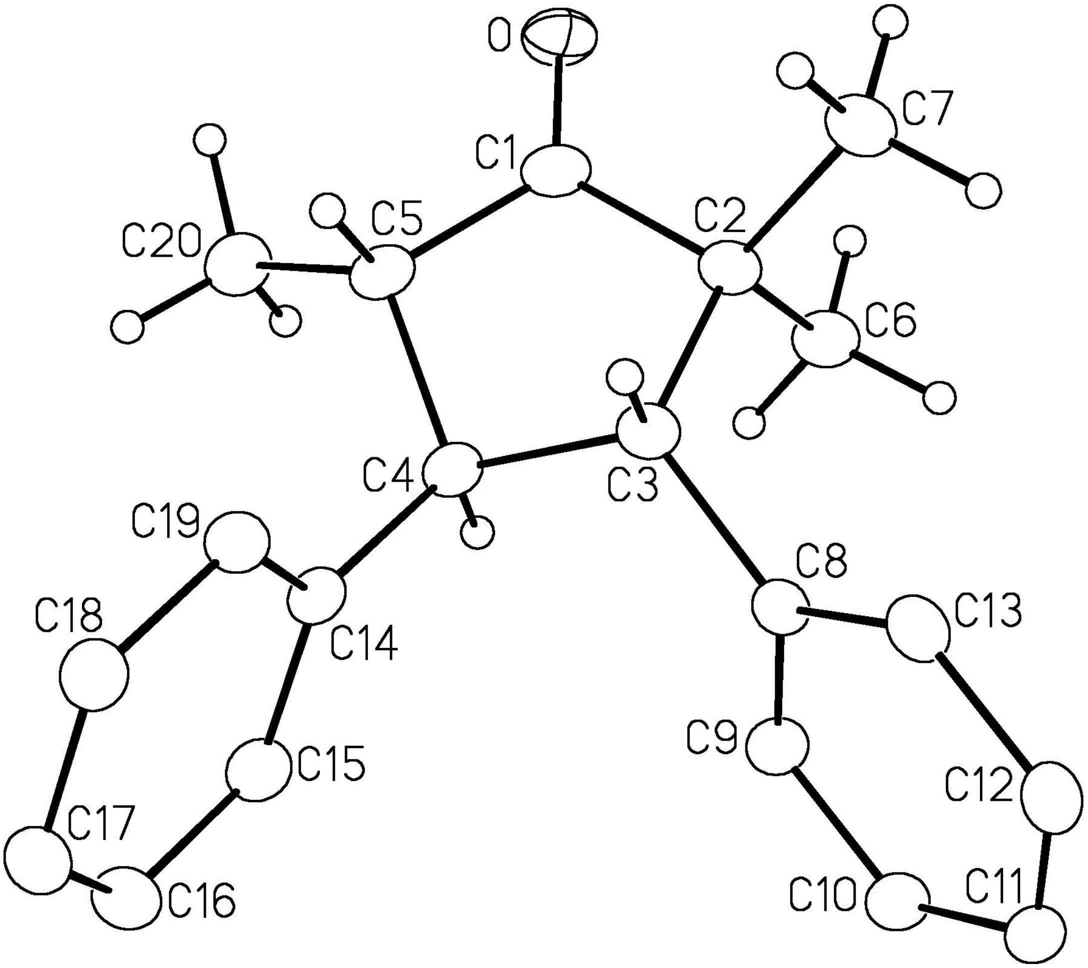
O
C7
C1
C5
C2
C20
C6
C4
C3
C19
C8
C18
C14
C13
C9
C15
C12
C17
C10
C11
C16

Figure 1. Perspective view of the 2,2,5-trimethyl-3,4-diphenylcyclopentanone molecule showing the atom labelling scheme. Non-hydrogen atoms are represented by Gaussian ellipsoids at the 20% probability level. Hydrogen atoms are shown with arbitrarily small thermal parameters except for phenyl-group hydrogens, which are not shown.

Table 1. Crystallographic Experimental Details

A. Crystal Data

formula	$C_{20}H_{22}O$
formula weight	278.38
crystal dimensions (mm)	0.36 × 0.24 × 0.21
crystal system	monoclinic
space group	$P2_1/c$ (No. 14)
unit cell parameters[a]	
a (Å)	12.2227 (2)
b (Å)	9.2606 (1)
c (Å)	15.2205 (3)
β (deg)	112.4602 (7)
V (Å^3)	1592.12 (4)
Z	4
ρ_{calcd} (g cm^{-3})	1.161
μ (mm^{-1})	0.532

B. Data Collection and Refinement Conditions

diffractometer	Bruker D8/APEX II CCD[b]
radiation (λ [Å])	Cu Kα (1.54178) (microfocus source)
temperature (°C)	–100
scan type	ω and ϕ scans (1.0°) (5 s exposures)
data collection 2θ limit (deg)	140.72
total data collected	10607 ($-14 \leq h \leq 14$, $-11 \leq k \leq 11$, $-17 \leq l \leq 18$)
independent reflections	2979 (R_{int} = 0.0138)
number of observed reflections (*NO*)	2796 [$F_o^2 \geq 2\sigma(F_o^2)$]
structure solution method	direct methods/dual space (*SHELXD*[c])
refinement method	full-matrix least-squares on F^2 (*SHELXL–97*[d])
absorption correction method	Gaussian integration (face-indexed)
range of transmission factors	0.8984–0.8300
data/restraints/parameters	2979 / 0 / 190
goodness-of-fit (*S*)[e] [all data]	1.057
final *R* indices[f]	
R_1 [$F_o^2 \geq 2\sigma(F_o^2)$]	0.0451
wR_2 [all data]	0.1223
largest difference peak and hole	0.313 and –0.165 e Å^{-3}

[a] Obtained from least-squares refinement of 9901 reflections with 7.82° < 2θ < 139.62°.

[b] Programs for diffractometer operation, data collection, data reduction and absorption correction were those supplied by Bruker. (continued)

Table 1. Crystallographic Experimental Details (continued)

[c] Schneider, T. R.; Sheldrick, G. M. *Acta Crystallogr.* **2002**, *D58*, 1772-1779.

[d] Sheldrick, G. M. *Acta Crystallogr.* **2008**, *A64*, 112–122.

[e] $S = [\Sigma w(F_o^2 - F_c^2)^2/(n - p)]^{1/2}$ (n = number of data; p = number of parameters varied; $w = [\sigma^2(F_o^2) + (0.0548P)^2 + 0.5705P]^{-1}$ where $P = [\mathrm{Max}(F_o^2, 0) + 2F_c^2]/3$).

[f] $R_1 = \Sigma||F_o| - |F_c||/\Sigma|F_o|$; $wR_2 = [\Sigma w(F_o^2 - F_c^2)^2/\Sigma w(F_o^4)]^{1/2}$.

Appendix VI: X-ray Crystallographic Data for Compound 3h

(Chapter 2)

STRUCTURE REPORT

XCL Code: FGW1208 **Date:** 17 August 2012

Compound: 6,7a-Dimethyl-5-phenylhexahydrocyclopenta[*b*]pyran-7(2*H*)-one
Formula: $C_{16}H_{20}O_2$

Supervisor: F. G. West

Crystallographer: R. McDonald

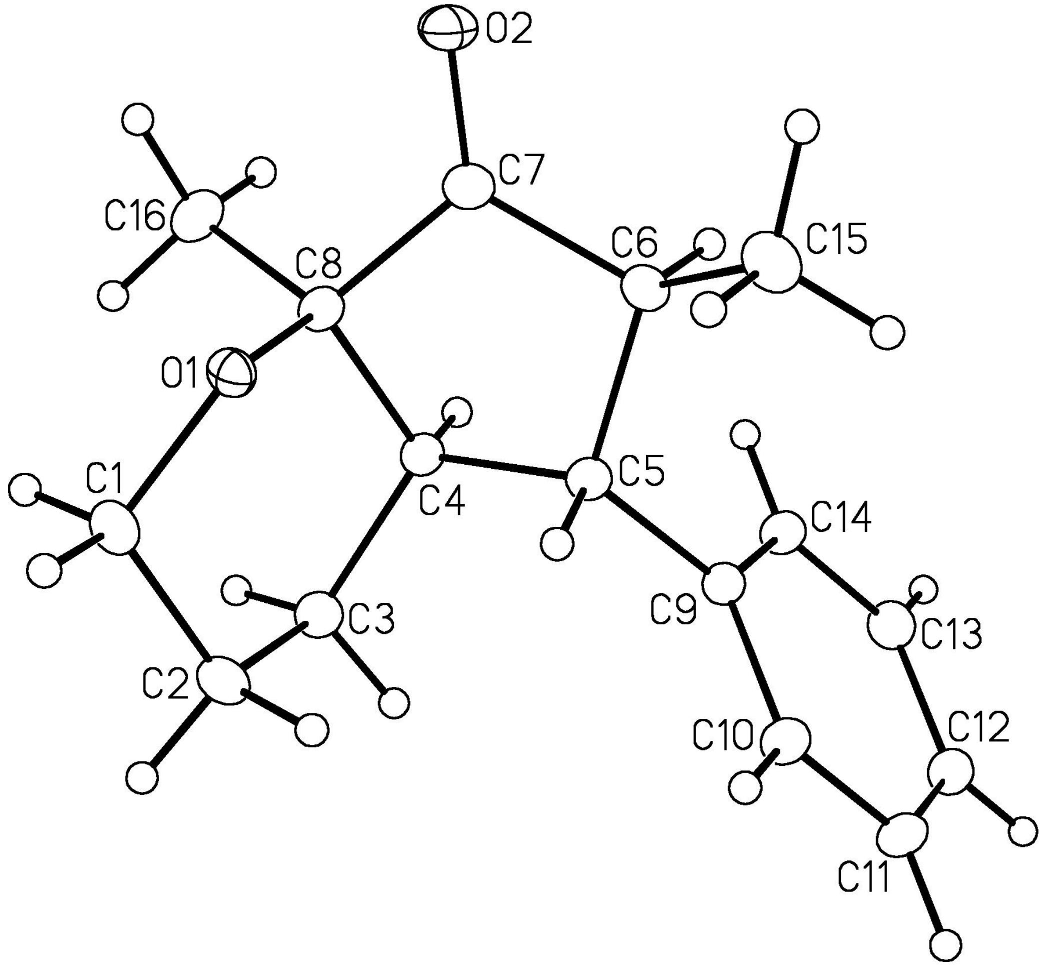
O2
C7
C16
C8
C6
C15
O1
C4
C5
C1
C14
C3
C9
C13
C2
C10
C12
C11

Figure 1. Perspective view of the 6,7a-dimethyl-5-phenylhexahydrocyclopenta[*b*]pyran-7(2*H*)-one molecule showing the atom labelling scheme. Non-hydrogen atoms are represented by Gaussian ellipsoids at the 20% probability level. Hydrogen atoms are shown with arbitrarily small thermal parameters.

Table 1. Crystallographic Experimental Details

A. Crystal Data

formula	$C_{16}H_{20}O_2$
formula weight	244.32
crystal dimensions (mm)	0.47 × 0.26 × 0.08
crystal system	monoclinic
space group	$P2_1$ (No. 4)
unit cell parameters[a]	
a (Å)	8.7213 (7)
b (Å)	7.2707 (6)
c (Å)	11.0792 (9)
β (deg)	109.3105 (9)
V (Å^3)	663.01 (9)
Z	2
ρ_{calcd} (g cm^{-3})	1.224
μ (mm^{-1})	0.079

B. Data Collection and Refinement Conditions

diffractometer	Bruker D8/APEX II CCD[b]
radiation (λ [Å])	graphite-monochromated Mo Kα (0.71073)
temperature (°C)	–100
scan type	ω scans (0.3°) (15 s exposures)
data collection 2θ limit (deg)	52.88
total data collected	5399 ($-10 \le h \le 10$, $-9 \le k \le 9$, $-13 \le l \le 13$)
independent reflections	2722 ($R_{\mathrm{int}} = 0.0193$)
number of observed reflections (*NO*)	2451 [$F_o^2 \ge 2\sigma(F_o^2)$]
structure solution method	direct methods/dual space (*SHELXD*[c])
refinement method	full-matrix least-squares on F^2 (*SHELXL–97*[d])
absorption correction method	Gaussian integration (face-indexed)
range of transmission factors	0.9936–0.9636
data/restraints/parameters	2722 / 0 / 164
Flack absolute structure parameter[e]	0.9(10)
goodness-of-fit (S)[f] [all data]	1.063
final R indices[g]	
R_1 [$F_o^2 \ge 2\sigma(F_o^2)$]	0.0336
wR_2 [all data]	0.0810
largest difference peak and hole	0.125 and –0.141 e Å^{-3}

[a] Obtained from least-squares refinement of 4164 reflections with $4.94° < 2\theta < 49.32°$.

[b] Programs for diffractometer operation, data collection, data reduction and absorption correction were those supplied by Bruker. (continued)

Table 1. Crystallographic Experimental Details (continued)

[c] Schneider, T. R.; Sheldrick, G. M. *Acta Crystallogr.* **2002**, *D58*, 1772-1779.

[d] Sheldrick, G. M. *Acta Crystallogr.* **2008**, *A64*, 112–122.

[e] Flack, H. D. *Acta Crystallogr.* **1983**, *A39*, 876–881; Flack, H. D.; Bernardinelli, G. *Acta Crystallogr.* **1999**, *A55*, 908–915; Flack, H. D.; Bernardinelli, G. *J. Appl. Cryst.* **2000**, *33*, 1143–1148. The Flack parameter will refine to a value near zero if the structure is in the correct configuration and will refine to a value near one for the inverted configuration. The low anomalous scattering power of the atoms in this structure (none heavier than oxygen) implies that the data cannot be used for absolute structure assignment, thus the Flack parameter is provided for informational purposes only. The compound was crystallized from a racemic mixture, and assignement of the relative stereochemistry is sufficient for the present study.

[f] $S = [\Sigma w(F_o^2 - F_c^2)^2/(n - p)]^{1/2}$ (n = number of data; p = number of parameters varied; $w = [\sigma^2(F_o^2) + (0.0377P)^2 + 0.0664P]^{-1}$ where $P = [\mathrm{Max}(F_o^2, 0) + 2F_c^2]/3$).

[g] $R_1 = \Sigma||F_o| - |F_c||/\Sigma|F_o|$; $wR_2 = [\Sigma w(F_o^2 - F_c^2)^2/\Sigma w(F_o^4)]^{1/2}$.

Appendix VII: X-ray Crystallographic Data for Compound 7a

(Chapter 2)

STRUCTURE REPORT

XCL Code: FGW1207 **Date:** 8 August 2012

Compound: 2-Ethyl-2,5-dimethyl-3,4-diphenylcyclopentanone
Formula: $C_{21}H_{24}O$

Supervisor: F. G. West

Crystallographer: R. McDonald

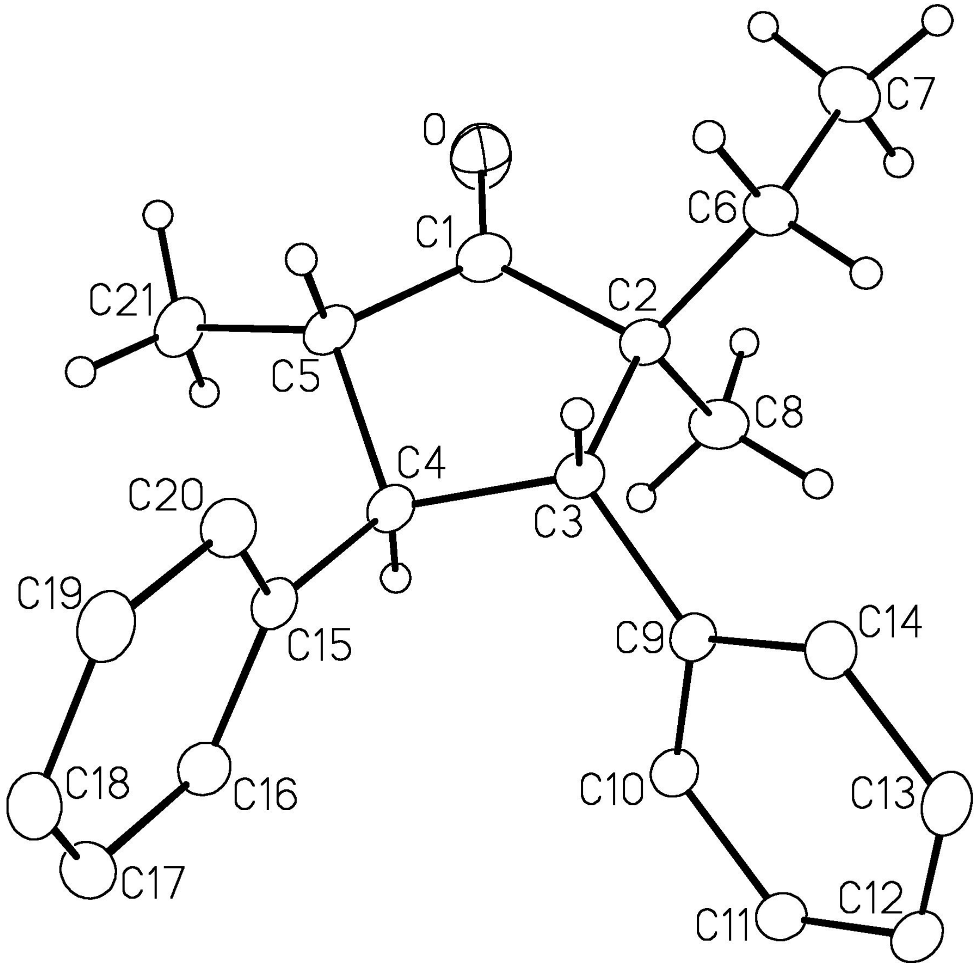
O
C1
C2
C3
C4
C5
C6
C7
C8
C9
C10
C11
C12
C13
C14
C15
C16
C17
C18
C19
C20
C21

Figure 1. Perspective view of the 2-ethyl-2,5-dimethyl-3,4-diphenylcyclopentanone molecule showing the atom labelling scheme. Non-hydrogen atoms are represented by Gaussian ellipsoids at the 20% probability level. Hydrogen atoms are shown with arbitrarily small thermal parameters except for phenyl-group hydrogens, which are not shown.

Table 1. Crystallographic Experimental Details

A. Crystal Data

formula	$C_{21}H_{24}O$
formula weight	292.40
crystal dimensions (mm)	0.47 × 0.46 × 0.43
crystal system	monoclinic
space group	$P2_1/n$ (an alternate setting of $P2_1/c$ [No. 14])
unit cell parameters[a]	
a (Å)	12.819 (3)
b (Å)	9.524 (2)
c (Å)	14.839 (3)
β (deg)	113.715 (2)
V (Å^3)	1658.7 (7)
Z	4
ρ_{calcd} (g cm^{-3})	1.171
μ (mm^{-1})	0.070

B. Data Collection and Refinement Conditions

diffractometer	Bruker D8/APEX II CCD[b]
radiation (λ [Å])	graphite-monochromated Mo Kα (0.71073)
temperature (°C)	–100
scan type	ω scans (0.3°) (15 s exposures)
data collection 2θ limit (deg)	53.56
total data collected	13283 ($-16 \leq h \leq 16$, $-12 \leq k \leq 12$, $-18 \leq l \leq 18$)
independent reflections	3530 (R_{int} = 3530)
number of observed reflections (*NO*)	2888 [$F_o^2 \geq 2\sigma(F_o^2)$]
structure solution method	direct methods/dual space (*SHELXD*[c])
refinement method	full-matrix least-squares on F^2 (*SHELXL–97*[d])
absorption correction method	Gaussian integration (face-indexed)
range of transmission factors	0.9709–0.9683
data/restraints/parameters	3530 / 0 / 199
goodness-of-fit (S)[e] [all data]	1.055
final R indices[f]	
R_1 [$F_o^2 \geq 2\sigma(F_o^2)$]	0.0474
wR_2 [all data]	0.1440
largest difference peak and hole	0.372 and –0.294 e Å^{-3}

[a] Obtained from least-squares refinement of 8300 reflections with 5.22° < 2θ < 52.96°.

[b] Programs for diffractometer operation, data collection, data reduction and absorption correction were those supplied by Bruker. (continued)

Table 1. Crystallographic Experimental Details (continued)

[c]Schneider, T. R.; Sheldrick, G. M. *Acta Crystallogr.* **2002**, *D58*, 1772-1779.

[d]Sheldrick, G. M. *Acta Crystallogr.* **2008**, *A64*, 112–122.

[e]$S = [\Sigma w(F_o^2 - F_c^2)^2/(n - p)]^{1/2}$ (n = number of data; p = number of parameters varied; $w = [\sigma^2(F_o^2) + (0.0736P)^2 + 0.3205P]^{-1}$ where $P = [\mathrm{Max}(F_o^2, 0) + 2F_c^2]/3$).

[f]$R_1 = \Sigma||F_o| - |F_c||/\Sigma|F_o|$; $wR_2 = [\Sigma w(F_o^2 - F_c^2)^2/\Sigma w(F_o^4)]^{1/2}$.

Appendix VIII: X-ray Crystallographic Data for Compound 8a’

(Chapter 2)

STRUCTURE REPORT

XCL Code: FGW1209 **Date:** 21 August 2012

Compound: 2-Cyano-2,5-dimethyl-3,4-diphenylcyclopentanone
Formula: $C_{20}H_{19}NO$

Supervisor: F. G. West

Crystallographer: R. McDonald

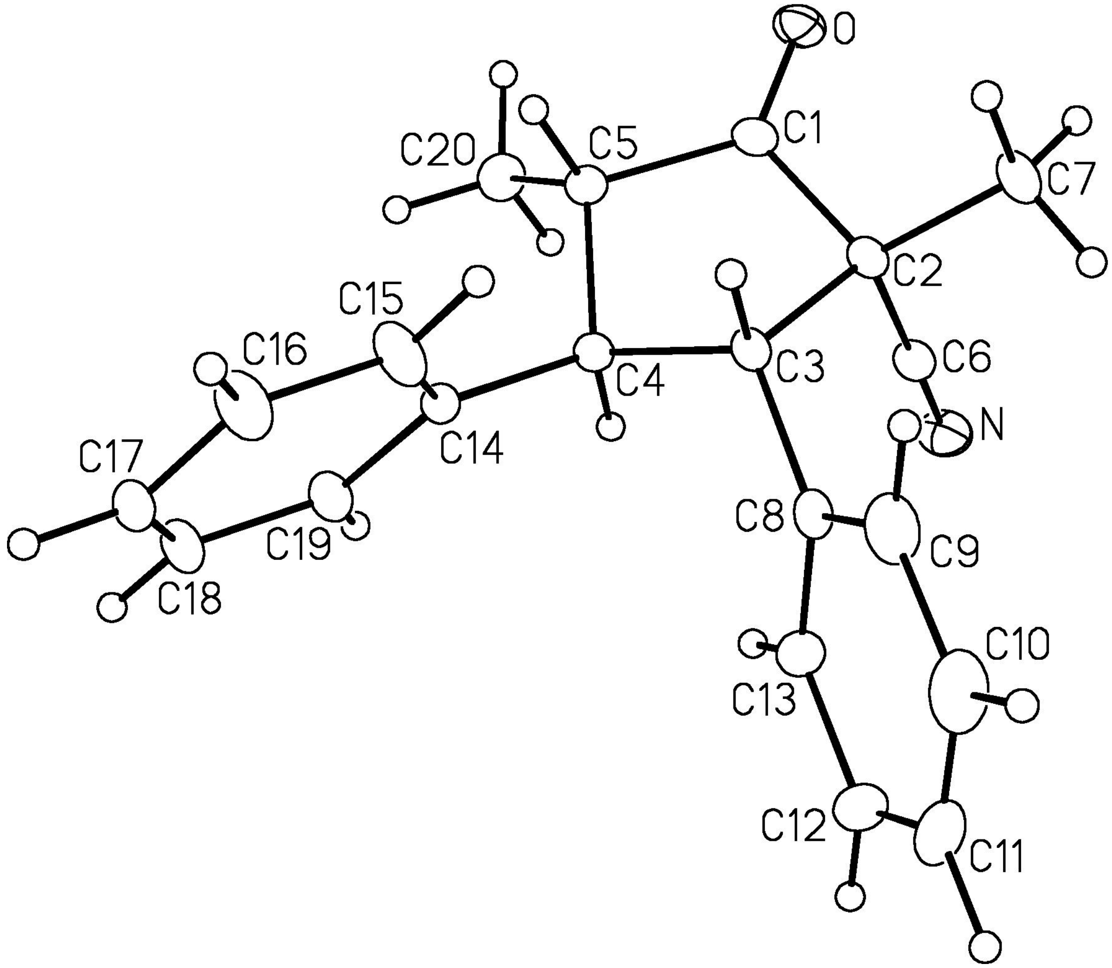
O
C1
C20
C5
C7
C2
C15
C16
C4
C3
C6
N
C14
C17
C8
C9
C19
C18
C10
C13
C12
C11

Figure 1. Perspective view of the 2-cyano-2,5-dimethyl-3,4-diphenylcyclopentanone molecule showing the atom labelling scheme. Non-hydrogen atoms are represented by Gaussian ellipsoids at the 20% probability level. Hydrogen atoms are shown with arbitrarily small thermal parameters.

Table 1. Crystallographic Experimental Details

A. Crystal Data

formula	$C_{20}H_{19}NO$
formula weight	289.36
crystal dimensions (mm)	0.45 × 0.20 × 0.19
crystal system	triclinic
space group	$P\bar{1}$ (No. 2)
unit cell parameters[a]	
a (Å)	6.4556 (5)
b (Å)	10.6376 (8)
c (Å)	11.9494 (9)
α (deg)	90.8324 (9)
β (deg)	93.9845 (10)
γ (deg)	98.3102 (9)
V (Å^3)	809.76 (11)
Z	2
ρ_{calcd} (g cm^{-3})	1.187
μ (mm^{-1})	0.073

B. Data Collection and Refinement Conditions

diffractometer	Bruker D8/APEX II CCD[b]
radiation (λ [Å])	graphite-monochromated Mo Kα (0.71073)
temperature (°C)	–100
scan type	ω scans (0.3°) (15 s exposures)
data collection 2θ limit (deg)	52.92
total data collected	6619 ($-8 \leq h \leq 8$, $-13 \leq k \leq 13$, $-14 \leq l \leq 14$)
independent reflections	3334 ($R_{\text{int}} = 0.0177$)
number of observed reflections (*NO*)	2599 [$F_o^2 \geq 2\sigma(F_o^2)$]
structure solution method	direct methods/dual space (*SHELXD*[c])
refinement method	full-matrix least-squares on F^2 (*SHELXL–97*[d])
absorption correction method	Gaussian integration (face-indexed)
range of transmission factors	0.9866–0.9678
data/restraints/parameters	3334 / 0 / 199
goodness-of-fit (S)[e] [all data]	1.062
final R indices[f]	
R_1 [$F_o^2 \geq 2\sigma(F_o^2)$]	0.0419
wR_2 [all data]	0.1115
largest difference peak and hole	0.218 and –0.199 e Å^{-3}

[a] Obtained from least-squares refinement of 3618 reflections with $5.10° < 2\theta < 52.78°$.

(continued)

Table 1. Crystallographic Experimental Details (continued)

[b] Programs for diffractometer operation, data collection, data reduction and absorption correction were those supplied by Bruker.

[c] Schneider, T. R.; Sheldrick, G. M. *Acta Crystallogr.* **2002**, *D58*, 1772-1779.

[d] Sheldrick, G. M. *Acta Crystallogr.* **2008**, *A64*, 112–122.

[e] $S = [\Sigma w(F_o^2 - F_c^2)^2/(n - p)]^{1/2}$ (n = number of data; p = number of parameters varied; $w = [\sigma^2(F_o^2) + (0.0497P)^2 + 0.1478P]^{-1}$ where $P = [\mathrm{Max}(F_o^2, 0) + 2F_c^2]/3$).

[f] $R_1 = \Sigma||F_o| - |F_c||/\Sigma|F_o|$; $wR_2 = [\Sigma w(F_o^2 - F_c^2)^2/\Sigma w(F_o^4)]^{1/2}$.

Appendix IX: X-ray Crystallographic Data for Compound 11a

(Chapter 2)

STRUCTURE REPORT

XCL Code: FGW1215 **Date:** 19 November 2012

Compound: 2-Azido-2,5-dimethyl-3,4-diphenylcyclopentanone
Formula: $C_{19}H_{19}N_3O$

Supervisor: F. G. West

Crystallographer: R. McDonald

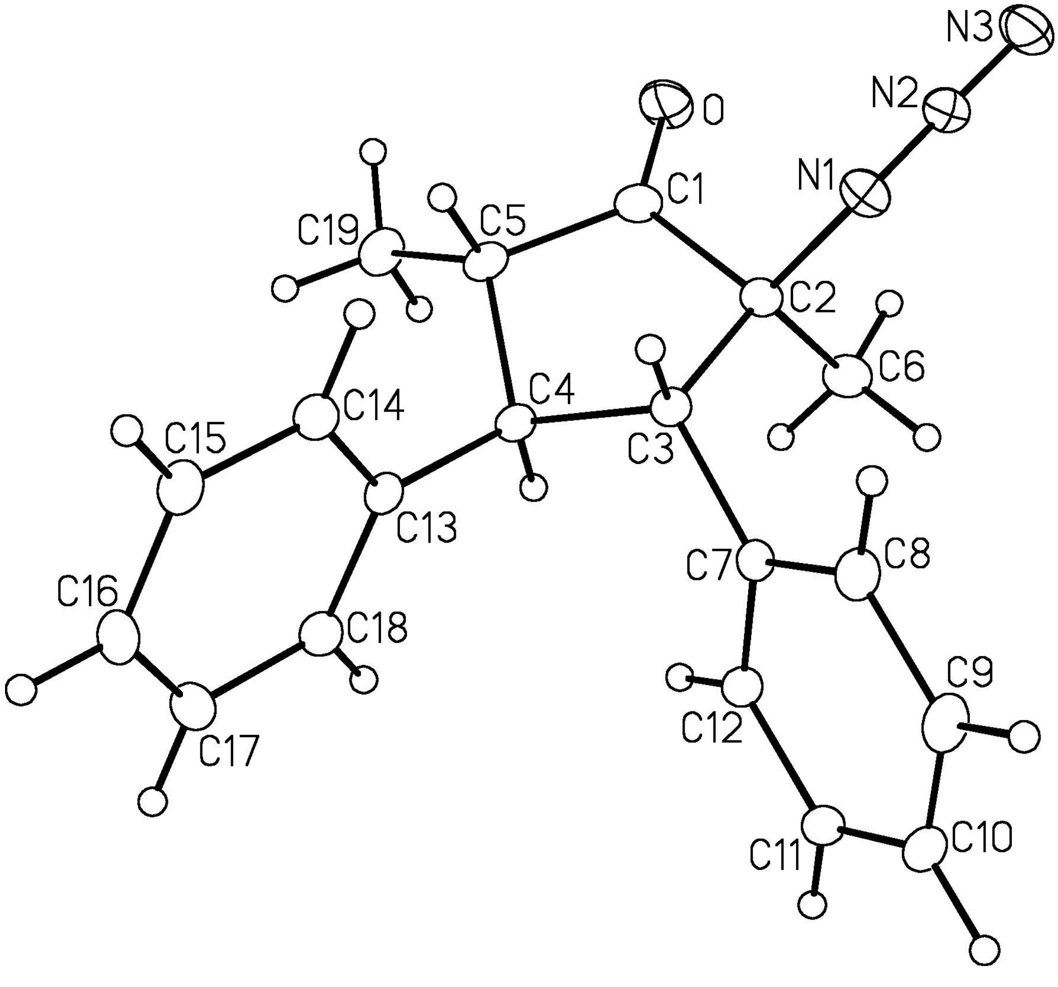
N3
N2
O
N1
C1
C19
C5
C2
C6
C14
C4
C15
C3
C13
C7
C8
C16
C18
C9
C12
C17
C11
C10

Figure 1. Perspective view of the 2-azido-2,5-dimethyl-3,4-diphenylcyclopentanone molecule showing the atom labelling scheme. Non-hydrogen atoms are represented by Gaussian ellipsoids at the 20% probability level. Hydrogen atoms are shown with arbitrarily small thermal parameters.

Table 1. Crystallographic Experimental Details

A. Crystal Data	
formula	$C_{19}H_{19}N_3O$
formula weight	305.37
crystal dimensions (mm)	0.56 × 0.53 × 0.47
crystal system	monoclinic
space group	$P2_1/n$ (an alternate setting of $P2_1/c$ [No. 14])
unit cell parameters[a]	
a (Å)	12.2479 (7)
b (Å)	9.7268 (6)
c (Å)	14.6819 (9)
β (deg)	113.8265 (6)
V (Å^3)	1600.03 (17)
Z	4
ρ_{calcd} (g cm^{-3})	1.268
μ (mm^{-1})	0.080
B. Data Collection and Refinement Conditions	
diffractometer	Bruker D8/APEX II CCD[b]
radiation (λ [Å])	graphite-monochromated Mo Kα (0.71073)
temperature (°C)	–100
scan type	ω scans (0.3°) (15 s exposures)
data collection 2θ limit (deg)	55.18
total data collected	14088 ($-15 \le h \le 15$, $-12 \le k \le 12$, $-19 \le l \le 19$)
independent reflections	3690 ($R_{\text{int}} = 0.0145$)
number of observed reflections (*NO*)	3215 [$F_o^2 \ge 2\sigma(F_o^2)$]
structure solution method	direct methods/dual space (*SHELXD*[c])
refinement method	full-matrix least-squares on F^2 (*SHELXL–97*[d])
absorption correction method	Gaussian integration (face-indexed)
range of transmission factors	0.9630–0.9560
data/restraints/parameters	3690 / 0 / 208
goodness-of-fit (S)[e] [all data]	1.050
final R indices[f]	
R_1 [$F_o^2 \ge 2\sigma(F_o^2)$]	0.0407
wR_2 [all data]	0.1192
largest difference peak and hole	0.276 and –0.304 e Å^{-3}

[a] Obtained from least-squares refinement of 7731 reflections with 5.18° < 2θ < 48.10°.

[b] Programs for diffractometer operation, data collection, data reduction and absorption correction were those supplied by Bruker. (continued)

Table 1. Crystallographic Experimental Details (continued)

[c]Schneider, T. R.; Sheldrick, G. M. *Acta Crystallogr.* **2002**, *D58*, 1772-1779.

[d]Sheldrick, G. M. *Acta Crystallogr.* **2008**, *A64*, 112–122.

[e]$S = [\Sigma w(F_o^2 - F_c^2)^2/(n - p)]^{1/2}$ (n = number of data; p = number of parameters varied; $w = [\sigma^2(F_o^2) + (0.0612P)^2 + 0.4349P]^{-1}$ where $P = [\mathrm{Max}(F_o^2, 0) + 2F_c^2]/3$).

[f]$R_1 = \Sigma||F_o| - |F_c||/\Sigma|F_o|$; $wR_2 = [\Sigma w(F_o^2 - F_c^2)^2/\Sigma w(F_o^4)]^{1/2}$.

Appendix X: X-ray Crystallographic Data for Compound 7a’

(Chapter 2)

STRUCTURE REPORT

XCL Code: FGW1315 **Date:** 23 August 2013

Compound: 2-Ethyl-2,5-dimethyl-3,4-diphenylcyclopentanone
Formula: $C_{21}H_{24}O$

Supervisor: F. G. West

Crystallographer: R. McDonald

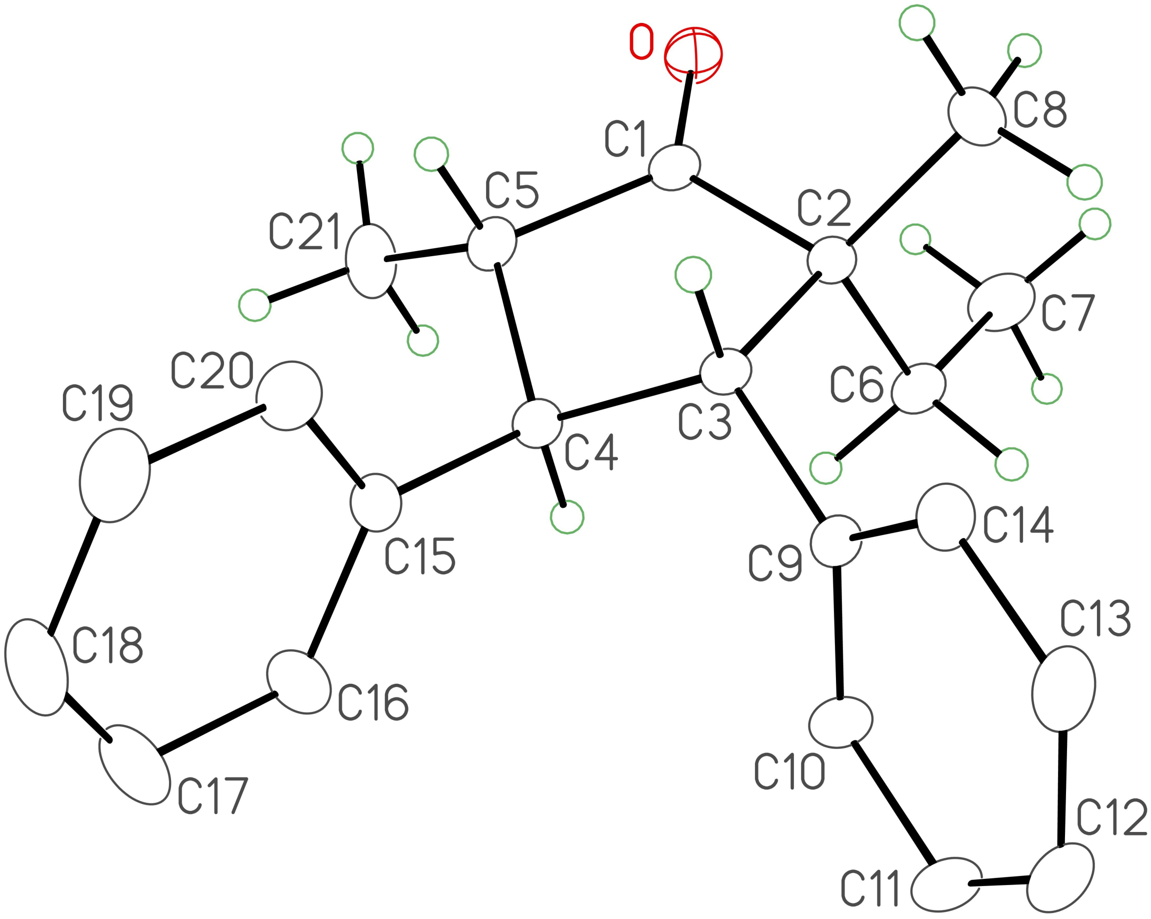
O
C1
C2
C3
C4
C5
C6
C7
C8
C9
C10
C11
C12
C13
C14
C15
C16
C17
C18
C19
C20
C21

Figure 1. Perspective view of the 2-ethyl-2,5-dimethyl-3,4-diphenylcyclopentanone molecule showing the atom labelling scheme. Non-hydrogen atoms are represented by Gaussian ellipsoids at the 20% probability level. Hydrogen atoms are shown with arbitrarily small thermal parameters except for phenyl-group hydrogens, which are not shown.

Table 1. Crystallographic Experimental Details

A. Crystal Data

formula	$C_{21}H_{24}O$
formula weight	292.40
crystal dimensions (mm)	0.37 x 0.27 × 0.20
crystal system	monoclinic
space group	$P2_1/c$ (No. 14)
unit cell parameters[a]	
a (Å)	13.7546 (12)
b (Å)	8.4867 (7)
c (Å)	15.9897 (14)
β (deg)	112.7092 (10)
V (Å^3)	1721.8 (3)
Z	4
ρ_{calcd} (g cm^{-3})	1.128
μ (mm^{-1})	0.067

B. Data Collection and Refinement Conditions

diffractometer	Bruker D8/APEX II CCD[b]
radiation (λ [Å])	graphite-monochromated Mo Kα (0.71073)
temperature (°C)	–100
scan type	ω scans (0.3°) (15 s exposures)
data collection 2θ limit (deg)	55.03
total data collected	14903 ($-17 \le h \le 17$, $-11 \le k \le 11$, $-20 \le l \le 20$)
independent reflections	3951 ($R_{\mathrm{int}} = 0.0166$)
number of observed reflections (*NO*)	3315 [$F_o^2 \ge 2\sigma(F_o^2)$]
structure solution method	direct methods/dual space (*SHELXD*[c])
refinement method	full-matrix least-squares on F^2 (*SHELXL–97*[d])
absorption correction method	Gaussian integration (face-indexed)
range of transmission factors	1.0000–0.9500
data/restraints/parameters	3951 / 0 / 199
goodness-of-fit (S)[e] [all data]	1.078
final R indices[f]	
R_1 [$F_o^2 \ge 2\sigma(F_o^2)$]	0.0453
wR_2 [all data]	0.1331
largest difference peak and hole	0.294 and –0.175 e Å^{-3}

[a] Obtained from least-squares refinement of 7016 reflections with $5.20° < 2\theta < 53.70°$.

[b] Programs for diffractometer operation, data collection, data reduction and absorption correction were those supplied by Bruker. (continued)

Table 1. Crystallographic Experimental Details (continued)

[c]Schneider, T. R.; Sheldrick, G. M. *Acta Crystallogr.* **2002**, *D58*, 1772-1779.

[d]Sheldrick, G. M. *Acta Crystallogr.* **2008**, *A64*, 112–122.

[e]$S = [\Sigma w(F_o^2 - F_c^2)^2/(n - p)]^{1/2}$ (n = number of data; p = number of parameters varied; $w = [\sigma^2(F_o^2) + (0.0652P)^2 + 0.4010P]^{-1}$ where $P = [\mathrm{Max}(F_o^2, 0) + 2F_c^2]/3$).

[f]$R_1 = \Sigma||F_o| - |F_c||/\Sigma|F_o|$; $wR_2 = [\Sigma w(F_o^2 - F_c^2)^2/\Sigma w(F_o^4)]^{1/2}$.

Appendix XI: X-ray Crystallographic Data for Compound 4a

(Chapter 3)

STRUCTURE REPORT

XCL Code: FGW1302 **Date:** 4 February 2013

Compound: 2-Hydroxy-2,5,5-trimethyl-3,4-diphenylcyclopentanone
Formula: $C_{20}H_{22}O_2$

Supervisor: F. G. West

Crystallographer: R. McDonald

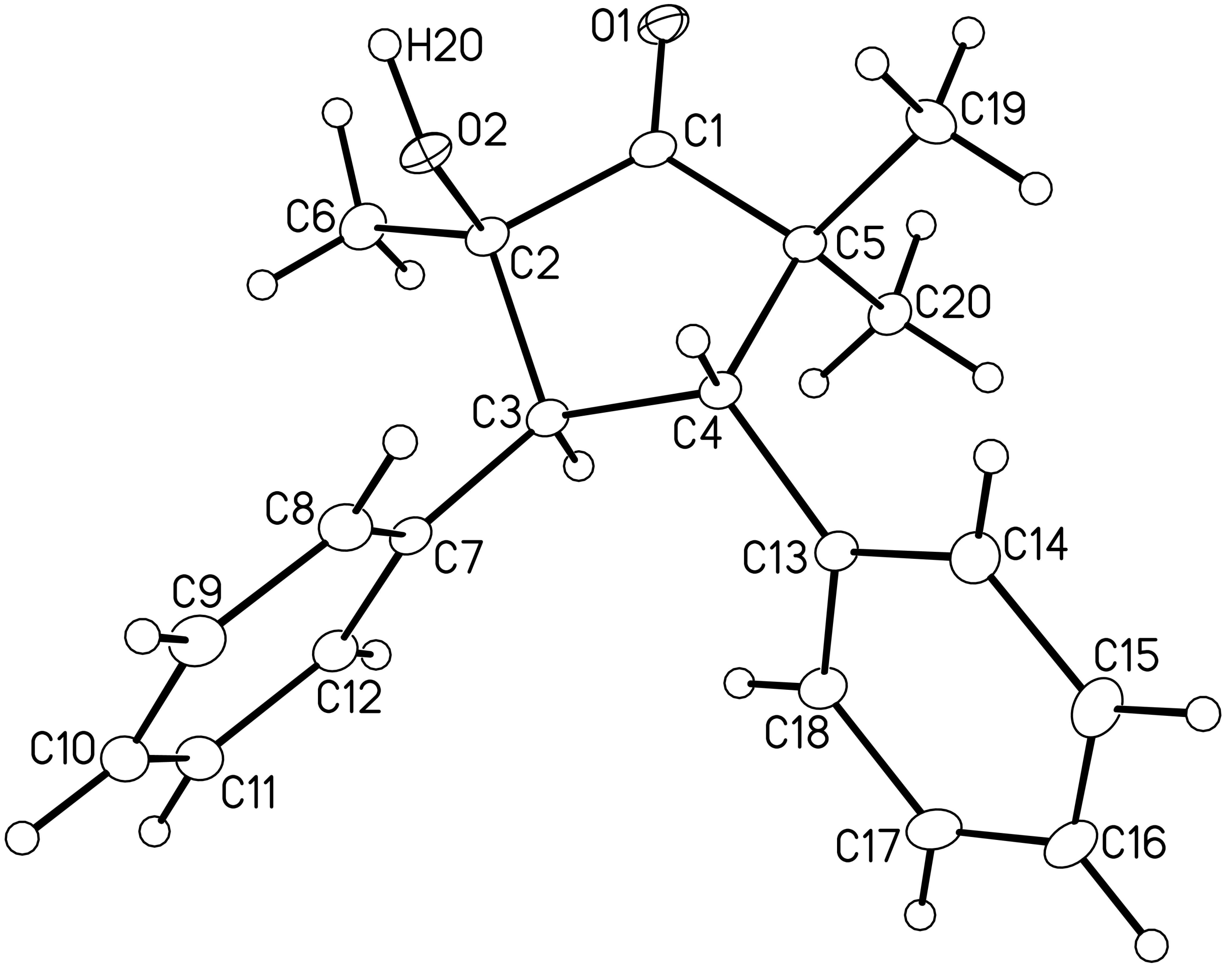
O1
H2O
O2
C1
C19
C6
C2
C5
C20
C3
C4
C8
C7
C13
C14
C9
C15
C12
C18
C10
C11
C17
C16

Figure 1. Perspective view of the 2-hydroxy-2,5,5-trimethyl-3,4-diphenylcyclopentanone molecule showing the atom labelling scheme. Non-hydrogen atoms are represented by Gaussian ellipsoids at the 20% probability level. Hydrogen atoms are shown with arbitrarily small thermal parameters.

Table 1. Crystallographic Experimental Details

A. Crystal Data	
formula	$C_{20}H_{22}O_2$
formula weight	294.38
crystal dimensions (mm)	0.46 × 0.11 × 0.03
crystal system	monoclinic
space group	$P2_1/n$ (an alternate setting of $P2_1/c$ [No. 14])
unit cell parameters[a]	
a (Å)	6.0600 (2)
b (Å)	17.8904 (7)
c (Å)	15.1129 (6)
β (deg)	96.9109 (16)
V (Å^3)	1626.57 (11)
Z	4
ρ_{calcd} (g cm^{-3})	1.202
μ (mm^{-1})	0.595
B. Data Collection and Refinement Conditions	
diffractometer	Bruker D8/APEX II CCD[b]
radiation (λ [Å])	Cu Kα (1.54178) (microfocus source)
temperature (°C)	–100
scan type	ω and ϕ scans (1.0°) (5 s exposures)
data collection 2θ limit (deg)	142.74
total data collected	10710 ($-7 \leq h \leq 7$, $-21 \leq k \leq 21$, $-18 \leq l \leq 18$)
independent reflections	3159 ($R_{\text{int}} = 0.0382$)
number of observed reflections (*NO*)	2836 [$F_o^2 \geq 2\sigma(F_o^2)$]
structure solution method	direct methods/dual space (*SHELXD*[c])
refinement method	full-matrix least-squares on F^2 (*SHELXL–97*[d])
absorption correction method	Gaussian integration (face-indexed)
range of transmission factors	0.9812–0.7730
data/restraints/parameters	3159 / 0 / 203
goodness-of-fit (*S*)[e] [all data]	1.045
final *R* indices[f]	
R_1 [$F_o^2 \geq 2\sigma(F_o^2)$]	0.0421
wR_2 [all data]	0.1184
largest difference peak and hole	0.221 and –0.291 e Å^{-3}

[a] Obtained from least-squares refinement of 9904 reflections with $4.94° < 2\theta < 142.68°$.

[b] Programs for diffractometer operation, data collection, data reduction and absorption correction were those supplied by Bruker.

(continued)

Table 1. Crystallographic Experimental Details (continued)

[c]Schneider, T. R.; Sheldrick, G. M. *Acta Crystallogr.* **2002**, *D58*, 1772-1779.

[d]Sheldrick, G. M. *Acta Crystallogr.* **2008**, *A64*, 112–122.

[e]$S = [\Sigma w(F_o^2 - F_c^2)^2/(n - p)]^{1/2}$ (n = number of data; p = number of parameters varied; $w = [\sigma^2(F_o^2) + (0.0693P)^2 + 0.3401P]^{-1}$ where $P = [\mathrm{Max}(F_o^2, 0) + 2F_c^2]/3$).

[f]$R_1 = \Sigma||F_o| - |F_c||/\Sigma|F_o|$; $wR_2 = [\Sigma w(F_o^2 - F_c^2)^2/\Sigma w(F_o^4)]^{1/2}$.

Appendix XII: X-ray Crystallographic Data for Compound 4e

(Chapter 3)

STRUCTURE REPORT

XCL Code: FGW1305 **Date:** 9 April 2013

Compound: 2-Hydroxy-2,5,5-trimethyl-3,4-diisopropylcyclopentanone
Formula: $C_{14}H_{26}O_2$

Supervisor: F. G. West

Crystallographer: R. McDonald

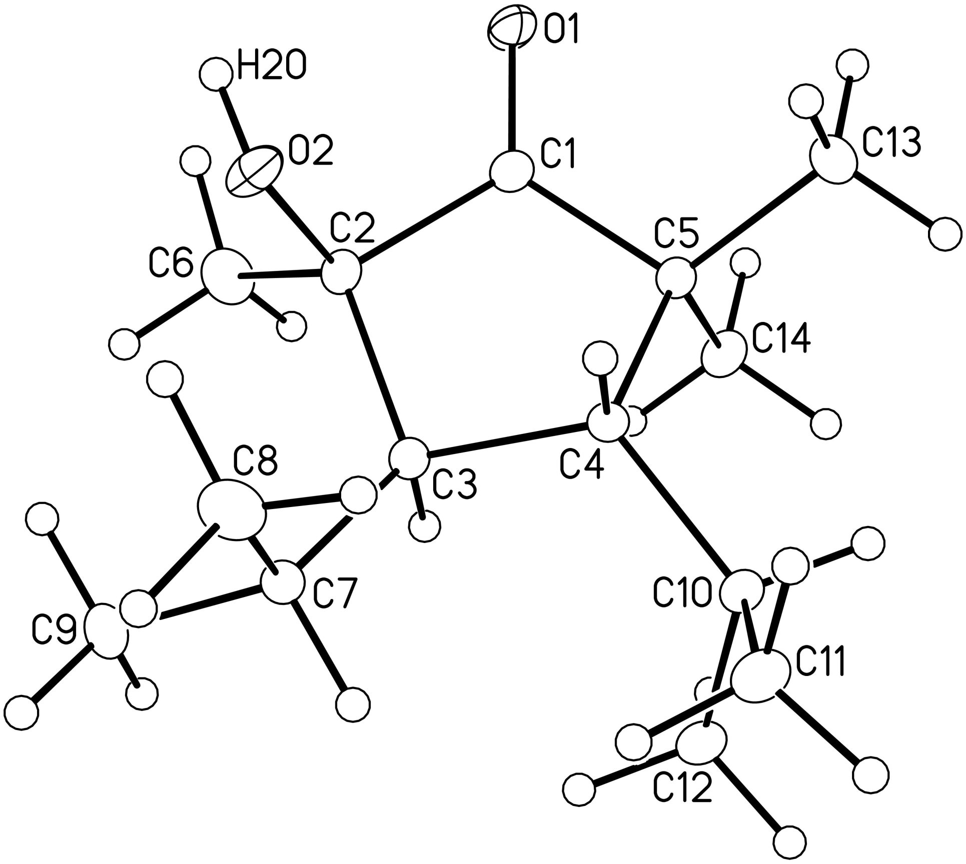
O1
H2O
O2
C1
C13
C2
C5
C6
C14
C8
C4
C3
C7
C10
C9
C11
C12

Figure 1. Perspective view of the 2-hydroxy-2,5,5-trimethyl-3,4-diisopropylcyclopentanone molecule showing the atom labelling scheme. Non-hydrogen atoms are represented by Gaussian ellipsoids at the 20% probability level. Hydrogen atoms are shown with arbitrarily small thermal parameters.

Table 1. Crystallographic Experimental Details

A. Crystal Data	
formula	$C_{14}H_{26}O_2$
formula weight	226.35
crystal dimensions (mm)	0.47 × 0.21 × 0.19
crystal system	triclinic
space group	$P\bar{1}$ (No. 2)
unit cell parameters[a]	
a (Å)	6.191 (2)
b (Å)	8.211 (3)
c (Å)	14.477 (5)
α (deg)	93.911 (4)
β (deg)	96.054 (5)
γ (deg)	109.796 (4)
V (Å^3)	684.3 (4)
Z	2
ρ_{calcd} (g cm^{-3})	1.098
μ (mm^{-1})	0.071
B. Data Collection and Refinement Conditions	
diffractometer	Bruker D8/APEX II CCD[b]
radiation (λ [Å])	graphite-monochromated Mo Kα (0.71073)
temperature (°C)	–100
scan type	ω scans (0.3°) (20 s exposures)
data collection 2θ limit (deg)	53.00
total data collected	5470 ($-7 \le h \le 7$, $-10 \le k \le 10$, $-18 \le l \le 18$)
independent reflections	2819 (R_{int} = 0.0199)
number of observed reflections (*NO*)	2247 [$F_o^2 \ge 2\sigma(F_o^2)$]
structure solution method	direct methods/dual space (*SHELXD*[c])
refinement method	full-matrix least-squares on F^2 (*SHELXL–97*[d])
absorption correction method	Gaussian integration (face-indexed)
range of transmission factors	0.9865–0.9678
data/restraints/parameters	2819 / 0 / 149
goodness-of-fit (S)[e] [all data]	1.088
final R indices[f]	
R_1 [$F_o^2 \ge 2\sigma(F_o^2)$]	0.0472
wR_2 [all data]	0.1310
largest difference peak and hole	0.255 and –0.198 e Å^{-3}

[a]Obtained from least-squares refinement of 2370 reflections with 5.30° < 2θ < 52.88°.

(continued)

Table 1. Crystallographic Experimental Details (continued)

[b] Programs for diffractometer operation, data collection, data reduction and absorption correction were those supplied by Bruker.

[c] Schneider, T. R.; Sheldrick, G. M. *Acta Crystallogr.* **2002**, *D58*, 1772-1779.

[d] Sheldrick, G. M. *Acta Crystallogr.* **2008**, *A64*, 112–122.

[e] $S = [\Sigma w(F_o^2 - F_c^2)^2/(n - p)]^{1/2}$ (n = number of data; p = number of parameters varied; $w = [\sigma^2(F_o^2) + (0.0578P)^2 + 0.2189P]^{-1}$ where $P = [\mathrm{Max}(F_o^2, 0) + 2F_c^2]/3$).

[f] $R_1 = \Sigma||F_o| - |F_c||/\Sigma|F_o|$; $wR_2 = [\Sigma w(F_o^2 - F_c^2)^2/\Sigma w(F_o^4)]^{1/2}$.

Appendix XIII: X-ray Crystallographic Data for Compound 5e

(Chapter 3)

STRUCTURE REPORT

XCL Code: FGW1306 **Date:** 9 April 2013

Compound: 2-Hydroxy-2,5,5-trimethyl-3,4-diisopropylcyclopentanone
Formula: $C_{14}H_{26}O_2$

Supervisor: F. G. West

Crystallographer: R. McDonald

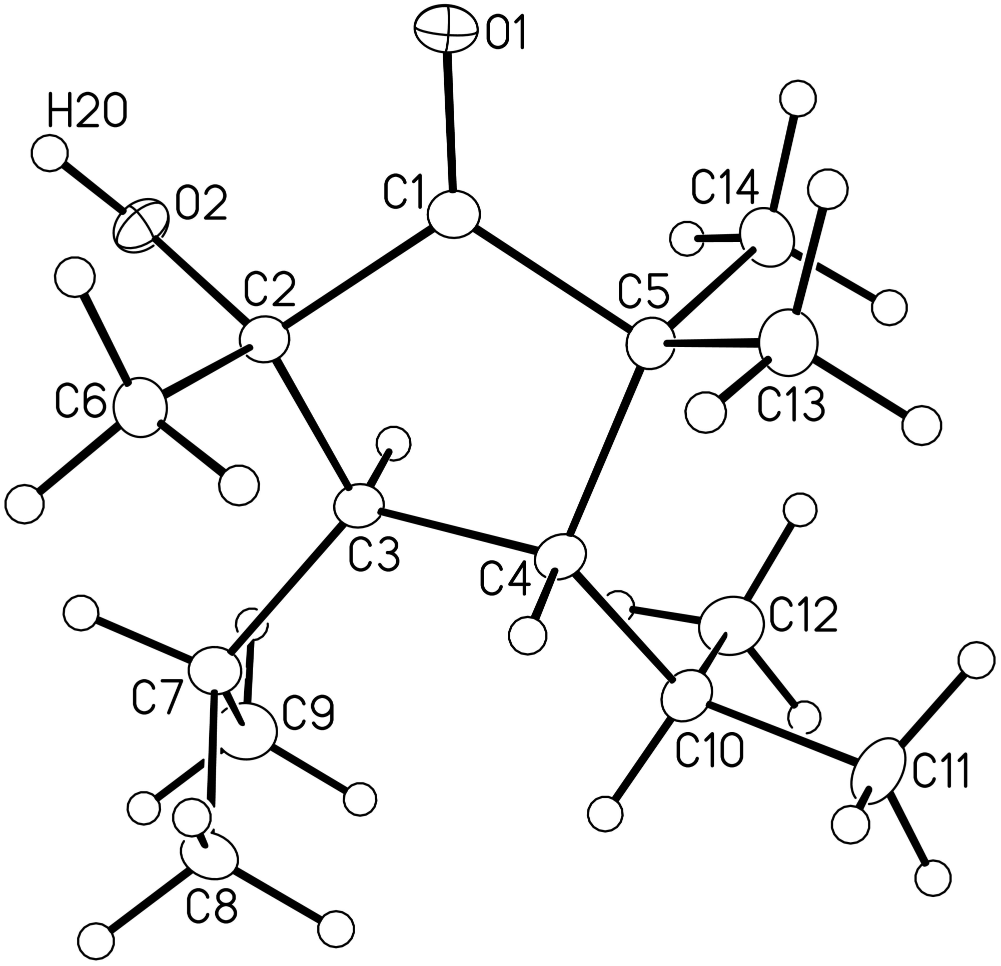

O1
H2O
O2
C1
C14
C2
C5
C6
C13
C3
C4
C12
C7
C9
C10
C11
C8

Figure 1. Perspective view of the 2-hydroxy-2,5,5-trimethyl-3,4-diisopropylcyclopentanone molecule showing the atom labelling scheme. Non-hydrogen atoms are represented by Gaussian ellipsoids at the 20% probability level. Hydrogen atoms are shown with arbitrarily small thermal parameters.

Table 1. Crystallographic Experimental Details

A. Crystal Data	
formula	$C_{14}H_{26}O_2$
formula weight	226.35
crystal dimensions (mm)	0.34 × 0.24 × 0.11
crystal system	monoclinic
space group	*C*2/*c* (No. 15)
unit cell parameters[a]	
a (Å)	28.5963 (16)
b (Å)	8.2309 (4)
c (Å)	11.4191 (6)
β (deg)	95.215 (3)
V (Å^3)	2676.6 (2)
Z	8
ρ_{calcd} (g cm^{-3})	1.123
μ (mm^{-1})	0.563
B. Data Collection and Refinement Conditions	
diffractometer	Bruker D8/APEX II CCD[b]
radiation (λ [Å])	Cu Kα (1.54178) (microfocus source)
temperature (°C)	–100
scan type	ω and ϕ scans (1.0°) (5 s exposures)
data collection 2θ limit (deg)	142.60
total data collected	8631 ($-34 \le h \le 34$, $-10 \le k \le 9$, $-14 \le l \le 13$)
independent reflections	2590 ($R_{\mathrm{int}} = 0.0204$)
number of observed reflections (*NO*)	2433 [$F_o^2 \ge 2\sigma(F_o^2)$]
structure solution method	direct methods/dual space (*SHELXD*[c])
refinement method	full-matrix least-squares on F^2 (*SHELXL–97*[d])
absorption correction method	Gaussian integration (face-indexed)
range of transmission factors	0.9401–0.8334
data/restraints/parameters	2590 / 0 / 149
goodness-of-fit (*S*)[e] [all data]	1.051
final *R* indices[f]	
R_1 [$F_o^2 \ge 2\sigma(F_o^2)$]	0.0575
wR_2 [all data]	0.1657
largest difference peak and hole	0.470 and –0.262 e Å^{-3}

[a] Obtained from least-squares refinement of 9845 reflections with $6.20° < 2\theta < 142.48°$.

[b] Programs for diffractometer operation, data collection, data reduction and absorption correction were those supplied by Bruker.

(continued)

Table 1. Crystallographic Experimental Details (continued)

[c] Schneider, T. R.; Sheldrick, G. M. *Acta Crystallogr.* **2002**, *D58*, 1772-1779.

[d] Sheldrick, G. M. *Acta Crystallogr.* **2008**, *A64*, 112–122.

[e] $S = [\Sigma w(F_o^2 - F_c^2)^2/(n - p)]^{1/2}$ (n = number of data; p = number of parameters varied; $w = [\sigma^2(F_o^2) + (0.0919P)^2 + 3.1559P]^{-1}$ where $P = [\mathrm{Max}(F_o^2, 0) + 2F_c^2]/3$).

[f] $R_1 = \Sigma||F_o| - |F_c||/\Sigma|F_o|$; $wR_2 = [\Sigma w(F_o^2 - F_c^2)^2/\Sigma w(F_o^4)]^{1/2}$.

Appendix XIV: X-ray Crystallographic Data for Compound 5g

(Chapter 3)

STRUCTURE REPORT

XCL Code: FGW1303 **Date:** 12 March 2013

Compound: 6-Hydroxy-6,7a-dimethyl-5-phenylhexahydrocyclopenta[*b*]pyran-7(2*H*)-one

Formula: $C_{16}H_{20}O_3$

Supervisor: F. G. West

Crystallographer: R. McDonald

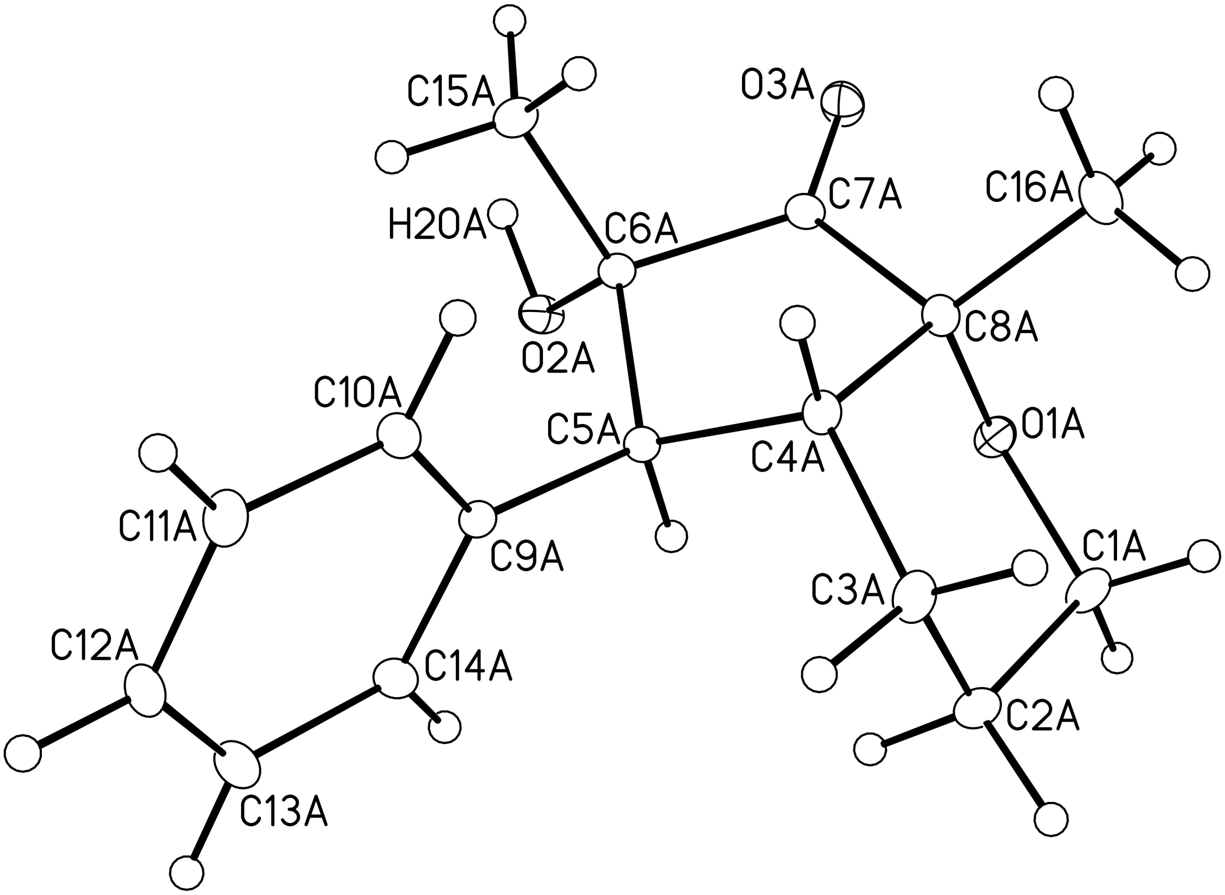
C15A
O3A
C7A
C16A
H2OA
C6A
C8A
O2A
C10A
C5A
O1A
C4A
C11A
C9A
C1A
C3A
C12A
C14A
C2A
C13A

Figure 1. Perspective view of one of the two crystallographically-independent molecules of 6-hydroxy-6,7a-dimethyl-5-phenylhexahydrocyclopenta[*b*]pyran-7(2*H*)-one (molecule A) showing the atom labelling scheme. Non-hydrogen atoms are represented by Gaussian ellipsoids at the 20% probability level. Hydrogen atoms are shown with arbitrarily small thermal parameters.

Table 1. Crystallographic Experimental Details

A. Crystal Data	
formula	$C_{16}H_{20}O_3$
formula weight	260.32
crystal dimensions (mm)	0.71 × 0.08 × 0.03
crystal system	orthorhombic
space group	$Pca2_1$ (No. 29)
unit cell parameters[a]	
a (Å)	22.5160 (6)
b (Å)	5.6843 (2)
c (Å)	21.2628 (6)
V (Å^3)	2721.38 (14)
Z	8
ρ_{calcd} (g cm^{-3})	1.271
μ (mm^{-1})	0.695
B. Data Collection and Refinement Conditions	
diffractometer	Bruker D8/APEX II CCD[b]
radiation (λ [Å])	Cu Kα (1.54178) (microfocus source)
temperature (°C)	–100
scan type	ω and ϕ scans (1.0°) (5 s exposures)
data collection 2θ limit (deg)	142.64
total data collected	17179 ($-27 \leq h \leq 27$, $-6 \leq k \leq 6$, $-26 \leq l \leq 26$)
independent reflections	5270 ($R_{\text{int}} = 0.0638$)
number of observed reflections (*NO*)	5028 [$F_o^2 \geq 2\sigma(F_o^2)$]
structure solution method	direct methods/dual space (*SHELXD*[c])
refinement method	full-matrix least-squares on F^2 (*SHELXL–97*[d])
absorption correction method	Gaussian integration (face-indexed)
range of transmission factors	0.9822–0.6390
data/restraints/parameters	5270 / 0 / 351
Flack absolute structure parameter[e]	0.34(17)
goodness-of-fit (*S*)[f] [all data]	1.033
final *R* indices[g]	
R_1 [$F_o^2 \geq 2\sigma(F_o^2)$]	0.0459
wR_2 [all data]	0.1159
largest difference peak and hole	0.274 and –0.224 e Å^{-3}

[a] Obtained from least-squares refinement of 7352 reflections with 8.32° < 2θ < 142.16°.

[b] Programs for diffractometer operation, data collection, data reduction and absorption correction were those supplied by Bruker.

(continued)

Table 1. Crystallographic Experimental Details (continued)

[c]Schneider, T. R.; Sheldrick, G. M. *Acta Crystallogr.* **2002**, *D58*, 1772-1779.

[d]Sheldrick, G. M. *Acta Crystallogr.* **2008**, *A64*, 112–122.

[e]Flack, H. D. *Acta Crystallogr.* **1983**, *A39*, 876–881; Flack, H. D.; Bernardinelli, G. *Acta Crystallogr.* **1999**, *A55*, 908–915; Flack, H. D.; Bernardinelli, G. *J. Appl. Cryst.* **2000**, *33*, 1143–1148. The Flack parameter will refine to a value near zero if the structure is in the correct configuration and will refine to a value near one for the inverted configuration. The low anomalous scattering power of the atoms in this structure (none heavier than oxygen) implies that the data cannot be used for absolute structure assignment, thus the Flack parameter is provided for informational purposes only.

[f]$S = [\Sigma w(F_o^2 - F_c^2)^2/(n - p)]^{1/2}$ (n = number of data; p = number of parameters varied; $w = [\sigma^2(F_o^2) + (0.0415P)^2 + 0.7502P]^{-1}$ where $P = [\mathrm{Max}(F_o^2, 0) + 2F_c^2]/3$).

[g]$R_1 = \Sigma||F_o| - |F_c||/\Sigma|F_o|$; $wR_2 = [\Sigma w(F_o^2 - F_c^2)^2/\Sigma w(F_o^4)]^{1/2}$.

Appendix XV: X-ray Crystallographic Data for Compound 4a

(Chapter 4)

STRUCTURE REPORT

XCL Code: FGW1214 **Date:** 8 December 2014

Compound: 2-(Hydroxymethyl)-2,5,5-trimethyl-3,4-diphenylcyclopentanone
Formula: $C_{21}H_{24}O_2$

Supervisor: F. G. West

Crystallographer: R. McDonald

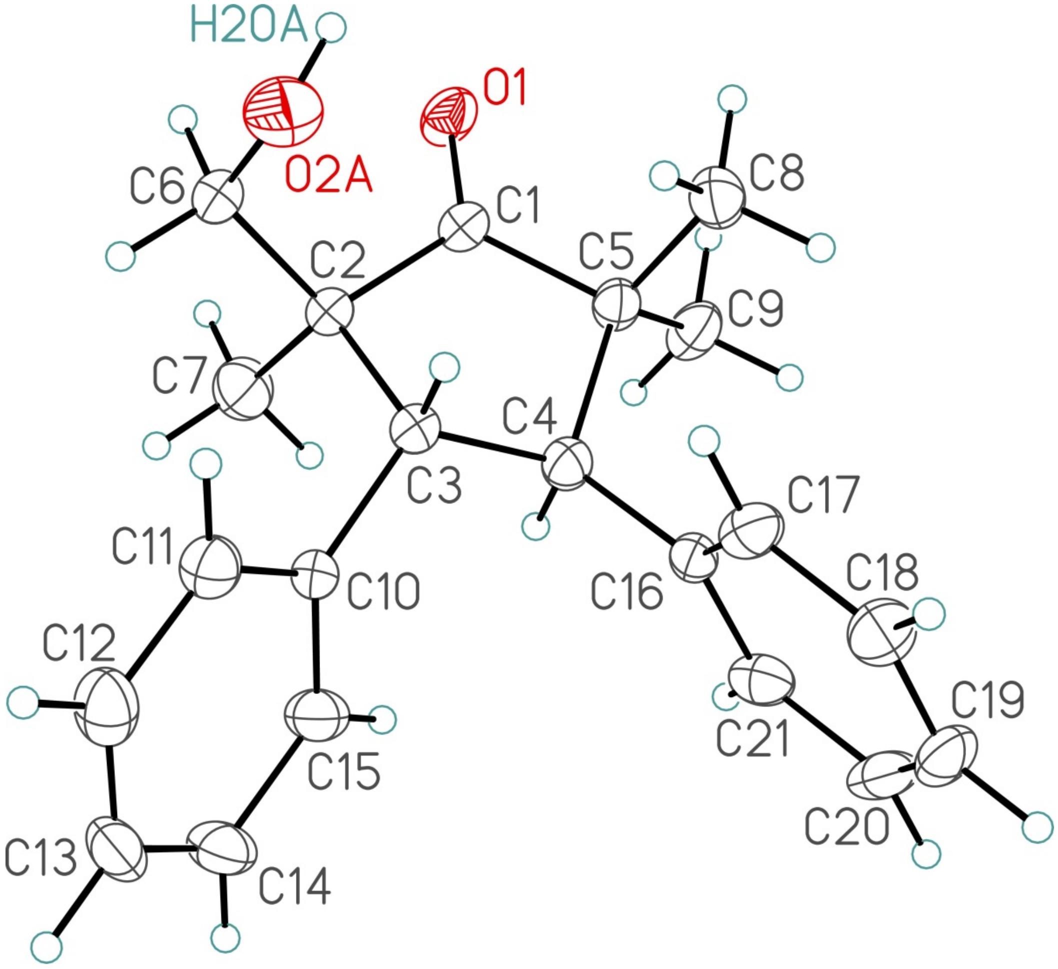
H2OA
O1
O2A
C6
C1
C8
C2
C5
C9
C7
C4
C3
C17
C11
C10
C16
C18
C12
C19
C21
C15
C20
C13
C14

Figure 1. Perspective view of the 2-(hydroxymethyl)-2,5,5-trimethyl-3,4-diphenylcyclopentanone molecule showing the atom labelling scheme. Non-hydrogen atoms are represented by Gaussian ellipsoids at the 30% probability level. Hydrogen atoms are shown with arbitrarily small thermal parameters.

Table 1. Crystallographic Experimental Details

A. Crystal Data	
formula	$C_{21}H_{24}O_2$
formula weight	308.40
crystal dimensions (mm)	0.37 × 0.34 × 0.27
crystal system	monoclinic
space group	$P2_1/c$ (No. 14)
unit cell parameters[a]	
a (Å)	15.6288 (4)
b (Å)	6.4934 (2)
c (Å)	17.2433 (4)
β (deg)	99.7513 (8)
V (Å^3)	1724.64 (8)
Z	4
ρ_{calcd} (g cm^{-3})	1.188
μ (mm^{-1})	0.583
B. Data Collection and Refinement Conditions	
diffractometer	Bruker D8/APEX II CCD[b]
radiation (λ [Å])	Cu Kα (1.54178) (microfocus source)
temperature (°C)	–100
scan type	ω and ϕ scans (1.0°) (5 s exposures)
data collection 2θ limit (deg)	142.84
total data collected	11053 ($-19 \le h \le 19$, $-7 \le k \le 7$, $-21 \le l \le 21$)
independent reflections	3325 ($R_{\mathrm{int}} = 0.0149$)
number of observed reflections (*NO*)	3287 [$F_o^2 \ge 2\sigma(F_o^2)$]
structure solution method	direct methods/dual space (*SHELXD*[c])
refinement method	full-matrix least-squares on F^2 (*SHELXL–2013*[d])
absorption correction method	Gaussian integration (face-indexed)
range of transmission factors	0.9219–0.8016
data/restraints/parameters	3325 / 0 / 215
goodness-of-fit (S)[e] [all data]	1.041
final R indices[f]	
R_1 [$F_o^2 \ge 2\sigma(F_o^2)$]	0.0800
wR_2 [all data]	0.2016
largest difference peak and hole	0.734 and –0.397 e Å^{-3}

[a] Obtained from least-squares refinement of 9454 reflections with 7.06° < 2θ < 142.46°.

[b] Programs for diffractometer operation, data collection, data reduction and absorption correction were those supplied by Bruker.

(continued)

Table 1. Crystallographic Experimental Details (continued)

[c] Schneider, T. R.; Sheldrick, G. M. *Acta Crystallogr.* **2002**, *D58*, 1772-1779.

[d] Sheldrick, G. M. *Acta Crystallogr.* **2008**, *A64*, 112–122.

[e] $S = [\Sigma w(F_o^2 - F_c^2)^2/(n - p)]^{1/2}$ (n = number of data; p = number of parameters varied; $w = [\sigma^2(F_o^2) + (0.0868P)^2 + 2.2518P]^{-1}$ where $P = [\mathrm{Max}(F_o^2, 0) + 2F_c^2]/3$).

[f] $R_1 = \Sigma||F_o| - |F_c||/\Sigma|F_o|$; $wR_2 = [\Sigma w(F_o^2 - F_c^2)^2/\Sigma w(F_o^4)]^{1/2}$.

Appendix XVI: X-ray Crystallographic Data for Compound 3f

(Chapter 4)

STRUCTURE REPORT

XCL Code: FGW1301 **Date:** 11 January 2013

Compound: 2-(Hydroxymethyl)-2,5,5-trimethyl-3-phenylcyclopentanone
Formula: $C_{15}H_{20}O_2$

Supervisor: F. G. West

Crystallographer: R. McDonald

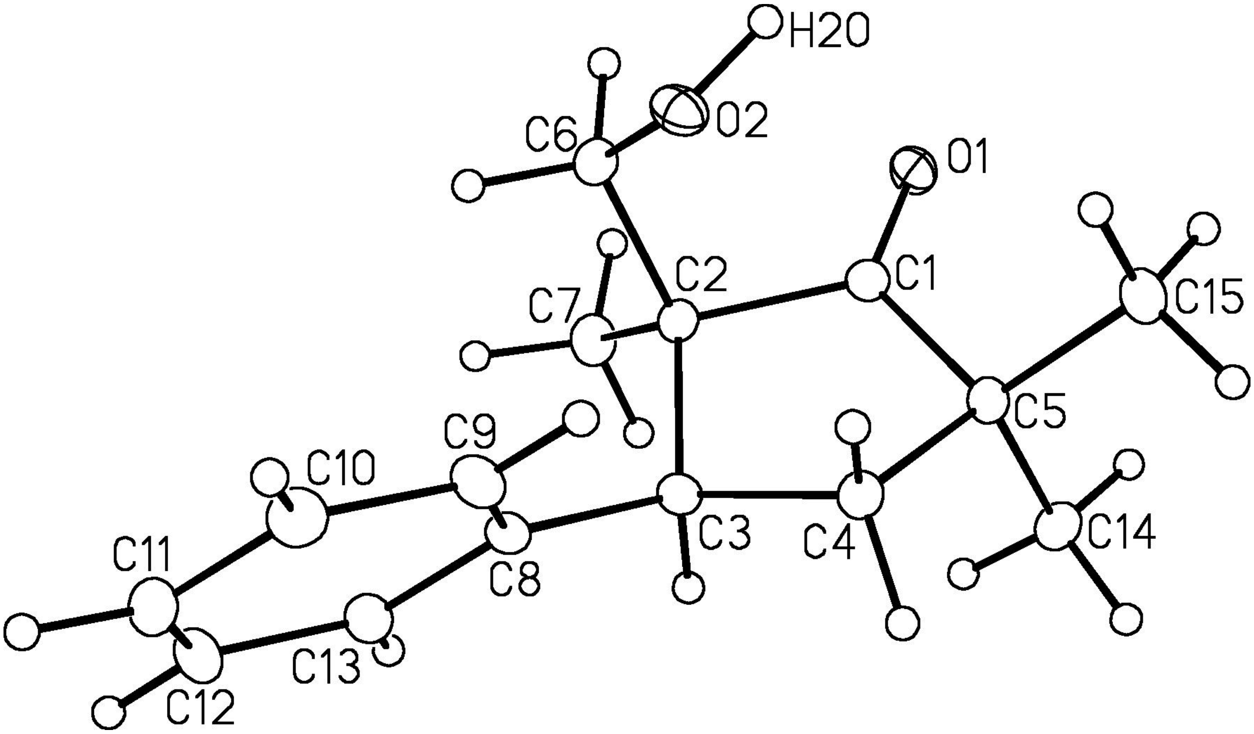

Figure 1. Perspective view of the 2-(hydroxymethyl)-2,5,5-trimethyl-3-phenylcyclopentanone molecule showing the atom labelling scheme. Non-hydrogen atoms are represented by Gaussian ellipsoids at the 20% probability level. Hydrogen atoms are shown with arbitrarily small thermal parameters.

Table 1. Crystallographic Experimental Details

A. Crystal Data

formula	$C_{15}H_{20}O_2$
formula weight	232.31
crystal dimensions (mm)	0.34 × 0.27 × 0.09
crystal system	monoclinic
space group	*C*2/*c* (No. 15)
unit cell parameters[a]	
a (Å)	21.799 (3)
b (Å)	6.4900 (10)
c (Å)	20.518 (3)
β (deg)	116.3214 (18)
V (Å^3)	2601.8 (7)
Z	8
ρ_{calcd} (g cm^{-3})	1.186
μ (mm^{-1})	0.077

B. Data Collection and Refinement Conditions

diffractometer	Bruker D8/APEX II CCD[b]
radiation (λ [Å])	graphite-monochromated Mo Kα (0.71073)
temperature (°C)	–100
scan type	ω scans (0.3°) (20 s exposures)
data collection 2θ limit (deg)	52.92
total data collected	10069 ($-27 \le h \le 27$, $-8 \le k \le 8$, $-25 \le l \le 25$)
independent reflections	2684 ($R_{\text{int}} = 0.0588$)
number of observed reflections (*NO*)	1813 [$F_o^2 \ge 2\sigma(F_o^2)$]
structure solution method	direct methods/dual space (*SHELXD*[c])
refinement method	full-matrix least-squares on F^2 (*SHELXL–97*[d])
absorption correction method	Gaussian integration (face-indexed)
range of transmission factors	0.9928–0.9744
data/restraints/parameters	2684 / 0 / 158
goodness-of-fit (*S*)[e] [all data]	1.045
final *R* indices[f]	
R_1 [$F_o^2 \ge 2\sigma(F_o^2)$]	0.0467
wR_2 [all data]	0.1310
largest difference peak and hole	0.267 and –0.223 e Å^{-3}

[a] Obtained from least-squares refinement of 1884 reflections with $4.42° < 2\theta < 39.94°$.

[b] Programs for diffractometer operation, data collection, data reduction and absorption correction were those supplied by Bruker. (continued)

Table 1. Crystallographic Experimental Details (continued)

[c]Schneider, T. R.; Sheldrick, G. M. *Acta Crystallogr.* **2002**, *D58*, 1772-1779.

[d]Sheldrick, G. M. *Acta Crystallogr.* **2008**, *A64*, 112–122.

[e]$S = [\Sigma w(F_o^2 - F_c^2)^2/(n - p)]^{1/2}$ (n = number of data; p = number of parameters varied; $w = [\sigma^2(F_o^2) + (0.0633P)^2 + 0.3485P]^{-1}$ where $P = [\mathrm{Max}(F_o^2, 0) + 2F_c^2]/3$).

[f]$R_1 = \Sigma||F_o| - |F_c||/\Sigma|F_o|$; $wR_2 = [\Sigma w(F_o^2 - F_c^2)^2/\Sigma w(F_o^4)]^{1/2}$.

Appendix XVII: X-ray Crystallographic Data for Compound 8a

(Chapter 4)

STRUCTURE REPORT

XCL Code: FGW1307 **Date:** 7 June 2013

Compound: 2-(hydroxymethyl)-2,5-dimethyl-3,4-diphenylcyclopentanone
Formula: $C_{20}H_{22}O_2$

Supervisor: F. G. West

Crystallographer: R. McDonald

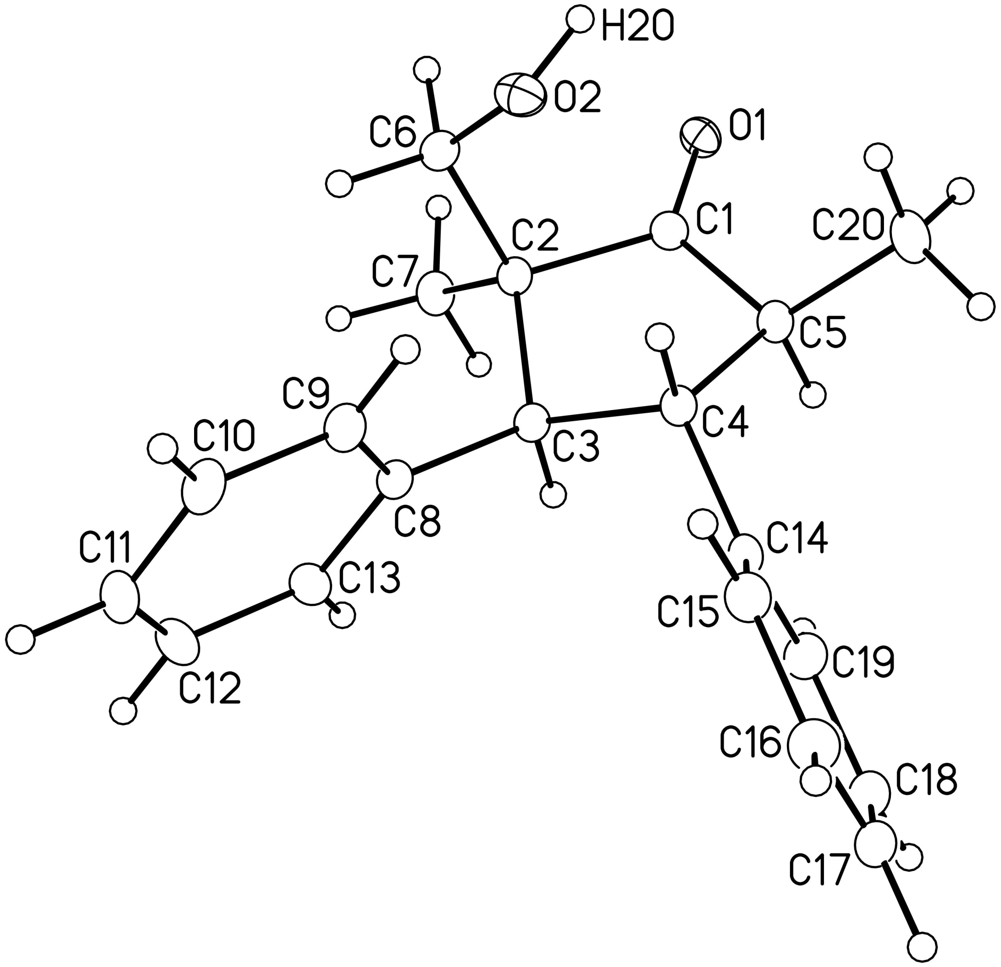
H2O
O2
O1
C6
C1
C20
C2
C7
C5
C9
C4
C10
C3
C8
C14
C11
C13
C15
C19
C12
C16
C18
C17

Figure 1. Perspective view of the 2-(hydroxymethyl)-2,5-dimethyl-3,4-diphenylcyclopentanone molecule showing the atom labelling scheme. Non-hydrogen atoms are represented by Gaussian ellipsoids at the 20% probability level. Hydrogen atoms are shown with arbitrarily small thermal parameters.

Table 1. Crystallographic Experimental Details

A. Crystal Data	
formula	$C_{20}H_{22}O_2$
formula weight	294.38
crystal dimensions (mm)	0.33 × 0.33 × 0.17
crystal system	monoclinic
space group	$P2_1/c$ (No. 14)
unit cell parameters[a]	
a (Å)	16.6340 (16)
b (Å)	6.4464 (6)
c (Å)	17.0969 (17)
β (deg)	116.3100 (11)
V (Å^3)	1643.4 (3)
Z	4
ρ_{calcd} (g cm^{-3})	1.190
μ (mm^{-1})	0.075
B. Data Collection and Refinement Conditions	
diffractometer	Bruker D8/APEX II CCD[b]
radiation (λ [Å])	graphite-monochromated Mo Kα (0.71073)
temperature (°C)	–100
scan type	ω scans (0.3°) (20 s exposures)
data collection 2θ limit (deg)	52.86
total data collected	12661 ($-20 \leq h \leq 20$, $-8 \leq k \leq 8$, $-21 \leq l \leq 21$)
independent reflections	3375 ($R_{\text{int}} = 0.0235$)
number of observed reflections (*NO*)	2775 [$F_o^2 \geq 2\sigma(F_o^2)$]
structure solution method	direct methods/dual space (*SHELXD*[c])
refinement method	full-matrix least-squares on F^2 (*SHELXL–97*[d])
absorption correction method	Gaussian integration (face-indexed)
range of transmission factors	0.9877–0.9756
data/restraints/parameters	3375 / 0 / 203
goodness-of-fit (S)[e] [all data]	1.065
final R indices[f]	
R_1 [$F_o^2 \geq 2\sigma(F_o^2)$]	0.0379
wR_2 [all data]	0.1023
largest difference peak and hole	0.241 and –0.188 e Å^{-3}

[a] Obtained from least-squares refinement of 5853 reflections with $4.78° < 2\theta < 52.54°$.

[b] Programs for diffractometer operation, data collection, data reduction and absorption correction were those supplied by Bruker. (continued)

Table 1. Crystallographic Experimental Details (continued)

[c] Schneider, T. R.; Sheldrick, G. M. *Acta Crystallogr.* **2002**, *D58*, 1772-1779.

[d] Sheldrick, G. M. *Acta Crystallogr.* **2008**, *A64*, 112–122.

[e] $S = [\Sigma w(F_o^2 - F_c^2)^2/(n-p)]^{1/2}$ (n = number of data; p = number of parameters varied; $w = [\sigma^2(F_o^2) + (0.0448P)^2 + 0.4161P]^{-1}$ where $P = [\mathrm{Max}(F_o^2, 0) + 2F_c^2]/3$).

[f] $R_1 = \Sigma||F_o| - |F_c||/\Sigma|F_o|$; $wR_2 = [\Sigma w(F_o^2 - F_c^2)^2/\Sigma w(F_o^4)]^{1/2}$.

Appendix XVIII: X-ray Crystallographic Data for Compound 9a

(Chapter 4)

STRUCTURE REPORT

XCL Code: FGW1310 **Date:** 26 July 2013

Compound: 2-(Hydroxymethyl)-2,5-dimethyl-3,4-diphenylcyclopentanone
Formula: $C_{20}H_{22}O_2$

Supervisor: F. G. West

Crystallographer: R. McDonald

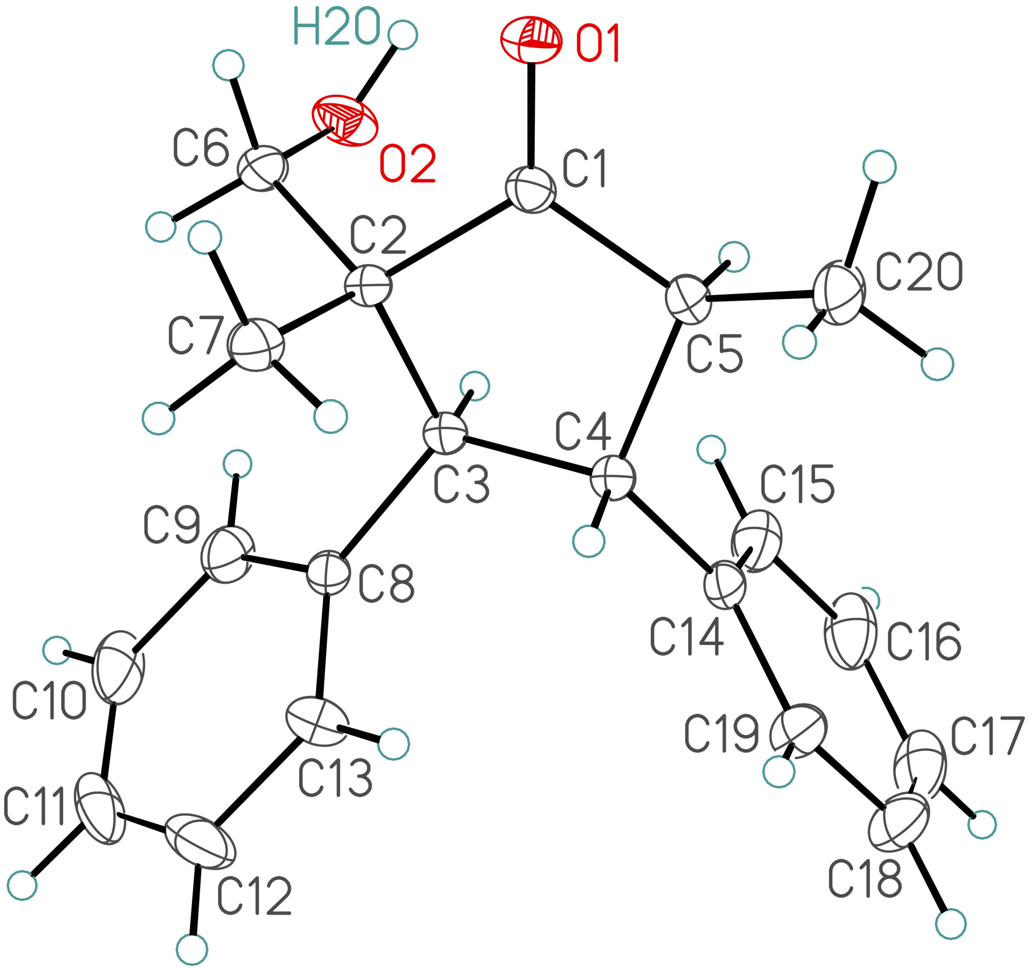
H2O
O1
C6
O2
C1
C2
C20
C7
C5
C4
C3
C15
C9
C8
C16
C14
C10
C19
C17
C13
C11
C18
C12

Figure 1. Perspective view of the 2-(hydroxymethyl)-2,5-dimethyl-3,4-diphenylcyclopentanone molecule showing the atom labelling scheme. Non-hydrogen atoms are represented by Gaussian ellipsoids at the 30% probability level. Hydrogen atoms are shown with arbitrarily small thermal parameters.

Table 1. Crystallographic Experimental Details

A. Crystal Data

formula	$C_{20}H_{22}O_2$
formula weight	294.37
crystal dimensions (mm)	0.30 × 0.19 × 0.17
crystal system	orthorhombic
space group	$Pna2_1$ (No. 33)
unit cell parameters[a]	
a (Å)	16.6139 (5)
b (Å)	15.7769 (5)
c (Å)	6.2842 (2)
V (Å^3)	1647.19 (9)
Z	4
ρ_{calcd} (g cm^{-3})	1.187
μ (mm^{-1})	0.075

B. Data Collection and Refinement Conditions

diffractometer	Bruker D8/APEX II CCD[b]
radiation (λ [Å])	graphite-monochromated Mo Kα (0.71073)
temperature (°C)	–100
scan type	ω scans (0.3°) (20 s exposures)
data collection 2θ limit (deg)	55.04
total data collected	14268 ($-21 \le h \le 21$, $-20 \le k \le 20$, $-8 \le l \le 8$)
independent reflections	3778 ($R_{\text{int}} = 0.0183$)
number of observed reflections (*NO*)	3581 [$F_o^2 \ge 2\sigma(F_o^2)$]
structure solution method	direct methods/dual space (*SHELXD*[c])
refinement method	full-matrix least-squares on F^2 (*SHELXL–97*[c])
absorption correction method	Gaussian integration (face-indexed)
range of transmission factors	1.0000–0.9366
data/restraints/parameters	3778 / 0 / 203
Flack absolute structure parameter[d]	0.3(3)
goodness-of-fit (S)[e] [all data]	1.042
final R indices[f]	
R_1 [$F_o^2 \ge 2\sigma(F_o^2)$]	0.0323
wR_2 [all data]	0.0861
largest difference peak and hole	0.184 and –0.160 e Å^{-3}

[a] Obtained from least-squares refinement of 8360 reflections with $4.90° < 2\theta < 50.94°$.

[b] Programs for diffractometer operation, data collection, data reduction and absorption correction were those supplied by Bruker.

(continued)

Table 1. Crystallographic Experimental Details (continued)

[c] Sheldrick, G. M. *Acta Crystallogr.* **2008**, *A64*, 112–122.

[d] Flack, H. D. *Acta Crystallogr.* **1983**, *A39*, 876–881; Flack, H. D.; Bernardinelli, G. *Acta Crystallogr.* **1999**, *A55*, 908–915; Flack, H. D.; Bernardinelli, G. *J. Appl. Cryst.* **2000**, *33*, 1143–1148. The Flack parameter will refine to a value near zero if the structure is in the correct configuration and will refine to a value near one for the inverted configuration. In this structure, both enantiomers of this compound are present, thus the value of the Flack parameter implies that the intermolecular structural 'handedness' (due to the noncentrosymmetric space group) cannot be accurately determined.

[e] $S = [\Sigma w(F_o^2 - F_c^2)^2/(n - p)]^{1/2}$ (n = number of data; p = number of parameters varied; $w = [\sigma^2(F_o^2) + (0.0463P)^2 + 0.2317P]^{-1}$ where $P = [\mathrm{Max}(F_o^2, 0) + 2F_c^2]/3$).

[f] $R_1 = \Sigma||F_o| - |F_c||/\Sigma|F_o|$; $wR_2 = [\Sigma w(F_o^2 - F_c^2)^2/\Sigma w(F_o^4)]^{1/2}$.

Appendix XIX: X-ray Crystallographic Data for Compound 14a

(Chapter 4)

STRUCTURE REPORT

XCL Code: FGW1304 **Date:** 12 March 2013

Compound: 2,2,5-Trimethyl-3,4-diphenyl-6,7-dioxabicyclo[3.2.1]octan-1-ol
Formula: $C_{21}H_{24}O_3$

Supervisor: F. G. West

Crystallographer: R. McDonald

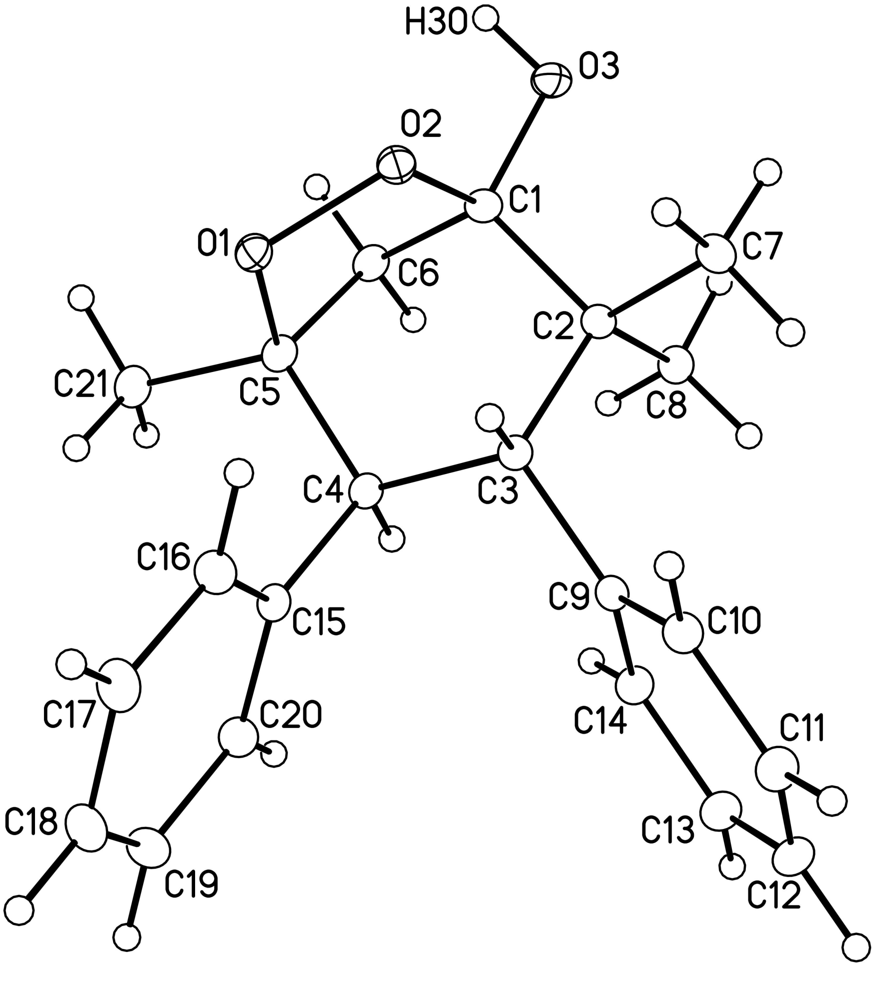
H3O
O3
O2
C1
O1
C6
C7
C2
C21
C5
C8
C4
C3
C16
C15
C9
C10
C17
C20
C14
C11
C18
C13
C19
C12

Figure 1. Perspective view of the 2,2,5-trimethyl-3,4-diphenyl-6,7-dioxabicyclo-[3.2.1]octan-1-ol molecule showing the atom labelling scheme. Non-hydrogen atoms are represented by Gaussian ellipsoids at the 20% probability level. Hydrogen atoms are shown with arbitrarily small thermal parameters.

Table 1. Crystallographic Experimental Details

A. Crystal Data	
formula	$C_{21}H_{24}O_3$
formula weight	324.40
crystal dimensions (mm)	0.50 × 0.09 × 0.06
crystal system	triclinic
space group	$P\bar{1}$ (No. 2)
unit cell parameters[a]	
a (Å)	6.1839 (3)
b (Å)	10.8563 (4)
c (Å)	12.9475 (5)
α (deg)	88.9254 (18)
β (deg)	87.588 (2)
γ (deg)	89.9685 (18)
V (Å^3)	868.30 (6)
Z	2
ρ_{calcd} (g cm^{-3})	1.241
μ (mm^{-1})	0.649
B. Data Collection and Refinement Conditions	
diffractometer	Bruker D8/APEX II CCD[b]
radiation (λ [Å])	Cu Kα (1.54178) (microfocus source)
temperature (°C)	–100
scan type	ω and ϕ scans (1.0°) (5 s exposures)
data collection 2θ limit (deg)	142.32
total data collected	5901 ($-7 \leq h \leq 7$, $-13 \leq k \leq 13$, $-15 \leq l \leq 15$)
independent reflections	3199 (R_{int} = 0.0208)
number of observed reflections (*NO*)	2821 [$F_o^2 \geq 2\sigma(F_o^2)$]
structure solution method	direct methods/dual space (*SHELXD*[c])
refinement method	full-matrix least-squares on F^2 (*SHELXL–97*[d])
absorption correction method	Gaussian integration (face-indexed)
range of transmission factors	0.9646–0.7362
data/restraints/parameters	3199 / 0 / 221
goodness-of-fit (*S*)[e] [all data]	1.079
final *R* indices[f]	
R_1 [$F_o^2 \geq 2\sigma(F_o^2)$]	0.0392
wR_2 [all data]	0.1102
largest difference peak and hole	0.283 and –0.188 e Å^{-3}

[a]Obtained from least-squares refinement of 8804 reflections with 6.84° < 2θ < 142.32°.

(continued)

Table 1. Crystallographic Experimental Details (continued)

[b] Programs for diffractometer operation, data collection, data reduction and absorption correction were those supplied by Bruker.

[c] Schneider, T. R.; Sheldrick, G. M. *Acta Crystallogr.* **2002**, *D58*, 1772-1779.

[d] Sheldrick, G. M. *Acta Crystallogr.* **2008**, *A64*, 112–122.

[e] $S = [\Sigma w(F_o^2 - F_c^2)^2/(n - p)]^{1/2}$ (n = number of data; p = number of parameters varied; $w = [\sigma^2(F_o^2) + (0.0547P)^2 + 0.2258P]^{-1}$ where $P = [\mathrm{Max}(F_o^2, 0) + 2F_c^2]/3$).

[f] $R_1 = \Sigma||F_o| - |F_c||/\Sigma|F_o|$; $wR_2 = [\Sigma w(F_o^2 - F_c^2)^2/\Sigma w(F_o^4)]^{1/2}$.

Appendix XX: X-ray Crystallographic Data for Compound 3a

(Chapter 5)

STRUCTURE REPORT

XCL Code: FGW1319 **Date:** 11 October 2013

Compound: 3,4-Diphenylhexa-2,5-dione
Formula: $C_{18}H_{18}O_2$

Supervisor: F. G. West

Crystallographer: R. McDonald

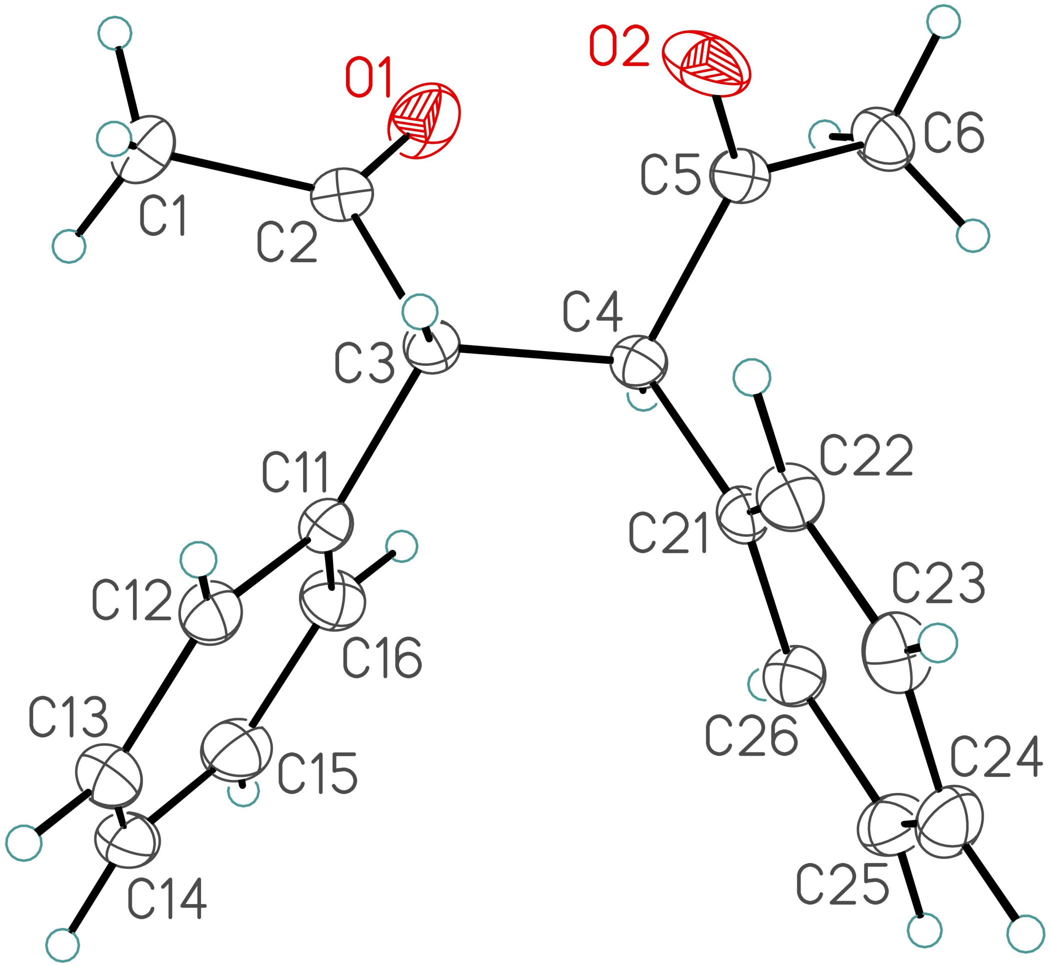
O1
O2
C1
C2
C3
C4
C5
C6
C11
C12
C13
C14
C15
C16
C21
C22
C23
C24
C25
C26

Figure 1. Perspective view of the 3,4-diphenylhexa-2,5-dione molecule showing the atom labelling scheme. Non-hydrogen atoms are represented by Gaussian ellipsoids at the 30% probability level. Hydrogen atoms are shown with arbitrarily small thermal parameters.

Table 1. Crystallographic Experimental Details

A. Crystal Data	
formula	$C_{18}H_{18}O_2$
formula weight	266.32
crystal dimensions (mm)	0.30 × 0.29 × 0.18
crystal system	orthorhombic
space group	$P2_12_12_1$ (No. 19)
unit cell parameters[a]	
a (Å)	7.7273 (5)
b (Å)	11.3507 (7)
c (Å)	16.7762 (10)
V (Å^3)	1471.45 (16)
Z	4
ρ_{calcd} (g cm^{-3})	1.202
μ (mm^{-1})	0.077
B. Data Collection and Refinement Conditions	
diffractometer	Bruker D8/APEX II CCD[b]
radiation (λ [Å])	graphite-monochromated Mo Kα (0.71073)
temperature (°C)	–100
scan type	ω scans (0.3°) (20 s exposures)
data collection 2θ limit (deg)	55.14
total data collected	13151 ($-10 \leq h \leq 10$, $-14 \leq k \leq 14$, $-21 \leq l \leq 21$)
independent reflections	3377 ($R_{\text{int}} = 0.0181$)
number of observed reflections (*NO*)	3171 [$F_o^2 \geq 2\sigma(F_o^2)$]
structure solution method	direct methods/dual space (*SHELXD*[c])
refinement method	full-matrix least-squares on F^2 (*SHELXL–2013*[d])
absorption correction method	Gaussian integration (face-indexed)
range of transmission factors	1.0000–0.9266
data/restraints/parameters	3377 / 0 / 183
Flack absolute structure parameter[e]	0.1(3)
goodness-of-fit (S)[f] [all data]	1.053
final R indices[g]	
R_1 [$F_o^2 \geq 2\sigma(F_o^2)$]	0.0325
wR_2 [all data]	0.0847
largest difference peak and hole	0.180 and –0.146 e Å^{-3}

[a] Obtained from least-squares refinement of 8121 reflections with $4.86° < 2\theta < 51.52°$.

[b] Programs for diffractometer operation, data collection, data reduction and absorption correction were those supplied by Bruker. (continued)

Table 1. Crystallographic Experimental Details (continued)

[c] Schneider, T. R.; Sheldrick, G. M. *Acta Crystallogr.* **2002**, *D58*, 1772-1779.

[d] Sheldrick, G. M. *Acta Crystallogr.* **2008**, *A64*, 112–122.

[e] Flack, H. D. *Acta Crystallogr.* **1983**, *A39*, 876–881; Flack, H. D.; Bernardinelli, G. *Acta Crystallogr.* **1999**, *A55*, 908–915; Flack, H. D.; Bernardinelli, G. *J. Appl. Cryst.* **2000**, *33*, 1143–1148. The Flack parameter will refine to a value near zero if the structure is in the correct configuration and will refine to a value near one for the inverted configuration. The low anomalous scattering power of the atoms in this structure (none heavier than oxygen) and the high value of the Flack parameter's standard uncertainty implies that these data cannot be used for absolute structure assignment. The crystal was grown from a racemic mixture, and establishment of the relative stereochemistry of this compound is satisfactory for this study.

[f] $S = [\Sigma w(F_o^2 - F_c^2)^2/(n-p)]^{1/2}$ (n = number of data; p = number of parameters varied; $w = [\sigma^2(F_o^2) + (0.0402P)^2 + 0.2349P]^{-1}$ where $P = [\mathrm{Max}(F_o^2, 0) + 2F_c^2]/3$).

[g] $R_1 = \Sigma||F_o| - |F_c||/\Sigma|F_o|$; $wR_2 = [\Sigma w(F_o^2 - F_c^2)^2/\Sigma w(F_o^4)]^{1/2}$.

Appendix XXI: X-ray Crystallographic Data for Compound 5a

(Chapter 5)

STRUCTURE REPORT

XCL Code: FGW1318 **Date:** 11 October 2013

Compound: 2,5-Dichloro-2,5-dimethyl-3,4-diphenylcyclopentanone
Formula: $C_{19}H_{18}Cl_2O$

Supervisor: F. G. West

Crystallographer: R. McDonald

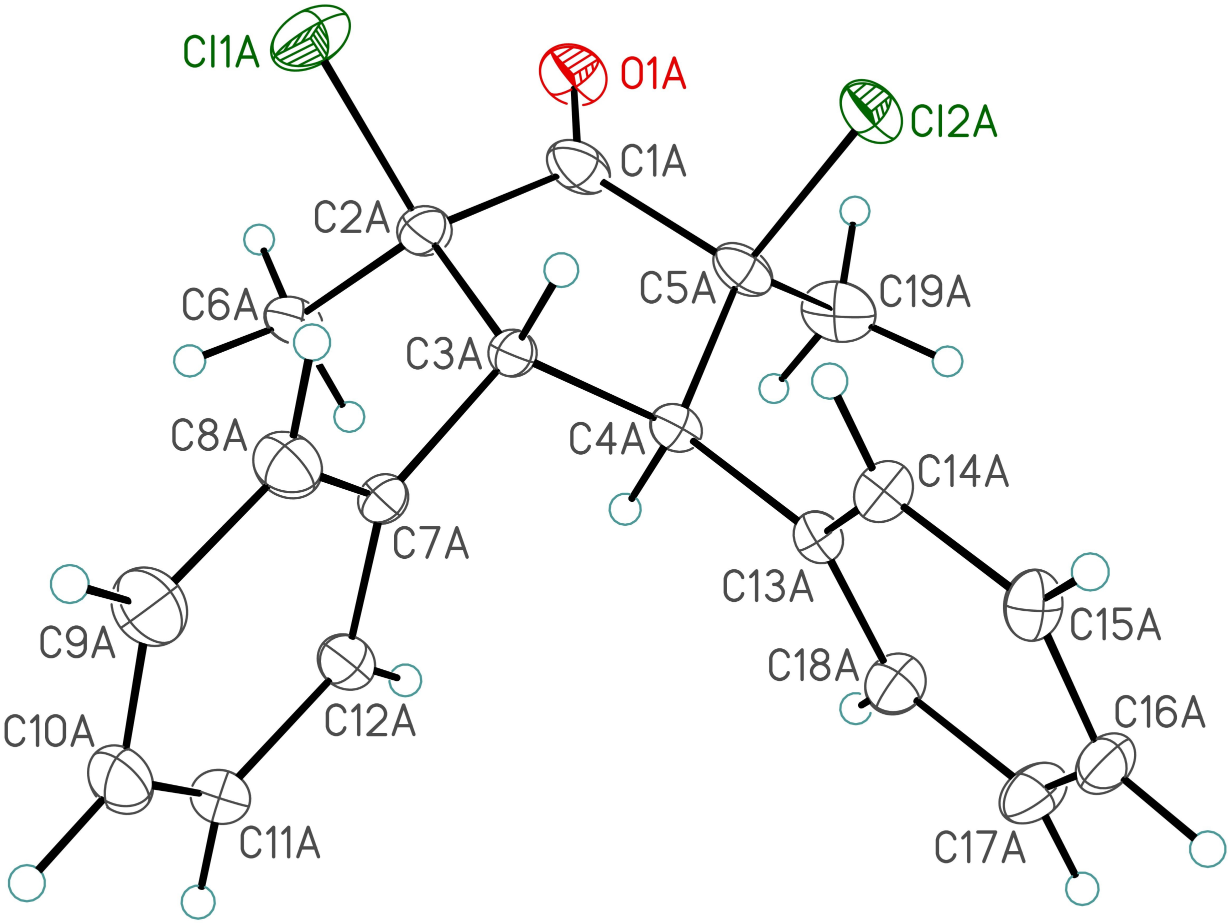
Cl1A
O1A
Cl2A
C1A
C2A
C5A
C19A
C6A
C3A
C4A
C8A
C14A
C7A
C13A
C9A
C15A
C18A
C16A
C12A
C10A
C11A
C17A

Figure 1. Perspective view of the majority (80%) disorder conformer of the 2,5-dichloro-2,5-dimethyl-3,4-diphenylcyclopentanone molecule showing the atom labelling scheme. Non-hydrogen atoms are represented by Gaussian ellipsoids at the 30% probability level. Hydrogen atoms are shown with arbitrarily small thermal parameters.

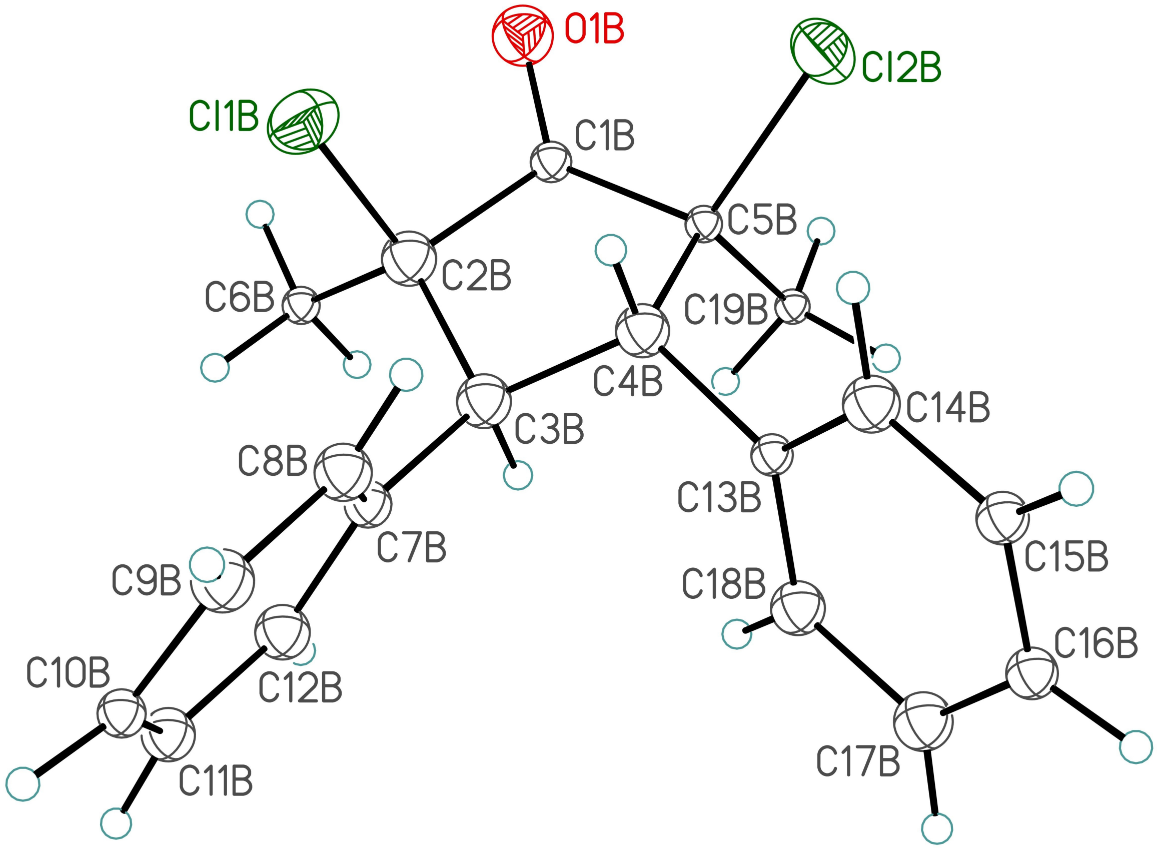
O1B
Cl1B
Cl2B
C1B
C5B
C2B
C6B
C19B
C4B
C3B
C14B
C8B
C13B
C7B
C15B
C9B
C18B
C16B
C10B
C12B
C17B
C11B

Figure 2. View of the minority (20%) disorder conformer of the 2,5-dichloro-2,5-dimethyl-3,4-diphenylcyclopentanone molecule.

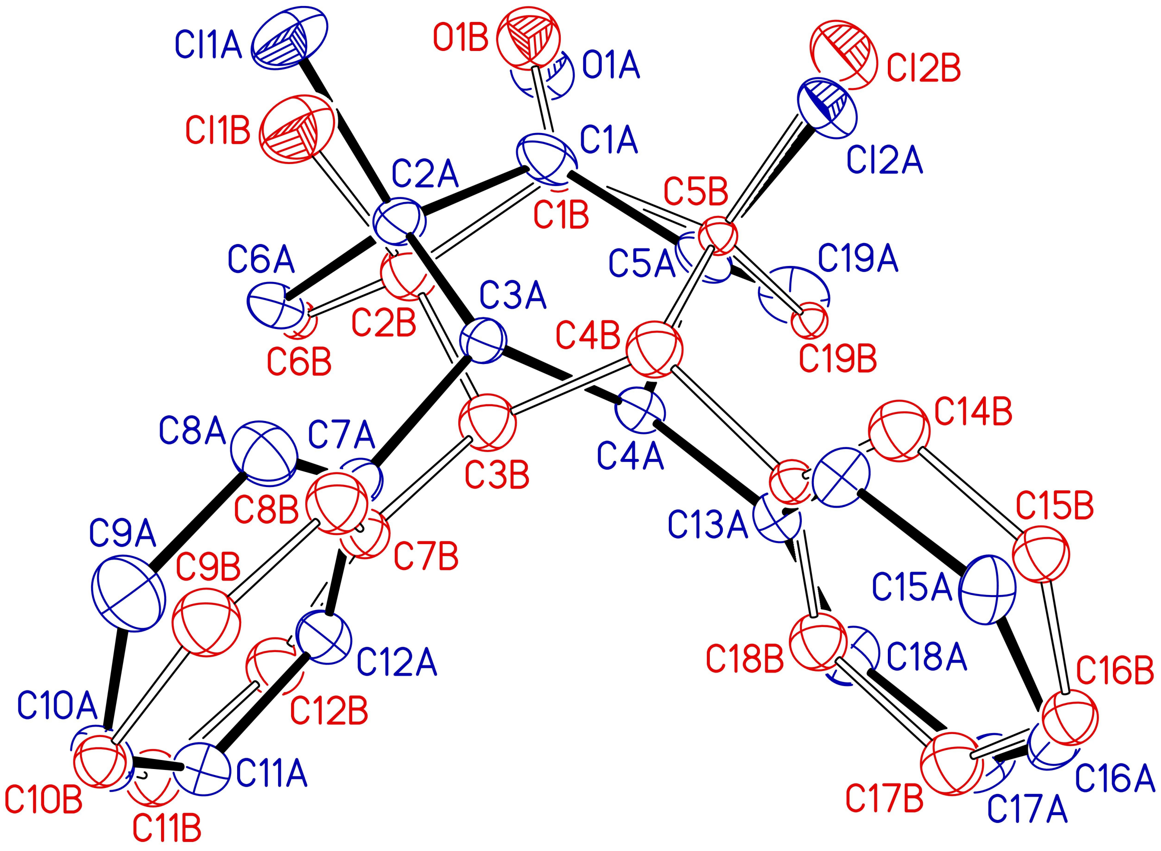
Cl1A
O1B
O1A
Cl2B
Cl1B
C1A
Cl2A
C2A
C5B
C1B
C19A
C6A
C5A
C3A
C2B
C4B
C19B
C6B
C14B
C8A
C7A
C3B
C4A
C8B
C15B
C13A
C9A
C7B
C9B
C15A
C12A
C18B
C18A
C16B
C10A
C12B
C11A
C16A
C10B
C11B
C17B
C17A

Figure 3. Illustration of the disorder mode of the molecule. The majority (80%) conformer is shown with solid bonds, while the minority (20%) conformer is shown with hollow bonds. Note that both conformers occupy approximately the same region in the unit cell lattice. These conformers represent opposite enantiomers, and although the local abundance ratio of the enantomers is 80:20, the centrosymmetric nature of the crystal's space group ensures that the enatiomers are equally abundant overall in the crystal (since there are positions in the crystal lattice that are related to this one via inversion symmtery).

Table 1. Crystallographic Experimental Details

A. Crystal Data	
formula	$C_{19}H_{18}Cl_2O$
formula weight	333.23
crystal dimensions (mm)	0.33 × 0.23 × 0.23
crystal system	orthorhombic
space group	*Pbca* (No. 61)
unit cell parameters[a]	
a (Å)	17.4006 (9)
b (Å)	9.0652 (5)
c (Å)	20.7592 (11)
V (Å^3)	3274.6 (3)
Z	8
ρ_{calcd} (g cm^{-3})	1.352
μ (mm^{-1})	0.395
B. Data Collection and Refinement Conditions	
diffractometer	Bruker D8/APEX II CCD[b]
radiation (λ [Å])	graphite-monochromated Mo Kα (0.71073)
temperature (°C)	–100
scan type	ω scans (0.3°) (20 s exposures)
data collection 2θ limit (deg)	55.00
total data collected	27260 ($-22 \leq h \leq 22$, $-11 \leq k \leq 11$, $-26 \leq l \leq 26$)
independent reflections	3760 ($R_{\text{int}} = 0.0559$)
number of observed reflections (*NO*)	3338 [$F_o^2 \geq 2\sigma(F_o^2)$]
structure solution method	direct methods/dual space (*SHELXD*[c])
refinement method	full-matrix least-squares on F^2 (*SHELXL–2013*[d])
absorption correction method	Gaussian integration (face-indexed)
range of transmission factors	0.9486–0.8665
data/restraints/parameters	3760 / 61[e] / 298
goodness-of-fit (*S*)[f] [all data]	1.155
final *R* indices[g]	
R_1 [$F_o^2 \geq 2\sigma(F_o^2)$]	0.0608
wR_2 [all data]	0.1645
largest difference peak and hole	0.464 and –0.429 e Å^{-3}

[a] Obtained from least-squares refinement of 9950 reflections with $4.56° < 2\theta < 53.40°$.

[b] Programs for diffractometer operation, data collection, data reduction and absorption correction were those supplied by Bruker.

(continued)

Table 1. Crystallographic Experimental Details (continued)

[c]Schneider, T. R.; Sheldrick, G. M. *Acta Crystallogr.* **2002**, *D58*, 1772-1779.

[d]Sheldrick, G. M. *Acta Crystallogr.* **2008**, *A64*, 112–122.

[f]All bond distances and 1,3-distances within bond angles involving corresponding atoms of the major (85%) and minor (15%) disorder components were constrained to be equal (within 0.03Å) during refinement, e.g. d(Cl1A–C2A) = d(Cl1B–C2B), d(O1A–-C1A) = d(O1B–C1B), d(Cl2A···C19A) = d(Cl2B···C19B) (for the Cl2A–C5A–C19A and Cl2B–C5B–C19B bond angles, respectively).

[f]$S = [\Sigma w(F_o^2 - F_c^2)^2/(n-p)]^{1/2}$ (n = number of data; p = number of parameters varied; $w = [\sigma^2(F_o^2) + (0.0565P)^2 + 3.8923P]^{-1}$ where $P = [\mathrm{Max}(F_o^2, 0) + 2F_c^2]/3$).

[g]$R_1 = \Sigma||F_o| - |F_c||/\Sigma|F_o|$; $wR_2 = [\Sigma w(F_o^2 - F_c^2)^2/\Sigma w(F_o^4)]^{1/2}$.